Quality Enhancement Techniques for Processing Fruits and Vegetables

Lead Guest Editor: Muhammad Faisal Manzoor
Guest Editors: Abid Hussain and Rana Muhammad Aadil

Quality Enhancement Techniques for Processing Fruits and Vegetables

Quality Enhancement Techniques for Processing Fruits and Vegetables

Lead Guest Editor: Muhammad Faisal Manzoor
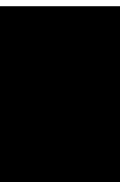Guest Editors: Abid Hussain and Rana Muhammad Aadil

María B. Pérez-Gago (iD), Spain
Anand Babu Perumal (iD), China
Gianfranco Picone (iD), Italy
Witoon Prinyawiwatkul, USA
Eduardo Puértolas (iD), Spain
Sneh Punia, USA
Sara Ragucci (iD), Italy
Miguel Rebollo-Hernanz (iD), Spain
Patricia Reboredo-Rodríguez (iD), Spain
Jordi Rovira (iD), Spain
Swarup Roy, India
Narashans Alok Sagar (iD), India
Rameswar Sah, India
El Hassan Sakar (iD), Morocco
Faouzi Sakouhi, Tunisia
Tanmay Sarkar (iD), India
Cristina Anamaria Semeniuc, Romania
Hiba Shaghaleh (iD), China
Akram Sharifi, Iran
Khetan Shevkani, India
Antonio J. Signes-Pastor (iD), USA
Amarat (Amy) Simonne (iD), USA
Anurag Singh, India
Ranjna Sirohi, Republic of Korea
Slim Smaoui (iD), Tunisia
Mattia Spano, Italy
Barbara Speranza (iD), Italy
Milan Stankovic (iD), Serbia
Maria Concetta Strano (iD), Italy
Antoni Szumny (iD), Poland
Beenu Tanwar, India
Hongxun Tao (iD), China
Ayon Tarafdar, India
Ahmed A. Tayel (iD), Egypt
Meriam Tir, Tunisia
Fernanda Vanin (iD), Brazil
Ajar Nath Yadav, India
Sultan Zahiruddin (iD), USA
Dimitrios I. Zeugolis (iD), Ireland
Chu Zhang (iD), China
Teresa Zotta (iD), Italy

Contents

WILEY | Hindawi

Review Article

Inactivating Food Microbes by High-Pressure Processing and Combined Nonthermal and Thermal Treatment: A Review

Prabhat K. Nema ⬡,[1] Rachna Sehrawat ⬡,[2] Chandrakala Ravichandran ⬡,[3] Barjinder Pal Kaur ⬡,[1] Anit Kumar ⬡,[4] and Ayon Tarafdar ⬡[5]

[1]Department of Food Engineering, National Institute of Food Technology Entrepreneurship and Management, Kundli, Sonepat 131028, Haryana, India
[2]Department of Food Process Engineering, National Institute of Technology Rourkela, Odisha 769008, India
[3]Department of Food Technology, Rajalakshmi Engineering College, Chennai-602105, Tamil Nadu, India
[4]Department of Food Technology, School of Chemical Technology, Harcourt Butler Technical University, Kanpur 208002, Uttar Pradesh, India
[5]Livestock Production and Management Section, ICAR-Indian Veterinary Research Institute, Izatnagar, Bareilly 243122, Uttar Pradesh, India

Correspondence should be addressed to Rachna Sehrawat; sehrawatrachna2017@gmail.com

High-pressure processing (HPP) is a mild technology alternative to thermal pasteurization and sterilization of different food products. HPP has emerged to provide enormous benefits to consumers, i.e., mildly processed food and additive-free food. It effectively retains bioactive compounds and extends the shelf life of food commodities by inactivating bacteria, yeast, mold, and virus. The limitation of HPP in inactivating spores can be overcome by using other thermal and nonthermal processing sequentially or simultaneously with HPP. This review summarizes the applications of HPP in the fruits and vegetables, dairy, meat, fish, and poultry sector. It also emphasizes microbial food safety and the effectiveness of HPP in the load reduction of microorganisms. Comprehensive information about the synergistic effect of HPP with different techniques and their effectiveness in ensuring food safety is reported. The summarized data would be handy to interested researchers and industry personnel.

1. Introduction

Most food commodities, i.e., fruits, vegetables, meat, poultry, seafood, milk, and their products, are perishable due to limited shelf life. The presence of moisture and environmental conditions (temperature and relative humidity) around food products during storage triggers physical, chemical changes, and microbiological growths leads to food deterioration or spoilage [1]. Spoilage can be defined as undesirable changes that render a product unsuitable for consumption due to physical, chemical, or microbiological changes. Physical changes include loss of moisture from dried foods, gain of moisture, and freeze burn. In many cases, physical changes in food products during storage also lead to chemical reactions and microorganism growth. Some undesirable chemical changes are staling, discolorations (by enzymatic browning and nonenzymatic browning), off-flavor development (due to oxidation of food leading to rancidity), etc. in the food products [2]. These chemical changes or reactions can be triggered by specific enzymes, i.e., lipases, peroxidases, polyphenol oxidases, and catalases. These changes reduce food quality and acceptability by consumers and are not recommended for consumption. Microbial spoilage can occur when bacteria, mold, and yeast grow in food or produce toxins harmful to humans. Apart from storage temperature and relative humidity, the growth of microorganisms in the food also depends on food composition. Since food is a rich source of nutrients and

water activity of most of the fresh commodities is high. So, it provides a very suitable environment for the microorganism to thrive on food. Food deterioration by the growth of pathogenic microorganisms is a significant concern [2]. As pathogenic bacteria are linked with outbreaks of fruits, vegetables, dairy, meat, and poultry-based products. Taiwan Food Drug Administration reported more than 2000 cases of food poisoning due to accidental consumption of fresh fruits, vegetables, and seafood products contaminated with pathogenic microbes [3]. So, it is important to process food commodities to keep them safe and as well as to extend their shelf life.

Different processing techniques (i.e., thermal and non-thermal technologies) are used to prevent physical contaminations, slow down the chemical, enzymatic reactions, and eliminate/reduce microbial spoilage. Although thermal processing (which involves applying heat) is the most used and is a well-established treatment in terms of its historical use, predictability, and cost, it impacts the nutritional quality due to the high temperature involved while processing. Nowadays, nonthermal techniques (which involve applications of pressure, short pulse electric field, light, and sound waves) are preferred over thermal techniques. As the temperature attained by the product during nonthermal processing is low, lower nutritional losses occur during food processing [4]. Moreover, consumers prefer minimally processed food with a clean label and products processed with nonthermal techniques. High-pressure processing (HPP), pulse electric field, irradiation, cold plasma, and ultrasound are some of the nonthermal processing techniques. Among these nonthermal techniques, HPP in compliance with consumer requirements, provide products similar to fresh, clean label, additives-free, and convenient with extended shelf life. It is a promising cold pasteurization technology and gaining importance worldwide [5–7].

For commercial processing, HPP utilizes the application of high pressure (100–600 MPa) for a particular time at room temperature to packaged food kept inside a vessel to inactivate microorganisms. The vessel contains solvent (i.e., water, propanol ethanol, etc.), which transmits the pressure equally and uniformly throughout the vessel [8]. HPP of food commodities leads to changes in the cell membrane, cell morphology, biochemical reactions, and alteration in the genetic mechanism responsible for microorganism inactivation. These effects vary with the type of microorganism and food composition. Hence, it is of utmost importance to optimize the process parameters (pressure/holding time/temperature) to ensure food safety with adequate margins [9].

Food with low pH values (pH values < 4.6) indicating high acid intensity is less likely to be spoiled by bacteria. But, low acid foods (pH values > 4.6) are less microbiologically stable, and bacteria tend to produce a dormant form known as spores in fresh food [10]. Spores are tough to kill/inactivate, and if they are not appropriately inactivated, they wait for favorable conditions to grow [11]. So, it is of utmost importance to kill spores. HPP at room temperature is not adequate to inactivate all the spores, especially in the case of low-acid foods. To achieve a higher efficacy in inactivating

pressure-resistant pathogens and spores, temperature (90–120°C) can simultaneously be increased during HPP. The combination of heat (90–120°C) with pressure sequentially or simultaneously has been reported to provide synergistic effects against spores on different food commodities [12]. Similarly, sequential use of other techniques like irradiation, preservatives along with HPP has shown synergistic and additive effects against spores/pathogens to achieve food commodities safety [13–15].

Keeping food safety in view, the main objective of this review is to summarize the existing data from the published research concerning the effects of high-pressure treatment to inactivate microorganisms in fruits and vegetables; milk and milk products; meat, poultry, and seafood, and their products. Sometimes, high pressure alone is ineffective for the complete inactivation of pathogens and spores; therefore, a different strategic combination of thermal and nonthermal techniques assisting high pressure is also assayed. The provided information would be beneficial to interested researchers and industry personnel.

2. High-Pressure Inactivation in Specific Food Sector

The effectiveness of treatment to inactivate microbial populations depends on the type of microorganism, species, types of food (plant or animal origin), and matrix of food. The lethal effect of HPP on microbial population is assumed to be due to simultaneous effects on cell membrane permeability, changes in cell morphology, altered biochemical reactions, interference in the genetic mechanism, which occurs in the cell of microorganism, and detailed mechanism has been reported by Sehrawat et al. [16].

2.1. Fruits, Vegetables, and Their Products. Fresh agricultural products are healthy and nutritious, but contamination by microorganisms has been reported during storage. Second, there is a huge demand for refrigerated stored salad, fresh-cut fruits, and vegetables available in the market. Apart from being healthy, the availability of these products from the market saves time and provides convenience to the customers. But during cutting and packaging, chances of growth of *E. coli* O157: H7 and *Salmonella* might occur. Recently, frequent food-borne pathogens outbreaks are linked with these products and are of major public health concern. Contamination of raw products with pathogenic microorganisms can be due to their direct growth or indirect sources such as insects, water, and soil. HPP has been proven to be an effective technology for eliminating these pathogens of concern [17]. The effectiveness of HPP in reducing the microbial population is given in Table 1.

Apart from providing microbial safety, another reason for considering HPP as an alternative to convention preservation techniques is its limited effects on covalent bonds resulting in an only minor modifications in nutritional and sensory aspects. Pressure-treated juices are now available on a commercial scale in many countries viz. France

TABLE 1: Effect of HPP to inactivate microorganisms in fruits, vegetables, and their products.

Product	Microflora	Treatment (MPa/min/°C)	Log reduction*	Shelf-life (days/°C)	Optimum conditions (MPa/min/°C)	Reference
Apple cubes	*Candida lipolytica*, *E. coli*	200–650/10/25, 40	6	90/5	600/10/25	Vercammen et al. [18]
Litchi fruits	Total aerobic mesophilesY&MPsychrotrophs	100–300/5–15/27	3.293.243.77	32/5	300/10–15/27	Kaushik et al. [19]
Orange comminuted	Aerobic bacteria	100–400/1–4/1–9	3–5	—	414/2/—	Serment-Moreno et al. [20]
Green beans	Total plate count	500/1/20	4	30/6	500/1/20	Krebbers et al. [21]
Sour Chinese cabbbage	Lactic acid bacteria (LAB)	200–600/10–30/25	6-7	60/4	600/10/25	Li et al. [22]
Sauerkraut	Aerobic mesophilic bacteria, LAB, coliforms	300/10/40	4-5	90/4	300/10/40	Penas et al. [23]
Green onion (soaked)	*Salmonella*; *E. coli* O157: H7	250–500/2/20–40	>5	15/4	400–450/2/20–40	Neetoo et al. [24]
	Salmonella enterica; *E. coli* O157: H7	300–500/2/20–40	>5	—	400/2/40	Neetoo et al. [25]
Carrot, spinach	*Salmonella typhimurium*	100–500/0–20/30	>5	—	500/5/30	Jung et al. [26]
Radish	Total plate countY&M	300–550/5/	5.57	90/4	550/5/-	Bao et al. [27]
Tomato puree	Total plate count	50–400/15/25	4	—	400/15/25	Plaza et al. [28]
Mango puree	*Saccharomyces cerevisiae*	207–552/5–15/25	5	27/3	552/5/25	Guerrero-Beltran et al. [29]
Granny smith apple puree	Total aerobic mesophiles; Y&M	400–600/5/20	3	21/5	400/5/20	Landl et al. [30]
Cantaloupe puree	Aerobic plate count, Y&M	300–500/5/8–15	3	10/4	400–500/5/15	Mukhopadhyay et al. [31]
Plum puree	Total aerobic mesophilic, Y&M	400–600/7/10	1-23	20/4	600/7/10	González-Cebrino et al. [32]
Mango pulp	Y&M	100–600/0–20/30	4.6	—	600/5/30	Kaushik et al. [33]
Orange juice	*Salmonella*	600/1/20	7	—	600/1/20	Teo et al. [34]
Valencia and navel orange juice	Total aerobic bacteria, Y&M,	600/1/20	>7>4	84/4	600/1/20	Bull et al. [35]
Orange juice	Aerobic plate count, Y&M	600/1/—	5–83–5	58/4	600/1/—	Timmermans et al. [36]
Cashew apple juice	*E. coli*Aerobic mesophilesYeast and fungi	250–400/3–7/25	643	56/4	400/3/25	Lavinas et al. [37]
Kiwifruit and pineapple juice	*E. coli*; *L. innocua*	300–375/(0–5)×2–10 pulses/−10, 0, 20	7	21/4, 7, 37	350/1×5 pulses/20	Buzrul et al. [38]
Pomegranate juice	Total plate count	400–600/5–10/25–50	4	—	400/5/25	Ferrari et al. [39]
Cantaloupe juice	Total plate count, *E. coli*, *Bacillus subtilis*	400–500/0–20/22	453	—	500/20/22	Ma et al. [40]
Mango juice	*L. mesenteroides*, *E. coli* O157: H7	250–550/0–60/20–23	6	28/4, 12, 20	500/1/-	Hiremath and Ramaswamy [41]
Papaya beverage	Total plate count, Y&M	350–650/5–10/-	43	40/4	350/5	Chen et al. [42]
Pomegranate juice	Aerobic mesophiles, Y&M	350–550/0.5–2.5/4	4	35/4	350/2.5/5	Varela-Santos et al. [43]
White grape juice	Aerobic plate count, coliforms, Y&M	300–600/3/20	21	20/4	600/3/20	Chang et al. [44]
Elephant apple juice	Total viable bacteria, Y&M	600/5/35	3-4	60/4	600/5/35	Nayak et al. [45]
Apple-brocooli juice	*Saccharomyces cerevisiae*), *Aspergillus flavus*, *E. coli*	250–500/5–20/15	>5	30/5	500/10/15	Houška et al. [46]

TABLE 1: Continued.

Product	Microflora	Treatment (MPa/min/°C)	Log reduction*	Shelf-life (days/°C)	Optimum conditions (MPa/min/°C)	Reference
Apple, orange, and tomato juices	*Alicyclobacillus acidoterrestris*	350/20/50	4	21/30	350/20/50	Alpas et al. [47]
Carrot juice	E. coli O157: H7 *Staphylococcus aureus*	200–400/0–15/40	55	—	—	Pilavtepe-Çelik et al. [48]
Carrot juice	Total plate count *L. monocytogenes*	500–600/1/20	46	22/4	500/1/20	Patterson et al. [49]
Wheatgrass juice	E. coli P36, *Listeria innocua* ATCC 51742, and *S. typhimurium* WG49	400–600/1–3/11	>5	—	500–600/1/11	Ali et al. [50]
Olive jam	Coliform; *Bacillus cereus, Salmonella*; *L. monocytogenes*	450–600/5/10	ND	540/4	600/5/10	Delgado-Adamez et al. [51]
Purple sweet potato nectar	Total aerobic bacteria, Y&M	400–600/2.5–10	64	84/4	—	Wang et al. [52]
Mango nectar	E. coli *Mesophiles*	275–414/0–5/17	7-87	——	414/2/17 or 315/4/17 414/4/17	Aguirre et al. [53]

ND = not detected; *log reductions are cited from the most lethal parameters after HPP treatment.

(Ultrifruit), Japan (Waka Food Industries), Portugal (Frabaca), the UK (Orchard House), the USA (Odwala), and Mexico (Grupo Jumex).

Different fruits and vegetables that have been processed using high-pressure are apples, litchi, orange, papaya, pomegranate, kiwi, plum, pineapple, cashew apple, green beans, cabbage, radish, carrot, spinach, wheat grass, onion, etc.

Different microflorae require different pressure treatments in order to inactivate them. Pathogenic E. coli was the most reported to be a more resistant bacterial strain than Listeria monocytogenes in mango juice to high-pressure treatment [41]. Around 6 log reduction of E. coli O157: H7 and 5 log reduction of L. monocytogenes were achieved at 400 MPa for 10 min and 500 MPa for 1 min; there were no survivors of E. coli. For Z. bailii, P. membranaefaciens, and L. mesenteroides, the pressure of 300 MPa was sufficient to reduce the count to less than 1 log CFU/mL [41]. So, the most resistant microorganism can be selected as the target microorganism to get the optimum conditions for the treatment. Pilavtepe-Çelik et al. [48] reported the inactivation of E. coli O157: H7 and Staphylococcus aureus by high-pressure treatment (200–400 MPa/0–40 min/40°C) in carrot juice and peptone water. The carrot juice medium showed pressure resistance to E. coli (add pressure treatment), whereas S. aureus (add pressure treatment) was more resistant to peptone water than the carrot juice medium. This specific effect on S. aureus is due to the release of naturally occurring constituents of phytoalexins (6-Methoxymellein from carrot root, which is an antimicrobial compound produced with the response to microbial infection) in cellular and vascular fluids, exerting a toxic effect. It was also evident from earlier literature that this 6-methoxymellein from carrot cells was more effective against Gram-positive bacteria than Gram-negative bacteria [54]. So, it is important to consider the medium in which treatment is given as it can have varied results. Another study on carrot juice

pressurization at 500 and 600 MPa for 1 min at 20°C showed a significant reduction in microbial count from (4 log reduction), and a shelf life of 22 days was reported at 4°C [49]. During the storage study, at 8°C count was higher, although it took a long time to reach the maximum level, it was lower than the control samples. Pressure treatment of carrot juice at 500 MPa/1 min/20°C followed by storage at 8°C, for 22 days inactivated the competitive microflora except for spore formers and L. lactis (non-spore former) [49]. It can be concluded that apart from the amount of pressure, duration of treatment, and storage temperature; the type of microorganism plays an important role.

The juice of wheatgrass was given different treatments, i.e., thermal (75°C/15 s), HPP (500 MPa/60 s), and ultraviolet-C light (254 nm/69.2 mJ/cm^2) to achieve 5 log CFU reduction of microorganisms. Although all the treatment conditions mentioned above were found to be effective in the inactivation of microorganisms like E. coli P36, L. innocua ATCC 51742, and S. typhimurium WG49. However, thermal processing leads to a reduction in chlorophyll content, antioxidant properties, and loss of color [50]. So, HPP was reported to be the preferred method of processing as it retained maximum nutrients and gave a higher yield, and was recommended for other beverages with the same equivalent treatments. Apart from the safety of food, quality is important and is given diligent consideration by processors and consumers. Similarly, in another study by Chang et al. [44]; HPP and thermal treatment were given to white grape juice. Thermal processing (90°C/60 s) and HPP (600 MPa/3 min) were found to be effective in increasing the shelf life of white grape juice for 20 days. Differences in HPP processed juice and fresh were not significant based on sensory analysis, but thermally processed juice showed low acceptance [44]. The initial population of aerobic plate count, Y&M, and coliform count for control juice were 3.2, 2.2, and 2.1 log CFU/mL. When compared to treatment at 300 MPa/3 min, 600 MPa/3 min showed a significant

reduction in aerobic plate count by more than 2.0 log CFU/mL, yeast and mold (Y&M), and coliforms to <1 log CFU/mL, respectively. The microbial reduction (600 MPa/3 min) was similar to the effect of traditional thermal treatment. At 20 days of storage, the control sample showed aerobic plate count Y&M, and CC as 4.9, 3.3, and 2.3 log CFU/mL, whereas HPP treatment at 600 MPa/3 min showed very low aerobic plate count and minimum detection limit of Y&M and coliforms. Besides, HPP preserves the color and odor of juices by mitigating the Maillard reaction that generally occurs in traditional thermal processing [44].

HPP treatment (600 MPa/5 min/35°C) of elephant apple juice extended the shelf life of juice by 60 days at 4°C (microorganism count was <1 CFU/mL), whereas the microbial count was higher in thermally processed and control samples during the shelf-life study. The untreated samples showed a continuous increase in microorganism number during the storage study and were unacceptable by the end of 10 days as total viable bacteria; Y&M were 6.23 and 4.06 CFU/mL, respectively [45].

For pressure treatment (400 MPa/10 min, 500 MPa/5 min, and 600 MPa/2.5 min) low acid foods like sweet potatoes reduced Y&M to below detection levels where the initial count was 6.06 log10 CFU/mL. Further, Y&M was not detected for up to 84 days when samples were stored at 4 and 25°C. However, better quality was reported in samples stored at 4°C, indicating the importance of storage temperature [52]. Similarly, in cantaloupe puree, pressure treatment of 400–500 MPa for 5 min drastically reduced Y&M, and no re-growth was observed up to 10 days of storage at 4°C [31]. A comparative effect of sustained pressure treatment, pressure pulses, and pressure cycles was done on pineapple juice and nectar inoculated with *B. nivea*. It was concluded that at 600 MPa pressure, the effect of cycles was more effective in *B. nivea* ascospore inactivation than treatment under sustained high pressure. In addition to ascospores, Y&M counts were also reduced to below detection levels [55].

Y&M spores are readily inactivated at 400 MPa except for certain ascospores of heat-resistant mold such as *Byssochlamys nivea*, *Neosartorya fischeri,* and *Talaromyces macrosporus*.[56]. In general, these ascospores are often associated with spoilage of pasteurized fruit products also, such as juice, jams, purees, and candied fruits. Besides, their presence in processed food may cause deleterious effects due to the production of mycotoxins. Santos et al. [57] identified twelve highly resistant mold species, including *Neosartorya fumigate* (23.6%), *N. fischeri* (19.1%), and *Byssochlamys nivea* (5.5%) being the predominant species in high acid pasteurized fruit products such as strawberry puree, orange juice, and apple puree. The resistance of these ascospores depends on the spore age and species. The older the spore higher its resistance to processing.

HPP has been successfully applied for the effective inactivation of different pathogens in various fruits, vegetables, and their products. The amount of pressure and time required to inactivate the microorganisms depends on the food category. Optimized process parameters conditions for one product cannot be generalized for all the products. Among the different factors that plays important role in achieving microorganism inactivation are type and age. As bacteria, Y&M against pressure offers varying resistance. Combination treatment is reported to be more effective against spores.

2.2. Milk and Milk Products.

Treating milk by high-pressure breaks only ionic and hydrophobic bonds of macromolecules (proteins) but does not denature bioactive proteins present in it. Very little or no effect on small molecules of milk components (vitamins, flavor, and amino acids) color, and other nutritional components have been reported along with effective microbial inactivation [58]. Other desirable changes induced are denaturation, gelling, and aggregation of proteins, which also influence the yield of dairy products produced from treated milk. Various researchers have successfully treated milk [59] and milk products like cheddar cheeses [60], gorgonzola cheese [61], and Queso Fresco cheese [62] using HPP for extended shelf life (Table 2).

Raw milk acts as a carrier for the transmission of bacteria like *E. coli*, *Salmonella*, shigella, and *S. aureus*. These microorganisms become part of untreated milk while milking milk from animals in barnyards, transporting milk, and storing milk at chilling centers. These food-borne pathogens are of public health concern. Yang et al. [66] worked on the inactivation of these bacteria in milk by HPP treatment. The duration of pressure treatment for 20, 30, 40, and 50 min at 300 MPa exhibited the highest inactivation rate of *Salmonella* and the lowest inactivation rate of *S. aureus*. The satisfactory duration for milk treatment was optimized to be 30 min. With an increase in pressure from 100 to 200 MPa, an increase in inactivation rates was observed. The inactivation was slower for *Salmonella* and *E. coli* and rapid for *Shigella* and *S. aureus*. It was concluded that a pressure of 300 MPa for 30 min at 25°C was sufficient to cause bacterial inactivation in milk. Most resistant *S. aureus* must be considered an indicator bacterium in milk when HPP was employed as a preservation technique. Efficacy of HPP in the destruction of *Mycobacterium avium* ssp. *Paratuberculosis* in milk was done by Donaghy et al. [64]. Pressure at 500 MPa for 10 min resulted in a 6.52 log reduction of the target microorganism.

A study was conducted by Narisawa et al. [72] to assess the injury and inactivation of *Escherichia coli* K-12 in different mediums, i.e., skimmed milk and its protein fractions (casein, whey, globulin, and albumin) by HPP treatment. It was revealed that skimmed milk had the most remarkable protective effect on inactivation. Moreover, the shielding effect was enhanced with an increase in the concentration of skimmed milk [72]. The presence of casein and lactose in milk also shields bacteria in milk during HPP [73]. The divalent cations Ca^{2+} and Mg^{2+} also shield bacteria against high-pressure-induced inactivation due to their stabilizing effect over the cellular membrane [16]. So, it is important to know the medium composition to optimize the pressure effective in overcoming the shielding effect provided to microorganisms by food.

Evidence of the repair mechanism of injured microbes in food, especially for low acid foods, has been reported, questioning the microbiological safety of foodstuffs.

TABLE 2: Effect of HPP to inactivate microorganisms in milk and milk products.

Product	Pathogens	Treatment (MPa/min/°C)	Log reduction[*]	Shelf-life (days/°C)	Optimum conditions (MPa/min/°C)	Reference
Milk	*L. monocytogenes*	400/0–25/20–25	5	—	400/4/20	Hayman et al. [63]
Milk	*Mycobacterium avium* ssp. *Paratuberculosis*	400–600/5–10/20	6.52	—	500/10/20	Donaghy et al. [64]
Milk	*S. aureus* ATCC 6538*E. coli* ATCC 25922*S. aureus* ATCC 25923*L. monocytogenes*ATCC 19115	400/21–31/0–50	6688	—	400/30/21–31	Viazis et al. [65]
Milk	*Salmonella, Staphylococcus aureus*	100–500/10–50/25	66	—	300/30/25	Yang et al. [66]
Cheese slurries	*Penicilliumroqueforti* IMI 297987, *E. coli* K-12	50–800/20/10–30	65	—	>600/20/20 or >400/20/30	O'Reilly et al. [67]
Cheddar cheese	*L. innocua*	200/five 1 min cycles/28	3–4	—	200/five 1 min cycles/28	Kheadr et al. [60]
Gorgonzola cheese	*L. monocytogenes*	400–700/1–15/—	5	—	600/10 or 700/5	Carminati et al. [61]
Soft-curd cheese	*S. aureus*	400/10/20	7	30/8	400/10/20	López-Pedemonte et al. [68]
Queso fresco	*L. monocytogenes*	200–600/5–20/20–40	5	84/4	600/5/20	Tomasula et al. [62]
Goat milk cheese	Mesophilic aerobic, *Enterobacteriaceae, Listeria* spp	400–600/7/10	1.61.11.5	60/4	600/7/10	Delgado et al. [69]
Yogurt	*Streptococcus thermophilus*	400–600/15/—	7	28/4	600/15/—	Jankowska et al. [70]
Whey-lime beverage	Mesophiles, yeast, coliforms	500/10/25	8	120/4	500/10/25	Bansal et al. [71]

[*]Log reductions are cited from the most lethal parameters after HPP treatment.

Mechanism of repair after injury of most pressure-resistant strains of two Gram-positive (*L. monocytogenes CA* and *S. aureus 485*) and Gram-negative bacteria (*E. coli* O157:H7 933 and *S. enteritidis FDA*) inoculated in milk, was studied [74]. Inoculated milk was given HPP treatment (350–550 MPa) and was stored at 4, 22, and 30°C. Three stages of microbes after pressure treatment were established: i.e., (i). Cells can form visible colonies plated in both selective and nonselective agar called active cells (AC), (ii). Cells that undergo structural injury like cell wall/cell membrane injury and can form colonies only on nonselective agar are called I1 injury or primary injury, (iii). Cells that undergo metabolic injury cannot form colonies in both selective and nonselective agar are called I2 injury or secondary injury. However, in the repair of I2 injury, cells can form colonies on nonselective agar, similar to I1 injury. Except for *L. monocytogenes CA*, other bacteria were inactivated or injured in milk at 350 MPa. *S. aureus* cells in milk after pressure treatment at 350 and 450 MPa observed on day 1 after storage at 22 and 30°C showed I1 type injury. Whereas pressure-treated milk samples at 350 MPa, after 1 day of storage, caused *E. coli* cells to repair from I1 state to active cell. Therefore, storage temperature and duration can alter the repair of bacterial cells, thereby influencing microbiological safety. Studies suggest that after the HPP of food, immediately injured cells might not be present but can recover during storage. So, a strategic combination with other processing techniques might effectively prevent the recovery of injured cells.

Yogurt is a fermented beverage prepared from milk in cooperation with two homofermentative bacteria *Streptococcus thermophilus* and *Lactobacillus delbrueckii* ssp. *Bulgaricus*. The excess lactic acid bacteria in yogurt have attributed beneficial effects; nonetheless, the post-acidification during the cold chain and modification of viable lactic acid bacteria count are bottlenecks. Thermal processing after fermentation, in this case, would not be a viable solution to preserve the lactic acid bacteria at desired levels, and therefore novel technique like HPP plays a role. The effect of high-pressure treatment on the microflora of yogurt was investigated by Jankowska et al. [70]. They found that high-pressure treatment at 500 MPa does not significantly decrease the inactivation rate. In contrast, pressure treatment at 600 MPa/15 min showed a significant increase in bacterial inactivation from the initial load of ~10^8–10^9 CFU/mL to ~10^2–10^3 CFU/mL. It was found that *Streptococcus thermophiles* were slightly more resistant to high pressure than *L. bulgaricus*. Besides, yogurt was found to maintain acidity throughout the storage period after HPP treatment as it sufficiently reduced the acidifying bacteria. It was concluded that pressure treatment of 550 MPa for 15 min was optimum for yogurt processing with good sensory and textural characteristics with a shelf life of 4 weeks at 4°C. Microbial survivability in yogurt depended on the initial bacterial load and acidity of the sample [70]. The development of uniformly consistent microstructure in probiotic yogurt with improved gel strength and viscosity was accomplished by

treating milk with HPP before fermentation. The development of uniformly consistent microstructure in probiotic yogurt with improved gel strength and viscosity was accomplished by treating milk with HPP before fermentation [75].

Cheese is a fermented dairy product in wide demand all over the world. Improved characteristics of cheese were reported after HPP. Studies showed that high pressure imparts the following: (i) e alters the proteolytic activity of cheese [76], (ii) Improve the softness of cheese [77], (iii) Affect the rennet coagulation of milk [76], (iv) Increase the shelf life [76], (v). Increase the cheese yield [76], and (vi) Improve the physicochemical properties of soft cheese [78]. In corresponding to microbial inactivation of cheese under high pressure, several studies have shown promising results in improving shelf life without affecting its inherent quality. The effect of high-dynamic pressure on different types of milk and its effect on the quality of the cheese was studied by Kheadr et al. [60]. They found that 3-4 log reduction in *L. innocua* and 2–4 log reduction in total viable bacteria count was achieved by pressurizing milk, specifically the reduction in the microbial count was higher in low-fat milk. The reason is that milk fat acts as a protective medium for bacteria under high dynamic pressure, thereby preventing its destruction [60]. Thus, applying high-pressure to skim milk or low-fat milk employed for cheese preparation resulted in cheese being firm, cohesive, less brittle, and compact protein matrix with satisfactory microbiological quality. The cheeses prepared from low-fat pressurized milk show an initial listeria count of 10^6 CFU/mL was decreased to 10^2 CFU/mL after 3 months of ripening. Delgado et al. [69] reported that HPP at 400 and 600 MPa for 7 min of raw goat milk cheese resulted in inactivation of Mesophilic, aerobic, *Enterobacteriaceae,* Lactic acid bacteria, and *Listeria* spp., and differences in texture were observed. But the differences in control and pressure-treated samples were not observed by trained panelists and consumers. López-Pedemonte et al. [68] investigated the effect of ultrahigh pressure homogenization (UHPH) and HHP processing on the inactivation of *S. aureus* CECT 976 in milk to be employed for cheese making. The UHPH was employed at 300 and 30 MPa at primary and secondary homogenization stage, resp., followed by HHP treatment at 400 MPa/10 min/20°C. They found that *S. aureus* was present in cheese initially at a load of 8.5 log10 CFU/g in control. After UHPH and HHP treatment of milk, the cheese after 15 days of ripening showed complete inactivation of *S. aureus* and its enterotoxin.

In general, flavor, color, and nutrients were significantly retained after the pressure treatment of milk and its products. However, to prevent the recovery of injured cells during storage, a strategic combination of HPP with other thermal and nonthermal treatments can be looked upon.

2.3. Meat, Poultry, and Seafood. Meat, poultry, and seafood are high in moisture content and rich in protein and thus, these products have been associated with frequent outbreaks of food poisoning and food-borne diseases. Major outbreaks

were linked with dog meat in China [79], red meat caused infectious intestinal infection disease outbreaks in the United Kingdom [80], and multiple outbreaks were due to frozen oyster in Australia [81]. A survey by FDA reported the presence of *L. monocytogenes* in cold-smoked salmon with a 17% frequency and 4% incidence in hot smoked fish and shellfish [82]. In Europe, 191 cases of death due to the eating of crustaceans and shellfish in which the presence of *Listeria* was reported in the year 2013 [83]. Listeriosis outbreak has been increasing in Europe for the last few years, with a fatality rate of 13.8% in 2017 EFSA (European Food Safety Authority) and ECDC (European Centre for Disease Prevention and Control) [84]. These implications could be minimized by using HPP, which also simultaneously retains the natural aroma, appearance, flavor, texture, and nutrient value of the products [85, 86].

The effect of high-pressure processing on deboned dry-cured hams was investigated by Perez-Baltar et al. [87]. They found that high pressure of 600 MPa for 5 min inactivated *L. monocytogenes* at the surface during 60 days of storage at 4 and 12°C. However, variation in the moisture content, water activity, and salt and nitrate content on the surface and interior of dry-cured ham showed variation in pathogen inactivation. Around 2 log reduction in surface and 3 log reduction in the interior of dry-cured hams were accomplished during HPP treatment. As per USDA and European criteria, food safety against *L. monocytogenes* could be attained by HPP treatment at 600 MPa/5 min. A study on the inactivation of Shiga Toxin-Producing *Escherichia coli* (STPE) by HPP treatment (400–600 MPa/0–18 min) was studied by Porto-Fett et al. [6]. Major conclusions drawn from the study were that refrigerated and frozen storage of meatballs prior to HPP resulted in similar pathogen reduction, i.e., 0.9 to 2.9 log CFU/g at 4°C and 1 to 3 log CFU/g −20°C. Only 1–3 min were required at 600 MPa as compared to 9 min at 400 MPa to achieve $a \geq 2.0$ log CFU/g. In another study, HPP treatment significantly reduced microbes in pork burgers [88]. The addition of 2% rice bran extract followed by HPP treatment at 600 MPa/5 min did not significantly affect microbial reduction but improved the quality of the pork burger. Rice bran extract acted as a natural antioxidant in maintaining the stability of burgers during refrigerated storage. Nevertheless, in comparison to rice bran extract, HPP treatment was effective in microbial inactivation and in extending the shelf life of pork burgers up to 21 days. Bonilauri et al. [89] reported the effect of the processing method and HPP on reducing *Salmonella* Spp. in Italian salami production. From the 20 different samples of salami, they identified a significant relationship between *salmonella* reduction and process parameters time/temperature of acidification/drying, time/temperature of seasoning, pH, and aw) during sausage production. The management of sausage production process parameters decreased the salmonella load by 0.97–4.67 Log CFU/g but was insufficient to achieve 5 log reduction requirements of export to the USA, whereas the additional hurdle in the form of HPP treatment resulted in 2.41–5.84 Log CFU/g. The study aimed to identify and implement appropriate HACCP plans to control the risk of *salmonella* in Italian Salami using the appropriate HPP technique.

Meat, poultry, and fish are perishable products with limited shelf life, and microorganisms easily thrive over them during various stages such as cutting, mincing, protein solubilizing with salt, product forming, or packaging [90]. HPP was used to inactivate the histamine-forming bacteria in tuna meat slurry, and HPP treatment resulted in morphological changes in the cells [91]. Direct HPP treatment caused morphological changes in the cell membrane, biochemical reactions, and the genetic mechanism of microorganisms, resulting in the microorganism inactivation. However, the effect is variable on microorganisms and depends upon different pressure and holding time. The total plate count and *Enterobacteriaceae* count of filleted tuna chunks decreased with an increase in pressure (100–300 MPa/5 min/25°C) compared to control tuna. The shelf life of filleted tuna chunks was increased up to 30 days at 2°C when packed in EVOH multilayered films after HPP treatment at 200 MPa [92]. However, in albacore tuna minced muscle, HPP treatments (275–310 MPa/2–6 min) resulted in a bacteriostatic effect on mesophiles and psychrophiles observed, i.e., were not able to kill microorganisms but were effective to prevent their proliferation during the shelf-life study. Treatment at 310 MPa for 6 min was most effective and improved the shelf life of minced albacore tuna for >22 days at 4°C and >93 days at −20°C. In addition, lipid stabilization, color, and texture improvement were also reported [93]. HPP can inactivate microorganisms and could be used for gelation without applying thermal treatment to achieve product characteristics close to fresh. HPP is currently employed in the USA by the oyster industry for shucking purposes, eliminating the need for costly skilled labor and reducing microbial risk to consumers by inactivating *Vibrio* spp. The oysters processed after HPP treatment in the USA (brand name plastic gold band) have received several national awards for quality products. Shelf-life of oysters was reported to be extended for 12 days at 4°C, and optimum conditions were found to be 300 MPa/2 min [94].

Several products such as minced mackerel [95], spreadable smoked salmon cream [96], raw chicken [90], pork paste [97], ready-to-eat meat [98], cold-smoked salmon [99], smoked salmon mince [100], oysters [101], albacore tuna minced muscle [93], black tiger shrimp [102, 103], and hilsa fillets [104] have been satisfactorily processed by HPP (Table 3).

Based on the reported literature on meat, poultry, and seafood, it can be concluded that HPP is a very effective technique for providing microbial safety and under optimized conditions HPP leads to an extension in shelf life by almost double or more. The pressure is also very effective in denaturing the proteins responsible for holding the meat within the shell of oysters, mussels, crabs, and shrimp. Therefore, a higher yield can be obtained as meat separation from the shell become more effortless and effective.

2.4. Other Products. HPP has also been utilized for products such as rice wine [121], ginger paste [122], maize [5], honey [123], and human milk [124]. Processing rice wine (non-heat pasteurized) at 392 MPa by Hara et al. [121] gave a shelf-stable product by inactivating Lactobacilli and yeast. The taste was equivalent to the untreated food sample. *Fusarium* mycotoxins, i.e., deoxynivalenol and zearalenone (produced by *F. graminearum)* were effectively decontaminated using HPP treatment (550 MPa/20 min/45°C) in maize [5].

A study on the effect of HPP on the reduction of native microflora of Mexican multifloral honey was reported by [123]. This study evidenced that high-pressure processing at 600 MPa for 12 min resulted in a reduction of 0.8 $\log_{10}$ of total mesophiles and 2.4 $\log_{10}$ of Y&M counts. A similar study by Akhmazillah et al. [125] on manuka honey has also reported that a high-pressure of more than 350 MPa at 40°C for 3 min reduced the bacterial load from 6 logN CFU/g to 3 logN CFU/g. Pressure-mediated treatment (600 MPa for 5 min) extended the shelf life of ginger paste for six months under refrigerated conditions. Both HPP and pasteurization were equally effective in reducing microbial population, but retention of bioactive components was more in HPP [122]. Rocha-Pimienta et al. [124] worked on the inactivation of *Bacillus cereus* and *S. aureus* vegetative cells in human milk by HPP. The pressure intensity and holding times needed for maximum inactivation up to 5.81 and 6.93 log CFU/mL were 593.96 MPa for 3.88 min. Waite et al. [126] indicated that the HPP of ranch dressing reduced the *Pediococcus acidilactici* by more than 6.4 log CFU/g. The studies carried out by eminent scientists proved that HPP is a viable process to improve the food safety of food products with extended shelf life.

In baked goods, cakes and batters were studied for their microbial, physical, and structural changes due to HPP [127]. The mesophilic aerobic bacteria Y&M were more susceptible to high pressure, causing a reduction from 4.3 to 3.8 log CFU/g and 1.7 to 1.0 log CFU/g, respectively, at 600 MPa for 6 min. The wheat dough also showed a similar reduction in the total aerobic mesophilic count, and Y&M count within 1 min of treatment at all pressures studied (50–250 MPa) [128].

Cereals and pulses being nonperishable commodities were not extensively studied for microbial aspects of high pressure. However, HPP was studied for its effect on starch modification, improving nutritional quality, water absorption, gelatinization, and development of quick-cooking rice [129–132]. Ravichandran et al. [133] investigated the effect of high pressure on water absorption and gelatinization of Paddy (*Basmati cv.*). Presoaked and unsoaked grains were pressure treated at 350, 450, and 550 MPa for a temperature of 30, 40, and 50°C for a duration of 300, 600, 900, and 1200 s. The highest moisture content of up to 50% (dB) was achieved at 550 MPa/50°C/1200 s in addition to 25% of gelatinization. Yu et al. [134] studied the effect of high pressure on cooked rice dominated with *Bacillus* spp. with *B. subtilis* and *B. cereus* population. They found that HPP treatment at 400 and 600 MPa increased the shelf life of cooked rice to 8 weeks at 25°C. HPP can be a very useful technique in reducing the microbial count of maize, honey, ranch dressing, and dough and in extending the shelf life of ginger paste and cooked rice.

TABLE 3: Effect of HPP to inactivate microorganisms in meat, poultry, and seafood.

Product	Microflora	Treatment (MPa/min/°C)	Log reduction	Shelf-life (days/°C)	Optimum conditions (MPa/min/°C)	Reference
Sliced vacuum-packaged dry-cured ham	Salmonella enteritidis	400–600/5/12	4.3	60/8	600/5/12	Alba et al. [105]
Poultry meat	MesophilesPsychrotrophs	60–450/15/20	3.2–3.85.2	—	450/15/20	Yuste et al. [106]
Bovine muscle	Total microflora	50–600/0–5/10	2.5	8/4	520/5/10	Jung et al. [107]
Raw marinated meats	Aerobic total count psychrotrophic bacteria, Yeast and Enterobacteriaceae	600/6/31	42	120/4	600/6/31	Garriga et al. [108]
Meat balls	Shiga toxin-producingEscherichia coli	400–600/0–18/—	<2		400/9/—600/3/	Porto-Fett et al. [6]
Low-fat pastramiStrassburg beefExport sausageCajun beef	Aerobic and anaerobic mesophiles, lactic acid bacteria, Listeria spp., Staphylococci, Brochothrix thermosphacta, coliforms, and fungi	600/3/20	4	98/4	600/3/20	Hayman et al. [98]
Smoked salmon mince	L. innocua, Micrococcus luteus Pseudomonas fluorescens	207/23/−20–25 (pressure shift freezing)	22.54.6	—	207/23/−20–25 with the release of pressure after 18 min	Picart et al. [100]
Oysters	Cryptosporidium parvum	305–550/0–360/—	6.5	—	550/3/—	Collins et al. [101]
Albacore tuna minced muscle	Total mesophiles and psychrophile	275–310/2–6/10	100–400 CFU/g	>22 days at 4°C and >93 days at −20°C.	310/6/10	Ramirez-Suarez and morrissey [93]
Oysters	Total aerobic count and anaerobic bacteria	260–600/5/20	2	31/2 on ice	400/5/20	Cruz-Romero et al. [109]
Minced trout	L. innocua	150–517/5/20	>4	—	414/5/20	Basaran-Akgul et al. [110]
Chicken breast fillet	E. coli KCTC 1682, S. typhimurium KCTC 1925, L. monocytogenes KCTC 3569	300–600/5/15	6–8	7–14/4	600/5/15	Kruk et al. [111]
Yellowfin tuna chunks	Total plate count, Enterobacteriaceae	100–300/5/25	11	20/4	200/5/25	[92]
Dry cured ham	Salmonella enteric	347–852/2.3–15.75/7.6–24.4	4	—	525/15.5/16525/12/7.6600/12.1/16600/5/23.5	Bover-Cid et al. [112]
Dry cured hamDry cured ham	EnterococcusfaecalisSerratia liquefaciens	347–852/2.3–15.8/7.6–24.4347–852/2.3–15.8/7.6–24.4	46	—	750/9.5	Belletti et al. [113].Belletti et al. [114]
Black shrimp	E. coli, S. aureus	100–435/5/25	1.531.16	—	435/5/25	Kaur et al. [102]
Beef (frozen)	E. coli O157: H7	551/4/−35	1.4–1.7	—	551/4/−35	Lowder [115]
Chicken meat	L. innocua	200–400/5–15/0–40	8	—	400/10/0	Bulut et al. [116]
Chicken nuggets	Enterobacteriaceae	300/5/27	3	30/4	300/5/27	Devatkal et al. [117]
Smoked rainbow trout fillets, Fresh European catfish fillets	L. monocytogenesE. coli	200–600/1–5/—	>6	41/47/4	600/5/—	Mengden et al. [118]

TABLE 3: Continued.

Product	Microflora	Treatment (MPa/min/°C)	Log reduction	Shelf-life (days/°C)	Optimum conditions (MPa/min/°C)	Reference
Vacuum packaged mutton patties	Total plate count	200–400/10/—	2–3	—	400/10/—	Banerjee et al. [119]
Mussels	Total plate count	100–400/5/30	2	28/2	300/5/30	Bindu et al. [120]
Oysters	Aerobic plate count	100–300/1–3/20	1.27	12/4	300/2/20	Rong et al. [94]
Deboned dry-cured hams	Listeriamonocytogenes	400–600/5–10/—	3	60/4	600/5/—	Perez-Baltar et al. [87]
Pork burger	Total aerobic mesophilic bacteria and psychotropic bacteria	600/5/10	3	21/4	600/5/10	[88]
Italian salami	Salmonella spp.	600/—/14	>5		600/—/14	Bonilauri et al. [89]

ND = not detected; *log reductions are cited from most lethal parameters after HPP treatment.

3. Microbial Inactivation by HPP Assisted by Other Processing Techniques

HPP is an effective technique to inactivate or eliminate vegetative microorganisms but does not substantially affect spores [135]. pH in the case of fruits is low (<4.6) due to inherent acidity. It is further reduced by compression, so partially injured cells of microorganisms by HPP will not be able to recover in such a hostile environment. The difficulty is in the case of low acid products (poultry, meat, and milk) where pH values are >4.6. Spores grow even after HPP as soon as they find a suitable environment to grow and ultimately spoil the food [12]. To achieve higher efficiency for spore inactivation present in food samples by HPP alone, spores need to be germinated at low pressure in the first stage. Then in the second stage, pressure needs to be elevated to inactivate germinated spores. But using HPP twice over a product increases the processing time and energy consumed and, subsequently cost of the product. Moreover, a combination of pressure and temperature (which can be increased along the HPP) eliminates the step of the spore's growth by HPP [136]. So, using a combination mode (HPP and temperature simultaneously) helps achieve rapid heating and cooling of products, reducing processing time and product cost [135].

Combining HPP with other nonthermal (irradiation, ultrasound, and pulsed electric field) and mild heat techniques (pasteurization, blanching, and drying) will be an additional hurdle for the microorganisms. Also, beyond 600 MPa pressure, there is an exponential increase in equipment cost, and not considered economical. Some authors proposed the use of antimicrobial preservatives (nisin, chitosans, and pediocin) to achieve a synergistic effect with pressure and to reduce process severity [13, 137–140]). Microbial inactivation by HPP assisted by other processing/preservation techniques has been attempted by eminent researchers such as irradiation of chicken breast [141], irradiation of lamb meat [142], irradiation of kefir [14]; ultrasonication of Rhodotorula rubra [143, 144]; use of

preservatives such as lysozyme, ethylene diamine tetraacetic acid (EDTA) [145], and nisin [146]. Hauben et al. [145] found that cells were more sensitive toward pressurization in the presence of preservatives. Effectiveness of hurdle technology consisting of HPP (400 MPa/30 min/70°C), pH (4), and nisin (0.8I U/mL) to completely eradicate spore of Bacillus coagulans (2.5 CFU/mL), whereas pressure alone (400 MPa) at ambient temperature and neutral pH had no significant effect on viable spores [146]. Paul et al. [142] showed that either irradiation (1.0 kGy) or HPP (200 MPa for 30 min) only reduced staphylococci ($10^4/g$) by 1 log cycle in lamb meat whereas, in combination, staphylococci can be completely eradicated. The complete deactivation of the microbial population (lactobacilli, lactococci, and yeast) of kefir was achieved using irradiation (5 kGy) and HPP (400 MPa/5 min/5°C) without changing structure and nutritional components (proteins and lipids) by Mainville et al. [14]. Treatment of Bacillus subtilis spores (400 MPa/30 min) and E. coli (300 MPa/10 min) using HPP followed by alternating current (50 Hz) leads to lethal damage to their cell component [147]. High pressure (500 kPa) in combination with heat (70°C) and ultrasound (117 db at 20 kHz) resulted in the inactivation of 99% of the Bacillus subtilis spore population [144]. Knorr [143] stated that HPP and ultrasonic individually were not adequate for inactivation of Rhodotorula rubra but complete inactivation was achieved in combination mode. The carbon dioxide-assisted HPP is one of the effective nonthermal technologies which has been applied successfully by different researchers for inactivating microorganisms and reported promising results [148]. This method utilizes moderate pressures (<50 MPa) sequentially or simultaneously with CO_2 to pasteurize liquid foods without compromising quality attributes. Pressure-ohmic-thermal sterilization is a novel technology involving the utilization of high-pressure in combination or consecutive application of ohmic heating for low acid foods to achieve a sterilization effect and simultaneously reduce the severity of the individual effect of temperature on quality attributes [149]. A study on ultrafiltration in combination with HPP

TABLE 4: Microbial inactivation by HPP assisted by other processing techniques.

| Technique | Treatment conditions | | Sample | Target Microorganism | Observations | Reference |
	HPP (MPa/min/°C)	Others				
Irradiation	200/30/—	1 kGy	Lamb meat	S. aureus	The count of *staphylococci* was below detection level when both techniques were applied in combination where as individual treatment reduced the count only by 1 log cycle	Paul et al. [142]
	680/20/80	2 kGy	Chicken breast	Clostridium sporogenes	The dose required to achieve the eradication of *C. sporogenes* reduced from 4.1 to 2 kGy in combination with HPP	Crawford et al. [141]
Modified atmospheres	150/10/5	50% O_2 + 50% CO_2	Atlantic salmon	L. monocytogenesS. typhimurium	The combined application was found to be more effective in retaining microbiological characteristics with the extended life of 10 days at 5°C.	Amanatidou et al. [153]
HPCD	10.3/15/36	Supercritical CO_2	Beef trimmings	Total plate count, E. coli O157: H7, E. coli, Salmonella spp.	Log reductions of 0.83, 0.93, 1.0, and 1.06 were observed in total plate count, *E. coli* O157: H7, *E. coli* and *Salmonella* sp, respectively	Meurehg [154]
	14/40/45	Supercritical CO_2	Soy sauce pasteMarinated porkLoins	E. coli, L. monocytogenes, S. typhimurium, E. coli O157: H7	Percentage reduction of 33.81, 37.96, 37.48, and 36.84% was achieved in *E. coli*, *L. monocytogenes*, *S. typhimurium*, and *E. coli* O157: H7, respectively.	Choi et al. [155]
	12/30/35	Supercritical CO_2	Boneless pork loins	E. coli, L. monocytogenes, S. typhimurium, E. coli O157: H7	Log reductions of 1.5 1.4, 1.56, and 1.0 were achieved in *E. coli*, *L. monocytogenes*, *S. typhimurium*, and *E. coli* O157: H7, respectively.	Choi et al. [156]
	10/10/50	Supercritical CO_2	Pears	S. cerevisiae	4 log reduction was achieved	Valverde et al. [157]
	22–25/2–10/ 43–60	Supercritical CO_2	Apple juice	Coliform, total aerobic bacteria, Y&M	Complete inactivation of coliform, Y&M was achieved, and 3.72 log cycle reduction was achieved in total aerobic bacteria	Xu et al. [158]
Thermosonication and HPP as pretreatment	600/15/—	Acoustic energy density 20.2 W/ mL	Orange juice	Alicyclobacillus acidoterrestris	HPP treatment with thermosonication was found to be most effective and the temperature used was 8°C lower than the temperature used in thermal treatment.	Evelyn and silva [151]
Heat Ultra-sonication Static pressure	300–500	Heat 70–90°C Ultrasonic 90–150 μm at 20 kHz	Buffer media	B. subtilis	Spores inactivation was observed to be highest at 70–90°C/300 kPa,/117 μm/ 20 kHz/6 min	Raso et al. [144]

TABLE 4: Continued.

Technique	Treatment conditions		Sample	Target Microorganism	Observations	Reference
	HPP (MPa/ min/°C)	Others				
Ultrafiltration	500/6/—	Ceramic membrane (0.05 μm)	Apple juice	Total plate count and Y&M	For ultrafiltration + HTST and ultrafiltration + HPP, both treatments apple juices were microbiologically safe but higher retention of phenol and lower degree of browning was observed in the later treatment.	Zhao et al. [150]
Modified atmospheres packaging (MAP)	300/5/20	30%CO_2/70% N_2	Fresh chicken breast fillets	*Total viable counts, Pseudomonas, LAB, Brochothrix thermosphacta, coliforms, E.coli*	Combination treatment extended the shelf life up to 28 days	Rodríguez-Calleja et al. [15]
Thermal pasteurization with Nisin	400/4/—500/2/ —	Pasteurization at °C/15 s with nisin-100 IU/mL	Cucumber juice drinks	Total plate count and Y&M	Longer shelf life was achieved with 500/2 with nisin compared to other treatments.	Zhao et al. [159]
Nisin Heat	300–700/ 7.5–17.5/30–70	Nisin-0 to333 IU/ mL.	UHT milk	*Clostridium botulinum spores*	To achieve 6 $\log_{10}$ cycle reduction best optimum conditions were 545 MPa/51°C/ 13.3 min and nisin at 129 IU/ml concentration.	Gao and ju [137]
Nisin; Ultrasound	300/3.3/5	1 mg/L34.6 W/30 s	Liquid whole egg	*L. seeligeri*	Nisin with HPP was more effective in reducing *Listeria seeligeri* (5 log reduction) as compared to HPP and ultrasound in combination.	Lee et al. [160]

Table 4: Continued.

Technique	Treatment conditions		Sample	Target Microorganism	Observations	Reference
	HPP (MPa/min/°C)	Others				
	700/2 pulse/80	80°C	Tomato puree	*B. stearothermophilus*	High-pressure in combination with elevated temperatures resulted in an ambient-stable product, in which all the spores were inactivated.	Krebbers et al. [161]
	400–700/0–5.5/105	105°C	Egg patties	*B. stearothermophilus*	4 log reductions using pressure-heat treatment at 700 MPa/5/105°C min were achieved as compared to 1.5 log reduction in thermal processing 121°C/15 min.	Rajan et al. [162]
	800/-/60–80	60–80°C	Hamster brain homogenate	Prion	Infectious scrapie prions were effectively inactivated at 800 MPa (3 × 5 min cycles) at 60 and 80°C	Heindl et al. [163]
	700–900/0–32/80–100	80–100°C	Milk	*Clostridium* sporogenes spores	Spores were more sensitive to temperature as compared to pressure	Ramaswamy et al. [164]
	600/3/60–70	60–70°C	Tris buffer, skimmed milk, and orange juice.	*B. subtilis*	Slow compression and slow decompression were more effective than fast compression and fast decompression.	Syed et al. [165]
Heat	600/-/75–105	75–105°C	Tomato juice	*B. coagulans*	Time taken to reduce the microbial counts were less using the combination treatment compared to individual treatment by thermal processing.	Daryaei and Balasubramaniam [166]
	200–350/0–2/105–150	105–150°C	Whole milk and phosphate-buffered saline	*B. amyloliquefaciens*	The temperature was the main driving force for inactivation and fat does not provide any shielding effect to microorganisms.	Dong et al. [167]
	300–900/1/60–80	60–80°C	Pumpkin puree	*Coliforms, Bacillus, E. coli, C. perfringens*	High-pressure-assisted thermal processing leads to a significant reduction in *Coliforms*, viable spores of *Bacillus* spp., mold and yeast. *E. coli* and *C. perfringens* were <1 log CFU g^{-1} (under limit)	García-Parra et al. [168]
	650/10/55–65	55–65°C	Soup	*B. subtilis*	Combined treatment reduced the *B. subtilis* by 4.5 logs. Also, this treatment took less time compared to static and agitating retort alone.	Ates et al. [169]
High pressure-assisted thermal processing	Step 1 = 100–200/7/−Step 2 = 586/10/23–77	80°C/10 min	Meat products	*C.perfringens*	The study purpose was activation of spores at low pressure (100–200 MPa/7 min) or elevated temperature (80°C/10 min); then germination at high temperature (80°C/10 min) followed by inactivation at high-pressure (586 MPa/23–73°C/10 min)	Akhtar et al. [170]

PEF: pulsed electric field; HPCD: high-pressure dense phase carbon dioxide.

Table 5: Microbial inactivation by HPP assisted by preservatives.

Technique	Treatment conditions HPP (MPa/ min/°C)	Treatment conditions Others	Sample	Target microorganism	Observations	Reference
Bacteriocin (Lacticin 3147)	150–600/ 30/25	10000–15000 AU ml^{-1}	Cheese	S. aureus, L. innocua	The combined treatment resulted in substantial cell death (>6 log reduction), which exceeded that observed with either of these treatments alone.	Morgan et al. [171]
Enterocins A and B, Sakacin K, Pediocin AcH nisin	400/10/17	—	Meat model system	E. coli, S. enterica, S. aureus, L. monocytogenes, Lactobacillus sakei, Leuconostoc carnosum	At 4°C no of survivors remains the same as after combination treatment.	Garriga et al. [172]
Pediocin + nisin	345/5/60	Pediocin + nisin-5000 AU/g	Roast beef	Clostridial species (C. sporogenes, C. perfringens, C. tertium, and C. laramie)	Combination treatment increased the shelf life to 7 days at 25°C and 84 days at 4°C where as HPP alone has a shelf life of 42 days only at 4°C	Kalchayanand et al. [140]
Nisin	250–500/5/ 20	0, 250, 500 IU/ml	Milk	E. coli; P. fluorescens; L. innocua; lactobacillus viridescens	Combining high-pressure and nisin resulted in a greater inactivation of microflora (>6.4 log reduction) than when either was applied individually.	Black et al. [13]
Lysozyme	300/15/25	224 UA/ml	Skim milk and banana juice	Gram-negative bacteria including, E. coli, Shigella flexneri, Yersinia enterocolitica, and S. typhimurium	Combination treatment enhanced the inactivation of 3.6–6.5 log cycles and 0.5–2.1 log units in banana and milk, respectively.	Nakimbugwe et al. [173]
Edible film	300/20/15	The film contains oregano, rosemary, and chitosan.	Cold-smoked sardine	Total counts, sulfide-reducing bacteria	Synergistic effects were observed in combination plant-based extract reduced the total counts whereas film containing chitosan reduced both.	Gomez-Estaca et al. [174]
Organic acids	300–600/ 10/—	Potassium lactate-3% Mixture potassium + sodium lactate-3%, potassium lactate + sodium diacetate- 2.5%	Spanish blood sausage (morcillas)	Total viable count, Enterobacteria, Pseudomonas, Lactic acid bacteria, Clostridium perfringens	15 days shelf life was achieved on the addition of potassium + sodium lactate followed by HPP as compared to other treatments.	Diez et al. [175]
Enterocins	400/10/17	Alginate films containing Enterocins 2000 AU/cm^2	Cooked ham	L. monocytogenes	A shelf life of 60 days was using combination treatment	Marcos et al. [176]

TABLE 5: Continued.

Technique	Treatment conditions HPP (MPa/min/°C)	Others	Sample	Target microorganism	Observations	Reference
Enterocins A and B, sakacin K, potassium lactate	400/10/17	Enterocins-200 or 2000 AU/cm², Sarkacin 200 AU/cm², nisin-200 AU/cm², potassium lactate-1.8%, and nisin (200 AU/g) plus potassium lactate (1.8%)	Sliced cooked ham	Salmonella spp.	A combination of HPP, antimicrobial packaging and refrigerated storage was an effective treatment to maintain a count <10CFU/g.	Jofre et al. [139]
Nisin and potassium lactate	600/5/10	Nisin-800 AU/g, potassium lactate-1.8%, nisin (800 AU/g) plus potassium lctate (1.8%)	Sliced cooked ham	Salmonella spp. L. monocytogenes and S. aureus	A combination of antimicrobials with HPP treatment with refrigerated storage was effective in controlling growth up to three months but HPP was effective in reducing the growth of Salmonella spp. L. monocytogenes at 1 and 6°C for three months	Jofre et al. [139]
Enterocins A and B	400/10/17	Enterocins A and B- 2000 AU/g	Fermented sausages	S. enterica, L. monocytogenes, and S. aureus	A combination of the ripening process, pressurization, and Enterocins was only effective in reducing the count of S. aureus.	Jofre, et al. [177]
Antimicrobial film	800/5/20	Films contained Carvacrol or allyl Isothiocyanate	Food model	Botrytis cinerea fungi	In combination lower intensity of both the treatment were utilized which would help develop low-cost technologies,	Raouche et al. [178]
Sodium lactate	600/2/20	2%	Cooked chicken	L. monocytogenes	After HPP treatment counts were below the detection limit but enhanced during storage within 21 days. Counts were below detection limit up to 105 days after combined treatment.	Patterson et al. [179]
Caprylic acid Purasal	110–700/10/5–40	Caprylic acid-0.15% Purasal (K-lactate + sodium diacetate)-2.5%	Cooked ham	Carnobacterium divergens, Leuconostoc carnosum, Brochothrix thermosphacta,L. innocua and E. coli, O157:H7	Carpylic or purasal addition in combination with HPP (600/10/10) enhanced the shelf life by 84 days	Vercammen et al. [18]
Mint essential oil	600/0–5/—	0.1 and 0.05%	Yogurt drink (ayran)	L. monocytogenes and L. innocua	To achieve the same level of inactivation combination treatment reduced the pressure by half (300 MPa) and time to 3.5 min	Evrendilek and balasubramaniam [180]

TABLE 5: Continued.

Technique	Treatment conditions HPP (MPa/ min/°C)	Treatment conditions Others	Sample	Target microorganism	Observations	Reference
Nisin	600/5/—	Nisin directly-200 AU/ cm² Nisin through film- 200 AU/cm²	Ready-to-eat (RTE) sliced dry-cured ham	*L. monocytogenes*	Up to 60 days at 8°C HPP treatment with direct application of nisin was more effective.	Hereu et al. [181]
Nisin	100–500/ 30–60/50	0–1000 IU/mL	Apple juice	*Alicyclobacillus acidoterrestris spores*	HPP (200 MPa for 45 min) of apple juice containing nisin (250 IU/mL) resulted in more than 6 log reduction of Alicyclobacillus acidoterrestris spores	Sokołowska et al. [182]
Bacteriocins nisin, cinnamon, and clove		Nisin 500 IU/g, cinnamon oil-0.2% and clove oil-0.25%,	Rice pudim	*S. aureus*	Even mild treatment in combination with additives was effective in reducing the log cycles against S. aureus	Pulido et al. [183]
Enterocin LM-2 at 256 and 2560 AU/g.	200–400/ 10/—	256 and 2560 AU/g.	Refrigerated shelf life of sliced cooked ham	*L. monocytogenes, Salmonella, S. aureus psychrotrophic bacteria, aerobic total plate count, LAB, Enterobacteriaceae*	Enterocin addition (2560 AU/ g), followed by HPP achieved >90 days shelf life.	Liu et al., [184]
Bacteriophages	200–600/5/ 10	1 : 1 of vB saus-phi-IPLA35 & vB saus-phi-IPLA88	Pasteurized whole milk	*S. aureus*	400 MPa was to be a promising treatment in combination with bacteriophages.	Tabla et al. [185]
Lactoperoxidase	250–450/ 10/—	Lactoperoxidase system	Smoked salmon	*L. monocytogenes*	Antimicrobial effects were observed after combination treatment but little alterations in quality attributes were also observed.	Montiel et al. [186]
Bovine lactoferrin	200–500/ 10/10	Bovine lactoferrin-0.5 mg/g.	Chicken filets	*E. coli O157: H7, Pseudomonas fluorescens*	Additional reduction of 2.3 log cycle was achieved in combined treatment of HPP (300 MPa) with bovine lactoferrin as compared to HPP alone	Del Olmo et al. [187]
Potassium lactate	600/6/10		Restructured hams	*Aerobic mesophilic total counts, Lactic acid bacteria, Enterobacteriaceae, L. monocytogenes, S. aureus, Salmonella spp.*	The addition of potassium lactate followed by HPP increased the reduction in the count.	Fulladosa et al. [188]

TABLE 5: Continued.

Technique	Treatment conditions		Sample	Target microorganism	Observations	Reference
	HPP (MPa/ min/°C)	Others				
Potassium chloride + potassium lactate, sodium chloride	600/13/5		Smoked dry-cured ham	L. monocytogenes Salmonella	After pressurization (600/5 min) elimination of the pathogen took 14 days in ham containing sodium chloride whereas mix additives (potassium chloride + potassium lactate) took 28 and 56 days to eliminate Salmonella and Listeria, respectively. It indicates ham containing sodium chloride has more stability	Stollewerk et al. [189]
Nisin	600/5/15	Nisin	Dry cured ham	L. monocytogenes	During HPP treatment L. monocytogenes were found to be resistant but the assistance of HPP with nisin enhanced the inactivation	Hereu et al. [181]
Bacteriocins nisin and pediocin	400–500/ 10/12	Nisin-100 IU/g Pediocin-0.6%	Dry-cured ham	E. coli	Individual addition of nisin and Pediocin does not affect E. coli. But combined treatment HPP (500) and nisin maintained a synergistic effect up to 60 days	Alba et al. [190]
Enterococcus strains	600/5/15	Enterococci strain (Enterococcus faecium CTC8005, Enterococcus devriesei CTC8006 and Enterococcus casseliflavus CTC800) at ca. 3×10^6 cfu/g	Low-acid fermented sausages	L. monocytogenes, S. aureus	A combination of HPP and E. faecium CTC8005 was the most effective treatment. Individual addition of Enterococcus strains without HPP was not able to affect Enterococcus strains.	Rubio et al. [191]
Essential oils or their chemical constituents	175–400/ 5–20/—	200 μL/L	Orange and apple juices	L. monocytogenes and E. coli	Promising synergistic effects were achieved.	Espina et al. [192]
Sodium chloride, antimicrobial packaging	600/5/12	600/5/12 PVOH films containing nisin-450 AU/cm	Sliced fermented sausages	L. monocytogenes	No extra protection was achieved using the combination	Marcos et al. [193]
Chitosan based-coating containing nanoemulsion of Mandarin essential oil	200–400/5/ 25	—	Green bean	L. innocua	Synergistic effect of antimicrobials with HPP was more promising than with pulse light.	Donsi et al. [194]

Table 5: Continued.

Technique	Treatment conditions		Sample	Target microorganism	Observations	Reference
	HPP (MPa/min/°C)	Others				
Virulent bacteriophages	150–550/5–13	Phages (a cocktail of 3 Shigella flexneri or single Vibrio cholerae phages, both applied at 109 PFU/mL)	S. flexneri in ground beef and V. cholerae in salmon and mussels	S. flexneriV. cholerae	To achieve an inactivation level similar to stand-alone treatment, combined treatment reduced the pressure and time there was more energy efficient pressure	Ahmadi et al. [195]
Marinating solutions (sodium chloride and citric acid)	300–600/5/—	1 or 2% for 18 hrs	Marinated beef	L. innocuaEnterococcus faecium	Combination treatment reduced both microorganisms by 6 log cycles and individual treatment with a marinating solution was not effective to reduce initial microbial count without HPP.	Rodrigues et al., [196]
HPP essential oils carvacrol and thymol, and thiol-reactive allyl-isothiocyanate and cinnamaldehyde	0.01–0.30%	450–600/3–15	Beef steaks	L. monocytogenes and enterohaemorrhagic E. coli	It was suggested by the author to use allyl-isothiocyanate and carvacrol practically to assist with HPP to achieve extended shelf life.	Li and Gänzle [197]

was conducted by Zhao et al. [150] and reported apple juice to be microbiologically safe with better quality attributes than UF + HTST (high-temperature short time) juice throughout the storage period of 60 days. Evelyn and Silva [151] used HPP as a pretreatment to enhance thermosonication effectiveness to eliminate *Alicyclobacillus acidoterrestris* spores in orange juice. To inactivate spores of pathogenic bacteria (*C. perfringens* and *B. cereus*) and spoilage microorganisms, i.e., bacteria (*Alicyclobacillus acidoterrestris)*, mold (*Byssochlamys nivea* and *Neosartorya fischeri*), and yeast (*S. cerevisiae)* present in food samples. HPP, thermal processing, high-pressure thermal processing, and thermal sonification was used. It was found that high-pressure thermal processing (600 MPa/20 min/70–75°C) was more effective in achieving reductions.

Moreover, a lower processing time was required to prepare a beef slurry, apple juice, strawberry puree, and beer [12]. Evelyn et al. [152] investigated the effect of high-pressure, high thermal treatments, and thermosonication treatments on the effect of *B. nivea* and *N. fischeri* mold spores. They identified that spores age has a profound effect on inactivation through HPP. For *B. nivea,* the reduction was 2.7 log for 4-week spores and 2 log for 12-week spores at 600 MPa/75°C/30 min. At the same treatment time, *N. fischeri* showed 2–4 log reduction, and 12-week-old spores were more resistant than 4-week-old spores indicating lower inactivation for older spores. On the other hand, thermosonic treatment at 0.33 W/mL at 75°C was not effective in the inactivation of ascospores. The high pressure of 600 MPa and temperature of 75°C would be appropriate while targeting the most resistant spores, i.e., old spores of >12 weeks.

Through combination treatment requirement of high temperature was reduced as required in individual thermal processing to achieve the same degree of inactivation with better quality and less energy. Similar results were found in the literature for using antimicrobial agents and preservatives. Treatments like ultrasonication and modified atmosphere packaging in combination with HPP were also found to provide a significant positive result in spores inactivation compared to individual treatment over food. Some of the literature describing the use of different techniques along with HPP is given in Tables 4 and 5.

4. Benefits of Technology and Engineering Challenges

Uniform and instantaneous pressure transmission are effective in causing the death of pathogenic microorganisms due to the permeabilization of cell membranes without much increase in product temperature. HPP can even be carried out at low temperatures. Cell membrane permeability changes are reversible at low pressure but irreversible at high-pressure. The effect of pressure occurs only on non-covalent bonds, and covalent bonds are not affected. Therefore, the characteristics of organoleptic and sensory properties remain unaltered, or the difference reported is not significant [16, 198]. Therefore, getting attention from the consumers and processors as the treated food is mildly processed and provides characteristics similar to fresh

products. It is also effective in reducing enzyme activity, thereby enhancing the product's yield, quality, and shelf life, especially in fruits and vegetables [199]. Technology is environment friendly as no residues or waste are generated.

A variety of products can be treated using the technology, i.e., solid foods (preferably vacuum packaged) and liquid foods (in a flexible package, having the ability to bear compression up to 15 to 20%), dry-cured or cooked meat products, fish, seafood, marinated products, ready to eat meals, sauces, fruits and vegetables, juices, marmalades, jams, cheeses, milk, and other dairy products and nutraceutical [200, 201]. Some foods that cannot be treated by high pressure are: food packaged in glass since glass containers will break on compression; products like bread and mousse that have air included in them; spices and dry fruits as these products have low moisture content.

The equipment cost is high, and processed products have a niche market, so the product is commercially processed only in developed countries. It is due to the limited availability or development of large pressure vessels that can handle large volumes of food and withstand high pressures. Using one large pressure vessel rather than multiple small pressure vessels in parallel would be more effective and reduce operating and capital costs. The operating cost of the product is also dependent upon the operating parameters, i.e., amount of pressure, holding time, and temperature of the solvent used. Therefore, it is pertinent to optimize processing variables [16]. Challenges to the commercial application of high-pressure technology include material handling, process optimization, limited knowledge in understanding kinetic data, the role of constituents cleaning, and disinfection of equipment.

5. Conclusions

This review illustrates the effectiveness of the nonthermal technique, i.e., HPP, on microorganism reduction and extension of the shelf life of different food products. Food composition, type and age of microorganism, amount of pressure, and treatment time play an important role in reducing the microorganism load. This novel technology is very effective against vegetative pathogens but has some limitations in the inactivation of spores. Effective and synergistic results in the inactivation of spores can be obtained when combined with other thermal and nonthermal techniques. This combination of hurdles reduces the severity of individual processing while retaining the nutritional quality of food products. Although initial equipment cost is high, recent advancements and an increase in the number of HPP units have resulted in the successful commercialization of HPP products in developed countries and are also getting acceptance worldwide. Still, further work can be done to reduce the equipment cost and further research on the resistance of microorganisms.

Data Availability

All data pertaining to this review are available within the article.

Conflicts of Interest

The authors declare that they have no conflicts of interest.

References

[1] G. Abera, "Review on high pressure processing of foods," *Cogent Food & Agriculture*, vol. 5, no. 1, Article ID e1568725, 2019.

[2] S. K. Amit, M. M. Uddin, R. Rahman, S. M. R. Islam, and M. S. Khan, "A review on mechanisms and commercial aspects of food preservation and processing," *Agriculture & Food Security*, vol. 6, no. 1, pp. 51–22, 2017.

[3] H.-W. Huang, C.-P. Hsu, and C.-Y. Wang, "Healthy expectations of high hydrostatic pressure treatment in food processing industry," *Journal of Food and Drug Analysis*, vol. 28, pp. 1–13, 2020.

[4] B. G. Nabi, K. Mukhtar, R. N. Arshad et al., "High-pressure processing for sustainable food supply," *Sustainability*, vol. 13, no. 24, Article ID 13908, 2021.

[5] N. K. Kalagatur, J. R. Kamasani, V. Mudili, K. Krishna, O. P. Chauhan, and M. H. Sreepathi, "Effect of high pressure processing on growth and mycotoxin production of *Fusarium graminearum* in maize," *Food Bioscience*, vol. 21, pp. 53–59, 2018.

[6] A. C. S. Porto-fett, A. Jackson-davis, L. S. Kassama et al., "Inactivation of shiga toxin-producing *Escherichia Coli* in refrigerated and frozen meatballs using high pressure processing," *Microorganisms*, vol. 8, no. 3, pp. 360–369, 2020.

[7] H. W. Woldemariam and S. A. Emire, "High pressure processing of foods for microbial and mycotoxins control: current trends and future prospects," *Cogent Food & Agriculture*, vol. 5, no. 1, Article ID 1622184, 2019.

[8] R. C. Bonfim, F. A. D. Oliveira, R. L. D. O. Godoy, and A. Rosenthal, "A review on high hydrostatic pressure for bivalve mollusk processing: relevant aspects concerning safety and quality," *Food Sci Technol*, vol. 39, no. 3, pp. 515–523, 2019.

[9] D. Daher, C. Pérez-Lamela, and C. Pérez-Lamela, "Effect of high pressure processing on the microbial inactivation in fruit preparations and other vegetable based beverages," *Agriculture*, vol. 7, no. 9, p. 72, 2017.

[10] M. Premi and K. A. Khan, "Role of canning technology in preservation of fruits and vegetables," in *Technological Interventions in Processing of Fruits and Vegetables*, R. Sehrawat, K. A. Khan, M. R. Goyal, and P. K. Paul, Eds., vol. 1, pp. 229–254, CRC press, Boca Raton, FL, USA, 2018.

[11] N. K. Rastogi, "High-pressure processing of plant products," in *Recent Developments in High Pressure Processing of Foods*, R. W. Hartel, Ed., University of Wisconsin-Madison, Madison, WI, USA, 2013.

[12] S. F. V. M. Evelyn, "Resistance of *Byssochlamys nivea* and *Neosartorya fischeri* mold spores of different age to high pressure thermal processing and thermosonication," *Journal of Food Engineering*, vol. 201716 pages, 2017.

[13] E. P. Black, A. L. Kelly, and G. F. Fitzgerald, "The combined effect of high pressure and nisin on inactivation of microorganisms in milk," *Innovative Food Science & Emerging Technologies*, vol. 6, no. 3, pp. 286–292, 2005.

[14] I. Mainville, D. Montpetit, N. Durand, and E. R. Farnworth, "Deactivating the bacteria and yeast in kefir using heat treatment, irradiation and high pressure," *International Dairy Journal*, vol. 11, no. 1-2, pp. 45–49, 2001.

[15] J. M. Rodríguez-Calleja, M. C. Cruz-Romero, M. G. O'Sullivan, M. L. García-López, and J. Kerry, "High-pressure-based hurdle strategy to extend the shelf-life of fresh chicken breast fillets," *Food Control*, vol. 25, no. 2, pp. 516–524, 2012.

[16] R. Sehrawat, B. P. Kaur, P. K. Nema, S. Tewari, and L. Kumar, "Microbial inactivation by high pressure processing: principle, mechanism and factors responsible," *Food Science and Biotechnology*, vol. 30, no. 1, pp. 19–35, 2021.

[17] O. S. Qadri, B. Yousuf, and A Srivastava, "Fresh-cut fruits and vegetables: critical factors influencing microbiology and novel approaches to prevent microbial risks—a review," *Cogent Food & Agriculture*, vol. 1, Article ID 1121606, 2015.

[18] A. Vercammen, K. G. A. Vanoirbeek, L. Lemmens, I. Lurquin, M. E. G. Hendrickx, and C. W. Michiels, "High pressure pasteurization of apple pieces in syrup: microbiological shelf-life and quality evolution during refrigerated storage," *Innovative Food Science & Emerging Technologies*, vol. 16, pp. 259–266, 2012.

[19] N. Kaushik, B. P. Kaur, and P. S. Rao, "Application of high pressure processing for shelf life extension of litchi fruits (*Litchi chinensis* cv. *Bombai*) during refrigerated storage," *Food Science and Technology International*, vol. 20, no. 7, pp. 527–541, 2013.

[20] V. Serment-Moreno, Z. Escobedo-Avellaneda, and J. Welti-Chanes, *High hydrostatic pressure (HHP) microbial kinetics in orange comminuted*, ICEF 11 International Congress on Engineering and Food, Athens, Greece, Europe, 2011.

[21] B. Krebbers, A. M. Matser, M. Koets, and R. Van den Berg, "Quality and storage-stability of high-pressure preserved green beans," *Journal of Food Engineering*, vol. 54, no. 1, pp. 27–33, 2002.

[22] L. Li, L. Feng, J. Yi et al., "High hydrostatic pressure inactivation of total aerobic bacteria, lactic acid bacteria, yeasts in sour Chinese cabbage," *International Journal of Food Microbiology*, vol. 142, no. 1-2, pp. 180–184, 2010.

[23] E. Penas, J. Frias, R. Gomez, and C. Vidal-Valverde, "High hydrostatic pressure can improve the microbial quality of sauerkraut during storage," *Food Control*, vol. 21, no. 4, pp. 524–528, 2010.

[24] H. Neetoo, S. Nekoozadeh, Z. Jiang, and H. Chen, "Application of high hydrostatic pressure to decontaminate green onions from *Salmonella* and *Escherichia coli* O157: H7," *Food Microbiology*, vol. 28, no. 7, pp. 1275–1283, 2011.

[25] H. Neetoo, Y. Lu, C. Wu, and H. Chen, "Use of high hydrostatic pressure to inactivate *Escherichia coli* O157: H7 and *Salmonella enterica* internalized within and adhered to preharvest contaminated green onions," *Applied and Environmental Microbiology*, vol. 78, no. 6, pp. 2063–2065, 2012.

[26] L. S. Jung, S. H. Lee, S. Kim, S. K. Lee, and J. Ahn, "Effect of high pressure processing on microbiological and physical qualities of carrot and spinach," *Food Science Biotechnology*, vol. 21, no. 3, pp. 899–904, 2012.

[27] R. Bao, A. P. Fan, X. Hu, X. J. Liao, and F. Chen, "Effects of high pressure processing on the quality of pickled radish during refrigerated storage," *Innovative Food Science & Emerging Technologies*, vol. 38, pp. 206–212, 2016.

[28] L. Plaza, M. Munoz, B. de Ancos, and M. P. Cano, "Effect of combined treatments of high pressure, citric acid and sodium chloride on quality parameters of tomato puree," *The Journal European Food Research and Technology*, vol. 216, no. 6, pp. 514–519, 2003.

[29] J. A. Guerrero-Beltran, G. V. Barbosa-Canovas, G. Moraga-Ballesteros, M. J. Moraga-Ballesteros, and B. G. Swanson,

"Effect of pH and ascorbic acid on high hydrostatic pressure processed mango puree," *Journal of Food Processing and Preservation*, vol. 30, no. 5, pp. 582–596, 2006.

[30] A. Landl, M. Abadias, C. Sárraga, I. Viñas, and P. A. Picouet, "Effect of high pressure processing on the quality of acidified Granny Smith apple purée product," *Innovative Food Science & Emerging Technologies*, vol. 11, no. 4, pp. 557–564, 2010.

[31] S. Mukhopadhyay, K. Sokorai, D. Ukuku, X. Fan, and V. Juneja, "Effect of high hydrostatic pressure processing on the background microbial loads and quality of cantaloupe puree," *Food Research International*, vol. 91, pp. 55–62, 2017.

[32] F. González-Cebrino, J. Garc´ıa-Parra, R. Contador, R. Tabla, and R. Ram´ırez, "Effect of high-pressure processing and thermal treatment on quality attributes and nutritional compounds of "Songold" plum puree," *Journal of Food Science*, vol. 77, no. 8, pp. 866–873, 2012.

[33] N. Kaushik, B. P. Kaur, P. S. Rao, and H. N. Mishra, "Effect of high pressure processing on color, biochemical and microbiological characteristics of mango pulp (*Mangifera indica* cv. Amrapali)," *Innovative Food Science & Emerging Technologies*, vol. 22, pp. 40–50, 2014.

[34] A. Y. L. Teo, S. Ravishankar, and C. E. Sizer, "Effect of low temperature, high pressure treatment on the survival of *Escherichia coli* O157: H7 and *Salmonella* in unpasteurized fruit juices," *Journal of Food Protection*, vol. 64, no. 8, pp. 1122–1127, 2001.

[35] M. K. Bull, K. Zerdin, E. Howe et al., "The effect of high pressure processing on the microbial, physical and chemical properties of valencia and navel orange juice," *Innovative Food Science & Emerging Technologies*, vol. 5, no. 2, pp. 135–149, 2004.

[36] R. A. H. Timmermans, H. C. Mastwijk, J. J. Knol et al., "Comparing equivalent thermal, high pressure and pulsed electric field processes for mild pasteurization of orange juice. Part I: impact on overall quality attributes," *Innovative Food Science & Emerging Technologies*, vol. 12, no. 3, pp. 235–243, 2011.

[37] F. C. Lavinas, M. A. L. Miguel, M. L. M. Lopes, and V. L. Valentemesquita, "Effect of high hydrostatic pressure on cashew apple (*Anacardium occidentale* L.) juice preservation," *Journal of Food Science*, vol. 73, no. 6, pp. 273–277, 2008.

[38] S. Buzrul, H. Alpas, A. Largeteau, and G. Demazeau, "Inactivation of *Escherichia coli* and *Listeria innocua* in kiwifruit and pineapple juices by high hydrostatic pressure," *International Journal of Food Microbiology*, vol. 124, no. 3, pp. 275–278, 2008.

[39] G. Ferrari, P. Maresca, and R. Ciccarone, "The application of high hydrostatic pressure for the stabilization of functional foods: pomegranate juice," *Journal of Food Engineering*, vol. 100, no. 2, pp. 245–253, 2010.

[40] Y. Ma, X. Hu, J. Chen et al., "Effect of UHP on enzyme, microorganism and flavor in cantaloupe (*Cucumis melo* L.) juice," *Journal of Food Process Engineering*, vol. 33, no. 3, pp. 540–553, 2009.

[41] N. D. Hiremath and H. S. Ramaswamy, "High-pressure destruction kinetics of spoilage and pathogenic microorganisms in mango," *Journal of Food Processing and Preservation*, vol. 36, no. 2, pp. 113–125, 2012.

[42] D. Chen, X. Pang, J. Zhao et al., "Comparing the effects of high hydrostatic pressure and high temperature short time on papaya beverage," *Innovative Food Science & Emerging Technologies*, vol. 32, pp. 16–28, 2015.

[43] E. Varela-Santos, A. Ochoa-Martinez, G. Tabilo-Munizaga et al., "Effect of high hydrostatic pressure (HHP) processing on physicochemical properties, bioactive compounds and shelf-life of pomegranate juice," *Innovative Food Science & Emerging Technologies*, vol. 13, pp. 13–22, 2012.

[44] Y. H. Chang, S. J. Wu, B. Y. Chen, H. W. Huang, and C. Y. Wang, "Effect of high-pressure processing and thermal pasteurization on overall quality parameters of white grape juice," *Journal of the Science of Food and Agriculture*, vol. 97, no. 10, pp. 3166–3172, 2017.

[45] P. K. Nayak, K. Rayaguru, and K. Radha Krishnan, "Quality comparison of elephant apple juices after high-pressure processing and thermal treatment," *Jorunal of Science Food Agriculture*, vol. 97, no. 5, pp. 1404–1411, 2017.

[46] M. Houška, J. Strohalm, K. Kocurova et al., "High pressure and foods-fruit/vegetable juices," *Journal of Food Engineering*, vol. 77, no. 3, pp. 386–398, 2006.

[47] H. Alpas, L. Alma, and F. Bozoglu, "Inactivation of alicyclobacillus acidoterrestris vegetative cells in model system, apple, orange and tomato juices by high hydrostatic pressure," *World Journal of Microbiology and Biotechnology*, vol. 19, no. 6, pp. 619–623, 2003.

[48] M. Pilavtepe-Çelik, S. Buzrul, H. Alpas, and F. Bozoglu, "Development of a new mathematical model for inactivation of *Escherichia coli* O157: H7 and *Staphylococcus aureus* by high hydrostatic pressure in carrot juice and peptone water," *Journal of Food Engineering*, vol. 90, no. 3, pp. 388–394, 2009.

[49] M. F. Patterson, A. M. McKay, M. Connolly, and M. Linton, "The effect of high hydrostatic pressure on the microbiological quality and safety of carrot juice during refrigerated storage," *Food Microbiology*, vol. 30, no. 1, pp. 205–212, 2012.

[50] N. Ali, V. Popović, T. Koutchma, K. Warriner, and Y. Zhu, "Effect of thermal, high hydrostatic pressure, and ultraviolet-C processing on the microbial inactivation, vitamins, chlorophyll, antioxidants, enzyme activity, and color of wheatgrass juice," *Journal of Food Process Engineering*, vol. 43, no. 1, 2019.

[51] J. Sánchez, J. Delgado-Adamez, M. N. Franco, C. De Miguel, M. R. Ramirez, and D. Martin-Vertedor, "Comparative effect of high pressure processing and traditional thermal treatment on the physicochemical, microbiology, and sensory analysis of olive jam," *Grasas Y Aceites*, vol. 64, no. 4, pp. 432–441, 2013.

[52] Y. T. Wang, F. X. Liu, X. M. Cao, F. Chen, X. Hu, and X. Liao, "Comparison of high hydrostatic pressure and high temperature short time processing on quality of purple sweet potato nectar," *Innovative Food Science & Emerging Technologies*, vol. 16, pp. 326–334, 2012.

[53] D. B. Aguirre, J. A. G. Beltran, G. V. B. Canovas, and J. W. Chanes, "Study of the inactivation of *E. coli* and pectin methylesterase in mango nectar under selected high hydrostatic pressure treatments," *Food Science and Technology International*, vol. 17, pp. 541–547, 2011.

[54] F. Kurosaki and A. Nishi, "Isolation and antimicrobial activity of the phytoalexin 6 methoxymellein from cultured carrot cells," *Phytochemistry*, vol. 22, no. 3, pp. 669–672, 1983.

[55] E. H. d R. Ferreira, A. Rosenthal, V. Calado, J. Saraiva, and S. Mendo, "*Byssochlamys nivea* inactivation in pineapple juice and nectar using high pressure cycles," *Journal of Food Engineering*, vol. 95, no. 4, pp. 664–669, 2009.

[56] F. Feroz, S. Nafisa, and R Noor, "Emerging technologies for food safety: high pressure processing (HPP) and cold plasma

technology (CPT) for decontamination of foods," *Bangladesh Journal of Microbiology*, vol. 36, no. 1, pp. 35–43, 2019.

[57] J. L. P. Santos, S. Samapundo, A. Biyikli et al., "Occurrence, distribution and contamination levels of heat-resistant moulds throughout the processing of pasteurized high-acid fruit products," *International Journal of Food Microbiology*, vol. 281, pp. 72–81, 2018.

[58] S. G. Sousa, I. Delgadillo, and J. A. Saraiva, "Human milk composition and preservation: evaluation of high-pressure processing as a non-thermal pasteurization technology," *Critical Reviews in Food Science and Nutrition*, vol. 56, no. 6, pp. 1043–1060, 2014.

[59] I. Sierra, V. C. Vidal, and F. R. Lopez, "Effect of high pressure on the vitamin B1 and B6 content of milk," *Milchwissenschaft*, vol. 55, pp. 365–436, 2000.

[60] E. E. Kheadr, J. F. Vachon, P. Paquin, and I. Fliss, "Effect of dynamic high pressure on microbiological, rheological and microstructural quality of Cheddar cheese," *International Dairy Journal*, vol. 12, no. 5, pp. 435–446, 2002.

[61] D. Carminati, M. Gatti, B. Bonvini, E. Neviani, and G. Mucchetti, "High pressure processing of gorgonzola cheese: influence on *Listeria monocytogenes* inactivation and on sensory characteristics," *Journal of Food Protection*, vol. 67, no. 8, pp. 1671–1675, 2004.

[62] P. M. Tomasula, J. A. Renye, D. Van Hekken et al., "Effect of high-pressure processing on reduction of *Listeria monocytogenes* in packaged Queso Fresco," *Journal of Dairy Science*, vol. 97, no. 3, pp. 1281–1295, 2014.

[63] M. Hayman, R. C. Anantheswaran, and S. J. Knabel, "The effects of growth temperature and growth phase on the inactivation of *Listeria monocytogenes* in whole milk subject to high pressure processing," *International Journal of Food Microbiology*, vol. 115, no. 2, pp. 220–226, 2007.

[64] J. A. Donaghy, M. Linton, M. F. Patterson, and M. T. Rowe, "Effect of high pressure and pasteurization on *Mycobacterium avium* ssp. *paratuberculosis* in milk," *Letters in Applied Microbiology*, vol. 45, no. 2, pp. 154–159, 2007.

[65] S. Viazis, B. E. Farkas, and L. A. Jaykus, "Inactivation of bacterial pathogens in human milk by high-pressure processing," *Journal of Food Protection*, vol. 71, no. 1, pp. 109–118, 2008.

[66] B. Yang, Y. Shi, X. Xia et al., "Inactivation of food borne pathogens in raw milk using high hydrostatic pressure," *Food Control*, vol. 28, no. 2, pp. 273–278, 2012.

[67] C. E. O'Reilly, P. M. O'Connor, A. L. Kelly, T. P. Beresford, and P. M. Murphy, "Use of hydrostatic pressure for inactivation of microbial contaminants in cheese," *Applied and Environmental Microbiology*, vol. 66, no. 11, pp. 4890–4896, 2000.

[68] T. López-Pedemonte, W. J. Brinẽz, A. X. Roig-Sagués, and B. Guamis, "Fate of *Staphylococcus aureus* in cheese treated by ultrahigh pressure homogenization and high hydrostatic pressure," *Journal of Dairy Science*, vol. 89, no. 12, pp. 4536–4544, 2006.

[69] F. J. Delgado, J. Delgado, J. González-Crespo, R. Cava, and R. Ramírez, "High-pressure processing of a raw milk cheese improved its food safety maintaining the sensory quality," *Food Science Technology International*, vol. 19, no. 6, pp. 493–501, 2013.

[70] A. Jankowska, A. Reps, A. Proszek, and M. Krasowska, "Effect of high pressure on microflora and sensory characteristics of yoghurt," *Polish Journal of Food Nutrition Sciences*, vol. 14, pp. 79–84, 2005.

[71] V. Bansal, K. Jabeen, P. S. Rao, P. Prasad, and S. K. Yadav, "Effect of high pressure processing (HPP) on microbial safety, physicochemical properties, and bioactive compounds of whey-based sweet lime (whey-lime) beverage," *Food Measure*, vol. 13, no. 1, pp. 454–465, 2019.

[72] N. Narisawa, S. Furukawa, T. Kawarai et al., "Effect of skimmed milk and its fractions on the inactivation of *Escherichia coli* K12 by high hydrostatic pressure treatment," *International Journal of Food Microbiology*, vol. 124, no. 1, pp. 103–107, 2008.

[73] H. S. Ramaswamy, H. Jin, and S. Zhu, "Effects of fat, casein and lactose on high-pressure destruction of *Escherichia coli* K12 (ATCC-29055) in milk," *Food and Bioproducts Processing*, vol. 87, pp. 1–6, 2009.

[74] F. Bozoglu, H. Alpas, and G. KaletunÃ, "Injury recovery of food borne pathogens in high hydrostatic pressure treated milk during storage," *FEMS Immunology & Medical Microbiology*, vol. 40, no. 3, pp. 243–247, 2004.

[75] A. L. B. Penna, G. Subbarao, and G. V. Barbosa-Cánovas, "High hydrostatic pressure processing on microstructure of probiotic low-fat yogurt," *Food Research International*, vol. 40, no. 4, pp. 510–519, 2007.

[76] C. E. O'Reilly, A. L. Kelly, P. M. Murphy, and T. P. Beresford, "High pressure treatment: applications in cheese manufacture and ripening," *Trends in Food Science & Technology*, vol. 12, no. 2, pp. 51–59, 2001.

[77] M. Capellas, M. Mor-Mur, E. Sendra, and B. Guamis, "Effect of high-pressure processing on physico-chemical characteristics of fresh goat's milk cheese (Mató)," *International Dairy Journal*, vol. 11, no. 3, pp. 165–173, 2001.

[78] C. O. R. Okpala, J. R. Piggott, and C. J. Schaschke, "Influence of high-pressure processing (HPP) on physico-chemical properties of fresh cheese," *Innovative Food Science & Emerging Technologies*, vol. 11, no. 1, pp. 61–67, 2010.

[79] J. Cui and Z. Q. Wang, "Outbreaks of human trichinellosis caused by consumption of dog meat in China," *Parasite*, vol. 8, pp. 74–77, 2001.

[80] W. J. Smerdon, G. K. Adak, S. J. O' Brien, I. A. Gillespie, and M. Reacher, "General outbreaks of infectious intestinal disease linked with red meat, England and Wales, 1992–1999," *Communicable Disease and Public Health*, vol. 4, pp. 259–267, 2001.

[81] R. J. Webby, K. S. Carville, M. D. Kirk et al., "Internationally distributed frozen oyster meat causing multiple outbreaks of norovirus infection in Australia," *Clinical Infectious Diseases*, vol. 44, no. 8, pp. 1026–1031, 2007.

[82] J. A. Torres and G. Velazquez, "Commercial opportunities and research challenges in the high pressure processing of foods," *Journal of Food Engineering*, vol. 67, no. 1-2, pp. 95–112, 2005.

[83] M. Ferreira, A. Almeida, I. Delgadillo, J. Saraiva, and A. Cunha, "Susceptibility of *Listeria monocytogenes* to high pressure processing: a review," *Food Reviews International*, vol. 32, no. 4, pp. 377–399, 2016.

[84] European Food Safety Authority, "The European union summary report on trends and sources of zoonoses, zoonotic agents and food-borne outbreaks in 2016," *EFSA Journal. European Food Safety Authority*, vol. 15, no. 12, Article ID e05077, 2017.

[85] L. W. Murchie, M. Cruz-Romero, J. P. Kerry et al., "High pressure processing of shellfish: a review of microbiological and other quality aspects," *Innovative Food Science & Emerging Technologies*, vol. 6, no. 3, pp. 257–270, 2005.

[86] U. Roobab, A. W. Khan, J. M. Lorenzo et al., "A systematic review of clean-label alternatives to synthetic additives in raw and processed meat with a special emphasis on high-pressure processing (2018–2021)," *Food Research International*, vol. 150, Article ID 110792, 2021.

[87] A. Perez-Baltar, A. Serrano, R. Montiel, and M. Medina, "*Listeria monocytogenes* inactivation in deboned dry-cured hams by high pressure processing," *Meat Science*, vol. 160, Article ID 107960, 2020.

[88] S. Martillanes, R. Ramírez, G. Amaro-Blanco, M. C. Ayuso-Yuste, M. V. Gil, and J. Delgado-Adámez, "Effect of rice bran extract on the preservation of pork burger treated with high pressure processing," *Journal of Food Process Preservation*, vol. 44, pp. 1–11, 2020.

[89] P. Bonilauri, M. S. Grisenti, P. Daminelli et al., "Reduction of *Salmonella* spp. populations in Italian salami during production process and high pressure processing treatment: validation of processes to export to the," *Meat Science*, vol. 157, Article ID e107869, 2019.

[90] J. K. O'Brien and R. T. Marshall, "Microbiological quality of raw ground chicken processed at high isostatic pressure," *Journal of Food Protection*, vol. 59, no. 2, pp. 146–150, 1996.

[91] Y. C. Lee, C. Y. Hsieh, M. L. Chen, C. Y. Wang, C. S. Lin, and Y. H. Tsai, "High-pressure inactivation of histamine-forming bacteria *Morganella morganii* and *Photobacterium phosphoreum*," *Journal of Food Protection*, vol. 83, no. 4, pp. 621–627, 2020.

[92] C. K. Kamalakanth, J. Ginson, J. Bindu et al., "Effect of high pressure on K-value, microbial and sensory characteristics of yellowfin tuna (*Thunnus albacares*) chunks in EVOH films during chill storage," *Innovative Food Science & Emerging Technologies*, vol. 12, no. 4, pp. 451–455, 2011.

[93] J. C. Ramirez-Suarez and M. T. Morrissey, "Effect of high pressure processing (HPP) on shelf life of albacore tuna (*Thunnus alalunga*) minced muscle," *Innovative Food Science & Emerging Technologies*, vol. 7, no. 1-2, pp. 19–27, 2006.

[94] C. Rong, Z. Ling, S. Huihui, and L. Qi, "Characterization of microbial community in high-pressure treated oysters by high-throughput sequencing technology," *Innovative Food Science & Emerging Technologies*, vol. 45, pp. 241–248, 2018.

[95] T. Fujii, M. Satomi, G. Nakatsuka, T. Yamaguchi, and M. Okuzumi, "Changes in freshness indexes and bacterial flora during storage of pressurized mackerel," *Journal of the Food Hygienic Society of Japan*, vol. 35, no. 2, pp. 195–200, 1994.

[96] G. Carpi, M. Buzzoni, S. Gola, A. Maggi, and P. Rovere, "Microbial and chemical shelf-life of high-pressure treated salmon cream at refrigeration temperatures," *IND Conserve*, vol. 70, pp. 386–389, 1995.

[97] K. Noeckler, V. Heinz, K. Lemkau, and D. Knorr, "Inactivation of *Trichinella spiralis* by high-pressure treatment," *Fleischwirtschaft*, vol. 81, pp. 85–88, 2001.

[98] M. M. Hayman, I. Baxter, P. J. O'Riordan, and C. M. Stewart, "Effects of high-pressure processing on the safety, quality, and shelf life of ready-to-eat meats," *Journal of Food Protection*, vol. 67, no. 8, pp. 1709–1718, 2004.

[99] R. Lakshmanan and P. Dalgaard, "Effects of high-pressure processing on *Listeria monocytogenes*, spoilage microflora and multiple compound quality indices in chilled cold-smoked salmon," *Jorunal of Applied Microbiology*, vol. 96, no. 2, pp. 398–408, 2004.

[100] L. Picart, E. Dumay, J. P. Guiraud, and C. Cheftel, "Combined high pressure-sub-zero temperature processing of smoked salmon mince: phase transition phenomena and inactivation of *Listeria innocua*," *Journal of Food Engineering*, vol. 68, no. 1, pp. 43–56, 2005.

[101] M. V. Collins, G. J. Flick, S. A. Smith et al., "The effect of high-pressure processing on infectivity of cryptosporidium parvum oocysts recovered from experimentally exposed eastern oysters (*Crassostrea virginica*)," *Journal of Eukaryotic Microbiology*, vol. 52, no. 6, pp. 500–504, 2005.

[102] B. P. Kaur, N. Kaushik, P. S. Rao, and O. P. Chauhan, "Effect of high-pressure processing on physical, biochemical, and microbiological characteristics of black tiger shrimp (*Penaeus monodon*)," *Food and Bioprocess Technology*, vol. 6, pp. 1390–1400, 2013a.

[103] B. P. Kaur, N. Kaushik, P. S. Rao, and H. N. Mishra, "Chilled storage of high pressure processed black tiger shrimp (*Penaeus monodon*)," *Journal of Aquatic Food Product Technology*, vol. 24, no. 3, pp. 283–299, 2013b.

[104] A. Chouhan, B. P. Kaur, and P. S. Rao, "Effect of high pressure processing and thermal treatment on quality of hilsa (*Tenualosa ilisha*) fillets during refrigerated storage," *Innovative Food Science & Emerging Technologies*, vol. 29, pp. 151–160, 2015.

[105] M. de Alba, R. Montiel, D. Bravo, P. Gaya, and M. Medina, "High pressure treatments on the inactivation of *Salmonella Enteritidis* and the physicochemical, rheological and color characteristics of sliced vacuum-packaged dry-cured ham," *Meat Science*, vol. 91, no. 2, pp. 173–178, 2012.

[106] J. Yuste, R. Pla, M. Capellas, E. Sendra, E. Beltran, and M. Mor-Mur, "Oscillatory high pressure processing applied to mechanically recovered poultry meat for bacterial inactivation," *Journal of Food Science*, vol. 66, no. 3, pp. 482–484, 2001.

[107] S. Jung, M. Ghoul, and M. de Lamballerie-Anton, "Influence of high pressure on the color and microbial quality of beef meat," *LWT-Food Science and Technology*, vol. 36, no. 6, pp. 625–631, 2003.

[108] M. Garriga, N. Grebol, M. T. Aymerich, J. M. Monfort, and M. Hugas, "Microbial inactivation after high-pressure processing at 600 MPa in commercial meat products over its shelf life," *Innovative Food Science & Emerging Technologies*, vol. 5, no. 4, pp. 451–457, 2004.

[109] M. Cruz-Romero, J. P. Kerry, and A. L. Kelly, "Changes in the microbiological and physicochemical quality of high-pressure-treated oysters (Crassostreagigas) during chilled storage," *Food Control*, vol. 19, no. 12, pp. 1139–1147, 2008.

[110] N. Basaran-Akgul, M. Mousavi-Hesary, P. Basaran, J. H. Shin, B. G. Swanson, and B. A. Rasco, "High pressure processing inactivation of Listeria innocua in minced trout (Oncorhynchus mykiss)," *Journal of Food Processing Preservation*, vol. 34, pp. 191–206, 2010.

[111] Z. A. Kruk, H. Yun, D. L. Rutley, E. J. Lee, Y. J. Kim, and C. Jo, "The effect of high pressure on microbial population, meat quality and sensory characteristics of chicken breast fillet," *Food Control*, vol. 22, no. 1, pp. 6–12, 2011.

[112] S. Bover-Cid, N. Belletti, M. Garriga, and T. Aymerich, "Response surface methodology to investigate the effect of high pressure processing on *Salmonella* inactivation on dry-cured ham," *Food Research International*, vol. 45, no. 2, pp. 1111–1117, 2012.

[113] N. Belletti, M. Garriga, T. Aymerich, and S. Bover-Cid, "High pressure inactivation of a virulent *Enterococcus faecalis* on dry-cured ham: modeling the effect of processing parameters," *Innovative Food Science & Emerging Technologies*, vol. 18, pp. 43–47, 2013.

[114] N. Belletti, M. Garriga, T. Aymerich, and S. Bover-Cid, "Inactivation of *Serratia liquefaciens* on dry-cured ham by high pressure processing," *Food Microbiology*, vol. 35, no. 1, pp. 34–37, 2013.

[115] A. C. Lowder, J. G. Waite-Cusic, and C. A. Mireles DeWitt, "High pressure-low temperature processing of beef: effects on survival of internalized *E. coli* O157: H7 and quality characteristics," *Innovative Food Science & Emerging Technologies*, vol. 26, pp. 18–25, 2014.

[116] S. Bulut, N. Chapleau, M. Lamballerie, and A. Le-Bail, "High pressure processing of chicken meat: change in total aerobic counts after pressure treatment and during chilled storage," *British Microbiology Research Journal*, vol. 4, pp. 4540–4549, 2014.

[117] S. Devatkal, R. Anurag, B. Jaganath, and S. Rao, "Microstructure, microbial profile and quality characteristics of high-pressure-treated chicken nuggets," *Food Science Technology International*, vol. 21, no. 7, pp. 481–491, 2014.

[118] R. Mengden, A. Röhner, N. Sudhaus, and G. Klein, "High-pressure processing of mild smoked rainbow trout fillets (*Oncorhynchus mykiss*) and fresh European catfish fillets (*Silurus glanis*)," *Innovative Food Science & Emerging Technologies*, vol. 32, pp. 9–15, 2015.

[119] R. Banerjee, K. Jayathilakan, O. P. Chauhan, B. M. Naveena, S. Devatkal, and V. V. Kulkarni, "Vacuum packaged mutton patties: comparative effects of high-pressure processing and irradiation," *Journal of Food Processing and Preservation*, vol. 41, 2016.

[120] J. Bindu, J. Ginson, C. K. Kamalakanth, and T. K. S. Gopal, "High pressure treatment of green mussel *Perna viridis* Linnaeus, 1758: effect on shucking and quality changes in meat during chill storage," *Indian Jorunal of Fisheries*, vol. 62, pp. 70–76, 2015.

[121] A. Hara, G. Nagahama, A. Ohbayashi, and R. Hayashi, "Effects of high pressure on inactivation of enzymes and microorganisms in non pasteurized rice wine (Namazake)," *Journal of the Agricultural Chemical Society of Japan*, vol. 64, no. 5, pp. 1025–1029, 1990.

[122] L. Unni, O. P. Chauhan, and P. S. Raju, "Quality changes in high pressure processed ginger paste under refrigerated storage," *Food Bioscience*, vol. 10, pp. 18–25, 2015.

[123] D. E. Leyva-Daniel, Z. Escobedo-Avellaneda, F. Villalobos-Castillejos, L. Alamilla-Beltrán, and J. Welti-Chanes, "Effect of high hydrostatic pressure applied to a Mexican honey to increase its microbiological and functional quality," *Food and Bioproducts Processing*, vol. 102, pp. 299–306, 2017.

[124] J. Rocha-Pimienta, S. Martillanes, R. Ramírez, J. Garcia-Parra, and J. Delgado-Adamez, "*Bacillus cereus* spores and *Staphylococcus aureus* sub. *aureus* vegetative cells inactivation in human milk by high-pressure processing," *Food Control*, vol. 113, Article ID 107212, 2020.

[125] N. Akhmazillah, M. M. Farid, and F. V. M. Silva, "High pressure processing of honey: preliminary study of total microorganism inactivation and identification of bacteria," *Journal of Science Technology*, vol. 4, pp. 1–12, 2012.

[126] J. G. Waite, J. M. Jones, E. J. Turek et al., "Production of shelf-stable ranch dressing using high-pressure processing," *Journal of Food Science*, vol. 74, no. 2, pp. M83–M93, 2009.

[127] B. Barcenilla, L. Román, C. Martínez, M. M. Martínez, and M. Gómez, "Effect of high pressure processing on batters and cakes properties," *Innovative Food Science & Emerging Technologies*, vol. 33, pp. 94–99, 2016.

[128] M. E. Bárcenas, R. Altamirano-Fortoul, and C. M. Rosell, "Effect of high pressure processing on wheat dough and bread characteristics," *LWT-Food Science and Technology*, vol. 43, no. 1, pp. 12–19, 2010.

[129] A. Ahromrit, D. Ledward, and K. Niranjan, "Kinetics of high pressure facilitated starch gelatinisation in Thai glutinous rice," *Journal of Food Engineering*, vol. 79, no. 3, pp. 834–841, 2007.

[130] M. Boluda-Aguilar, A. Taboada-Rodríguez, A. López-Gómez, F. Marín-Iniesta, and G. V. Barbosa-Cánovas, "Quick cooking rice by high hydrostatic pressure processing," *LWT-Food Science and Technology*, vol. 51, no. 1, pp. 196–204, 2013.

[131] H. Katopo, Y. Song, and J. L. Jane, "Effect and mechanism of ultrahigh hydrostatic pressure on the structure and properties of starches," *Carbohydrate Polymers*, vol. 47, no. 3, pp. 233–244, 2002.

[132] B. Wang, D. Li, L. J. Wang, Y. L. Chiu, X. D. Chen, and Z. H. Mao, "Effect of high-pressure homogenization on the structure and thermal properties of maize starch," *Journal of Food Engineering*, vol. 87, no. 3, pp. 436–444, 2008.

[133] C. Ravichandran, P. C. Badgujar, P. Gundev, and A. Upadhyay, "Review of toxicological assessment of d-limonene, a food and cosmetics additive," *Food and Chemical Toxicology*, vol. 120, pp. 668–680, 2018.

[134] L. Yu, S. Muralidharan, N. A. Lee et al., "The impact of variable high pressure treatments and/or cooking of rice on bacterial populations after storage using culture-independent analysis," *Food Control*, vol. 92, pp. 232–239, 2018.

[135] U. Roobab, R. Afzal, M. M. A. N. Ranjha, X. A. Zeng, Z. Ahmed, and R. M. Aadil, "High pressure-based hurdle interventions for raw and processed meat: a clean-label prospective," *International Journal of Food Science & Technology*, vol. 57, no. 2, pp. 816–826, 2022.

[136] V. Heinz and D. Knorr, "High pressure inactivation kinetics of *Bacillus subtilis* cells by a three-state-model considering distributed resistance mechanisms," *Food Biotechnology*, vol. 10, no. 2, pp. 149–161, 1996.

[137] Y. L. Gao and X. R. Ju, "Exploiting the combined effects of high pressure and moderate heat with nisin on inactivation of *Clostridium botulinum* spores," *Journal of Microbiological Methods*, vol. 72, no. 1, pp. 20–28, 2008.

[138] A. Jofre, T. Aymerich, and M. Garriga, "Assessment of the effectiveness of antimicrobial packaging combined with high pressure to control *Salmonella* sp. in cooked ham," *Food Control*, vol. 19, no. 6, pp. 634–638, 2008.

[139] A. Jofre, M. Garriga, and T. Aymerich, "Inhibition of *Salmonella* sp. *Listeria monocytogenes* and *Staphylococcus aureus* in cooked ham by combining antimicrobials, high hydrostatic pressure and refrigeration," *Meat Science*, vol. 78, no. 1-2, pp. 53–59, 2008.

[140] N. Kalchayanand, C. P. Dunne, A. Sikes, and B. Ray, "Inactivation of bacterial endospores by combined action of hydrostatic pressure and bacteriocins in roast beef," *Journal of Food Safety*, vol. 23, no. 4, pp. 219–231, 2003.

[141] Y. J. Crawford, E. A. Murano, D. G. Olson, and K. Shenoy, "Use of high hydrostatic pressure and irradiation to eliminate *Clostridium sporogenes* in chicken breast," *Journal of Food Protection*, vol. 59, no. 7, pp. 711–715, 1996.

[142] P. Paul, S. P. Chawala, P. Thomas, and P. C. Kesavan, "Effect of high hydrostatic pressure, gamma-irradiation and combined treatments on the microbiological quality of lamb meat during chilled storage," *J Food Saf*, vol. 16, pp. 263–271, 1997.

[143] D. Knorr, "Hydrostatic pressure treatment of food: microbiology (1995)," in *The New Methods for Food Preservation*, G. W. Gould, Ed., Blackie Academic, London, UK, 1995.

[144] J. Raso, M. L. Calderón, M. Góngora, G. V. Barbosa-Cánovas, and B. G. Swanson, "Inactivation of *Zygosaccharomyces Bailii* in fruit juices by heat, high hydrostatic pressure and pulsed electric fields," *Journal of Food Science*, vol. 63, no. 6, pp. 1042–1044, 2006.

[145] K. J. A. Hauben, E. Y. Wuytack, C. C. F. Soontjens, and C. W. Michiels, "High pressure transient sensitization of *Escherichia coli* to lysozyme and nisin by disruption of outer membrane permeability," *Journal of Food Protection*, vol. 59, no. 4, pp. 350–355, 1996.

[146] C. M. Roberts and D. G. Hoover, "Sensitivity of *Bacillus coagulans* spores to combinations of high hydrostatic pressure, heat acidity, and nisin," *Journal of Applied Bacteriology*, vol. 81, no. 4, pp. 363–368, 1996.

[147] R. Shankar, "High pressure processing- changes in quality characteristic of various food material processed under high pressure technology," *International Journal of Innovation Science and Research*, vol. 3, pp. 168–186, 2014.

[148] G. Ferrentino and S. Spilimbergo, "High pressure carbon dioxide pasteurization of solid foods: current knowledge and future outlooks," *Trends in Food Science & Technology*, vol. 22, no. 8, pp. 427–441, 2011.

[149] S. H. Park, V. Balasubramaniam, and S. K. Sastry, "Quality of shelf-stable low-acid vegetables processed using pressure-ohmic-thermal sterilization," *LWT-Food Science and Technology*, vol. 57, no. 1, pp. 243–252, 2014.

[150] L. Zhao, Y. Wang, D. Qiu, and X. Liao, "Effect of ultrafiltration combined with high-pressure processing on safety and quality features of fresh apple juice," *Food and Bioprocess Technology*, vol. 7, no. 11, pp. 3246–3258, 2014.

[151] S. F. V. M. Evelyn and F. V. Silva, "High pressure processing pretreatment enhanced the thermosonication inactivation of *Alicyclobacillus acidoterrestris* spores in orange juice," *Food Control*, vol. 62, pp. 365–372, 2016.

[152] M. E. Evelyn, E. Milani, and F. V. Silva, "Comparing high pressure thermal processing and thermosonication with thermal processing for the inactivation of bacteria, moulds, and yeasts spores in foods," *Journal of Food Engineering*, vol. 214, pp. 90–96, 2017.

[153] A. Amanatidou, O. Schlüter, K. Lemkau, L. G. M. Gorrisa, E. J. Smid, and D. Knorr, "Effect of combined application of high pressure treatment and modified atmospheres on the shelf life of fresh Atlantic salmon," *Innovative Food Science & Emerging Technologies*, vol. 1, no. 2, pp. 87–98, 2000.

[154] T. C. A. Meurehg, *Control of Escherichia Coli O157: H7, Generic Escherichia Coli, and Salmonella spp. on Beef Trimmings Prior to Grinding using a Controlled Phase Carbon Dioxide (cpCO2) System*, Kansas State University, Manhattan, Kansas, USA, 2006.

[155] Y. M. Choi, Y. Y. Bae, K. H. Kim, B. C. Kim, and M. S. Rhee, "Effects of supercritical carbon dioxide treatment against generic *Escherichia coli, Listeria monocytogenes, Salmonella typhimurium*, and *E. coli* O157: H7 in marinades and marinated pork," *Meat Science*, vol. 82, no. 4, pp. 419–424, 2009a.

[156] Y. M. Choi, O. Y. Kim, K. H. Kim, B. Kim, and M. S. Rhee, "Combined effect of organic acids and supercritical carbon dioxide treatments against nonpathogenic *Escherichia coli, Listeria monocytogenes, Salmonella typhimurium* and *E. coli* O157:H7 in fresh pork," *Letters in Applied Microbiology*, vol. 49, no. 4, pp. 510–515, 2009b.

[157] M. T. Valverde, F. Marın-Iniesta, and L. Calvo, "Inactivation of *Saccharomyces cerevisiae* in conference pear with high pressure carbon dioxide and effects on pear quality," *Journal of Food Engineering*, vol. 98, no. 4, pp. 421–428, 2010.

[158] Z. Xu, L. Zhang, Y. Wang, X. Bi, R. Buckow, and X. Liao, "Effects of high pressure CO_2 treatments on microflora, enzymes and some quality attributes of apple juice," *Journal of Food Engineering*, vol. 104, no. 4, pp. 577–584, 2011.

[159] L. Zhao, S. Wang, F. Liu et al., "Comparing the effects of high hydrostatic pressure and thermal pasteurization combined with nisin on the quality of cucumber juice drinks," *Innovative Food Science & Emerging Technologies*, vol. 17, pp. 27–36, 2013.

[160] D. U. Lee, V. Heinz, and D. Knorr, "Effects of combination treatments of nisin and high-intensity ultrasound with high pressure on the microbial inactivation in liquid whole egg," *Innovative Food Science & Emerging Technologies*, vol. 4, no. 4, pp. 387–393, 2003.

[161] B. Krebbers, A. M. Matser, S. W. Hoogerwerf, R. Moezelaar, M. M. M. Tomassen, and R. W. van den Berg, "Combined high-pressure and thermal treatments for processing of tomato puree: evaluation of microbial inactivation and quality parameters," *Innovative Food Science & Emerging Technologies*, vol. 4, pp. 377–385, 2003.

[162] S. Rajan, S. Pandrangi, V. M. Balasubramaniam, and A. E. Yousef, "Inactivation of *Bacillus stearothermophilus* spores in egg patties by pressure-assisted thermal processing," *LWT-Food Science and Technology*, vol. 39, no. 8, pp. 844–851, 2006.

[163] P. Heindl, A. F. Garcia, P. Butz et al., "High pressure/temperature treatments to inactivate highly infectious prion subpopulations," *Innovative Food Science & Emerging Technologies*, vol. 9, no. 3, pp. 290–297, 2008.

[164] H. S. Ramaswamy, Y. Shao, and S. Zhu, "High-pressure destruction kinetics of *Clostridium sporogenes* ATCC 11437 spores in milk at elevated quasiisothermal conditions," *Journal of Food Engineering*, vol. 96, no. 2, pp. 249–257, 2010.

[165] Q. A. Syed, K. Reineke, J. Saldo, M. Buffa, B. Guamis, and D. Knorr, "Effect of compression and decompression rates during high hydrostatic pressure processing on inactivation kinetics of bacterial spores at different temperatures," *Food Control*, vol. 25, no. 1, pp. 361–367, 2012.

[166] H. Daryaei and V. M. Balasubramaniam, "Kinetics of Bacillus coagulans spore inactivation in tomato juice by combined pressure-heat treatment," *Food Control*, vol. 30, no. 1, pp. 168–175, 2013.

[167] P. Dong, E. S. Georget, K. Aganovic, V. Heinz, and A. Mathys, "Ultra high pressure homogenization (UHPH) inactivation of *Bacillus amyloliquefaciens* spores in phosphate buffered saline (PBS) and milk," *Front Microbiol*, vol. 6, pp. 712–811, 2015.

[168] J. García-Parra, F. González-Cebrino, J. Delgado, R. Cava, and R. Ramírez, "High pressure assisted thermal processing of pumpkin purée: effect on microbial counts, color, bioactive compounds and polyphenoloxidase enzyme," *Food and Bioproducts Processing*, vol. 98, pp. 124–132, 2016.

[169] M. B. Ates, D. Skipnes, T. M. Rode, and O. I. Lekang, "Comparison of spore inactivation with novel agitating retort, static retort and combined high pressure-temperature treatments," *Food Control*, vol. 60, pp. 484–492, 2016.

[170] S. Akhtar, D. Paredes-Sabja, J. A. Torres, and M. R. Sarker, "Strategy to inactivate *Clostridium perfringens* spores in meat products," *Food Microbiology*, vol. 26, no. 3, pp. 272–277, 2009.

[171] S. M. Morgan, R. P. Ross, T. Beresford, and C. Hill, "Combination of hydrostatic pressure and lacticin 3147 causes increased killing of Staphylococcus and Listeria," *Journal of Applied Microbiology*, vol. 88, no. 3, pp. 414–420, 2000.

[172] M. Garriga, M. T. Aymerich, S. Costa, J. M. Monfort, and M. Hugas, "Bactericidal synergism through bacteriocins and high pressure in a meat model system during storage," *Food Microbiology*, vol. 19, no. 5, pp. 509–518, 2002.

[173] D. Nakimbugwe, B. Masschalck, M. Atanassova, A. Zewdie-Bosüner, and C. W. Michiels, "Comparison of bactericidal activity of six lysozymes at atmospheric pressure and under high hydrostatic pressure," *International Journal of Food Microbiology*, vol. 108, no. 3, pp. 355–363, 2006.

[174] J. Gomez-Estaca, P. Montero, B. Gimenez, and M. C. Gomez-Guillen, "Effect of functional edible films and high pressure processing on microbial and oxidative spoilage in cold-smoked sardine (*Sardina pilchardus*)," *Food Chemistry*, vol. 105, no. 2, pp. 511–520, 2007.

[175] A. M. Diez, E. M. Santos, I. Jaime, and J. Rovira, "Application of organic acid salts and high-pressure treatments to improve the preservation of blood sausage," *Food Microbiology*, vol. 25, no. 1, pp. 154–161, 2008.

[176] B. Marcos, A. Jofre, T. Aymerich, J. M. Monfort, and M. Garriga, "Combined effect of natural antimicrobials and high pressure processing to prevent *Listeria monocytogenes* growth after a cold chain break during storage of cooked ham," *Food Control*, vol. 19, no. 1, pp. 76–81, 2008.

[177] A. Jofre, T. Aymerich, N. Grebol, and M. Garriga, "Efficiency of high hydrostatic pressure at 600 MPa against food-borne microorganisms by challenge tests on convenience meat products," *LWT-Food Science and Technology*, vol. 42, no. 5, pp. 924–928, 2009.

[178] S. Raouche, M. Mauricio-Iglesias, S. Peyron, V. Guillard, and N. Gontard, "Combined effect of high pressure treatment and anti-microbial bio-sourced materials on microorganisms' growth in model food during storage," *Innovative Food Science & Emerging Technologies*, vol. 12, no. 4, pp. 426–434, 2011.

[179] M. F. Patterson, A. Mackle, and M. Linton, "Effect of high pressure, in combination with antilisterial agents, on the growth of *Listeria monocytogenes* during extended storage of cooked chicken," *Food Microbiology*, vol. 28, no. 8, pp. 1505–1508, 2011.

[180] G. A. Evrendilek and V. M. Balasubramaniam, "Inactivation of *Listeria monocytogenes* and *Listeria innocua* in yogurt drink applying combination of high pressure processing and mint essential oils," *Food Control*, vol. 22, no. 8, pp. 1435–1441, 2011.

[181] A. Hereu, P. Dalgaard, M. Garriga, T. Aymerich, and S. Bover-Cid, "Modeling the high-pressure inactivation kinetics of *Listeria monocytogenes* on RTE cooked meat products," *Innovative Food Science & Emerging Technologies*, vol. 16, pp. 305–315, 2012.

[182] B. Sokołowska, S. Skąpska, M. Fonberg-Broczek et al., "The combined effect of high pressure and nisin or lysozyme on the inactivation of *Alicyclobacillus acidoterrestris* spores in apple juice," *High Pressure Research*, vol. 32, no. 1, pp. 119–127, 2012.

[183] R. Pérez Pulido, J. Toledo del Árbol, M. J. Grande Burgos, and A. Galvez, "Bactericidal effects of high hydrostatic pressure treatment singly or in combination with natural antimicrobials on *Staphylococcus aureus* in rice pudding," *Food Control*, vol. 28, no. 1, pp. 19–24, 2012.

[184] G. Liu, Y. Wang, M. Gui, H. Zheng, R. Dai, and P. Li, "Combined effect of high hydrostatic pressure and enterocin LM-2 on the refrigerated shelf life of ready-to-eat sliced vacuum-packed cooked ham," *Food Control*, vol. 24, no. 1-2, pp. 64–71, 2012.

[185] R. Tabla, B. Martínez, J. Rebollo et al., "Bacteriophage performance against *Staphylococcus aureus* in milk is improved by high hydrostatic pressure treatments," *International Journal of Food Microbiology*, vol. 156, no. 3, pp. 209–213, 2012.

[186] R. Montiel, D. Bravo, M. de Alba, P. Gaya, and M. Medina, "Combined effect of high pressure treatments and the lactoperoxidase system on the inactivation of *Listeria monocytogenes* in cold-smoked salmon," *Innovative Food Science & Emerging Technologies*, vol. 16, pp. 26–32, 2012.

[187] A. Del Olmo, J. Calzada, and M. Nuñez, "Effect of lactoferrin and its derivatives, high hydrostatic pressure, and their combinations, on *Escherichia coli* O157: H7 and *Pseudomonas fluorescens* in chicken filets," *Innovative Food Science & Emerging Technologies*, vol. 13, pp. 51–56, 2012.

[188] E. Fulladosa, X. Sala, P. Gou, M. Garriga, and J. Arnau, "K-lactate and high pressure effects on the safety and quality of restructured hams," *Meat Science*, vol. 91, pp. 56–61, 2012.

[189] K. Stollewerk, A. Jofré, J. Comaposada, J. Arnau, and M. Garriga, "The effect of NaCl-free processing and high pressure on the fate of *Listeria monocytogenes* and *Salmonella* on sliced smoked dry-cured ham," *Meat Science*, vol. 90, no. 2, pp. 472–477, 2012.

[190] M. de Alba, D. Bravo, and M. Medina, "Inactivation of *Escherichia coli* O157: H7 in dry-cured ham by high-pressure treatments combined with biopreservatives," *Food Control*, vol. 31, no. 2, pp. 508–513, 2013.

[191] R. Rubio, S. Bover-Cid, B. Martin, M. Garriga, and T. Aymerich, "Assessment of safe enterococci as bioprotective cultures in low-acid fermented sausages combined with high hydrostatic pressure," *Food Microbiology*, vol. 33, no. 2, pp. 158–165, 2013.

[192] L. Espina, D. Garcıa-Gonzalo, A. Laglaoui, B. M. Mackey, and R. Pagán, "Synergistic combinations of high hydrostatic pressure and essential oils or their constituents and their use in preservation of fruit juices," *International Journal of Food Microbiology*, vol. 161, no. 1, pp. 23–30, 2013.

[193] B. Marcos, T. Aymerich, M. Garriga, and J. Arnau, "Active packaging containing nisin and high pressure processing as postprocessing listericidal treatments for convenience fermented sausages," *Food Control*, vol. 30, no. 1, pp. 325–330, 2013.

[194] F. Donsì, E. Marchese, P. Maresca et al., "Green beans preservation by combination of a modified chitosan based-coating containing nanoemulsion of Mandarin essential oil with high pressure or pulsed light processing," *Postharvest Biology and Technology*, vol. 106, pp. 21–32, 2015.

[195] H. Ahmadi, H. Anany, M. Walkling-Ribeiro, and M. W. Griffiths, "Biocontrol of *Shigella flexneri* in ground beef and *Vibrio cholerae* in seafood with bacteriophage-assisted high hydrostatic pressure (HHP) treatment," *Food and Bioprocess Technology*, vol. 8, no. 5, pp. 1160–1167, 2015.

[196] I. Rodrigues, M. A. Trindade, F. R. Caramit, K. Candŏgan, P. R. Pokhrel, and G. V. Barbosa-Cánovas, "Effect of high pressure processing on physicochemical and microbiological properties of marinated beef with reduced sodium content," *Innovative Food Science & Emerging Technologies*, vol. 38, pp. 328–333, 2016.

[197] H. Li and M. Gänzle, "Effect of hydrostatic pressure and antimicrobials on survival of *Listeria monocytogenes* and enterohaemorrhagic *Escherichia coli* in beef," *Innovative Food Science & Emerging Technologies*, vol. 38, pp. 321–327, 2016.

[198] A. Kumar, R. Sehrawat, T. L. Swer, and A. Upadhyay, "High pressure processing of fruits and vegetables," in *Technological Interventions in Processing of Fruits and Vegetables*, R. Sehrawat, K. A. Khan, M. R. Goyal, and P. K. Paul, Eds., vol. 1, pp. 165–184, CRC press, Boca Raton, FL, USA, 2018.

[199] R. S. Chavan, R. Sehrawat, P. K. Nema et al., "High pressure processing of dairy products," in *Dairy Engineering Advanced Technologies and Their Applications,* Apple Academic Press, Palm Bay, FL, U.S.A, 2017.

[200] C. A. Pinto, S. A. Moreira, L. G. Fidalgo, R. S. Inácio, F. J. Barba, and J. A. Saraiva, "Effects of high-pressure processing on fungi spores: factors affecting spore germination and inactivation and impact on ultrastructure," *Comprehensive Reviews in Food Science and Food Safety*, vol. 19, no. 2, pp. 553–573, 2020.

[201] S. Tewari, R. Sehrawat, P. K. Nema, and B. P. Kaur, "Preservation effect of high-pressure processing on ascorbic acid of fruits and vegetables: a review," *Journal of Food Biochemistry*, vol. 41, no. 1, Article ID e12319, 2016.

WILEY | Hindawi

Research Article

Effect of Fermentation Time on Physiochemical Properties of Kombucha Produced from Different Teas and Fruits: Comparative Study

Siying Li,[1] Yang Zhang,[1] Jingrong Gao,[2] Tong Li,[3] Huizhen Li,[1] Adele Mastroyannis,[4] Shan He [1,5,6] Abdul Rahaman [2] and Kun Chang[6]

[1]*School of Chemistry and Chemical Engineering, Guangzhou University, Guangzhou, China*
[2]*School of Food Science and Engineering, South China University of Technology, Guangzhou, China*
[3]*Labudio Flavor and Distillation Biotech Laboratory, Shandong, Jinan, China*
[4]*Centre for Marine Bioproducts Development, College of Medicine and Public Health, Flinders University, Bedford Park, Australia*
[5]*Institute for NanoScale Science and Technology, College of Science and Engineering, Flinders University, Bedford Park, Australia*
[6]*Peats Soil and Garden Supplies, Whites Valley, SA, Australia*

Correspondence should be addressed to Shan He; he0091@gmail.com and Abdul Rahaman; rahaman_knabdul@ymail.com

This study aimed to investigate the impact of fermentation time on antioxidative activities and phenolic composition and sensory quality of kombucha fermented from different teas (green, black, and oolong) and fruits (grape, dragon, and guava). Results: the highest antioxidative activity was observed in kombucha from green tea and grapefruit fermented for 6-7 days at 25–30°C and 48 h at 37°C, respectively. Further analysis revealed that the antioxidative activity of grape kombucha was significantly improved due to an increase in polyphenols' concentration as compared to original green tea kombucha. Furthermore, the sensory evaluation of grape kombucha suggested that grape-flavoured kombucha is more acceptable by the young-aged group. In conclusion, this study provides a potential and promising method for the first time to produce fruit-flavoured kombucha with increased bioactive compounds in very short fermentation time (48 h) which could fulfil the nutritional requirement for human health.

1. Introduction

Kombucha is a fermented beverage which is prepared under aerobic conditions by fermenting tea with sugar and by applying a symbiotic culture of bacteria and yeast, generally for 10–15 days. It originated from northeast China in about 220 B.C. and spread round the globe through trade routes [1, 2]. After fermentation, kombucha becomes a cocktail of chemical components, including sugars, polyphenols, organic acids, fiber, ethanol, amino acids, essential elements, and water-soluble vitamins [3]. Due to these bioactive compounds and the chemical composition of kombucha, it is considered as a popular functional food for human health. Several in vivo and in vitro studies have been carried out to

establish the existence of antioxidant [4], antimicrobial [5], and anti-inflammatory [6] properties. Recently, kombucha has transitioned from a homemade fermented beverage to a commercialized drink in the market. In 2016, PepsiCo purchased KeVita, a popular functional probiotic and kombucha beverage maker [2].

In the USA alone, the kombucha market is expected to exhibit a strong growth rate of 17.5% between 2019 and 2024. From the year 2017 onwards, retail sales of kombucha have increased by over 30% each year globally. As per the recent report, kombucha is the fastest growing product in the functional beverage market, and in the coming time, it would become one of the most popular low-alcoholic fermented beverages in the world [2]. Despite the claim of

several health benefits of kombucha such as reduced blood pressure, healed peptic ulcer, diabetes, courage weight loss, and detoxification, the microbial contents still need to be investigated. With the growing consumption of kombucha drinks, the risk of safety is also a matter of concern. Several disease-causing microorganisms are found in kombucha drinks because of raw materials, vessels, and during packaging and fermentation methods that may sometime produce toxic metabolites and antinutritional substances such as cyanogenic glycosides, phytates, tannins, and protein inhibitors [7]. Along with these drawbacks, other hurdles in producing kombucha are the long-time fermentation period. As it has been noticed that the kombucha fermentation takes at least 3 to 60 days based on the microbial cultured used in. The fermentation of kombucha is usually performed at room temperature. Therefore, standard production methods are required to produce kombucha drinks [8].

To overcome these problems and development of kombucha with high bioactive compounds with short fermentation period, for the first time, we have tried to develop fruit-flavored kombucha drinks using a unique method and analyzed their quality characteristics. Besides the original flavor, kombucha has been developed with different flavors, which would provide a better fruit-flavored kombucha drink with improved antioxidant properties for human health. However, this approach and their comprehensive strategy has not been used before. This study aimed to develop the kombucha drink with a unique fruit flavor at different fermentation periods and compare the antioxidative activities and phenolic composition of the drink fermented from green, black, and oolong tea, along with grape, dragon, and guava fruits.

2. Materials and Methods

2.1. Materials. Green, black, and oolong tea were purchased from a local supermarket in Guangzhou. The grape, dragon, and guava fruits were also purchased from a local fresh food market in Guangzhou, China. Kombucha start culture (original kombucha mushroom solution) was purchased from Shenzhen Care Pack. Co. Ltd. (Shenzhen, China).

2.2. Preparation of Original Kombucha. Original kombucha was prepared using green, oolong, and black tea. In brief, 100 g of sucrose was dissolved in 800 mL of distilled water by maintaining the temperature at 98°C for 15 min. Then, 4 g of the tea leaves were soaked in the prepared sugar solution and heated at 98°C for 12 min. Furthermore, the tea leaves were filtered out after soaking, and the solutions were cooled down to 25°C. Furthermore, the solution was inoculated with 600 ml of kombucha start culture, and fermentation was carried out for 15 days at 25, 30, and 35°C temperatures, respectively. Samples were collected and analyzed on a daily basis during fermentation.

2.3. Preparation of Fruit Kombucha. Grape, dragon, and guava fruits were selected to produce fruit kombucha drinks due to their availability in the market and frequent

consumption by the consumers in China. In brief, the fruit was smashed, blended, and stored into a 500 mL bottle of original kombucha produced under the identified optimized processing conditions. The ratio of smashed fruit to original kombucha was 6 g to 100 mL. Bottles with original kombucha and smashed fruits were sealed with caps. The sealed bottles were placed into a water bath at a temperature of 37°C and fermented for 72 h. Samples were collected and analyzed at 0, 24, 48, and 72 h during fermentation. The formulated grape kombucha beverage was prepared with a formulation of 40% (w/w) grape kombucha, 55% (w/w) sparkling water, and 5% (w/w) sugar, without fermentation, and considered as a control sample.

2.4. Measurement of the Total Polyphenol Content. The total phenolic content (TPC) of kombucha drink was determined using the method of Ahmed and Hikal [9] with slight modifications. In brief, 250 μL of kombucha was mixed with 125 μL of 0.2 mol/L Folin–Ciocalteu phenol reagent and then incubated in the dark at room temperature for 5 min on a shaking table. Furthermore, after 5 min of incubation, 250 μL of 5% (w/v) sodium carbonate was added, which was prepared in deionized water. The mixture was gently shaken in the dark at room temperature for 60 min. Furthermore, the phenolic content was recorded at the absorbance of 725 nm using a spectrophotometer (Ultraviolet visible spectrophotometer; UV-2100; Beijing Ruili Analytical Instrument Co. Ltd.). The TPC was determined in micrograms of gallic acid equivalents (GAE) per gram of barley flour (μg GAE/g).

2.5. Measurements of the Total Flavonoid Content. The total flavonoid content of kombucha was determined according to Jakubczyk et al. [10] with slight modifications. In brief, 4 mL of distilled water was mixed with 1 mL of kombucha in test tubes. Additionally, 0.3 mL of 5% sodium nitrite solution was added to 0.3 mL of 10% aluminum chloride solution followed by incubation at room temperature for 5 minutes and further addition of 2 mL (1 M sodiumhydroxide). This stock solution was diluted with 10 mL of water. The solution turned into pink color, was mixed with vortex, and transferred into the glass cuvette, and the absorbance was recorded at 510 nm using a spectrophotometer. Aqueous solutions of catechin concentrations in the range of 50–100 mg/L were used for calibration, and the results were shown as milligrams of catechin equivalents (CEQ) per gram of the sample.

2.6. Measurement of Antioxidative Activity. The methods determining ferric-reducing antioxidant power (FRAP) and 2,2′-azino-bis(3-ethylbenzothiazoline-6-sulfonic acid (ABTS) radical scavenging ability were applied to measure the antioxidative activity of kombucha samples.

2.6.1. FRAP Assay. The FRAP assay was analyzed according to Sethi et al. [11] with slight modifications. The FRAP reagent contained 10 mM of TPTZ in 40 Mm of hydrochloric acid/20 mM ferric chloride/acetate buffer (0.3 M, pH

3.6), mixed in a ratio of 1 : 1:10 (v/v). Test tubes containing 1 mL of each sample in 5 ml of FRAP reagent were incubated at 37°C for 20 min, and the absorbance was recorded at a wavelength of 593 nm with a spectrophotometer. The results were calculated using standard solutions of ferrous sulphate at different concentrations (100–1400 μM) as FRAP values (μM Fe^{2+}). The standard curve equation was $y = 2.01x + 0.081$ ($R^2 = 0.999$).

2.6.2. ABTS Radical Scavenging Ability Assay. The ABTS radical scavenging ability of kombucha was examined according to Jayabalan and Subathradevi [12] with slight modifications. In brief, ABTS solution (7 mM aqueous solution of ABTS with 2.45 mM aqueous solution of $K_2S_2O_8$) was made in the dark and left for incubation at room temperature for 16 h. Furthermore, ABTS solution was diluted with ethanol to an absorbance of 0.70 (±0.02) at 734 nm and equilibrated at 30°C. Furthermore, 0.3 ml of each kombucha sample was added with 1.2 ml of ABTS solution and left for 6 min incubation, and then the absorbance was recorded at 734 nm using a spectrophotometer. The capability of scavenging ABTS was calculated using the following equation:

$$\text{ABTS radical scavenging ability} \, (\%) = \left[\frac{A_{\text{control}} - B_{\text{sample}}}{A_{\text{control}}} \right] \times 100\%. \quad (1)$$

Here, A is the absorbance of the blank sample, and B is the absorbance of the kombucha samples.

2.7. Phenolic Analysis by High-Performance Liquid Chromatography (HPLC). Quantification of individual polyphenolic compositions was carried out by reverse-phase HPLC analysis using the method described by Garzoli et al. [13] with slight modifications. In brief, kombucha samples were injected into a Waters HPLC system. It was composed of a 1525 binary pump, a thermostat, and a 717+ autosampler linked to the Waters 2996 diode array and an EMD 1000 single quadrupole detector with an ESI probe (Waters, Milford, MA, USA). Polyphenols were separated using a Symmetry C-18 RP column (125 mm × 4 mm i.d., 5 μm particle size). The mobile phase was prepared from 0.1% formic acid (eluent A) and acetonitrile (eluent B) at a flow rate of 1.2 mL/min. The gradient profile was as follows: 0–20 min, linear gradient from 10 to 25% B; 20–40 min, linear gradient up to 45% B. Then, the gradient returned to 15% B followed by an additional 5 min of equilibration time. An optimal mobile phase inflow was obtained by a post-column flow splitter (ASI, Richmond, CA, USA) with a 5/1 split ratio for the ESI probe. Chromatograms were constructed by employing a 3D mode equipped with extracted signals at specific wavelengths for different compounds (367, 326, 309, and 204 nm). To compare the literature, data, retention times, were used to qualitatively measure the compounds detected in the samples. The pure standard method and compounds were used as references for the concentration and retention time for quantitative analysis [14]. The peaks from the data acquisition and spectral evaluation were identified using the Waters Empower2 Software (Waters, Milford, USA).

2.8. Food Safety Tests. Standard United States Environmental Protection Agency (USEPA) methods 6010B and 6020 (USEPA 1996) were used to examine the trace element content by inductively coupled plasma mass spectrometry and inductively coupled atomic emission spectrometry. Australian Standard/New Zealand Standard 1766: Food Microbiology (Standards of Australia and Standards, New Zealand 1998) was applied for microbiological testing.

2.9. Sensory Tests. Sensory tests were conducted according to Qinzhu et al. [15] with slight modifications. In brief, forty volunteers in 2 different age groups (<30 years old and >30 years old) were recruited. The sensory evaluation was performed in private booths equipped with Sensory Management System hardware (2006) and computerized sensory software (Sensory Integrated Management System, Morristown, N.J., U.S.A.). The volunteers received 1 h training on discrimination testing. The sensory evaluation involved rating the color, taste, and aroma. Each characteristic was rated from 0 (extreme dislike) to 1 (extreme like).

2.10. Statistical Analysis. All parameters of each sample were measured in triplicate. The least significant difference (LSD) and one-way variance analysis (ANOVA) was performed on the data using the means and standard deviations, and the statistical significance of the F value ($P < 0.05$) was determined. These analyses were performed using v15 MINITAB statistical software.

3. Results and Discussion

3.1. Process Optimization of Fruit Kombucha Production. The grape, dragon, and guava fruits were used to develop the fruit kombucha. These three fruits are very commonly consumed by consumers throughout China. The original green tea kombucha was produced under optimal conditions and served as the control shown in Figures 1 and 2. It was found that the antioxidative activity of the control showed a slight decline after fermentation for 7 days. However, further fermentation by blending smashed fruits with original green tea kombucha (used as the start culture) for fruit flavour extraction showed significantly increased antioxidative activity in comparison with control. The highest level (4.5 mM Fe^{2+} to 7.5 mM Fe^{2+}) of antioxidant activity was observed in grape kombucha measured by the FRAB method as shown in Figure 1. The same trend of antioxidant capacity was observed by the ABTS radical scavenging method as shown in Figure 2. All three types of fruit kombucha demonstrated a substantial increase in antioxidative activity during fermentation in comparison with the control. The highest level of antioxidant capacity was observed in grape kombucha fermented for 48 h. Therefore, the optimum fermentation processing condition for grape kombucha was identified as 48 h at 37°C. Grape kombucha was produced for further development of a formulated grape kombucha beverage (see Figure 3).

The highest level of antioxidative activity of kombucha was demonstrated in green tea kombucha fermented at 25

(a)

(b)

(c)
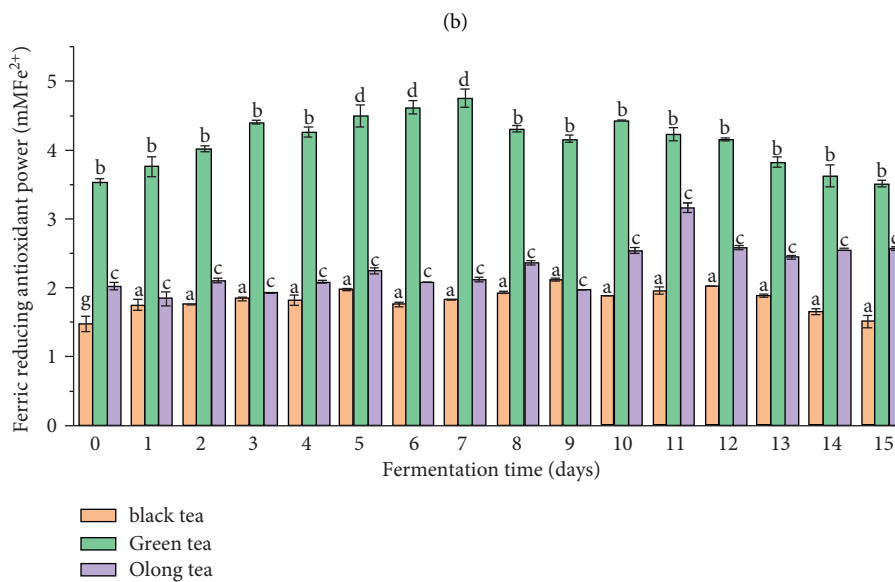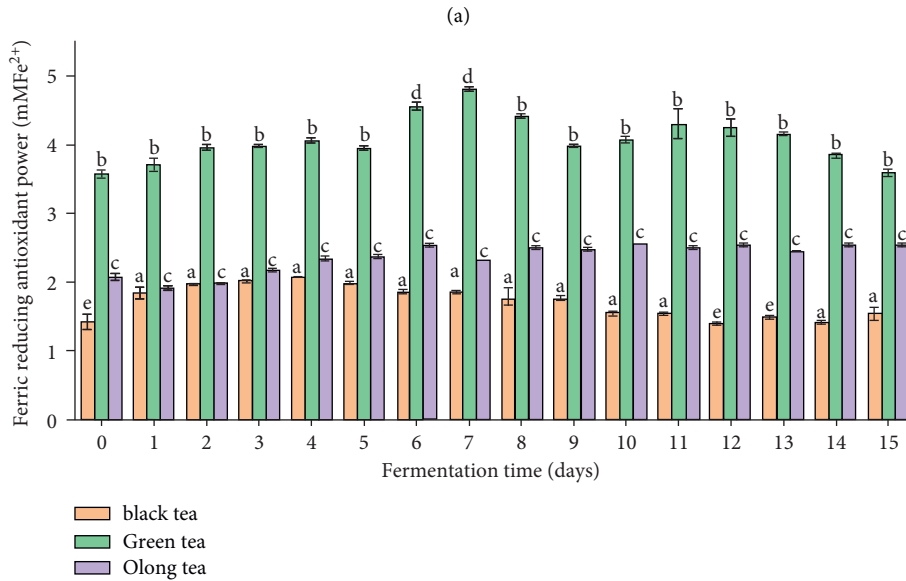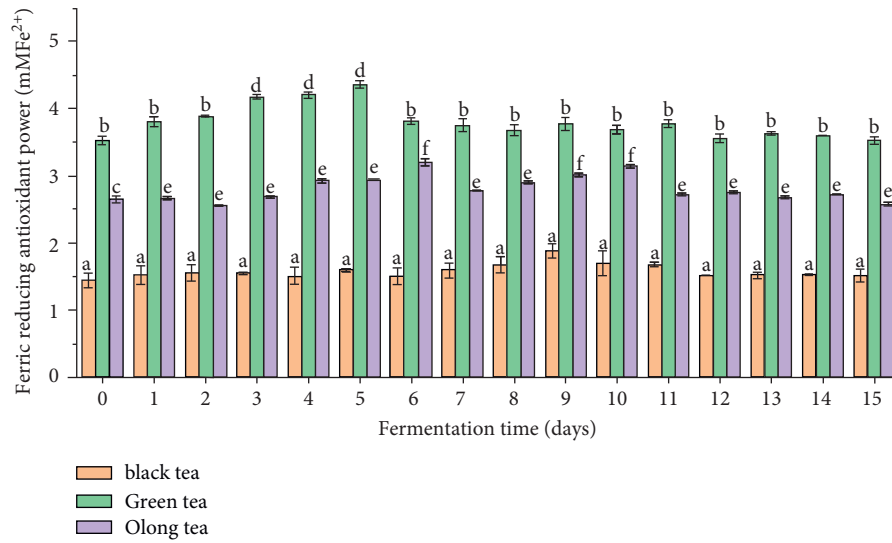
Figure 1: Changes in antioxidative activity of kombucha fermented from three different teas at different temperatures ((a) 35°C; (b) 30°C; (c) 25°C) measured by ferric reducing antioxidant power. Different letters in the same graph indicate significant difference ($P < 0.05$).
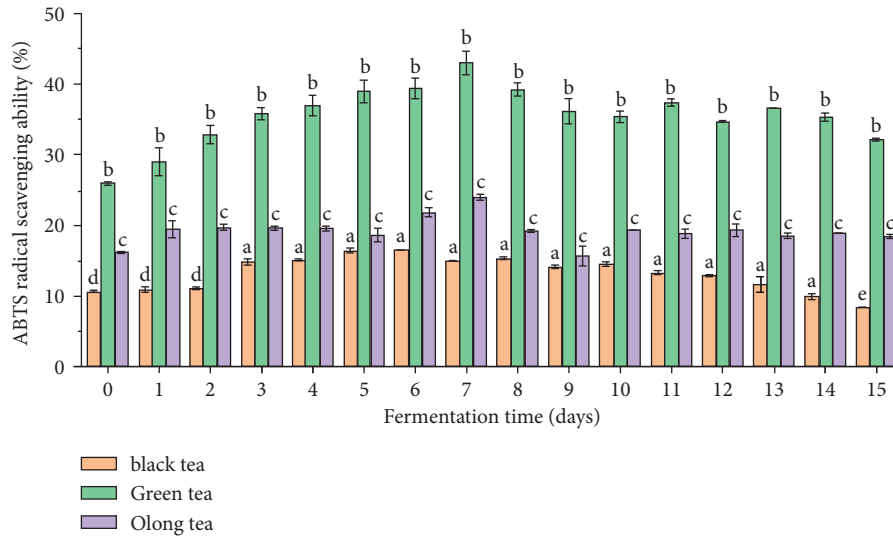
(a)
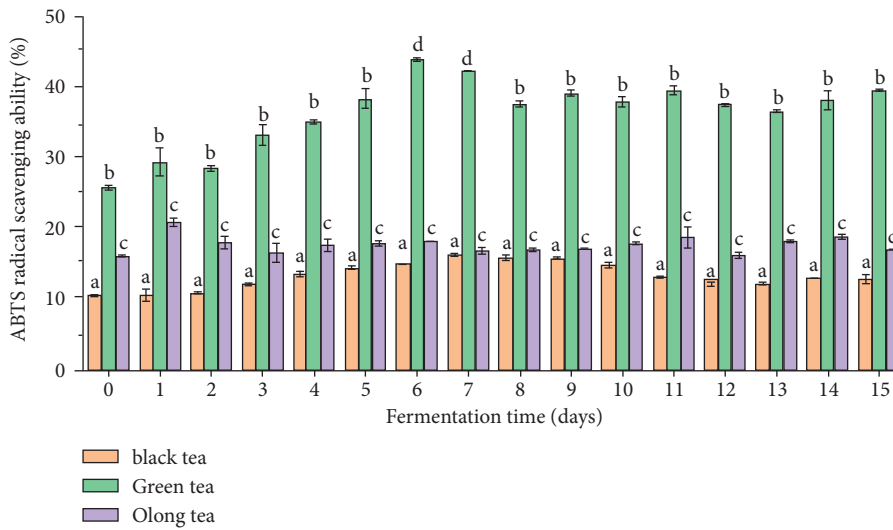
(b)
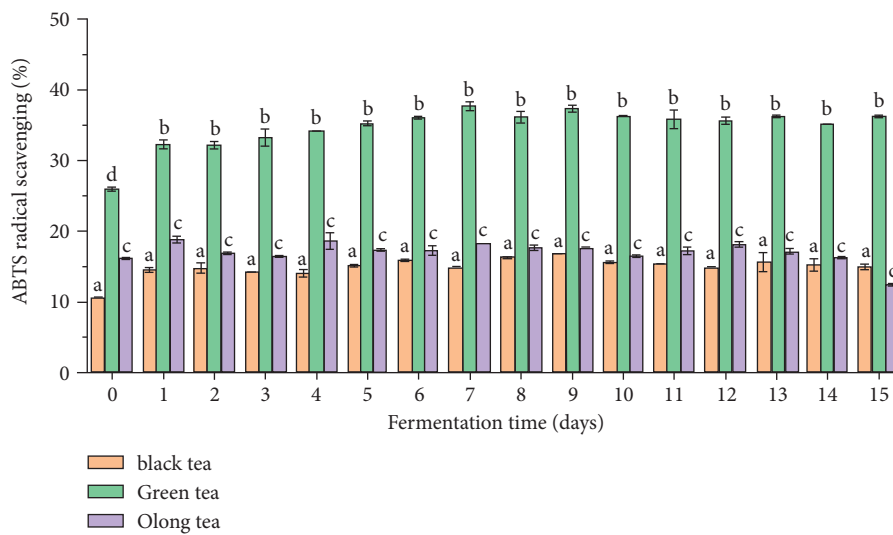
(c)

FIGURE 2: Changes in antioxidative activity of kombuchas fermented from three different teas at different temperatures ((a) 35°C; (b) 30°C; (c) 25°C) measured by ABTS radical scavenging ability. Different letters in the same graph indicate significant difference ($P < 0.05$).

(a)

(b)
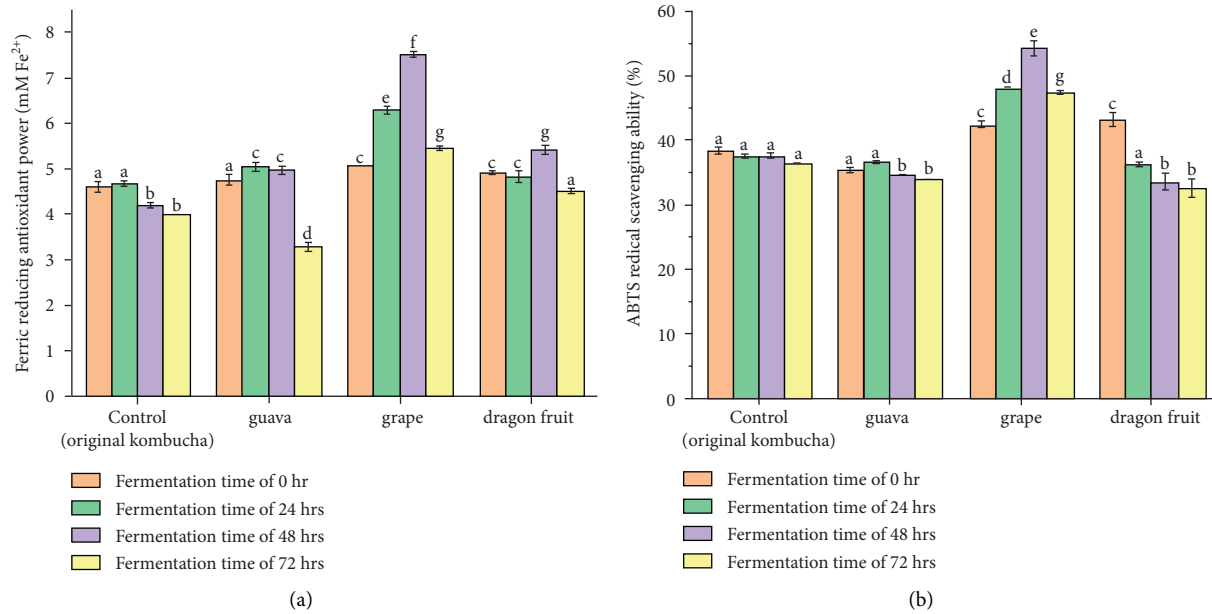
FIGURE 3: Antioxidative activity of original green tea kombucha and three fruit kombuchas fermented for different durations measured by ferric reducing antioxidant power (a) and ABTS radical scavenging ability (b). Different letters in the same graph indicate significant difference ($P < 0.05$).

and 30°C for 7 days (4.6 mM Fe^{2+}) (Figure 1) and 45% after fermentation at 30°C for 6 days (Figure 2). Previous studies also reported that the optimum temperatures for original kombucha fermentation are 25 and 30°C [16]. A recent study suggested that kombucha fermentation was 28°C [17]. Furthermore, an investigation proved that the optimum temperature for fermentation of black tea kombucha was 28 ± 2°C. It can be seen in Figures 1 and 2, initially, that the antioxidative activity of green tea kombucha sharply increased up to 7 days of fermentation. However, after 7 days, the antioxidative activity of green tea kombucha either declined (Figure 1) or stagnated (Figure 2). The same trend has also been reported by Jakubczyk [10]; the author stated that the antioxidative activity of green tea and white tea kombucha during fermentation was highest at 7 days. Therefore, the optimal fermentation temperature and time were 25/30°C and 6 to 7 days, respectively. The green tea kombucha was made under this optimal condition and used as a starter culture to produce fruit-flavoured kombuchas.

3.2. Total Polyphenol Content and Flavonoid Content.

The total polyphenol content in the original kombucha and grape kombucha processed under optimized conditions is shown in Figure 4. Green tea without fermentation (the green tea sample with a fermentation time of 0 days in Figures 1 and 2) served as the control sample as shown in Figure 4. The active antioxidants in plant-based products are exhibited mainly due to polyphenols. The mechanisms involved in the antioxidant activity of polyphenols include the suppression of reactive oxygen species (ROS) formation by either inhibition of enzymes involved in their production or upregulation of antioxidant defenses [18]. The content of polyphenols and the antioxidant properties were determined in fermented
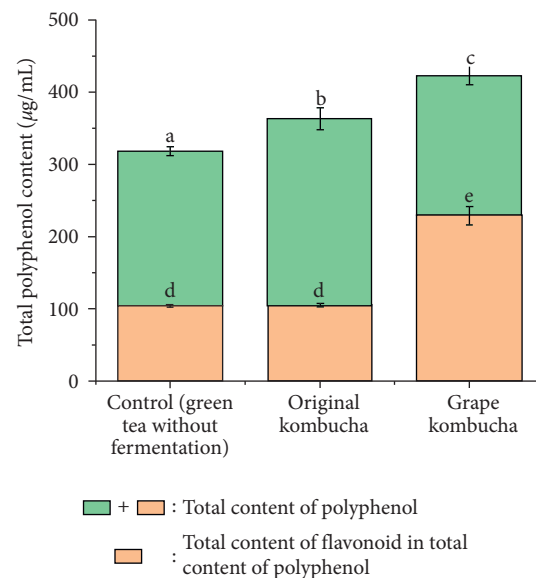
FIGURE 4: Total polyphenol and flavonoid in green tea without fermentation (control), original green tea kombucha, and grape kombucha. Different letters indicate significant difference ($P < 0.05$).

soybean and tempeh. The highest concentration (5.307 mg/g) of polyphenols was observed in soybean fermented for 4 days, and the strength of antioxidant activity was also the highest and exhibited 12 times higher than in unfermented material after fermentation for 4 days [19].

The same correlation has also been reported in fermented cornelian cherry beer, Joanna et al. [10] and *Asparagus* cochin chinensis root [20]. Wu et al. [18] compared polyphenol-rich cranberry fruit extract and non-

polyphenol-rich cranberry fruit extracts and revealed that the former offered an efficacious and safe means to prevent colonic tumorigenesis in humans due to its greater antioxidative activity attributed to polyphenols. Hence, green tea was identified as the optimal type of tea for original kombucha production.

Our findings also suggested that increasing polyphenolic contents lead to an increase in the antioxidative activity of kombucha drinks, as shown in Figures 1, 2, and 4. The polyphenol concentration increases from 318.21 to 362.89 μm/mL in green tea before and after fermentation (kombucha). A similar result was reported by Hassoun et al. [21]; the author stated that the antioxidants found in green tea powder exhibited higher antioxidant activity followed by rosemary and mate at a given concentration due to the higher content of polyphenols in the green tea. Green tea contained approximately 30% of polyphenols on the dry weight basis. However, the oolong and black tea both contain only 5% of polyphenols on a dry weight basis [21]. This number was further elevated to 428.68 μm/mL in grape kombucha. Among the different categories of polyphenols, flavonoids have been reported as an undisputedly superb antioxidant effect. It exhibits anti-inflammatory properties and supports the immune system [22]. It can be seen from Figure 4 that the increasing polyphenols from original kombucha to grape kombucha is due to the increase in flavonoids.

3.3. Polyphenolic Compositions of Green Tea, Original Kombucha, and Grape Kombucha. The polyphenolic compositions of green tea without fermentation (control), original kombucha, and grape kombucha are shown in Table 1. Major differences in the polyphenolic profiles of the original kombucha are the reductions in epicatechin gallate and epigallocatechin gallate and increasing epicatechin and epipagglcatechin compared to control. It has been reported that the biotransformation of epicatechin gallate and epigallocatechin gallate to epicatechin and epipagglcatechin by enzymes excreted by start culture during fermentation is the reason for the increasing content of epicatechin and epipagglcatechin in original kombucha [10]. There are some flavonoid compounds which exist in grape kombucha, such as quercetin, narigenin, and hespertin. This explains the increased contents of flavonoids and polyphenols in grape kombucha as shown in Figure 4. It has been reported that quercetin, narigenin, and hespertin uniquely exist in grapefruit [23]. Many studies have proven that most of the flavonoid compounds that exist in plants are combined with protein, fat, and insoluble fibers. Fermentation induces structural changes in the plant cells which causes a reaction between enzymes secreted from microorganisms in the start culture and the complex combined with flavonoids and other materials. This reaction facilitates the release of flavonoids from the plant to the fermented grape kombucha.

3.4. Analysis of the Formulated Grape Kombucha Beverage. Among all tea and fruits, the grape kombucha was selected to produce at industrial scale for the consumers' after optimizing the processing conditions and due to the best physiochemical properties shown after analysis and short fermentation period. The sparkling water was applied in the final grape kombucha beverage to achieve a similar mouth feel of kombucha beverages available in the market. The final formulation was fixed as 40% (w/w) grape kombucha blended with 55% (w/w) sparkling water and 5% (w/w) sugar. The antioxidative activity of the grape kombucha formulated in this study was compared with grape kombucha flavor that currently exists in the market (Table 2). Regardless of the measurement methods, the former showed superior antioxidative activity. This finding concludes that the grape kombucha formulated in this study would provide more benefits to human health.

3.5. Food Safety Tests for the Formulated Grape Kombucha Beverage. Trace element content and microbiology testing were carried out for the formulated grape's kombucha beverage prior to the sensory test. Table 3 presents the acceptable standards for the trace element of the formulated grape kombucha beverage according to Australia/New Zealand Food Standard 1.4.1. Human body needs to obtain a sufficient number of essential elements, such as sodium and calcium to maintain adequate physiological functions. However, humans might be exposed to health risks from harmful nonessential elements by drinking water and consuming fresh and processed foods [24]. For instance, skin cancer and organ cancers can be initiated by excess arsenic intake. In addition, excess cadmium intake can affect renal tubule function, and reabsorption of proteins, sugars, and amino acids leads to irreversible impairment. Having an excessive amount of trace elements in food may lead to serious health damage; however, as shown in Table 3, all trace element contents in the formulated grape kombucha beverage were lower than the standard levels.

The microbial analysis of grape kombucha is shown in Table 4. These can be compared with the reference standards obtained from Australia/New Zealand Food Standard 1.3.4 in Table 4 as well. The comparative reference standards for total viable counts are indicated in the guidelines for the microbiological examination of ready-to-eat foods for *Escherichia coli, Salmonella, Enterobacteriacea,* yeast, and molds. It was found that the overall formulated grape kombucha beverage is fit for consumption by considering all food safety standards. Food safety is the paramount component of any food product. Therefore, it is necessary to carry out food safety tests for the formulated grape kombucha beverage prior to its sensory evaluation.

3.6. Sensory Evaluation of the Formulated Grape Kombucha Beverage. The sensory evaluation of grapes kombucha was performed by choosing two groups of panels. The sensory evaluation by these two groups revealed that the acceptance of the formulated grape kombucha beverage was susceptible for the young age group (<30) as the average score can be seen in Figure 5. There was a significant difference regarding the acceptance of the formulated grape kombucha beverage between different age groups. Although, the acceptance of the color was similar between the two age groups. However, the

TABLE 1: The concentration of monomeric phenolic compounds determined in green tea without fermentation (control), original green tea kombucha, and grape kombucha.

Phenolic compounds	Concentration (μg/mL)*		
	Green tea without fermentation (control)	Original green tea kombucha	Grape kombucha
Acid compounds			
Gallic acid	$34.12^a \pm 0.02$	$48.13^b \pm 0.01$	$44.33^c \pm 0.01$
Isoferulic acid	$5.96^a \pm 0.01$	$5.24^b \pm 0.01$	$6.83^c \pm 0.01$
p-coumaric acid	$5.36^a \pm 0.03$	$9.63^b \pm 0.02$	$11.69^c \pm 0.02$
Caffeine	$86.63^a \pm 1.23$	$92.32^b \pm 0.23$	$82.33^c \pm 0.01$
Flavonoid compounds			
Epicatechin gallate	$28.08^a \pm 0.03$	$17.50^b \pm 0.03$	$20.80^c \pm 0.01$
Gallocatechin gallate	$5.23^a \pm 0.02$	$6.58^b \pm 0.02$	$4.50^c \pm 0.01$
Epigallocatechin gallate	$51.19^a \pm 0.36$	$40.39^b \pm 0.23$	$38.71^c \pm 0.52$
Catehin gallate	$6.96^a \pm 0.01$	$4.41^b \pm 0.01$	$6.17^c \pm 0.01$
Gallocatechin	$6.23^a \pm 0.02$	$4.86^b \pm 0.02$	3.88 ± 0.02
Epigallocatechin	$4.96^a \pm 0.03$	$13.61^b \pm 0.04$	$15.97^c \pm 0.02$
Catechin	$3.01^a \pm 0.01$	$5.07^b \pm 0.01$	$3.66^c \pm 0.01$
Epicatechin	$2.56^a \pm 0.01$	$9.61^b \pm 0.01$	$7.56^c \pm 0.01$
Rutin	$1.98^a \pm 0.02$	$2.68^b \pm 0.02$	$4.88^c \pm 0.02$
Quercetin	Nd	Nd	$2.34^c \pm 0.01$
Naringenin	Nd	Nd	$26.92^c \pm 0.23$
Hesperetin	Nd	Nd	$3.03^c \pm 0.02$

nd: not detected; *: mean ± standard deviation ($n = 3$); different letters in each row indicate significant difference ($P < 0.05$) according to one-way ANOVA and LSD test.

TABLE 2: Comparison of antioxidative activity between grape kombucha in this study and kombucha with grape flavor in market.

	Antioxidative activity*	
	FRAP (mM Fe^{2+})	ABTS radical scavenging ability (%)
Grape kombucha in this study	$1.53^a \pm 0.24$	$23.68^d \pm 2.25$
Kombucha with grapeflavor in market	$0.52^b \pm 0.31$	$12.54^c \pm 2.51$

*: mean ± standard deviation ($n = 3$); different letters in each column indicate significant difference ($P < 0.05$), according to one-way ANOVA and LSD test.

TABLE 3: Trace elements determined in grape kombucha.

Trace elements	Content (mg/L)	
	Sample	Reference (Australia New Zealand Food Standard 1.4.1)
Arsenic	0.58	2
Cadmium	<0.01	0.05
Lead	0.004	0.5
Mercury	0.033	0.5
Tin	0.24	250

TABLE 4: Microbiological test (cfu/ml) of grape kombucha.

Microbes	Cell counts	
	Sample	Reference (Australia New Zealand Food Standard 1.3.4)
Total viable count (g)	230	$<10^4$
E. coli (mL)	Not detected	<3
Salmonella (25 mL)	Not detected	Not detected
Enterobacteriacea (g)	<10	$<10^2$
Yeast (g)	<10	<10
Mould (g)	<10	<10
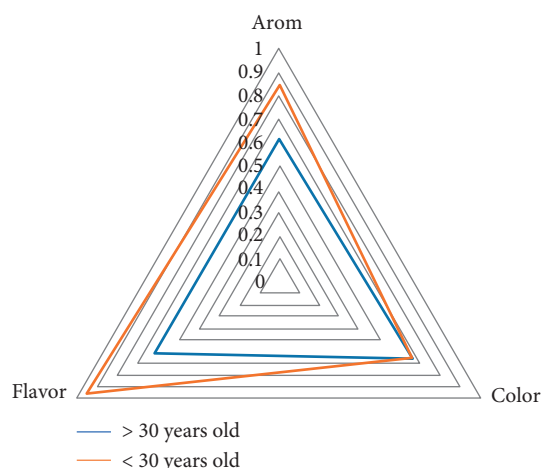
Figure 5: Sensory evaluation of grape kombucha by two age groups of participants.

higher acceptance of grape kombucha was noticed among young age group volunteers (<30 years) based on aroma and flavor. It was reported that kombucha is more favorable for the younger generation. This sensory evaluation further confirmed that the market promotion of the formulated grape kombucha beverage developed in this study should be focused on new generations, such as millennials.

4. Conclusion

A comprehensive analysis of antioxidative activities and phenolic composition and sensory analysis in kombucha beverages fermented from different teas and fruits have been carried out in this study. The processing conditions to produce tea and fruit kombucha are optimized. It was found that the best processing and fermentation conditions for the production of green tea kombucha would be at 25–30°C for 6-7 days. Furthermore, the investigation stated that the fermentation at 37°C for 48 h would be the more reliable processing condition for the development of grape kombucha with better physiochemical properties such high antioxidant, phenolic compounds, and texture which may help to fulfil the nutritional requirement for the consumers. The antioxidative activity of grape kombucha was significantly improved in comparison with the original green kombucha due to the increase in the polyphenol contents. After the comparative physiochemical analysis of kombucha from green, black, and oolong tea along with dragon and guava fruit, the formulated grape kombucha beverage was selected for industrial scale production. The sensory test of the formulated grape kombucha suggested that people at the age of <30 would be the most preferable consumers in the market. This study has found a novel channel to produce value-added grapes' kombucha drinks in a short fermentation period for consumers with improved nutritional quality at an industrial scale.

Data Availability

The data used to support the findings of this study are available from the corresponding author upon request.

Conflicts of Interest

The authors declare that there are no conflicts of interest.

Authors' Contributions

All the authors have read and approved the final manuscript. Siying Li and Yang Zhang contributed equally to this work.

Acknowledgments

References

[1] R. M. D. Coelho, A. L. d. Almeida, R. Q. G. d. Amaral, R. N. d. Mota, and P. H. M. d. Sousa, "Kombucha: review," *International Journal of Gastronomy and Food Science*, vol. 22, Article ID 100272, 2020.

[2] J. Kim and K. Adhikari, "Current trends in kombucha: marketing perspectives and the need for improved sensory Research," *Beverages*, vol. 6, no. 1, p. 15, 2020.

[3] J. M. Kapp and W. Sumner, "Kombucha: a systematic review of the empirical evidence of human health benefit," *Annals of Epidemiology*, vol. 30, pp. 66–70, 2019.

[4] H. Amarasinghe, N. S. Weerakkody, and V. Y. Waisundara, "Evaluation of physicochemical properties and antioxidant activities of kombucha "Tea Fungus" during extended periods of fermentation," *Food Sciences and Nutrition*, vol. 6, no. 3, pp. 659–665, 2018.

[5] H. Shahbazi, H. Hashemi Gahruie, M.-T. Golmakani, M. H. Eskandari, and M. Movahedi, "Effect of medicinal plant type and concentration on physicochemical, antioxidant, antimicrobial, and sensorial properties of kombucha," *Food Sciences and Nutrition*, vol. 6, no. 8, pp. 2568–2577, 2018.

[6] B. S. Sivamaruthi, P. Kesika, M. I. Prasanth, and C. Chaiyasut, "A mini review on antidiabetic properties of fermented foods," *Nutrients*, vol. 10, no. 12, p. 1973, 2018.

[7] S. M. Mousavi, S. A. Hashemi, M. Zarei et al., "Recent progress in chemical composition, production, and pharmaceutical effects of kombucha beverage: a complementary and alternative medicine," *Evidence-Based Complementary and Alternative Medicine*, vol. 18, 2020.

[8] J. Martínez Leal, L. Valenzuela Suarez, R. Jayabalan, J. Huerta Oros, and A. Escalante-Aburto, "A review on health benefits of kombucha nutritional compounds and metabolites," *CyTA—Journal of Food*, vol. 16, no. 1, pp. 390–399, 2018.

[9] R. F. Ahmed, M. S. Hikal, and K. A. Abou-Taleb, "Biological, chemical and antioxidant activities of different types Kombucha," *Annals of Agricultural Science*, vol. 65, no. 1, pp. 35–41, 2020.

[10] K. Jakubczyk, J. Kaldunska, J. Kochman, and K Janda, "Chemical profile and antioxidant activity of the kombucha beverage derived from white, green, black and red tea," *Antioxidants*, vol. 9, no. 5, p. 447, 2020.

[11] S. Sethi, A. Joshi, B. Arora, A. Bhowmik, R. R. Sharma, and P. Kumar, "Significance of FRAP, DPPH, and CUPRAC assays for antioxidant activity determination in apple fruit extracts," *European Food Research and Technology*, vol. 246, pp. 591–598, 2020.

[12] R. Jayabalan, P. Subathradevi, S. Marimuthu, M. Sathishkumar, and K. Swaminathan, "Changes in free-radical scavenging ability of kombucha tea during fermentation," *Food Chemistry*, vol. 109, no. 1, pp. 227–234, 2008.

[13] S. Garzoli, F. Cairone, S. Carradori et al., "Effects of processing on polyphenolic and volatile composition and fruit quality of clery strawberries," *Antioxidants*, vol. 9, no. 7, p. 632, 2020.

[14] D. Keser, G. Guclu, H. Kelebek et al., "Characterization of aroma and phenolic composition of carrot daucus carota 'nantes' powders obtained from intermittent microwave drying using GC–MS and LC–MS/MS," *Food and Bioproducts Processing*, vol. 119, pp. 350–359, 2020.

[15] Z. Qinzhu, C. Yan-ling, S. Dong-xiao, B. Tian, Y. Yang, and H. Shan, "Process optimization and anti-oxidative activity of peanut meal Maillard reaction products," *Lwt-Food Science and Technology*, vol. 97, pp. 573–580, 2018.

[16] C. Tu, S. Tang, F. Azi, W. Hu, and M. Dong, "Use of kombucha consortium to transform soy whey into a novel functional beverage," *Journal of Functional Foods*, vol. 52, pp. 81–89, 2019.

[17] D. Bhattacharya, S. Bhattacharya, M. M. Patra et al., "Antibacterial activity of polyphenolic fraction of kombucha against enteric bacterial pathogens," *Current Microbiology*, vol. 73, no. 6, pp. 885–896, 2016.

[18] X. Wu, L. Xue, A. Tata, M. Song, C. C. Neto, and H. Xiao, "Bioactive components of polyphenol-rich and non-polyphenol-rich cranberry fruit extracts and their chemopreventive effects on colitis-associated colon cancer," *Journal of Agricultural and Food Chemistry*, vol. 68, no. 25, pp. 6845–6853, 2020.

[19] M. Kuligowski, K. Pawłowska, I. Jasińska-Kuligowska, and J. Nowak, "Isoflavone composition, polyphenols content and antioxidative activity of soybean seeds during tempeh fermentation," *CyTA—Journal of Food*, vol. 15, no. 1, pp. 27–33, 2017.

[20] K. Y. Koo, W. B. Kim, S. H. Park et al., "Antioxidative properties of *Asparagus cochinchinensis* root," *Journal of the Korean Society of Food Science and Nutrition*, vol. 45, no. 4, pp. 524–532, 2016.

[21] A. Hassoun, M. Carpena, M. A. Prieto et al., "Use of spectroscopic techniques to monitor changes in food quality during application of natural preservatives: a review," *Antioxidants*, vol. 9, no. 9, p. 882, 2020.

[22] M. Rondanelli, M. A. Faliva, A. Miccono et al., "Food pyramid for subjects with chronic pain: foods and dietary constituents as anti-inflammatory and antioxidant agents," *Nutrition Research Reviews*, vol. 31, no. 1, pp. 131–151, 2018.

[23] N. Terahara, "Flavonoids in foods: a review," *Natural Product Communications*, vol. 10, no. 3, pp. 521–528, 2015.

[24] B. Pilarczyk, A. Tomza-Marciniak, R. Pilarczyk, J. Udala, B. Kruzhel, and M. Ligocki, "Content of essential and non-essential elements in wild animals from western Ukraine and the health risks associated with meat and liver consumption," *Chemosphere*, vol. 244, Article ID 125506, 2020.

WILEY | Hindawi

Research Article

A Rapid Integration Method of Wild Ornamental Plant Resources Based on Improved Clustering Algorithm

Linlin Cong [ID][1,2] **and Dong Han** [ID][1,2]

[1]*College of Tourism & Landscape Architecture, Guilin University of Technology, Guilin 541004, China*
[2]*Graduate School of Technical Design Staff, Kookmin University, Seoul 02707, Republic of Korea*

Correspondence should be addressed to Dong Han; 2019021@glut.edu.cn

Wild ornamental plants are beneficial as well as dangerous for the environment. Because the introduction of attractive plants that are not suited to the local ecosystem can result in significant environmental damage, a quick integration strategy based on an enhanced clustering algorithm is proposed for wild ornamental plant resources. The technique is enhanced with density stratification by integrating the k-means distance measurement formula and establishing the objective function of clustering optimization. The cluster termination condition is controlled by the number of clusters k, and the wild plant data categories are continually merged. Uneven density distribution is used to deal with the wild plant distribution dataset. To obtain the distribution of wild ornamental plants in different regions, to estimate the optimal parameters of wild plant samples, to combine with maximum likelihood classification to obtain the plant flora differentiation degree, and to complete the resource integration, remote sensing images were used. Comprehensive survey and systematic sampling were used to conduct a complete survey of the protected area. The heat map of the plant size distribution shows that there is a clear negative correlation between the spatial scale difference and the overall density difference of the plant distribution, that is, it appears spatially. From the experimental analysis, it is observed that the high-density small-scale and low-density large-scale agglomeration distribution characteristics delay is 1.96 s.

1. Introduction

Wild plant resources have been in a natural and self-growth state for a long time. Many species have distinct flower kinds and blossoming times, as well as high stress tolerance (drought resistance, cold resistance, disease and insect resistance, salt and alkali resistance, heat resistance, and so on) and environmental adaptation. It is a natural gene bank that contains extraordinarily rich genetic information, as well as mankind's valuable assets and the foundation of modern garden plants [1]. The protective development and utilization of wild plant resources can not only increase the beauty of urban greening and beautification but also increase the urban biodiversity index and reduce the serious losses caused by the introduction of ornamental plants that are not suitable for the local environment [2, 3].

A series of abnormal changes have occurred in the natural world as a result of the emergence of climate change and ecosystem instability, particularly with the expansion of human activities, changes in production systems, and predatory development. Wild plants are facing the dilemma of resource loss and endangerment [3, 4]. Approximately 29% of the country's wild plant populations are under jeopardy, and natural resources of a range of therapeutic materials are rare, with just a tiny number of commodities accessible or none at all. In order to provide a theoretical basis for the future management and protection of wild plant resources in Zhouzhi Nature Reserve, providing suggestions and ideas for the rational planning and utilization of plant resources [4] is suggested [5, 6]. China has a vast territory and abundant resources of wild ornamental plants. There are about 30000 kinds of higher plants and more than 6000 kinds of ornamental garden plants. There are many different

types of high-quality decorative plants available in China, and ornamental plant cultivation has a long history. As early as in the Western Zhou Dynasty from the 11th century B.C. to the 7th century B.C., the working people of the country had cultivated flowers and trees in gardens. However, there are not many kinds of plants used for urban greening in China [5]. For example, Nanjing, Hangzhou, Ningbo, and other cities generally have 200–300 species, while Shanghai has nearly 400 species. Furthermore, with the exception of areas with extremely unique living conditions, such as tropical, frigid, or arid regions, there is no discernible difference in the greening of most Chinese cities. The repetitive and similar plant materials produce a condition similar to one city in a thousand, which does not correspond to the position of a large nation with many plant resources.

Flower production is widely acknowledged as a successful agribusiness branch, despite the fact that floriculture crops are not classified among the primary agricultural commodities. Low labour costs, as well as ecologically and occupationally unsustainable practices, have all contributed to this rise in Kenya, Ethiopia, Colombia, Brazil, and Thailand [6]. The fast increase of flower production in emerging nations is aided by seasonal and meteorological benefits [7]. Pesticides are still used more in the flower business than in any other agricultural crop. Because the safety guidelines for pesticide usage are less severe than those for other horticultural crops, large volumes of pesticides are regularly used to maintain the attractiveness of flowers and plants [8]. But due to the use of huge pesticides, there is a growth of wild ornamental plant resources which is hazardous. The greenhouse growing technique boosts production and assures a year-round supply of high-quality ornamental plant produce. Climate variables like temperature and humidity, on the other hand, are designed to boost crop development in such protected areas [9]. Hence, an enhanced clustering approach is proposed in this research work to ornamental plant resource integration.

The rest of the study is organized as follows: Section 2 discusses the improved clustering algorithm with rapid integration of wild ornamental plant resources. In Section 3, experimental results are discussed, followed by conclusion in Section 4.

2. Proposed Method

The work in this study focuses on the enhanced clustering algorithm for quick integration of wild ornamental plant resources. The steps of the proposed work are elaborated as follows.

(i) An enhanced clustering approach is proposed for quick integration of wild ornamental plant resources

(ii) The goal function of clustering optimization is defined using the k-means distance measurement formula, and the technique is enhanced by combining it with density stratification. The clustering termination condition is dictated by the number of clusters K.

(iii) The wild plant data classes are continuously merged to deal with the wild plant distribution resource dataset with uneven density distribution. The distribution of wild ornamental plants in different regions was determined using remote sensing photos, and the ideal parameters of wild plant samples were computed.

(iv) The differentiation degree of flora and species was derived using a combination of maximum likelihood classification, and resource integration was accomplished.

2.1. Improved Clustering Algorithm. The k-means is an unsupervised algorithm for clustering data objects. The k-means clustering technique separates n data items into k-clusters, each of which contains the data object with the closest mean value. Each group's data items are compact, whereas the objects in the other group are disjunct [10, 11]. The sum of squares is used in the k-means algorithm to construct groups of diverse items. The input parameter of the algorithm is the number of cluster centers. Then, the distance between each element and the center of each cluster is calculated. The distance between the calculated data elements and each cluster center is compared, and the data elements are assigned to the nearest cluster center. The distance measured in k-means clustering is the Euclidean distance. The distance between sample x_i and x_j is defined in the following equation:

$$D\left(x_i, x_j\right) = \left(x_{i1} - x_{j1}\right)^2 + \left(x_{i2} - x_{j2}\right)^2 + \cdots = \sum_{d=1}^{D} \left(x_{i\,d} - x_{i\,d}\right)^2. \tag{1}$$

Equation (1) can be used to calculate the distance between each data element and the cluster center. Data elements are allocated to the cluster center with the minimum distance. The cluster center is the mean value of all data points in the group. Each cluster center with a data element set is called a cluster [10].

In cluster analysis, a cluster is defined as the sample set with the minimum dispersion (or maximum compactness), and the dispersion is measured by the distance from the sample to the cluster center. Combined with the k-means distance measurement formula, the objective function of clustering optimization is defined in the following equations:

$$J\left(\Pi, W\right) = \sum_{k=1}^{K} \sum_{x_i \in \pi_k} \sum_{d=1}^{D} \left(x_{i\,d} - v_{k\,d}\right)^2, \tag{2}$$

$$v_{k\,d} = \frac{1}{|\pi_k|} \sum_{x_i \in \pi_k} x_{i\,d}. \tag{3}$$

The more compact the samples in the cluster are, the less discrete they are from the standpoint of data distribution [11]. The implementation steps of clustering algorithm are as follows:

Input: according to the number of clusters k, randomly select k samples from N sample data to make $X = \{X_1, X_2, X_3, \ldots, X_k\}$

Output: select the object to be clustered from the data object set as the initial cluster, which is also $c_1, c_2, c_3, \ldots, c_{kn}$.

Procedure: the dataset is divided randomly, and the arithmetic mean of each cluster is calculated.

According to (1), the distance from the sample to the center of each cluster is calculated as given in the following equation:

$$\left| X_k - c_j \right| = \min \sqrt{\sum_{k=1}^{m} \left(X_k - c_j \right) x^2}. \tag{4}$$

The sample is divided into the nearest cluster, the cluster center c_k is recalculated as shown in the following equation, and the sample is divided until the cluster does not change.

$$c_k = \frac{1}{x_k} \sum_{X_i \subset X_k} X_i. \tag{5}$$

The enhanced method is a density-based agglomerative hierarchical clustering technique that requires the number of clusters to be determined in advance as the clustering termination condition [12, 13]. At first, each data object is regarded as a separate class, and then, the classes are merged until the termination condition is satisfied.

The points in the dataset with a minimal density of roughly 10% are eliminated as deviation points in the modified method, and the remaining data points are hierarchically grouped on the two layers of maximum and minimum densities. On the basis of hierarchical clustering, the whole dataset after excluding deviation points is integrated into agglomerative hierarchical clustering, and finally, the deviation points are divided into the nearest clustering. The number of classes in the known dataset is k, and the total number of data points is N. The implementation steps of the improved algorithm are as follows:

(A) Calculate the density of each data point in dataset D.

The point density is the number of points in a certain area and is defined in the following equations:

$$\rho_i = \sum_{j \in D} \chi \left(d_{ij} - d_c \right), \tag{6}$$

$$\chi(x) = \begin{cases} 1, & x < 0, \\ 0, & x \geq 0, \end{cases} \tag{7}$$

where d_{ij} represents the distance between point i and point j. d_c is the cutoff distance. The selection principle is that the average number of adjacent data points is 1–3% of the total number of data points, and the average number of data points for a dataset within 1000 is generally about 10. The density of data point i is as follows: the number of points whose distance to point i is less than the cutoff distance d_c.

(B) Take about 10% of the data points with the smallest density in dataset D as deviating points to form dataset P and exclude them and combine the remaining data points in D to form dataset S.

The deviation point is the point where the density is less than the cutoff density p_c, and the process of obtaining the deviation point is the process of continuously adjusting the cutoff density p_c. Initially, set a cutoff density p_c and find the number of points n whose density is less than the cutoff density and is calculated as given in the following equation:

$$n = \sum_{i \in D} \chi \left(\rho_i - \rho_c \right). \tag{8}$$

If $n > 0.12N$, adjust the truncation density to $\rho_c = 0.8\rho_c$, if $n < 0.08N$, adjust the truncation density to $\rho_c = 1.2\rho_c$, update ρ_c, and then calculate the number of points ρ_c again. Keep adjusting $0.08N \leq n \leq 0.12N$ until the number of points n meets ρ_c, at which point ρ_c is the final cutoff density. Knowing the final result, we can determine which points in the dataset D have a density less than the cutoff density, so as to determine the deviation points and form the dataset P. The red points shown in Figure 1 are deviated points from the dataset P and the black points are deviated points from the dataset S.

(C) The dataset B is composed of about 25% of the points with the highest density in the dataset S, and the dataset B is clustered into about $2k$ categories according to the agglomerated hierarchical clustering method. The process of obtaining dataset B is similar to the process of finding deviating points. The green points are about 25% of the points with the highest density in the dataset S. These green points are deviated points from the dataset B. The clustering of dataset B is agglomerated hierarchical clustering, that is, initially treat each point in B as a separate class and then continuously merge the classes with the smallest distance between classes until there are only 8 categories in B; the final clustering effect is shown in Figure 2.

Assuming that i, j are different data points, the distance between the two clusters u, p is defined in the following equation:

$$d_{up} = \min_{i \in u, \, j \in p} d_{ij}. \tag{9}$$

(D) Finally, the deviating points in the dataset P are divided into the nearest k classes in S, and the clustering of the entire dataset D is completed. Because the points in the dataset P are all deviating points and there is no complete new class in the point set P, there is no need to perform hierarchical clustering on the points in P separately. Just divide these deviating points into the nearest existing k categories. Figure 3 shows the dataset clustering impact before and after off-point processing. According to the clustering effect, the improved algorithm is suitable for spherical clusters.

The parameters cutoff distance and cutoff density have a minor impact on the enhanced method [14]. The enhanced algorithm is based on a straightforward concept. The entire clustering process relies on the calculation of the distance between data points, and there is no complicated formula [15, 16]. The method of excluding some points with the smallest density makes the improved algorithm insensitive to outliers and noise [17, 18]. The

(a)

(b)
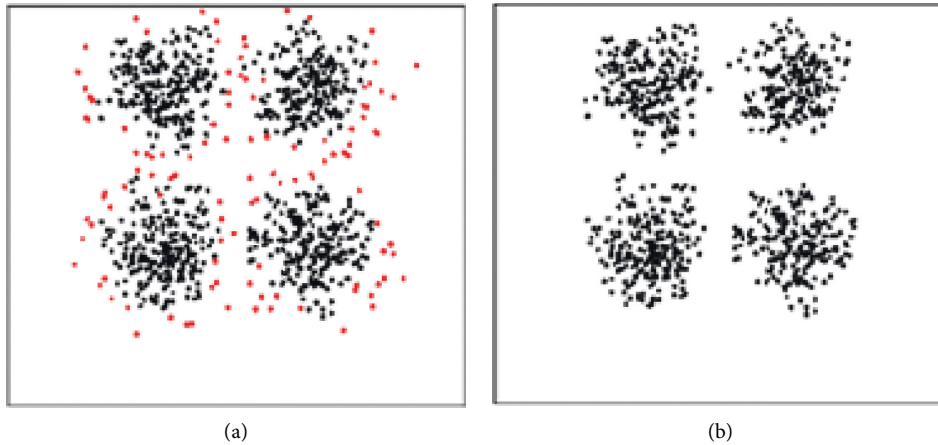
FIGURE 1: The distribution of deviation point set *P* and dataset *S*.

(a)

(b)
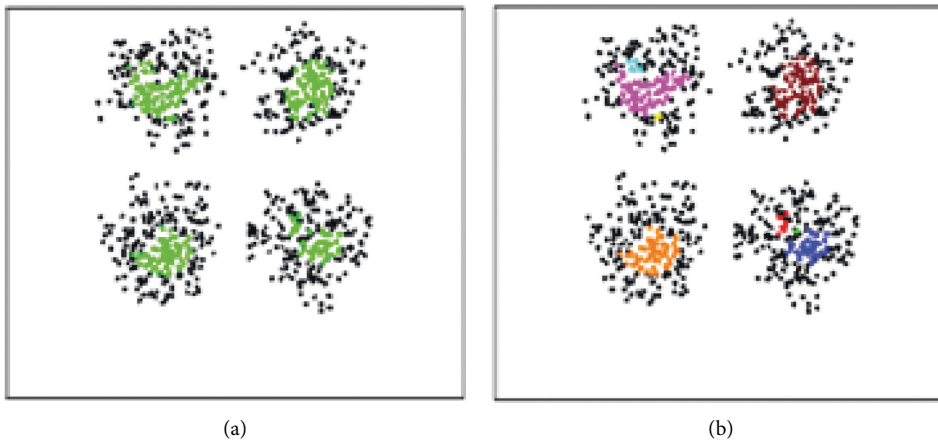
FIGURE 2: The distribution of dataset *B* and its clustering effect.

(a)

(b)
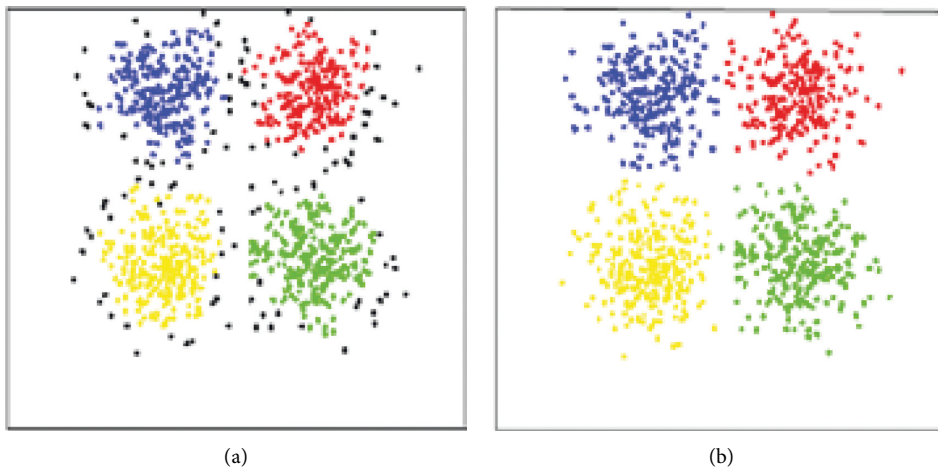
FIGURE 3: The clustering effect of dataset D before and after the deviation point processing.

enhanced technique is stratified by density, and the notion of hierarchical clustering in the greatest, and lowest density layers can not only increase the algorithm's performance but also allow it to handle datasets with unequal density distribution.

2.2. Rapid Integration of Wild Ornamental Plant Resources

2.2.1. Location. Hebei Wu'an National Forest Park is located in the Taihang Mountains in the west of Handan City, Hebei Province, within the territory of Wu'an City, bounded by the

west edge of Wu'an City in the east and Shexian County in the south. It is adjacent to the Fengfeng Mining Area of Ci County and Zuoquan County in the west. The geographical coordinates are $113°45'-114°22'$ east longitude and $36°28'-37°01'$ north latitude. The total area of the park is $40500 \, km^2$. The forest park is full of peaks, crisscross ravines, undulating terrain, and complex and diverse landforms.

2.2.2. Topography.

It is located in the first-order structure of the New Cathaysia, the contact part of the Taihang Mountain uplift and the subsidence zone of the North China Plain. The soil types are mainly leached cinnamon soil and brown soil, which are distributed vertically with the altitude. From top to bottom, they are mainly mountain brown soil, grassy brown soil, and cinnamon soil (eluvial cinnamon soil, mountain cinnamon soil, and carbonate cinnamon). The landform features are complex, and the terrain slopes from northwest to southeast. It is known as Sanhe, Wuchuan, and Jiugou. The highest peak in the territory is Qingyazhai with a height of 1898.7 m and the lowest Yonghe village with a height of 87 m. The terrain is relatively undulating. There are two main mountains, Xiaomotianling and Shibapan.

2.2.3. Climate and Hydrology.

It belongs to a warm temperate continental monsoon climate. The main characteristics are four distinct seasons, rain and heat in the same season. The annual average temperature is 11°C–13.5°C, the extreme minimum temperature is −19.9°C, and the extreme maximum temperature is 35.5°C; the annual average sunshine hours is 2297 h, the annual average frost-free period is 230 d, and the average annual precipitation is 600–800 mm. Most of them are concentrated in June to August, with the characteristics of rain and hot in the same season and distinct dry and wet. Figure 4 shows the wild ornamental plants.

2.2.4. Plant Resource Integration.

The plant characteristics and habits of wild ornamental plants are very different; their adaptability and resistance abilities are also not the same, and the value of development and utilization is also different [19, 20]. As a result, before developing and utilizing wild plant resources, evaluation standards should be established based on the development and utilization's purpose and main objectives, and targeted screening should be conducted to achieve key and orderly rational utilization, as well as increase the development and utilization efficiency of wild ornamental plants. Table 1 provides the distribution of wild ornamental plants in different regions.

Analyzed from the perspective of the main color distribution, the distribution of the main color will affect the combination effect of the plant landscape configuration. When the main color distribution of the plant landscape is relatively sparse, the beauty value is higher, and when the main color distribution of the plant landscape is more concentrated, the beauty value is lower. It indicates that people prefer the plant landscape configuration with scattered colors. In terms of the main color ratio, the main color ratio of the plant landscape configuration with a higher degree of beauty is more regular. While, the main color ratio of the plant landscape configuration with a lower degree of beauty is more irregular. So, the main color ratio affects the beautiful degree value of the plant landscape configuration, in terms of color coordination. It is the color coordination which directly affects people's judgment on the plant landscape configuration, and people like the plant landscape configuration with higher contrast tones and degrees. In terms of hierarchical structure, a good plant landscape configuration hierarchy has a higher beauty value, and a weak plant landscape configuration hierarchy has a lower beauty value, indicating that the strength of the color hierarchy affects the beauty value of the plant landscape configuration. From the point of view, when cool colors account for a larger proportion, it can greatly increase the value of plant landscape configuration [14, 15].

Based on high-resolution remote sensing images, the basic data and characteristics of the current urban landscape pattern are extracted, and n groups of sample observation values are randomly selected from the fusion results of the fused high-resolution remote sensing images. According to the characteristics and values of the samples, the optimal parameter estimation of the wild plant samples is performed [19, 20]. Assuming that the classification feature index of the fused remote sensing image has the condition of multivariate normal distribution, calculate the covariance matrix and average vector of each type of training sample, and using the following equation, calculate the probability of the wild plant distribution information X in the ith category.

$$P(X \mid i) = (2\pi)\frac{d}{2}|T_i|^{-(1/2)} \times \exp\left[-\frac{1}{2}(X - u_i)^T T_i^{-1}(X - u_i)\right].$$

$$(10)$$

$NDVI = (NIR - R)/(NIR + R)$ and T_i^{-1}, respectively, represents the total mutation matrix and its inverse matrix. The expression of T_i is shown as follows:

$$T_i = \begin{bmatrix} S_{11} & S_{12} & \Lambda & S_{1d} \\ S_{21} & S_{22} & \Lambda & S_{2d} \\ M & M & O & M \\ S_{d1} & S_{d2} & \Lambda & S_{dd} \end{bmatrix},$$

$$(11)$$

where d is the number of feature classes, S_{ij} is the covariance of the X and j^{th} classes, and u_i is the average vector of the ith class. In addition, X represents the sample feature represented by the d-dimensional matrix, and its expression is given as follows:

$$X = \begin{bmatrix} x_1 \\ x_2 \\ M \\ x_d \end{bmatrix}.$$

$$(12)$$

Using the maximum likelihood classification method expressed in the above equation, the classification results of remote sensing images are obtained. Then, normalize the

(a)   (b)

FIGURE 4: Picture of wild ornamental plants.

TABLE 1: Distribution of wild ornamental plants in different regions.

Image number	Wild plant image	Ornamental plant distribution
6		Chongyang wood + flower leaf Yanshan ginger + *Ophiopogon japonicus* + weeping willow + Yunnan Huangshu Xin + red photinia
10		White orchid + *Liriodendron* + weeping willow + golden leaf ball + red lorops
17		False betel nut + brown bamboo + bright leaf banana + golden leaf + false *Forsythia*
21		Chongyang wood + Mi Zilan + bright leaf banana + *Ophiopogon japonicus* + paper *Broussonetia*
35		Banyan + white orchid + crape myrtle + flower leaf Yanshan ginger + Buddha moon bamboo + red lorops
42		Banyan tree + *Rhododendron sylvestris* + *Quercus* fern + safflower *Loropia chinensis* + *Sphaerotheca* fern

plant distribution index to realize the extraction of wild plant information from remote sensing images. The extraction process is shown in the following equation:

$$NDVI = \frac{NIR - R}{NIR + R}. \tag{13}$$

Massive resources are classified by their diverse integration of wild ornamental plant resources. The problem to be solved by classification is to analyze and predict resource data. A classification function is mined on the basis of existing data. Therefore, this article uses a decision tree to generate the classification function. The calculation amount

is within the allowable range, and it can handle continuous and discrete fields. It can also clearly indicate the important field. Without considering the noise, the real data may have some field incompleteness or errors. In the case of noise, it will affect the classification performance of the decision tree. Therefore, pruning is needed to simplify the decision tree structure and make it easier to understand. First, establish a decision tree and use the evaluation equation in each classification node to obtain the test set with the largest function as the optimal condition to complete the node division. This research study uses the method test function as the information gain rate function as shown in the following equations:

$$\text{Gain ratio} = \frac{\text{gain}(A)}{\text{spliti}(A)}, \tag{14}$$

$$\text{Spliti}(A) = -\sum_{1}^{v} \frac{p_i}{m} \log\left(\frac{p_i}{m}\right), \tag{15}$$

where $\text{gain}(A)$ represents information gain, A is the attribute of the decision tree, v represents the number of discrete values of A, and p_i represents the number of positive examples.

Use floristic species differentiation (SD) to reflect the degree of differentiation of different flora as in the following equation:

$$SD = \frac{n_2}{n_1} + \frac{n_3}{n_2}, \tag{16}$$

where SD represents the degree of differentiation of the flora. The larger the value of SD, the higher the degree of differentiation of the flora in this area, and vice a versa the lower the degree of differentiation. n_1, n_2, n_3, respectively, represent the value of family, genus, and species in a flora.

3. Results

A comprehensive survey of the protected area shall be carried out using a survey method combining line survey and systematic sampling. Shrubs use a $100\,\text{m} \times 10\,\text{m}$ sample line method with 4 repetitions, and herb plants use a $1\,\text{m} \times 1\,\text{m}$ sample method with 4 repetitions. The survey content includes statistics on all plant species and their habitats, latitude and longitude, coverage, abundance, frequency, height, and aboveground biomass. At the same time, observation records are closely related to the ornamental value, biological characteristics, resource potential, economic value, and ecological value. Plant type, ornamental parts, flower and fruit color, flower diameter, leaf shape and leaf color, ecological habits, and other indicators are noted, and take photos and collect specimens. A total of 235 sample lines and samples were investigated in the past two years.

The "hot spot" detection tool is used to generate a heat map of the plant size distribution in the protected area. The red region shown in Figure 5 represents a hot location where high values congregate, whereas the blue area represents a cold place where low values congregate. Spatial hot spot detection (Getis-Ord G_i^*) is used to test whether the spatial scale has statistically significant high and low values in a local area. Visualization methods can be used to reveal the "hot spot" and "cold spot" areas for the study of the spatial scale of plants. The statistical calculation of Getis-Ord G_i^* is given in the following equation:

$$G_i^* = \frac{\sum_{j=1}^{n} w_{ij} x_j - x}{\sqrt{\left(\sum_{j=1}^{n} w_{ij} x_j - \left(\sum_{j=1}^{n} w_{ij}^z\right)\right) / (n-1)}}. \tag{17}$$

It can be seen from Figure 5 that there are obvious differences in the spatial distribution of wild plant landscapes in this area, roughly showing high north and low south, and the northern region has a ring-shaped surrounding feature of "low central and high surroundings." There is an obvious negative correlation between the difference in the spatial scale of the plant distribution and the difference in density, that is, the spatial distribution characteristics of high-density small-scale and low-density large-scale agglomeration.

The various integration techniques are turned into programme codes and then entered into the created test platform. In order to ensure that the integration method can run in the experimental environment, the relevant parameters are configured. The corresponding integration result is shown in Figure 6.

Integration runtime delay is calculated as in the following equation:

$$R = \frac{\sum_{(a,b)} N^{\text{ext}}(a,b) \oplus N^{\text{ref}}(a,b)}{\sum_{(a,b)} N^{\text{ref}}(a,b)}, \tag{18}$$

where (a,b) represents a pixel, N^{ref} represents an image segmentation area, N^{ref} describes a remote sensing image target segmentation area, and arithmetic symbol $\oplus$ represents a logical addition.

Take the running data of the background program in the experimental environment, extract the relevant data about the running time, and input it into the Excel data processing software.

As shown in Figure 7, the running delays of the integrated methods presented in reference [5], cholinesterase inhibition [8], and genic simple sequence repeat markers (eSSRs) [9] are compared. It takes 4.64 s, 3.86 s, and 2.94 s running delay, respectively, by these three algorithms, whereas the proposed methods of clustering discussed in the study has a delay of 1.96 s which is minimal among all approaches. The designed integration based on the improved clustering method runs faster and integrate the results. The main reason is that the method introduces an improved clustering algorithm which shows optimal results in lesser iterations and minimum time. The improved algorithm is not sensitive to outliers and noise. It is stratified according to the density and the idea of hierarchical clustering that the maximum and minimum densities can not only improve the efficiency of the algorithm but also can handle datasets with uneven density distribution.
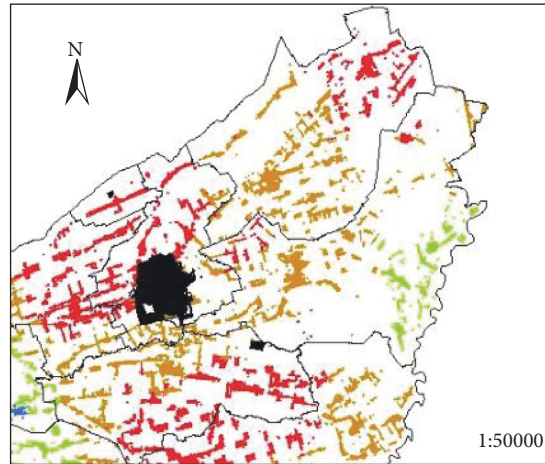
Hot spot analysis of
rural settlement area

■ Cold spot area

■ Subcooling zone

■ Sub hotspot area

■ Hot spot area

■ Township border

□ Towns and townships

FIGURE 5: "Hot spot" map of plant size difference.

Comparative prediction results

Experimental prediction results

Sea area
Farmland
Orchard
Woold land
Built-up area
Silt beach
Breed
Water body
Brine pan
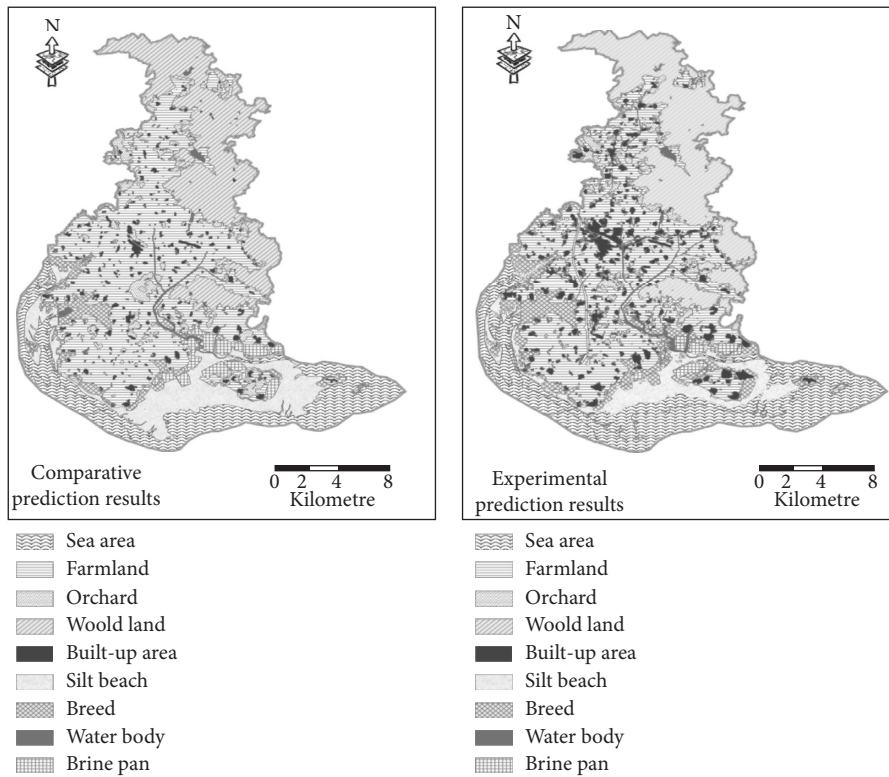
FIGURE 6: Legend of wild plant pattern prediction results before and after the application of the improved clustering algorithm.
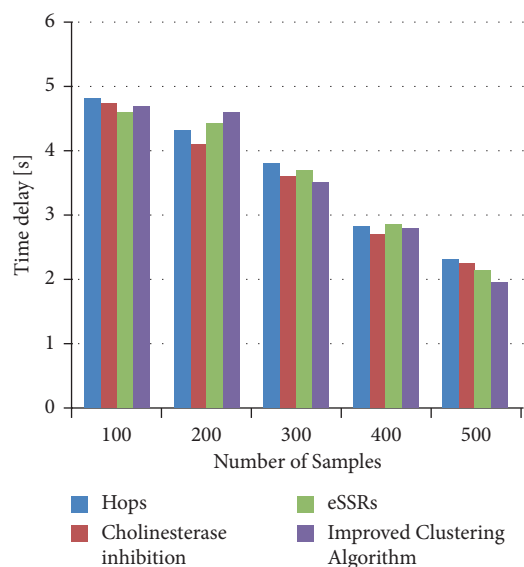
FIGURE 7: The execution delays of the integrated methods.

4. Conclusion

This study proposes a rapid integration of wild ornamental plant resources based on an enhanced clustering algorithm to prevent the substantial losses caused by the introduction of ornamental plants that are not suited for the local environment. To increase the algorithm's efficiency, density stratification is combined to continue integration of wild plant data categories. Wild plant distribution resource datasets with uneven density distribution are processed, and hierarchical clustering at the highest and lowest density levels is performed which are suitable for processing datasets with uneven density distribution. To obtain the distribution of wild ornamental plants in different regions, to estimate the optimal parameters of wild plant samples, to combine with maximum likelihood classification to obtain the plant flora differentiation degree, and to complete the resource integration, remote sensing images were used. The difference in spatial scale and density of plant distribution as a whole, as shown in the heat map of plant size distribution, demonstrates the features of high-density small-scale and low-density large-scale agglomeration distribution in space. The integrated running time delay is 1.96 s.

Data Availability

The data used to support the findings of this study are available from the corresponding author upon request.

Conflicts of Interest

The authors declare that there are no conflicts of interest.

Acknowledgments

References

[1] M. E. Dulloo and N. Maxted, "Special issue: plant genetic resources conservation and utilization–crop wild relatives," *Plant Genetic Resources*, vol. 17, no. 2, pp. 1-2, 2019.

[2] Y. Gong, T. Zhou, P. Wang et al., "Fundamentals of ornamental plants in removing benzene in indoor air," *Atmosphere*, vol. 10, no. 4, p. 221, 2019.

[3] Y. Jiang, R. Qian, W. Zhang et al., "Composition and biosynthesis of scent compounds from sterile flowers of an ornamental plant clematis Florida cv. "Kaiser"," *Molecules*, vol. 25, no. 7, p. 1711, 2020.

[4] I. Karagöz and G. Yücel, "Use of super absorbent polymers with euonymus plants (Euonymus Japonicus "Aureomarginatus") in ornamental plant cultivation," *Tarim Bilimleri Dergisi*, vol. 26, no. 2, pp. 201–211, 2020.

[5] A. H. A. Khan, I. Nawaz, Z. G. Qu, T. A. Butt, S. Yousaf, and M. Iqbal, "Reduced growth response of ornamental plant Nicotiana alata L. upon selected heavy metals uptake, with co-application of ethylenediaminetetraacetic acid," *Chemosphere*, vol. 241, Article ID 125006, 2019.

[6] W. E. Klingeman, J.-H. Chong, C. Harmon, L. Ames, A. V. LeBude, and P. Chandran, "Scale insect records from ornamental plants help to prioritize plant health resource development," *Plant Health Progress*, vol. 21, no. 4, pp. 278–287, 2020.

[7] J. L. Mccallum, M. H. Nabuurs, S. T. Gallant, C. W. Kirby, and A. A. S. Mills, "Phytochemical characterization of wild hops (humulus lupulus ssp. lupuloides) germplasm resources from the maritimes region of Canada," *Frontiers of Plant Science*, vol. 10, p. 1438, 2019.

[8] P. P. M. Nassar and M. G. Ribeiro, "Considerations for cholinesterase biomonitoring in flower and ornamental plant greenhouse workers," *The Science of the Total Environment*, vol. 711, no. 1, Article ID 135228, 2019.

[9] M. Nowicki, E. E. Schilling, S. L. Boggess et al., "Development and characterization of genic microsatellites for the ornamental plant green and gold (Chrysogonum virginianum)," *Hort Science*, vol. 54, no. 2, pp. 395–400, 2019.

[10] F. A. Hale, D. D. Hensley, and R. A. Cloyd, *Using Pesticides in Geenhouses (No. PB 1595(Rev))*, University of Tennessee Extension. Institute of Agriculture. University of Tennessee, Knoxville, TN, USA, 2018.

[11] S. Saheb, "Medicinal plant resources and conservation in Gundlabrahmeswaram wild life sanctuary," *Journal of the Radio Research Laboratories*, vol. 24, no. 1, pp. 115–117, 2019.

[12] P. Saxena and S. Sonwani, "Remediation of ozone pollution by ornamental plants in indoor environment," *Global Journal of Environmental Science and Management*, vol. 6, no. 4, pp. 497–508, 2020.

[13] Z. Song, T.-Q. Li, Z.-H. Liu, K. Jiang, and X.-B. Ou, "The complete chloroplast genome of Tagetes erecta (Asteroideae), a wildly cultivated ornamental plant," *Mitochondrial DNA Part B*, vol. 5, no. 1, pp. 79-80, 2020.

[14] L. Wang, Q. Sheng, Y. Zhang, J. Xu, H. Zhang, and Z. Zhu, "Tolerance of fifteen hydroponic ornamental plant species to formaldehyde stress," *Environmental Pollution*, vol. 265, no. Pt B, p. 115003, 2020.

[15] F. Wen, F. Min, Y. J. Zhang, and C. Yang, "Crude oil price shocks, monetary policy, and China's economy,"

International Journal of Finance & Economics, vol. 24, no. 2, pp. 812–827, 2019.

[16] M. Kaur, "Elitist multi-objective bacterial foraging evolutionary algorithm for multi-criteria based grid scheduling problem," *2016 International Conference on Internet of Things and Applications (IOTA)*, pp. 431–436, 2016.

[17] C. Damalas and S. Koutroubas, "Farmers' exposure to pesticides: toxicity types and ways of prevention," *Toxics*, vol. 4, no. 1, pp. 1–10, 2016.

[18] L. Jiang, S. R. Sakhare, and M. Kaur, "Impact of industrial 4.0 on environment along with correlation between economic growth and carbon emissions," *International Journal of System Assurance Engineering and Management*, 2021.

[19] M. Kenis, L. Tonina, R. Eschen et al., "Non-crop plants used as hosts by *Drosophila suzukii* in Europe," *Journal of Pest Science*, vol. 89, no. 3, pp. 735–748, 2016.

[20] K. S. Sankaran, N. Vasudevan, and V. Nagarajan, "Plant disease detection and recognition using K means clustering," in *Proceedings of the 2020 International Conference on Communication and Signal Processing (ICCSP)*, pp. 1406–1409, Chennai, India, July 2020.

WILEY | Hindawi

Review Article

Lipopeptide Biosurfactants from *Bacillus* spp.: Types, Production, Biological Activities, and Applications in Food

Nawazish Ali [1,2] **Zhengjun Pang,**[2] **Fenghuan Wang** [1,2] **Baocai Xu** [1,2] **and Hesham R. El-Seedi**[3,4]

[1]*Beijing Advanced Innovation Center for Food Nutrition and Human Health, Beijing Technology & Business University (BTBU), Beijing 100048, China*
[2]*School of Light Industry, Beijing Technology & Business University (BTBU), Beijing 100048, China*
[3]*Pharmacognosy Group, Department of Pharmaceutical Biosciences, Uppsala University, Biomedical Centre, Box 591, SE-751 24, Uppsala, Sweden*
[4]*International Research Center for Food Nutrition and Safety, Jiangsu University, Zhenjiang 212013, China*

Correspondence should be addressed to Fenghuan Wang; wangfenghuan@th.btbu.edu.cn and Baocai Xu; xubaoc@btbu.edu.cn

Received 1 December 2021; Revised 30 January 2022; Accepted 3 March 2022; Published 27 April 2022

Academic Editor: Abid Hussain

Biosurfactants are a functionally and structurally heterogeneous group of biomolecules produced by multiple filamentous fungi, yeast, and bacteria, and characterized by their distinct surface and emulsifying ability. The genus *Bacillus* is well studied for biosurfactant production as it produces various types of lipopeptides, for example, lichenysins, bacillomycin, fengycins, and surfactins. *Bacillus* lipopeptides possess a broad spectrum of biological activities such as antimicrobial, antitumor, immunosuppressant, and antidiabetic, in addition to their use in skincare. Moreover, *Bacillus* lipopeptides are also involved in various food products to increase the antimicrobial, surfactant, and emulsification impact. From the previously published articles, it can be concluded that biosurfactants have strong potential to be used in food, healthcare, and agriculture. In this review article, we discuss the versatile functions of lipopeptide *Bacillus* species with particular emphasis on the biological activities and their applications in food.

1. Introduction

Biosurfactants (BSs) could be found on the surface of microbial cell and transferred into the extracellular space by multiple filamentous fungi, and yeast (*Starmerella, Candida, Ustilago, Saccharomyces, Trichosporon,* and *Pseudozyma*) and bacteria (*Nocardia, Rhodococcus, Acinetobacter, Arthrobacter,* and *Gordonia*) [1]. They are primarily classified according to their structural characteristics, associated microorganisms, and molecular weight (MW) [2].

BSs have a hydrophobic region and a hydrophilic end consisting of hydrocarbons acids, diverse fatty acids (saturated, unsaturated, linear, or branched long-chain) and carbohydrate cyclic peptide, alcohol, carboxylic acid, amino acid, and phosphate. This amphipathic framework provides an ability to reduce the surface tension at the interfaces of phases with divergent polarities, which includes emulsion (liquid-liquid) and suspension (liquid-solid), which is collectively named "dispersion" [3, 4]. BSs have also the capacity to produce molecular aggregates, for example, micelles, like the ones patented at the critical micelle concentration (CMC). The CMC of BSs is normally 1–200 mg/L, which is 10–40 times lower than that formed with chemical surfactants [5].

BSs are produced through microbial fermentation, which includes yeast, fungi, and bacterial strains (*Pseudomonas*, *Lactobacillus*, *Acinetobacter*, *Halomonas*, *Rhodococcus*, *Bacillus*, *Enterococcus*, and *Arthrobacter*). Among all microbes, genus *Bacillus* is well studied for its biosurfactant production as it produces various types of cyclic lipopeptides/lipoproteins such as lichenysins, bacillomycin, fengycins, and surfactins [6].

Lipopeptides and glycolipids are highly efficient and popular group of BSs such as surfactin and rhamnolipids, with low-MW [7–9], whereas the high-MW BSs are lipoprotein, phospholipids, and emulsion [10, 11]. Lipopeptide BSs are composed of two different regions: an acyl tail (s) and a short linear oligopeptide sequence, containing an amide bond. The hydrophobic tail contains a hydrocarbon chain, whereas the hydrophilic head contains the lipopeptide BSs peptide sequence. The peptide module includes cationic and anionic residues, as well as nonproteinaceous amino acids [12].

Taking into account the unique properties of *Bacillus* cyclic lipopeptides, and their applications in medicine, healthcare, environment, agriculture, and food industries, their biocompatibility, bioavailability, and structural diversity attracted further attention in the last decade [13–15]. The nonribosomal peptide synthetase (NRPS) enzyme is associated with the formation of cyclic lipopeptides. Lipopeptide surfactants are classified according to their structure, with isoforms comprising a variety of D and L amino acids [16, 17]. The demand for new lipopeptides is increasing in order to broaden their application. Earlier, various studies have been conducted to establish the biotechnological production, functional qualities, and physical properties of lipopeptide surfactants. In this review article, a comprehensive study is carried out to describe the contributions of *Bacillus* lipopeptides in the food industry and biological activities.

2. Classes of Lipopeptides Produced by *Bacillus spp*

Lipopeptides are a subgroup of microbial surfactants, for example, surfactin, fengycin, iturin, lichenysin, and kurstakin [18]. The types or classifications of lipopeptides surfactants are mainly based on the amino acid sequences and various strains of *Bacillus spp*. producing lipopeptides such as *B. subtilis, B. cereus, B. thuringiensis, B. globigii, B. amyloliquefaciens, B. megaterium, B. pumilus*, and *B. licheniformis*. [19–22] (Table 1 and Figure 1).

2.1. Surfactin. Surfactin belongs to the lipopeptides family, which was firstly isolated by Arima et al. in 1968 and produced by many *Bacillus* with surfactant activities [66]. Surfactin (1036 Da) is an amphipathic cyclic lipopeptide biosurfactant produced by many strains of the bacterial genus *Bacillus*. The surfactin molecule was firstly screened from the culture media of *B. subtilis* strains and applied as a clotting inhibitor [67, 68].

Surfactin is composed of a heptapeptide (ELLVDLL) along with chiral sequence LLDLLDL linked with β-hydroxy (fatty acid chain) of carbon chain (C12–C16) and forms a close cyclic lactone ring structure. The structure of surfactin consists of both hydrophobic (located at 2–4, 6, and 7) and hydrophilic (located at 1 and 5) part [69]. Surfactin displays a stable and conserved folding in aqueous solutions, and negatively charged amino acids, Glu and Asp, exhibit polar domain. Moreover, it is also soluble in organic solvents, for

example, dichloromethane, ethanol, chloroform, butanol, and methanol [70].

The peptide part represents topology like "horse-saddle" and is called the β-sheet structure in the backbone folding, which believe that these structural traits contribute to the broad spectrum of biological properties of surfactin [71, 72].

Naturally, many isoforms of surfactin present, which only differ with their physicochemical properties such as (1) type of amino acid of peptide ring at 2nd, 4th, and 7th positions, and (2) branching of hydroxyl fatty acid moiety and chain length. What's more, isoforms also depend upon the *Bacillus* strain and other factors such as media, environmental, and nutritional conditions of substrate [73, 74]. Previously, studies reported that surfactin shows potent antitumoral, antiviral, anticoagulant, inhibitors of enzymes, and antimicoplasma activities [75].

2.2. Lichenysin. Lichenysin a lipopeptide produced most of *B. licheniformis* strains, and it has excellent surfactant and chelating agent for Ca^{2+} and Mg^{2+} [76–79]. Lichenysin was also reported to exert antimicrobial, anti-inflammatory, antitumor, and immunosuppressive properties. Besides good biological activities, it also has hemolytic activity [79]. These traits of lichenysin are caused by the amphiphilic nature of the lipopeptide. Structurally, lichenysin consists of amino acids (7) and a β-hydroxy fatty acid along with C12–C17 carbon atoms. Many isoforms of lichenysin are present in nature, for example, lichenysin A [80–82]. The structure of lichenysin is very similar to surfactin and differs with the substitution of glutamine with glutamic acid in the first amino acid position [82]. However, this small difference markedly increases the surfactant properties of lichenysin [79].

2.3. Kurstakin. Kurstakin is a low-molecular-weight lipopeptide mainly produced and isolated from *Bacillus thuringiensis kurstakin HD-1*. The amino acid sequence of kurstakin was reported as follows: Thr-Gly-Ala-Ser-His-Gln-Gln. The fatty acyl chain of kurstakin is linked with N-terminal amino acid residue by amide bond, and every lipopeptide consists of lactone linkage among carboxyl terminal amino acid and hydroxyl group in the side chain of the serine residue [83, 84].

2.4. Iturin. Iturin are an important class of lipopeptides with a molecular mass of ~1.1 kDa. Iturin A consists of two parts: (a) C14–C17 (amino fatty acids) and (b) seven amino acid residues (heptapeptides; Asn-Tyr-Asn-Gln-Pro-Asn-Ser). Iturin (D and E) varies from iturin A due to the presence of a free carboxyl group in iturin D and carboxymethyl group in iturin E. The structure of iturin shows that it has an amphiphilic character [85, 86]. Iturin molecule is of great interest because of their biological activities and physicochemical traits and used in oil, pharmaceutical, and food industries. Almost all strains of *Bacillus subtilis* produce iturin lipopeptide, and its operon ranges from 38 to 40 kb in size and contains four open reading frames such as *ItuA,*

TABLE 1: Lipopeptide-producing strains and their applications.

Lipopeptides	LP-producing bacterial strain	Biological application	Ref.
Surfactin	B. methylotrophicus DCS1	Antioxidant, antimicrobial, and antiadhesive activities	[23]
	B. mojavensis A21	Diesel biodegradation	[24]
	B. mojavensis PRC101	Antagonism against Fusarium verticillioides (fungal species infecting maize)	[25]
	B. subtilis	Inhibitory activity against phytopathogenic Fusarium sp.	[26]
	B. atrophaeus L193	Aphicidal activity against the aphid Rhopalosiphum padi (pest in cereal crops)	[27]
	B. subtilis SAS-1 B. amyloliquefaciens BR-15	Engine oil degradation efficiently augmented (75–94%)	[28]
	B. subtilis SPB1	Antioxidant activity, chelating activity, histological study proved effective treatment of complicated wound healing and skin diseases	[29]
	B. subtilis strain ATCC6633	Microbial enhanced oil recovery	[30]
	B. subtilis 573	Decreased viability of breast cancer cell lines, T47D and MDA-MB-231 and nontumor fibroblast cell line (MC-3 T3-E1)	[31]
	B. natto TK-1	Therapeutic agent, anti-inflammation	[32]
	B. subtilis ANR 88	Effective in the synthesis of silver as well as gold nanoparticles	[33]
	B. pumilus	Silver nanoparticles produced as antimicrobial and nematicide	[34]
	B. subtilis LSFM-05	Nontoxic dispersion in biotechnology and nanotoxicology.	[35]
	B. (SPB) NH-100 and NH-217	Biocontrol agent against bakanae diseases in rice	[36]
Surfactin A	B. stratosphericus sp. A15	Antioxidant and antibacterial activity, wound healing activity by connective tissue regeneration, thickened epidermal layer, and keratinocyte formation	[37]
Pumilacidin	B. stratosphericus FLU5	Hydrocarbon removal from contaminated soil, negligible cytotoxic effect against the mammalian cells HEK293	[38]
Lipopeptide	B. subtilis SPB1	Anti-obesity effect through the inhibition of lipid digestive and liver dysfunction enzymes	[39]
Iturin A, fengycin	B. amyloliquefaciens DSM 23117	Biocontrol agent against a common fungal phytopathogen botrytis cinerea	[40]
Bacillomycin D	B. amyloliquefaciens fiply 3A	Killing human cancer cell line viz. A549 (alveolar adenocarcinoma), A498 (renal carcinoma) and HCT-15 (colon adenocarcinoma) while not effecting the normal cell line L-132 (pulmonary epithelial cells)	[41]
Iturin A	B. subtilis	Inhibiting chronic myelogenous leukemia in vitro via paraptosis, apoptosis, and inhibition of autophagy	[42]
Lipopeptide	B. mojavensis ifo 15718	Pharmaceutical applications as it possesses antibacterial activity against pathogen S. aureus and lack of toxicity to PC12 and PBMC cells	[43]
Iturin A	B. amyloliquefaciens PPCB004	Activity against postharvest fungal pathogens on stored fruits	[44]
Fengycin	B. amyloliquefaciens FZB42	Antifungal activity against fusarium moniliforme (rice bakanae disease), fusarium oxysporum (root rot) and trichoderma atroviride (ear rot and root rot)	[45]
Surfactin homologs	B. amyloliquefaciens MD4-12	Synergistic Antimicrobial effects against various gram-positive and Gram-negative bacteria	[46]
	B. subtilis NH 217, B. amyloliquefaciens FZB42	Excellent biofilm formation, antifungal activity against various phytopathogen and their associated diseases	[47]
Bacillomycin, Fengycin	B. methylotrophicus XT1 CECT 8661	Effective biocontrol agent against B. cinerea infection, antioxidant triggerer in different fruits	[48]
Iturin A, Fengycin C	B. Subtilis EA-CBOO15	Iturin A inhibited M. fijiensis mycelial growth, and fengycin C displayed strong inhibitory activity on ascospore germination	[49]
Iturin A, surfactin	B. Subtilis	Broad hypocholesterolemic activities, immune-modulators, toxins, and enzyme inhibitors	[50]
Surfactin, Fengycin	B. subtilis fmbj (CGMCC no. 0934)	Effective against Newcastle disease virus (NDV) and infectious bursal disease virus (IBDV)	[51]
Lichenysin	B. licheniformis VS16	Biofilm inhibition, removal of heavy metals	[52]
	B. licheniformis Ali5	Enhanced oil recovery and motor oil removal from contaminated sand	[53]
	B. licheniformis W16	Excellent emulsification and microbial enhanced oil recovery	[54]
Surfactin	B. subtilis C9	Effective biocontrol agent controlling cladoceran grazers in algal cultivation system	[55]
Lipopeptide biosurfactant	B. pseudomycoides OR 1	Biocontrol agent against food-borne pathogens E. coli (MTTC 43), Klebsiella pneumoniae (MTVV 530) and staphylococcus aureus (MTCC 96)	[56]
Novel cyclic lipopeptide C18	B. pseudomycoides BS6	Bioremediation and recycling waste cooking oil	[57]

TABLE 1: Continued.

Lipopeptides	LP-producing bacterial strain	Biological application	Ref.
Pumilacidin	*B. safensis* CCMA-560	Thermal stable and microbial enhanced oil recovery	[58]
Lipopeptide	*B. sp.* H20-1	Antagonistic effect against sulfate-reducing bacteria	[59]
Lipopeptide	*B. cereus* UCP1615	Bioremediation of petroleum derivative in soil and water with above 90% removal	[60]
Paenibacterin	*Paenibacillus elgii* HOA73	Effective bio-pesticide against diamondback moth Plutella xylostella (destructive insect pest)	[61]
Paenibacterin	*Paenibacillus thiaminolyticus*OSY-SE	Minimized endotoxemia showed low toxicity against human kidney sell line (ATCC CRL-2190)	[62]
Lipopeptide	*B. altitudinis* MS16	Promising emulsification and antifungal activity	[63]
Lipopeptide	*B. brevis*	Excellent emulsifier and antibacterial effects	[64]
Lipopeptide	*B. subtilis* SPB1	Toothpaste formulation	[65]
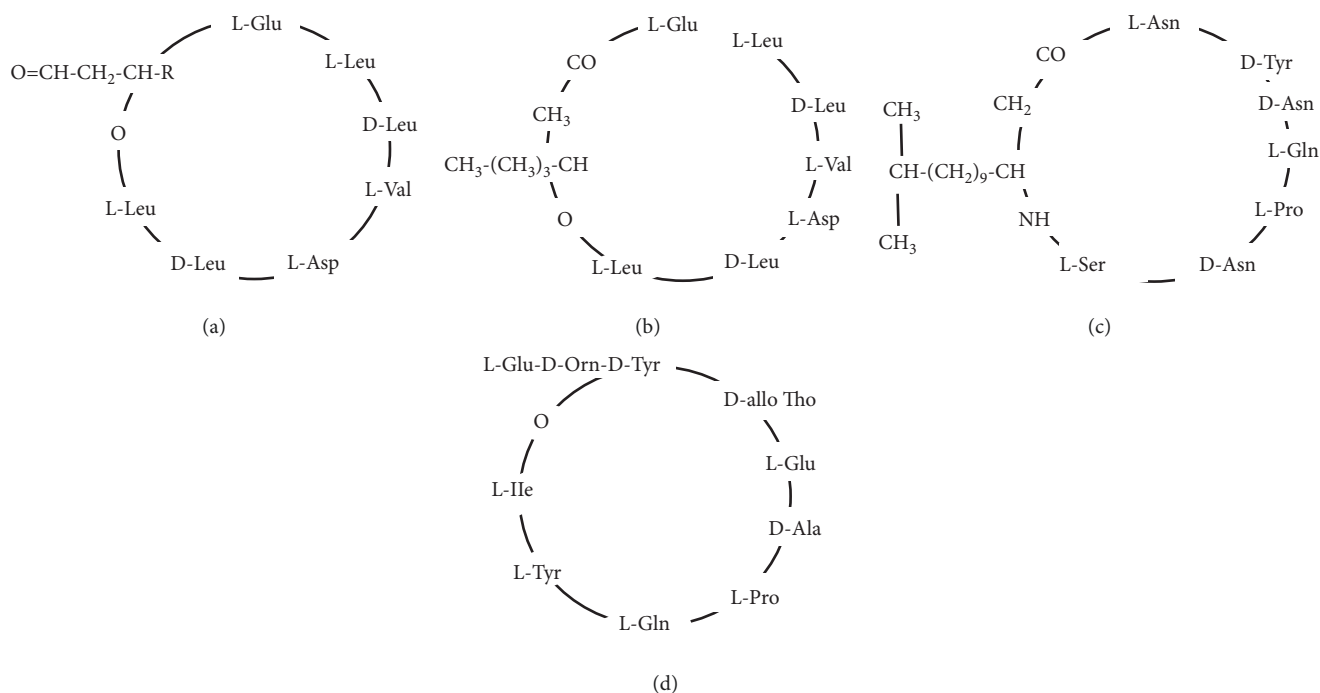
FIGURE 1: Chemical structures of some lipopeptides: (a) surfactin, (b) lichenysin, (c) iturin, (d) fengycin.

ItuB, ItuC, and *ItuD* [87]. Iturin lipopeptide also contains mojavensin, mycosubtilin, bacillomycin D, bacillomycin F, and bacillomycin L, which differ in amino acid sequences of the heptapeptides [88]. Iturin was reported to exert potent antifungal activity against, *Botrytis cinerea*, *Alternaria alternate*, and *Penicillium expansum*. Moreover, it also has strong surface activity and destabilizing effect [89].

2.5. Fengycins. Fengycins are lipopeptides mainly produced by the genera of *Bacillus* and *Paenibacillus*. Fengycins have strong antifungal activity and markedly affect filamentous fungi [90]. Fengycins are decapeptides and C14–C19 to β-hydroxy fatty acid chain, which showed potent antifungal activity [91, 92]. There are two subclasses of Fengycins, namely, Fengycin A and Fengycin B, that only differ from each by the amino acid attached at position 6. Fengycin B contains Val at position 6, whereas Fengycin A contains Ala.

Fengycins (A and B) were firstly reported in *B. subtilis* strain by Vanittanakom et al. [93]. The closely related fengycin type was reported and named plipastatin due to the position of amino acids L- Tyr and D- Tyr [94].

3. Production, Isolation, and Characterization of *Bacillus* Lipopeptides

Lipopeptide surfactants are produced by many microbes including bacteria, fungi, and yeast. However, herein, we mainly focus on the production of *Bacillus* lipopeptides. The biosurfactants are synthesized from the extracellular or intracellular part of microbes. Notably, biosurfactants are produced during the stationary and exponential phase, whereas the biosurfactant production is predominate in the death phase. Reduction in surface tension to 8 mJm^{-2} is the minimum value to be considered when producing the biosurfactant. The various strains of *Bacillus spp.* produced

novel lipopeptides such as *B. licheniformis,* and *B. circulans*. Furthermore, details of lipopeptide production from various *Bacillus* along with fermentation conditions are presented in Tables 1 and 2.

3.1. Substrates. Many substrates mainly consist of hydrophobic mixtures, vegetable oils, waste products, dairy products, etc. and are used for the production of lipopeptide-based surfactants. To minimize the production cost of lipopeptide-based surfactants, renewable and low-cost substrates were applied as presented in Tables 1 and 2. Moreover, it is also necessary to select substrates with a high nutritional value for the growth of microbes. One of the best methods used is to apply organic matter such as industrial waste, oil substrate, and agro-based materials. Interestingly, these waste materials provide distinct energy source for microbes with effective surfactants production.

3.2. Production of Biosurfactants by Using Agro-Industrial Waste. Agro-industrial waste is an ideal choice for the production of lipopeptide and helps in the industrial waste management. Agro-industrial wastes contain both carbon and lipids along with other necessary nutrients, which are the major requirement for the growth of biosurfactant-producing microbes. Previously, many researchers successfully utilized various agro-industrial wastes such as sugarcane molasses, date molasses, cassava flour, rice straw, corn, fruits and vegetable wastes, bran, and others for the production of biosurfactant [115, 140–146].

Molasses is the key waste product of sugar and date industries, and it has gained a lot of attention for the production of biosurfactant. This popularity to use as a substrate for biosurfactant production is mainly due to its low cost and rich source of dry matter (75%), protein (2.5%), nonsugar organic matter (9–12%), minerals (potassium, calcium, phosphorus, and magnesium), and other components (thiamine, biotin, inositol, and pantothenic acid). The sugar content in the molasses ranges from 48 to 56%, making it ideal for the growth of various microorganisms [147–149].

Makkar and Cameotra [150], Saimmai et al. [142], and Joshi et al. [151] reported the biosurfactant production from *Bacillus subtilis* strains (MTTCC 2423, MTCC1427, and SA9) and *Bacillus licheniformis* TR7) by using molasses as carbon source. In another study, Joshi et al. [54] documented that cane molasses and date molasses used as a carbon source enhance the production of lichenysin-A-like lipopeptide by using *Bacillus licheniformis* W16. Rane et al. [33] conducted a study to utilized agro-industrial wastes (molasses, banana peels, orange peels, whey, potato peels, and bagasse) as a substrate for the production of biosurfactant by *Bacillus subtilis* ANR 88. Their study results revealed that biosurfactant production in the molasses substrate as a carbon source was higher (0.24 g/L) compared to other agro-industrial wastes. Moreover, they also found that by optimizing the conditions (ammonium ferric citrate 0.25%, molasses 4%, and pH 7), the yield of biosurfactant significantly increases to 2-fold (0.513 g/L).

Recently, Al-Dhabi et al. [141] used date molasses as a carbon source for the production of biosurfactant from *Bacillus subtilis* strain Al-Dhabi-130. They found that using date molasses as a carbon source yields the biosurfactant to 74 mg/g substrate and can be used for the large-scale production of biosurfactant .

Peanut oil cake is a novel agro-waste, which can be used for the production of lipopeptide. Nalini et al. [152] reported that maximum lipopeptide production was obtained (8.18 g) from peanut oil cake as a substrate by using *B. cereus* strain SNAU01. Paraszkiewicz et al. [153] also observed that lipopeptide surfactants such as surfactin and iturin can be produced by *Bacillus* strains using carrot peel as substrate.

3.3. Production of Lipopeptides by Using Oil Waste. Wastes from oil processing industries represent one of the best and readily available renewable substrates for microbial biosurfactant production. The hydrophobic substrate containing media such as oil helps microbes to produce lipopeptide surfactant. Sunflower, olive oil, coconut oil, and canola are the main oil made from oil industries and considered the best carbon source for biosurfactant production [22, 38, 143, 154].

Ostendorf et al. [143] reported the excellent production of lipopeptide biosurfactants by *Bacillus stratosphericus* strain FLU5 using waste vegetable oils (olive oil, corn oil, and residual frying oil). In another study, Md Badrul Hisham et al. [155] observed the excellent yield of surfactin by *Bacillus* sp. HIP3 when using used cook oil as a substrate (2%).

4. Isolation, Purification, and Characterization of Lipopeptides

Lipopeptides are mostly synthesized by bacterial genus *Bacillus*. The bacterial cells are grown in their respective media with specific conditions (varied from strains to strains) to produce lipopeptides prior to their separation by centrifugation. Malfanova et al. [156] grew bacterial cells (60 h at 28°C) subjected to centrifugation (13,000 rpm for 10 min) to obtain crude lipopeptides. The obtained supernatant was acidified by using HCl acid, while the precipitate was extracted with methanol and further concentrated by vacuum evaporation [156, 157]. The crude extract was purified by many methods such as gel filtration in Sephadex column and high-performance liquid chromatography, and the collected eluent was further subjected to MALDI-TOF-MS/LC-MS/MS-MS/NMR/FTIR [53].

5. Pharmacological Activities

5.1. Anticancer. *Bacillus* lipopeptides are considered versatile bioactive compounds with potent antitumor activity. For example, surfactin has been documented to exert antitumor activity towards human colon carcinoma cell lines (HCT15 and HT29), Ehrlich's ascites carcinoma cells, and breast cancer cell lines (T47D and MDA-MB-231) [31, 104, 158]. Surfactin inhibits the growth of transformed

Table 2: Strategies and mechanisms used to enhance lipopeptide production by *Bacillus sp.*

Strategy used	Factors evaluated	Strain	Results	BS nature	Ref.
RSM, CCD	Brewery waste and (carbon, nitrogen, agitation speed, temperature, pH)	*B. subtilis* N3–1P	657 g.l^{-1}	Surfactin	[95]
RSM, BBD	(d-glucose, sucrose, xylose), hydrocarbons (hexadecane, diesel, benzene, heptane), nitrogen source (NaNO$_3$, NH$_4$NO$_3$, (NH$_4$)$_2$SO$_4$, NaHCO$_3$, urea)	*Bacillus sp.* SS105	2.65 g.l^{-1}	Surfactin	[96]
CCD, PBD	Sucrose, glucose, starch, peanut oil, potato), nitrogen source (peptone, beef extract, trypsin, yeast extract), other variables (MgSO$_4$, KCl, KH$_2$PO$_4$, FeSO$_4$.6H$_2$O, NH$_4$Cl, MnSO$_4$, CuSO$_4$, sodium glutamate)	*B. subtilis* N7	0.706 g.l^{-1}	Surfactin	[97]
RSM, PBD, (TFAT) two factors at time	Nitrogen source ((NH$_4$)$_2$SO$_4$, KNO$_3$, NaNO$_3$, NH$_4$Cl, beef extract, yeast extract)	*B. subtilis* KLP2015	0.98 g.l^{-1}	Surfactin	[98]
RSM, OFAT one factor at a time	Carbon source (glucose, fructose, sucrose, xylose, rhamnose, soluble starch), nitrogen source (NH$_4$Cl, C$_6$H$_{17}$N$_3$O$_7$, urea, peptone, soybean meal), metal ions (ZN^{2+}, Fe^{3+}, Mg^{2+}, Mn^{2+}, Ca^{2+}, K$^+$)	*Bacillus sp.* BH072	0.027 g.l^{-1}	IturinA A	[99]
OFAT	Single and multidose Fe^{2+}	*B. megaterium*	4.2 g.l^{-1}	Surfactin	[100]
2^2 factorial design, RSM	Glucose and yeast extract	*B. subtilis* EA-CB0015	0.78, 0.355 g.l^{-1}	Fengycin, Iturin A	[101]
PBD, CCD	Carbon source (glucose, maltose, dextrose, mannitol, sorbitol, galactose, xylose, starch), nitrogen source (KNO$_3$, (NH$_4$)$_2$SO$_4$, NaNO$_3$, soy flour, peptone, casein hydrolysate, yeast extract urea)	*B. amyloliquefaciens* MD4-12	1.25 g.l^{-1}	Surfactin	[102]
CCD, Fed-batch strategy	Fed-batch strategy (pH-stat, DO-stat, constant rate feeding, combined feeding), Sunflower oil, NaNO$_3$, MgSO$_4$.7H$_2$O, yeast extract	*Aneurinibacillus thermoaerophilus* HAKO1	11.2 g.l^{-1}	Surfactin	[103]
ANN-GA	Glucose, urea, SrCl$_2$, and MgSo$_4$	*B. circulans* MTCC 8281	4.38 g.l^{-1}	Unidentified	[104]
ANN-GA	Lp concentration, Ca^{2+}, pH	*B. licheniformis, B. megaterium*	45% oil recovery	Lipopeptide	[105]
BBD	Glucose, glutamic acid, temperature, NaCl	*B. mojavensis* 14	4.12 g.l^{-1}	Lipopeptide	[106]
BBD	Optimization of non-nutritional factors (inoculum age and size, pH, agitation, aeration, temperature)	*B. subtilis* SPB1	3.3 g.l^{-1}	Lipopeptide	[107]
	Nitrogen source ((NH$_4$)$_2$SO$_4$, KNO$_3$, NH$_4$NO$_3$, NH$_4$Cl, peptone, beef extract, yeast extract), carbon source (glucose, sucrose, fructose, maltose, sorbitol, starch)	*B. velezensis* KLP2016	2.5 g.l^{-1}	Lipopeptide	[108]
Media composition and characteristics	n-paraffin, n-dodecane, n-hexadecane, sunflower oil, canola oil, sucrose, glycerol, diesel fuel, n-tetradecane, nitrogen source ((NH$_4$)$_2$SO$_4$, NaNO$_3$, KNO$_3$, urea, peptone, yeast extract, beef extract), metal and sulfur source (FeSO$_4$, MnSO$_4$, MgSO$_4$), and C/N ratio, pH	*Paenibacillus sp.* D9	4.11 g.l^{-1}	New lipopeptide	[109]
	Different culture media, shaking speed of shaker, liquid and solid fermentation, attapulgite powder	*B. natto* NT-6	1.94-fold increased	Iturin A, surfactin	[110]
	Different culture media, vine-trimming shoots, glucose, hemicellulosic hydrolysate, and cellulosic hydrolysate	*B. tequilensis* ZSB10	1.52 g.l^{-1}	Lipopeptide	[111]
Taguchi method	Carbon source (sucrose, whey, crude oil)), NaCl, Na$_2$HPO$_4$, NaH$_2$PO$_4$, and (NH$_4$)$_2$SO$_4$	*B. cereus*	1.8 g.l^{-1}	Lipopeptide	[112]

TABLE 2: Continued.

Strategy used	Factors evaluated	Strain	Results	BS nature	Ref.
Use of cheap substrate/raw material	Carbon source (orange peel, citrus medica peels, banana peels, and potato peels), inoculum size, incubation time, temperature, substrate concentration	B. licheniformis KC710973	1.796 g.l^{-1}	Lichenysin	[113]
	(Butter milk, poultry-transforming waste flour, inoculum size), submerged fermentation	B. subtilis SPB1	12.61 g.l^{-1}	Lipopeptide	[114]
	Corn steep liquor (CSL), iron, manganese, and magnesium	B. subtilis #573	4.8 g.l^{-1}	Surfactin	[115]
	Potato peels, temperature, pH, saline conditions	B. pumilus DSVP18	3.2 g.l^{-1}	Iturin A	[116]
	Grape seed flour	B. amyloliquefaciens C5	0.80 g.l^{-1}	Bacillomycin D	[117]
	Distiller grains (DGS, coculture fermentation with B. B. amyloliquefaciens X82	B. amyloliquefaciens MT45	3.4 g.l^{-1}	Surfactin	[118]
	Palm oil, waste glycerol, immobilized on chitosan	Bacillus Sp. GY 19	9.8 g.l^{-1}	Lipopeptide	[119]
Solid state fermentation (SSF)	Soybean flour, rice straw, starch, yeast extract, kinetic parameters (iso- and nonisothermal process, isothermal and nonisothermal process in fermenter)	B. amyloliquefaciens XZ-173	(55.83 mg/gds)	Lipopeptide	[120]
	Soybean flour, rice straw, glycerol, maltose, pH, water content, inoculum size, fermentation time, temperature	B. amyloliquefaciens XZ-173	15.03 mg/gds	Surfactin	[121]
	Wheat bran, rice straw, soybean flour, temperature, pH, water content, inoculum size	B. subtilis CCTCCM207209	70.90 mg/gds	Lipopeptide	[122]
	Rice bran husk, sunflower oil, coconut oil cake, cotton oil cake, corn cob, orange peel, jackfruit peel, sugarcane leaf, pineapple peel, banana leaf, cheese whey, dry yeast cells, pongamia seed cake, jatropha seed cake ground oil cake, glucose with MSM	B. amyloliquefaciens	3-fold increased	Iturin A	[123]
	Olive leaf residue flour, olive cake flour	B. subtilis SPB1	0.3067 g.l^{-1}	Lipopeptide	[124]
Mutagenesis induced enhanced yield	UV and gamma ray-induced mutagenesis	B. subtilis HS0121	2-fold increased	Surfactin	[125]
	Random mutagenesis using gamma irradiation	B. subtilis UTB1	1.8-fold increased	Iturin A	[126]
	UV irradiation, nitrosoguanidine, and ion beam mutagenesis	B. amyloliquefaciens ES-2-4	10.3-fold increased	Lipopeptide	[127]
	Combination of UV irradiation and nitrous acid treatment	B. subtilis SPB1	2-fold increased	Lipopeptide	[51]
Genome shuffling	Genome shuffling	B. amyloliquefaciens FMB38	2-fold increased	Surfactin	[128]
	Genome shuffling and gene (fenA) expression	B. amyloliquefaciens ES-2-4	8.30-fold increased	Fengycin	[129]
	Mutagenesis (UV, nitrosoguanidine, atmospheric, and room temperature plasma)	B. amyloliquefaciens LZ-5	2.03-fold increased	Iturin A	[130]
	Protoplast fusion	B. mojavensis JF-2	0.382 g.l^{-1}	Lipopeptide	[131]

TABLE 2: Continued.

Strategy used	Factors evaluated	Strain	Results	BS nature	Ref.
Recombinant strains for higher yield	Surfactin promoter THY-15 was replaced to THY-15/pg3-srfA. Then introduced a Vitreoscilla hemoglobin (VHb) gene into engineered strain to obtain a novel THY-15/pg3-srfA (VHb)	*B. subtilis THY-15*	10.02 g.l^{-1}	Surfactin C15	[132]
	Loc gene expressed, the fosmid N13 with whole *Loc* gene screened from B. velezensis 916 genomic library, the cassette fused with IPTG inducible promoter Pspac induced in the fosmid N13 resulted N13+spec and N13+PSSpec transformed to obtained derivative strains FZBNPLOC and FZBPSLOC	*B. velezensis FZB42*	15-fold increased	Locillomycins	[133]
	Enhanced transcription of iturin A biosynthetic genes was implemented by inserting a strong promoter C2up into upstream of the *itu* operon, fermentation optimization using RSM and furthermore, overexpression of pleiotropic regulator DegQ	*B. amyloliquefaciens LL3*	8-fold increased	Iturin A	[134]
	Cloning of the biosurfactant genes sfp, sfp0, sfpA into BioS a, BioS b, BioS c, recombinant strains after cloning of biosurfactant genes in to *E. coli*. (*E. coli* DH5ά)	*B. subtilis* SK320	2-fold increased	Lipopeptide	[135]
	Wild type, overexpression of THY-7-P$_{grac}$-*ycxA*, overexpression of THY-7-P$_{grac}$-*krsE*, overexpression of THY-7-P$_{grac}$-*yerP*	*B. subtilis* 168	0.55, 1.15, 0.93, 1.67 g.l^{-1}	Surfactin	[136]
	Using CRISPRi 20 genes were repressed, *yrpC, racE, murC* genes were inhibited individually. Furthermore, combination inhibition of *bkdAA* and *bkdA*B genes	*B. subtilis*	4.69-fold increased	Surfactin	[137]
	Replacement of PsrfA with P$_{g3}$	B. subtilis	0.55–9.74 g l^{-1}	Surfactin	[138]
	Insertion of *sfp* gene from Paenibacillus sp. D9 into *E. coli*	Paenibacillus sp. D9	3-fold increased	Paenibacterin	[139]

cells via cell cycle arrest and induction of apoptosis and suppresses ERK (extracellular-signal-regulated kinase) and PI3 K/Akt pathway [158]. In another study, Liu et al. [159] reported that surfactin-like lipopeptides purified from *B. subtilis* Hs0121 exert cytotoxicity towards Bcap-37 breast cancer cells (IC$_{50}$: $29 \pm 2.4 \mu M$). Surfactin was also documented to inhibit the LoVo colon cancer cells (IC$_{50}$: $26 \mu M$) [158] (Figure 2). What's more, Wang et al. [160] observed that *B. subtilis* natto T-2 with crude cyclic lipopeptides (CLPs) showed a cytotoxic effect against human K562 leukemia cells. Surfactin was also reported to exhibit the cytotoxic effect on hepatocellular carcinoma [159, 160]. Recently, Hong et al. [161] have reported that five Surfactin isomers produced by *B. pumilus* HY1 during Cheonggukjang fermentation markedly inhibited the growth of two cancer cell lines (MCF-7 and Caco-2).

Fengycin, a lipopeptide produced by various strains of *B. subtilis*, was reported to exert strong anticancer activity on colon cancer cell line HT29 and human lung cancer cell line 95D [162, 163]. Similarly, *Bacillus* lipopeptide (iturin) was also reported to possess a broad spectrum of anticancer activity on several cell lines (e.g., HepG2, Caco-2, BT474, MDA-MB-231, MCF-7, HUVEC, BIU-87, BRL-3A, A549, and K562 cells [42, 164–171].

5.2. Hemolytic Activity. The lipopeptide surfactants induce the hemolysis of human erythrocytes due to their detergent effect and membrane forming ability. Therefore, lipopeptide surfactants are used as potent inhibitors of fibrin clot formation. Arima et al. [172] reported for the first time that the surfactin potently inhibits the fibrin clot formation via abrogating the conversion of fibrin monomer into fibrin polymer. Bernheimer and Avigad studied the inhibition of fibrin clot formation and hemolysis of erythrocyte by subtilysin derived from *B. subtilis* since 1970 [173] (Figure 2).

The hemolytic activity of lipopeptide iturin A was studied by Aranda et al. They documented that iturin dependently exerts hemolytic activity on human erythrocytes. The underlying mechanism of action was that iturin A induced hemolysis via colloid-osmotic mechanism and K$^+$ leakage followed by hemoglobin release [85]. In another study, Dehghan-Noudeh et al. [174] documented that *B. subtilis* ATCC 6633-derived lipopeptide surfactant attenuated potent hemolytic effect in comparison with chemical surfactants such as hexadecyl trimethyl ammonium bromide, sodium dodecyl sulfate, tetradecyl trimethyl ammonium bromide, and benzalkonium chloride.
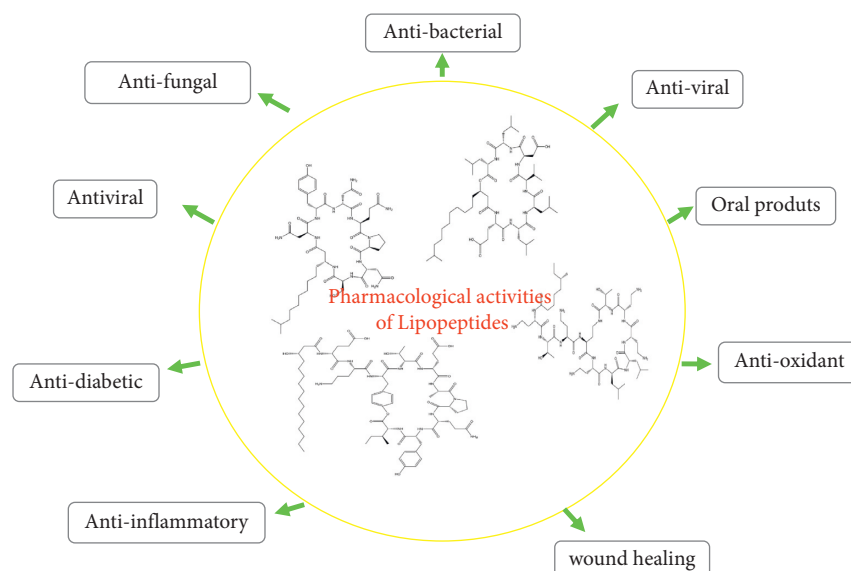
Figure 2: Pharmacological activities of lipopeptides.

5.3. Anti-Inflammatory. Previously, it was reported that lipopeptides exert anti-inflammatory activities via several pathways such as modulation of the TLR4 (Toll-like receptor 4), inhibition of lipoteichoic acid (LTA)-induced NF-κB, activator of transcription-1 (STAT-1), interaction with cytosolic phospholipase A2 (PLA2), and increase in the phosphorylation of STAT-3 [88] (Figure 3).

Moreover, it also impairs the antigen-presenting function of macrophages, suppresses the LPS-induced expression of cluster of differentiations (CD40, CD54, CD80), and inhibits the activation of CD4$^+$ T-cells [32, 88].

It was also documented that surfactin markedly inhibits the overproduction pro-inflammatory mediators (IL-6, tumor necrosis factor alpha or TNF-alpha, and interleukin beta or IL-1β), prostaglandin E2, monocyte chemoattractant protein-1, NO, and reactive oxygen species (ROS), and suppresses the expression of MMP-9 (matrix metallopeptidase 9), COX-2 (cyclooxygenase-2), and iNOS (inducible nitric oxide synthase) [175].

5.4. Antibacterial Activity. The demand for new antimicrobial agents significantly increases due to the resistance of pathogenic microorganisms towards already present antimicrobial drugs. Surfactin, a lipopeptide, was reported to exert antibacterial activity against various pathogenic bacteria. Beside surfactin, other Bacillus-related lipopeptides were also reported to possess well-known inhibitory activity towards the growth of pathogenic bacteria [176–179].

Huang et al. [178] reported that surfactin and fengycin produced by the strain B. subtilis fmbj effectively inactivate endospores of B. cereus. The lipopeptide mainly damages the surface structure of the spores. B. velezensis strain H3-isolated surfactin isoforms were reported to active against P. aeruginosa, St. aureus, Klebsiella pneumoniae, and Mycobacterium [179].

In another study, fengycin isoforms isolated from marine Bacillus strain markedly inhibited the growth of various bacteria such as K. aerogenes, Citrobacter fruendii, Micrococcus flavus, Proteus vulgaris, Alcaligenes faecalis, E. coli, and Serratia marcescens [180].

Lipopeptide antibiotic subtulene A isolated from the culture filtrate of B. subtilis SSE4 was reported to inhibit the growth of Gram-positive and Gram-negative bacterial strains such as Stenotrophomonas maltophilia, Enterobacter cloacae, and Xanthomonas campestris [181]. Fengycin and surfactin lipopeptides containing culture filtrate of the endophytic B. amyloliquefaciens was reported to potently inhibited the growth of all tested Gram-negative ones except Ochrobactrum anthropi and all Gram-positive bacteria tested except B. [157].

Recently, a study conducted by Lv et al. [177] has also reported that B. amyloliquefaciens C-1 fermentation supernatant contains a mixture containing surfactin and fengycin, which inactivate the growth of Clostridium difficile (bacteria that can infect the bowel and cause diarrhoea). Iturin analog isolated from Bacillus strain was reported to inactivate the growth of Xanthomonas arboricola and Pseudomonas syringae [176].

5.5. Antifungal and Biocontrol. It has been documented that Bacillus lipopeptides exert a wide array of antifungal activities. Briefly, iturin markedly inhibits the growth of nematophagous fungi, wood-staining fungi, Aspergillus flavus, Penicillium roqueforti, and Colletotrichum demiatium [19, 182–186], whereas fengycin was reported to inhibit the Fusarium graminearum, Botrytis cinerea, and Podosphaera fusca [187, 188].

More detailed investigations conducted by various researchers reported that lipopeptides exert morphological changes such as hyphal swellings, changed organization of mitochondria, decreased intracellular pH, esterases, and mitochondria activities, and decreased hydrophobicity of the hyphae [48, 189].
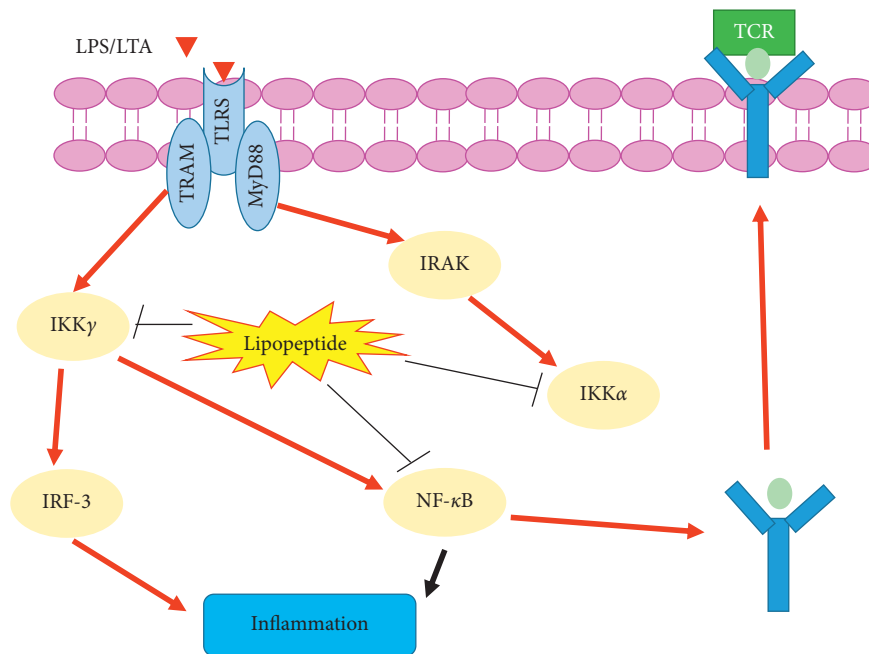
FIGURE 3: The proposed anti-inflammatory mechanism of *Bacillus subtilis* lipopeptides.

Desmyttere et al. [190] conducted a study to explore the antifungal activities of lipopeptides isolated from *B. subtilis* against apple scab disease causing *Venturia inaequalis* strains. Their study results revealed that *Bacillus subtilis* lipopeptide mixtures containing (fengycin, surfactin, and mycosubtilin) markedly inhibited the growth of *V. inaequalis* S755 and *V. inaequalis* rs552.

Han et al. [191] documented that *B. amyloliquefaciens* L-H15-derived peptides (iturin A with C15β-amino fatty acid and cyclic peptide with a molecular weight of 852.4 Da) exhibited strong antagonism against *Fusarium oxysporum*, *Rhizoctonia solani*, and *Phytophthora capsici*.

Dimkić et al. [176] studied five different lipopeptide-producing strains of *Bacillus* (SS-10.7, SS-12.6, SS-13.1, SS-27.2, and SS-38.4), and their extracts were further tested against *Pseudomonas syringae* pv. *aptata* (P16) and *Xanthomonas arboricola* pv. *juglandis* (301, 311, and 320). The results revealed that *Bacillus* strains mostly produced kurstakins, iturins, surfactins, and fengycins lipopeptides. Moreover, they reported that ethyl acetate extracts exert more favorable effect on phytopathogens.

Botrytis cinerea is a necrotrophic fungi, which infects more than 200 plant species including fruits and vegetables. Toral et al. [48] conducted a study to determine anti-*B. cinerea* activity of lipopeptides isolated from *Bacillus* XT1 CECT 8661. They observed that lipopeptide-rich extract mainly containing surfactin, bacillomycin, and fengycin potently inhibits the growth of *B. cinerea*. What's more, SEM (scanning electron microscope) and TEM (transmission electron microscope) analysis revealed that lipopeptides alter the morphology of the phytopathogen.

5.6. Antiviral Activity.

It has been well documented that lipopeptides such as surfactin possess a broad spectrum of antiviral activity against SARS-CoV-2, herpes simplex virus

(HSV-1 and HSV-2), Newcastle disease virus, Semliki Forest virus, murine encephalomyocarditis virus, Simian immunodeficiency virus, vesicular stomatitis virus, transmissible gastroenteritis virus, porcine parvovirus feline calicivirus, pseudorabies virus, and bursal disease virus, porcine epidemic diarrhoea virus, and viral hemorrhagic septicemia virus. The chemical structure of surfactin lipopeptide, for example, length of the carbon chain, makes it fit for the inactivation of various viruses [51, 192–194]. Moreover, it was also observed that surfactin more significantly inactivates the enveloped viruses such as herpes viruses and retroviruses compared with nonenveloped viruses [195]. This may be due to the physicochemical interaction among membrane active property of surfactin and the virus lipid membrane [196]. Surfactin permeates into the lipid bilayer and results in the complete disintegration of the envelope containing the viral proteins involved in virus adsorption and penetration to the target cells [195].

5.7. Antiadhesion and Antibiofilm.

Surface adhesion and biofilm formation are the mechanisms by which most of bacteria are used for their survival. Lipopeptides have the potential to decrease the interfacial tension and surface of biofilms. In numerous ways, lipopeptides disrupt the membrane structure. For example, surfactin gets inserted into the lipid bilayers, chelates monovalent and divalent cations, solubilizes the fluid phospholipid phase, and modifies the membrane permeability [197]. Surfactin may form voltage-independent channels in biofilms, and these channels disturb the membrane integrity and permeability, leading to membrane disruption [13, 198]. Iturin isoform (mycosubtilin) produced by *B. subtilis* interacts with membranes via its sterol alcohol group and exhibits resistance to fungi [199]. *B. circulans* strain showed

antiadhesive property towards many bacteria species [200]. Similarly, various *Bacillus* strains inhibit biofilm formation [6, 78–80].

5.8. Others. *Bacillus* lipopeptides were also reported in wound healing and oral care products [65]. Zouari et al. [29] documented how the *B. subtilis* SPB1 biosurfactant supplementation improves the liver function, hyperlipidemia, and hypertriglyceridemia in high-fat-high-fructose (HFHF) diet-fed rats. In another study, the same research group also observed that *B. subtilis* SPB1 biosurfactant treatment improves the renal functions and inhibits angiotensin I-converting enzyme (ACE) in HFHF diet-fed rats [39]. Moreover, *B. subtilis* strain containing surfactin was shown to effectively kill the larval and pupal stages of mosquito species, for example, *Aedes aegypti*, *Culex quinquefasciatus,* and *Anopheles stephensi* [195].

6. Lipopeptide Applications in Food

Lipopeptides have well-defined antiadhesive, antibacterial, antiviral, and anticancer properties, ensuring their role in the cosmetics, pharmaceutical, and even food industries. Lipopeptides are mainly employed as surfactants in the food industry. Moreover, rhamnolipids and surfactins are positively exploited in the baking industry, providing good texture, volume, and product stability. They are also used to promote the emulsification process in the fat tissue to regulate fat globule agglomeration. Certain lipopeptides derived from *Enterobacter cloacae* have recently been presented into the food market with their high emulsifying characteristics owing to the potential to improve viscosity even at extreme acidic conditions. In terms of economic growth, the most significant increases in food additives have been seen in emulsifiers and hydrocolloids that were up to 10.5% and 6.0%, respectively.

The vulnerability of biologically active peptides as an antimicrobial agent in the food preservation is rare due to their limits to proteases. The usage of ring-structured peptides like lipopeptides, on the other hand, can prevent this susceptibility. There are two types of lipopeptides: a cyclic heptapeptide acylated with β-amino fatty acids that have a chain length of C14–C16, and the fengycin group containing a β-hydroxy fatty acid with uncommon amino acids including allo-threonine and ornithine. They also consisted of cyclic heptapeptide that makes a lactone linkage with β-hydroxy fatty acids. They are enzyme-insensitive (particular protease), suppressing the development of a broad variety of pathogenic fungi (*Fusarium graminearum*, *Rhizoctonia solani,* and *Aspergillus flavus*) as well as postharvest pathogens such as *Botrytis cinerea* and *Penicillium expansum*.

Gandhi and his coworkers revealed that the rhamnolipid emulsifier with a concentration of 0.10% significantly improved the texture, moisture content, and appearance of muffins for longer periods. Surfactin inclusion in many fermented food products, like natto, a Japanese soybean meal, is extremely favorable for acceptance as an ingredient or addition. Juola et al. [201] determined the surfactin content of various natto types. Notably, the greatest concentrations discovered were close to 2.2 mg/g, which corresponds to 80–100 mg surfactin per 50 g natto. Additional research is required to establish the surfactant's recommended daily intake (RDI) to pronounce it harmless and is usually considered to be a generally recognized as safe (GRAS) organism. Therefore, surfactin has strong potential to be used in the food sector.

Zouari et al. [202] prepared the cookies using sesame peel flour partially replaced with white wheat flour. When additional sesame peel flour was employed, the characteristics such as toughness, water content, and spread factor had been degraded. Interestingly, adding 0.1% *B. subtilis* SPB1 biosurfactant significantly enhanced the textural profile, even when compared to the standard surfactant glycerol monostearate [202]. In another research, the possible lipopeptides from *Bacillus spp.* reduced the *Ochratoxin* and *A. carbonarius* that were found in the processing of wine-making [203]. In the wine-making process, the concentration of *Ochratoxin* should not surpass 2.0 μg/L as it is a carcinogenic mycotoxin. Additionally, this compound has a detrimental effect on yeast fermentation behaviour. Lipopeptides also had higher antifungal capabilities than SO_2 and stimulated yeast growth as well as the generation of esters and acids that are involved in the olfactory profile [203].

7. Conclusion

Lipopeptides are very useful molecules due to their multiple applications. Most *Bacillus* lipopeptides have been applied in food, cosmetic, biotechnology, pharmaceutical industries, where emulsifying, antimicrobial, and surfactant properties are used. The application and production of lipopeptides are very promising trend; however, the high cost of production makes them unfit for large-scale synthesis. Furthermore, even though there are many reports displaying the thrombolytic, antitumor, and anti-inflammatory activity of lipopeptides, the few numbers of clinical trials warrant more significant efforts. In future, extensive studies should be carried out to verify previously published author findings, which further help with the utilization of these miracle compounds. In summary, *Bacillus* lipopeptides have strong potential application in various fields and a lot of work will be needed to formulate strategies for improved large-scale biosynthesis of lipopeptides.

Data Availability

No data were used in this article.

Conflicts of Interest

The authors declare no conflicts of interest.

Acknowledgments

References

[1] T. Morita, Y. Ishibashi, N. Hirose et al., "Production and characterization of a glycolipid biosurfactant, mannosylerythritol lipid B, from sugarcane juice by ustilago scitaminea NBRC 32730," *Bioscience Biotechnology and Biochemistry*, vol. 75, 2011.

[2] R. Jahan, A. M. Bodratti, M. Tsianou, and P. Alexandridis, "Biosurfactants, natural alternatives to synthetic surfactants: physicochemical properties and applications," *Advances in Colloid and Interface Science*, vol. 275, Article ID 102061, 2020.

[3] T. Tadros, "Stabilisation of dispersions using a graft copolymer of hydrophobically modified polyfructose," *Colloids and Surfaces A: Physicochemical and Engineering Aspects*, vol. 519, pp. 11–19, 2017.

[4] M. Usman, C. Zhang, P. J. Patil et al., "Potential applications of hydrophobically modified inulin as an active ingredient in functional foods and drugs-a review," *Carbohydrate Polymers*, vol. 252, Article ID 117176, 2020.

[5] C. Ceresa, L. Fracchia, E. Fedeli, C. Porta, and I. M. Banat, "Recent advances in biomedical, therapeutic and pharmaceutical applications of microbial surfactants," *Pharmaceutics*, vol. 13, no. 4, p. 466, 2021.

[6] S. S. Giri, E. Ryu, and S. C. Park, "Antioxidant, antibacterial, and anti-adhesive activities of biosurfactants isolated from Bacillus strains," *Microbial Pathogenesis*, vol. 132, pp. 66–72, 2019.

[7] J. Chen, Q. Wu, Y. Hua, J. Chen, H. Zhang, and H. Wang, "Potential applications of biosurfactant rhamnolipids in agriculture and biomedicine," *Applied Microbiology and Biotechnology*, vol. 101, no. 23, pp. 8309–8319, 2017.

[8] W.-C. Chen, R.-S. Juang, and Y.-H. Wei, "Applications of a lipopeptide biosurfactant, surfactin, produced by microorganisms," *Biochemical Engineering Journal*, vol. 103, pp. 158–169, 2015.

[9] S. Shekhar, A. Sundaramanickam, and T. Balasubramanian, "Biosurfactant producing microbes and their potential applications: a review," *Critical Reviews in Environmental Science and Technology*, vol. 45, no. 14, pp. 1522–1554, 2015.

[10] D. J. McClements and C. E. Gumus, "Natural emulsifiers—biosurfactants, phospholipids, biopolymers, and colloidal particles: molecular and physicochemical basis of functional performance," *Advances in Colloid and Interface Science*, vol. 234, pp. 3–26, 2016.

[11] K. Ramani, S. C. Jain, A. B. Mandal, and G. Sekaran, "Microbial induced lipoprotein biosurfactant from slaughterhouse lipid waste and its application to the removal of metal ions from aqueous solution," *Colloids and Surfaces B: Biointerfaces*, vol. 97, pp. 254–263, 2012.

[12] M. H. Mondal, A. Sarkar, T. K. Maiti, and B. Saha, "Microbial assisted (pseudomonas sp.) production of novel bio-surfactant rhamnolipids and its characterisation by different spectral studies," *Journal of Molecular Liquids*, vol. 242, pp. 873–878, 2017.

[13] M. Inès and G. Dhouha, "Lipopeptide surfactants: production, recovery and pore forming capacity," *Peptides*, vol. 71, pp. 100–112, 2015.

[14] T. Janek, L. R. Rodrigues, and Z. Czyżnikowska, "Study of metal-lipopeptide complexes and their self-assembly behavior, micelle formation, interaction with bovine serum albumin and biological properties," *Journal of Molecular Liquids*, vol. 268, pp. 743–753, 2018.

[15] I. Mnif, A. Grau-Campistany, J. Coronel-León et al., "Purification and identification of Bacillus subtilis SPB1 lipopeptide biosurfactant exhibiting antifungal activity against Rhizoctonia bataticola and Rhizoctonia solani," *Environmental Science and Pollution Research*, vol. 23, no. 7, pp. 6690–6699, 2016.

[16] S. A. Cochrane and J. C. Vederas, "Lipopeptides from Bacillus and Paenibacillus spp.: a gold mine of antibiotic candidates," *Medicinal Research Reviews*, vol. 36, no. 1, pp. 4–31, 2016.

[17] I. Mnif and D. Ghribi, "Review lipopeptides biosurfactants: mean classes and new insights for industrial, biomedical, and environmental applications," *Peptide Science*, vol. 104, no. 3, pp. 129–147, 2015.

[18] P. Das, S. Mukherjee, and R. Sen, "Antimicrobial potential of a lipopeptide biosurfactant derived from a marine Bacillus circulans," *Journal of Applied Microbiology*, vol. 104, no. 6, pp. 1675–1684, 2008.

[19] G. Y. Yu, J. B. Sinclair, G. L. Hartman, and B. L. Bertagnolli, "Production of Iturin A by Bacillus amyloliquefaciens suppressing Rhizoctonia solani," *Soil Biology and Biochemistry*, vol. 34, no. 7, pp. 955–963, 2002.

[20] J. Vater, B. Kablitz, C. Wilde, P. Franke, N. Mehta, and S. S. Cameotra, "Matrix-assisted laser desorption ionization-time of flight mass spectrometry of lipopeptide biosurfactants in whole cells and culture filtrates of Bacillus subtilis C-1 isolated from petroleum sludge," *Applied and Environmental Microbiology*, vol. 68, no. 12, pp. 6210–6219, 2002.

[21] M. T. Pueyo, C. Bloch, A. M. Carmona-Ribeiro, and P. Di Mascio, "Lipopeptides produced by a soil Bacillus megaterium strain," *Microbial Ecology*, vol. 57, no. 2, pp. 367–378, 2009.

[22] V. Nihorimbere, H. Cawoy, A. Seyer, A. Brunelle, P. Thonart, and M. Ongena, "Impact of rhizosphere factors on cyclic lipopeptide signature from the plant beneficial strain Bacillus amyloliquefaciens S499," *FEMS Microbiology Ecology*, vol. 79, no. 1, pp. 176–191, 2012.

[23] N. Jemil, H. Ben Ayed, A. Manresa, M. Nasri, and N. Hmidet, "Antioxidant properties, antimicrobial and anti-adhesive activities of DCS1 lipopeptides from Bacillus methylotrophicus DCS1," *BMC Microbiology*, vol. 17, no. 1–11, p. 144, 2017.

[24] N. Hmidet, H. Ben Ayed, P. Jacques, and M. Nasri, "Enhancement of surfactin and fengycin production by Bacillus mojavensis A21: application for diesel biodegradation," *BioMed Research International*, vol. 2017, Article ID 5893123, 8 pages, 2017.

[25] A. A. Blacutt, T. R. Mitchell, C. W. Bacon, and S. E. Gold, "Bacillus mojavensis RRC101 lipopeptides provoke physiological and metabolic changes during antagonism against Fusarium verticillioides," *Molecular Plant-Microbe Interactions*, vol. 29, no. 9, pp. 713–723, 2016.

[26] H. B. Ayed, M. C. Azabou, N. Hmidet, M. A. Triki, and M. Nasri, "Economic production and biocontrol efficiency of lipopeptide biosurfactants from Bacillus mojavenis A21," *Biodegradation*, vol. 30, no. 4, pp. 273–286, 2019.

[27] M. Rodríguez, A. Marín, M. Torres, V. Béjar, M. Campos, and I. Sampedro, "Aphicidal activity of surfactants produced by Bacillus atrophaeus L193," *Frontiers in Microbiology*, vol. 9, no. 1–12, p. 3114, 2018.

[28] R. Sharma, J. Singh, and N. Verma, "Production, characterization and environmental applications of biosurfactants from Bacillus amyloliquefaciens and Bacillus subtilis,"

Biocatalysis and Agricultural Biotechnology, vol. 16, pp. 132–139, 2018.

[29] R. Zouari, D. Moalla-Rekik, Z. Sahnoun, T. Rebai, S. Ellouze-Chaabouni, and D. Ghribi-Aydi, "Evaluation of dermal wound healing and in vitro antioxidant efficiency of *Bacillus subtilis* SPB1 biosurfactant," *Biomedicine & Pharmacotherapy*, vol. 84, pp. 878–891, 2016.

[30] T. Park, M.-K. Jeon, S. Yoon, K. S. Lee, and T.-H. Kwon, "Modification of interfacial tension and wettability in oil-brine-quartz system by in situ bacterial biosurfactant production at reservoir conditions: implications for microbial enhanced oil recovery," *Energy and Fuels*, vol. 33, no. 6, pp. 4909–4920, 2019.

[31] C. Duarte, E. J. Gudiña, C. F. Lima, and L. R. Rodrigues, "Effects of biosurfactants on the viability and proliferation of human breast cancer cells," *AMB Express*, vol. 4, pp. 40–12, 2014.

[32] Y. Zhang, C. Liu, B. Dong et al., "Anti-inflammatory activity and mechanism of surfactin in lipopolysaccharide-activated macrophages," *Inflammation*, vol. 38, 2014.

[33] A. N. Rane, V. V. Baikar, V. Ravi Kumar, R. L. Deopurkar, M. Alejandra, and D. Rienzo, "Agro-industrial wastes for production of biosurfactant by *Bacillus subtilis* ANR 88 and its application in synthesis of silver and gold nanoparticles," *Frontiers in Microbiology*, vol. 8, p. 492, 2017.

[34] W. M. Mahmoud, T. S. Abdelmoneim, A. M. Elazzazy, and F. Walsh, "The impact of silver nanoparticles produced by *Bacillus pumilus* as antimicrobial and nematicide," *Frontiers in Microbiology*, vol. 207, 2016.

[35] D. Stéfani, T. Martinez, A. F. Faria et al., "Exploring the use of biosurfactants from *Bacillus subtilis* in bionanotechnology: a potential dispersing agent for carbon nanotube ecotoxicological studies," *Process Biochemistry*, vol. 49, pp. 1162–1168, 2014.

[36] A. Sarwar, M. N. Hassan, M. Imran et al., "Biocontrol activity of surfactin A purified from Bacillus NH-100 and NH-217 against rice bakanae disease," *Microbiological Research*.vol. 209, 2018.

[37] S. Sana, A. Mazumder, S. Datta, and D. Biswas, "Towards the development of an effective in vivo wound healing agent from Bacillus sp. derived biosurfactant using Catla catla fish fat," *RSC Advances*, vol. 7, no. 22, pp. 13668–13677, 2017.

[38] D. Hentati, A. Chebbi, F. Hadrich et al., "Production, characterization and biotechnological potential of lipopeptide biosurfactants from a novel marine *Bacillus stratosphericus* strain FLU5," *Ecotoxicology and Environmental Safety*, vol. 167, pp. 441–449, 2019.

[39] R. Zouari, K. Hamden, A. E. Feki et al., "Protective and curative effects of *Bacillus subtilis* SPB1 biosurfactant on high-fat-high-fructose diet induced hyperlipidemia, hypertriglyceridemia and deterioration of liver function in rats," *Biomedicine & Pharmacotherapy*, vol. 84, pp. 323–329, 2016.

[40] D. Pretorius, J. van Rooyen, and K. G. Clarke, "Enhanced production of antifungal lipopeptides by *Bacillus amyloliquefaciens* for biocontrol of postharvest disease," *New Biotechnology*, vol. 32, no. 2, pp. 243–252, 2015.

[41] S. N. Hajare, M. Subramanian, S. Gautam, and A. Sharma, "Induction of apoptosis in human cancer cells by a *Bacillus* lipopeptide bacillomycin D," *Biochimie*, vol. 95, no. 9, pp. 1722–1731, 2013.

[42] H. Zhao, L. Yan, X. Xu et al., "Potential of *Bacillus subtilis* lipopeptides in anti—cancer I: induction of apoptosis and paraptosis and inhibition of autophagy in k562 cells," *AMB Express*, vol. 8, 2018.

[43] M. Fanaei and G. Emtiazi, "Microbial assisted (*Bacillus mojavensis*) production of bio-surfactant lipopeptide with potential pharmaceutical applications and its characterization by MALDI-TOF-MS analysis," *Journal of Molecular Liquids*, vol. 268, 2018.

[44] E. Arrebola, R. Jacobs, and L. Korsten, "Iturin A is the principal inhibitor in the biocontrol activity of *Bacillus amyloliquefaciens* PPCB004 against postharvest fungal pathogens," *Journal of Applied Microbiology*, vol. 108, no. 2, pp. 386–395, 2010.

[45] A. Hanif, F. Zhang, P. Li et al., "Fengycin produced by *Bacillus amyloliquefaciens*," *Toxins*, vol. 11, 2019.

[46] P. Sudarmono, A. Wibisana, L. W. Listriyani, and S. Sungkar, "Characterization and synergistic antimicrobial evaluation of lipopeptides from *Bacillus amyloliquefaciens* isolated from oil-contaminated soil," *Internet Journal of Microbiology*, vol. 2019, Article ID 3704198, 8 pages, 2019.

[47] A. Sarwar, G. Brader, E. Corretto et al., "Qualitative analysis of biosurfactants from Bacillus species exhibiting antifungal activity," *PLoS One*, vol. 13, Article ID e0198107, 2018.

[48] L. Toral, M. Rodríguez, V. Béjar, and I. Sampedro, "Antifungal activity of lipopeptides from Bacillus XT1 CECT 8661 against *Botrytis cinerea*," *Frontiers in Microbiology*, vol. 9, pp. 1315–1412, 2018.

[49] L. M. González-jaramillo, F. José, J. Antonio, V. Villegas-escobar, and A. Ortiz, "Colloids and surfaces B: biointerfaces antimycotic activity of fengycin C biosurfactant and its interaction with phosphatidylcholine model membranes," *Colloids and Surfaces B: Biointerfaces*, vol. 156, pp. 114–122, 2017.

[50] K. R. Meena and S. S. Kanwar, "Lipopeptides as the antifungal and antibacterial agents: applications in food safety and therapeutics," *BioMed Research International*, vol. 2015, Article ID 473050, 9 pages, 2015.

[51] X. Huang, Z. Lu, H. Zhao, X. Bie, F. Lü, and S. Yang, "Antiviral activity of antimicrobial lipopeptide from *Bacillus subtilis* fmbj against pseudorabies virus, porcine parvovirus, newcastle disease virus and infectious bursal disease virus in vitro," *International Journal of Peptide Research and Therapeutics*, vol. 12, no. 4, pp. 373–377, 2006.

[52] S. S. Giri, S. S. Sen, J. W. Jun, V. Sukumaran, and S. C. Park, "Role of *Bacillus licheniformis* VS16-derived biosurfactant in mediating immune responses in carp rohu and its application to the food industry," *Frontiers in Microbiology*, vol. 8, 2017.

[53] N. Ali, F. Wang, B. Xu et al., "Production and application of biosurfactant produced by *Bacillus licheniformis* Ali5 in enhanced oil recovery and motor oil removal from contaminated sand," *Molecules*, vol. 24, pp. 1–18, 2019.

[54] S. J. Joshi, Y. M. Al-Wahaibi, S. N. Al-Bahry et al., "Production, characterization, and application of *Bacillus licheniformis* W16 biosurfactant in enhancing oil recovery," *Frontiers in Microbiology*, vol. 7, 2016.

[55] J. Yun, D. Cho, B. Lee, H. Kim, and Y. K. Chang, "Application of biosurfactant from *Bacillus subtilis* C9 for controlling cladoceran grazers in algal cultivation systems," *Scientific Reports*, vol. 8, 2018.

[56] O. R. Chittepu, "Isolation and characterization of biosurfactant producing bacteria from groundnut oil cake dumping site for the control of foodborne pathogens," *Grain & Oil Science and Technology*, vol. 2, pp. 15–20, 2019.

[57] J. Li, M. Deng, Y. Wang, and W. Chen, "Production and characteristics of biosurfactant produced by *Bacillus pseudomycoides* BS6 utilizing soybean oil waste," *International Biodeterioration & Biodegradation*, vol. 112, 2016.

[58] L. G. C. Lorraine de Araujo, L. G. P. Sodré, R. Laísa, D. F. Brasil, and D. Valéria, "Microbial enhanced oil recovery using a biosurfactant produced by Bacillus safensis isolated from mangrove microbiota-part I biosurfactant characterization and oil displacement test," *Journal of Petroleum Science and Engineering*, vol. 180, pp. 950–957, 2019.

[59] E. Korenblum, L. V. de Araujo, C. R. Guimarães et al., "Purification and characterization of a surfactin-like molecule produced by Bacillus sp. H2O-1 and its antagonistic effect against sulfate reducing bacteria," *BMC Microbiology*, vol. 12, p. 252, 2012.

[60] I. Amaro, A. Helena, M. Resende, and N. M. Padilha, "Aplication of biosurfactants produced by *Bacillus cereus* and *Candida sphaerica* in the bioremediation of petroleum derivative in soil and water," *Chemical Engineering Transactions.*vol. 64, pp. 2283–9216, 2018.

[61] S. Neung, X. H. Nguyen, K. W. Naing, Y. S. Lee, K. Y. Kim, and K. Y. Kim, "Insecticidal potential of *Paenibacillus elgii* HOA73 and its combination with organic sulfur pesticide on diamondback moth, *Plutella xylostella*," *Journal of the Korean Society for Applied Biological Chemistry*, vol. 57, no. 2, pp. 181–186, 2014.

[62] E. Huang and A. E. Yousef, "Paenibacterin, a novel broad-spectrum lipopeptide antibiotic, neutralises endotoxins and promotes survival in a murine model of *Pseudomonas aeruginosa*-induced sepsis," *International Journal of Antimicrobial Agents*, vol. 44, no. 1, pp. 74–77, 2014.

[63] M. Goswami and S. Deka, "Biosurfactant production by a rhizosphere bacteria Bacillus altitudinis MS16 and its promising emulsification and antifungal activity," *Colloids and Surfaces B: Biointerfaces*, vol. 178, pp. 285–296, 2019.

[64] F. E. Mouafi, M. M. Abo Elsoud, and M. E. Moharam, "Optimization of biosurfactant production by *Bacillus brevis* using response surface methodology," *Biotechnology Reports*, vol. 9, pp. 31–37, 2016.

[65] M. Bouassida, N. Fourati, F. Krichen, R. Zouari, S. Ellouz-chaabouni, and D. Ghribi, "Potential application of *Bacillus subtilis* SPB1 lipopeptides in toothpaste formulation," *Journal of Advanced Research*, vol. 8, no. 4, pp. 425–433, 2017.

[66] A. Théatre, C. Cano-Prieto, M. Bartolini et al., "The surfactin-like lipopeptides from Bacillus spp.: natural biodiversity and synthetic biology for a broader application range," *Frontiers in Bioengineering and Biotechnology*, vol. 9, p. 118, 2021.

[67] F. Peypoux, J. M. Bonmatin, and J. Wallach, "Recent trends in the biochemistry of surfactin," *Applied Microbiology and Biotechnology*, vol. 51, no. 5, pp. 553–563, 1999.

[68] J.-M. Bonmatin, O. Laprevote, and F. Peypoux, "Diversity among microbial cyclic lipopeptides: iturins and surfactins. Activity-structure relationships to design new bioactive agents," *Combinatorial Chemistry & High Throughput Screening*, vol. 6, no. 6, pp. 541–556, 2003.

[69] E. J. Gudiña, V. Rangarajan, R. Sen, and L. R. Rodrigues, "Potential therapeutic applications of biosurfactants," *Trends in Pharmacological Sciences*, vol. 34, no. 12, pp. 667–675, 2013.

[70] A. M. Abdel-Mawgoud, M. M. Aboulwafa, and N. A.-H. Hassouna, "Characterization of surfactin produced by *Bacillus subtilis* isolate BS5," *Applied Biochemistry and Biotechnology*, vol. 150, no. 3, pp. 289–303, 2008.

[71] L. Jin, V. M. Garamus, F. Liu et al., "Interaction of a biosurfactant, surfactin with a cationic gemini surfactant in aqueous solution," *Journal of Colloid and Interface Science*, vol. 481, pp. 201–209, 2016.

[72] Y. Ishigami, M. Osman, H. Nakahara, Y. Sano, R. Ishiguro, and M. Matsumoto, "Significance of β-sheet formation for micellization and surface adsorption of surfactin," *Colloids and Surfaces B: Biointerfaces*, vol. 4, no. 6, pp. 341–348, 1995.

[73] F. Peypoux and G. Michel, "Controlled biosynthesis of Val7- and leu7-surfactins," *Applied Microbiology and Biotechnology*, vol. 36, pp. 515–517, 1992.

[74] M. Kowall, J. Vater, B. Kluge, T. Stein, P. Franke, and D. Ziessow, "Separation and characterization of surfactin isoforms produced by *Bacillus subtilis* OKB 105," *Journal of Colloid and Interface Science*, vol. 204, no. 1, pp. 1–8, 1998.

[75] M. Ongena and P. Jacques, "*Bacillus lipopeptides*: versatile weapons for plant disease biocontrol," *Trends in Microbiology*, vol. 16, no. 3, pp. 115–125, 2008.

[76] J. Coronel-León, A. M. Marqués, J. Bastida, and A. Manresa, "Optimizing the production of the biosurfactant lichenysin and its application in biofilm control," *Journal of Applied Microbiology*, vol. 120, no. 1, pp. 99–111, 2016.

[77] H. T. Rønning, E. H. Madslien, T. N. Asp, and P. E. Granum, "Identification and quantification of lichenysin–a possible source of food poisoning," *Food Additives & Contaminants: Part A*, vol. 32, no. 12, pp. 2120–2130, 2015.

[78] E. H. Madslien, H. T. Rønning, T. Lindbäck, B. Hassel, M. A. Andersson, and P. E. Granum, "Lichenysin is produced by most *Bacillus licheniformis* strains," *Journal of Applied Microbiology*, vol. 115, no. 4, pp. 1068–1080, 2013.

[79] I. Grangemard, J. Wallach, R. Maget-Dana, and F. Peypoux, "Lichenysin: a more efficient cation chelator than surfactin," *Applied Biochemistry and Biotechnology*, vol. 90, no. 3, pp. 199–210, 2001.

[80] R. Mikkola, M. Kolari, M. A. Andersson, J. Helin, and M. S. Salkinoja-Salonen, "Toxic lactonic lipopeptide from food poisoning isolates of *Bacillus licheniformis*," *European Journal of Biochemistry*, vol. 267, no. 13, pp. 4068–4074, 2000.

[81] M. M. Yakimov, W.-R. Abraham, H. Meyer, L. Laura Giuliano, and P. N. Golyshin, "Structural characterization of lichenysin A components by fast atom bombardment tandem mass spectrometry," *Biochimica et Biophysica Acta*, vol. 1438, no. 2, pp. 273–280, 1999.

[82] D. Konz, S. Doekel, and M. A. Marahiel, "Molecular and biochemical characterization of the protein template controlling biosynthesis of the lipopeptide lichenysin," *Journal of Bacteriology*, vol. 181, pp. 133–140, 1999.

[83] M. Béchet, T. Carade, W. Hussein et al., "Structure, biosynthesis, and properties of kurstakins, nonribosomal lipopeptides from Bacillus spp," *Applied Microbiology and Biotechnology*, vol. 95, pp. 593–600, 2012.

[84] Y. Hathout, Y.-P. Ho, V. Ryzhov, P. Demirev, and C. Fenselau, "Kurstakins: a new class of lipopeptides isolated from *Bacillus thuringiensis*," *Journal of Natural Products*, vol. 63, no. 11, pp. 1492–1496, 2000.

[85] F. J. Aranda, J. A. Teruel, and A. Ortiz, "Further aspects on the hemolytic activity of the antibiotic lipopeptide iturin A," *Biochimica et Biophysica Acta*, vol. 1713, no. 1, pp. 51–56, 2005.

[86] F. Besson and G. Michel, "Isolation and characterization of new iturins: iturin D and iturin E," *Journal of Antibiotics*, vol. 40, pp. 437–442, 1987.

[87] K. Tsuge, T. Akiyama, and M. Shoda, "Cloning, sequencing, and characterization of the iturin A operon," *Journal of Bacteriology*, vol. 183, no. 21, pp. 6265–6273, 2001.

[88] H. B. Zhao, D. Y. Shao, C. M. Jiang et al., "Biological activity of lipopeptides from Bacillus," *Applied Microbiology and Biotechnology*, vol. 101, no. 15, pp. 5951–5960, 2017.

[89] M. E. Cozzolino, J. S. Distel, P. A. García et al., "Control of postharvest fungal pathogens in pome fruits by lipopeptides from a Bacillus sp. isolate SL-6," *Scientia Horticulturae*, vol. 261, Article ID 108957, 2020.

[90] M. Deleu, M. Paquot, and T. Nylander, "Effect of fengycin, a lipopeptide produced by *Bacillus subtilis*, on model bio-membranes," *Biophysical Journal*, vol. 94, no. 7, pp. 2667–2679, 2008.

[91] C.-Y. Wu, C.-L. Chen, Y.-H. Lee et al., "Nonribosomal synthesis of fengycin on an enzyme complex formed by fengycin synthetases," *Journal of Biological Chemistry*, vol. 282, no. 8, pp. 5608–5616, 2007.

[92] X.-Y. Li, Y. H. Wang, and Y. Q. He, "Diversity and active mechanism of fengycin-type cyclopeptides from Bacillus subtilis XF-1 against plasmodiophora brassicae," *Journal of Microbiology and Biotechnology*, vol. 23, no. 3, pp. 313–321, 2013.

[93] N. Vanittanakom, W. Loeffler, U. Koch, and G. Jung, "Fengycin—a novel antifungal lipopeptide antibiotic produced by *Bacillus subtilis* F-29-3," *Journal of Antibiotics*, vol. 39, no. 7, pp. 888–901, 1986.

[94] P. S. Kumar and P. T. Ngueagni, "A review on new aspects of lipopeptide biosurfactant: types, production, properties and its application in the bioremediation process," *Journal of Hazardous Materials*, vol. 407, Article ID 124827, 2021.

[95] B. Moshtagh, K. Hawboldt, and B. Zhang, "Optimization of biosurfactant production by *Bacillus subtilis* N3-1P using the brewery waste as the carbon source," *Environmental Technology*, vol. 40, no. 25, pp. 3371–3380, 2019.

[96] N. Maheshwari, M. Kumar, I. Shekhar, and S. Srivastava, "Bioresource technology recycling of carbon dioxide by free air CO 2 enriched (FACE) Bacillus sp. SS105 for enhanced production and optimization of biosurfactant," *Bioresource Technology*, vol. 242, 2017.

[97] Y. Luo, G. Zhang, Z. Zhu, X. Wang, W. Ran, and Q. Shen, "Optimization of medium composition for lipopeptide production from *Bacillus subtilis* N7 using response surface methodology," *Korean Journal of Microbiology and Biotechnology*, vol. 41, pp. 52–59, 2013.

[98] K. R. Meena, A. Sharma, R. Kumar, and S. S. Kanwar, "Two factor at a time approach by response surface methodology to aggrandize the *Bacillus subtilis* KLP2015 surfactin lipopeptide to use as antifungal agent," *Journal of King Saud University Science*, vol. 32, no. 1, pp. 337–348, 2020.

[99] X. Zhao, Y. Han, X.-q. Tan, J. Wang, and Z.-j. Zhou, "Optimization of antifungal lipopeptide production from Bacillus sp. BH072 by response surface methodology," *Journal of Microbiology*, vol. 52, no. 4, pp. 324–332, 2014.

[100] V. Rangarajan, G. Dhanarajan, R. Kumar, R. Sen, and M. Mandal, "Time-dependent dosing of Fe^{2+} for improved lipopeptide production by marine *Bacillus megaterium*," *Journal of Chemical Technology & Biotechnology*, vol. 87, no. 12, pp. 1661–1669, 2012.

[101] S. Mosquera, L. M. González-Jaramillo, S. Orduz, and V. Villegas-Escobar, "Multiple response optimization of *Bacillus subtilis* EA-CB0015 culture and identification of antifungal metabolites," *Biocatalysis and Agricultural Biotechnology*, vol. 3, no. 4, pp. 378–385, 2014.

[102] A. Wibisana, W. Sumaryono, W. Sumaryono, T. Mirawati Sudiro, and P. Pudjilestari Sudarmono, "Optimization of surfactin production by *Bacillus amyloliquefaciens* MD4-12 using response surface methodology," *Microbiology Indonesia*, vol. 9, no. 3, pp. 120–128, 2015.

[103] H. Hajfarajollah, B. Mokhtarani, A. Tohidi, S. Bazsefidpar, and K. Akbari Noghabi, "Overproduction of lipopeptide biosurfactant by *Aneurinibacillus thermoaerophilus* HAK01 in various fed-batch modes under thermophilic conditions," *RSC Advances*, vol. 9, no. 52, pp. 30419–30427, 2019.

[104] C. Sivapathasekaran, S. Mukherjee, A. Ray, A. Gupta, and R. Sen, "Artificial neural network modeling and genetic algorithm based medium optimization for the improved production of marine biosurfactant," *Bioresource Technology*, vol. 101, no. 8, pp. 2884–2887, 2010.

[105] G. Dhanarajan, V. Rangarajan, C. Bandi et al., "Biosurfactant-biopolymer driven microbial enhanced oil recovery (MEOR) and its optimization by an ANN-GA hybrid technique," *Journal of Biotechnology*, vol. 256, pp. 46–56, 2017.

[106] I. Ghazala, A. Bouallegue, A. Haddar, and S. Ellouz-Chaabouni, "Characterization and production optimization of biosurfactants by *Bacillus mojavensis* I4 with biotechnological potential for microbial enhanced oil recovery," *Biodegradation*, vol. 30, no. 4, pp. 235–245, 2019.

[107] I. Mnif, S. Ellouze-Chaabouni, and D. Ghribi, "Optimization of inocula conditions for enhanced biosurfactant production by *Bacillus subtilis* SPB1, in submerged culture, using box-behnken design," *Probiotics and Antimicrobial Proteins*, vol. 5, no. 2, pp. 92–98, 2013.

[108] K. R. Meena, T. Tandon, A. Sharma, and S. S. Kanwar, "Lipopeptide antibiotic production by *Bacillus velezensis* KLP2016," *Journal of Applied Pharmaceutical Science*, vol. 8, pp. 91–98, 2018.

[109] A. A. Jimoh and J. Lin, "Enhancement of paenibacillus sp. D9 lipopeptide biosurfactant production through the optimization of medium composition and its application for biodegradation of hydrophobic pollutants," *Applied Biochemistry and Biotechnology*, vol. 187, no. 3, pp. 724–743, 2019.

[110] D. Sun, J. Liao, L. Sun et al., "Effect of media and fermentation conditions on surfactin and iturin homologues produced by *Bacillus natto* NT-6: LC–MS analysis," *AMB Express*, vol. 9, 2019.

[111] S. Cortés-Camargo, N. Pérez-Rodríguez, R. P. Oliveira, S. B. E. B. Huerta, and J. M. Domínguez, "Production of biosurfactants from vine-trimming shoots using the halotolerant strain *Bacillus tequilensis* ZSB10," *Industrial Crops and Products*, vol. 79, pp. 258–266, 2016.

[112] H. Amani, M. Haghighi, M. H. Sarrafzadeh, M. R. Mehrnia, and F. Shahmirzaee, "Optimization of the production of biosurfactant from Iranian indigenous bacteria for the reduction of surface tension and enhanced oil recovery," *Petroleum Science and Technology*, vol. 29, no. 3, pp. 301–311, 2011.

[113] A. P. Kumar, A. Janardhan, B. Viswanath, K. Monika, J. Y. Jung, and G. Narasimha, "Evaluation of orange peel for biosurfactant production by *Bacillus licheniformis* and their

ability to degrade naphthalene and crude oil," *3 Biotech*, vol. 6, p. 43, 2016.

[114] R. Zouari, S. Ellouze-Chaabouni, and D. Ghribi, "Use of butter milk and poultry-transforming wastes for enhanced production of *Bacillus subtilis* SPB1 biosurfactant in submerged fermentation," *Journal of Microbiology, Biotechnology and Food Sciences*, vol. 4, no. 5, pp. 462–466, 2015.

[115] E. J. Gudiña, E. C. Fernandes, A. I. Rodrigues, J. A. Teixeira, and L. R. Rodrigues, "Biosurfactant production by *Bacillus subtilis* using corn steep liquor as culture medium," *Frontiers in Microbiology*, vol. 6, p. 59, 2015.

[116] D. Sharma, M. J. Ansari, S. Gupta, A. Al Ghamdi, P. Pruthi, and V. Pruthi, "Structural characterization and antimicrobial activity of a biosurfactant obtained from bacillus pumilus DSVP18 grown on potato peels," *Jundishapur Journal of Microbiology*, vol. 8, Article ID e21257, 2015.

[117] S. Soussi, R. Essid, J. Hardouin et al., "Utilization of grape seed flour for antimicrobial lipopeptide production by *Bacillus amyloliquefaciens* C5 strain," *Applied Biochemistry and Biotechnology*, vol. 187, no. 4, pp. 1460–1474, 2019.

[118] Y. Zhi, Q. Wu, and Y. Xu, "Production of surfactin from waste distillers' grains by co-culture fermentation of two *Bacillus amyloliquefaciens* strains," *Bioresource Technology*, vol. 235, pp. 96–103, 2017.

[119] N. Khondee, S. Tathong, O. Pinyakong et al., "Lipopeptide biosurfactant production by chitosan-immobilized Bacillus sp. GY19 and their recovery by foam fractionation," *Biochemical Engineering Journal*, vol. 93, pp. 47–54, 2015.

[120] G. Seghal Kiran, T. Anto Thomas, J. Selvin, B. Sabarathnam, and A. P. Lipton, "Optimization and characterization of a new lipopeptide biosurfactant produced by marine *Brevibacterium aureum* MSA13 in solid state culture," *Bioresource Technology*, vol. 101, no. 7, pp. 2389–2396, 2010.

[121] Z. Zhu, F. Zhang, Z. Wei, W. Ran, and Q. Shen, "The usage of rice straw as a major substrate for the production of surfactin by *Bacillus amyloliquefaciens* XZ-173 in solid-state fermentation," *Journal of Environmental Management*, vol. 127, pp. 96–102, 2013.

[122] P. Zhao, Y. Wang, S. Lie, X. Zhao, C. Jiang, and D. Y. Shao, "Junlin shi production of lipopeptide in solid state fermentation and their application in antifungal and heavy metal removal," *Brazilian Archives of Biology and Technology.*vol. 128, pp. 401–408, 2019.

[123] P. Narendra Kumar, T. H. Swapna, M. Y. Khan, G. Reddy, and B. Hameeda, "Statistical optimization of antifungal iturin A production from *Bacillus amyloliquefaciens* RHNK22 using agro-industrial wastes," *Saudi Journal of Biological Sciences*, vol. 24, no. 7, pp. 1722–1740, 2017.

[124] R. Zouari, S. Ellouze-chaabouni, and D. Ghribi-aydi, "Optimization of Bacillus subtilis SPB1 biosurfactant production under solid-state fermentation using by-products of a traditional olive mill factory," *Achievements of Life Sciences*, vol. 8, no. 2, pp. 162–169, 2015.

[125] Y. Meng, W. Zhao, J. You, and H. Gang, "Structural analysis of the lipopeptide produced by the *Bacillus subtilis* mutant R2-104 with mutagenesis," *Applied Biochemistry and Biotechnology*, vol. 179, pp. 973–985, 2016.

[126] H. Afsharmanesh, M. Ahmadzadeh, M. Javan-nikkhah, and K. Behboudi, "Improvement in biocontrol activity of *Bacillus subtilis* UTB1 against *Aspergillus flavus* using gamma-irradiation," *Crop Protection*, vol. 60, pp. 83–92, 2014.

[127] J. Zhao, Y. Li, C. Zhang et al., "Genome shuffling of *Bacillus amyloliquefaciens* for improving antimicrobial lipopeptide production and an analysis of relative gene expression using FQ RT-PCR," *Journal of Industrial Microbiology and Biotechnology*, vol. 39, no. 6, pp. 889–896, 2012.

[128] J. Zhao, L. Cao, C. Zhang, L. Zhong, J. Lu, and Z. Lu, "Differential proteomics analysis of *Bacillus amyloliquefaciens* and its genome-shuffled mutant for improving surfactin production," *International Journal of Molecular Sciences*, vol. 15, pp. 19847–19869, 2014.

[129] J. Zhao, C. Zhang, J. Lu, and Z. Lu, "Enhancement of fengycin production in *Bacillus amyloliquefaciens* by genome shuffling and relative gene expression analysis using RT-PCR," *Canadian Journal of Microbiology*, vol. 62, no. 5, pp. 431–436, 2016.

[130] J. Shi, X. Zhu, Y. Lu, H. Zhao, F. Lu, and Z. Lu, "Improving iturin A production of *Bacillus amyloliquefaciens* by genome shuffling and its inhibition against *Saccharomyces cerevisiae* in orange juice," *Frontiers in Microbiology*, vol. 9, p. 2683, 2018.

[131] X. Liang, R. Shi, M. Radosevich et al., "Anaerobic lipopeptide biosurfactant production by an engineered bacterial strain for in situ microbial enhanced oil recovery," *RSC Advances*, vol. 7, no. 33, pp. 20667–20676, 2017.

[132] Q. Wang, H. Yu, M. Wang, H. Yang, and Z. Shen, "Enhanced biosynthesis and characterization of surfactin isoforms with engineered *Bacillus subtilis* through promoter replacement and Vitreoscilla hemoglobin co-expression," *Process Biochemistry*, vol. 70, pp. 36–44, 2018.

[133] C. Luo, Y. Chen, X. Liu et al., "Engineered biosynthesis of cyclic lipopeptide locillomycins in surrogate host *Bacillus velezensis* FZB42 and derivative strains enhance antibacterial activity," *Applied Microbiology and Biotechnology*, vol. 103, no. 11, pp. 4467–4481, 2019.

[134] Y. Dang, F. Zhao, X. Liu et al., "Enhanced production of antifungal lipopeptide iturin A by *Bacillus amyloliquefaciens* LL3 through metabolic engineering and culture conditions optimization," *Microbial Cell Factories*, vol. 18, 2019.

[135] K. K. Sekhon, S. Khanna, and S. S. Cameotra, "Enhanced biosurfactant production through cloning of three genes and role of esterase in biosurfactant release," *Microbial Cell Factories*, vol. 10, no. 1, p. 49, 2011.

[136] F. François, J. Niehren, D. Dhali, M. John, V. Cristian, and J. Philippe, "Modeling leucine' s metabolic pathway and knockout prediction improving the production of surfactin , a biosurfactant from *Bacillus subtilis*," *Biotechnology Journal*, vol. 10, pp. 1216–1234, 2015.

[137] C. Fact, C. Wang, Y. Cao, Y. Wang, L. Sun, and H. Song, "Enhancing surfactin production by using systematic CRISPRi repression to screen amino acid biosynthesis genes in *Bacillus subtilis*," *Microbial Cell Factories*, vol. 18, 2019.

[138] S. Jiao, X. Li, H. Yu, H. Yang, X. Li, and Z. Shen, "In situ enhancement of surfactin biosynthesis in *Bacillus subtilis* using novel artificial inducible promoters," *Biotechnology and Bioengineering*, vol. 114, 2016.

[139] A. Adekilekun and J. Johnson, "Heterologous expression of S fp - type phosphopantetheinyl transferase is indispensable in the biosynthesis of lipopeptide biosurfactant," *Molecular Biotechnology*, vol. 61, pp. 836–851, 2019.

[140] F. F. C. Barros, A. N. Ponezi, and G. M. Pastore, "Production of biosurfactant by *Bacillus subtilis* LB5a on a pilot scale using cassava wastewater as substrate," *Journal of Industrial Microbiology & Biotechnology*, vol. 35, no. 9, pp. 1071–1078, 2008.

[141] N. A. Al-Dhabi, G. A. Esmail, and M. Valan Arasu, "Enhanced production of biosurfactant from *Bacillus subtilis* strain Al-Dhabi-130 under solid-state fermentation using

date molasses from Saudi arabia for bioremediation of crude-oil-contaminated soils," *International Journal of Environmental Research and Public Health*, vol. 17, no. 22, p. 8446, 2020.

[142] A. Saimmai, V. Sobhon, and S. Maneerat, "Molasses as a whole medium for biosurfactants production by Bacillus strains and their application," *Applied Biochemistry and Biotechnology*, vol. 165, no. 1, pp. 315–335, 2011.

[143] T. A. Ostendorf, I. A. Silva, A. Converti, and L. A. Sarubbo, "Production and formulation of a new low-cost biosurfactant to remediate oil-contaminated seawater," *Journal of Biotechnology*, vol. 295, pp. 71–79, 2019.

[144] I. J. B. Durval, A. H. M. Resende, M. A. Figueiredo, J. M. Luna, R. D. Rufino, and L. A. Sarubbo, "Studies on biosurfactants produced using Bacillus cereus isolated from seawater with biotechnological potential for marine oil-spill bioremediation," *Journal of Surfactants and Detergents*, vol. 22, no. 2, pp. 349–363, 2018.

[145] A. J. Das and R. Kumar, "Utilization of agro-industrial waste for biosurfactant production under submerged fermentation and its application in oil recovery from sand matrix," *Bioresource Technology*, vol. 260, pp. 233–240, 2018.

[146] M. J. Chaprão, R. d. C. F. S. da Silva, R. D. Rufino, J. M. Luna, V. A. Santos, and L. A. Sarubbo, "Production of a biosurfactant from Bacillus methylotrophicus UCP1616 for use in the bioremediation of oil-contaminated environments," *Ecotoxicology*, vol. 27, no. 10, pp. 1310–1322, 2018.

[147] P. R. F. Marcelino, G. F. D. Peres, R. Terán-Hilares et al., "Biosurfactants production by yeasts using sugarcane bagasse hemicellulosic hydrolysate as new sustainable alternative for lignocellulosic biorefineries," *Industrial Crops and Products*, vol. 129, pp. 212–223, 2019.

[148] Z. A. Raza, M. S. Khan, and Z. M. Khalid, "Physicochemical and surface-active properties of biosurfactant produced using molasses by a Pseudomonas aeruginosa mutant," *Journal of Environmental Science and Health. Part A, Toxic/hazardous Substances & Environmental Engineering*, vol. 42, pp. 73–80, 2007.

[149] Z. A. Raza, A. Rehman, M. S. Khan, and Z. M. Khalid, "Improved production of biosurfactant by a Pseudomonas aeruginosa mutant using vegetable oil refinery wastes," *Biodegradation*, vol. 18, pp. 115–121, 2007.

[150] R. S. Makkar and S. S. Cameotra, "Utilization of molasses for biosurfactant production by two Bacillus strains at thermophilic conditions," *Journal of the American Oil Chemists' Society*, vol. 74, no. 7, pp. 887–889, 1997.

[151] S. Joshi, C. Bharucha, S. Jha, S. Yadav, A. Nerurkar, and A. J. Desai, "Biosurfactant production using molasses and whey under thermophilic conditions," *Bioresource Technology*, vol. 99, no. 1, pp. 195–199, 2008.

[152] S. Nalini, R. Parthasarathi, and V. Prabudoss, "Production and characterization of lipopeptide from Bacillus cereus SNAU01 under solid state fermentation and its potential application as anti-biofilm agent," *Biocatalysis and Agricultural Biotechnology*, vol. 5, pp. 123–132, 2016.

[153] K. Paraszkiewicz, P. Bernat, A. Kusmierska, J. Chojniak, and G. Płaza, "Structural identification of lipopeptide biosurfactants produced by Bacillus subtilis strains grown on the media obtained from renewable natural resources," *Journal of Environmental Management*, vol. 209, pp. 65–70, 2018.

[154] M. Rani, J. T. Weadge, and S. Jabaji, "Isolation and characterization of biosurfactant-producing bacteria from oil well batteries with antimicrobial activities against food-borne and plant pathogens," *Frontiers in Microbiology*, vol. 11, p. 64, 2020.

[155] N. H. Md Badrul Hisham, M. F. Ibrahim, N. Ramli, and S. Abd-Aziz, "Production of biosurfactant produced from used cooking oil by Bacillus sp. HIP3 for heavy metals removal," *Molecules*, vol. 24, no. 14, p. 2617, 2019.

[156] N. Malfanova, L. Franzil, B. Lugtenberg, V. Chebotar, and M. Ongena, "Cyclic lipopeptide profile of the plant-beneficial endophytic bacterium Bacillus subtilis HC8," *Archives of Microbiology*, vol. 194, pp. 893–899, 2012.

[157] L. Sun, Z. Lu, X. Bie, F. Lu, and S. Yang, "Isolation and characterization of a co-producer of fengycins and surfactins, endophytic Bacillus amyloliquefaciens ES-2, from Scutellaria baicalensis Georgi," *World Journal of Microbiology and Biotechnology*, vol. 22, pp. 1259–1266, 2006.

[158] S.-Y. Kim, J. Y. Kim, S.-H. Kim et al., "Surfactin from Bacillus subtilis displays anti-proliferative effect via apoptosis induction, cell cycle arrest and survival signaling suppression," *FEBS Letters*, vol. 581, no. 5, pp. 865–871, 2007.

[159] X. Liu, X. Tao, A. Zou, S. Yang, L. Zhang, and B. Mu, "Efect of the microbial lipopeptide on tumor cell lines: apoptosis induced by disturbing the fatty acid composition of cell membrane," *Protein Cell*, vol. 1, pp. 584–594, 2010.

[160] C. L. Wang, T. B. Ng, F. Yuan, Z. K. Liu, and F. Liu, "Induction of apoptosis in human leukemia K562 cells by cyclic lipopeptide from Bacillus subtilis natto T-2," *Peptides*, vol. 28, pp. 1344–1350, 2007.

[161] S.-Y. Hong, D.-H. Lee, J.-H. Lee, M. A. Haque, and K.-M. Cho, "Five surfactin isomers produced during Cheonggukjang fermentation by Bacillus pumilus HY1 and their properties," *Molecules*, vol. 26, no. 15, p. 4478, 2021.

[162] W. Cheng, Y. Q. Feng, J. Ren, D. Jing, and C. Wang, "Antitumor role of Bacillus subtilis fmbJ-derived fengycin on human colon cancer HT29 cell line," *Neoplasma*, vol. 63, pp. 215–222, 2016.

[163] H. Yin, C. Guo, Y. Wang et al., "Fengycin inhibits the growth of the human lung cancer cell line 95D through reactive oxygen species production and mitochondria-dependent apoptosis," *Anti-Cancer Drugs*, vol. 24, no. 6, pp. 587–598, 2013.

[164] G. Dey, R. Bharti, P. K. Ojha et al., "Therapeutic implication of "Iturin A" for targeting MD-2/TLR4 complex to overcome angiogenesis and invasion," *Cellular Signalling*, vol. 35, pp. 24–36, 2017.

[165] G. Dey, R. Bharti, I. Banerjee et al., "Pre-clinical risk assessment and therapeutic potential of antitumor lipopeptide "Iturin A" in an in vivo and in vitro model," *RSC Advances*, vol. 6, no. 75, pp. 71612–71623, 2016.

[166] H. Zhao, X. Xu, S. Lei et al., "Iturin A-like lipopeptides from Bacillus subtilis trigger apoptosis, paraptosis, and autophagy in Caco-2 cells," *Journal of Cellular Physiology*, vol. 234, no. 5, pp. 6414–6427, 2019.

[167] H. Zhao, X. Zhao, S. Lei et al., "Effect of cell culture models on the evaluation of anticancer activity and mechanism analysis of the potential bioactive compound, iturin A, produced by Bacillus subtilis," *Food & Function*, vol. 10, no. 3, pp. 1478–1489, 2019.

[168] J. Jiang, H. Zhang, C. Zhang et al., "Production, purification and characterization of "iturin A-2"a lipopeptide with antitumor activity from Chinese sauerkraut bacterium Bacillus velezensis T701," *International Journal of Peptide Research and Therapeutics*, vol. 27, 2021.

[169] H. Zhao, J. Li, Y. Zhang et al., "Potential of iturins as functional agents: safe, probiotic, and cytotoxic to cancer cells," *Food & Function*, vol. 9, no. 11, pp. 5580–5587, 2018.

[170] H. Zhao, L. Yan, L. Guo et al., "Effects of *Bacillus subtilis* iturin A on HepG2 cells in vitro and vivo," *AMB Express*, vol. 11, no. 1, pp. 1–12, 2021.

[171] F. Yan, C. Li, X. Ye, Y. Lian, Y. Wu, and X. Wang, "Antifungal activity of lipopeptides from Bacillus amyloliquefaciens MG3 against *Colletotrichum gloeosporioides* in loquat fruits," *Biological Control*, vol. 146, Article ID 104281, 2020.

[172] K. Arima, A. Kakinuma, and G. Tamura, "Surfactin, a crystalline peptidelipid surfactant produced by *Bacillus subtilis*: isolation, characterization and its inhibition of fibrin clot formation," *Biochemical and Biophysical Research Communications*, vol. 31, no. 3, pp. 488–494, 1968.

[173] I. Geetha and A. M. Manonmani, "Surfactin: a novel mosquitocidal biosurfactant produced by *Bacillus subtilis* ssp. subtilis (VCRC B471) and influence of abiotic factors on its pupicidal efficacy," *Letters in Applied Microbiology*, vol. 51, pp. 406–412, 2010.

[174] G. Dehghan-Noudeh, M. Housaindokht, and B.-S. Fazly Bazzaz, "Isolation, characterization, and investigation of surface and hemolytic activities of a lipopeptide biosurfactant produced by *Bacillus subtilis* ATCC 6633," *Journal of Microbiology*, vol. 43, pp. 272–276, 2005.

[175] S. Y. Park, J.-H. Kim, S. J. Lee, and Y. Kim, "Involvement of PKA and HO-1 signaling in anti-inflammatory effects of surfactin in BV-2 microglial cells," *Toxicology and Applied Pharmacology*, vol. 268, no. 1, pp. 68–78, 2013.

[176] I. Dimkić, S. Stanković, M. Nišavić et al., "The profile and antimicrobial activity of *Bacillus lipopeptide* extracts of five potential biocontrol strains," *Frontiers in Microbiology*, vol. 8, p. 925, 2017.

[177] J. Lv, R. Da, Y. Cheng et al., "Mechanism of antibacterial activity of bacillus amyloliquefaciens c-1 lipopeptide toward anaerobic *Clostridium difficile*," *Biomed Research International*, vol. 2020, Article ID 3104613, 12 pages, 2020.

[178] X. Huang, Z. Lu, X. Bie, F. Lü, H. Zhao, and S. Yang, "Optimization of inactivation of endospores of Bacillus cereus by antimicrobial lipopeptides from *Bacillus subtilis* fmbj strains using a response surface method," *Applied Microbiology and Biotechnology*, vol. 74, no. 2, pp. 454–461, 2007.

[179] X. Liu, B. Ren, M. Chen et al., "Production and characterization of a group of bioemulsifiers from the marine *Bacillus velezensis* strain H3," *Applied Microbiology and Biotechnology*, vol. 87, pp. 1881–1893, 2010.

[180] C. Sivapathasekaran, S. Mukherjee, R. Samanta, and R. Sen, "High-performance liquid chromatography purification of biosurfactant isoforms produced by a marine bacterium," *Analytical and Bioanalytical Chemistry*, vol. 395, no. 3, pp. 845–854, 2009.

[181] B. H. Williams, Y. Hathout, and C. Fenselau, "Structural characterization of lipopeptide biomarkers isolated from *Bacillus globigii*," *Journal of Mass Spectrometry*, vol. 37, no. 3, pp. 259–264, 2002.

[182] A. L. Moyne, R. Shelby, T. E. Cleveland, and S. Tuzun, "Bacillomycin D: an iturin with antifungal activity against *Aspergillus flavus*," *Journal of Applied Microbiology*, vol. 90, pp. 622–629, 2001.

[183] G. S. Chitarra, P. Breeuwer, M. J. R. Nout, A. C. van Aelst, F. M. Rombouts, and T. Abee, "An antifungal compound produced by *Bacillus subtilis* YM 10-20 inhibits germination of *Penicillium roqueforti* conidiospores," *Journal of Applied Microbiology*, vol. 94, no. 2, pp. 159–166, 2003.

[184] S. Hiradate, S. Yoshida, H. Sugie, H. Yada, and Y. Fujii, "Mulberry anthracnose antagonists (iturins) produced by *Bacillus amyloliquefaciens* RC-2," *Phytochemistry*, vol. 61, pp. 693–698, 2002.

[185] Y. M. Li, N. I. A. Haddad, S. Z. Yang, and B. Z. Mu, "Variants of lipopeptides produced by Bacillus licheniformis HSN221 in different medium components evaluated by a rapid method ESI-MS," *International Journal of Peptide Research and Therapeutics*, vol. 14, pp. 229–235, 2008.

[186] N. Velmurugan, M. S Choi, S. S Han, and Y. S Lee, "Evaluation of antagonistic activities of *Bacillus subtilis* and *Bacillus licheniformis* against wood-staining fungi: in vitro and in vivo experiments," *Journal of Microbiology*, vol. 47, pp. 385–392, 2009.

[187] J. Wang, J. Yao, J. Liu, H. Chen, and J. Yao, "Characterization of *Fusarium graminearum* inhibitory lipopeptide from *Bacillus subtilis* IB," *Applied Microbiology and Biotechnology*, vol. 76, pp. 889–894, 2007.

[188] D. Romero, A. de Vicente, R. H. Rakotoaly et al., "The iturin and fengycin families of lipopeptides are key factors in antagonism of *Bacillus subtilis* toward *Podosphaera fusca*," *Molecular Plant-Microbe Interactions*, vol. 20, pp. 430–440, 2007.

[189] M. Hansen, C. Thrane, S. Olsson, and J. Sorensen, "Confocal imaging of living fungal hyphae challenged with the fungal antagonist viscosinamide," *Mycologia*, vol. 92, pp. 216–221, 2000.

[190] H. Desmyttere, C. Deweer, J. Muchembled et al., "Antifungal activities of *Bacillus subtilis* lipopeptides to two *Venturia inaequalis* strains possessing different tebuconazole sensitivity," *Frontiers in Microbiology*, vol. 10, p. 2327, 2019.

[191] S. R. Han, H. M. Munang'andu, I. K. Yeo, and S. H. Kim, "Bacillus subtilis inhibits viral hemorrhagic septicemia virus infection in olive flounder (*Paralichthys olivaceus*) intestinal epithelial cells," *Viruses*, vol. 13, no. 1, p. 28, 2021.

[192] R. K. Singla, H. D. Dubey, and A. K. Dubey, "Therapeutic spectrum of bacterial metabolites," *Indo Global Journal of Pharmaceutical Sciences*, vol. 2, no. 2, pp. 52–64, 2014.

[193] T. Chowdhury, P. Baindara, and S. M. Mandal, "LPD-12: a promising lipopeptide to control COVID-19," *International Journal of Antimicrobial Agents*, vol. 57, no. 1, Article ID 106218, 2021.

[194] L. Yuan, S. Zhang, J. Peng, Y. Li, and Q. Yang, "Synthetic surfactin analogues have improved anti-PEDV properties," *PLoS One*, vol. 14, no. 4, Article ID e0215227, 2019.

[195] G. Seydlová, R. Čabala, and J. Svobodová, "Biomedical engineering, trends, research and technologies," in *Surfactin—Novel Solutions for Global Issues*, vol. 13, pp. 306–330, InTech, Rijeka, Croatia, 2011.

[196] D. Vollenbroich, M. Özel, J. Vater, R. M. Kamp, and G. Pauli, "Mechanism of inactivation of enveloped viruses by the biosurfactant surfactin from *Bacillus subtilis*," *Biologicals*, vol. 25, no. 3, pp. 289–297, 1997.

[197] M. Deleu, J. Lorent, L. Lins et al., "Effects of surfactin on membrane models displaying lipid phase separation," *Biochimica et Biophysica Acta (BBA) - Biomembranes*, vol. 1828, no. 2, pp. 801–815, 2013.

[198] O. S. Ostroumova, V. V. Malev, M. G. Ilin, and L. V. Schagina, "Surfactin activity depends on the membrane dipole potential," *Langmuir*, vol. 26, no. 19, pp. 15092–15097, 2010.

[199] M. N. Nasir and F. Besson, "Interactions of the antifungal mycosubtilin with ergosterol-containing interfacial

monolayers," *Biochimica et Biophysica Acta*, vol. 1818, no. 5, pp. 1302–1308, 2012.

[200] P. Das, S. Mukherjee, and R. Sen, "Antiadhesive action of a marine microbial surfactant," *Colloids and Surfaces B: Biointerfaces*, vol. 71, no. 2, pp. 183–186, 2009.

[201] M. Juola, K. Kinnunen, K. F. Nielsen, and A. von Right, "Surfactins in Natto: the surfactin production capacity of the starter strains and the actual surfactin contents in the products," *Journal of Food Protection*, vol. 77, no. 12, pp. 2139–2143, 2014.

[202] R. Zouari, S. Besbes, S. Ellouze-Chaabouni, and D. Ghribi-Aydi, "Cookies from composite wheat–sesame peels flours: dough quality and effect of *Bacillus subtilis* SPB1 biosurfactant addition," *Food Chemistry*, vol. 194, pp. 758–769, 2016.

[203] C. Jiang, X. Chen, S. Lei, H. Zhao, Y. Liu, and J. Shi, "Lipopeptides from *Bacillus subtilis* have potential application in the winemaking process: inhibiting fungal and ochratoxin A contamination and enhancing esters and acids biosynthesis," *Australian Journal of Grape and Wine Research*, vol. 23, no. 3, pp. 350–358, 2017.

WILEY | Hindawi

Research Article
"*Pseudomonas fluorescens*" as an Antagonist to Control Okra Root Rotting Fungi Disease in Plants

Harsha Sharma [ID],[1] **Mohd Anul Haq** [ID],[2] **Ashok Kumar Koshariya** [ID],[3] **Anil Kumar** [ID],[4] **Sandeep Rout** [ID],[5] and **Karthikeyan Kaliyaperumal** [ID][6]

[1]*Faculty of Science, Motherhood University, Roorkee, Haridwar, Uttarakhand, India*
[2]*Department of Computer Science, College of Computer Science and Information Science, Majmaah University, AL-Majmaah 11952, Saudi Arabia*
[3]*Department of Plant Pathology, School of Agriculture, Lovely Professional University Jalandhar, Jalandhar, Punjab, India*
[4]*Department of Botany, DDU Gorakhpur University, Gorakhpur 273009, India*
[5]*Faculty of Agriculture, Sri Sri University, Cuttack, Odisha 754006, India*
[6]*IT @ IoT - HH Campus, Ambo University, Ambo, Ethiopia*

Correspondence should be addressed to Karthikeyan Kaliyaperumal; karthikeyan@ambou.edu.et

The common bacteria found in fruit and vegetables are *Pseudomonas fluorescens* which is Germ-negative and is rod-shaped. *Pseudomonas fluorescens* has been originated from the rhizosphere of Roorkee-grown okra. The presented work involves recognizing and controlling the isolates of *Pseudomonas fluorescens*. The scope of the proposed work is that the technique used here is a unique strategy to plant protection and control of rotting fungus diseases based on the recognition and management of *Pseudomonas fluorescens* isolates. Antagonist effect occurs commonly in vegetable and fruit plants. The main goal of this study is to isolate, identify, and evaluate the development of these bacteria which effects on plant growth. In this research work, five isolates have been chosen for further research based on their morphological, biochemical, and physiological characteristics. All five isolates have been identified as *Pseudomonas fluorescens* from Bergey's Manual for the determination of bacteriology. Catalase, urease, amylase, and citrate utilization test were all positive in all of the isolates. PFTT4 was identified to be a likely strain for all plant growth promoting exercises such as age of IAA, HCN, ammonia, and phosphate solubilization subsequent to being assessed for their plant development advancing properties. Further, in vitro exploring uncovered that PFTT4 diminished the development of phytopathogens such as *Fusarium solani* and extraordinarily further developed seed germination just as all development boundaries like shoot and root length. Furthermore, *Pseudomonas* sp. PFTT4's plant growth promoting and antifungal activities put forward to it could be there used because of bioinoculant agents for *Abelmoschus esculentus*.

1. Introduction

For plant health, the rhizosphere (the area of soil around and enveloping the plant root) is crucial. *Pseudomonas* is an important rhizosphere chemical, and a specific strain, together with lady finger, has been demonstrated to boost plant physical condition in a variety of crops. Pseudomonads are being researched intensively over the world to determine if they can be employed as crop protection and soil health maintainers. They are the bacterial groups in the rhizosphere with the most metabolic and functional flexibility. Interactions between soil bacteria and plants in the rhizosphere can help, hinder, or impair plant growth. The growth and development of biological control agents as an alternative, ecologically friendly technique for protecting agricultural and horticultural crops against bacterial and fungal diseases have sparked attention due to environmental and customer concerns. Furthermore, protection against many illnesses is

necessary for plant and animal development. The initial effort to separate PGPR from the rhizosphere top soil of Roorkee-developed okra is depicted in flow. The rhizosphere provides an ideal home for soil microorganisms due to the high supplement accessibility via root exudates. The plant rhizosphere is an important soil biological environment for plant-microbe interactions. Contingent upon the sort of microorganisms, soil supplement status, protection framework, and soil climate, colonization through a scope of microbes in and around the roots can result in symbiotic, associative, naturalistic, or parasitic relationship inside the plant. Okra (*Abelmoschus esculentus*), a popular vegetable in many nations, has global economic and nutritional significance. This vegetable crop is widely produced and used for economical purposes on the planet. The pseudomonads are now being studied extensively over the world to see whether they can be used to protect groupings. Plant growth can be aided, delayed, or hampered by interactions between soil bacteria crops and preserve soil health. They are the rhizosphere's most metabolically and functionally flexible bacterial and plants in the rhizosphere.

Pseudomonads are the world's generally assorted and naturally applicable bacterial gathering. *Pseudomonas* strains secrete many of the chemicals such as gibberellins and solubilize phosphate, cytokinins, and auxins, they generate HCN and siderophores, and lytic enzymes stimulate plant development and are hence referred to be plant growth promoting rhizobacteria. All nonpathogenic rhizobacteria and a few separates of *Pseudomonas aeruginosa*, *Pseudomonas aureofaciens*, *Pseudomonas fluorescens*, and *Pseudomonas putida* smothered soil-borne microorganisms by creating optional metabolites, for example, antitoxins, protease, HCN, and siderophore. The rhizobacteria is enhancing plant development while also acting as biocontrol agents which might be a feasible solution. According to various researches, pseudomonads have been found to protect okra from infections that cause illness.

Vegetable developing spaces of the world, *Fusarium* spp. and *Rhizoctonia solani,* are significant soil-borne contagious contaminations of both nursery and field created ladies fingers, causing cataclysmic sicknesses, for example, root spoils and shrink, and at last diminished yield creation and quality. Chemical fungicides are mostly used to combat these infections. However, the widespread use of these chemicals poses a threat to the environment as well as human health.

As a result, alternate techniques to plant disease control should be highlighted. Plant growth promoting rhizobacteria with biocontrol capacity could be a viable option. Pseudomonads have been shown to prevent pathogens that cause disease in okra, according to several. The goal of this study was to seclude, distinguish, and assess the development advancing and adversarial impacts of a few *Pseudomonas fluorescens* effects on okra plants in Roorkee, India.

2. Materials and Method

2.1. Isolation of Pseudomonas Fluorescens from the Rhizospheric Soil. Okra seedlings were tenderly eliminated from different fields in Roorkee; these all transported toward the laboratory into sterilized plastic bags. Until further processing, each one trial is kept into the refrigerator on 4°-5°C (showed in Table 1). Okra rhizospheric dirt was removed and dried by air. 1 gram of soil was weighed, and successive dilutions were performed before plating on King's *B* plates and incubating for 24–36 hours at 28°C. Pure cultures were kept for further use lying slant on NAM (nutrient agar medium) at 4°-5°C temperature [1].

2.2. Gram Staining for Identification. I took a clean slide and prepared thin smear of old culture be created and heat fixed. For about 1 minute, a couple of drops of precious crystal violet reagent are put on the smear. Using running tap water, I washed the slide. I used Gram's iodine to flood the smear and let it sit for 2 minutes. Drop by drop, ethyl alcohol (95%) was used to decolorize the stain. For 2–4 minutes, I poured a few drops of safranine. I washed the slide in faucet water and mount it in oil emulsion or glycerine before taking a gander at it under a magnifying lens (microscope) [2].

2.3. CT (Catalase Test). A drop of hydrogen peroxide (30%) was applied to the test culture on a clean slide, and the reported to result of bubbles was seen [3].

2.4. IP (Indole Production) Test. After autoclaving, each bacterial culture was injected separately in test tubes containing 5 ml tryptone broth. One test tube was preserved when in charge of, with no bacterial culture inoculated. 1 ml of Kovac's reagent was added to each tube, including the control, after 48 hours of incubation. After a 10–15-minute break, the tubes were gently moistened. [4] To allowing the reagent to rise to the top, the tubes were allowed to stand [5].

2.5. MRVP (Methyl Red and Voges-Proskauer) Test. Before autoclaving, the MRVP broth prepared and 6 ml of it were poured in each test tube. Four test tubes were kept as controls, and the bacterial culture was put into all of the others. The test was incubated at 28°–32°C for 24–48 hours. 05 drops of MR indicator were added to each test tube [6]. The control and the color change was observed. In the same way, for incubated test tubes and the control, 8–10 drops of Voges-Proskauer-I reagent and 2 drops of Voges-Proskauer-II reagent were used. The color change in the test tubes was observed and compared to the control [7].

2.6. CU (Citrate Utilization) Test. Simmon's citrate agar slants were formed and the bacterial culture was streaked on them. For 36–48 hours, the tubes were incubated at 28°–32°C. It was noticed that the slants' color changed [8].

2.7. Urease Production Test. Sticking an inoculating loop into the butt (bottom of the tube) and streaking the slants in a wavy pattern were used to inoculate urea agar slants [9]. The results were seen after 24 hours of incubation at 27°-28°C. The tubes were placed in front of a control.

TABLE 1: Morphological and biochemical characterization of *Pseudomonas fluorescens*.

Parameter	Isolates				
	PFTT1	PFTT2	PFTT3	PFTT4	PFTT5
Shape	Coccus	Coccus	Rod	Rod	Rod
Colonies	Circle	Circle	Circle	Circle	Circle
Colony growth	Slow growth	Fast growth	Slow growth	Fast growth	Fast growth
Colonies growth	Light greenish	Yellowish green	Yellowish green	Yellowish green	Light green
Gram staining	+	+	+	+	+
MR test	+	−	+	+	+
VP test	−	+	−	−	−
Citrate utilization test	−	−	−	−	−
Urease test	+	+	−	+	+
Starch hydrolysis test	−	−	+	−	−
Catalase test	+	+	−	+	+
Indole test	−	−	+	−	−
Carbohydrate fermentation					
Mannitol	+	+	+	+	+
Dextrose	−	+	−	−	+
Lactose	+	+	+	+	+
Sucrose	−	+	−	−	+

2.8. Starch Hydrolysis Test. Inoculated cultures were placed on starch agar plates and incubated at 28–30°C for 48 hours. Plates with healthy bacteria were soaked with iodine solution for 30 seconds using a dropper. The surplus iodine solution was poured out [10]. The result showed the formation of clear and clean zones around each isolate's line of growth, for example, a change in medium color.

2.9. CFT (Carbohydrate Fermentation Test). First, we took the tubes of broth that had been sweetened with 4 different color sweeteners (0.5% of each, for example, dextrose, mannitol, lactose, and sucrose); one Durham tube has been submerged in each tube [11]. The test culture tubes were cultured for 24–26 hours at 28°–30°C. Signs of acid or gas generation, such as a change in color or the creation of bubbles, were examined for in the tubes.

2.10. IAA (Indole Acetic Acid) Production. Mansoor's description of IAA manufacturing was confirmed (2007) [12]. L-Tryptophan (0.1 g/l) was injected into bacterial colonies in nutrient broth. At 4°C, exponentially growing cultures were centrifuged for 15 minutes at 10000 rpm [12]. Two drops of Salkowski reagent were added to the supernatant (2 ml) (1 ml of 0.5 M $FeCl_3$ in 50 ml of 35 percent $HClO_4$). The appearance of pink color confirmed the presence of IAA.

2.11. Phosphate Solubilization. The capability of isolates to solubilize phosphate was tested using Pikovskaya's agar plates [13]. The plates were checked and used for the appearance of clearing zones surrounding the colonies after 4 days of incubation at 281°C (appropriate to solubilization of inert phosphate by producing macrobiotic acid by microorganisms).

2.12. Zinc Solubilization. Zinc solubilization by microbes was carried out according to Sayyed's method (2005) [6]. The bacteria were identified using Tris-minimal media plates

containing zinc phosphate and a pH indicator called bromophenol blue [14].

2.13. HCN Production. Modified approach was used to determine HCN production (2010). Isolates' exponentially growing cultures (108 cells/ml) were streaked on solid agar plates supplemented with 4.4 g glycine/I, filter paper soaked in 0.5% picric acid in 1% Na_2CO_3 added to the upper lid of the plates at the same time [15]. Para film was used to seal the plates. After 48–72 hours of incubation at 281°C, the hue changed from yellow to light brown, sensible brown, or strong brown, indicating possible HCN production [16, 17].

2.14. Ammonia Production. A bacterial isolate will be tested in peptone water to see if it can generate ammonia. 48-hour-old cultures were incubated in 08 ml peptone water and incubated at 28°–30°C for 70–72 hours [18, 19]. On the culture broth over the slide, 0.5 mL Nessler's reagent was applied. A yellow to brown precipitation emerged within a few minutes, indicating moderate to high ammonia production Chen et al. [20].

2.15. Antagonistic Activities. The development of secluded strains contrary to the parasitic infection *Fusarium solani* was measured using a dual culture approach (MTCC 3871) [21, 22]. Agar blocks (5 mm in diameter) were inserted in the centre of the assay plate from the margin of a 5-day-old fungal pathogen culture. One loop (24-hour-old) isolated strain culture founded 02 cm away from the pathogen. Plates were incubated for 3–7 days at 281°C [23]. The hindrance zone was determined utilizing the recipe: inhibition zone (rate) = 100C−T/C, where C addresses spiral development in charge and T addresses outspread development in double culture Aarab et al. [24].

2.16. Bacterization of Seed. Bacterial strains (PFTT1–PFTT5) were refined in supplement stock for 48 hours in a shaker at 281°C. At 4°C, the cultures were centrifuged for 15 minutes at 8000 rpm. To achieve a final population density of 1 108 cells/ml, the way of life supernatants were disposed of and the pellets were washed and suspended in sterile refined water. Independently, bacterial cell suspensions were joined with 1% CMC answers for structure slurry, which was then covered on the outer layer of seeds. Okra seeds covered with a 1% CMC slurry were utilized as a manage.

2.17. Germination of Seed. For the pot examine, sterile nursery soil was utilized. The dirt was ground into fine particles before being sanitized in a 160°C broiler for 2 hours. Okra seeds were gathered from the Roorkee neighborhood market. We picked solid seeds that were comparative in structure and size in sets of three, bacterized seeds were planted in the pots. Seeds treated with just 1% CMC were utilized as a benchmark grouping. As necessary, the pots are watered. The following were the treatments: T1, *Pseudomonas* spp. bacterized seeds PFTT1; T2, *Pseudomonas* spp. bacterized seeds PFTT2; T3, *Pseudomonas* spp. bacterized seeds PFTT3; T4; *Pseudomonas* spp. bacterized seeds PFTT4; T5, *Pseudomonas* spp. bacterized seeds PFTT5. Up to 21 DAS, root weight, shoot length, shoot weight, root length, and germination percentage were considered.

3. Result

3.1. Isolation of Pseudomonas fluorescens. Rhizobacteria samples were secluded from okra using King's medium and a serial dilution approach. On the basis of early investigation, total 5 isolates (PFTT1, PFTT2, PFTT3, PFTT4, and PFTT5) were examined. The urease, citrate utilization, catalase production, and MRVP synthesis all were positive, whereas indole production was negative in all five. Furthermore, IAA production was reported in all isolates, with PFTT5 exhibiting the brightest pink hue. The experiment's outcomes are depicted in a variety of tables and flowcharts. It was discovered that PFTT4 may be used as bioinoculants for okra and other harvests because it has excellent plant growth and boosting properties such as IAA age and phosphate solubility.

3.2. Gram Staining and Morphological Characteristics. Isolate colonies form is described as spherical and yellow green in color. Gram negative and rod-shaped isolates were discovered in every case.

3.3. Biochemical Characterization. The whole of the disengaged (PFTT1, PFTT2, PFTT3, PFTT4, and PFTT5) were observed to be positive for urease, citrate usage, and catalase creations and starch hydrolysis however was negative for indole creation and MRVP creation (Table 1).

3.4. Indole Acetic Acid Production. IAA production was discovered in all five *Pseudomonas* spp. isolates (PFTT1,

PFTT2, PFTT3, PFTT4, and PFTT5). The deepest pink color produced by PFTT5 indicated the highest indole acetic acid production (Table 2).

3.5. Phosphate Solubilization and Zinc Solubilization. On Pikovskaya's agar plate, all of the confines are fit to make clear corona around the spot vaccination. Phosphate solubilization ability was demonstrated in such clearing zones around the bacteria (Table 2). Because there were no halo zones around the colonies, not any of the isolate was capable to solubilization of zinc (Table 2).

3.6. HCN and Ammonia Production. Aside from PFTT3, the whole disengage of *Pseudomonas fluorescens* framed HCN is shown through a change in channel paper tone. As shown by the serious earthy colored shade of the pass through a channel paper, PFTT4 delivered the most HCN (Table 2). In peptone stock, all of disengage produced alkali by creating yellowish earthy colored accelerates (Table 2 and Figure 1).

3.7. Antagonist Activity. The whole of the *Pseudomonas* disconnects were tried for *Fusarium solani* opposing action. The development of test microorganisms on PDA plates at 28°C was stifled by *Pseudomonas* spp. PFTT4. The term of hatching compares to an expansion in parasitic restraint. Following 7 days of hatching, *Pseudomonas* spp. PFTT4 had the option to obstruct 42% of *Fusarium solani*, as per the normal outspread development restraint rate (Table 2).

3.8. Pot Trial Studies. *Pseudomonas* spp. disconnects were utilized to bacterize okra seeds of uniform shape and size (PFTT1 to PFTT5). Following 22 days of planting in pots, seeds closed up with the aforementioned microbial inoculants showed initiated vegetative qualities. *Pseudomonas* sp. PFTT4 had the best seed germination, shoot, and root length. Shoot new and dry weight, just as root new and dry weight, showed comparative expansion propensities. The medicines with *Pseudomonas* spp. PFTT1, PFTT4, and PFTT5 delivered the best number of plants. *Pseudomonas* sp. PFTT4 bacterized okra seeds brought about an extensive expansion in seed germination rate (82.2%), trailed by PFTT5 (75.8%). Seed germination was 40% in the control treatment (Table 3). In contrast with the control, each of the measurements was upgraded and was huge at 1% and additionally 5%. Figure 2 shows the graph scale of *Pseudomonas fluorescens* effect on seed germination and vegetative growth of okra.

In a pot trial investigation, okra seed bacterized with *Pseudomonas fluorescens* PFTT5 showed critical expansion in shoot length, root length, and dried shoot and root weight. PFTT4 and PFTT5 treated seeds germination rates were 83.3 percent and 76.7 percent, separately.

4. Discussion

Flow research depicts the starting exertion finished to isolate PGPR from the rhizospheric top soil of Roorkee-developed okra. Due to the high supplement accessibility as root

TABLE 2: Plant growth promoting activities of *Pseudomonas fluorescens* and *Abelmoschus esculentus*.

Isolations	IAA	Zinc solubilization	Phosphate solubilization	Ammonia production	HCN production	Antagonist
PFTT1	+	++	−	−	+	−
PFTT2	++	+	−	++	+++	+
PFTT3	++	+	−	+	+	−
PFTT4	+	++	−	−	+	−
PFTT5	++	+	−	++	+++	+

A−, IAA positive; IAA negative, +, B−, +, phosphate solubilization positive, −, phosphate solubilization negative, +, little radiances <0.5 cm wide encompassing provinces; −, absence of corona development; ++, medium coronas >0.5 cm wide encompassing settlements; +++, enormous radiances >1.0 cm wide encompassing states.
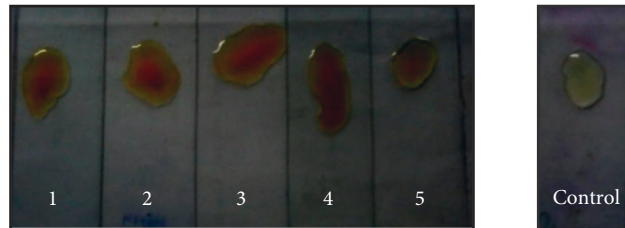
FIGURE 1: Plant growth promoting activities of *Pseudomonas fluorescens*.

TABLE 3: *Pseudomonas fluorescens* effect on seed germination and vegetative growth of okra.

Isolates	Seed germination (%)	Root length (cm)	Shoot length (cm)	Root weight (g)		Shoot weight (g)	
				Fresh wt.	Dry wt.	Fresh wt.	Dry wt.
PFTT1	65.7	3.567*	4.80**	0.0210*	0.1**	0.232**	0.10*
PFTT2	62.5	4.325	3.465**	0.016**	0.012**	0.215^{ns}	0.90^{ns}
PFTT3	60.00	3.68**	3.44**	0.112^{ns}	0.006^{ns}	0.186^{ns}	0.103*
PFTT4	82.2	5.896**	4.322**	0.32*	0.012**	0.432*	0.117**
PFTT5	75.8	4.100^{ns}	3.400**	0.018^{ns}	0.007*	0.240^{ns}	0.220*
Control	39.0	55.7	2.57*	4.70**	0.210*	0.01**	0.22**
SEM		52.5	4.25	2.45**	0.16**	0.011**	0.25^{ns}
CD at 1%		060.0	3.867^{ns}	3.444**	0.0112^{ns}	0.006^{ns}	0.186^{ns}
CD at 5%		65.7	3.567*	4.25**	0.21*	0.01**	0.23**

SEM = standard blunder mean; CD = critical differences. values are mean of 3 arbitrarily chose plants from each set; **huge at 01%; *huge at 5% when contrasted with control; NS = nonhuge when contrasted with control (nonfactorized seeds).

exudates, the rhizosphere gives an optimal environment to soil microorganisms. The number of inhabitants in organic entities that live in a given climate is special and is impacted by the physical and natural components that exist in that climate. Additionally, Patel et al. utilized King's medium to extricate 10 fluorescent pseudomonad strains from assorted rhizospheric soil of yield plants such as rice, maize, and bazar [11]. Kumar et al. recognized 115 *Pseudomonas fluorescens* isolates from the rhizosphere of soybean in Cirebon, Plumbon, Indonesia [5]. All of the detaches tried positive for catalase, citrate use, urease age, and starch hydrolysis, yet negative for indole blend and MRVP.

IAA production was discovered in all of the isolates. In PBRI, Haridwar, India, bacteria that produce indole acetic acid have been shown to stimulate root elongation and plant growth. The development of natural acids, for example, gluconic, acidic, lactic, fumaric, and succinic acids is connected to phosphate solubilization by bacterial separates. The easiest way of plant bacterial identification is physical evaluation of crop heredity and set up of appropriate samples. Through this way, we can easily detect and diagnosed plant diseases. But, the modern techniques such as AI

play crucial role in detecting the plant diseases in early stages and diagnosed in time.

Natural corrosive amalgamation brings down soil pH, bringing about the age of H^+, which replaces Ca^{2+} and discharges HPO_4^{2-} into the dirt arrangement. *Pseudomonas* and *Bacillus* were recognized as the essential phosphate solubilizes by Ashrafuzzaman et al. [21]. Immunization utilizing phosphate solubilizing microbes further developed maize development and grain yield, cut compost uses, and brought down ozone depleting substance outflows, as per Mandal et al. [13]. As per Verma et al., 70% of their detached is suitable for solubilize phosphate in the scope of 5.8 to 13.45 mg/100 ml and advance chickpea improvement [3]. These investigations back up our decision.

Except for PFTT3, all detaches that twisted the shade of the channel paper from yellow to orange-brown were assigned HCN makers [4]. *Pseudomonas* spp. produces HCN, which represses the development of phytopathogens, as per Saad [8]. The plant growth promoting activities play an important role for the development of plant through many ways. Plant growth can be aided, delayed, or hampered by interactions between soil bacteria crops and preserve soil
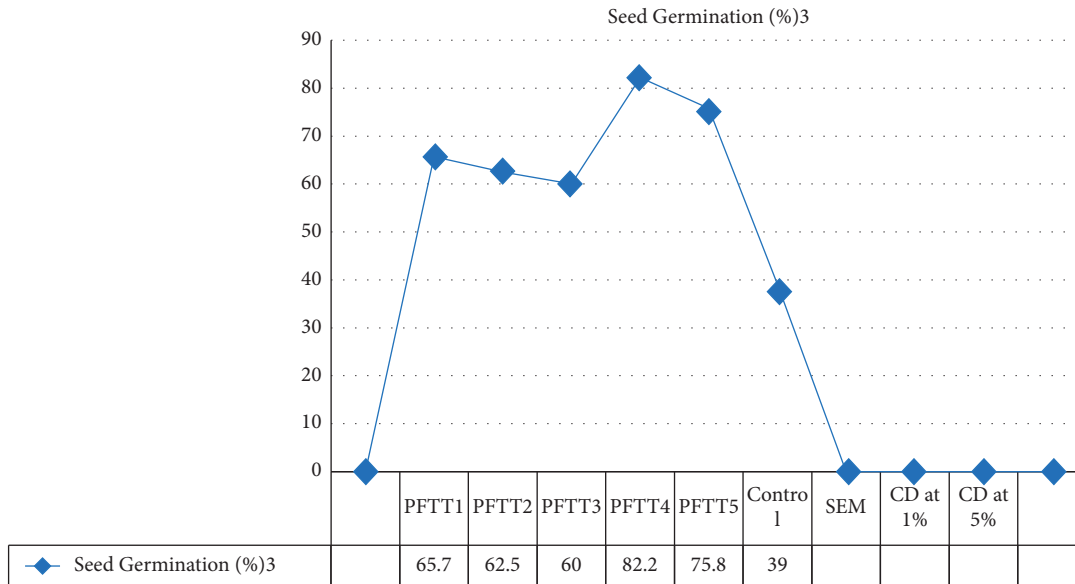
FIGURE 2: Graph scale of *Pseudomonas fluorescens* effect on seed germination and vegetative growth of okra.

health. Furthermore, in vitro studies revealed that PFTT4 inhibited the growth of phytopathogens such as *Fusarium solani* and significantly improved seed germination, as well as all development parameters such as shoot and root length.

HCN is a wide range antibacterial atom occupied with organic control of root contaminations by various plant connected fluorescent pseudomonads, as indicated by León et al. [25]. In this examination, every one of the disconnected life forms was observed to be acceptable smelling salt makers. Also, Kaur and Sharma discovered smelling salts age in 95% of *Bacillus* secludes and 94.2 percent of *Pseudomonas* disconnects, which upholds our discoveries [15]. The shading changes from brown to yellow tone were a positive test for alkali creation [11].

PFTT4 was observed in the direction of suppressing *Fusarium solani* growth (in vitro) in our investigation. Wahyudi et al. found that *Pseudomonas* spp. have antifungal efficacy against *Fusarium solani* [2]. Mansoor et al. discovered that using *P. aeruginosa* and *P. lilacinus* alone or in combination effectively controlled *F. solani*. In the benchmark group, only 40% of seeds developed (uninoculated seeds) [12]. These discoveries are like those of Sayyed et al.'s who found that immunizing wheat seed with *P. fluorescens* NCIM 5096 expanded the pace of germination by 10% [6]. Ashrafuzzaman et al. showed an increment in seed germination when rice seeds were pretreated with plant growth promoting rhizobacteria detaches [21]. Likewise asserting this, plant growth promoting rhizobacteria worked on nut development and seed rise.

As a consequence, alternative plant disease control approaches should be promoted. Rhizobacteria that enhance plant development while also acting as biocontrol agents might be a feasible solution. According to various researches, pseudomonads have been found to protect okra from infections that cause illness. Regarding plant-microbe interactions, the plant rhizosphere is a crucial biological habitat in the soil. Colonization by a variety of microbes

outside the roots can result in a symbiosis, associative, naturalistic, or parasitic interaction within the plant, depending on the kind of microorganisms, soil supplement status, protective framework, and soil temperature.

Therefore, it is feasible to presume that *Pseudomonas* spp. bacterial strains will gather more consideration in the field of biofertilization and natural control due to their multifunctional capacities. *Pseudomonas* spp. (PFTT4), which have great plant development boosting characteristics such as IAA age, phosphate solubilization, HCN creation, alkali creation, and biocontrol, could be utilized as bioinoculants for okra and different harvests, as per the current review [20].

5. Conclusion and Future Scope

Due to environmental and consumer concerns, the development of biological control agents as an alternative, environmentally acceptable strategy for safeguarding agricultural and horticultural crops against bacteria, and fungi diseases has generated interest. Moreover, the growth of plants and animals depends on protection from various diseases. *Pseudomonas fluorescens* is a Germ-negative, rod-shaped bacterium commonly found in fruits and vegetables. *Pseudomonas fluorescens* has been derived from the rhizosphere of Roorkee-grown okra. The work provided here focuses on identifying and managing *Pseudomonas fluorescens* isolates. The presented work is a novel approach towards protection and to control rotting fungi diseases in plants by recognisation and controlling the isolates of *Pseudomonas fluorescens*. The entire focus of the study is to seclude, distinguish, and assess the development advancing the impacts of these bacteria on plant growth. Five different isolates were chosen which are based on their morphological, biochemical, and physiochemical characteristics. These are PFTT1, PFTT2, PFTT3, PFTT4, and PFTT5. All five were observed to be positive for urease, citrate usage, catalase

creation, and MRVP creation, however, negative for indole production. Moreover, IAA production was discovered for all isolates and it was found that deepest pink color was observed in PFTT5. The results of the experiment have been illustrated though various tables and flowcharts. It was observed that PFTT4, having great plant development and boosting characteristics such as IAA age and phosphate solubilisation, can be used as bioinoculants for okra and different harvests. However, further understanding of the components involved, as well as the signaling interaction between antagonist, pathogen, soil, and plants is required in the future to promote biocontrol agents as broadly applicable biofertilizers.

Data Availability

The data shall be made available on request.

Conflicts of Interest

The authors declare that they have no conflicts of interest.

References

[1] M. Yazdani, M. A. Bahmanyar, H. Pirdashti, and M. A. Esmaili, "Effect of phosphate solubilization microorganisms (PSM) and plant growth promoting rhizobacteria (PGPR) on yield and yield components of corn (*Zea mays* L.)," *World Academy of Science, Engineering and Technology*, vol. 49, pp. 90–92, 2009.

[2] A. T. Wahyudi, R. I. Astuti, and N. Giyanto, "Screening of *Pseudomonas* sp. isolated from rhizosphere of soybean plant as plant growth promoter and biocontrol agent," *American Journal of Agricultural and Biological Sciences*, vol. 6, no. 1, pp. 134–141, 2011.

[3] J. P. Verma, J. Yadav, and K. N. Tiwari, "Application of *Rhizobium* sp. BHURC01 and plant growth promoting rhizobactria on nodulation, plant biomass and yields of chickpea (*Cicer arietinum* L.)," *International Journal of Agricultural Research*, vol. 5, no. 3, pp. 148–156, 2010.

[4] K. V. B. R. Tilak, N. Ranganayaki, K. K. Pal et al., "Diversity of plant growth and soil health supporting bacteria," *Current Science*, vol. 89, pp. 136–150, 2005.

[5] A. Suresh, P. Pallavi, P. Srinivas, P. V. Kumar, J. S. Chandran, and R. S. Reddy, "Plant growth promoting activities of fluorescent pseudomonads associated with some crop plants," *African Journal of Microbiology Research*, vol. 4, no. 14, pp. 1491–1494, 2010.

[6] R. Sayyed, M. D. Badgujar, H. M. Sonawane, M. M. Mhaske, and S. B. Chincholkar, "Production of microbial ironchelators (siderophores) by fluorescent pseudomonads," *Indian Journal of Biotechnology*, vol. 4, pp. 484–490, 2005.

[7] V. S. Saravanan, S. R. Subramoniam, and S. A. Raj, "Assessing in vitro solubilization of different zinc solubilizing bacterial (ZBS) isolates," *Brazilian Journal of Microbiology*, vol. 34, pp. 121–125, 2003.

[8] M. M. Saad, "Destruction of *Rhizoctonia solani* and *Phytophthora capsici* causing okra root-rot by *Pseudomonas fluorescens* lytic enzymes," *Research Journal of Agriculture and Biological Sciences*, vol. 2, pp. 274–281, 2006.

[9] A. Ramette, M. Frapolli, G. Défago, and Y. Moënne-Loccoz, "Phylogeny of HCN synthase-encoding hcnBC genes in biocontrol fluorescent pseudomonads and its relationship with host plant species and HCN synthesis ability," *Molecular Plant-Microbe Interactions*, vol. 16, no. 6, pp. 525–535, 2003.

[10] C. L. Patten and B. R. Glick, "Role of *Pseudomonas putida* indole acetic acid in the development of host plant root system," *Canadian Journal of Microbiology*, vol. 59, pp. 220–224, 2002.

[11] R. R. Patel, V. R. Thakkar, and B. R. Subramanian, "A *Pseudomonas guariconensis* strain capable of promoting growth and controlling collar rot disease in *Arachis hypogaea* L." *Plant and Soil*, vol. 390, no. 1-2, pp. 369–381, 2015.

[12] F. Mansoor, V. Sultana, and S. Ehteshamul-Haque, "Enhancement of biocontrol potential of *Pseudomonas aeroginosa* and *Paecilomyces lilacinus* against root rot of mungbean by a medicinal plant *Launaeanudi caulis* L." *Pakistan Journal of Botany*, vol. 39, pp. 2113–2119, 2007.

[13] S. Mandal, N. Mallick, and A. Mitra, "Salicylic acid-induced resistance to *Fusarium oxysporum* f. sp. lycopersici in tomato," *Plant Physiology and Biochemistry*, vol. 47, no. 7, pp. 642–649, 2009.

[14] D. Ushakov, L. Cherkasova, and K. Shatila, "Environmental management system and its impact on productivity," *IOP Conference Series: Earth and Environmental Science*, vol. 937, no. 2, Article ID 022037, 2021.

[15] N. Kaur and P. Sharma, "Screening and characterization of native *Pseudomonas* sp. as plant growth promoting rhizobacteria in chickpea (*Cicerarietinum* L.) rhizosphere," *African Journal of Microbiology Research*, vol. 7, no. 16, pp. 1465–1474, 2013.

[16] M. Karthikeyan, K. Radhika, S. Mathiyazhagan, R. Bhaskaran, R. Samiyappan, and R. Velazhahan, "Induction of phenolics and defense-related enzymes in coconut (*Cocos nucifera* L.) roots treated with biocontrol agents," *Brazilian Journal of Plant Physiology*, vol. 18, no. 3, pp. 367–377, 2006.

[17] K. D. Kamble and D. K. Galerao, "Indole acetic acid production from *Pseudomonas* species isolated from rhizosphere of garden plants in Amravati," *International Journal of Advances in Pharmacy Biology and Chemistry*, vol. 4, no. 1, pp. 23–31, 2015.

[18] O. Sivash, D. Ushakov, and M. Ermilova, "Investment process resource provision in the agricultural sector," *IOP Conference Series: Earth and Environmental Science*, vol. 272, no. 3, Article ID 032118, 2019.

[19] R. Dey, K. K. Pal, D. M. Bhatt, and S. M. Chauhan, "Growth promotion and yield enhancement of peanut (*Arachis hypogaea* L.) by application of plant growth-promoting rhizobacteria," *Microbiological Research*, vol. 159, no. 4, pp. 371–394, 2004.

[20] Y. Chen, X. Shen, H. Peng, H. Hu, W. Wang, and X. Zhang, "Comparative genomic analysis and phenazine production of *Pseudomonas chlororaphis*, a plant growth-promoting rhizobacterium," *Genomics Data*, vol. 4, pp. 33–42, 2015.

[21] M. Ashrafuzzaman, F. A. Hossen, M. R. Ismail et al., "Efficiency of plant growth promoting rhizobacteria (PGPR) for the enhancement of rice growth," *African Journal of Biotechnology*, vol. 8, pp. 1247–1252, 2009.

[22] G. Roland, S. Kumaraperumal, S. Kumar, A. D. Gupta, S. Afzal, and M. Suryakumar, "PCA (principal component analysis) approach towards identifying the factors determining the medication behavior of Indian patients: an empirical study," *Tobacco Regulatory Science*, vol. 7, no. 6-1, pp. 7391–7401, 2021.

[23] M. F. Abdel-Monaim, "Induced systemic resistance in okra plants against fusarium wilt disease," in *Proceedings of the 2nd*

Minia Conference for Agriculture and Environmental Science, pp. 253–263, Minia, Egypt, March 2010.

[24] S. Aarab, F. J. Ollero, M. Megías, A. Laglaoui, M. Bakkali, and A. Arakrak, "Isolation and screening of bacteria from rhizospheric soils of rice fields in northwestern Morocco for different plant growth promotion (PGP) activities: an *in vitro* study," *International Journal of Current Microbiology and Applied Sciences*, vol. 4, no. 1, pp. 260–269, 2015.

[25] R. H. León, D. R. Solís, M. C. Pérez et al., "Characterization of the antifungal and plant growth-promoting effects of diffusible and volatile organic compounds produced by *Pseudomonas fluorescens* strains," *Biological Control*, vol. 81, pp. 83–92, 2015.

WILEY | Hindawi

Research Article

Design and Evaluation of a Hybrid Technique for Detecting Sunflower Leaf Disease Using Deep Learning Approach

Arun Malik [ID],[1] Gayatri Vaidya [ID],[2] Vishal Jagota [ID],[3] Sathyapriya Eswaran [ID],[4] Akash Sirohi [ID],[1] Isha Batra [ID],[1] Manik Rakhra [ID],[1] and Evans Asenso [ID][5]

[1]*Department of Computer Science and Engineering, Lovely Professional University, Phagwara, Punjab 144411, India*
[2]*Department of Studies in Food Technology, Davangere University, Davangere, Karnataka, India*
[3]*Department of Mechanical Engineering, Madanapalle Institute of Technology & Science, Madanapalle, Andhra Pradesh, India*
[4]*Department of Agricultural Extension, Amrita School of Agricultural Sciences, Amrita Vishwa Vidyapeetham University, Coimbatore 642109, India*
[5]*Department of Agricultural Engineering, School of Engineering Sciences, University of Ghana, Accra, Ghana*

Correspondence should be addressed to Evans Asenso; easenso@ug.edu.gh

Agriculture and plants, which are a component of a nation's internal economy, play an important role in boosting the economy of that country. It becomes critical to preserve plants from infection at an early stage in order to be able to treat them. Previously, recognition and classification were carried out by hand, but this was a time-consuming operation. Nowadays, deep learning algorithms are frequently employed for recognition and classification tasks. As a result, this manuscript investigates the diseases of sunflower leaves, specifically *Alternaria* leaf blight, *Phoma* blight, downy mildew, and *Verticillium* wilt, and proposes a hybrid model for the recognition and classification of sunflower diseases using deep learning techniques. VGG-16 and MobileNet are two transfer learning models that are used for classification purposes, and the stacking ensemble learning approach is used to merge them or create a hybrid model from the two models. This work makes use of a data set that was built by the author with the assistance of Google Images and comprises 329 images of sunflowers divided into five categories. On the basis of accuracy, a comparison is made between several existing deep learning models and the proposed model using the same data set as the original comparison.

1. Introduction

Sunflower originated in 2100 BCE in Mexico, and it is also known as *Helianthus*. Sunflower seeds and their leaves have several uses and benefits. Sunflower can be used for food because it has many nutrients in its seeds and leaves. Sunflower roots have the soaking ability by which it is able to soak the radioactive substance too. It is also a good source of vitamins. Due to its therapeutic properties, sunflower is also used in the treatment of various diseases such as malaria, arthritis by reducing swelling, gastroenteritis, chest pain, and respiratory tract disorders. Sunflower leaves have properties that can cure insect bites, snake bites, spider bites, headaches, etc. Its leaves have diuretic properties by which it can

cure bladder disorders, and it can also act as an antioxidant. Sunflower leaves have several uses in animal husbandry and many industries. Sunflower leaves are affected by many diseases, but in this thesis, *Alternaria* leaf blight, *Phoma* blight, downy mildew, and *Verticillium* wilt are considered:

Alternaria leaf blight: *Alternaria helianthi* is the fungal plant pathogen responsible for *Alternaria* leaf blight, as shown in Figure 1. South Africa is the major area of *Alternaria* diseases. It is a potential disease occurring in the producing areas of sunflower.

Symptoms: concentric rings of 0.2–0.5 mm diameter with dark brown to black lesion appear on the leaves and stems. When the spores on the leaves or stems

FIGURE 1: *Alternaria* leaf blight.

FIGURE 2: Downy mildew.

come in the contact of moisture and start penetrating, then the infection process starts.

Treatment: fungicides are sprayed directly on infected plants, coupled with improved sanitation and crop rotation.

Downy mildew: this disease is caused by a plant pathogen called *Plasmopara halstedii*. *Plasmopara halstedii* oospores produce thin walls, which are resistant structures, sexually produced that are fundamental for its continuation, as shown in Figure 2. Entering a territory, the annihilation of the microbe is troublesome because of the arrangement of oospores, which can stay in soil for a long time.

Symptoms: initial symptoms are visible on the upper surface like large, angular or blocky, yellow areas. They rapidly expand and become brown-like lesions, mature. The under surface of infected leaves appears water-soaked.

Phoma blight: this disease is caused by the plant pathogenic fungus called *Phoma macdonaldii*, as shown in Figure 3, and it is also a common disease caused by soil-borne fungi.

Symptoms: this is perceived as a huge dull sore on the stem, begins from the leaf and reaches the petiole. The enormous patches on the tail become generally perceptible after the petal drops.

Treatment: 4-year crop rotation is a good treatment for curing *Phoma* blight, which reduces the disease by controlling stem weevil.

Verticillium wilt: *Verticillium dahliae*, a soil-borne fungus, is the main cause of the disease. It is also called "Vert," and it starts from the lower leaves and moves to the whole leaves, as shown in Figure 4.

Sunflower and its leaves have various uses and benefits. They are beneficial for human beings, animals, and the environment; so if it gets infected, then it is a big loss to the environment. If we can identify or recognize the diseases in the initial stage, then we can save the sunflower plant and its leaves, thus saving the environment and source of many nutrients. There are some ancient methods and some

FIGURE 3: *Phoma* blight.

FIGURE 4: *Verticillium* wilt.

computer vision methods to classify or recognize the diseases in the earlier stage.

In the past, diseases were classified manually without the use of electronic devices, which required more time, was more expensive, and had a higher chance of error because the entire process was carried out by humans. However, computer vision (also known as machine learning) has made it possible to reduce the processing time of classification and also provide better accuracy than the manual method. It is also capable of classifying multiple images at the same time. In the field of machine learning, there are three main learning approaches: supervised learning, unsupervised

learning, and reinforcement learning. In machine learning, there are many different approaches, such as linear regression, decision tree, logistic regression, SVM, random forest, Naive Bayes, KNN, and k-means. Although machine learning algorithms give decent accuracy, they fall short of the target, i.e., we were unable to identify images with high accuracy when employing machine learning algorithms. When it comes to text value prediction and categorization, machine learning algorithms are the most effective tools. Deep learning began to have an influence on picture categorization at around this time.

Early identification and prediction of plant diseases is one of the most crucial needs for developing agriculture, which is important to our country's economy. It supports the economy and feeds a large population. And, by earlier detection, we can conserve the plants and avoid losses. Deep learning techniques are frequently used to classify or forecast outcomes [1, 2]. Deep learning techniques are used as active methods for the classification of plant diseases [3], and the main classifier used is convocational neural network (CNN). The CNN is one of the most recommended models for the classification or recognition with the help of images whether we have a large or small data set [4]. As deep learning dynamically analyses structured characteristics, there is no need to manually design the feature extraction function and classifier. Deep learning methods surpass machine learning as image classifiers with CNN being the best. The CNN is widely recognized as the finest and most effective image classifier on both small and large data sets, and it serves as the foundation for all deep learning models [5, 6]. It is a basic deep learning model used for the classification of images according to some patterns or features. One of the best properties is that CNN trained in a supervised manner with the help of existing data [7]. The CNN is a basic architecture over which many models are formed such as AlexNet, GoogLeNet, and LeNet. The CNN architecture is presented in Figure 5. The CNN attains the name of best image recognition system and is the most recommended system for the purpose of recognition and classification [8]. It performs well in the plant disease detection task. It is the finest technique for object identification. Any neural architecture should be able to be paired with any feature exactor, depending on the requirements. Data preprocessing is necessary for models to operate correctly. Many infections (viral or fungal) may be difficult to identify due to overlapping signs [9, 10].

Other strategies are based on ensemble learning, which is used to develop several models and then merge the models with the assistance of ensemble methods to enhance the results. Most of the time, the ensemble technique outperforms the single model in terms of performance. Some of the ensemble approaches are bagging (also known as boosting), majority voting (also known as weighted average), and stacking (also known as stacking ensemble). In this research, two approaches of ensemble learning technique—namely, stacking ensemble and weighted average technique—are applied, and the outcomes of the both are compared with one another.

2. Related Work

Zhong and Zhao [11] used the DenseNet-121 deep learning technique to classify the 6 apple diseases with three methods for which they used the data set of 2462 images, and they concluded that their proposed method gave the accuracy of 93.51%, 93.31%, and 93.71%, respectively.

Ji et al. [12] proposed a CNN based on an integrated method to classify the grape leaf diseases for which they used a data set from the PlantVillage database, and they concluded that their proposed method gave 99.17% and 98.57% accuracy for validation and test, respectively.

Uguz and Uysal [13] developed a CNN model to classify the olive leaf diseases, i.e., *Aculus olearius* and olive peacock spot disease. They used the data set of 3400 olive images from Turkey and used the transfer learning techniques, i.e., VGG-16 and VGG-19, and they concluded that their proposed model gave an accuracy of 95%.

Nanehkaran et al. [14] proposed a CNN method for the detection of leaf diseases, and they divided their method into two parts—image segmentation and image classification; they also proposed a segmentation algorithm based on intensity and LAB. They concluded that their proposed method gave a detection accuracy of 75.59%.

Jiang et al. [15] proposed the hybrid method of CNN and SVM to classify rice diseases. They used CNN for the feature extraction of disease images and then used SVM for the classification of the diseases with a 10-fold cross-validation method. They concluded that their proposed method gave a test accuracy of 96.8%.

Ghosal et al. [16] developed a CNN model with the help of VGG-16 for the classification of rice leaf diseases, and to train the model, they created their own data set of rice images and concluded that their method gave an accuracy of 92.46%.

Jasim et al. [3] proposed a method for the detection and classification of tomatoes, pepper, and potato leaf diseases. They collected 20,636 images from the PlantVillage database to make their data set. They classified 12 leaf disease classes and 3 healthy leaf classes with the help of the CNN method concluded that their model gave a training accuracy of 98.29%, and 98.029% for testing.

Md. Rasel Howlader et al. in [17] have studied guava leaf diseases, using deep CNN to see infection, and their designs characterise for important diseases, for example, algal leaf area, whitefly, and rust. They collected their own data set and even developed their own model. They conclude that their model gave an accuracy of 98.74%.

The mango leaf disease called anthracnose was managed by Singh et al. [18]. In their study, they tried to suggest a concept in addition to a monetarily savvy program for which they make use of a multilayer convolutional neural community (MCNN). They prepared their model with a continuing image on the Faculty of J&K. They concluded their unit provided an accuracy of 97.13% for sickness called anthracnose.

Geetharamani and Arun [19] proposed a disease ID type of a novel grow leaf which is determined by Deep CNN. They prepared the model of theirs with a receptive dataset of thirty-nine photos as well as groundwork photographs. This
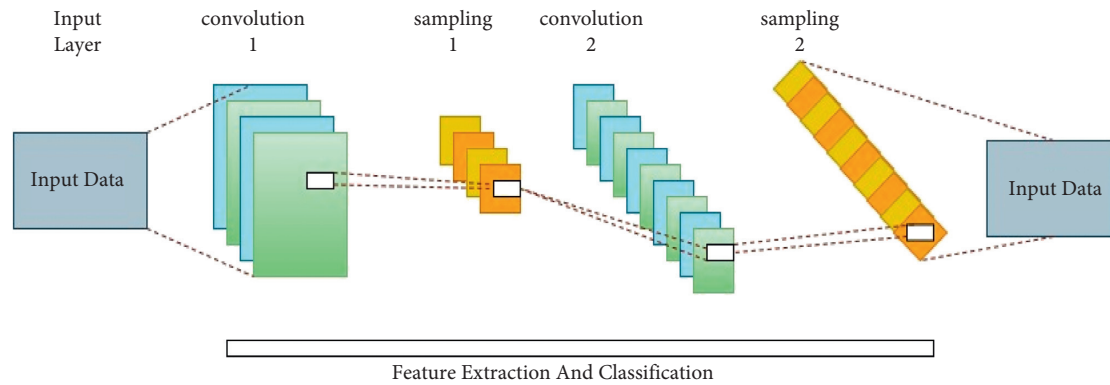
Figure 5: CNN architecture.

study includes six parameters on photos as turn, gamma remedy, clamor infusion, PCA, and scaling, and then photo flipping is utilized by them. They declared due to the exercise exhibitions on the purposed method are expanded. They contrast the model of theirs and also the previous body as well as the main reason which their unit provides much better results with 96.46% exactness.

Jiang et al. [20] took care of 5 types of infection in apple leaves by making use of the deep learning approach based on improved convolutional neural structures. Same authors prepared the model of theirs with frequent photographs of apple leaf within the wake of using a few images controlling methods. They used the GoogLeNet system in addition to upgraded CNN and the utilisation of INAR (SSD with Inception component as well as Rainbow connection) when designing a Panasonic phone. The proposed model yields 78.80 percent exactness with an excellent place velocity of 23.13 fps, which was substantially better than prior versions.

Akshay and Vani [21] made sure that the convolutional neural structure would become the greatest technique to perceive the maladies. They proposed a unit to evaluate the infection of tomato foliage and created their very own data set from the PlantVillage database. They stated that their model provided 99.25% precision. They compared their model with different neural networks such as ResNet-50, VGGNet, and also LeNet.

Hasan et al. [22] tried to find the right technique to figure out the jute diseases (chlorosis along with yellowish mosaic). Jute was selected for the very first time. They used 600 images as a data set and also inferred their proposed method provided 96% exactness without using any image-creating method.

Mohit Agarwal et al. in [23] tried to find out the diseases within apple foliage through the use of neural telephone system strategies. They released a data set from the town's grow the town initiative. They utilised a multilayer neural network to create their suggested style and also compare it to two CNN models, InceptionV3 and VGG16, to determine which model is more specific than the others and also provides 99% accuracy, as well as additionally determine which their unit captures seven seconds for screening.

A neural method to cluster the ailments of vegetation using an image was proposed by Sijiang Huang et al. in [24]. A unique deep neural network structure in this study is used that can accurately categorise plant kinds and illness using a single picture of a plant leaf. The proposed model is composed of two sub-models: a leaf segmentation model that utilises a U-Net to effectively separate the leaves in the original image from the background, and a plant disease classification model that utilises two-head network to classify plant diseases using features extracted from various popular pre-trained models. Experiments reveal that final model obtains a classification accuracy of 0.9807 for plants and a disease identification accuracy of 0.8745.

Singh [25] focused on the use of sunflower in oil production and agriculture areas. He mentioned that it is difficult to detect the damage or disease of sunflower for a full farm. Therefore, he proposed an algorithm for segmenting and classifying the images of sunflower leaf. The practical swarm optimization method is used for the classification of disease.

Sujithra and Ukrit [26] identified that it is not easy to figure out the disease on the leaf as most of the leaves are found damaged. They analyzed various deep leaning and image processing methods to classify the disease. Furthermore, it was said that neutral network algorithms like support vector help identifying and classifying leaf diseases.

Montecchia et al. [27] recognized that the soil-borne disease that affect sunflower is SVW (sunflower *Verticillium* wilt and leaf mottle). They carried out their work in infected fields of the Argentina region. This paper highlights the various disease descriptors depending on disease incidence and severity. This paper presents a way for resisting the SVW of sunflower.

Huu Quan Cap et al. in [28] ascertain that identification of growing diseases was accomplished in a couple of ways: they used only a small photo, i.e., a few of the tips of the photograph as information, and on the off chance that they used a continuous photo, they saved additional time by utilising a leaf limitation method with deep understanding. Additionally, their technical precision was 78 percent within 2.0fps.

Zhang et al. [29] dealt with the ID and also evaluation of maize leaf problems. It basically focused on the various

TABLE 1: Summary of various crops, their diseases, and the referred models and their accuracy.

Author	Crop	Disease	Model used	Accuracy
Yong Zhong and Ming Zhao	Apple	All disease	DenseNet-121	93.71%
Miaomio Ji et al.	Grape	Black rot, esca, and isariopsis leaf spot	CNN	99.17% (validation) and 98.57% (testing)
Sinan Uguz and Nese Uysal	Olive	*Aculus olearius* and olive peacock spot diseases	VGG-16 and VGG-19	95%
Junde Chen et al.	Plants	Common	MobileNet-V2	99.85% (public data set) and 99.11% (collected data set)
Y.A. Nanehkaran et al.	Plants	Common	CNN + LAB	75.59%
Shreya Ghosal et al.	Rice	Leaf blast, leaf blight, and brown spot	VGG-16	92.46%
Marwan Adnan Jasim et al.	Tomato, pepper, and potato	Common	CNN	98.29% (training) and 98.029% (testing)
Junde Chen et al.	Plants	Common	VGGNet + ImageNet	91.83% and 92%
Md. Rasel Howlader et al.	Guava	Whitefly, algal leaf spot, and rust	D-CNN	98.74%
Uday Pratap Singh et al.	Mango	Anthracnose	MCNN	97.13%
Geetharamani G. and Arun Pandian	Plants	Common	D-CNN	96.46%
Md. Zahid Hasan et al.	Jute	Chlorosis and yellow mosaic	CNN	96%
Sijiang Huang et al.	Plants	Common	U-Net and ResNet	98.07% (classification) and 87.45% (recognition)
S. Santhana Hari et al.	Plants	Common	CNN	86%
Sammy V. Militante et al.	Plants	Common	CNN	96.5%
Mercelin Francis and C. Deisy	Apple and tomato	Common	CNN	87%
Jayme Garcia Arnal Barbedo	Plants	Common	CNN	87%
Md. Helal Sheikh et al.	Maize and peach	Gray leaf spot corn, common rust corn, and bacterial spot peach	CNN	99.28%
Mehmet Metin Ozguven and Kemal Adem	Sugar beet	Low, severe, and low and severe	Faster R-CNN	95.48%
Malik Hashmat Shadab et al.	Sugarcane	*Cercospora* leaf spot, helminthosporium leaf spot, rust, red rot, and yellow leaf disease	YOLO + FR-CNN	93.20%
Radhamadhab dalai and Kishore Kumar Senapati	Plants	Bacterial canker, gray mold, blossom end rot, and whitefly	R-CNN	75.43%, 67.85%, 72.13%, and 49.87%
A.S.M. Farhan Al Haque et al.	Guava	Anthracnose, fruit rot, and fruit canker	CNN	95.61%
Sukhvir Kaur et al.	Plants	Common	Machine learning	—
Siddharth Singh Chouhan et al.	Plants	Common	BRBFNN	89%
Huu Quan Cap et al.	Plants	Common	CNN	78%
Robert G. de Luna et al.	Tomato	*Phoma* rot, leaf miner, and target spot	FR-CNN	91.67%
Rutu Gandhi et al.	Plants	Common	CNN + GANs	—
Konstantinos P. Feretinos	Plants	Common	VGG	99.53%
K.R. Aravind et al.	Maize	*Cercospora* leaf spot, common rust, and leaf blight	SVM	83.7%
Edna Chebet Too et al.	Plants	Common	DenseNet	99.75%
Halil Durmus et al.	Tomato	Yellow leaf curl, bacterial spot, early blight, late blight, leaf mold, Septoria leaf spot, spider mites, target spot, and mosaic virus	AlexNet and SqueezeNet	95.65% and 94.3%
Usama Mokhtar et al.	Tomato	Powdery mildew and early bright	SVM	99.5%
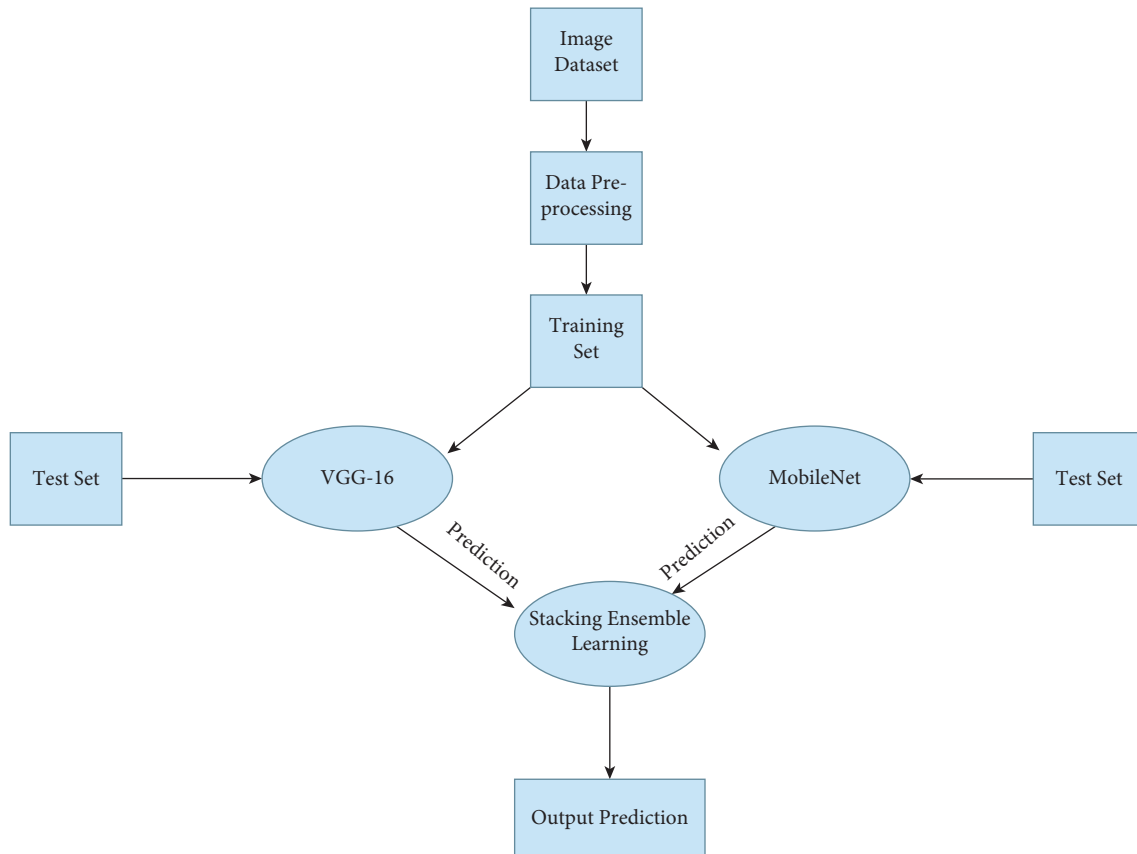
FIGURE 6: Proposed hybrid technique's work flow.

diseases on maize leaf that can occur and also focused on how to mitigate those diseases. With the assistance of the CIFAR10, they found nine distinct diseases and also to increase precision of the model on various epochs the model was hyper-tuned. After hyper-tuning, the model researchers obtained 98.9 percent accuracy, while with Cifar10, accuracy achieved was 98.8 percent. They demonstrate how it is possible to increase precision by increasing the number of pooling activities, and they also supplied the long-term value by consolidating brand-new calculations to increase precision or even discriminate brand-new maize diseases.

de Luna et al. [30] had taken a go from the 3 ailments of tomato leaves: *Phoma* rot, target spot, and leaf miner. They used Diamante Max's kind of tomato for examining. They produced a motor-controlled image-capturing package that catches images from every side of a leaf. They used CNN of deep learning; they compared their model with previous designs such as Fast R-CNN giving 80% accuracy and transfer learning providing 95.57% exactness and inferred that their model provided 91.67% accuracy.

Table 1 presents a summary of various crop diseases and their detection models. Thus, it is understood that the detection of crop diseases is crucial for agricultural production, quality management, and decision-making. Several projects in this field have focused on deep learning, namely, deep

CNN. Although CNNs are powerful and required image processing, deep CNNs are need to be used to diagnose plant diseases [31, 32].

3. Proposed Hybrid Model for Detecting Sunflower Leaf Diseases

This work proposes a hybrid deep learning model for classifying sunflower illnesses using images, which is based on a deep learning hybrid model. Two models—VGG-16 and MobileNet—are combined, and one of the ensemble learning techniques, stacking, is used to learn the new model combination. Due to the fact that ensemble models outperform single models in terms of accuracy, the ensemble learning approach is applied in this situation. The accuracy of some existing deep learning techniques was calculated in order to select these two models. It was discovered that VGG-16 and MobileNet provide better results than the others, with 81% and 86% accuracy, respectively. Furthermore, pretrained networks are best suited for small size data sets, and because our data set is small in size, these two pretrained networks were selected for this work. The approaches of ensemble learning stacking and weighted average are used in conjunction with each other. The work flow of the proposed technique is shown in Figure 6.

Geometric transformations such as rotation, shifts, scale, zoom, and flip were accomplished via the use of image

```
       start:
 (1)   import numpy, sklearn, tensorflow, keras as np1, sk, tf, kr
 (2)   def convert_img_array(img):
       If img not None:
       Return array of img
       else
       Return np1.array[]
 (3)   for I in imgdir://....imgdir contains list of images
       imgList[].append(convert_img_array(img))
       labelList[].append(i.label)//...i.label gives label or class of each images
 (4)   modify labelList with label_binarizer library
 (5)   image_list = np1.array(imgList, dtype = np.float16)/225.0
 (6)   train_test_split(image_list, labelList, 0.2,3)
 (7)   do Augmentation with Keras.ImageDataGenerator()
 (8)   Implement Models:
       from keras.applications.vgg16 import VGG16
       from keras.applications.mobilenet import MobileNet
 (9)   models[].append(VGG16() & MobileNet)
(10)   for i in range models:
       Models[i].fit_transform();//to train the models
(11)   Now combine prediction values;
       For i in range models:
       Yhat = models[i].prediction(); //stacked data set
(12)   Now create stacked model
       stackedx = call process 11
       Model = LogisticRegression();
13     Now to train the stacked model:
       Model.fit(stackedx, test_x);
(14)   Now store prediction value of stacked model:
       Yhat = Model.predict(stackedx)
(15)   Now calculate accuracy:
       Sklearn.accuracy_score(yhat, test_y)
       end;
```

ALGORITHM 1: Technique for detecting sunflower leaf disease.
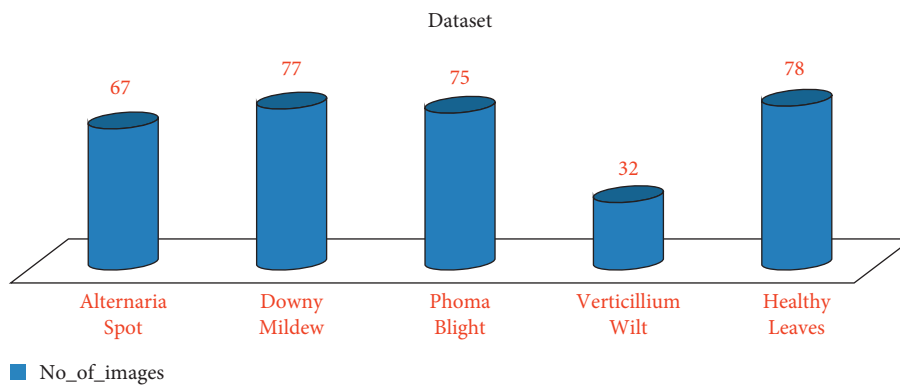
FIGURE 7: Data set.

augmentation in this paper. The ImageDataGenerator from Keras was used for the data augmentation process. In addition to improving the images, this strategy helps to prevent overfitting by using a batch size number that selects images for training purposes in a random manner. The algorithm for the suggested hybrid approach is detailed in the next section.

4. Results and Discussion

This section compares the proposed hybrid technique with the existing techniques on the basis of recognition or classification of sunflower leaf diseases. Data sets play an important role in classification or anything because if we do not have any data, then there is no meaning for
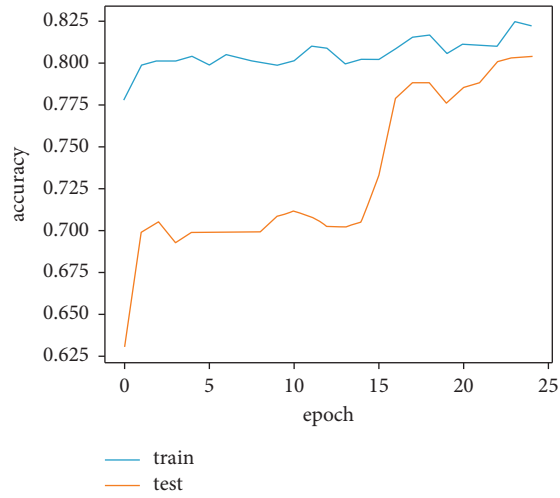
FIGURE 8: AlexNet.
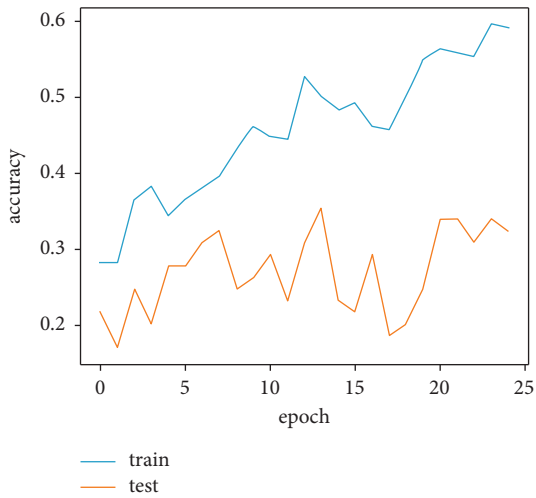
FIGURE 9: CNN.
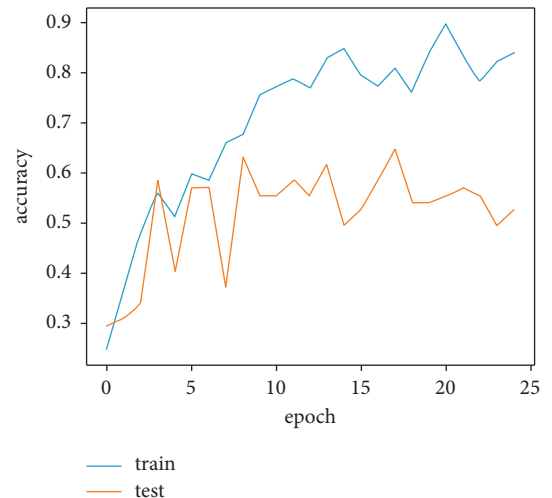
FIGURE 11: Inception_V3.
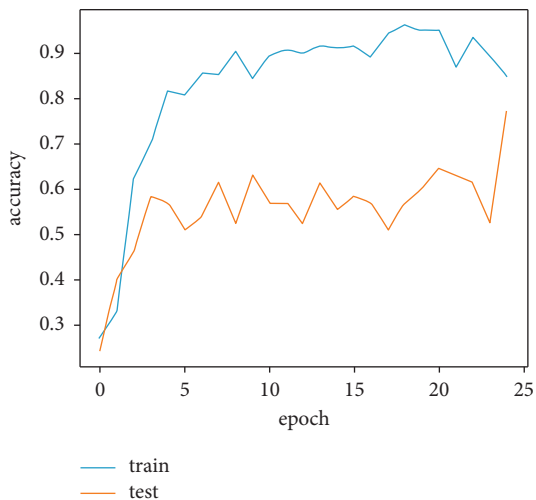
FIGURE 10: DenseNet-121.
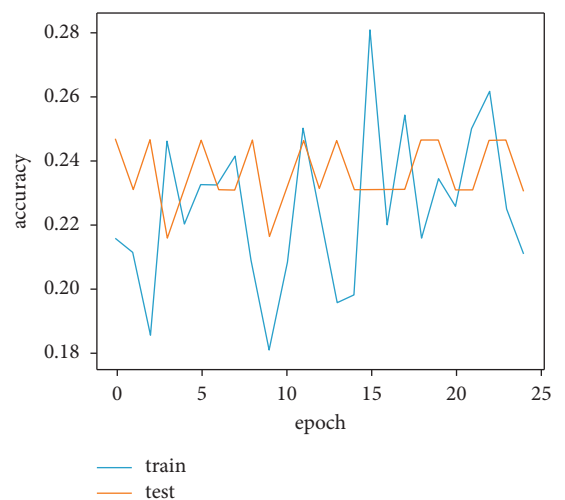
FIGURE 12: LeNet5.
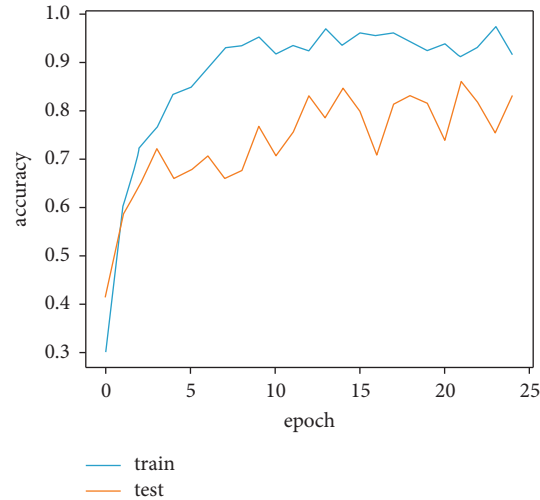
FIGURE 13: MobileNet.
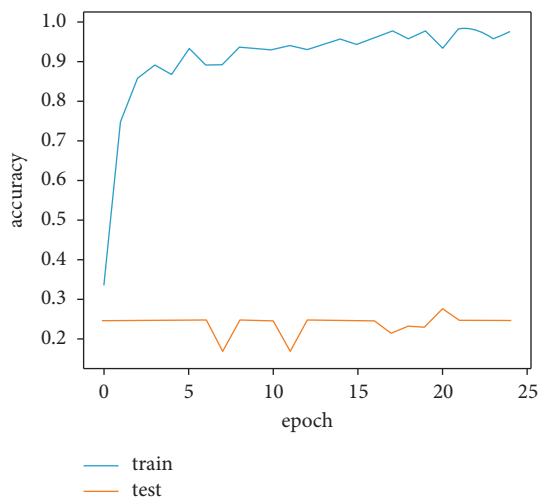
FIGURE 14: ResNet-50.
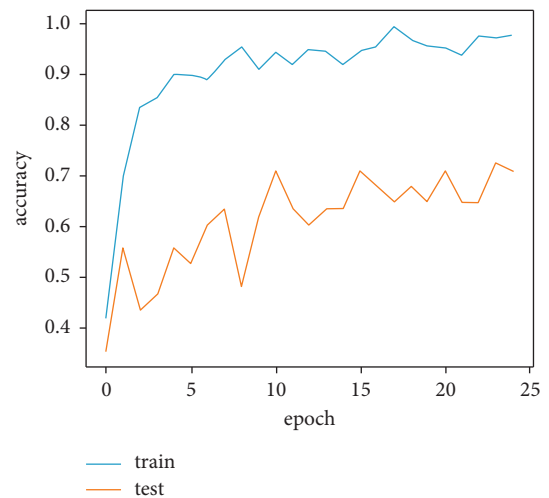
FIGURE 15: ResNet50V2.

calculating something or predicting something; so to achieve high accuracy in any work, we should have a proper and well-organized data set. In this work, an organized data set or the images containing diseases of sunflower is used. The data set used in this paper was taken from Google Images. In total, the data set contains 329 images including 67 images of *Alternaria* leaf spot, 78 images of healthy sunflower leaf, 77 images of downy mildew, 75 images of *Phoma* blight, and 32 images of *Verticillium* wilt. Later, the data set was split in the ratio of 80% and 20%, in which 80% images for training and 20% images for testing. In this data set, all the images are of high quality, which helps in increasing the accuracy and somehow increasing the processing speed. Figure 7 shows bifurcation of the data set used.

Initially, some existing deep learning techniques such as AlexNet, DenseNet-121, ResNet-101, ResNet-50, ResNet-50v2, Inception_v3, LeNet5, VGG-16, MobileNet, and CNNs are implemented with 7 layers. For the implementation of these techniques, the same process as of the proposed model till step 7 is used, and after that with the help of Keras library, the object of individual technique is initialized and then finally it is trained with the used data set. The accuracies of various techniques were evaluated, and Figures 8–17 show the graph between accuracy and epoch of individual model. This basically depicts that with more epoch of the model, the accuracy is increased and the model is making real predictions.

After calculating the accuracy of these models, i.e., AlexNet, CNN, DenseNet-121, Inception_V3, ResNet-50, ResNet50V2,
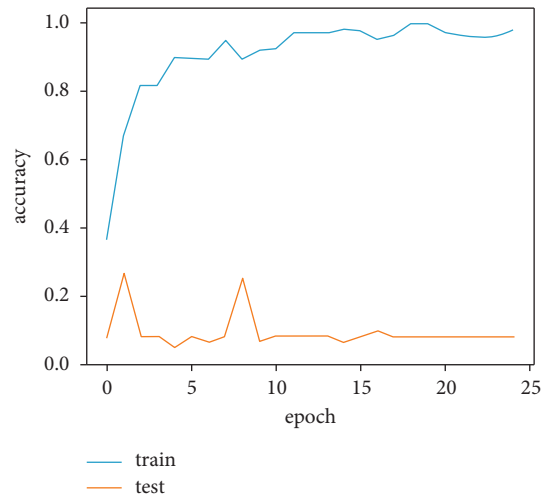
Figure 16: ResNet-101.
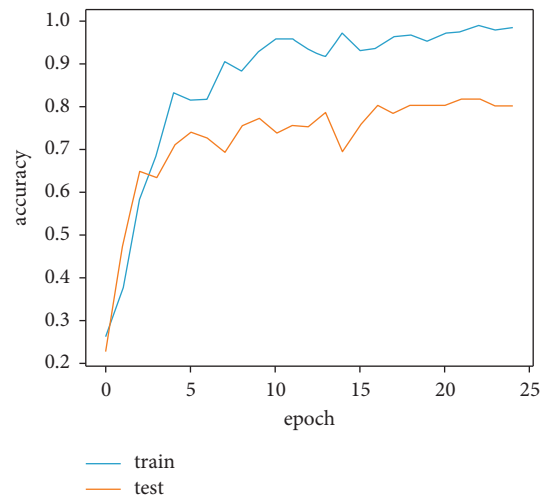
Figure 17: VGG-16.
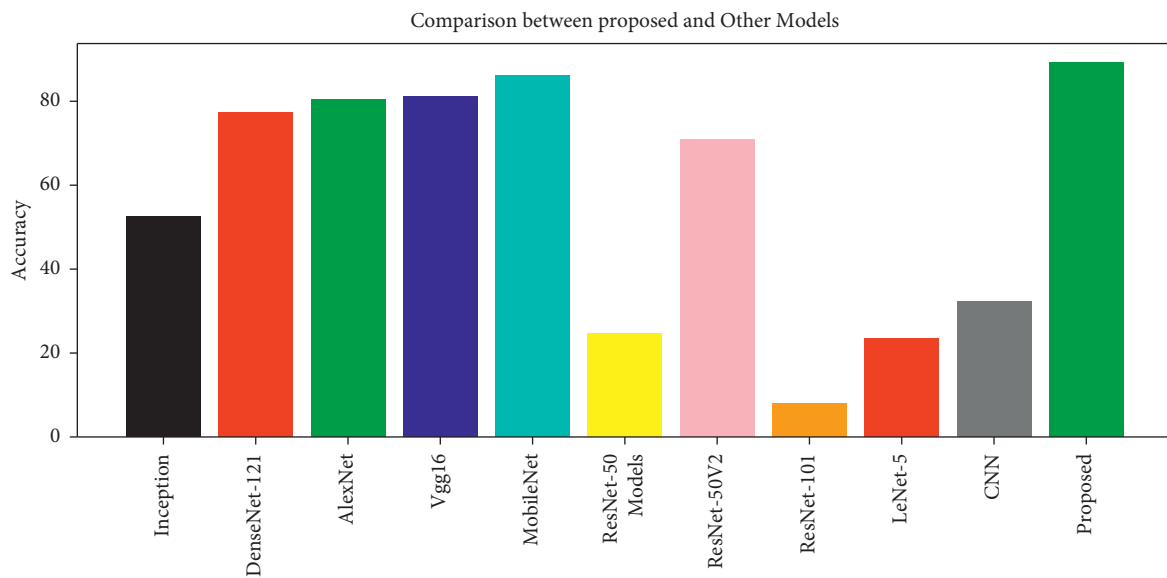
Figure 18: Comparison between the proposed and other models.

ResNet-101, and VGG-16, it can be concluded that proposed technique gives a better accuracy than the others.

5. Conclusion and Future Trends

Sunflower has several advantages, and its leaves and seeds are used in a variety of disciplines, making sunflower plants essential to our well-being as well as to the environment. The importance of detecting or recognizing infections in sunflower plants at an early stage cannot be overstated. However, this may be challenging to do manually. It is made simple by using deep learning methods or models. In this publication, a hybrid approach for the classification or identification of sunflower leaf diseases is suggested, which makes use of deep learning techniques to achieve this classification or recognition. This paper discusses four sunflower diseases, namely, *Alternaria* leaf blight, downy mildew, *Phoma* blight, and *Verticillium* wilt. *Alternaria* leaf blight is a kind of leaf blight that affects the leaves of sunflower plants. The last step is to do a comparison between the current approaches and the proposed technique. With the same data set, the proposed approach exceeds the competition, with an accuracy of 89.2%. The creation of a well-organized collection of sunflower illnesses, either by manually gathering the images of sunflowers or by utilizing a high-configuration system with many epochs, would allow for improved accuracy in the future. The graphical comparison between the proposed technique and other techniques is presented in Figure 18.

Data Availability

The data used to support the findings of this study are available from the corresponding author upon request.

Conflicts of Interest

The authors declare that there are no conflicts of interest regarding the publication of this paper.

References

[1] S. O. Mezan, S. M. A. Absi, A. H. Jabbar, M. S. Roslan, and M. A. Agam, "Synthesis and characterization of enhanced silica nanoparticle (SiO_2) prepared from rice husk ash immobilized of 3-(chloropropyl) triethoxysilanea," *Materials Today: Proceedings*, vol. 42, pp. 2464–2468, 2021.

[2] S. F. Suhel, V. K. Shukla, S. Vyas, and V. P. Mishra, "Conversation to automation in banking through chatbot using artificial machine intelligence language," in *Proceedings of the 2020 8th International Conference on Reliability, Infocom Technologies and Optimization (Trends and Future Directions) (ICRITO)*, pp. 611–618, IEEE, Noida, India, June 2020.

[3] M. A. Jasim, M. Jamal, and AL-Tuwaijari, "Plant leaf diseases detection and classification using image processing and deep learning techniques," in *Proceedings of the 2020 International Conference on Computer Science and Software Engineering (CSASE)*, IEEE, April 2020.

[4] J. Chen, D. Zhang, and Y. A. Nanehkaran, "Identifying plant diseases using deep transfer learning and enhanced lightweight network," *Multimedia Tools and Applications*, vol. 79, pp. 1–19, 2020.

[5] G. Rastogi and R. Sushil, "Cloud computing implementation: key issues and solutions," in *Proceedings of the 2015 2nd International Conference on Computing for Sustainable Global Development (INDIACom)*, pp. 320–324, IEEE, New Delhi, India, March 2015.

[6] T. K. Lohani, M. T. Ayana, A. K. Mohammed, M. Shabaz, G. Dhiman, and V. Jagota, "A comprehensive approach of hydrological issues related to ground water using GIS in the Hindu holy city of Gaya, India," *World Journal of Engineering*, p. 6, 2021.

[7] K. P. Ferentinos, "Deep learning models for plant disease detection and diagnosis," *Computers and Electronics in Agriculture*, vol. 145, pp. 311–318, 2018.

[8] J. Ma, K. Du, F. Zheng, L. Zhang, Z. Gong, and Z. Sun, "A recognition method for cucumber diseases using leaf symptom images based on deep convolutional neural network," *Computers and Electronics in Agriculture*, vol. 154, pp. 18–24, 2018.

[9] S. Vyas and D. Bhargava, "Big data analytics and cognitive computing in smart health systems," in *Smart Health Systems* Springer, Singapore, 2021.

[10] S. N. H. Bukhari, A. Jain, E. Haq et al., "Machine learning-based ensemble model for zika virus T-cell epitope prediction," *Journal of Healthcare Engineering*, vol. 2021, Article ID 9591670, 10 pages, 2021.

[11] Y. Zhong and M. Zhao, "Research on deep learning in apple leaf disease recognition," *Computers and Electronics in Agriculture*, vol. 168, Article ID 105146, 2020.

[12] M. Ji, L. Zhang, and Q. Wu, "Automatic grape leaf diseases identification via UnitedModel based on multiple convolutional neural networks," *Information Processing in Agriculture*, vol. 7, no. 3, pp. 418–426, 2020.

[13] S. Uğuz and N. Uysal, "Classification of olive leaf diseases using deep convolutional neural networks," *Neural Computing & Applications*, pp. 1–17, 2020.

[14] Y. A. Nanehkaran, "Recognition of plant leaf diseases based on computer vision," *Journal of Ambient Intelligence and Humanized Computing*, pp. 1–18, 2020.

[15] F. Jiang, Y. Lu, Y. Chen, D. Cai, and G. Li, "Image recognition of four rice leaf diseases based on deep learning and support vector machine," *Computers and Electronics in Agriculture*, vol. 179, p. 105824, 2020.

[16] S. Ghosal and K. Sarkar, "Rice leaf diseases classification using CNN with transfer learning," in *Proceedings of the IEEE Calcutta Conference (CALCON)*, IEEE, Kolkata, India, February 2020.

[17] Howlader and M. Rasel, "Automatic recognition of Guava leaf diseases using deep convolution neural network," in *Proceedings of the 2019 International Conference on Electrical, Computer and Communication Engineering (ECCE)*, IEEE, February 2019.

[18] U. P. Singh, S. S. Chouhan, S. Jain, and S. Jain, "Multilayer convolution neural network for the classification of mango leaves infected by anthracnose disease," *IEEE Access*, vol. 7, pp. 43721–43729, 2019.

[19] G. Geetharamani and P. Arun, "Identification of plant leaf diseases using a nine-layer deep convolutional neural network," *Computers & Electrical Engineering*, vol. 76, pp. 323–338, 2019.

[20] P. Jiang, Y. Chen, B. Liu, D. He, and C. Liang, "Real-time detection of apple leaf diseases using deep learning approach

based on improved convolutional neural networks," *IEEE Access*, vol. 7, pp. 59069–59080, 2019.

[21] A. Kumar and M. Vani, "Image based tomato leaf disease detection," in *Proceedings of the 2019 10th International Conference on Computing, Communication and Networking Technologies (ICCCNT)*, July 2019.

[22] M. Z. Hasan, "Recognition of jute diseases by leaf image classification using convolutional neural network," in *Proceedings of the 2019 10th International Conference on Computing, Communication and Networking Technologies (ICCCNT)*, July 2019.

[23] M. Agarwal, "FCNN-LDA: a faster convolution neural network model for leaf disease identification on apple's leaf dataset," in *Proceedings of the 2019 12th International Conference on Information & Communication Technology and System (ICTS)*, July 2019.

[24] S. Huang, "Development and validation of a deep learning algorithm for the recognition of plant disease," in *Proceedings of the IEEE 21st International Conference on High Performance Computing and Communications; IEEE 17th International Conference on Smart City; IEEE 5th International Conference on Data Science and Systems (HPCC/SmartCity/DSS)*, IEEE, August 2019.

[25] V. Singh, "Sunflower leaf diseases detection using image segmentation based on particle swarm optimization," *Artificial Intelligence in Agriculture*, vol. 3, pp. 62–68, 2019.

[26] J. Sujithra and M. F. Ukrit, "A review on crop disease identification and classification through leaf images," *European Journal of Molecular & Clinical Medicine*, pp. 1168–1183, 2020.

[27] J. F. Montecchia, M. I. Fass, I. Cerrudo et al., "On-field phenotypic evaluation of sunflower populations for broad-spectrum resistance to Verticillium leaf mottle and wilt," *Scientific Reports*, vol. 11, no. 1, pp. 11644–11714, 2021.

[28] H. Q. Cap, "A deep learning approach for on-site plant leaf detection," in *Proceedings of the 2018 IEEE 14th International Colloquium on Signal Processing & its Applications (CSPA)*, March 2018.

[29] X. Zhang, Y. Qiao, F. Meng, C. Fan, and M. Zhang, "Identification of maize leaf diseases using improved deep convolutional neural networks," *IEEE Access*, vol. 6, pp. 30370–30377, 2018.

[30] de Luna, G. Robert, E. P. Dadios, and A. A. Bandala, "Automated image capturing system for deep learning-based tomato plant leaf disease detection and recognition," in *Proceedings of the TENCON 2018-2018 IEEE Region 10 Conference*, October 2018.

[31] F. Ajaz, M. Naseem, S. Sharma, M. Shabaz, and G. Dhiman, "COVID-19: challenges and its technological solutions using IoT," *Current Medical Imaging Formerly Current Medical Imaging Reviews*, vol. 18, no. 2, pp. 113–123, 2022.

[32] Z. Yan, Y. Yu, and M. Shabaz, "Optimization research on deep learning and temporal segmentation algorithm of video shot in basketball games," *Computational Intelligence and Neuroscience*, vol. 2021, Article ID 4674140, 10 pages, 2021.

WILEY | Hindawi

Research Article

Quality Improvement in Vegetable Greenhouse by Cadmium Pollution Remediation

Zhihui Yu [1,2] **and Jie Tang** [2]

^{1}*Forestry College of Beihua University, Jilin 132013, China*
^{2}*College of New Energy and Environment, Jilin University, Changchun 130012, China*

Correspondence should be addressed to Zhihui Yu; yuzhihui@beihua.edu.cn

Greenhouse vegetable production (GVP) has grown in importance as a source of public vegetable consumption as well as income for farmers. Due to the high cropping index, substantial agricultural input, and confined environment, numerous contaminants can accumulate in GVP. Polluted soil is treated with metal cadmium pollution remediation technology in order to improve the quality of vegetable greenhouse soil and increase crop yields. The heavy metal cadmium-contaminated soil in vegetable greenhouses is rectified utilizing three methods: chemical remediation, bioremediation, and physical remediation. Soil restoration with broom sedge planting might result in a 9.78 percent reduction in cadmium pollution. Planting broom sedge has a root > stem > leaf effect on pollution remediation. The elimination of cadmium from the soil around the anode can be as high as 75.1 percent. The clearance rate of the soil near the anode was 75.1 percent and 77.9 percent, respectively, when the anode cadmium mass fraction dropped fast. Hence this paper focuses on the reduction of cadmium pollution to improve the quality of GVP crop to yield more benefit. Chemical leaching is faster, more efficient, and less dangerous, with a higher application value. The approach of bioremediation is of low cost and creates no secondary contaminants. Physical electrodynamics is easy to understand and has a distinct effect.

1. Introduction

Greenhouse vegetable production (GVP) is a method of agricultural production that uses a lot of energy. As a link between the inorganic and organic boundaries, soil plays an important role in protecting the environment and maintaining ecological balance [1]. Heavy metal cadmium has infiltrated the soil through numerous means in recent years, causing contamination, due to the emission of three wastes, incorrect agricultural product usage, and sewage irrigation. Cadmium (Cd) is a nonessential natural component found in plants and in the ecosystem. Cadmium is a hazardous heavy metal contaminant found in soil. It may be found in the environment, meta sediments, and soils naturally. Cadmium contamination is one of the most prevalent types of heavy metal pollution in farming, and it causes the greatest amount of damage. The major natural causes of Cd

contamination include geological weathering of rocks and human sources such as pesticide application or soil pollution from the disposal or reuse of industrial or municipal wastes [2].

Human activity such as urban waste disposal, mining, metal manufacture, and the use of artificial phosphate fertilizer increases Cd risks to the ecosystem and is hazardous to human health. In recent decades, the frequent pollution accidents caused by heavy metal cadmium have brought much harm to human beings. Cd is a very hazardous, soil-persistent, main heavy metal pollutant [3], which is relatively easily absorbed by plant roots, contaminating the food chain and resulting in bioaccumulation in the human body, causing hazardous consequences [4]. There are a number of parameters that might influence Cd absorption by plants, with pH being one of the most important. The adsorptive capacity of soils for Cd triples with each pH unit rise in the

range [4–7]. Related research shows that waste water with cadmium discharges into the paddy and makes the rice dead and accumulates in the liver and kidneys through the food chain, causing acute or chronic poisoning. This makes people pay great attention to the problem of heavy metal pollution in farmland soil, and the problem of soil safety and soil management cannot be ignored [5].

Cd absorption from the soil and distribution among shoots and roots is a carefully controlled process involving a number of critical players: root cell plasma membrane metal transporters, xylem and phloem loading/unloading, and leaf/shoot sequestration and detoxifying [6]. Cadmium must pass the cell membrane to reach the root cells (symplast), which is made easier by the existence of several outlets and metal exchangers. Conventional heavy metal cleanup approaches, such as physical and chemical procedures, are being employed; however, they are ecologically damaging, costly, and difficult to apply. Numerous studies on heavy metal bioremediation employing biological material such as live plants or microorganisms from contaminated soil and water have been published. Phytoremediation, a rapidly advancing technique, is an environmentally benign, low-tech, premium, and green solution to these problems [7]. Cadmium causes water shortages, ionic imbalances, discoloration, necrosis, and eventually cell mortality, genotoxicity, and yield decrease in plants. Cadmium may enter and persist in crops through the soil and then pass through the food chain and impact the human body. It damages the liver, kidneys, and bones of the human body. As a result, the objective of this research paper was to minimize heavy metal cadmium contamination in vegetable greenhouse soil by chemical remediation, bioremediation, and physical remediation.

The rest of the paper is organized as follows: in Section 2 a detailed study of vegetable greenhouse cadmium pollution of chemical remediation technology, physical remediation technology, and bioremediation technology is elaborated. In Section 3, the detailed analysis and discussion of the experiment carried out on samples of plant using chemical remediation technology, physical remediation technology and bioremediation technology are presented. In Section 4, conclusions are presented followed by references.

2. Material and Method

2.1. Vegetable Greenhouse Cadmium Pollution Chemical Remediation Technology. Engineering methods and chemical remedies are both used in soil remediation technologies. Adding fresh soil, removing topsoil, electrical remediation technology, leaching method, and washing method are some of the engineering measures. Chemical reagents and soil heavy metal ions are used in the leaching and washing methods to decrease heavy metal concentrations in soil [3]. Chemical remediation, as indicated in Table 1, is the use of chemical remediation in soil, which includes complicated leaching, in situ passivation, and other approaches. The key to this technology is the selection of the passivator, eluent, and the determination of the dosage [4]. Chemical repair is an early, relatively mature, and effective method [5],

including chemical leaching technology, chemical oxidation remediation technology, and soil performance improvement technology.

2.1.1. Chemical Passivator Type. The commonly used passivators include inorganic passivator and organic passivator. Inorganic passivators mainly include industrial waste, lime, red mud, fly ash, silicon fertilizer, calcium magnesium phosphate, dolomite, clay mineral, and antagonistic substances. Organic passivators are mainly derived from livestock manure, crop straw, peat, leguminous green manure and composting, and natural extraction of polymer compound. Lime is widely used passivator in the present experimental research.

(i) Passivation Mechanism The mechanism of chemical passivation is mainly to reduce the activity of cadmium in the soil by changing the soil properties, which involves precipitation fixation, adsorption and ion exchange, ion antagonism, and chelation. Most passivators work with a variety of mechanisms.

(ii) Precipitation/Fixation With this mechanism, most passivators reduce the availability of cadmium in soil. The application of alkaline substances like lime can obviously improve the soil pH value and reduce the solubility and activity of cadmium in the soil. In addition, when the passivator with carbonate ion, silicate ion, and hydroxyl ion is added to the soil, cadmium ions can react with these anions to produce hardly dissolved sediment, which can reduce the availability of soil cadmium [6].

(iii) Adsorption and Ion Exchange Clay minerals such as zeolite have strong ion exchange ability, and the availability of cadmium in soil can be reduced by ion exchange and specific adsorption of cadmium ions [7]. In addition, lime can increase soil pH value, increase the negative charge on the soil colloid surface, enhance the adsorption of cadmium ions, and reduce the bioavailability of cadmium in soil.

(iv) Ion Antagonism According to studies, cadmium interacts with a variety of nutrients, including zinc, selenium, copper, manganese, iron, calcium, potassium, phosphorus, and nitrogen, in ways that are either synergistic, antagonistic, or unrelated [8]. Therefore, the application of zinc can suppress the absorption of cadmium. The antagonists of cadmium are zinc sulphate and lanthanum.

(v) Chelation Organic amendments contain a variety of organic ligands, such as amino, imido, ketone, hydroxyl, and thioether, that can chelate with heavy metal ions like cadmium to create insoluble chelate, lowering heavy metal ion bioavailability.

2.2. Vegetable Greenhouse Cadmium Pollution Bioremediation Technology. Bioremediation, which includes animal remediation, phyto remediation, and micro bioremediation,

TABLE 1: Chemical remediation of cadmium pollution in soil.

Method	Complexation and leaching	In situ passivation
Definition	Cleaning the cadmium in the soil with a drenching agent and then concentrating on the cadmium in the leaching solution.	It reduces the solubility, diffusivity, and biological toxicity of pollutants after various chemical reactions after adding passivating agent to contaminated soil.
Advantage	It is fast and efficient.	It is simple and easy to choose the suitable passivating agent according to the degree of contaminated soil and the property of the soil. Most of the passivating agents are the byproduct of industry and having the lower cost.
Shortcoming	The remediation effect is affected by soil types, eluent resistance, and the occurrence form of cadmium. The eluent is expensive and may pollute groundwater, causing nutrient loss and soil fertility decline. The development of technology and equipment is relatively backward.	Only the occurrence of cadmium has been changed and it is not completely removed from the soil. Long-term monitoring is needed to prevent activation.
Remarks	It is suitable for sandy soil and sandy loam with good water permeability and heavy pollution. The selection and treatment of leaching solution is the key technology.	It is the key to find the passivating agent with low price, friendly environment, and continuous effect.

is the utilization of specific organisms' habits to adapt, inhibit, and ameliorate cadmium pollution, as indicated in Table 2.

2.3. Animal Remediation. The employment of parasitic organisms in the soil, such as earthworms and rodents, to absorb heavy metals is known as animal remediation. Researches on the use of lower animals to remediate cadmium pollution are still limited to the laboratory stage. The earthworm has a significant cadmium enrichment capacity, according to the findings, and the earthworm's enrichment steadily increases when the earthworm culture period is extended [9]. The efficiency of animal remediation is low, which is not an ideal remediation technique.

2.4. Phytoremediation. Plant extraction, plant volatilization, plant degradation, plant root filtration, and rhizosphere microbial degradation are all examples of phytoremediation techniques that employ plants to absorb, disintegrate, alter, or immobilise toxic and harmful contaminants in the soil. Plant extraction remediation, or the use of hyper accumulator plant features to remediate cadmium and other heavy metal polluted soil, is the most extensively utilised method [10]. More than 10 hyper accumulator plants, including cruciferae and cramineae, are with better remediation effect of cadmium contaminated soil. Some ornamental plants, cropland weeds, and woody plants are also the source of hyper accumulator plants for remediation of cadmium contaminated soil [11].

The tolerance mechanisms of cadmium hyper-accumulator plant are mainly compartmentation, anti-oxidation, and chelation. The compartmentation effect utilizes a large number of ligand residues in plant cell walls, including heavy metal ions, ion exchange, adsorption, and complexation, to influence the diffusion of heavy metal ions into cells [12]. The advantages of phytoremediation technology are simple implementation, less investment, and little damage to the environment, but there are also some shortcomings. These plants have usually slow growing, low

biomass, long repair cycle, and difficulty to be widely applied.

Phytoremediation technology has the advantages of being easy to implement, little investment, and little environmental impact, but it also has certain drawbacks, such as sluggish growth, low biomass, a long remediation cycle, and a limited applicability [13].

2.5. Micro Bioremediation

2.5.1. Method. Some microbes can be employed to fix, migrate, or convert heavy metals in the soil, therefore lowering toxicity and facilitating detoxification. The mechanisms include cell metabolism, absorption, precipitation, and redox reaction. The metabolites of some microbes, such as S^{2-} and PO_4^{3-}, can react with Cd^{2+} to produce precipitation and reduce the toxicity of cadmium [14]. Microorganisms currently used for remediation of cadmium contaminated soil include bacteria, fungi, and some small algae.

2.5.2. Mechanism of Action. Obligate microorganism can promote the composition of heavy metal and micro object. Therefore, inoculation of obligatory microorganisms into polluted soil can help microorganisms absorb heavy metals [15]. The common obligate microorganisms include bacteria, fungi, endophytic mycorrhizae, and ectomycorrhizae [16]. In conclusion, these microbes can be used to immobilise heavy metals in soil and reduce the mobility of heavy metals in soil from the absorption of heavy metals [17].

2.6. Vegetable Greenhouse Cadmium Pollution Physical Remediation Technology. Physical remediation refers to the use of physical method to dilute, remove, and fix cadmium in soil in order to reduce the impact on the soil environment. The classification of physical remediation is shown in Table 3. The change of soil method is commonly used, including adding new soil, changing soil, topsoil, and deep ploughing [18]. Adding new soil entails adding a specified

TABLE 2: Bioremediation of cadmium pollution in soil.

Method	Animal repair	Microbioremediation	Phytoremediation
Definition	The use of earthworms, voles, and other soil animals to absorb soil cadmium	Reducing, adsorbing, accumulating cadmium, or changing the rhizosphere environment by microorganisms to promote the uptake of cadmium in plants	Extract: the use of hyperaccumulator plants to enrich the cadmium in the soil on the parts of the plant harvested and concentrated
			Volatilization: the use of plants to absorb cadmium in the soil and convert it into gas to volatilize into the atmosphere Stable: cadmium activity in soil by cadmium - resistant or super - resistant plants
Advantage	Improving soil structure and enhancing soil fertility	In situ remediation, improvement of soil environment, soil improvement, low cost	Low cost, low cost, in situ remediation, little impact on the environment, increase soil fertility and organic matter content, and concentrate on the above ground part to reduce two times of pollution, clean and beautify the social environment, and repair the soil and surrounding water
Shortcoming	Unable to deal with high concentration of cadmium contaminated soil	Strong specificity, concentration limit, difficult to separate from soil	With a single nature and selectivity, compared with other remediation methods, the cycle will be longer. Soil environment and artificial conditions may lead to biological invasion. If plants are not collected in time, there will be two pollution types and limited cadmium tolerance.
Remarks	Further study	Development potential and application prospect	Extract: the key is to find plants with high yield and hyper concentration Volatilization: more soil for the remediation of se, hg, as contaminated soil Stable: more used for remediation of contaminated soils, smelters, sludge, and other contaminated soils

amount of clean soil. The term "soil change" refers to the process of removing polluted soil and replacing it with clean soil. The polluted topsoil is turned into the bottom layer by deep ploughing [19]. Soil leaching is a method of transferring cadmium from solid soil to liquid via a leaching solution, followed by wastewater recovery.

Thermodynamic remediation method uses high frequency voltage to generate electromagnetic wave, which heats the soil, so that the pollutant is desorbed from the soil particles [20]. Electrokinetic remediation refers to the insertion of electrodes in the contaminated soil to obtain the direct movement of cadmium ions in the soil under the action of electric field, so as to achieve the purpose of clearing cadmium.

3. Results

3.1. Cadmium Contaminated Soil Remediation by Chemical Technology

3.1.1. Case Study of Chemical Leaching Remediation of Cadmium Contaminated Soil in the United States. Chemical leaching to remediate heavy metal polluted soil has reached a commercial level in the United States. Table 4 shows the demonstration projects of chemical leaching remediation of cadmium contaminated soil in the United States.

3.1.2. Passivation Restoration Experiment of Vegetable Greenhouse Contaminated Soil by Clay Mineral and Fertilizer. To investigate the remediation effect of single and compound treatments on cadmium pollution in vegetable fields of the northern sewage irrigated area and to find a better passivation treatment, clay minerals, sepiolite, phosphate bone meal, and organic fertilizer humic acid were chosen as passivators.

3.1.3. Experimental Setup. Clay mineral sepiolite is purchased from Yixian, Hebei. The chemical formula is $Mg_4Si_6O_{15}(OH)_2 \cdot 6H_2O$. The surface area is 22.7 $m^2 \cdot g^{-1}$ and the pH value is 10.1. The phosphate fertilizer bone meal is purchased from the Tengzhou Chemical Plant in Shandong. The pH value is 9.51, and the effective phosphorus content is 9.5%. The main chemical components are hydroxyapatite $[Ca_{10}(PO_4)_6(OH)_2]$ and amorphous calcium hydrogen phosphate ($CaHPO_4$). Organic manure humic acid is purchased from Shanxi and processed by lignite. The vegetable for test is lettuce. The test site is located in northern sewage irrigated area of Tianjin. The soil type is the tidal soil. The basic physicochemical properties of the tested soil are as follows: the pH value is 8.38, the cation exchange amount is 19.2 $cmol \cdot kg^{-1}$, the organic matter content is 2.14%, the soil cadmium content is 1.71 $mg \cdot kg$, and 1.12 passivation treatments are set up in the test. Test

TABLE 3: Physical remediation of cadmium pollution in soil.

Method	Definition	Advantage	Shortcoming	Remarks
Soil	Adding a large amount of uncontaminated soil to contaminated soil, covering the surface, or mixing the contaminated soil.	Not restricted by soil conditions, the effect is remarkable, and it is completely stable.	It requires a lot of manpower, material resources, high cost, land occupation, leakage, and secondary pollution. It destroys soil structure and reduces soil fertility.	Suitable for shallow root plant planting areas and polluted areas with poor mobility of pollutants
Change of soil	Replace the contaminated soil in part or all with nonpolluted soil			The thickness of soil change is greater than that of the plough layer
Go to the topsoil	According to the characteristics of cadmium contaminated surface soil, tillage activated the lower layer of soil			Prevent the two pollution types of the changed soil
Turn the soil depth	To spread the accumulation of cadmium on the surface to a wider range, so as to dilute it to a bearable value.			Suitable for heavy soil contaminated areas with fertilizer
Heat treatment	Heating the contaminated soil to evaporate the cadmium from the soil	Simple process	The destruction of organic and structural water in the soil and the disposal of the volatile matter	More suitable for volatile heavy metals: Hg, As
Electric repair	DC voltage is applied at both ends of the contaminated soil, and cadmium in the soil is taken to the electrode under the action of an electric field to collect soil samples	The economy is feasible, the operation is simple, the cycle is short, and the efficiency is high.	The effect of remediation is influenced by soil environment, soil components and heavy metals, which can easily lead to the change of soil basic physical and chemical changes.	The clay silt, which is used for low permeability, is still in the experimental stage and less successful.
Vitrification	Melting the polluted soil at high temperature and forming vitreous material after cooling	Permanent cadmium fixation	Energy consumption, complex technology, and difficult practical operation	

TABLE 4: The chemical leaching remediation of cadmium contaminated soil in greenhouse experiment in the United States.

Experimental sample	Target heavy metal	Eluent
Vegetable fields 1	Hg, Cd	KI solution
Vegetable fields 2	Ag, Cr, Cu, Cd	Leaching test
Vegetable fields 3	Cd, Cu, Cr, Hg, Pb	Acid
Vegetable fields 4	Cr, Pb, Cd	Leaching test

scheme and the type and dosage of passivation materials are shown in Table 5. Each processing set is repeated 3 times and arranged according to the random group.

3.1.4. Test Plant Sample Preparation. Passivators are uniformly dispersed on the soil surface and mixed with soil (20 cm depth) by human or mechanical means, followed by the planting of vegetables a month later. Passivators were applied in May, 2014, and the lettuce was sowed and planted in June, 2014. The lettuce is harvested and collected in 30 days after the emergence of the seedling. Rinse the veggies two times with distilled water after harvesting. Dry out with filter paper, and weigh and record the fresh weight. After the sample is placed in a blast oven at 105°C for 30 min, it is dried at 70°C for 48 h, and the weight of dry weight is recorded. The dried sample is comminuted and mixed with a small pulverizer, and the wet digestion is used. The soil sample is sampled by using S sampling method, and the fresh soil in

plough layer (0–20 cm) is collected in each cell. It is grinded after air drying and followed by 1 mm and 0.15 mm aperture sieves for spare. The effective cadmium in soil sample is extracted by TCLP method. The leaching solution with the pH value 2.88 ± 0.05 is prepared by analysis of pure glacial acetic acid. The ratio of soil to solution is 1 : 20 and the solution is centrifugally filtered after 20 h at room temperature [21].

3.1.5. Determination of Cadmium Content. The cadmium content of plant sample and the available cadmium content in soil are determined by ICP-MS. Statistical analysis of experimental data is carried out with Excel 2010 and SPSS 13.0. The significance of differences between different passivators is analyzed by variance analysis of and multicomparison (LSD method). Figure 1 shows the effects of different passivators on the cadmium content in the edible part of lettuce. Figure 2 shows the effect of passivators on the available cadmium content of soil.

TABLE 5: Experimental treatment of passivation repair.

Number	Handle	Consumption
Ck	Control 1	0
Bom	Bone meal	0.5
Hua	Humic acid	0.5
Sep1	Sepiolite 1	0.5
Sep2	Sepiolite 2	1
Sep3	Sepiolite 3	1.5
Sep1+bom	Sepiolite 1+ bone powder	0.5 + 0.5
Sep2+bom	Sepiolite 2+ bone powder	1.0 + 0.5
Sep3+bom	Sepiolite 3+ bone powder	1.5 + 0.5
Sep1+hua	Sepiolite 1+ humic acid	0.5 + 0.5
Sep2+hua	Sepiolite 2+ humic acid	1.0 + 0.5
Sep3+hua	Sepiolite 3+ humic acid	1.5 + 0.5
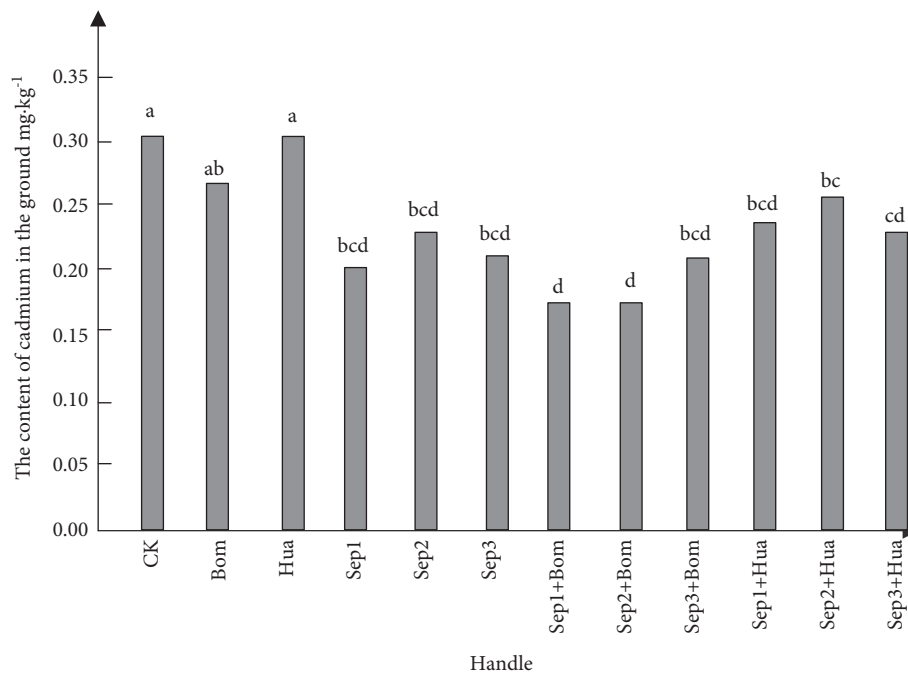
FIGURE 1: Effect of passivation treatment on the content of cadmium in the upper part of lettuce.

From Figure 1, it can be seen that, after passivation treatment, cadmium in the shoot of lettuce has an obvious decreasing trend with the decrease of 3.3%–39.7%. For the single passivation, the effect of sepiolite is the best and the decrease of the cadmium content in the shoot of lettuce is up to 30.8%. The second is bone meal with the decrease of 16.1%. Humic acid has no significant effect on the absorption of cadmium in lettuce. In addition, the effect of compound treatment is better than single treatment. The effect of Sep2+Bom treatment on reducing the cadmium content in lettuce is best, with the decrease of 39.7%, which is lower than the limit of cadmium content in leafy vegetables specified by GB2762-2012 0.2 mg·kg-1.

For improvement of the heavy metal pollution in 4 (Table 4) vegetable greenhouses, chemical leaching is used for remediation. Experimental results show that the chemical leaching can effectively remediate the pollution of heavy metal cadmium in soil. The cost of chemical leaching is relatively high. There is no cost report of leaching technology in China at present. In the United States, the cost of chemical leaching is 120–200 dollars/t.

From Figure 2, it can be seen that sepiolite and its compound treatment can obviously reduce the available cadmium content in soil, with the decrease of 12.16%–55.64%. The reduction effect of bone meal and compound treatment with sepiolite and bone meal is better, with the decrease of 55.64% and 54.12%, respectively.

3.2. Cadmium Contaminated Soil Remediation by Biotechnology.
Different planting years (0, 5, 10, 15, 20, 25, 30 years) of soil samples in vegetable greenhouse are collected. Taking broom sedge as the research object, the remediation effect and accumulation characteristics of broom
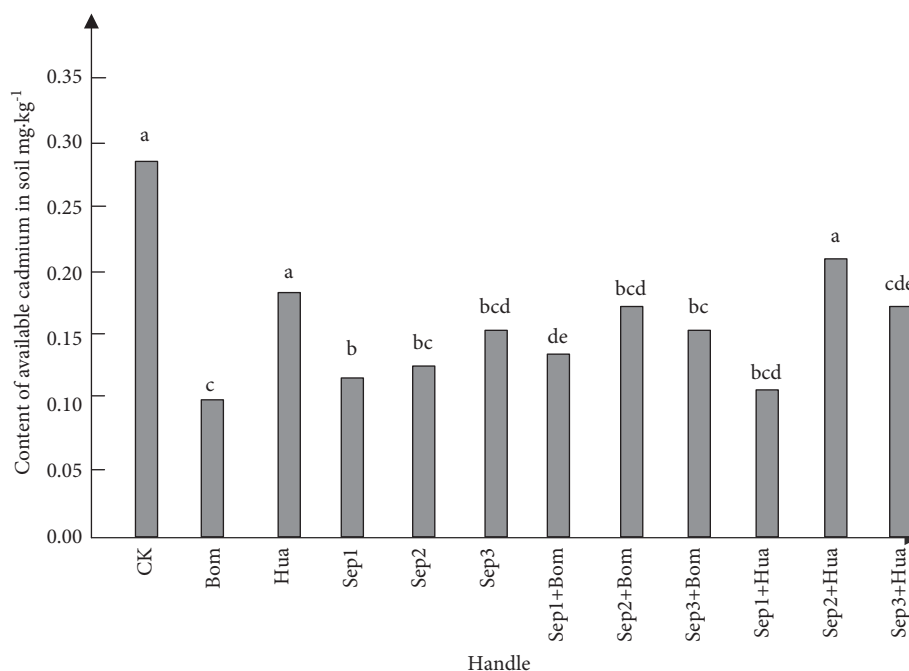
FIGURE 2: Effect of passivation treatment on the content of available cadmium in soil.

sedge planting on the contaminated soil with different planting years are researched.

3.2.1. Experimental Material and Measure. The test material is a broom sedge that was gathered in 2014 (wild specie). The location of the collection is the suburb of Xinxiang, Henan Province, with a geographical position of north latitude 35°21' and east longitude 113°50'. The soil sample is collected in harmless vegetable production base of Muye District, Xinxiang, in March 26, 2010. S multipoint (20 point) mixed sampling method is used for sampling soil. The planting years are 0, 5, 10, 15, 20, 25, and 30 years and the sampling depth is 0–20 cm. The plant roots, leaves, and rocks are removed from the air dried soil sample. The soil sample is filtered by 2 mm soil sieve and used for the cultivation of broom sedge. The other part is filtered by 1.0 mm and 0.2 mm soil sieve after being ground with agate mortar. Then it is stored in the polythene bag for determination of heavy metal content in soil.

The treated seven soil samples are placed in the seedling tray (square 50 hole) and sowing. The sample is cultured for 40 days after emergence. When the height of the seedling is 15–20 cm, the seedling is pulled out from the cavern and cleaned. After drying, the roots, stems, and leaves are separated. Then it is put into the oven at 105 °C for 2h and dried to constant weight at 70 °C. It is ground to powder and loaded into a polythene bag.

3.2.2. Determination of Heavy Metal Content. Microwave digestion inductively coupled plasma emission spectrometry is used for determination of heavy metal content.

3.2.3. Determination of Mass Fraction of Heavy Metal in Soil. The soil samples before and after planting broom sedge (filtered by 0.2 mm soil sieve) are weighed for 0.5 g (accurate to 0.0001) and put in PTFE digestion tank. 8 ml nitric acid, 2 ml perchloric acid, and 2 ml hydrofluoric acid are added in turn. After mixture and uniform encryption seal, it is put in the MAS microwave digestion instrument for digestion. After the digestion tank is cooled, the solution is transferred to the 50 ml polytetrafluoroethylene beaker and placed in the electric heating plate at 170 °C to dry up the acid. After adding 2ml0.2%HNO3 to dissolve the residue, it is transferred to the bottle with 25 ml capacity (GG-17 glass) and then to the polyethylene plastic bottle after shaking. The mass fraction of heavy metal cadmium is determined by Optima 2100DV inductively coupled plasma emission spectrometer.

3.2.4. Determination of Mass Fraction of Heavy Metal in Broom Sedge. The root, stem, and leaf of broom sedge are taken 0.5 g and put in microwave digestion tank. For each digestion tank, 5 ml concentrated nitric acid (95%) and 2 ml hydrogen peroxide are added in order. After digestion, the solution is transferred to a small beaker and the digestion tank is cleaned with 0.2% dilute nitric acid for 3 times. The small beaker is put on the electric heating plate 170 C to drive acid to the near dry. After adding 2 ml 0.2% nitric acid to dissolve the residue, it is transferred to the 25 ml volumetric bottle and finally fixed the volume with 0.2% dilute nitric acid solution. Mass fraction of heavy metal cadmium is determined by inductively coupled plasma emission spectrometer. Experimental results are shown in Figures 3 and 4. Figure 3 shows the remediation effect and Figure 4 shows the absorption and accumulation characteristics.
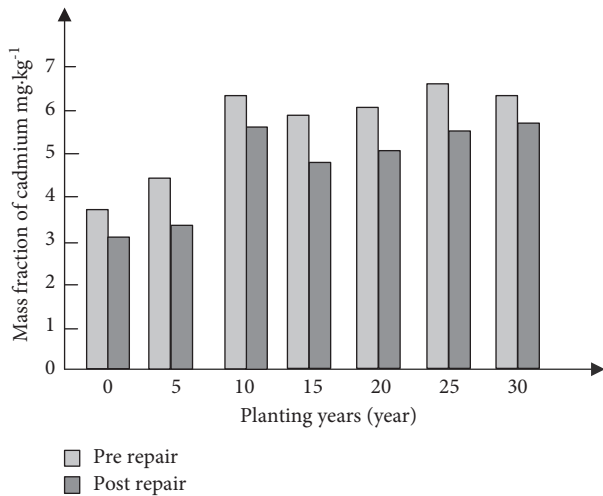
FIGURE 3: Effect of repair of greenhouse in different planting years of broom sedge vegetable soil cadmium.
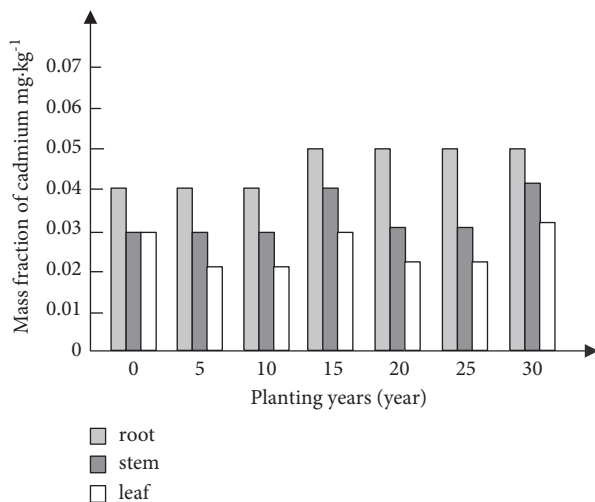
FIGURE 4: The characteristics of greenhouse vegetable soil with different planting years of cadmium absorption and accumulation of broomsedge.

From Figure 3, it can be known that, after planting broomsedge, the content of cadmium pollution decreased significantly. With broomsedge planting, the absorption and accumulation of the heavy metal cadmium are related with the concentration and the remediation efficiency is unrelated with the planting year. From Figure 4, the sorting of the accumulation of cadmium in the root, stem, and leaf is root > stem > leaf. The remediation efficiency of broomsedge on vegetable greenhouse cadmium contaminated soil is 9.78%.

3.3. Electrokinetic Remediation of Cadmium Pollution in Soil

3.3.1. Experimental Setup and Measure. Platform scale, electronic balance, atomic absorption meter, pH meter, centrifuge, and mixer spectrophotometry are the primary instruments and equipment utilized in electrokinetic remediation. Electrolyzer is a self-designed 25 cm × 5 cm×10 cm organic glass trough. High purity graphite electrode is used as electrode material. Experimental reagents are mainly cadmium sulphate, copper sulphate, concentrated sulfuric acid, concentrated nitric acid, phosphoric acid, hydrochloric acid, and sodium hydroxide. All of the reagents employed are of analytical purity. Soil sample is collected in the wild field. Heavy metal pollution solution is compounded according to the demand for pollutants and added to the quantitative soil sample to form the contaminated soil. The moisture content of the contaminated soil samples is 44.3%. The contaminated soil is then layered into the electrolyzer and compacted evenly. The experimental model is stably stabilized in the laboratory for 72 h. The mass fraction of heavy metals in pollutants is determined by atomic absorption spectrometry and determination of pH value and temperature of samples is obtained by acidity meter and thermometer.

3.3.2. Experimental Result. The selected heavy metal pollution factors are Cd and Cu. The used voltage is 0.5 V/cm. In the experiment, 50 ml working fluid with the 0.05 mol·L-1concentration is added into the electrode chamber. Remediation experiment is carried out after connecting the reaction unit with the power supply. The pH value and mass fraction of heavy metal contaminants are measured at a fixed time interval. The cumulative time of the experiment is 32 h. Changes of the mass fraction of heavy metal in all samples and the pH value in the electrolyzer are shown in Figures 5 and 6 ("+" represents the anode, "-" to represent the cathode).

From Figures 5 and 6, it can be seen that the method of point dynamic remediation can effectively reduce the cadmium content in soil. Figures 5 and 6 show the change of cadmium mass fraction of cadmium near the two poles of soil after electrokinetic remediation. The cadmium content near the anode decreases gradually from the initial state of 575.8 mg 575.8 mg·kg-1 to the end of 143.5 mg·kg-1. Therefore, cadmium is migrated to the cathode under the action of electric field, and the mass fraction of cadmium decreases faster in the vicinity of the anode. The migration rate of cadmium in the vicinity of the anode is greater than the migration efficiency of cadmium far from the anode. In the experiment, the removal efficiency of cadmium in the soil near the anode is 75.1% and 77.9%. Electrokinetic technology can effectively remove cadmium in the contaminated soil, which is convenient and effective.

In the chemical remediation technology, the passivation effect increases with the increase of the amount of passivator and the time of passivation. The appropriate addition of lime in lateritic red soil decreases the soil available cadmium content greatly. After adding 0.7% lime for 30 d to the southern acid soil, the effective cadmium in the soil is reduced by 28.17%. The release of calcium, magnesium, and phosphate fertilizer in acid soil can significantly increase the pH value in soil and reduce the content of exchangeable and effective cadmium. With the base fertilizer of 5 g/kg alkaline coal cinder, the content of cadmium in brown rice of early
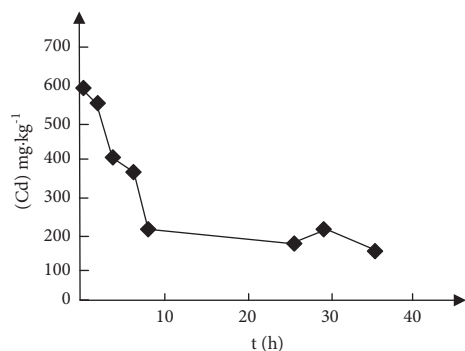
FIGURE 5: The change curve of cadmium in soil (+).
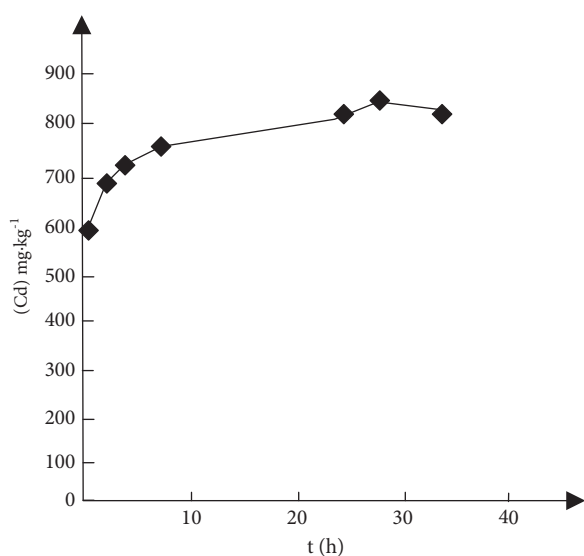
FIGURE 6: The change curve of cadmium in soil (-).

rice could be reduced by 75.4%, and the content of cadmium in brown rice of late rice decreased by 87.9%. The adsorption capacity of red mud to cadmium is up to 22.25 g/kg. The content of effective cadmium after the treatment of red mud can be reduced by 31% compared with the control treatment.

4. Conclusion

Cadmium pollution in agriculture soil is quite harmful, and the source of contamination is widespread. Therefore, it is necessary to remediate the cadmium contaminated soil. Zeolite can reduce the cadmium concentration in the leaves of potted lettuce by 86%. Sepiolite can significantly promote the growth of spinach and reduce the cadmium content in water spinach. Spraying zinc and selenium can reduce the absorption of cadmium by 37.01% and 31.63%. The content of cadmium in Chinese cabbage treated by rare Earth is 89.4%–98.08% compared with the control treatment. Organic fertilizer can promote the conversion of exchangeable cadmium to organic binding state and manganese oxide bound cadmium, thus reducing the available cadmium content in soil. Because of the particularity of the passivation

mechanism, most passivators only temporarily reduce the effective form of cadmium by various effects. Therefore, the passivation remediation could introduce secondary pollution to the soil in the later period. It is proposed that the study is improved from the following elements for the remediation of cadmium contamination in vegetable greenhouse. Attention should be paid to the development of high efficiency and low cost cadmium pollution barrier, passivation products, and standardization technology. A single remediation method is often difficult to adapt to the remediation of a variety of heavy metal contaminated soil. It is necessary to adopt the combination of chemical and biological methods for remediation and optimization. Chemical remediation can be combined with other remediation methods, such as phytoremediation and micro bioremediation. For the selection of the passivator, it is necessary to ensure that the passivation effect of the heavy metal is obvious and simple.

Data Availability

The data used are available from the corresponding author upon request.

Conflicts of Interest

The authors declare that there are no conflicts of interest regarding the publication of this paper.

References

[1] D. Mohan, H. Kumar, A. Sarswat, M. Alexandre-Franco, and C. U. Pittman, "Cadmium and lead remediation using magnetic oak wood and oak bark fast pyrolysis bio-chars," *Chemical Engineering Journal*, vol. 236, no. 2, pp. 513–528, 2014.

[2] C. Sulmon, F. Ramel, G. Gouesbet, and I. Couée, "Improvement of environmental remediation by on-site phytoremediating greenhouses," *Environmental Science and Technology*, vol. 48, no. 11, pp. 6055-6056, 2014.

[3] S. Adiloğlu, A. Adiloğlu, and F. E. Açıkgöz, "Phytoremediation of cadmium from soil using patience dock (rumex patientia l.)," *Analytical Letters*, vol. 49, no. 4, pp. 601–606, 2016.

[4] S. Kushwaha, B. Sreedhar, R. Bhatt, and P. P. Sudhakar, "Spectroscopic characterization for remediation of copper, cadmium and mercury using modified palm shell powder," *Journal of the Taiwan Institute of Chemical Engineers*, vol. 46, no. 46, pp. 191–199, 2015.

[5] B. V. Tangahu, S. R. Sheikh Abdullah, H. Basri, M. Idris, N. Anuar, and M. Mukhlisin, "A review on heavy metals (As, Pb, and Hg) uptake by plants through phytoremediation," *International Journal of Chemical Engineering*, vol. 2011, pp. 1–31, 2011.

[6] M. Gildiaz, A. Gonzalez, and J. Alonso, "Evaluation of the stability of a nanoremediation strategy using barley plants," *Journal of Environmental Management*, vol. 165, no. 1, p. 150, 2015.

[7] K. R. Hladun, D. R. Parker, and J. T. Trumble, "Cadmium, copper, and lead accumulation and bioconcentration in the vegetative and reproductive organs of raphanus sativus:

implications for plant performance and pollination," *Journal of Chemical Ecology*, vol. 41, no. 4, pp. 386–395, 2015.

[8] Z. Lei, "The contamination characteristic of cadmium in soil and green plant in the downtown area of zhaoyuan city," in *Proceedings of the 2012 International Conference on Biomedical Engineering and Biotechnology*, pp. 1791–1794, Macau, China, May 2012.

[9] C. L. Nagodavithane, B. Singh, and Y. Fang, "Effect of ageing on surface charge characteristics and adsorption behaviour of cadmium and arsenate in two contrasting soils amended with biochar," *Soil Research*, vol. 52, no. 2, pp. 155–163, 2014.

[10] B. Yousaf, G. Liu, R. Wang et al., "Investigating the potential influence of biochar and traditional organic amendments on the bioavailability and transfer of Cd in the soil-plant system," *Environmental Earth Sciences*, vol. 75, no. 5, p. 374, 2016.

[11] T. Tang Chunfang, L. Li Kelin, Y. Ling Dingxun, and L. Dingxun, "Influence of Co-planting on Cd accumulation in oilseed rape and pai-tsai plants," in *Proceedings of the 2011 Third International Conference on Measuring Technology and Mechatronics Automation*, pp. 410–413, Shangshai, China, January 2011.

[12] S. Ghafoor and S. Ata, "Synthesis of carboxyl-modified fe3o4@sio2 nanoparticles and their utilization for the remediation of cadmium and nickel from aqueous solution," *Journal of the Chilean Chemical Society*, vol. 62, no. 3, pp. 3588–3592, 2017.

[13] X. Y. Xi, M. Y. Liu, Y. Huang, Y. Chen, Y. Zhang, and Y. Y. Chen, "Response of flue-cured tobacco plants to different concentration of lead or cadmium," in *Proceedings of the 2010 4th International Conference on Bioinformatics and Biomedical Engineering*, pp. 1–4, Chengdu, China, June 2010.

[14] S. Colombano, S. Andriatsihoarana, and S. Ouali, "Effect of remediation treatments on polar PACs in soils; degradation vs. formation," *Brain Research*, vol. 674, no. 2, pp. 291–298, 2015.

[15] M. Ahmad, A. U. Rajapaksha, J. E. Lim et al., "Biochar as a sorbent for contaminant management in soil and water: a review," *Chemosphere*, vol. 99, no. 3, pp. 19–33, 2014.

[16] R. Bian, S. Joseph, L. Cui et al., "A three-year experiment confirms continuous immobilization of cadmium and lead in contaminated paddy field with biochar amendment," *Journal of Hazardous Materials*, vol. 272, no. 4, pp. 121–128, 2014.

[17] J. Gómez-Pastora, E. Bringas, and I. Ortiz, "Recent progress and future challenges on the use of high performance magnetic nano-adsorbents in environmental applications," *Chemical Engineering Journal*, vol. 256, no. 8, pp. 187–204, 2014.

[18] H.-S. Kim, K.-R. Kim, H.-J. Kim et al., "Effect of biochar on heavy metal immobilization and uptake by lettuce (Lactuca sativa L.) in agricultural soil," *Environmental Earth Sciences*, vol. 74, no. 2, pp. 1249–1259, 2015.

[19] C. Li, J. G. Huang, and S. Pang, "Detection model simulation of soil pollution degree of garbage leachate," *Computer Simulation*, vol. 31, no. 5, pp. 264–267, 2014.

[20] F. Liu, X. Liu, L. Zhao, C. Ding, J. Jiang, and L. Wu, "The dynamic assessment model for monitoring cadmium stress levels in rice based on the assimilation of remote sensing and the WOFOST model," *Ieee Journal of Selected Topics in Applied Earth Observations and Remote Sensing*, vol. 8, no. 3, pp. 1330–1338, 2015.

[21] Y. Zhang, H. Liang, Y. Pan, G. Dai, G. Deng, and D. Li, "Identification of anthocyanin biosynthesis genes in rice pericarp using PCAMP," *Plant Biotechnology Journal*, vol. 17, no. 9, pp. 1700–1702, 2019.

WILEY | Hindawi

Research Article

Optimal Matching Metaheuristic Algorithm for Potential Areas of Agricultural Economic Resources Development Based on Spatial Relationship

Jianying Zhang [ID] **and Xuebin Feng** [ID]

Vocational and Technical College, Inner Mongolia Agricultural University, Hohhot 104109, China

Correspondence should be addressed to Jianying Zhang; ndzjying@imau.edu.cn

The agriculture sector is the backbone of the economies of many Asian countries such as India, China, and Bangladesh. The agriculture sector can contribute a major share to the GDP of such countries where the main occupation of the citizens is agriculture or the dependency of the citizens is mainly on the agricultural productivity. It is important to study the potential areas of agricultural economic resource development. The existing methods are not efficient enough to map the potential areas of agricultural productivity with economic resource development, and hence, it has motivated us to study the aspects which impact the economic resource development based on agricultural productivity. There are numerous factors such as low productivity, high irrigation amount, high labor charges, low proportion of planning optimization, and low crop yield that should be considered to study the correlation between economic development and agricultural productivity. Firstly, the spatial relationship of potential areas of agricultural economic resources development is analyzed in this paper. Secondly, the multiobjective linear programming model is proposed. Based on this multiobjective model, the optimal matching model for potential areas of agricultural economic resource development is constructed, and the improved genetic algorithm is used to solve the model to realize the optimal matching of potential areas of agricultural productivity and economic resource development. The experimental results show that the proposed method has high economic benefit, low irrigation amount, and high proportion of planning optimization with high crop yield.

1. Introduction

Water resource is an important factor for promoting agriculture-based economic growth and agriculture is the largest water resource consumer in China [1]. Due to the influence of market price and water consumption of different crops, different allocation of water resources among crops can bring different economic benefits [2]. In order to make the full utilization of water resources and achieve the maximum benefit, it is necessary to adjust the crop planting structure with differently available agricultural water resources [3]. Water resources are needed for ensuring regional food security and a reasonable output structure of crop products [1]. Especially for the arid and semiarid areas, it is of great practical importance for regional agricultural development

to adjust the regional planting structure under the constraints of limited agriculturally available water resources. Other resources are also important, but not as much as those of water resources. Soil quality, humidity for plants, weather conditions, climate, exposure to sunlight, pesticides, quality of seeds, temperature, economic markets, and export-import policies all contribute as factors of influence on agricultural productivity. The motivation of this paper is to study the impact of these factors on agricultural productivity and the correlation between agricultural productivity and economic resource development.

In [4], the authors proposed a matching algorithm for resource development potential regions based on linear programming. The algorithm took the highest economic benefit under different irrigation technology proportions as

the goal and added the calculation of a comprehensive ecological environment index to the conventional constraints such as total agricultural planting area and water consumption of agricultural planting. Based on this, the ecological benefit of optimization results was evaluated, and a linear programming model was established. To achieve area matching, the algorithm did not consider the crop planting structure and had the problem of low proportion of planning optimization. In [5], the authors proposed a matching algorithm for potential regions of agricultural resource development based on IBM software. Wheat, corn, cotton, rice, sugar beet, and potato were selected as the research objects. On the basis of using the Penman–Monteith formula to calculate the unit virtual water yield of 6 main crops in 14 prefectures and 64 main producing counties in Xinjiang, the algorithm proposed a matching algorithm for potential regions of agricultural resource development based on IBM SPSS software and the unit virtual water value of main crops was obtained. With the help of IBM SPSS for correspondence analysis, this paper studied the planting preference and layout of main crops in Xinjiang from the perspective of virtual water value. The algorithm did not consider the water consumption of agricultural plantings and had the problem of high irrigation water. In [6], the authors proposed an area matching algorithm for agricultural resource development potential based on multitemporal Sentinel-2A. The algorithm used multitemporal Sentinel-2A remote sensing images as a data source and calculated the time series normalized vegetation index (NDVI) and red edge normalized vegetation index (RBNDVI) and their combination characteristics. It analyzed crop characteristic curves and used the random forest method to match five characteristic parameters as classification characteristics. The algorithm did not consider the yield and benefit and had the problems of low economic benefit and low crop yield.

In [7], the authors explored the usage of IT and its applications in the area of agriculture. The role of IT in the development of agricultural productivity and its impact on the economy were studied in the paper. It certainly helped the agriculture sector to improve its traditional way of doing things and in adding more value to the country's economy. In [8], the authors concluded that the contribution of agriculture in GDP was decreasing significantly over the periods with the evolution of manufacturing and other industries. The economy was still growing due to the agriculture sector and could collapse if the agriculture sector was ignored. The importance of agricultural products would prevail in the growth of the economy. In [9], the authors studied the impact of outdated irrigation methods adopted by the farmers in small villages. The lack of knowledge led to the generation of poor income due to the adoption of obsolete methods for irrigation and agriculture. Economic growth and food security were concerned with the yield of crops. The major issue of poverty was revealed to be poor irrigation methods. In [10], the authors presented a structural model which revealed the direct and indirect impact of dam-driven water for irrigation on the revenue of the crops. The results concluded that the revenue was directly proportional to the availability of water. The availability of water could aid in generating high revenues.

Apart from water resources, we have made an attempt to study more factors that affect productivity and economic resource development. The major highlights are given as follows:

(i) There are numerous factors such as low productivity, high irrigation amount, high labor charges, low proportion of planning optimization, and low crop yield which are considered to study the correlation between economic development and agricultural productivity in this paper rather than focusing on just one factor like water/irrigation resources.

(ii) In the first phase, the spatial relationship of potential areas of agricultural economic resources development is analyzed to get an idea about the factors influencing agricultural productivity and economic growth.

(iii) Then, the multiobjective linear programming model is proposed. The multiobjective model considers constraints and optimizes multiple objectives simultaneously.

(iv) Based on the multiobjective model, the optimal matching model for potential areas of agricultural economic resource development is constructed, and the improved genetic algorithm is used to solve the model to realize the optimal matching of potential areas of agricultural productivity and economic resource development.

The paper discusses the proposed model in two phases, and the next section explains the proposed model. The third section focuses on the results of the proposed research. The last section summarizes the research work presented in this paper.

2. Proposed Research

This section explains the best match model for the potential area of agricultural economic resources development.

2.1. The Proposed Mapping Model for Agricultural Productivity and Economic Resources. Based on the spatial relationship, the optimal matching algorithm for the potential area of agricultural economic resources development considers the spatial relationship between the development potential areas and constructs the optimal matching model for the potential area of agricultural economic resources development through three submodels as discussed below.

(1) The multiobjective optimal allocation model of flow and time in main and branch canals is constructed, and the two objectives of minimum fluctuation of water distribution flow and minimum loss of water conveyance are realized at the same time.

(2) Branch canal and bucket canal's round irrigation group division model are constructed to minimize

water distribution time and obtain the distribution flow and time of branch canal and bucket canal, thereby obtaining optimized water distribution.

(3) Based on the results of water distribution in main and branch canals, a linear fractional programming model based on chance-constrained programming is constructed to optimize the planting structure of various crops in an irrigation area, so as to obtain the maximum benefit per unit planting area.

The specific process is shown in Figure 1.

2.1.1. Multiobjective Linear Programming Model of Flow and Time Allocation in Canal System.

The branch canals are known as continuous irrigation channels. Water is available in the canals throughout the water distribution cycle in China [11, 12]. The modeling idea of the proposed algorithm is to optimize the flow and water distribution time of the main and branch channels in the irrigation area and satisfy the following clauses:

(1) The actual water distribution is within the range of available water in the irrigation area.

(2) The water distribution time is within the specified rotation period.

(3) The actual water distribution should meet the requirements of crop irrigation.

(4) At any time, the sum of the water distribution flows of each lower channel is equal to the water distribution flows of the upper channel, and the water distribution flow of the upper and lower channels should be changed between 0.6 and 1.2 times the design flow as far as possible, so as to meet the requirements of the water distribution level of the channel and prevent the collapse caused by the overflow of the channel. According to the above modeling idea, a multiobjective linear programming model for water distribution in main and branch canals is constructed. The first objective function is to consider the minimum fluctuation of water distribution flow in superior canals at different times; the second objective function is to minimize the water loss of the canal system, which can reflect the actual situation of the canal system to meet the requirements of the canal system.

The objective function (1) of the model is given by equation (1) and the substitute is devised by equation (2).

Objective function (1) is given as follows:

$$\min Z_1 = \min \frac{\sum_{t=1}^{T} \left(Q_{st} - \overline{Q}_s\right)^2}{T - 1}, \quad \forall t = 1, 2, \ldots, T, \tag{1}$$

where

$$Q_{st} = \sum_{n=1}^{N} q_n^* f_{tn}(x), \quad \forall t = 1, 2, \ldots, T. \tag{2}$$

Objective function (2) is given by equation (3) and the substitute is devised by equation (4).

$$\min Z_2 = V_s + V_d = \frac{\sum_{t=1}^{T} W_{st}(1 - \eta_s)}{\eta_s} + \sum_{t=1}^{T} W_{dn}^*(1 - \eta_{dn}). \tag{3}$$

Where,

$$\begin{cases} W_{st} = Q_{st} t_{st} \times 60 \times 60, \\ W_{dn}^* = q_n^* \times t_{1n} \times 60 \times 60. \end{cases} \tag{4}$$

The constraints of the multiobjective method are shown from equations (5) to (8).

The constraint of irrigation water supply is given in the following equation:

$$\frac{W_{st}}{\eta_s} \leq W_{at}, \quad \forall t = 1, 2, \ldots, T. \tag{5}$$

A round constraint is given by the following equation:

$$\begin{cases} 0 \leq t_{0n} \leq T, \\ t_{2n} \leq T, \quad \forall t = 1, 2, \ldots, T. \\ t_{0n} + t_{1n} = t_{2n}, \end{cases} \tag{6}$$

A flow constraint of lower channel is given in the following equation:

$$a \times qd_n \leq q_n^* \leq qd_n, \quad \forall t = 1, 2, \ldots, N. \tag{7}$$

Flow constraints of superior channel node are given in the following clubbed equation:

$$\begin{cases} \text{Node } A: aQ_A \leq \sum_{n=1}^{N} q_n^* f_{tn}(x) \leq bQ_A, \quad \forall n = 1, 2, \ldots, N, \\ \text{Node } B: aQ_B \leq \sum_{n=1}^{N} q_n^* f_{tn}(x) \leq bQ_B, \quad \forall n = 1, 2, \ldots, 5, \\ \text{Node } C: aQ_C \leq \sum_{n=1}^{N} q_n^* f_{tn}(x) \leq bQ_C, \quad \forall n = 6, 7, \ldots, N, \\ \text{Node } D: aQ_D \leq \sum_{n=1}^{N} q_n^* f_{tn}(x) \leq bQ_D, \quad \forall n = 6, 7, \ldots, 15, \\ \text{Node } E: aQ_E \leq \sum_{n=1}^{N} q_n^* f_{tn}(x) \leq bQ_E, \quad \forall n = 16, 17, \ldots, 19. \end{cases} \tag{8}$$

In the above equations, t is the time, n is the number of lower-level channels, N is the number of branch canals in a round irrigation group, q_n^* is the gross distribution flow of the lower-level channels of each round irrigation group, t_{0n} is the start time of the n th lower-level channel, t_{1n} is the irrigation time of the n-th lower-level channel, t_{2n} is the irrigation end time of the n th lower-level channel, and n is the time step of the t th period. T is the rotation irrigation cycle and Q_{st} is the net water distribution of the upper-level channel at time t which is equal to the sum of the flow of the lower-level water distribution channel at this moment.

$f_{tn}(x)$ is a continuous function that describes the continuous water distribution state of the channel during the
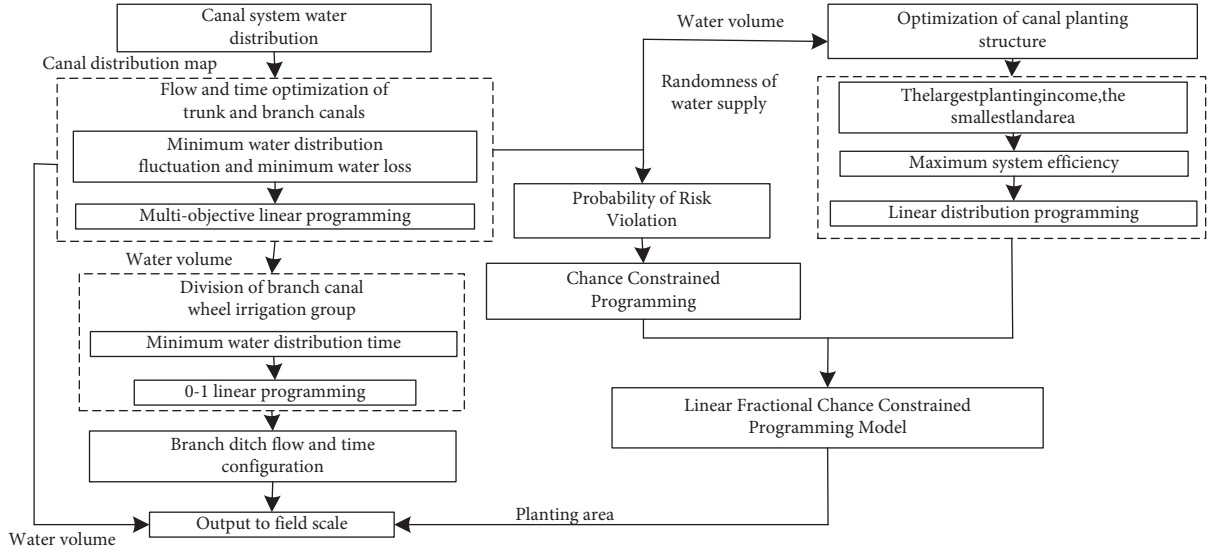
Figure 1: Schema of the proposed research.

rotation period. If $t_{0n} \leq t \leq t_{2n}$, then $f_{tn}(x) = 1$, otherwise, $f_{tn}(x) = 0$; W_{st} is the net water distribution of the upper-level channel, W^*_{dn} is the gross water distribution of the n th lower channel; η_s is the water utilization coefficient of the upper channel canal system; η_{dn} is the water utilization coefficient of the n th lower channel; qd_n is the design flow rate of the n th lower channel. Q_A, Q_B, Q_C, Q_D, and Q_E are the design flow of the superior channel corresponding to each node A, B, C, D, and E respectively. a and b are the allowable threshold coefficients of channel running flow, respectively, and W_{at} is the water available for irrigation in time period of t.

2.1.2. Optimization of Crop Planting Structure. The optimization of crop planting structures on the scale of a canal system is to study the proportion of crop planting in each canal through a reasonable arrangement to reduce irrigation water demand and increase irrigation income [13, 14]. The research on the deterministic model of crop planting structure optimization at home and abroad includes single-objective models and multiobjective models. The single-objective models generally aim to maximize the economic benefits of the whole irrigation area, and the calculation method generally adopts the linear programming method [15]. The single-objective model is relatively simple, but it fails to achieve the overall development of negotiation and coordination between decision-makers and models [16, 17]. With the concept of sustainable development in irrigation areas, many scholars began to study the multiobjective planning model of crop planting structure [18]. The commonly used multiobjective optimization methods for planting structure include the objective weight method, grey analysis, compromise constraint, fuzzy optimization theory, and order degree mode [19]. These studies have a certain guiding significance for the adjustment of crop planting structures, but most of the multiobjective models of crop planting structures based on the above methods have

subjective factors in the calculation of coefficient and the determination of index weight of the objective function [20]. In order to overcome the above shortcomings, the proposed algorithm introduces fractional programming into the multiobjective optimization model of planting structure. Considering the randomness of available water supply, stochastic change-constrained programming is introduced to construct the multiobjective uncertainty model of the planting structure based on fractional programming and stochastic chance-constrained programming. The expression of the model is given in equation (9) and constraint conditions are given in equations (10) and (11).

Objective function is given as follows:

$$\max f = \frac{\max f_1}{\min f_2} = \frac{\max \left[\sum_{s=1}^{S} C_s Y_s a_s - \text{EC} \right]}{\min \sum_{s=1}^{S} m_s a_s}. \tag{9}$$

Available water constraint is given as follows:

$$\Pr \left\{ \sum_{s=1}^{S} m_s a_s - Q_{yl} \right\} \geq 1 - p. \tag{10}$$

Planting area constraint is given as follows:

$$\begin{cases} \sum_{s=1}^{S} a_s \leq A_{\max}, \\ \sum_{s_j=1}^{S_j} a_{s_j} \leq A_{s_j, \max}, a_s \geq a_{s, \min}, a_2 \leq a_{2, \max}, \sum_{s_j=1}^{S_j} a_{s_j} \geq A'_{\min}. \end{cases} \tag{11}$$

In the above equations, f is the objective function, f_1 is the economic benefit target, f_2 is the irrigation water target, s is the crop variety, C_s is the unit price of the sth crop, Y_s is the yield per unit area of the sth crop, a_s is the planting area of the sth crop, a_{s_j} is the planting area of cash crops, and a_2 is the planting area of summer miscellaneous goods. EC is the operational cost of the irrigation area including management fees, maintenance fees, and operating expenses.

m_s is the irrigation quota of the sth crop, Q_{yl} is the net useable water resources of irrigation area, $A_{\max}$ is the maximum total irrigation area of the irrigation area, $A_{s_j, \max}$ and $A'_{\min}$ are the maximum planting area of cash crops and the minimum planting area of food crops respectively, and $a_{s, \min}$ is the minimum planting area of sth crops.

As the above model is a single-layered programming model, there are differences in its solution methods. The solution idea is to transform the single-layer fractional linear programming model into an ordinary linear programming model and then solve it. A typical fractional programming model can be expressed as given in the following equation:

$$\begin{cases} \max f(x) = \dfrac{cx + \alpha}{dx + \beta}, \\ \\ Ax \le b, x \ge 0. \end{cases} \tag{12}$$

In the above equation, A is a $m \times n$ matrix, x and b are n-dimensional and m-dimensional column vectors, respectively, c and d are n-dimensional row vectors, respectively, and α and β are parameters. If the above formula is satisfied, then the following will applicable.

$d = 0$. $dx + \beta > 0$.

(1) For all x, $dx + \beta > 0$

(2) The objective function is continuously differentiable

(3) The feasible area is nonempty and bounded

Then the above formula can be transformed into the following equation:

$$\begin{cases} \min g(y, z) = z, \\ A^T y + d^T z \ge c^T, \\ -b^T y + \beta z = \alpha, \\ y \ge 0. \end{cases} \tag{13}$$

In the above equation, T represents the transpose of the matrix, y is a column vector with m elements, and z is a scalar. The above formula is a general linear programming model, and its optimal solution $(\widehat{y}, \widehat{z})$ can be easily obtained. The relaxation column vector $\widehat{v}$ is introduced with $\widehat{v} = a^T \widehat{y} + d^T \widehat{z} - c^T$ and $\widehat{v} \ge 0$. Let $\widehat{x}$ be the optimal solution of model and $\widehat{u}$ be the relaxation column vector, then $a\widehat{x} + \widehat{u} = b$ and $\widehat{u} \ge 0$. According to the relaxation theorem, if $\widehat{x}_j \widehat{v}_j = 0$ and $\widehat{y}_j \widehat{u}_j = 0$, models (12) and (13) have the same optimal solutions. Therefore, the linear fractional programming model can be solved by the above conversion.

2.1.3. Division Model of Round Irrigation Group in Canal System.
The modeling idea has some assumptions. The water flow from the branch canal is determined when the water is distributed to the ditch and the ditch takes the specified amount of water from the branch canal in a constant flow to the required agricultural areas [21]. Once each ditch is opened, it is required to deliver water continuously within the specified time to maintain its stable flow until the specified amount of water reaches the destined place [22]. The result of optimal water distribution is to minimize the leakage loss of the ditch. When dividing each ditch in the branch canal into round irrigation groups, only one ditch in each group is required to divert water [23]. The outlet of any lower ditch is only opened once in the rotation period [24]. When the diversion of the ditch in a group is about to be completed, the diversion flow in the branch canal should be kept unchanged [25]. At this time, the sum of the diversion flow of the ditch plus the leakage loss is in balance with the diversion flow of the branch canal. In order to facilitate the management, the water diversion duration of each round irrigation group is equal or similar.

Taking the minimum irrigation time of a round irrigation group as the objective function, 0-1 integer programming is used to establish the division model of the round irrigation group for branch canal and bucket canal; the constraints such as the maximum net irrigation amount and rotation period are considered. The expression of the model is given in the following equation:

$$\begin{cases} \min Z = \displaystyle\sum_{g=1}^{G} \sum_{m=1}^{M} x_{gm} t_m, \\ \\ t_m = \dfrac{W_{gm} + W_{sm}}{q_{mm}}. \end{cases} \tag{14}$$

In the above equation, Z is the sum of the water delivery time of each round of irrigation group, g is the ordinal number of round irrigation group in branch canal/bucket canal, G is the number of each bucket canal, m is the ordinal number of branch canal/bucket canal, M is the number of round irrigation group, t_m is the water delivery time of each branch canal/bucket canal in the round irrigation group, and W_{gm} is the net water demand of the mth branch canal/bucket canal. W_{sm} represents the leakage loss of the mth branch canal/bucket canal, q_{mm} is the gross flow rate of the mth branch canal/bucket canal, the decision variable is $x_{gm} = \{0, 1\}$ which means the switch state of the mth branch canal/ bucket canal of the g th round irrigation group, and x_{gm} is equal to 0, when the branch canal/bucket canal gate is closed. x_{gm} equal to 1 means that the gate of the branch canal/ bucket canal is opened. The constraint functions are expressed in equations (15) and (16).

Round constraints are given as follows:

$$T_{\min} \le \sum_{m=1}^{M} x_{gm} t_m \le T_{\max}. \tag{15}$$

One time diversion constraint is given as follows:

$$\sum_{g=1}^{G} x_{gm} = 1. \tag{16}$$

0-1 constraints: $x_{gm} = \{0, 1\}$. $T_{\max}$ and $T_{\min}$ are the maximum and minimum diversion time of the upper branch canal.

Combined with the above model, the best matching model of agricultural economic resources development potential is constructed as shown in the following equation:

$$F = \min Z_1 + \min Z_2 + \max f + \min Z. \qquad (17)$$

3. Mapping Model for Agriculture Productivity and Economic Development

For mapping the potential area of agricultural economic resources development based on spatial relationship, the improved genetic algorithm (GA) is used to solve the best matching model for the potential area of agricultural economic resources development to achieve the best matching. Specific steps are as follows:

(1) Encoding mode: the encoding mode is using binary encoding.

The coding symbol set used in binary coding is composed of "0" and "1", and the binary symbol string constitutes the individual genotype [22]. Assuming that the value range of a parameter is $[U_{min}, U_{max}]$, and the length of the binary code symbol string representing this parameter is l, the corresponding relationship between parameter codes is given by the following equation:

$$
\begin{aligned}
000000 \cdots 000000 &= 0 \longrightarrow U_{min}, \\
000000 \cdots 000000 &= 1 \longrightarrow U_{min} + \delta, \\
&\vdots \\
111111 \cdots 111111 &= 2^l - 1 \longrightarrow U_{max}.
\end{aligned}
\qquad (18)
$$

Then the coding accuracy of binary coding is given by the following equation:

$$\delta = \frac{U_{max} - U_{min}}{2^l - 1}. \qquad (19)$$

If the code of an individual is $X: a_l a_{l-1} \cdots a_2 a_1$, the corresponding decoding formula is given by

$$x = U_{min} + \left(\sum_{i=1}^{l} a_i \times 2^{i-1} \right) \frac{U_{max} - U_{min}}{2^l - 1}. \qquad (20)$$

(2) Initial population: For the generation of the initial population, the random generation method is adopted.

(3) The fitness function is given by the following equation:

$$
\text{Fitness} =
\begin{cases}
\dfrac{1}{1 + \exp\left[\left(f - f_{avg} \right)/c \right]}, & g \geq 30\% n, \\[4mm]
\dfrac{1}{1 + \exp\left(f - f_{avg} \right)}, & g < 30\% n.
\end{cases}
\qquad (21)
$$

f is the original fitness value. If there is a need to find the minimum then f is considered as the objective function. If the problem is to find the maximum then the problem needs to be transformed into a problem of finding the minimum. f_{avg} is the average of the fitness of each individual in the contemporary population. The difference between the f value of each individual and f_{avg} is calculated, g represents the number of individuals whose difference range is $(-10, 10)$, and c represents the magnitude of the maximum absolute value of the difference between the value of f and f_{avg}.

(4) Selection operation: A strategy combining roulette selection and optimal preservation strategy is used to replace the last M individuals in the population after crossover and mutation with the M individuals with the top fitness value in the parent genes, so that the offspring and the parent can participate in the competition together [17].

Implementation steps are as follows:

(a) All the individuals in the current population are ranked according to the fitness value, and M individuals in the front row are selected.

(b) Let all individuals in the contemporary population participate in crossover and mutation operation to produce the next generation population.

(c) All individuals in the next generation population are ranked according to the fitness value, and the next M individuals are found.

(d) The M individuals from 1 is used to replace the M individuals from 3 to produce a new generation.

(e) Crossover operator: A single point crossover operator is used, and the crossover probability is calculated by the following equation:

$$
p_c =
\begin{cases}
p_{c3} - \dfrac{p_{c3} - p_{c2}}{1 + \exp\left[A\left(2 - 3(f_{max} - f')/\left(f_{max} - f_{avg} + r \right) \right) \right]}, & f' \geq f_{avg}, \\[5mm]
p_{c2} - \dfrac{p_{c2} - p_{c1}}{1 + \exp\left[A\left(1 - 3\left(f_{avg} - f' \right)/\left(f_{avg} - f_{min} + r \right) \right) \right]}, & f' < f_{avg},
\end{cases}
\qquad (22)
$$
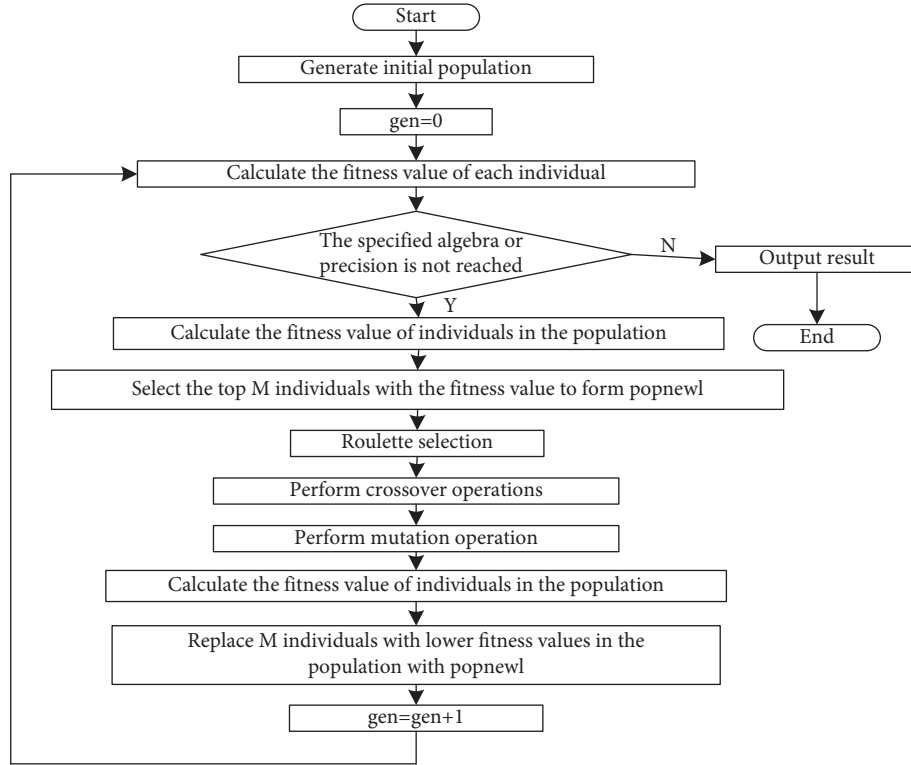
FIGURE 2: Solution flow using GA.

where, $f_{\max}$ is the largest individual fitness value and $f_{\min}$ is the smallest individual fitness value.

(5) Mutation operator: The basic unit mutation operator is used, and the mutation probability is calculated by the following formula as given in equation:

$$p_m = \begin{cases} p_{m2} - \dfrac{p_{m2} - p_{m1}}{1 + \exp\left[A\left(3\left(f_{\max} - f\right)/\left(f_{\max} - f_{\text{avg}} + r\right) - 2\right)\right]}, & f \geq f_{\text{avg}}, \\[4mm] p_{m3} - \dfrac{p_{m3} - p_{m2}}{1 + \exp\left[A\left(3\left(f_{\text{avg}} - f'\right)/\left(f_{\text{avg}} - f_{\min} + r\right)\right) - 1\right]}, & f < f_{\text{avg}}. \end{cases} \tag{23}$$

(6) Set the number of iterations. If the maximum number of iterations is reached, the optimal solution of the best matching model for the potential area of agricultural economic resources development is found. The specific flow chart is shown in Figure 2.

4. Results and Discussion

In order to verify the overall effectiveness of the proposed optimal matching algorithm for the potential region of agricultural economic resources development based on spatial relationships, it is necessary to evaluate the performance and compare it with the other existing methods. The proposed optimal algorithm is termed as "Algorithm 1" in the results. The other comparative approaches considered for the comparative study are algorithm-2 (presented in the reference paper [4]), algorithm-3 (presented in the reference

paper [5]), and algorithm-4 (presented in the reference paper [6]). The maximum benefit and minimum irrigation amount of the above algorithms are compared. The test results are shown in Figure 3.

By analyzing the results in Figure 3, it can be seen that compared with algorithm-2 [4], algorithm-3 [5], and algorithm-4 [6], the proposed "algorithm-1" obtains maximum economic benefits in different agricultural areas. On the contrary, the minimum irrigation water requirement by the proposed algorithm is relatively lesser as compared to other approaches. It indicates that algorithm-1 can obtain greater economic benefits with lesser requirements of irrigation water. As Algorithm-1 constructs a multiobjective linear programming model for canal system flow and time configuration, it can obtain greater economic benefits with the lowest amount of irrigation water.

(a)

(b)

(c)

(d)
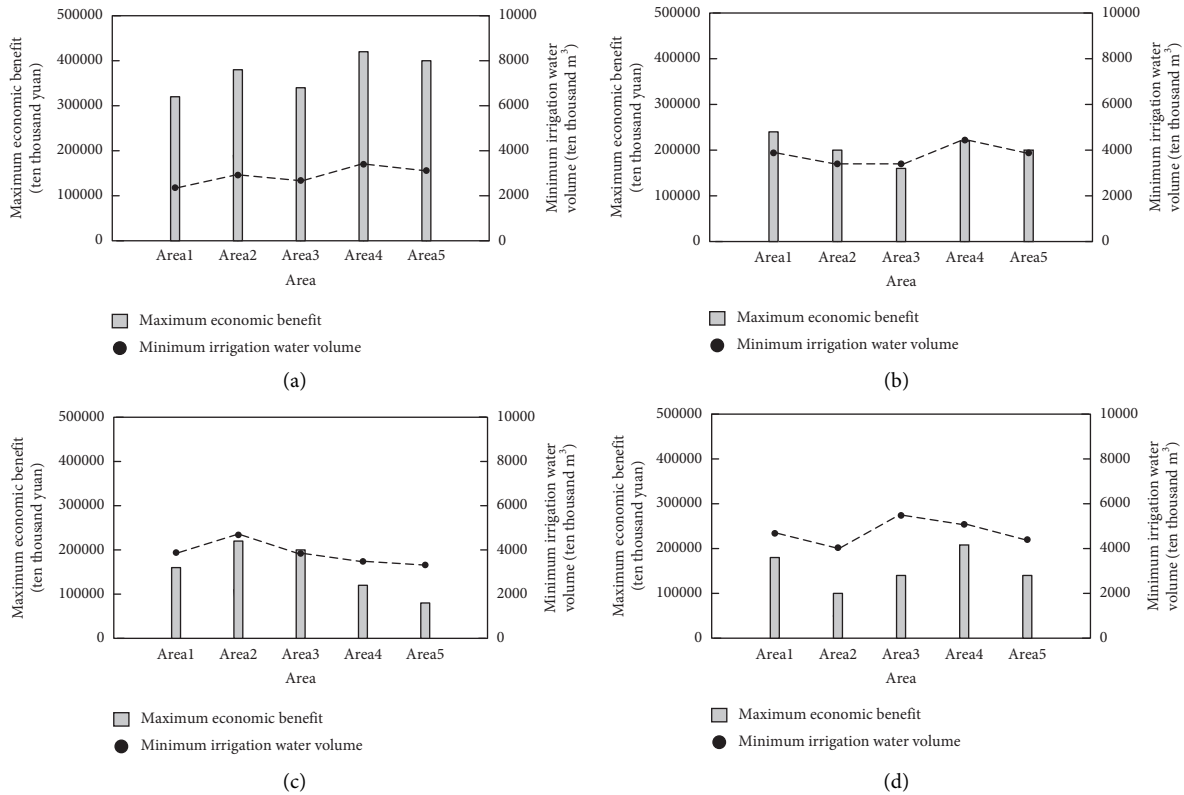
Figure 3: Maximum economic benefit and minimum irrigation water quantity by different algorithms. (a) The maximum economic benefit and minimum irrigation water quantity of algorithm-1, (b) the maximum economic benefit and minimum irrigation water quantity of algorithm-2, (c) the maximum economic benefit and minimum irrigation water quantity of algorithm-3, and (d) the maximum economic benefit and minimum irrigation water quantity of algorithm-4.
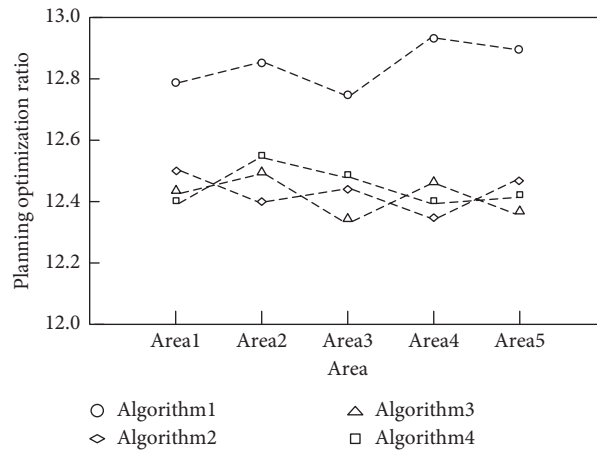
Figure 4: Optimal proportion of different algorithms.

The effectiveness of algorithm-1, algorithm-2 [4], algorithm-3 [5], and algorithm-4 [6] is tested by taking the planning optimization ratio as the test index. The test results are shown in Figure 4.

By analyzing the results in Figure 4, it can be seen that the optimization proportion of algorithm-1 is higher than that of algorithm-2 [4], algorithm-3 [5], and algorithm-4 [6] in different areas. The higher planning proportion is an indicator for the reasonable proportion of crops in the area.

From the above analysis, it can be seen that algorithm-1 can effectively and reasonably realize crop allocation in resource development potential areas. Since algorithm-1 constructs a multiobjective uncertainty model of planting structure, it can reasonably allocate the planting areas and areas of different crops in the region and can improve the planning optimization proportion of the algorithm.

The crop yields of algorithm-1, algorithm-2 [4], algorithm-3 [5], and algorithm-4 [6] are shown in Figure 5.

(a)
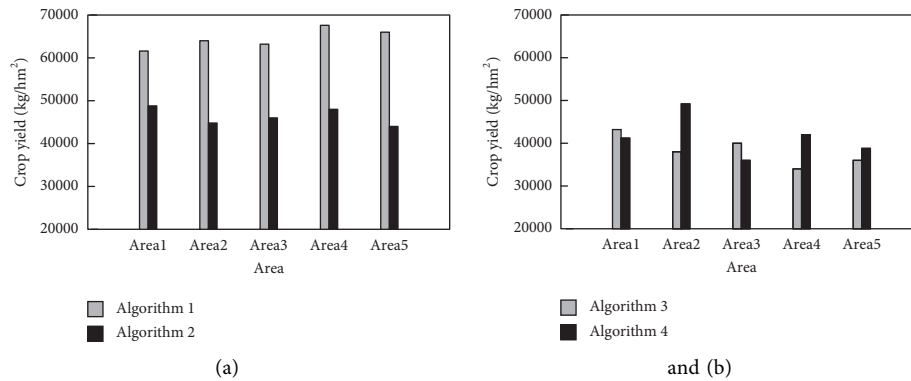
and (b)

Figure 5: Crop yield of different algorithms. (a) Crop yield of algorithm-1 and algorithm-2 and (b) crop yield of algorithm-3 and algorithm-4.

According to the data in Figure 5, the crop yield obtained by the proposed algorithm-1 is much higher than that of algorithm-2 [4], algorithm-3 [5], and algorithm-4 [6] in multiple areas. Since algorithm-1 constructs the division model of the canal system, it optimizes the water distribution, minimizes the leakage loss of the ditch, and improves the regional crop yield.

5. Conclusion

The development of water-saving and efficient agriculture is a strategic choice for sustainable agricultural development. The rational allocation of agricultural water and soil resources is an important way to improve the utilization efficiency of agricultural resources to improve the economic growth of the country. The allocation of agricultural water and soil resources in different spatial scales has different characteristics and impacts on the agriculture produce. Climate change and human activities lead to the uncertainty of optimal utilization of agricultural water and soil resources. Therefore, it is of great significance to study the multiobjective model that can map the agriculture requirements with the available natural resources. The potential growth of agricultural economic resources is certain by devising an intelligent mechanism to map the demand with the available resources and our proposed method is capable of mapping the requirements with the available resources for optimal utilization of agriculture resources for economic development. This paper constructs the optimal mapping model for optimal utilization of agricultural resources. The results prove that the proposed model enhances the economic benefit by minimizing water requirements and also enhances the yield of the crops for economic development.

Data Availability

The data used are available from the corresponding author upon request.

Conflicts of Interest

The authors declare that there are no conflicts of interest regarding the publication of this study.

References

[1] B. J. Du, J. Zhang, Z. M. Wang, D. H. Mao, M. Zhang, and B. F. Wu, "Crop classification using sentinel-2a ndvi time series and object-oriented decision tree method," *Journal of Geo-Information Science*, vol. 21, no. 05, pp. 740–751, 2019.

[2] Z. Zhou, S. Y. Li, K. Zhang, and Y. Y. Shao, "Crop distribution mapping based on cnn and crop spectral texture features," *Remote Sensing Technology and Application*, vol. 34, no. 04, pp. 694–703, 2019.

[3] X. H. Li, B. Y. Jia, Z. W. Fan, Y. F. Hong, F. Lu, and B. L. Liu, "Community test study on the influence of typical crops on soil erosion," *Water Conservancy and Hydropower Technology*, vol. 50, no. 02, pp. 95–100, 2019.

[4] Y. Li, C. X. Wang, and X. L. He, "Research on optimization model of agricultural planting structure under water-saving irrigation technology," *Agricultural Research in the Arid Areas*, vol. 37, no. 03, pp. 104–109, 2019.

[5] F. Fang and Q. Ma, "Research on planting preference and layout of Xinjiang's main crops from the perspective of virtual water value," *Water Saving Irrigation*, vol. 07, pp. 95–100, 2019.

[6] Z. Sun, J. Chen, Y. Han, R. Huang, Q. Zhang, and S. Guo, "An optimized water distribution model of irrigation district based on the genetic backtracking search algorithm," *IEEE Access*, vol. 7, pp. 145692–145704, 2019.

[7] L. Li and X. Hu, "Information technology and agricultural economic development," in *Proceedings of the 2020 2nd International Conference on Economic Management and Model Engineering (ICEMME)*, pp. 218–220, Chongqing, China, November 2020.

[8] W. Xuezhen, W. Shilei, and G. Feng, "The relationship between economic growth and agricultural growth: the case of China," in *Proceedings of the 2010 International Conference on E-Business and E-Government*, pp. 5315–5318, Guangzhou, China, May 2010.

[9] A. V. Vempati, G. I. Aswath, S. Radhakrishnan et al., "Agricultural problems and technology-based sustainable solutions for an impoverished village of Bihar, India," in *Proceedings of the 2020 IEEE 8th R10 Humanitarian Technology Conference (R10-HTC)*, pp. 1–5, Kuching, Malaysia, December 2020.

[10] M. C. Zewdie, S. Van Passel, J. Cools et al., "Direct and indirect effect of irrigation water availability on crop revenue in northwest Ethiopia: a structural equation model," *Agricultural Water Management*, vol. 220, pp. 27–35, 2019.

[11] M. B. Francisco, J. L. J. Pereira, G. A. Oliver, F. H. S. da Silva, S. S. da Cunha, and G. F. Gomes, "Multiobjective design optimization of CFRP isogrid tubes using sunflower optimization based on metamodel," *Computers & Structures*, vol. 249, no. 12, Article ID 106508, 2021.

[12] U. L. C. Baldos, T. W. Hertel, and F. C. Moore, "Understanding the spatial distribution of welfare impacts of global warming on agriculture and its drivers," *American Journal of Agricultural Economics*, vol. 101, no. 5, pp. 1455–1472, 2019.

[13] V. Yakavenka, I. Mallidis, D. Vlachos, E. Iakovou, and Z. Eleni, "Development of a multi-objective model for the design of sustainable supply chains: the case of perishable food products," *Annals of Operations Research*, vol. 294, no. 1-2, pp. 593–621, 2020.

[14] M. Kaur and S. Kadam, "Discovery of resources over Cloud using MADM approaches," *International Journal for Engineering Modelling*, vol. 32, no. 2–4, pp. 83–92, 2019.

[15] L. A. Alejo, V. B. Ella, R. M. Lampayan, and A. A. Delos Reyes, "Assessing the impacts of climate change on irrigation diversion water requirement in the Philippines," *Climatic Change*, vol. 165, no. 3-4, p. 58, 2021.

[16] D. Masseroni, A. Castagna, and C. Gandolfi, "Evaluating the performances of a flexible mechanism of water diversion: application on a northern Italy gravity-driven irrigation channel," *Irrigation Science*, vol. 39, no. 1, pp. 1–11, 2021.

[17] B. Mareschal, M. Kaur, V. Kharat, and S. S. Sakhare, "Convergence of smart technologies for digital transformation," *Tehnički glasnik*, vol. 15, no. 1, pp. II–IV, 2021.

[18] M. Kaur, "FastPGA based scheduling of dependent tasks in grid computing to provide QoS to grid users," in *Proceedings of the 2016 International Conference on Internet of Things and Applications (IOTA)*, pp. 418–423, Pune, India, January 2016.

[19] Y. Zhang, W. Liu, S. U. Khan, B. Swallow, C. Zhou, and M. Zhao, "An insight into the drag effect of water, land, and energy on economic growth across space and time: the application of improved Solow growth model," *Environmental Science and Pollution Research*, vol. 29, no. 5, pp. 6886–6899, 2022.

[20] W. Lingjun, W. Xinlei, H. Dongbing, and Y. Jianfeng, "Calculation and analysis of the contribution rate of agricultural technological progress in guizhou province," in *Proceedings of the 2021 International Conference on Public Management and Intelligent Society (PMIS)*, pp. 268–272, Shanghai, China, Feburary 2021.

[21] F.-y. Jiao and L.-n. Liu, "Contribution of fiscal expenditure on supporting agriculture to promoting agricultural economic growth—empirical study based on Northeast panel data," in *Proceedings of the 2009 International Conference on Management Science and Engineering*, pp. 944–949, Moscow, Russia, September 2009.

[22] S. P. Raflesia, A. K. Pamosoaji, S. Nurmaini, Firdaus, and D. Lestarini, "Conceptual modeling for intelligent knowledge-based system in agriculture: case study of Indonesia," in *Proceedings of the 2018 International Conference on Electrical Engineering and Computer Science (ICECOS)*, pp. 397–402, Pangkal, Indonesia, October 2018.

[23] E. Malaj, K. Liber, and C. A. Morrissey, "Spatial distribution of agricultural pesticide use and predicted wetland exposure in the Canadian Prairie Pothole Area," *The Science of the Total Environment*, vol. 718, Article ID 134765, 2019.

[24] M. N. Kumar, V. Jagota, and M. Shabaz, "Retrospection of the optimization model for designing the power train of a formula student race car," *Scientific Programming*, vol. 2021, Article ID 9465702, 9 pages, 2021.

[25] V. Jagota and R. K. Sharma, "Interpreting H13 steel wear behavior for austenitizing temperature, tempering time and temperature," *Journal of the Brazilian Society of Mechanical Sciences and Engineering*, vol. 40, pp. 1–12, Article ID 219, 2018.

WILEY | Hindawi

Research Article

Study on Double-Layer Stereo Ecological Cultivation Technology of Greenhouse Gardening Fruit Trees

Gang Chen [1] **and Rajasekhar Boddu** [2]

[1]*Agronomy College of Jilin Agricultural Science and Technology University, Jilin 132101, China*
[2]*Department of Software Engineering, College of Computing and Informatics, Haramaya University, Dire Dawa, Ethiopia*

Correspondence should be addressed to Gang Chen; chengang2999@126.com and
Rajasekhar Boddu; rajsekhar.boddu@haramaya.edu.et

Global food demand can be met by agricultural technology. But the increase in demand also needs effective planting and sufficient illumination in order for crops to grow. In order to solve the problems of low planting efficiency and insufficient illumination in traditional greenhouse horticultural fruit tree planting, we propose a three-dimensional double-layer ecological cultivation technology for greenhouse horticultural fruit trees. The design is a double-layered three-dimensional cultivation model. After the growth rate of horticultural fruit trees is determined, the optimal distance between the two-dimensional cultivation layers is determined by weighted Euclidean distance, and the double-layer three-dimensional ecological cultivation mode of greenhouse horticultural fruit trees is designed. Through the analysis of the irradiance of the double bed planting mode, the design of the light environment in horticultural fruit tree planting is completed. A principal component analysis was used to determine the amount of soil components in double-layer three-dimensional ecological cultivation of greenhouse horticultural fruit trees, and the technology of double-layer three-dimensional ecological cultivation was developed. The results show that the planting efficiency of horticultural fruit trees planted by the technology is always higher than 90%, and the illumination in the planting environment is sufficient.

1. Introduction

The increasing contradiction between man and land, the decrease of arable land, pollution, destruction of land resources, the serious shortage of water resources, the low efficiency of water production, and the low utilization rate of fertilizer have become the important factors restricting the sustainable development of agriculture in China. As a result, the planting area of fruit trees is decreasing, and facility cultivation has become a key method for growing fruit trees in recent years [1]. It is for this reason that facility cultivation is one of the important signs of agricultural modernization in seasons or areas that are not conducive to growing fruit trees and other crops [2, 3]. It is done by artificially designing and controlling the facilities and environment in order to meet the needs of fruit trees and to produce products of high

quality for the people [4, 5]. Application of water and fertilizer integration in fruit tree cultivation is more conducive to controlling temperature and humidity in facilities, optimizing water fertilization, controlling diseases and insect pests, improving the soil microbial environment, improving work efficiency, and resulting in high quality and yielding fruit trees [6, 7]. In recent years, with the increase of facility cultivation in China, the obstacles associated with soil continuous cropping, as well as soil salinization, have intensified due to excessive emphasis on high yields, multiple species, flood irrigation, and excessive fertilization [8–10]. Therefore, designing a new ecological cultivation technology for fruit trees has become a hot topic in current research [11, 12].

In reference [2], a new type of steel-structured solar greenhouse suitable for off-season cultivation of fruit trees

was proposed. Planting fruit trees in this environment can improve the survival efficiency and quality of fruit trees. Based on the new greenhouse structure of "two coverings and three films" and "one covering and two films," this method is innovated. After three years of research, the steel structure solar greenhouse is summarized. The greenhouse has a high ridge, a large span, increased internal space, and is more suitable for off-season cultivation of fruit trees. At the same time, the greenhouse has strong resistance to natural disasters such as strong wind, snow pressure, and long life. The results showed that the peach in the greenhouse grew well, and the fruit coloring stage and ripening stage were basically the same or earlier than those in the greenhouse structure of "two coverings and three films." The quality of fruit trees cultivated in this environment is good, and the designed greenhouse environment is suitable for the growth of fruit trees. Nevertheless, planting horticultural fruit trees in this environment has not been successful, and there are still many shortcomings in the quality, quantity, and shape of fruit trees.

The paper [4] puts forward a new facility for strawberry stereoscopic cultivation mode. In order to improve the land-use efficiency of facility strawberries, a new three-dimensional cultivation mode of facility strawberries was designed. A Hongyan strawberry was used as the experimental material. The light conditions, plant nutrition growth, fruit yield and quality, economic benefits, and other indicators of new H-type and traditional cultivation modes were analyzed and compared. Also, the actual production performance of the new H-type three-dimensional cultivation mode was comprehensively evaluated. The results showed that the number of plants, input, yield, total income, and net profit of the new H-type three-dimensional cultivation mode increased by 20%, 44.455%, 20.240%, 35.269%, and 25.876%, respectively. It was preliminarily confirmed that the overall performance of the new H-type three-dimensional cultivation mode was better than that of the traditional cultivation mode. It improves the efficiency of land use. Similar methods have been applied to horticultural fruit tree planting, which can also improve the planting efficiency of fruit trees, but there are still better techniques to be explored [13, 14].

The effect of microridge mulching on soil moisture in the root zone of dwarf horticultural fruit trees was analyzed in literature [15]. This method is mainly used to study the effect of root zone soil on the growth length of dwarf horticultural fruit trees. In this method, three treatments (microridge mulching, straw mulching, and clear tillage) were set up to analyze the changes in soil water storage, orchard water consumption, fruit yield, and water use efficiency of apple trees under different precipitation years. The average soil water storage of 0–300 cm of soil layer in horticultural fields with micro ridges increased by 6.88%, 8.02%, 1.64%, and 2.92%, respectively compared to clear tillage and straw mulching treatment. This significantly improved the soil water storage and water supply capacity of the main root distribution layer of fruit trees and improved the regulation and storage of deep soil water. The effect of microridge mulching on deep soil water storage is better than straw

mulching, and its effect on the balance of soil water storage is closely related to the precipitation in the middle and later stages of fruit tree growth and development. Furthermore, compared with clear tillage, fruit tree transpiration water consumption increased by 16.57% and 12.09%, and evaporation and transpiration did not differ significantly from straw. A microridge mulching system increased yield and water use efficiency significantly in an underwater year and a normal water year, respectively, but there was no difference in fruit yield and water use efficiency when compared to straw. Microridge mulching in horticultural fields can be used as an effective water storage and moisture conservation technology in dwarf apple cultivation systems in Weibei dryland. This technology improves the growth quality of horticultural fruit trees, but the planting area is limited, which leads to some restrictions on the yield of horticultural fruit trees.

The paper [16] describes a system that is based on Arduino and automatically monitors the physical conditions of a greenhouse and controls or regulates them as needed. The system measures the humidity, temperature, soil moisture, etc., of the greenhouse and controls or regulates them accordingly. The greenhouse gardening industry is rapidly expanding, so the use of this automatic control system could be very useful for farmers. This will result in improved productivity and quality of crops. In paper [6], authors have proposed a new feature selection technique called modified recursive feature elimination (MRFE) for selecting appropriate features from a data set for crop prediction. By using a ranking method, the proposed MRFE technique selects and ranks salient features. The results demonstrate that the MRFE method selects the best features while the bagging technique helps determine an accurate crop prediction. The proposed work [17] describes an autonomous style of gardening, which operates autonomously with the assistance of autonomous robots. The robots use sensors to monitor the plants and maintain a database of such information. In this study [18], using artificial neural networks, sensitivity analysis is applied to predict greenhouse tomato yield and determine the most influencing factors for tomato production. Data was collected using a face-to-face survey of 25 greenhouse tomato farms in Biskra Province, Algeria. Despite the high energy inputs, the energy ratio of 1.055 indicates low energy efficiency. As cities grow denser [19], urban planners understand the importance of encouraging and promoting climate and environment-friendly urban areas. Ensuring adequate and easily accessible green public spaces can help shape a healthy urban environment. This study examines how heritage combined with urban gardening can serve to revitalize areas that need it the most. In areas in need of regeneration, heritage combined with urban agriculture is an effective method.

On the basis of the above planting technology, this paper proposes to design a double-layer three-dimensional ecological cultivation technology for greenhouse horticultural fruit trees. As part of the development of a double-layer three-dimensional ecological cultivation model for greenhouse horticultural fruit trees, this paper proposes a bed-type double-layer three-dimensional cultivation model. First

of all, the double-layer three-dimensional cultivation mode of greenhouse horticultural fruit trees was designed. After determining the growth rate of horticultural fruit trees, the optimal distance between layers of the double-layer three-dimensional cultivation mode of greenhouse horticultural fruit trees was determined by weighted Euclidean distance. Then, by analyzing the irradiance of the double bed planting mode, the light environment design of horticultural fruit tree planting was completed. To determine the soil component content in greenhouse horticultural fruit tree double-layer three-dimensional ecological cultivation, principal component analysis methods are used. In this study on greenhouse horticultural fruit tree double-layer three-dimensional ecological cultivation, we have used an optical fiber tracking algorithm to assume that the surface elements of a double-layer plantation and maintenance structure for greenhouse horticultural fruit trees are smooth and transparent.

The organization of this paper is as follows:

After determining the growth rate of horticultural fruit trees, the optimal distance between two layers was determined by weighted Euclidean distance, and the double-layer ecological cultivation mode of horticultural fruit trees in a greenhouse was designed. By analyzing the irradiance of the double bed planting mode, the light environment design of horticultural fruit tree planting was completed. With the help of the principal component analysis method to determine the content of soil components in greenhouse horticultural fruit tree double-layer three-dimensional ecological cultivation, the research on greenhouse horticultural fruit tree double-layer three-dimensional ecological cultivation technology was completed. In the last section, experimental analysis and conclusion are added.

2. Proposed Method

2.1. Design of Double-Dimensional Ecological Cultivation Pattern of Greenhouse Horticulture Fruit Tree.
In the design of the three-dimensional ecological cultivation mode of fruit tree gardening, spatial three-D cultivation expands the cultivation area and saves certain land. This planting model makes full use of space and provides planting per area. The general principle of the planting mode is that the height of the double-layer stereo ecological cultivation mode bed is determined according to the height of the planting fruit tree, with the middle and upper trees having less light in the lower layer. The planting pattern extends the planting length north and south. The basic model is shown in Figure 1.

In the greenhouse horticultural fruit tree double-layer ecological cultivation mode, horticultural fruit trees were planted in both the upper and lower layers. Since the growth cycle of each fruit tree is different, the growth rate is also different. Therefore, the height of fruit tree growth should be taken into account in double-layer stereoscopic ecological cultivation, and its growth rate can be expressed as follows:

$$H = L \times w \sum p. \tag{1}$$

In the above formula, H represents the height of horticultural fruit trees, L represents the initial height of the horticultural fruit trees, and w represents the growth factor.

After assuming the growth rate of horticultural fruit trees, the optimal space between the lower layer and the upper layer should be considered in the double-layer stereoscopic ecological cultivation model, and the distance between them determines the quality of horticultural fruit tree growth. The Euclidean distance [10] is used to determine the optimal distance between them.

In Euclidean distance calculation, the distance between the upper and lower vectors is expressed in the following equation:

$$\text{dis}(x, y) = \sqrt{\sum_{i=1}^{n} (x_i - y_i)^2}. \tag{2}$$

In the above formula, $\text{dis}(x, y)$ represents the Euclidean distance, n represents the dimensions, x_i represents the components of a vector in i dimensions, and y_i represents the component of the vector on the i dimension.

In formula (2), it is only the traditional European distance between double layers, and it is impossible to determine whether this distance is the optimal distance between double bed plantings. On this basis, this paper weighted it to obtain the optimal distance [11] in the stereo ecological cultivation mode of greenhouse gardening fruit trees as expressed in the following equation:

$$\text{dis}'(x, y) = \sqrt{\sum_{i=1}^{n} \left(\frac{T'}{T} k (x_i - y_i)^2 \right)}. \tag{3}$$

In the above formula, (T'/T) represents the weights, k represents the regulator between the bilayers, and value range of [1].

In the design of the double-layer three-dimensional ecological cultivation model of greenhouse horticultural fruit trees, this paper designs a bed-type double-layer three-dimensional cultivation model. After determining the growth rate of horticultural fruit trees, the optimal distance between bed-type double-layer three-dimensional cultivation layers were determined by weighted European distance. The design of the double-layer ecological cultivation model of greenhouse horticultural fruit trees was completed.

2.2. Light Environment Design of Double-Dimensional Ecological Cultivation Pattern of Greenhouse Horticulture Fruit Tree.
According to the above design of double-layer three-dimensional ecological planting mode, in order to achieve the realization of this research technology, the temperature environment of fruit trees in the greenhouse is designed. In this design, the planting temperature and humidity in the greenhouse are controlled by the Internet of Things technology and adjusted according to its needs. Due to the horticultural fruit trees's growth process, light demand is very critical [11]. Therefore, in the study of greenhouse environmental temperature, the problem of light in the greenhouse is mainly analyzed. In the greenhouse environment, the greenhouse ground and the inner surface of the envelope exhibit different brightnesses. This is due to the interaction of solar radiation, indoor supplementary
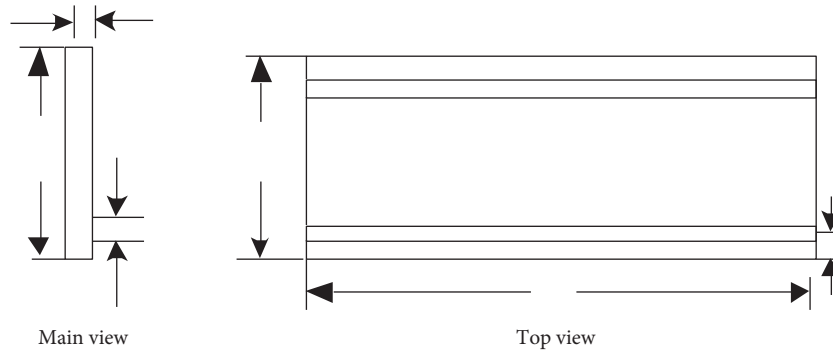
FIGURE 1: Double-dimensional ecological cultivation pattern of greenhouse horticulture fruit trees.

lighting, and the surface of the enclosure. The problem to be solved by the light environment model is how to use the mathematical model to calculate the light radiation energy received at any point in the greenhouse. The brightness of the object surface radiated in a given direction in space can be calculated by the light environment model [12]. In terms of the light energy composition received by the research site, the solar radiation energy can be the light energy transmitted and reflected by the inner surface of the greenhouse envelope (the light supplement lamps directly provide the light energy for the indoor surface). Transmitted light can be divided into direct transmission light and indirect transmission light [13]. Surface reflected light can also be divided into direct and indirect reflected light, which is produced by solar radiation directly incident on a certain surface or repeatedly reflected by other surfaces. Therefore, the greenhouse light environment model can be simply divided into the local light environment model and the overall light environment model. The local light environment model does not consider the mutual reflection and transmission between the surfaces. The overall light environment model reflects the distribution of light energy more completely, and the calculation of the model is much larger than that of the local model. In greenhouse horticulture, fruit tree planting, light is very important [14]. In this study, the light in the greenhouse is regarded as light energy flow, and the angle of light is analyzed according to a certain law of physical conservation so as to determine the angle and duration of light for fruit trees.

It is assumed that the angle of greenhouse horticultural fruit trees exposed to light is a solid cone angle as expressed in the following equation (4):

$$z = \frac{aS}{b^2}. \tag{4}$$

In the above formula, aS represents the light-illuminated corner heart of greenhouse gardening trees and b represents the cross-sectional area on the cone-angle sphere.

The light exposure angle of greenhouse horticultural fruit trees is shown in Figure 2.

According to the angle analysis of the light illumination, the luminous intensity of the greenhouse gardening fruit tree surface in one direction is defined as the light flux in the unit stereo angle in that direction as expressed in the following equation (5):

$$E = \frac{dF}{as}. \tag{5}$$

In the above formula, dF represents luminous flux.

A major problem to be solved in greenhouse gardening and fruit tree planting is the solar radiation intensity acceptable to fruit trees on the greenhouse cultivation bed or on the canopy.

If the vS represents the luminous surface that contributes light energy to the sun, h represents the brightness of the radiation, the incident and stereo angles of the greenhouse horticultural trees are represented as β and ϑ, respectively, and the light flux$x$ of solar radiation can be expressed as in the following equation:

$$dF = h \cos \beta vS \cos \vartheta. \tag{6}$$

Through the calculation of luminous flux, we can clearly understand the radiation illumination that greenhouse horticultural fruit trees can receive. In this paper, the optical fiber tracking algorithm is used to assume that the surface elements of the double-layer planting and maintenance structure of greenhouse horticultural fruit trees are smooth and transparent, and the irradiance distribution of the sun can be expressed as in the following equation:

$$G_m = \begin{cases} \dfrac{1}{dc_i} & V = R. \\ 0 & others \end{cases} \tag{7}$$

In the above formula, R represents the solar irradiation light reflection vector. At this point, the ideal rule projection light energy distribution function can be expressed as the following equation:

$$G_t = \begin{cases} \dfrac{1}{dg_i} & V = R. \\ 0 & others \end{cases} \tag{8}$$

By analyzing the light irradiance of double bed planting mode, the light environment design of horticultural fruit trees is completed, which lays a foundation for subsequent planting.
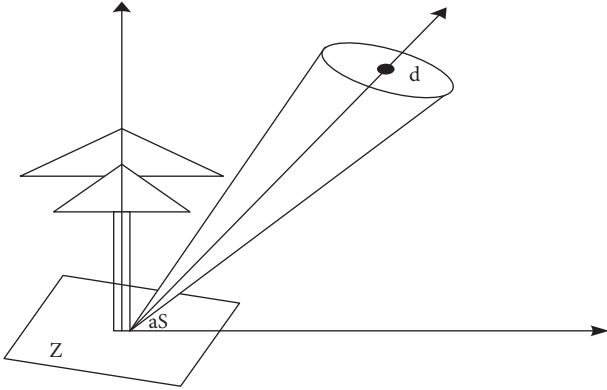
Figure 2: Angle of greenhouse gardening fruit trees.

2.3. Design of Three-Dimensional Ecological Cultivation Soil Environment. Soil is an important support for the growth of horticultural fruit trees in double-layer ecological cultivation of greenhouse horticultural fruit trees. This paper examines the soil environment for double-layer ecological cultivation of greenhouse horticultural fruit trees. Firstly, the comprehensive scores of soil nutrients in the upper and lower layers were calculated by principal component analysis. In this process, the soil nutrient data should be standardized to avoid the analysis of different nutrient levels affecting the soil environment of fruit tree planting. The conversion of soil nutrients to standard data is given by the following equation:

$$Y_i = \frac{y_a - y_b}{y}. \tag{9}$$

In the above formula, Y_i represents the standardized values for greenhouse gardening, y_a represents the initial soil nutrient index for the cultivation of greenhouse horticultural fruit trees y_b on behalf of the greenhouse horticultural fruit tree planting soil nutrient initial index average, and y represents the initial standard deviation.

In the design of the double-layer ecological cultivation soil environment of greenhouse horticultural fruit trees, the higher the comprehensive score, the higher the nutrient content, and the higher the soil fertility degree [10, 18]. Therefore, according to the eigenvalue and eigenvector of the relationship matrix calculated by the standard deviation matrix of the double-layer ecological cultivation soil of greenhouse horticultural fruit trees, the fertility of the soil is determined by the following equation:

$$f_m^2 = \frac{1}{n-1} \sum_{i=1}^n (y_a - y_b)^2. \tag{10}$$

In the above formula, f_m^2 represents the fertility of the soil.

The results of the above calculation are shown in Table 1.

In the principal component analysis of chemical components in the soil environment of double-layer ecological cultivation of greenhouse horticultural fruit trees, the eigenvalue of each principal component can represent the amount of original information of the corresponding components described as shown in Figure 3.

In Figure 3, the cumulative contribution rate of the first two principal components is high, so the extraction of the first two principal components can generalize most of the information. That is, the first two principal components can be used as a summary of soil nutrient characteristics. The soil organic matter, total nitrogen, and available phosphorus in the soil held a high load on the first principal component; that is, the correlation with the first principal component was strong. Also, organic matter had a significant correlation with total nitrogen and available phosphorus, indicating that organic matter is a major carrier of total nitrogen and available phosphorus in soil.

3. Results and Analysis

3.1. Experimental Scheme Design. In order to verify the effectiveness of the proposed technology, an experimental analysis was carried out. According to this method, the two-layer planting pattern of horticultural planting is designed to plant low horticultural fruit trees to watch apple trees and ornamental orange trees. The growth period of the fruit tree is 3 months, and the height is about 50 cm. In this space, 50 low apple trees and 50 ornamental orange trees are planted in the upper layer. It was observed for 3 months and the final experimental results were analyzed. The same way is planted with literature [2] methods and literature [15], and then the effectiveness of the three methods is compared.

3.2. Experimental Index Design. To verify the effectiveness of this method, we compared [2] and [15] techniques. The results of the planting efficiency of the gardening trees and the illumination of plantings are described in this section.

3.3. Analysis of Experimental Results

3.3.1. Analysis of Planting Efficiency of Horticultural Fruit Trees with Different Methods. To verify the effectiveness of the proposed technique, the experimental analysis is compared with the literature [2] technique and the literature [15] technique. The purpose of this comparative study is to analyze the efficiency of sample horticultural fruit tree plantings. In this experiment, the planting efficiency is compared with the survival rate of horticultural fruit trees after planting. The results are shown in Table 2.

It is estimated that more than 90% of plants will have survived after planting technology, about 85% of plants will survive after planting technology, and about 86% of plants will survive after planting technology. In contrast, the survival rate of trees planted by the [15] technique is higher, which is due to the composition of the double planting environment and soil environment, which improves the survival rate of horticultural fruit trees.

In order to demonstrate the high efficiency of horticultural fruit trees, in this paper, the plot area used for the cultivation of sample fruit trees by three methods is analyzed experimentally to ensure the survival rate. The results are shown in Table 3.

TABLE 1: Specific environment of greenhouse gardening fruit trees.

	Organic matter (g kg^{-1})	Total nitrogen (g kg^{-1})	Rapidly available phosphorus (mg kg^{-1})	Available potassium (mg kg^{-1})
Organic matter/g kg^{-1}	1.000	0.906	0.606	0.126
Total nitrogen/g kg^{-1}		1.000	0.541	0.167
Rapidly available phosphorus/mg kg^{-1}				−0.019
Available potassium/mg kg^{-1}				1.000
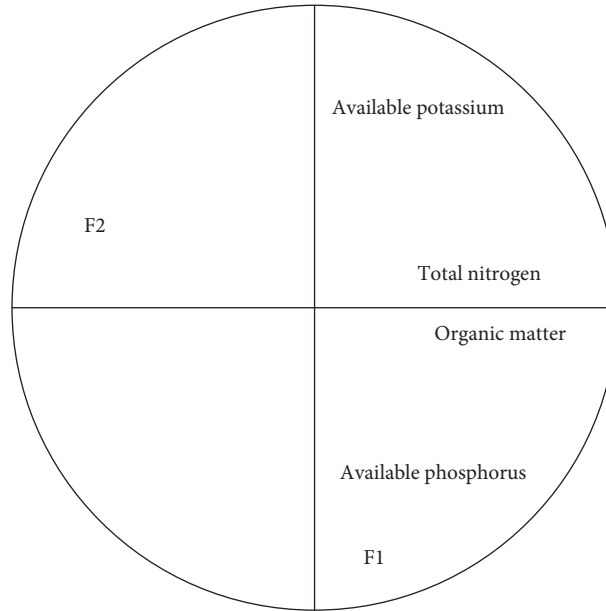
FIGURE 3: Analysis of the main chemical composition of the cultivated soil environment.

TABLE 2: Analysis of fruit yield of sample trees under different planting techniques (%).

Number of planted trees	Methods of this paper	Protemics [2]	Hort technology [15]
10	90	80	80
20	95	80	70
30	96	85	86
40	94	84	70
50	95	82	85

TABLE 3: Analysis of planting area of sample fruit trees under different techniques (m^2).

Number of planted trees	Methods of this paper	Hort technology [15]	Protemics [2]
10	5	10	11
20	5	20	22
30	10	30	33
40	10	40	44
50	15	50	55

The data in Table 3 show that with the change of the number of fruit trees planted in the sample, there are some differences in the planting area of fruit trees cultivated by three techniques. Among them, the proposed technology planting area is always lower than the other two existing techniques. This is because the planting method designed in this paper is based on double-layer planting, which saves the land area and verifies the effectiveness of this method.

3.3.2. Analysis of Illumination in Sample Gardening Fruit Trees. The key factors affecting the growth of horticultural fruit trees are illumination. Therefore, the light intensity of plants in the process of planting is analyzed in the experiment. By comparing the ideal temperature change with the actual temperature, the effectiveness of this method is verified. The experimental results are shown in Figure 4.
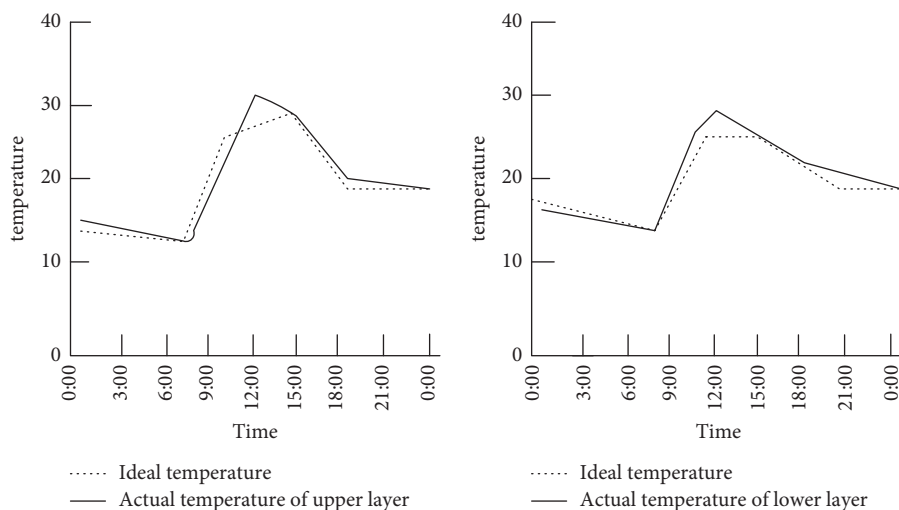
Figure 4: Results of light illumination in the planting of horticultural fruit trees.

The experimental results in Figure 4 show that the illumination of horticultural fruit trees varies under different time periods. Among them, the double-layer planting temperature and the ideal temperature are more consistent. When the light is most intense between 9:00 am and 12:00 pm in the upper layer, the temperature increases, but it is also within the tolerance of horticultural plants. However, the change curve is close to the ideal temperature, which verifies the effectiveness of this technique.

4. Conclusion

In order to maximize the efficiency of greenhouse gardening and save planting land, this paper proposes a double-layer ecological cultivation technique for greenhouse horticultural fruit trees. By using weighted European distances, we determined the optimal interlayer distance of double-layer stereoscopic cultivation of greenhouse horticultural fruit trees. We then developed an ecological cultivation model for double layer stereoscopic ecological cultivation of greenhouse horticultural fruit trees. When we compare the proposed method with the traditional method, it was observed that the planting efficiency of horticultural fruit trees planted by the proposed technology is always higher than 90%, and the planting land area is less. Along with that, the horticultural fruit trees planted with the proposed technology have sufficient illumination and are suitable for horticultural fruit trees. In the future, we can increase the layers in the ecological cultivation technique to increase the amount of healthy fruit growth.

Data Availability

All the data used in this article is included within the article itself.

Conflicts of Interest

The authors declare that there are no conflicts of interest regarding the publication of this paper.

References

[1] L. Yang, F. Gong, E. Xiong, and W. Wang, "Proteomics: a promising tool for research on sex-related differences in dioecious plants," *Frontiers of Plant Science*, vol. 6, p. 954, 2015.

[2] L.-H. Gao, M. Qu, H.-Z. Ren, X.-L. Sui, Q.-Y. Chen, and Z.-X. Zhang, "Structure, function, application, and ecological benefit of a single-slope, energy-efficient solar greenhouse in China," *Hort Technology*, vol. 20, no. 3, pp. 626–631, 2010.

[3] Y. Y. Huang, S. W. Liu, Y. K. Chen, X. Liu, H. Y. Zheng, and T. Wang, "Construction of water and fertilizer integrated fertilization system for greenhouse substrate cultivation," *Jiangsu Agricultural Sciences*, vol. 47, no. 12, pp. 278–281, 2019.

[4] P. Liao, P. Liu, Y. Wang et al., "Stereoscopic cultivation of Panax notoginseng: a new approach to overcome the continuous cropping obstacle," *Industrial Crops and Products*, vol. 126, pp. 38–47, 2018.

[5] B. Mareschal, M. Kaur, V. Kharat, and S. Sakhare, "Convergence of smart technologies for digital transformation," *Tehnički Glasnik - Technical Journal*, vol. 15, p. 1, 2021, https://doi.org/10.31803/tg-20210225102651.

[6] G. Mariammal, A. Suruliandi, S. P. Raja, and E. Poongothai, "Prediction of land suitability for crop cultivation based on soil and environmental characteristics using modified recursive feature elimination technique with various classifiers," *IEEE Transactions on Computational Social Systems*, vol. 8, no. 5, pp. 1132–1142, 2021.

[7] M. Kaur and S. Kadam, "Bio-inspired workflow scheduling on HPC platforms," *Tehnički glasnik*, vol. 15, no. 1, pp. 60–68, 2021, https://doi.org/10.31803/tg-20210204183323.

[8] E. Rodríguez-Caballero, Y. Cantón, S. Chamizo, R. Lázaro, and A. Escudero, "Soil loss and runoff in semiarid ecosystems: a complex interaction between biological soil crusts, micro-

topography, and hydrological drivers," *Ecosystems*, vol. 16, no. 4, pp. 529–546, 2013.

[9] P. Sun, R. X. Lin, H. Bao, and J. S. Shen, "Ecological high value stereoscopic cultivation techniques of grape strawberry dendrobium officinale," *Northern Horticulture*, vol. 14, no. 10, pp. 200–203, 2018.

[10] P. Y. Wang, P. G. Tian, W. G. Wu, T. T. Cao, and F. Y. Shen, "Study on cultivation techniques of Pitaya in greenhouse in North China," *Agriculture & Technology*, vol. 41, no. 2, pp. 103–105, 2021.

[11] V. Jagota, M. Luthra, J. Bhola, A. Sharma, and M. Shabaz, "A secure energy-aware game theory (SEGaT) mechanism for coordination in WSANs," *International Journal of Swarm Intelligence Research*, vol. 13, no. 2, pp. 1–16, 2022, https://doi.org/10.4018/ijsir.287549.

[12] K. Y. Yeung and W. L. Ruzzo, "Principal component analysis for clustering gene expression data," *Bioinformatics*, vol. 17, no. 9, pp. 763–774, 2019.

[13] H. F. Zhang and H. Zhang, "The extraordinary mode in the three-dimensional magnetized plasma photonic crystals with layer-by-layer lattices containing the function dielectric," *The European Physical Journal*, vol. D73, no. 7, pp. 1424–1428, 2019.

[14] Z. Y. Zhang, H. Zhu, Q. Cheng et al., "Low polarization-dependent-loss double-layer grating coupler for three-dimensional photonic integration," *Optics Communications*, vol. 445, no. 12, pp. 1414–1421, 2019.

[15] P. Zhou, J. Qian, W. Yuan et al., "Effects of interval flooding stress on physiological characteristics of apple leaves," *Horticulturae*, vol. 7, no. 10, p. 331, 2021.

[16] P. Kumar, S. Saroj, S. Kumar, and C. Azad, "Automated monitoring and regulation of user-friendly greenhouse using Arduino," in *Proceedings of the Fourth International Conference on Microelectronics, Computing and Communication Systems*, pp. 43–59, Singapore, June 2021.

[17] D. Ruth Anita Shirley, K. Ranjani, G. Arunachalam, and D. A. Janeera, "Automatic distributed gardening system using object recognition and visual servoing," in *Inventive Communication and Computational Technologies*Springer, Singapore, 2021.

[18] S. Mikhailova, L. Mikhailov, G. Ismailova, N. Kenes, R. Yersaiyn, and R. Mahmutov, "Solar-powered smart window design with aerosol trap and greenhouse gardening," *Materials Today Proceedings*, vol. 49, pp. 2527–2531, 2022.

[19] G. Swensen, V. E. Stafseng, and V. K. Simon Nielsen, "Visionscapes: combining heritage and urban gardening to enhance areas requiring regeneration," *International Journal of Heritage Studies*, vol. 27, pp. 1–27, 2022.

WILEY | Hindawi

Research Article

A Comparative Analysis of Business Machine Learning in Making Effective Financial Decisions Using Structural Equation Model (SEM)

A. V. L. N. Sujith (ID),[1] **Naila Iqbal Qureshi** (ID),[2] **Venkata Harshavardhan Reddy Dornadula** (ID),[3] **Abinash Rath** (ID),[4] **Kolla Bhanu Prakash** (ID),[5] **and Sitesh Kumar Singh** (ID)[6]

[1]*Department of Computer Science and Engineering, Anantha Lakshmi Institute of Technology and Sciences, Ananthapuramu, India*
[2]*Department of Business Administration, College of Business Administration, Princess Nourah Bint Abdulrahman University, Riyadh, Saudi Arabia*
[3]*IT & ITES Department, Startups Mentoring Society, Tirupati, Andhra Pradesh 517501, India*
[4]*School of Business, The Assam Kaziranga University, Jorhat, India*
[5]*Department of Computer Science Engineering, K L Deemed to Be University, Green Fields, Vaddeswaram, Guntur District, A.P., India*
[6]*Department of Civil Engineering, Wollega University, Nekemte, Oromia, Ethiopia*

Correspondence should be addressed to Sitesh Kumar Singh; sitesh@wollegauniversity.edu.et

Globally, organisations are focused on deriving more value from the data which has been collected from various sources. The purpose of this research is to examine the key components of machine learning in making efficient financial decisions. The business leaders are now faced with huge volume of data, which needs to be stored, analysed, and retrieved so as to make effective decisions for achieving competitive advantage. Machine learning is considered to be the subset of artificial intelligence which is mainly focused on optimizing the business process with lesser or no human interventions. The ML techniques enable analysing the pattern and recognizing from large data set and provide the necessary information to the management for effective decision making in different areas covering finance, marketing, supply chain, human resources, etc. Machine learning enables extracting the quality patterns and forecasting the data from the data base and fosters growth; the machine learning enables transition from the physical data to electronically stored data, enables enhancing the memory, and supports with financial decision making and other aspects. This study is focused on addressing the application of machine learning in making the effective financial decision making among the companies; the application of ML has emerged as a critical technology which is being applied in the current competitive market, and it has offered more opportunities to the business leaders in leveraging the large volume of data. The study is intended to collect the data from employees, managers, and business leaders in various industries to understand the influence of machine learning in financial decision making .

1. Introduction

Business leaders around the globe are now using the advanced techniques of machine leaning (ML) and deep learning (DL) as they offer enhanced benefits in decision making. The replication of human intellectual processes by machines, particularly computer systems, is known as artificial intelligence. The approaches and other aspects of artificial intelligence (AI) tend to support in creating better risk management models and estimate the requirement of cash and other aspects based on the historical data. With its immense potential, AI tools like ML are being applied for

enhanced financial decision making, mainly in stock markets to forecast the price of the securities and enable the management of the risk efficiently [1]. It is estimated that nearly $41 billion annually is being spent on AI, mainly in the financial industry for effective decision making.

The critical aspect of AI is that it is being implemented for algorithmic trading, enables management of the risk, supports in process automation, and manages the cash movement effectively. The most relevant aspect of AI method is focused on machine learning as they offer supporting aspects in forecasting the data and information based on the collated information [2]. Furthermore, ML is used in performing high end statistical modelling and analysis using the data, also supporting in creating better dashboard reports. Also, AI and ML approaches are mainly applied in the front office of major financial institutions, banking, and other sectors so as to provide effective services to the customers. Moreover, they enable assessing the credit quality of the customers and managing the critical reports in an effective manner [3].

With the increased scrutiny by the regulators related to financial transaction, companies are required to collect and maintain the database of the customers for complying antimoney laundering, knowing your customer, and other information. Hence, the banking and financial institutions are holding a large amount of data which needs to be stored and retrieved and reports need to be generated for better decision making [2, 4]. Moreover, the application of ML based technologies supports in creating better interaction with the customers and enables addressing their queries in an effective manner. The application of machine learning algorithms in discovering better concepts, analysing the data effectively, and providing the information for taking better financial decisions [5]. The ML algorithms usually create customised reports depending on available data, resulting in simple and straightforward information being delivered to various levels of management. Employees and management tend to deploy such technologies for recognising the pattern, focusing on estimating the price of the security and taking adequate steps in managing the risk effectively [4]. One of the critical aspects of AI is the application of natural language processing (NLP). NLP is a field of artificial intelligence (AI) that provides computers the capacity to read text and spoken language in a manner similar to that of humans which supports in analysing the data, offers more potential in integrating the large volume of information, supports in predicting the pattern, and extrapolates the information for effective analysis on the broader market [6]. Machine learning can be applied to various financial decision making for the management as it enables making extensive analysis covering regression, vector machines, etc. These aspects support in understanding the pattern based on the available data and classifies the information in order to make quick and better decisions. The management can also enable forecasting the prices of the securities and predict the bullish or bearish phase in the security price or the broader market index.

Based on the increased demand in delivering high end customer services, banks and financial institutions have intended to apply novel AI and ML methods to cater to the needs of the customers. The implementation of the ML approaches supports in reducing the cost, optimizing the overall productivity, supports in risk management, and engages the customers effectively for enhanced financial decision making. Furthermore, the ML algorithms tend to offer customised reports based on the available data and thereby clear and concise information is being provided to the different level of management so as to ensure organised decision making.

The development of different technological advancements in the financial industry has enabled the creation of specific data sets and also reduced the investment in IT infrastructure as they can save more information through cloud computing. Hence, this study is focused on analysing the critical factors of machine learning in effective financial decision making; the major factors considered are the usage of ML in risk management, identification of areas of financial performance, and managing the cash and other resources effectively. These are highly critical financial decision making and hence the study is revolved around these factors.

2. Review of Literature

Thematic modelling is the application of ML to NLP; therefore we supplement our study with a symbiotic element using ML techniques to understand ML research in finance [7]. As far as we know, ML's ability in financial decision making was examined for the first time from a research perspective, with emphasis on neural networks as a tool for economic decision making. In the 2010s, the *Journal of Banking & Finance* also published a series of preliminary studies reflecting the future benefits for the banking sector, examining whether ML can improve lending decisions and credit risk management [8]. The researchers used neural networks to rank Italian companies based on the probability of financial difficulties, but applied genetic learning algorithms to the same subject. New research in financial journals continued to focus on forecasting, but switched to deep learning techniques and other advanced ML techniques. These latest apps include understanding default recovery speeds, learning the coverage rates for the best options, and modelling of the investment environment.

Artificial intelligence and machine learning can be used to manage risks through earlier, more accurate risk assessments. ML is extremely beneficial to the organisation in making improved risk management decisions, and the second biggest relationship is discovered in efficiently managing the organisation's cash. For example, if artificial intelligence and machine learning allow decisions to be made based on past relationships between the values of different assets, financial institutions will be better able to manage these risks [9]. Tools to reduce driving risks can be particularly beneficial for the entire system. [5]. In addition, artificial intelligence and machine learning can be used to predict and detect the risk of fraud, suspicious transactions, late payments, and cyber-attacks, which can lead to better risk management. But tools based on artificial intelligence

and machine learning can also omit new types of dangers and events, as they can potentially "over-educate" previous events [10]. While artificial intelligence and machine learning tools can improve risk management, the latest developments in these strategies mean that they have not yet been tested to manage risks in changing economic conditions. This research article is organised as follows: Section 1 describes the introduction, and Section 2 describes the literature work. The methodology is described in Section 3. Section 4 summarizes the outcomes and research findings, and Section 5 concludes with a conclusion and future scope. The use of artificial intelligence and machine learning creates risk "black boxes" in decision making that can cause complex problems, especially at the end of events. It can be difficult for financial users—and regulators in particular—to understand how decisions such as those relating to trade and investment were made. Artificial intelligence and machine learning are problematic not just because of the lack of clarity, but also because of potential biases acquired by the techniques from human preconceptions and collecting artefacts buried in the training data, which may result in unfair or incorrect choices. In addition, the communication mechanism used by these tools may be incomprehensible to humans, which causes monitoring problems for human operators of such solutions [11]. When in doubt, users of these artificial intelligence and machine learning tools can simultaneously pull their "shut-off switches," that is, turn off the systems manually. Following such incidents, users can only reactivate the systems if other users in the market do so in a coordinated manner. This can increase system-wide voltage risks and the need for proper switches.

Artificial intelligence and machine learning can facilitate "more personal" and "more personal" financial services through big data analytics [12]. For example, artificial intelligence and machine learning can facilitate big data analysis, thereby clarifying the characteristics of individual consumers and / or investors and allowing companies to design well-targeted services. However, the use of consumer data can lead to privacy and information security issues. In addition, since analytical artificial intelligence and machine learning data can analyse the characteristics of individual customers through public data, it would be necessary to consider customer results. It must be protected while protecting the anonymity of individual consumers and facilitating the safe and efficient use of big data for better services [13]. Deep learning algorithms, in particular, offer benefits for organisational decision making, such as supporting employees with information processing, so augmenting their analytical capacities and maybe assisting them in transitioning to more design output. In addition, in order to protect consumers and investors, it would be important to establish well-designed governance structures for financial service providers using artificial intelligence and machine learning.

3. Methodology

The purpose of the article is to explore the significance of machine learning approaches in supporting the financial decision making of the organisation. For the purpose of the study

the researchers have considered the selection of private banking companies and financial institutions in India and the data are collated from the respondents. Machine learning algorithms play a crucial role in finance to identify fraud, simplify trading processes, and give financial advice to clients. Without being explicitly taught, machine learning can examine lots of data sets in a short period of time to improve results [14]. The researchers have focused on using the descriptive research design as the area of application of machine learning in financial decision making is gaining importance in the emerging economies. Moreover, business leaders are looking to implement new technologies so that they can effectively manage the risk, optimise the cash inflows and outflows, support in better pricing of the securities, and apprehend the areas to generate better financial returns [15].

The data are collected through the questionnaire from the respondents, nonprobability sampling methods were applied, and the researchers have generated only 229 completed data from the sample population and hence all were considered for performing the analysis [16]. Using closed ended questionnaire enables the researchers to get the responses from the sample population in an effective manner; in order to convert the overall responses into quantitative aspect, the Likert scale principle is applied [1: strongly disagree and 5: strongly agree]. The authors intend to test the data using basic descriptive analysis of the demographic variables, and then apply AMOS for implementing the structural equation model (SEM) [17]. The SEM model enables measuring the overall association of the independent variables towards the dependent variables.

Hypothesis

Ho: there is no significant association between the application of machine learning in risk management and effective financial decision making in the organisation.

Ho: there is no significant association between the application of machine learning in analysing the area of enhancing financial performance and effective financial decision making in the organisation.

Ho: there is no significant association between the cash management and effective financial decision making in the organisation.

3.1. Analysis. This section provides detailed analysis based on the data collected by the authors; the major analysis includes percentage analysis, correlation analysis, and SEM model analysis.

From Table 1, the analysis reveals that 86% of the sample population were male and the remaining were female, also 30.6% of the respondents were in the age group of 31–40 years, 28.8% were in the age group of less than 30 years, 27.5% were above 50 years and remaining were in the age group between 41–50 years. 52% of them were living in the joint family, 61.6% were working in banking companies, and the remaining 38.4% were working in financial and

TABLE 1: Demographic analysis.

Demographic variables	Features	Frequency	Percent
Gender category	Male	197	86.00
	Female	32	14.00
Age category	Less than 30 years	66	28.80
	31–40 years	70	30.60
	41–50 years	30	13.10
	Above 50 years	63	27.50
Type of family currently living	Joint family	119	52.00
	Nuclear family	110	48.00
Nature of industry	Banking companies	141	61.60
	Financial and nonbanking companies	88	38.40
Management cadre	Lower level management	62	27.10
	Middle level management	134	58.50
	Process head	33	14.40
Total experience	Less than 3 years of experience	60	26.20
	4–8 years	54	23.60
	8–12 years	32	14.00
	12–16 years	19	8.30
	Above 16 years	64	27.90

nonbanking corporations. 58.5% were in the middle level management, 27.10% were junior level management, and the remaining were working as process head in the current organisation. 26.2% possess experience of less than 3 years, 23.6% were possessing experience between 4 – 8 years, and 14% were having experience of 8–12 years.

The researcher intends to analyse the role of machine learning in offering more opportunities for the management in taking more decisions [18]. Based on Table 2, it is noted that 41.5% of the respondents have strongly agreed that the machine learning tends to provide more opportunities for the management in taking better decision; also 31.9% of the respondents have agreed to the statement; however, 13.5% of the respondents have been neutral, 7.9% of the respondents have disagreed, and 5.2% of the respondents have strongly disagreed to the statement. Figure 1 introduces a chart that represents the opportunities possessed by machine learning. Machine learning is useful because compute is plentiful and inexpensive. The volume of data we are gathering, as well as development in capabilities of machine learning algorithms, has been driven by abundant and low-cost computation.

The authors have also tested the respondents to understand whether the application of machine learning supports in managing the overall operational costs. From Table 3, it is identified that 39.3% of the respondents have strongly agreed to the statement, and 30.1% of the respondents have agreed to the same. Meanwhile, 15.7% of the respondents have been neutral, 9.6% of them have disagreed, and 5.2% of the respondents have strongly disagreed. Support of machine learning in managing the cost effectiveness is shown in Figure 2. This figure represents a chart which is based on different respondents values; these values have measured through strongly disagree, disagree, neutral, agree, and strongly agree.

3.2. Correlation. The correlation analysis is one of the useful statistical tools to measure the overall association between

TABLE 2: Machine learning possesses more opportunities.

More opportunities	Frequency	Percent
Strongly disagree	12	5.2
Disagree	18	7.9
Neutral	31	13.5
Agree	73	31.9
Strongly agree	95	41.5
Total	229	100
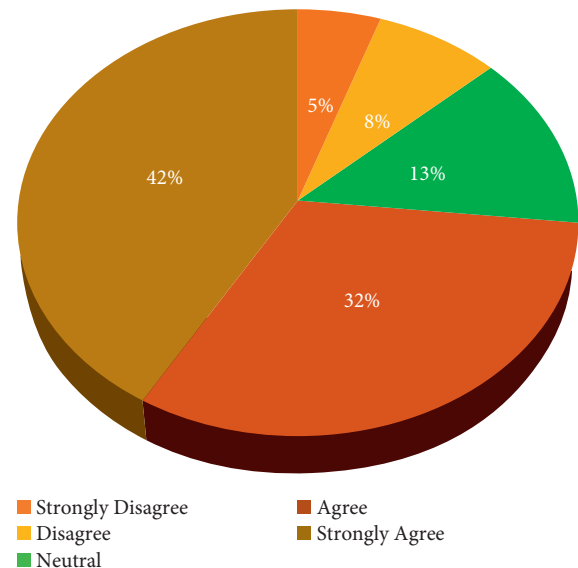
FIGURE 1: Chart representing that machine learning possesses more opportunities.

the variables; in the study the researchers have considered three key independent variables, viz., risk management, areas of enhancing financial performance, and managing the cash, and its relationship towards the dependent variable enhances financial decision making.

TABLE 3: Machine learning supports in managing the cost effectively.

Cost management	Frequency	Percent
Strongly disagree	12	5.2
Disagree	22	9.6
Neutral	36	15.7
Agree	69	30.1
Strongly agree	90	39.3
Total	229	100
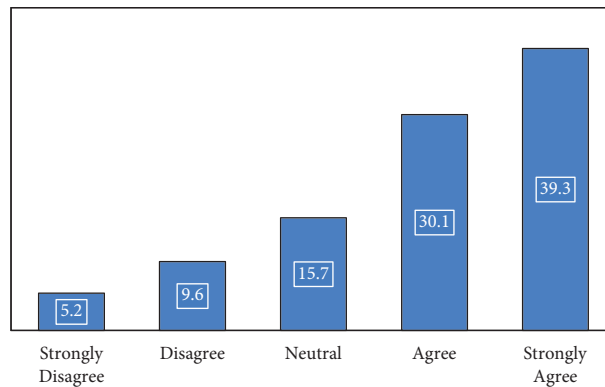
FIGURE 2: Chart representing the machine learning supports in managing the cost effectively.

TABLE 4: Correlation analysis.

	Risk management	Areas of financial performance	Managing cash effectively	ML in financial decision making
Risk management	1	0.660**	0.891**	0.927**
Areas of financial performance	0.660**	1	0.745**	0.724**
Managing cash effectively	0.891**	0.745**	1	0.894**
ML in financial decision making	0.927**	0.724**	0.894**	1

Based on table of the correlation analysis shown in Table 4, it is identified that the variables possess higher positive association as the values are more than +0.700, higher correlation is identified between financial decision making and risk management; hence ML is highly helpful for the organisation in taking improvised decision making related to risk management; also the next highest association is noted between managing the cash of the organisation effectively. Businesses get cash inflows through sales and other aspects, which are to be utilised effectively so that the cost is minimised so that the profits can be maximized; hence machine learning technologies support in making quick decisions.

3.3. Structural Equation Modelling Approach (SEM). The SEM is considered as an exhaustive multivariate approach which enables the researcher to use the combination of factor analysis and regression analysis; moreover it is used to assess the overall structural association between the measured variables and the constructs [19]. Hence, this model is highly supported by the scholars and practitioners as it estimates the multiple and other dependence through the analysis; furthermore, the analysis can consider both endogenous and exogenous variables. This has been shown in Figure 3.

From Table 5 of the analysis, it is noted that the *P* value of all the independent variables towards the financial decision making is less than 5% level of significance (value is at 0.05); hence the null hypothesis is rejected and alternate hypothesis is accepted.

Therefore, the statement of hypothesis is stated as Table 6.

4. Findings and Discussion

Therefore, for the overall analysis, it can be stated that the key independent variables like risk management and analysing the area to enhance financial performance and cash management using machine learning are highly helpful in making quick financial decisions. Business leaders are highly poised to focus on critical areas where they can enhance the business profits, managing the risk is a key attribute, and implementation of machine learning tools and techniques can forecast the outcomes; thereby appropriate financial decision making can be made by the leaders for maximising the profits [20]. Furthermore other areas like the operational cost and expenses can be analysed so that they can be reduced using different strategies,
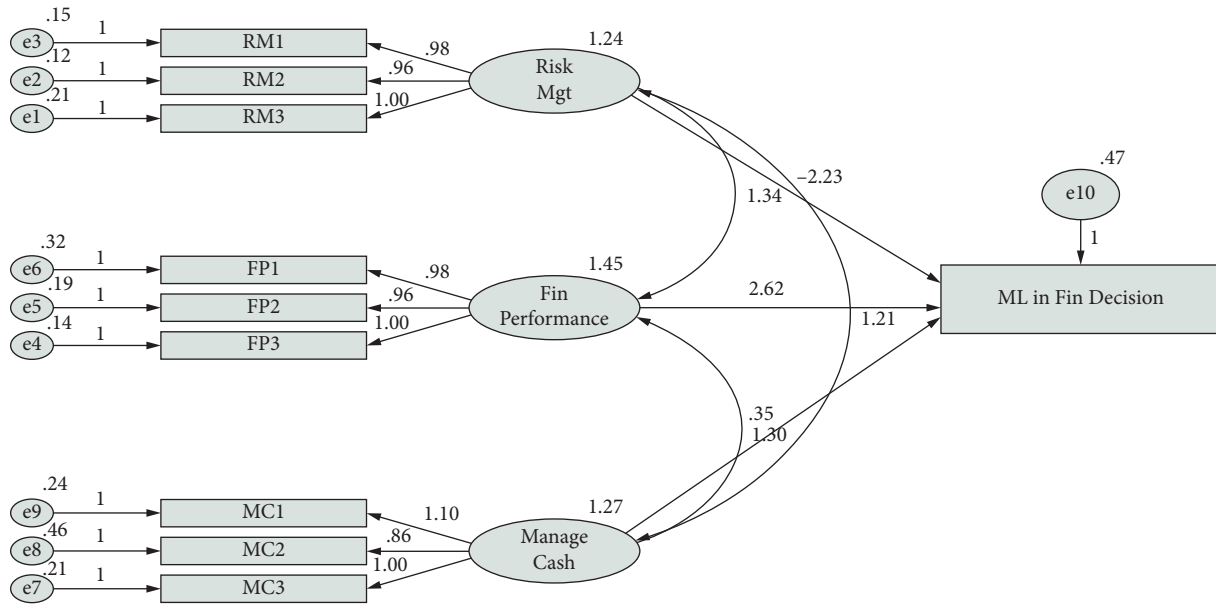
FIGURE 3: Chart representing the SEM between the independent and dependent variables.

TABLE 5: Regression weights.

Dependent variable	Independent variable	Estimate	S.E.	C.R.	P
Financial decision	Risk_Mgt	−2.228	5.745	−0.388	≤0.001
Financial decision	Fin_Performance	2.618	4.503	0.581	≤0.001
Financial decision	Manage_Cash	0.353	0.96	0.368	≤0.001

TABLE 6: Hypothesis analysis.

Hypothesis	Decision
There is a significant association between the application of machine learning in risk management and effective financial decision making in the organisation	Accept
There is a significant association between the application of machine learning in analysing the area of enhancing financial performance and effective financial decision making in the organisation	Accept
There is a significant association between the cash management and effective financial decision making in the organisation	Accept

also the managers understand that cash is one of the critical factors in production and hence it needs to be managed effectively. Using machine learning models, the management can forecast the requirement of cash so that better decision can be made.

5. Conclusion

Machine learning is seen as a subset of artificial intelligence that mainly focuses on optimizing business processes with little or no human intervention. ML technologies allow the model to be analysed and identified from a large set of data and provide management with the information they need to make effective decisions in several areas of finance, marketing, and supply chain. A key aspect of artificial intelligence is that it applies algorithmic transactions, can manage risks, supports process automation, and efficiently manages cash flow. The most relevant aspect of the AI method focuses on machine learning as it provides support aspects for predicting data

and information based on the information collected. In addition, the use of ML-based technology helps to better interact with customers and answer their questions effectively. Use machine learning algorithms to discover better concepts, provide efficient data analysis, and provide the information you need to make better financial decisions. Employees and management tend to develop such techniques to recognize the pattern, focus on the valuation of securities, and take appropriate measures to effectively manage risks. Using ML methods helps reduce costs, optimise overall productivity, support risk management, and engage customers to make better financial decisions. In addition, ML algorithms tend to generate personal reports based on available data, providing clear and concise information at various levels of management for organised decision making.

Data Availability

The data shall be made available on request.

Conflicts of Interest

The authors declare that they have no conflicts of interest.

References

[1] S. Mullainathan and J. Spiess, "Machine learning: an applied econometric approach," *The Journal of Economic Perspectives*, vol. 31, no. 2, pp. 87–106, 2017.

[2] A. Mishra, D. Irwin, P. Shenoy, J. Kurose, and T. Zhu, "Smartcharge: cutting the electricity bill in smart homes with energy storage," in *Proceedings of the 3rd International Conference on Future Energy Systems: Where Energy, Computing and Communication Meet*, p. 29, ACM, Madrid, Spain, May 2012.

[3] R. Ghasemiyeh, R. Moghdani, and S. S. Sana, "A hybrid artificial neural network with metaheuristic algorithms for predicting stock price," *Cybernetics & Systems*, vol. 48, no. 4, pp. 365–392, 2017.

[4] M. Kampouridis and F. E. B. Otero, "Heuristic procedures for improving thepredictability of a genetic programming financial forecasting algorithm," *Soft Computing*, vol. 21, no. 2, pp. 295–310, 2017.

[5] C. Worasucheep, "Forecasting currency exchange rates with an Artificial Bee Colony-optimized neural network," in *Proceedings of the 2015 IEEE Congress on Evolutionary Computation (CEC)*, pp. 3319–3326, IEEE, Sendai, Japan, May 2015.

[6] A. J. Hussain, D. Al-Jumeily, H. Al-Askar, and N. Radi, "Regularized dynamic self-organized neural network inspired by the immune algorithm for financial time series prediction," *Neurocomputing*, vol. 188, pp. 23–30, 2016.

[7] S. Kumar, P. K. Baag, and K. V. Shaji, "Impact of ESG integration on equity performance between developed and developing economy: evidence from S and P 500 and NIFTY 50," *Empirical Economics Letters*, vol. 20, no. 4, pp. 01–16, 2021.

[8] B. Weng, L. Lu, X. Wang, F. M. Megahed, and W. Martinez, "Predicting short-term stock prices using ensemble methods and online data sources," *Expert Systems with Applications*, vol. 112, pp. 258–273, 2018.

[9] S. Sanober, I. Alam, S. Pande et al., "An enhanced secure deep learning algorithm for fraud detection in wireless communication," in *Wireless Communications and Mobile Computing*, V. Shanmuganathan, Ed., vol. 2021, Hindawi Limited, Article ID 6079582, 14 pages, Hindawi Limited, 2021.

[10] V. Panwar, D. K. Sharma, K. V. P. Kumar, A. Jain, and C. Thakar, "Experimental investigations and optimization of surface roughness in turning of EN 36 alloy steel using response surface methodology and genetic algorithm," *Materials Today Proceedings*, vol. 46, 2021.

[11] A. Piepenbrink and E. Nurmammadov, "Topics in the literature of transition economies and emerging markets," *Scientometrics*, vol. 102, no. 3, pp. 2107–2130, 2015.

[12] S. Oprea, "Informatics solutions for electricity consumption optimization," in *Proceedings of the 2015 16th IEEE International Symposium on Computational Intelligence and Informatics (CINTI)*, pp. 193–198, IEEE, Budapest, Hungary, November 2015.

[13] A. Jain and A. K. Pandey, "Multiple quality optimizations in electrical discharge drilling of mild steel," *Sheet" Material Today Proceedings*, vol. 8, pp. 7252–7261, 2019.

[14] A. Jain, A. K. Yadav, and Y. Shrivastava, "Modelling and optimization of different quality characteristics in electric discharge drilling of titanium alloy sheet" Material," *Today Proceedings*, vol. 21, pp. 1680–1684, 2019.

[15] A. Jain and A. Kumar Pandey, "Modeling and optimizing of different quality characteristics in electrical discharge drilling of titanium alloy (Grade-5) sheet," *Materials Today Proceedings*, vol. 18, pp. 182–191, 2019.

[16] S. Kumar, "Effective hedging strategy for us treasury bond portfolio using principal component analysis," *Academy of Accounting and Financial Studies Journal*, vol. 26, no. 2, pp. 1–17, 2022.

[17] K. Mahajan, U. Garg, and M. Shabaz, "CPIDM: a clustering-based profound iterating deep learning model for HSI segmentation," in *Wireless Communications and Mobile Computing*, V. Shanmuganathan, Ed., vol. 2021, Hindawi Limited, Article ID 7279260, 12 pages, Hindawi Limited, 2021.

[18] D. S. Ushakov, V. V. Shepelev, and Y. O. Patlasov, "Marketing researches of the modified starch market and the technologies of its production," *IOP Conference Series: Earth and Environmental Science*, vol. 422, no. 1, Article ID 012128, 2020.

[19] W. Xu, Z. Zhang, D. Gong, and X. Guan, "Neural network model for the risk prediction in cold chain logistics," *International Journal of Multimedia and Ubiquitous Engineering*, vol. 9, no. 8, pp. 111–124, 2014.

[20] S. Tirunillai and G. J. Tellis, "Mining marketing meaning from online chatter: strategic brand analysis of big data using latent dirichlet allocation," *Journal of Marketing Research*, vol. 51, no. 4, pp. 463–479, 2014.

WILEY | Hindawi

Research Article

Effect of Freeze-Drying on Apple Pomace and Pomegranate Peel Powders Used as a Source of Bioactive Ingredients for the Development of Functional Yogurt

Munir Ahmed [ID],[1] Anwar Ali [ID],[2,3,4] Aleena Sarfraz [ID],[5] Qin Hong [ID],[6] and Hu Boran [ID][1]

[1]*School of Food Science and Engineering, Yangzhou University, Yangzhou, China*
[2]*Department of Epidemiology and Health Statistics, Xiangya School of Public Health, Central South University, Changsha, China*
[3]*Hunan Provincial Key Laboratory of Clinical Epidemiology, Xiangya School of Public Health, Central South University, Changsha, China*
[4]*Food and Nutrition Society Gilgit-Baltistan, Skardu, Pakistan*
[5]*Department of Chemistry, University of Engineering and Technology, Lahore, Pakistan*
[6]*Department of Nutrition and Food Hygiene, School of Public Health, Central South University, Changsha, China*

Correspondence should be addressed to Hu Boran; huboran@yzu.edu.cn

Agro-industrial by-products of fruits have turned into an essential source of bioactive products. This study examined the effect of freeze-drying on apple pomace powder (APP) and pomegranate peel powder (PPP) and their utilization in functional yogurt development at different concentrations. Freeze-dried powders in functional yogurt were investigated by chemical profile and bioactive characterization of total phenolic content (TPC), total flavonoid content (TFC), and antioxidant activity. The highest concentration of TPC (4.64) mg GAE/g, TFC (1.73 ± 0.00) CE mg/g, and antioxidant activity (83.87 ± 0.02) % was investigated in the yogurt sample T_6, having the maximum amount of PPP in it, which was significantly higher compared to the treatments having APP. Yogurt samples were analyzed for their sensory attributes, which showed a decline with the increase in both APP and PPP concentrations in contrast by introducing the optimum levels of APP and PPP (3% or 6%); hence, no significant loss in sensory profile was found as compared to the control samples. The results were found to be significant at the level ($p < 0.05$). In terms of the freeze-dried APP and PPP results, the APP samples had the most complete chemical composition, with the exception of fiber and ash concentration. Treatments of functional yogurt were prepared for their physicochemical profile, which demonstrated a straight proportionate relationship between the proportions of both powders in the meantime. Protein and fat levels were likely to decrease as both dry powder levels increased. Hence, apple pomace and pomegranate peel can be used after freeze-drying as a rich source of bioactive compounds in functional yogurt in the food industry.

1. Introduction

The agro-industrial waste is rich in dietary fiber, phytochemicals, and other essential nutrients [1, 2]. A substantial amount of this waste is often burned or dumped; however, it holds many important and beneficial nutrients [3]. Apple pomace is considered one of the essential and major industrial wastes, which contain significantly higher amounts of dietary fiber, bioactive compounds, and other essential nutrients. With time, the term "food by-products" has been progressively utilized. This term enlightens biological material as waste can be appropriately treated and altered into more valuable market-conscious derivatives [4]. The term "food waste" refers to "fractions of food and inedible parts of food" removed from the food supply chain [5]. Definitions become more complicated when it comes to the sector of fruits and vegetables. Fruit and vegetable waste can be defined as unpalatable parts of vegetables being discarded throughout the reception, handling, transportation, and different processing stages [6].

Due to the higher biodegradability of fruits and vegetable waste, this can cause environmental compilations. Apart from biological and nutritional losses, economic loss is also present. That is why in the last few decades, great efforts were made for the development of advanced methods and policies for waste [7]. Fruits and vegetables are a significant source of nutrition, especially their residues or wastes left behind after processing in fruit juice processing industries [8]. Fruit wastes or residues can be converted into a consumable form or utilized as a processing aid in food products because they are a portion of the fruit left behind after juice extraction. Apple pomace and pomegranate peel are excellent sources of dietary fiber and higher bioactive potential; therefore, the food products developed by employing these waste plant residues will significantly affect the health of the textural properties of the prepared products. These fruits residues can play a vital role in regulating the body's proper working as they contain sufficient amounts of bioactive compounds, resulting in reducing oxidative stress [9]. All over the globe, apple pomace is being utilized to develop different functional dairy products such as bakery items (e.g., spinach-flavoured ice cream made up of vegetable fat and fiber-supplemented dairy yogurt) [10].

Human beings have been familiar with fermentation techniques since the Stone Age. It is one of the oldest preservation techniques that convert milk into more nutritional products and prolong its shelf life at a significant level. The accurate beginning of the fermentation technique is almost unknown, but it is considered that it could be existing from 15000 years ago [11]. Yogurt is one of the most consumed milk products around the globe [12]. The production of yogurt is mainly done by either fermentation of fresh milk or reconstituted milk with lactic acid bacteria. It is popular among customers due to its benefits on the intestinal environment and body immunity [13]. Yogurt has a unique flavour, texture and good sensory characteristics. Yogurt is also beneficial for our gut microflora. Yogurt can be obtained by treating the pasteurized milk with lactic acid fermentation via *Streptococcus thermophilus* and *Lactobacillus bulgaricus* or with other cultures of bacteria [14, 15].

Nevertheless, the abovementioned health-endorsing characteristics prompt food entrepreneurs to focus on pomegranate peel phytochemicals containing food preparations including food supplements, nutraceuticals, and phenolic enriched diets [16]. In addition to their nutraceutical significance, PoP and PoPx show essential practical purposes (antioxidant, antimicrobial, colorant, and flavouring). They might also act as excellent natural additives for food preservation and quality improvement. The medical industry observed a significant improvement due to peel-extracted derivatives' high nutritional and nutraceutical capabilities [17].

Freeze-dried products hold much of their original flavour, phytochemical properties and are found to be very light and crispy at the same time [18]. Still, there is no single method of moisture removal suitable for all commodities of food products since each organic material (food) has its exclusive characteristics and subsequently, the requirements are diverse. There is a dire need to stop burning and wasting

these nutritious leftovers that can be easily transferred into new products and recover the nutritional loss in existing products and enhancements in their shelf life. The purpose of this research is to confirm that apple pomace and pomegranate peel powder can be employed in the preparation of high-fiber fermented functional products, such as yogurt. For this, the freeze-dried apple pomace and pomegranate peel powder and their bioactive potential at various stages of the yogurt development process have been analyzed.

2. Materials and Methods

2.1. Procurement of Raw Material. Raw milk, apple, and pomegranate were purchased from dairy, fruits, and vegetable stores, respectively, situated in Lahore, India. Apples and pomegranates were transferred into plastic bags; however, milk was collected in a sterile glass bottle with a 500 mL capacity to avoid contamination. Furthermore, the raw materials were transferred to the fruits and vegetable laboratory at the Department of Food Science, Government College University Faisalabad, for further examination. The raw form of apple pomace and pomegranate peel is shown in Figure 1(b).

2.2. Handling of Raw Material. Apple, pomegranate, and milk were brought in to the laboratory for further processing. First, apple and pomegranates were thoroughly washed with distilled water and inner seeds in case of apple were removed using apple seed corer. However, milk container was placed in the refrigerator at $7^\circ C$ until apple pomace and pomegranates peel were developed.

2.3. Drying of Apple Pomace and Pomegranate Peel. Apple pomace and pomegranate peel were dried using the freeze-drying technique as prescribed by [19] with some needed modifications. For this purpose, a laboratory freeze-dryer (ALPHA 1-2 LD Plus, Christ, USA) was employed. Different parameters were settled for wet apple pomace and pomegranate peel freeze-drying, such as freezing temperature, T_{sh} temperature, P_{kch} (mbr) vacuum pressure, and residual moisture content, as shown in Table 1. Furthermore, wet apple pomace and pomegranate peel were conveyed in a freeze-dryer for drying. Then, the dried powders were collected and stored in aluminum pouches at room temperature for further analysis. After drying, apple pomace and pomegranate peel were ground to make fine powder for further analysis and development of functional yogurt as shown in Figures 1(c) and 1(d).

2.4. Product Development. APP and PPP were weighed and directly added to the pasteurized milk before fermentation, as shown in Table 2. Furthermore, for fermentation, cultures containing *Lactobacillus bulgaricus* and *Streptococcus thermophilus* were introduced into milk and mixed at $46^\circ C$ and allowed to ferment for 12–24 hrs. Further analysis was conducted after fermentation.

(a)

(b)

(c)

(d)
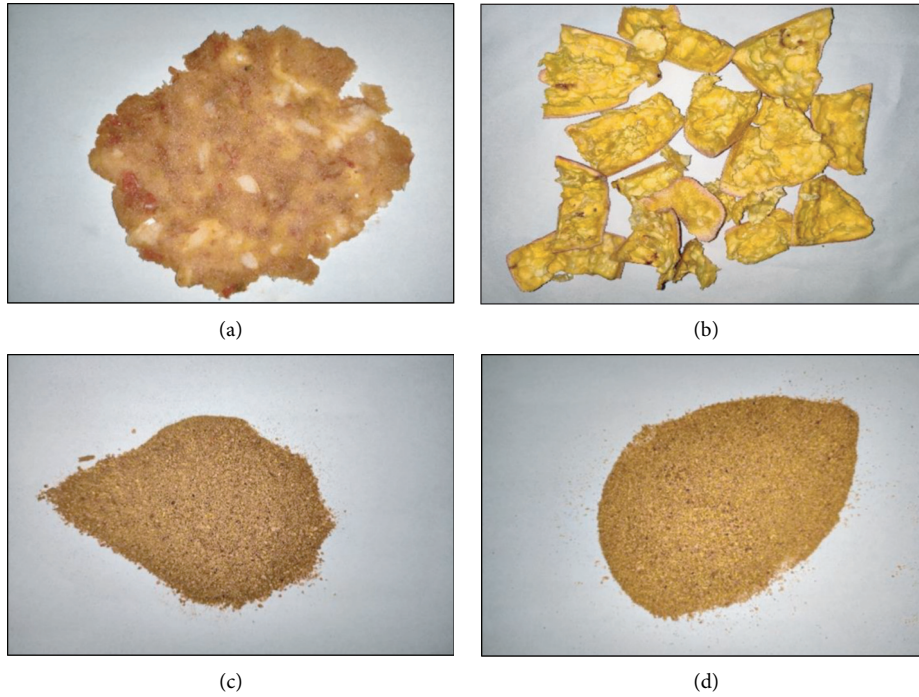
Figure 1: (a) Fresh apple pomace. (b) Fresh pomegranate peel. (c) Dried apple pomace. (d) Dried pomegranate peel.

Table 1: Different optimized conditions in freeze-dryer.

Product	Factors				
	Blanched at 100°C	Freezing temp. (°C)	T_{sh} (°C)	P_{kch} (mbr)	RM (%)
AP	+	−27	90	1.3	2.1
PP	+	−80	90	1.5	1.3

PP = pomegranate peel. AP = apple pomace.

Table 2: Treatment table.

Treatments		Levels (%)
T_0	Control	0%
T_1		3%
T_2	Apple pomace (dried)	6%
T_3		9%
T_4		3%
T_5	Pomegranate peel powder (dried)	6%
T_6		9%
T_7	APP + PPP	2.5 + 2.5%

PPP = pomegranate peel powder. APP = apple pomace powder.

2.5. *Chemical Composition.* The basic chemical composition such as moisture, fat, crude protein, ash, and carbohydrate content of freeze-dried PPP and APP was examined according to the standard procedures prescribed by the Association of Official Analytical Chemists (AOAC, 2010). Moisture content was evaluated by taking exactly 2 g of dried powder sample and drying in an oven at about $100 \pm 5°C$ for approximately 3 hrs and then reweighed. Protein and fat content were further examined by employing the Kjeldahl and Soxhlet apparatus. In addition, the ash content was measured by subjecting 2 g sample under the controlled environment of the muffle furnace at 400°C for 3 hrs. The crude fiber was also examined in this particular effort. Meanwhile, carbohydrate- or nitrogen-free extracts were calculated by employing the following expression:

$$\%\text{Carbohydrates (NFE)} = 100 - (\text{Fat} + \text{Protein} + \text{Moisture} + \text{Ash} + \text{Crude Fiber}). \tag{1}$$

2.6. *Rheological Analysis of Yogurt.* The samples were measured right after making to reduce the effects of sample shear history. Tests were conducted using an Anton Paar Physica MCR 301 controlled stress rheometer (Anton Paar Germany GmbH, Ostfildern, Germany) with a measuring cell (PPTD 120) equipped with a Peltier temperature control. A humidity chamber was used to prevent water loss during evaluation. A Julabo circulator (Julabo West, Inc., CA, USA)

was used as a temperature control system for the Peltier element. A parallel plate geometry (PP50) was used at 0.5 mm gap. The test was conducted at 4°C. Using a farinograph (Brabender, Duisburg, Germany) according to AAAC methods (2000), the influence of apple pomace and pomegranate peel powders on the mixing profile of the dough was investigated. Extensograph (Brabender, Duisburg, Germany) was used to investigate the dough's elastic characteristics according to AAAC methods (2000). The visco-amylograph (Brabender, Duisburg, Germany) was used to determine the blends' pasting properties according to AAAC methods (2000).

2.7. Bioactive Characterization of Yogurt

2.7.1. Sample Extraction. Freeze-dried pomegranate peels and apple pomace samples were ground into a fine powder using a KMF grinder at 9676.8 g. Prepared ground samples were kept in sterile bags to prevent contamination at −40°C until further extraction. Methyl alcohol, ethyl alcohol, and water were employed to prepare extracts. Accurately, 0.5 g of dried sample was added into a flask followed by exactly 100 mL ethyl acetate and stirred at 20°C for 3 hrs. The mixture was centrifuged (Harrier 18/80 refrigerated centrifuge) (SANYO, MSE, UK) at 9676.8 g for 30°C. Furthermore, the supernatant was filtered by Whatman filter paper (No. 1, Ø 155 mm). However, the prepared extracts were stored at 4°C for further analysis as followed by [20, 21].

2.7.2. Antioxidant Activity (DPPH Assay). Antioxidant activity was examined by the method (2,2-diphenyl-1-picryl hydroxyl) prescribed by [19] with slight modifications as mentioned above. For this purpose, accurately 15 μl extracts were added into a test tube followed by 735 μl methanol and 750 μl 0.1 mM DPPH solution and thoroughly mixed until the extract dissolved in methanol. Then, the mixture was incubated for exactly 30 min in the dark to avoid any exposure to light. A UV-visible spectrophotometer measured the absorbance was measured at 517 nm by employing a UV-visible spectrophotometer (Thermo Scientific Technologies, Madison, WI, USA). A suitable calibration curve was prepared using ascorbic acid as the standard solution. The obtained results were expressed as mM ascorbic acid (AA) equivalent g^{-1} of extracts.

2.7.3. Total Phenolic Content (TPC). Prepared extracts were examined for their TPC by the Folin–Ciocalteu method as prescribed by [1]. For this purpose, 70 μL of the prepared extracts was accurately added in a test tube of 10 mL capacity, followed by 250 μL of Folin–Ciocalteu reagent and 750 μL of Na_2Co_3 (1.9 M). However, a total volume of exactly 5 ml was made up by adding distilled water and then mixed by using a vortex mixer for about 1 minute before incubation for 2 hrs in the dark. Consequently, the absorbance was measured by utilizing a Spectrophotometer (Thermo-Spectronic, Surrey, England) at 765 nm wavelength. A calibration curve was prepared by employing controlled

solutions of gallic acid. Obtained results were expressed as gallic acid equivalents (GAE) in mg^{-g} dry solids.

2.7.4. Total Flavonoid Content (TFC). TFC of the freeze-dried apple pomace and pomegranate peel extract was determined by a method as prescribed by [1]. For this purpose, exactly 1 mL of the prepared extract was placed in to a test tube (10 mL) already containing 4 mL of distilled water. At an instant, 0.3 mL of 5% sodium nitrite was added into the test tube. However, after 5 min accurately, 0.3 mL of 10% aluminium chloride was placed in the same test tube. Then, after 6 min, exactly 2 mL of 1 M sodium hydroxide was added to the test tube and mixed. Instantly, the test tube was diluted with the addition of 2.4 mL of distilled water and thoroughly mixed.

At last, the absorbance of the pink coloured mixture was examined at 510 nm and water was used as a blank. Different amounts of catechin solutions were used to create an appropriate calibration curve. The results were expressed in mg catechin equivalent (CE) per g of dried solids.

2.8. Syneresis Analysis. Accurately 5 ml of sample was taken in falcon tubes and the tubes was centrifuged at 500 rpm for 15–20 minutes at 4-5 degrees centigrade. The whey was separated after 1-2 minutes. The whey amount was expressed as volume of whey separated per 100 ml of yogurt. The syneresis was checked and measured during 0, 7th, 14th, and 21st [13].

2.9. Sensory Evaluation. A 9-point hedonic scale was used to assess the sensory evaluation of yogurt samples. Sensory attributes were judged by a panel of different trained judges relevant to the field of study. The parameters on the scale were as follows: 1 = dislike, 2 = dislike slightly, 3 = neither like or dislike, 4 = like moderately, 5 = like very much, 6 = like extremely, 7 = good, 8 = very good, and 9 = excellent.

2.10. Statistical Analysis. The obtained data were analyzed by analysis of variance (ANOVA) through SPSS. Duncan's Multiple Range (LSD) test was utilized to determine the significance level between the mean values obtained.

3. Results

3.1. Chemical Profile. In Table 3, the average chemical compositions of PPP and APP were elaborated, which depicts that APP samples were examined to exhibit the highest protein (8.16) g/100 g and fat (1.10) g/100 g contents, whereas PPP samples were investigated to have much higher ash (3.53) g/100 g, fiber (35.19) g/100 g along with moisture (8.43) g/100 g, and carbohydrate (61.34) % levels in contrast to APP samples.

3.2. Bioactive Potential of APP and PPP. In Table 4, freeze-dried APP and PPP were studied for their bioactive potential, which clearly shows a significantly higher TPC (221.77 ± 1.79) mg GAE/g content and TFC (26.15 ± 1.00)

TABLE 3: Proximate chemical analysis of apple pomace powder and pomegranate peel powder.

Attributes	APP	PPP
Moisture (g/100 g)	7.88	8.43
Protein (g/100 g)	8.16	3.26
Fat (g/100 g)	1.10	0.55
Fiber (g/100 g)	12.70	35.19
Ash (g/100 g)	1.53	3.35
Carbohydrates (%)	53.12	61.34

APP: apple pomace powder. PPP: pomegranate peel powder.

TABLE 4: Bioactive profile of apple pomace powder and pomegranate peel powder.

Attributes	APP	PPP
TPC (GAE mg^{-g})	52.36 ± 1.22^b	221.77 ± 1.79^a
TFC (CE mg^{-g})	8.40 ± 0.13^b	26.15 ± 1.00^a

Means that do not share a letter in a column respective to their factor are significantly different at level ($p < 0.05$). APP: apple pomace powder. PPP: pomegranate peel powder. TPC: total phenolic content. TFC: total flavonoid content. Values in mean column are given in (mean ± SD).

CE mg/g levels in samples from PPP in contrast to the TPC (52.36 ± 1.22) mg GAE/g and TFC (8.40 ± 0.13) CE mg/g found in APP samples.

3.3. Rheological Analysis of Yogurt. The average yogurt contains (14.60 ± 0.67) g/100 g protein content, though, the maximum content was observed in T_0 (15.27) g/100 g sample having 0% dried APP and PPP; on the other hand, least protein content (13.98) g/100 g was determined in T_6 sample with 9% freeze-dried PPP. The fat analysis depicts that on average (3.89 ± 0.38) g/100 g yogurt contains fat content, though, the highest content was found in T_0 (4.11) g/100 g sample having 0% freeze-dried APP and PPP, whereas the minimum fat concentration was determined in T_6 (3.69) g/100 g sample having 9% PPP. Brix determination clearly shows that on average (13.61 ± 0.35) w/w % yogurt contains total soluble solids content; however, the maximum concentration was detected in T_6 (14.26) w/w % sample having 9% freeze-dried PPP; on the other hand, minimum TSS content was examined in T_0 (control) (13.07) w/w % sample with 0% freeze-dried powder. Solid not fat analysis depicts that on average (10.24 ± 0.60) w/w % yogurt contains solid, not fat content though, the highest amount was examined in T_6 (11.21) w/w % sample having 0% dried APP and PPP, whereas least SNF content was examined in T_0 (Control) (9.17 ± 0.01) w/w % sample with 0% freeze-dried APP and PPP. pH determination can be used as an accurate acidity indicator of milk and provide H+ value or absorption in milk. The association between acidity and pH value is only a loose-end estimation. pH determination clearly shows that on average (4.49 ± 0.04) yogurt contains pH content; however, the highest value was detected in T_3 (4.56) sample having 9% freeze-dried APP; in contrast, the least pH value was examined in T_6 (4.43 ± 0.01) sample with 9% PPP.

After a sample of furnace oil has been entirely burnt, the ash content indicates the incombustible component that remains. The ash content of the developed functional yogurt was determined. This certain type of analysis was conducted to observe the concentration and nature of minerals (inorganic mass) in food. Ash analysis depicts that, on average, the ash content is (2.08 ± 0.16) g/100 g yogurt while the maximum content was found in T_6 (3.37 ± 0.01) g/100 g sample having 9% freeze-dried PPP; on the other hand, least ash content was detected in T_0 (control) (1.85 ± 0.01) g/100 g sample with 0% dried powder. The rheological profile of yogurt is exhibited in Table 5.

The Brix, ash, SNF, and pH values except for fat and protein levels of different treatments were tending to increase with the increase in APP or PPP concentrations as shown in Figure 2. Moreover, adding freeze-dried PPP contents in the developed functional yogurt increased significantly higher than APP incorporated treatments at level ($p < 0.05$).

3.4. Bioactive Profile of Functional Yogurt. In Table 6, the descriptive analysis for total phenolic contents analysis depicts that on average (4.07 ± 0.37) mg GAE/g concentrations were found. However, the maximum content was detected in T_6 (4.64) mg GAE/g sample having 9% freeze-dried PPP; on the other hand, least TPC was inspected in T_0 (control) (3.39) mg GAE/g sample with 0% freeze-dried powder. TFC analysis elaborates that on mean (1.44 ± 0.17) CE mg/g concentrations were found. However, the highest level was investigated in T_6 (1.73) CE mg/g sample having 9% freeze-dried PPP, whereas the lowest TFC was inspected in T_0 (control) (1.21) CE mg/g sample with 0% freeze-dried powder. Antioxidant activity examination explains that on average (70.58 ± 9.43) % was calculated. Meanwhile, the extreme activity was diagnosed in T_6 (83.87) % sample having 9% freeze-dried PPP; besides, the least antioxidant activity or DPPH inhibition was measured in T_0 (control) (59.51) % sample with 0% freeze-dried powder as shown in Figure 3.

3.5. Syneresis in Functional Yogurt. Prepared functional yogurt samples comprising of T_0, T_1, T_2, T_3, T_4, T_5, T_6, and T_7 were analyzed for their syneresis at different intervals of time (day 0, day 7, day 14, and day 21) by using a method as described in Materials and Methods. Descriptive analysis was conducted; however, maximum concentration was observed and detected in T_0 (1.82 ± 0.01) g/100 g at 21st day of storage, whereas minimum syneresis concentration was observed and detected in T_6 (1.32 ± 0.01) g/100 g at day 0 of storage. Three times replications were made for each treatment as shown in Table 7.

3.6. Sensory Evaluation. In Table 8, the developed functional yogurt with the addition of APP and PPP at different levels was conducted. As far as the descriptive analysis is concerned, the maximum scores for appearance (8.50), texture (7.70), flavour (7.40), taste (8.50), and consistency (7.70) were observed and detected in T_0 (control) sample having absolutely no *APP and *PPP concentrations; on the other

TABLE 5: Effect of adding apple pomace powder and pomegranate peel powder on the rheological profile of yogurt. Values in mean column are given in (mean ± SD).

Treatments	Parameters					
	TSS %	SNF %	pH	Ash %	Fat %	Protein %
T_0	13.07 ± 0.02^f	9.17 ± 0.01^g	4.48 ± 0.05^d	1.85 ± 0.03^g	4.11 ± 0.02^a	15.27 ± 0.02^a
T_1	13.35 ± 0.01^e	9.77 ± 0.02^f	4.51 ± 0.03^c	1.96 ± 0.01^f	4.03 ± 0.02^b	15.09 ± 0.02^b
T_2	13.61 ± 0.04^c	10.13 ± 0.02^e	4.54 ± 0.04^b	2.08 ± 0.03^d	3.91 ± 0.01^c	14.57 ± 0.06^e
T_3	13.83 ± 0.01^b	10.34 ± 0.01^c	4.56 ± 0.01^a	2.21 ± 0.02^b	3.84 ± 0.04^d	14.17 ± 0.08^g
T_4	13.53 ± 0.01^{cd}	10.20 ± 0.01^d	4.46 ± 0.03^e	2.02 ± 0.01^e	3.85 ± 0.06^d	14.75 ± 0.02^c
T_5	13.87 ± 0.17^b	10.90 ± 0.03^b	4.45 ± 0.04^e	2.16 ± 0.04^c	3.77 ± 0.01^e	14.29 ± 0.03^f
T_6	14.26 ± 0.01^a	11.21 ± 0.02^a	4.43 ± 0.06^f	2.37 ± 0.03^a	3.71 ± 0.02^f	13.98 ± 0.04^h
T_7	13.39 ± 0.03^e	10.16 ± 0.01^{de}	4.46 ± 0.04^e	1.98 ± 0.00^{ef}	3.89 ± 0.04^c	14.68 ± 0.06^d
Average	13.61 ± 0.35	10.24 ± 0.60	4.49 ± 0.34	2.08 ± 0.16	3.89 ± 0.38	14.60 ± 0.67

Means that do not share a letter in a column are significantly different at level ($p < 0.05$). $T_0 = 0\%$ control. $T_1 = 3\%$ apple pomace powder. $T_2 = 6\%$ apple pomace powder. $T_3 = 9\%$ apple pomace powder. $T_4 = 3\%$ pomegranate peel powder. $T_5 = 6\%$ pomegranate peel powder. $T_6 = 9\%$ pomegranate peel powder. $T_7 = 2.5 + 2.5\%$ apple pomace powder + pomegranate peel powder.

FIGURE 2: Effect of adding APP and PPP on the rheological properties of yogurt.

FIGURE 3: Effect of adding APP and PPP on the biological properties of yogurt.

TABLE 6: Effect of adding apple pomace powder and pomegranate peel powder on the bioactive profile of yogurt. Values in mean column are given in (mean ± SD).

Treatments	Parameters		
	Antioxidant activity (%)	TPC (mg GAE/ g)	TFC (CE mg/ g)
T_0	59.51 ± 0.04^h	3.39 ± 0.01^h	1.21 ± 0.01^g
T_1	61.80 ± 0.02^g	3.67 ± 0.04^g	1.24 ± 0.03^f
T_2	63.85 ± 0.01^f	3.99 ± 0.03^e	1.35 ± 0.02^e
T_3	65.13 ± 0.02^e	4.12 ± 0.04^c	1.46 ± 0.04^d
T_4	79.46 ± 0.01^c	4.08 ± 0.02^d	1.53 ± 0.00^c
T_5	82.67 ± 0.02^b	4.28 ± 0.03^b	1.61 ± 0.03^b
T_6	83.87 ± 0.02^a	4.64 ± 0.05^a	1.73 ± 0.05^a
T_7	68.33 ± 0.03^d	3.79 ± 0.02^f	1.34 ± 0.04^e
Average	70.58 ± 9.43	4.00 ± 0.37	1.44 ± 0.17

Means that do not share a letter in a column are significantly different at level ($p < 0.05$). TFC: total flavonoid content. TPC: total phenolic content. $T_0 = 0\%$ control. $T_1 = 3\%$ apple pomace powder. $T_2 = 6\%$ apple pomace powder. $T_3 = 9\%$ apple pomace powder. $T_4 = 3\%$ pomegranate peel powder. $T_5 = 6\%$ pomegranate peel powder. $T_6 = 9\%$ pomegranate peel powder. $T_7 = 2.5 + 2.5\%$ apple pomace powder + pomegranate peel powder.

hand, least scores for appearance (4.80), texture (4.70), flavour (4.20), and taste (3.30) were investigated in T_6 sample with 9% PPP. Overall acceptability scores were found to be significantly higher than other analyzed treatments. In this study, sensory attributes tended to decrease with the increase in freeze powder concentrations; however, by adding APP in yogurt, sensorial scores did not decrease significantly compared to the treatments having PPP in them. Estimated marginal means for sensory evaluation of samples were conducted and textured to ease in comparison as shown in Figure 4.

4. Discussion

Fruit juice processing enterprises generate a large amount of industrial waste, such as apple pomace and pomegranate peel. The moisture is removed from pomegranate peel and apple pomace using a freeze-drying method. The moisture content of PPP was determined to be in the range of 8.3–7.9 g/100 g using the freeze-drying procedure [22].

TABLE 7: Descriptive analysis for syneresis in different treatments. Values are given in (mean ± SD).

Attribute	Treatments	Time intervals				Means
		Day 0	Day 7	Day 14	Day 21	
	Control	1.65 ± 0.00	1.73 ± 0.00	1.78 ± 0.01	1.82 ± 0.00	1.75 ± 0.07^A
	T_1	1.61 ± 0.00	1.64 ± 0.00	1.67 ± 0.01	1.71 ± 0.00	1.66 ± 0.04^B
	T_2	1.58 ± 0.00	1.61 ± 0.00	1.63 ± 0.00	1.66 ± 0.00	1.62 ± 0.03^{CD}
	T_3	1.37 ± 0.00	1.39 ± 0.00	1.44 ± 0.00	1.48 ± 0.00	1.42 ± 0.05^E
Syneresis (g/100 g)	T_4	1.60 ± 0.00	1.62 ± 0.00	1.65 ± 0.00	1.68 ± 0.00	1.64 ± 0.03^C
	T_5	1.55 ± 0.00	1.59 ± 0.00	1.61 ± 0.00	1.64 ± 0.00	1.60 ± 0.03^D
	T_6	1.32 ± 0.00	1.35 ± 0.00	1.39 ± 0.00	1.42 ± 0.00	1.37 ± 0.04^F
	T_7	1.59 ± 0.00	1.61 ± 0.00	1.66 ± 0.00	1.69 ± 0.00	1.64 ± 0.04^{BC}
	Means	1.54 ± 0.12^D	1.57 ± 0.13^C	1.61 ± 0.12^B	1.64 ± 0.12^A	

Means that do not share a letter are significantly different at level ($p < 0.05$). $T_0 = 0\%$. $T_1 = 3\%$ apple pomace powder. $T_2 = 6\%$ apple pomace powder. $T_3 = 9\%$ apple pomace powder. $T_4 = 3\%$ pomegranate peel powder. $T_5 = 6\%$ pomegranate peel powder. $T_6 = 9\%$ pomegranate peel powder. $T_7 = 2.5 + 2.5\%$ apple pomace powder + pomegranate peel powder.
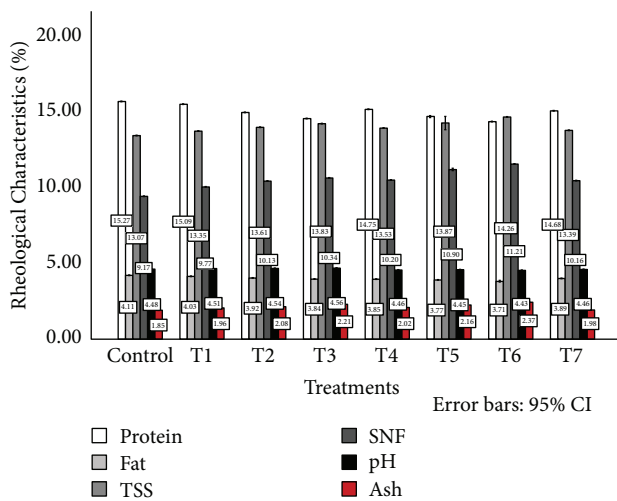
TABLE 8: Effect of adding apple pomace powder and pomegranate peel powder on the sensory profile of yogurt. Values are given in (mean ± SD).

Sensory attributes	Treatments							
	T_0 (Control)	T_1	T_2	T_3	T_4	T_5	T_6	T_7
Appearance	8.50^a	7.40^b	6.30^e	5.40^g	7.30^c	6.10^f	4.80^h	6.30^d
Texture	7.70^a	7.30^b	5.80^d	5.20^g	7.10^c	5.60^e	4.70^h	5.30^f
Flavour	7.40^a	7.00^b	6.10^d	5.40^g	6.90^c	5.90^e	4.20^h	5.80^f
Taste	8.50^a	7.20^b	6.50^d	5.70^f	6.80^c	5.40^g	3.30^h	5.60^e
Consistency	7.70^a	7.50^c	7.20^e	6.80^h	7.60^b	7.30^d	6.90^g	7.10^f
Overall acceptability	7.80^a	7.30^b	6.40^d	5.70^g	7.15^c	6.10^f	4.80^h	6.00^e

Means that do not share a letter in a row are significantly different at level ($p < 0.05$). $T_0 = 0\%$ control. $T_1 = 3\%$ apple pomace powder. $T_2 = 6\%$ apple pomace powder. $T_3 = 9\%$ apple pomace powder. $T_4 = 3\%$ pomegranate peel powder. $T_5 = 6\%$ pomegranate peel powder. $T_6 = 9\%$ pomegranate peel powder. $T_7 = 2.5 + 2.5\%$ apple pomace powder + pomegranate peel powder.
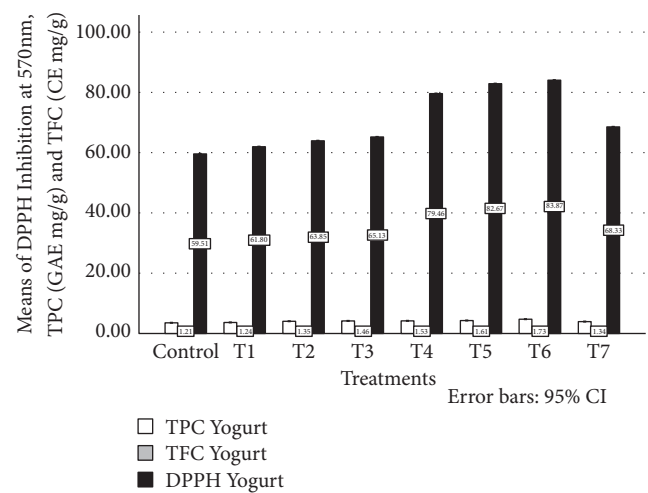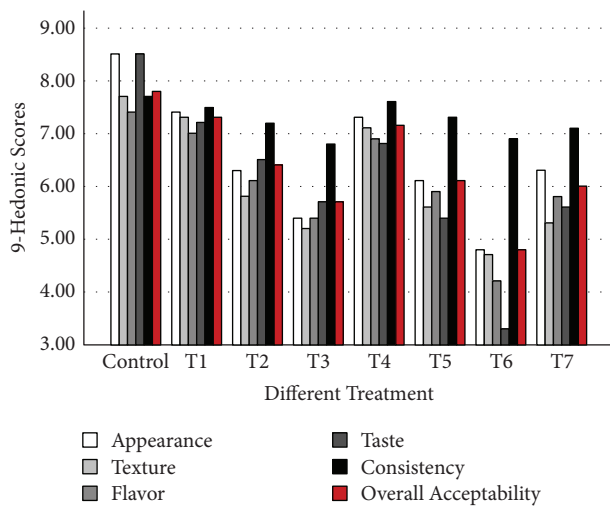

FIGURE 4: Estimated marginal means for sensory evaluation in functional yogurt samples were conducted and textured to ease in comparison.

Another study [1] undertaken during the production of fiber-enriched cookies found that by incorporating freeze-drying, moisture content of 8.90–9.15 g/100 g could be attained, which was observed in a similar range of 7.88 g/100 g as reported in the current effort. In contrast to APP, PPP samples had the greatest fiber 35.19 g/100 g and ash 3.53 g/100 g; these results were observed in form as resulted in the range of 34.05–39.13 g/100 g and 3.30–3.41 g/100 g for protein and ash, respectively, in PPP samples [23].

The TPC of APP samples ranging from 28.91 to 30.17 mg GAE/g as studied by [24] contradicts with the results of current report and this contradiction may be due to the difference in extraction solution aqueous, methanolic or ethanolic. The highest TPC (221.71) mg GAE/g and TFC (26.15) mg GAE/g was discovered in freeze-dried PPP samples; similar outcomes were reported by [21] in methanolic extracts. Thermal treatments have negative impact on polyphenols in the food system as predicted by [19].

Another study was reported by [25], stating that during the air-drying of red pepper as temperature rises polyphenolic concentrations tend to decrease significantly. According to [26], this might be because the majority of phenolic compounds are attached to cellular structures, and subsequent dehydration procedures tend to liberate the bound biologically active compounds from the food system, making them more bio-accessible during the extraction process. A study also stated that freeze-drying is generally considered as one of the best and most effective dehydration approaches coupled with enhanced shelf span [19], while [27] states that freeze-drying is the technique that allows the best preservation of phytochemicals and their bioactivity in fruit and vegetable powders. With reference to the present study, freeze-drying can be adopted for the maximum recovery of bioactive compounds (i.e., TPC and TFC from apple pomace and pomegranate peel).

pH level in response to the addition of APP has been observed to be increased, whereas after the incorporation of PPP the pH levels were examined to decrease significantly at higher concentrations. Similar phenomenon was observed during the development of peanut milk fermented curd as reported by [28]. Thus, in the case of apple pomace, pH tends to increase which shows a decline in the acidity of yogurt, which may be due to the dilution factor. After introducing APP and PPP in inclining order, total soluble solid along with solid not fat and ash levels was found to be increased significantly. Some similar increases reported in TSS and SNF levels when incorporated in the development of fiber-enriched yogurt [14, 29]. Fat and protein levels were found to be remarkably affected by the introduction of increasing APP and PPP concentration order; in validation, the Food Drug Administration (FDA) standards for drinkable yogurt postulate >8.25% milk (SNF), fat levels to satisfy nonfat yogurt (<0.5%), low-fat yogurt (2%), and yogurt (>3.25%) before the addition of other ingredients. Thus, fiber-enriched yogurt with APP and PPP can be termed as low-fat yogurt.

Syneresis was also examined where maximum concentration was observed and detected in T_0 (1.82 ± 0.01) g/100 g at 21st day of storage, whereas minimum syneresis concentration was observed and detected in T_6 (1.32 ± 0.01) g/100 g at day 0 of storage. Syneresis concentrations tended to decrease by the addition of APP and PPP. Meanwhile, treatments having pomegranate peel powder (1.42 ± 0.01) g/100 g as compared to apple pomace powder (1.71 ± 0.01) g/100 g were observed to show significantly less syneresis concentrations at the 21st day of storage.

Highest TPC (4.69) GAE/g and TFC (1.78) CE/g level was observed in T_6 having 9% PPP in it. In the current study, TPC as well as TFC was found to be increased significantly as APP and PPP concentration tend to incline in yogurt. Meanwhile, by introducing PPP and APP, remarkably higher increment was found in bioactive components in oppose to the treatments having APP in it. A similar increase has been stated in TPC and TFC compounds during the development of probiotic yogurt fortified with apple pomace flour [30]. Highest TPC and TFC were found in a study during the characterization of 12 widely used spices [31]. It has been reported that by fortifying pomegranate peel extracts during the development of stirred yogurt, TPC and TFC were found to be significantly increased and found in the ranges of 3.39–5.97 mg GAE/g and 1.11–2.18 mg CE/g, respectively [29]. TPC and TFC concentrations of different developed treatments were found directly proportional to APP and PPP concentrations; moreover, by incorporating freeze dried PPP, TPC concentrations in developed functional yogurt was observed increased significantly higher as compared to freeze-dried APP. These results were found in engagement with the studies led by [13, 23].

Antioxidant activity scavenges free radicals and it is directly proportional to the phenolic and flavonoid compounds in a particular food systems. As the previous trend extends, a significant increment in the antioxidant activity was examined as APP and PPP concentrations, which tend to increase gradually. The antioxidant activity of different developed treatments were observed to be directly proportional to APP and PPP concentrations; moreover, by incorporating freeze dried PPP, antioxidant activity in developed functional yogurt increased significantly higher as compared to freeze-dried APP [13, 23]. Previously, studies reported by [23, 28, 30] emphasize that by the introduction of APP as well as PPP, the antioxidant activity of yogurt increases.

5. Conclusion

In this study, we prepared functional yogurt by the addition of APP and PPP that was examined for its bioactive profile such as TPC, TFC, and DPPH inhibition, also known as antioxidant activity. First, apple pomace and pomegranate peel were freeze-dried and further introduced into yogurt. Chemical composition and the bioactive investigation clearly showed that PPP was far more superior to APP except for protein and fat content, which was found to be significantly higher in APP samples. Moreover, adding APP or PPP rheological attributes of functional yogurt was found to be increased marginally in comparison to the control sample. In addition, bioactive characterization of functional yogurt was also done, which exhibits significantly higher outcomes in treatments having PPP. Developed functional yogurt samples were also investigated for their sensory parameters, which describes that by introducing higher levels of either APP or PPP in both cases, the sensory profile tends to decrease; this decline was found to be more prominent in PPP (T_4, T_5, and T_6) added treatments in contrast to APP (T_1, T_2, and T_3) introduced ones. The APP-enriched and PPP-enriched yogurt were found to be the most suitable in terms of appearance, body/consistency, flavour, and overall acceptance in this study, indicating that apple pomace and pomegranate peel can be utilized as a source of bioactive compounds in yogurt after freeze-drying in the food industry.

Data Availability

The data set supporting the conclusions of this article is included within the article.

Conflicts of Interest

The authors declare that they have no conflicts of interest regarding the publication of this paper.

References

[1] M. Usman, S. Ahmed, A. Mehmood et al., "Effect of apple pomace on nutrition, rheology of dough and cookies quality," *Journal of Food Science & Technology*, vol. 57, no. 9, pp. 3244–3251, 2020.

[2] N. Leyva-López, C. E. Lizárraga-Velázquez, C. Hernández, and E. Y. Sánchez-Gutiérrez, "Exploitation of agro-industrial waste as potential source of bioactive compounds for aquaculture," *Foods*, vol. 9, no. 7, p. 843, 2020.

[3] W. Willett, J. Rockström, B. Loken et al., "Food in the anthropocene: the EAT–Lancet Commission on healthy diets from sustainable food systems," *The Lancet*, vol. 393, no. 10170, pp. 447–492, 2019.

[4] J. C. M. Barreira, A. A. Arraibi, and I. C. F. R. Ferreira, "Bioactive and functional compounds in apple pomace from juice and cider manufacturing: potential use in dermal formulations," *Trends in Food Science & Technology*, vol. 90, pp. 76–87, 2019.

[5] I. Esparza, N. Jiménez-Moreno, F. Bimbela, C. Ancín-Azpilicueta, and L. M. Gandía, "Fruit and vegetable waste management: conventional and emerging approaches," *Journal of Environmental Management*, vol. 265, Article ID 110510, 2020.

[6] P. A. R. Fernandes, S. S. Ferreira, R. Bastos et al., "Apple pomace extract as a sustainable food ingredient," *Antioxidants*, vol. 8, no. 6, p. 189, 2019.

[7] F. Younas, A. Mustafa, Z. U. R. Farooqi et al., "Current and emerging adsorbent technologies for wastewater treatment: trends, limitations, and environmental implications," *Water*, vol. 13, no. 2, p. 215, 2021.

[8] N. Ahmed, A. Ali, S. Riaz, A. Ahmad, and M. Aqib, "Vegetable proteins: nutritional value, sustainability, and future perspectives," in *Vegetable Growing* IntechOpen, London, UK, 2021.

[9] N. A. Sagar, S. Pareek, S. Sharma, E. M. Yahia, and M. G. Lobo, "Fruit and vegetable waste: bioactive compounds, their extraction, and possible utilization," *Comprehensive Reviews in Food Science and Food Safety*, vol. 17, no. 3, pp. 512–531, 2018.

[10] M. Faustino, M. Veiga, P. Sousa, E. Costa, S. Silva, and M. Pintado, "Agro-food byproducts as a new source of natural food additives," *Molecules*, vol. 24, no. 6, Article ID 1056, 2019.

[11] H. Vatanparast, N. Islam, R. P. Patil et al., "Consumption of yogurt in Canada and its contribution to nutrient intake and diet quality among Canadians," *Nutrients*, vol. 11, no. 6, Article ID 1203, 2019.

[12] A. Rakhmanova, Z. A. Khan, and K. Shah, "A mini review fermentation and preservation: role of lactic acid bacteria," *MOJ Food Processing & Technology*, vol. 6, no. 5, pp. 414–417, 2018.

[13] K. Issar, P. C. Sharma, and A. Gupta, "Utilization of apple pomace in the preparation of fiber-enriched acidophilus yoghurt," *Journal of Food Processing and Preservation*, vol. 41, no. 4, Article ID e13098, 2017.

[14] S. Nagaoka, "Yogurt production," *Lactic Acid Bacteria*, Humana Press, New York, NY, USA, pp. 45–54, 2019.

[15] S. Jauhar, M. A. R. Nor-Khaizura, W. Z. W. Ibadullah, and M. R. Ismail-Fitry, "Review on different extraction methods of polyphenol compounds from pomegranate (Punica granatum)," in *Proceedings of the 5th International Conference on Applied Sciences and Engineering (ICASEA, 2018)*, Cameron Highlands Malaysia, Sukoharjo, Indonesia, October 2018.

[16] K. S. Ganesh, A. Sridhar, and S. Vishali, "Utilization of fruit and vegetable waste to produce value-added products: conventional utilization and emerging opportunities-a review," *Chemosphere*, vol. 287, no. 3, Article ID 132221, 2021.

[17] D. Donno, M. G. Mellano, I. Riondato et al., "Traditional and unconventional dried fruit snacks as a source of health-promoting compounds," *Antioxidants*, vol. 8, no. 9, p. 396, 2019.

[18] R. R. Mphahlele, O. A. Fawole, N. P. Makunga, and U. L. Opara, "Effect of drying on the bioactive compounds, antioxidant, antibacterial and antityrosinase activities of pomegranate peel," *BMC Complementary and Alternative Medicine*, vol. 16, no. 1, p. 143, 2016.

[19] U. A. Fischer, R. Carle, and D. R. Kammerer, "Identification and quantification of phenolic compounds from pomegranate (Punica granatum L.) peel, mesocarp, aril and differently produced juices by HPLC-DAD-ESI/MSn," *Food Chemistry*, vol. 127, no. 2, pp. 807–821, 2011.

[20] M. Zahin, F. Aqil, and I. Ahmad, "Broad spectrum antimutagenic activity of antioxidant active fraction of Punica granatum L. peel extracts," *Mutation Research: Genetic Toxicology and Environmental Mutagenesis*, vol. 703, no. 2, pp. 99–107, 2010.

[21] A. Al-Rawahi, G. Edwards, M. Al-Sibani, G. Al-Thani, A. S. Al-Harrasi, and M. S. Rahman, "Phenolic constituents of pomegranate peels (Punica granatum L.) cultivated in Oman," *European Journal of Medicinal Plants*, vol. 4, no. 3, pp. 315–331, 2014.

[22] A. S. Al-Rawahi, M. S. Rahman, N. Guizani, and M. M. Essa, "Chemical composition, water sorption isotherm, and phenolic contents in fresh and dried pomegranate peels," *Drying Technology*, vol. 31, no. 3, pp. 257–263, 2013.

[23] X. Wang, E. Kristo, and G. LaPointe, "Adding apple pomace as a functional ingredient in stirred-type yogurt and yogurt drinks," *Food Hydrocolloids*, vol. 100, Article ID 105453, 2020.

[24] A. Vega-Gálvez, K. Di Scala, K. Rodríguez et al., "Effect of air-drying temperature on physico-chemical properties, antioxidant capacity, colour and total phenolic content of red pepper (Capsicum annuum, L. var. Hungarian)," *Food Chemistry*, vol. 117, no. 4, pp. 647–653, 2009.

[25] A. Wojdylo, J. Oszmianski, and R. Czemerys, "Antioxidant activity and phenolic compounds in 32 selected herbs," *Food Chemistry*, vol. 105, no. 3, pp. 940–949, 2007.

[26] R. M. S. C. Morais, A. M. M. B. Morais, I. Dammak et al., "Functional dehydrated foods for health preservation," *Journal of Food Quality*, vol. 2018, Article ID 1739636, 29 pages, 2018.

[27] M. Jovanovic, M. Petrovic, J. Miocinovic et al., "Bioactivity and sensory properties of probiotic yogurt fortified with apple pomace flour," *Foods*, vol. 9, no. 6, p. 763, 2020.

[28] R. C. Chandan and K. R. O'Rell, "Manufacture of various types of yogurt," *Manufacturing Yogurt and Fermented Milks*, Wiley, Hoboken, NJ, USA, pp. 211–236, 2006.

[29] M. M. El-Said, H. F. Haggag, H. M. Fakhr El-Din, A. S. Gad, and A. M. Farahat, "Antioxidant activities and physical properties of stirred yoghurt fortified with pomegranate peel extracts," *Annals of Agricultural Science*, vol. 59, no. 2, pp. 207–212, 2014.

[30] D. N. Yadav, K. K. Singh, S. N. Bhowmik, and R. T. Patil, "Development of peanut milk-based fermented curd," *International Journal of Food Science and Technology*, vol. 45, no. 12, pp. 2650–2658, 2020.

[31] A. Ali, H. Wu, E. N. Ponnampalam, J. J. Cottrell, F. R. Dunshea, and H. A. R. Suleria, "Comprehensive profiling of most widely used spices for their phenolic compounds through LC-ESI-QTOF-MS2 and their antioxidant potential," *Antioxidants*, vol. 10, no. 5, p. 721, 2021.

WILEY | Hindawi

Research Article

Effect of Microwave Heat Processing on Nutritional Indices, Antinutrients, and Sensory Attributes of Potato Powder-Supplemented Flatbread

Muhammad Waseem [1], **Saeed Akhtar,**[1] **Nazir Ahmad** [3], **Tariq Ismail** [1,2]
Claudia E. Lazarte,[2] **Majid Hussain,**[1] **and Muhammad Faisal Manzoor** [4,5]

[1]*Institute of Food Science & Nutrition, Bahauddin Zakariya University, Multan, Pakistan*
[2]*Department of Food Technology, Engineering and Nutrition, Lund University, Lund, Sweden*
[3]*Department of Nutritional Sciences, Faculty of Medical Sciences, Government College University, Faisalabad, Pakistan*
[4]*School of Food Science and Engineering, South China University of Technology, Guangzhou, China*
[5]*School of Food and Biological Engineering, Jiangsu University, Zhenjiang, China*

Correspondence should be addressed to Nazir Ahmad; drnazirahmad@gcuf.edu.pk, Tariq Ismail;
ammarbintariq@yahoo.com, and Muhammad Faisal Manzoor; 201712800025@mail.scut.edu.cn

This study aims at evaluating nutritional, toxicological, and sensory attributes of microwave heat-treated potato powder-supplemented unleavened flatbread. Straight-grade wheat flour (SGF) was substituted with potato powder at the rate of 2.5–10% d.w. A comparison was made for nutritional, antinutrient, and organoleptic attributes of microwave heat-treated potato powder and SGF—potato powder composite flour-based flatbreads. The results suggest processed potato powder supplementation in SGF to significantly ($p < 0.05$) improve ash (0.48 to 0.63 g/100 g), dietary fiber (2.15 to 2.61 g/100 g), and protein (8.33 to 9.91 g/100 g) contents of composite chapatis. Likewise, significant ($p < 0.05$) improvement in the concentration of microelements and trace elements was observed including Ca, Na, K, Fe, and Zn contents, which were increased from 29.7 to 33.5 mg/100 g, 2.8 to 6.3 mg/100 g, 376 to 466 mg/100 g, 3.1 to 3.4 mg/100 g, and 3.17 to 3.25 mg/100 g, respectively. Microwave heating of potato powder was observed to reduce the load of alkaloids, oxalates, tannins, and phytates of the raw potato powder at the rate of 76%, 80%, 84%, and 82%, respectively, thus anticipating a promising response to minimize toxicant load in supplemented flatbread. Supplementing potato powder in SGF elucidated significant ($p < 0.05$) improvement in color values, i.e., a^* (1.89–2.32) and b^* (10.95–13.22), and increased product hardness from 3.17 to 7.9 N. The study concludes that microwave heat-treated potato powder yield improved nutritional and safety concerns of the consumers when used alone or as a supplement for developing composite flours based on value-added products.

1. Introduction

Potato (*Solanum tuberosum* L.), a staple tuber crop of the Solanaceae family, is considered the fourth most vital staple food crop afterward wheat, rice, and corn. With a worldwide 17.3 MH area of crop cultivation, global production of potato was recorded as more than 370 million metric tons in 2019 with the People's Republic of China, India, Russia, and Ukraine as the leading potato-producing countries [1].

Historical data on potato and potato products suggest their application as a fresh crop for table consumption. Contrary to their conventional uses, recent global potato consumption trends are suggesting a shift from their fresh uses to value-added products like frozen potato, dehydrated potato flacks, and potato powder. Long-standing applications of the value-added potato products have been reported in snack foods, bakery, meat, culinary spices and seasoning, dairy industry, pharmaceuticals, textile, thermoplastic starch foams, and

animal feed industry [2, 3]. Dehydrated potatoes are considered a value-added ingredient for developing products including extruded snacks, soups, muffins, cakes, steamed noodles, steamed bread, and biscuits [4–6]. Earlier literature on potatoes indicates health-promising features owing to various health-promoting bioactive compounds such as phenolics, i.e., flavones, isoflavones and flavonoids, and antioxidants that play their significant role in the prevention of numerous health calamities including different cancers, peptic ulcer, inflammation, acidity, cardiovascular maladies, and atherosclerosis [7, 8].

Potatoes are featured with substantial amounts of protein, inorganic mineral substances, vitamins, dietary fibers, bioactive phenolic compounds, carotenoids, and anthocyanins, which play their pivotal role in promoting health. Potato proteins are preferred over cereal proteins for their food applications due to the presence of balanced amino acid composition [9]. The existing pool of information on intrinsic toxins in potatoes reports the presence of numerous antinutrients such as oxalates, tannins, phytates, phytic acid, glycoalkaloids (solanine and chaconine), cyanide, and saponins [10, 11]. Several preliminary processing techniques such as soaking, microwaving, blanching, germination, fermentation, autoclaving, and steaming have been suggested to reduce antinutrients and improve nutrient bioavailability in tuber crops [12, 13].

Among bakery products, chapatti–the unleavened flatbread, and its variants have a strong position as a staple food in different cultures of Southeast Asia. On account of their wide acceptability as a cultural food, wheat flour and chapatti are used as potential carriers for food fortificants and other replacers bearing improved functional and health-promoting properties [14]. Low-carbon footprint and relatively lesser requirements of water for cultivation make potato a better choice to be considered as a staple food crop in emerging challenges of the future, i.e., climate change and food insecurity [15]. An intelligent shift from conventional staple cereals to nonconventional edible resources may reduce the emerging risks of food insecurity and malnutrition in resource-restrained countries. Alternate starch sources like potato powder, partial to substantial replacement of wheat, in staple foods are necessitated to reduce the burden on conventional staples and to promote dietary diversification. This study was, therefore, planned to reduce the antinutrient load of potato powder by microwave heat processing and to explore functional, nutritional, and sensory acceptability of unleavened flatbread developed from wheat–potato powder composite flours. This study also highlights the differences in key attributes of the product developed with raw and microwave heat-treated potato powder supplementation.

2. Materials and Methods

2.1. Procurement of Raw Materials, Chemicals, and Reagents. Fresh potatoes and straight-grade wheat (*Triticum aestivum*) flour were procured from the vegetables and grain market of Multan, Pakistan. Samples were stored at ambient room temperature till further appraisal. Analytical grade chemicals and reagents were purchased from Sigma Chemical Co., Ltd. (St. Louis, MO). Standard solutions used for the preparation of stock solutions for estimation of macroinorganic and microinorganic substances were procured from BDH Chemicals Ltd. (Shanghai, China).

2.2. Raw and Processed Potato Powder Preparation. Potatoes were inspected for physical and insect damages, diseases, and blemishes. Healthy potato tubers were washed and manually peeled. A known amount of peeled potatoes was mechanically sliced (Pamico Technologies, Pakistan) and microwave processed at 1.1 kW for 2 minutes. Microwaved processed potatoes were cabinet dried at $50 \pm 2°C$ for 10–12 hours to the final moisture contents in a range between 8 and 15%. Dehydrated potatoes were converted into fine potato powder (mesh size~70–80 mm) using a commercial attrition mill (Pamico Technologies, Pakistan). Raw and processed potato powder samples were stored at ambient room temperature in airtight polyethylene bags for further appraisal [16, 17].

2.3. Nutritional Composition and Mineral Quantification. Proximate nutrient composition, i.e., moisture (protocol no. 925.10), crude ash (protocol no. 923.03), fat (protocol no. 920.85), fiber (protocol no. 32–10), and protein (protocol no. 920.87) and mineral contents of the raw and processed potato powder, and potato powder-supplemented chapatis were estimated by the standard protocols as laid down in Official Methods of Analysis [18]. Carbohydrate contents and energy were derived using equation (1), respectively.

$$\text{Carbohydrates}\,(\%) = [100 - (\text{moisture} + \text{ash} + \text{fat} + \text{protein} + \text{fiber})],$$
$$\text{energy}\,(\text{kcal/g}) = 9.00\,(\%\text{fat}) + 4.00\,(\%\text{carbohydrates} + \%\text{protein}). \tag{1}$$

2.4. Product Development

2.4.1. Raw and Processed Potato Powder-Supplemented Chapati Premix Preparation. Composite premixes of SGF and potato powder were developed by replacing SGF with raw and processed potato powder at the rate of 2.5–10%. Premix formulations were stored in airtight plastic containers at $25 \pm 2°C$ for further applications.

2.4.2. Development of Composite Flour Unleavened Flatbread. SGF and composite flour-based unleavened

flatbreads were made by the method followed by Waseem et al. [19] with slight modification. Briefly, SGF and the premixes were mixed with potable water to make 50 g dough. Dough developed was allowed a rest period of 30 minutes and rolled into thin sheets to a diameter of 12 cm and a thickness of 2 mm. Evenly rolled unleavened flatbread dough was baked from both sides onto the iron plate at $210 \pm 5°C$. Baked chapatis were cooled and analyzed for various sensory and biochemical parameters.

2.5. Antinutrient Determination.

Alkaloid contents in raw and processed potato powder and supplemented unleavened flatbread were determined using the method followed by Onwuka [20], wherein 5.0 g of each sample was poured in 50 mL, 10% acetic acid solution in ethanol and filtered using Whatman filter paper No. 41. Filtrates were titrated against conc. ammonium hydroxide and then with 1% solution of ammonium hydroxide. Alkaloid precipitates were oven-dried at 55°C for 30 minutes and were calculated using differences in initial and final weights. Amin et al. [21] method was adopted to determine the oxalate contents. One gram sample in 190 mL distilled water was acid digested in 10 mL (6 M, HCl) and centrifuged (2,000 rpm, 10 minutes). Subsequently, 50 mL of the supernatant was concentrated to 25 mL and filtered. The precipitates were washed with concentrated ammonia solution and $CaCl_2$ (10 mL, 5%) to obtain oxalate precipitates, which were titration against 0.05 M $KMnO_4$ to a pink-colored endpoint. Oxalates were calculated by multiplying the titer value by 0.1125. Tannins were assessed by Amin et al. [21]. About 0.5 g sample was boiled in 7.5 mL distilled water and centrifuged at 2,000 rpm for 20 minutes. Afterward, 1 mL of centrifuged supernatant was mixed with 5 mL Folin-Denis reagent and 10 mL (7.5%) sodium carbonate solution to adjust the final volume to 10 mL using distilled water. Spectrophotometric absorptions for tannic acid determination were measured at 700 nm against the tannic acid standard curve (10–100 mg/1000 g). However, spectrophotometric absorptions for phytate measurements were measured following the protocols as laid down by Haug and Lantzsch [22]. About 1 g of cabbage powder was extracted with 0.2 N, 10 mL HCl for phytates. Thereafter, o.5 mL extract was boiled in 1 mL ferric solution (i.e., 0.2 g $NH_4Fe(SO_4)_2$ in 2 N HCl to a volume 1 L). Afterward, centrifugation (Hermle, Z236K) was performed for 30 min at 3,000 rpm. Now, 1 mL extract was mixed with 1.5 mL 2-2′ -bipyridine solution (i.e., 25 mL of 0.25 g thioglycolic acid and 0.25 g 2-2′ -bipyridine). Spectrophotometric absorbance (UV-Vis 3000, ORI, Germany) of phytic acid standards, reagent blank, and samples was recorded at 519 nm, and contents of phytates were measured.

2.6. Color and Textural Properties.

Color variables including L^*, a^*, and b^* values, the textural attributes of raw and processed potato powder, and supplemented baked goods were determined using Hunter Color Lab (Hunter Associates Laboratory Inc., Reston, VA, USA) and texture analyzer (TA, Stable Microsystems, TAXT-2i Texture Analyser,

Godalming, Surrey, UK) by the methods as outlined by Liu et al. [23] and Kiumarsi et al. [24], respectively.

2.7. Puffed Height.

Puffing heights of the SGF and raw and processed potato powder-based composite unleavened flatbreads were determined by the method suggested by Rao et al. [25], wherein the cooked flatbreads were shifted to an adjacent heater for puffing for 10–15 seconds. Afterward, the puffing heights of flatbreads were measured using a sterilized stainless steel scale (cm).

2.8. Sensory Evaluation.

Sensory assessment of SGF, and raw and processed potato powder composite flour-based unleavened flatbread was evaluated for color, taste, folding ability, appearance, texture, and overall acceptability. Based on product discriminative ability, a panel of 20 trained graduate students from the Institute of Food Science and Nutrition, Bahauddin Zakariya University, was taken on board to perform preference mapping of the baked products on a 9-point hedonic scale, i.e., 9 = like extremely; 8 = like very much; 7 = like moderately; 6 = like slightly; 5 = no liking no disliking; 4 = dislike slightly; 3 = dislike moderately; 2 = dislike very much; and 1 = dislike extremely [24]. The panelists were prebriefed about the objectives of the study and instructed about the evaluation of the finished product. The organoleptic evaluation was performed in a well-lit sensory study room free from odors and sounds, which may interfere with the results of panelists.

2.9. Statistical Analysis.

Two replicates of each analysis were performed, and the values were stated as mean ± standard deviation. Statistical data on nutritional and textural quality parameters of SGF, raw and processed potato powder composite flours, and the unleavened flatbreads derived thereof were statistically analyzed using analysis of variance technique on Statistix 8.1 (Tallahassee, FL). The least significant difference (LSD) was used to assess the significance level among the means at a $p < 0.05$ confidence interval.

3. Results and Discussion

3.1. Nutritional Composition of SGF, Raw and Processed Potato Powder, and Supplemented Chapatis.

The nutritional composition of SGF, raw and processed potato powder, and potato powder-supplemented chapatis is presented in Table 1. The data suggest nonsignificant differences in fat, fiber, protein, and NFE contents of the raw and processed potato powders, while a significant ($p < 0.05$) moisture and ash contents of the microwave-treated dehydrated potato were relatively lower than the raw potato flour. Concerning the SGF carrying 0.4 g/100 g ash and 2.6 g/100 g crude fiber, potato powders, either raw or processed, were carrying higher concentrations of inorganic matters and crude fibers, i.e., 2.44–2.54 g/100 g and 5.76–6.26 g/100 g, respectively. Likewise, fat (0.8–0.9 g/100 g) and NFE contents (70.7–72.1 g/100 g) of the potato powder were significantly lesser than those observed in SGF, i.e., 1.32 g/100 g and

TABLE 1: Nutritional composition of straight-grade wheat flour (SGF), raw and processed (microwave heat treated) potato powder, and supplemented chapatis (g/100 g).

Treatments	Moisture	Ash	Fat	Fiber	Protein	NFE[†]
SGF	10.92 ± 0.05^a	0.41 ± 0.03^c	1.32 ± 0.03^a	2.60 ± 0.05^b	8.89 ± 0.09^a	75.87 ± 0.14^a
Raw PP	9.39 ± 0.09^b	2.54 ± 0.01^a	0.90 ± 0.03^b	6.26 ± 0.07^a	10.23 ± 0.67^a	70.69 ± 0.74^b
Processed PP	8.85 ± 0.07^c	2.44 ± 0.05^b	0.81 ± 0.02^b	5.76 ± 0.07^a	10.00 ± 0.57^{ab}	72.14 ± 0.54^b
T_0	35.65 ± 0.07^a	0.48 ± 0.01^c	1.85 ± 0.02^a	2.15 ± 0.02^c	8.33 ± 0.01^d	51.52 ± 0.07^b
T_1	34.21 ± 0.16^b	0.49 ± 0.01^c	1.65 ± 0.01^b	2.24 ± 0.06^c	9.13 ± 0.19^c	52.27 ± 0.42^b
T_2	31.06 ± 0.08^c	0.51 ± 0.01^c	1.59 ± 0.01^c	2.36 ± 0.09^{bc}	9.43 ± 0.12^{bc}	55.04 ± 0.33^a
T_3	30.25 ± 0.07^d	0.55 ± 0.01^b	1.43 ± 0.04^d	2.51 ± 0.01^{ab}	9.63 ± 0.19^{ab}	55.62 ± 0.23^a
T_4	29.75 ± 0.07^e	0.63 ± 0.01^a	1.31 ± 0.01^e	2.61 ± 0.16^a	9.91 ± 0.16^a	55.79 ± 0.38^a

Values are means $\pm$ S.D. ($n = 2$). Values having identical lettering in each column are nonsignificant at $p > 0.05$. $T_0 = 100\%$ straight-grade wheat powder chapatis (control), $T_1 = 2.5\%$ processed potato powder (PP), $T_2 = 5\%$ processed PP, $T_3 = 7.5\%$ processed PP, and $T_4 = 10\%$ processed PP. [†]Nitrogen-free extract = 100−(moisture + ash + fat + fiber + protein).

75.9 g/100 g, respectively (Table 1). Product analysis yielded significantly ($p < 0.05$) lower moisture contents in potato powder-supplemented flatbread, i.e., 29.8 g/100 g than observed for 100% SGF-based control (35.7 g/100 g). Such a reduction that may be attributed to reduced water-binding ability of the potato powder resulted in higher NFE contents of the supplemented flatbread at 5–10% level of substitution. Potato powder supplementation also improved ash, crude fiber, and crude protein contents of the composite flour flatbread from 0.48 to 0.63 g/100 g, 2.2 to 2.6 g/100 g, and 8.3 to 9.9 g/100 g, respectively.

Improved inorganic residues in potatoes have also been reported to yield better ash contents of the baked goods developed with potato powder supplementation at a level <10% [23]. The referred study had also reported lower fat contents in the potato powder-supplemented steam bread that may be attributed to the proportionally lower lipid profile of the potato powder. Substituting conventional cereal produce like wheat flour with fat devoid and a balanced protein composition may improve consumer acceptability and reduce the likelihood of chronic ailments such as cardiovascular disease [4].

Potato powder as a promising carrier of dietary fibers can yield value-added baked goods with better fiber contents as has been observed in this study, wherein fiber contents of the 100% SGF-based flatbread increased from 2.15% to 2.6% at 10% substitution. Improved fiber contents of the steam bread supplemented with raw potato powder have also been reported by Liu et al. [23] suggesting relatively higher fiber contents in the supplemented bread when compared with our findings. Such a difference may be attributed to the difference in potato cultivar bearing relatively higher fiber contents when compared with our findings.

Potato powder is considered to hold balanced amino acid composition [26], which offers the product a significant place to replace cereal proteins. Dehydrated potatoes accentuate about 18 amino acids including all essential amino acids, i.e., valine, isoleucine, methionine, histamine, phenylalanine, and threonine, and semiessential amino acids, e.g., arginine and lysine [26]. Our study reported raw and processed potato powder to offer significantly ($p < 0.05$) comparable protein contents to those of the SGF suggesting wheat flour value addition with potato powder to anticipate comparable protein contents and improved protein quality.

Supplementing potato powder @10% of the recipe has also yielded ~19% improvement in protein contents of the composite flatbread suggesting partial replacement of SGF with potato powder to also anticipate better protein yield. Compositing cereals with grains and other nonconventional food ingredients holding relatively better nutrient composition has been termed to serve as a complementary approach in addressing various functional and nutritional shortcomings to foods. Earlier, the substitution of wheat flour with potato peel powder @ 5% has been reported to demonstrate better protein and fiber contents of the composite cake with good sensory attributes [27]. The study suggests potato peel powder as a health-oriented product with higher fiber and comparatively low-caloric contents. The essential amino acid composition of potato protein had been reported comparable to egg protein for some amino acids including lysine, tryptophan, and leucine, while a moderate amount of isoleucine, phenylalanine, threonine, valine, histidine, arginine, and methionine is the key differentials between the quality of potato and cereal protein [28]. Thus, potato powder supplementation or partially substituting wheat flour with potato powder may help in improving nutritional inadequacies in staple foods of communities that rely more on wheat as their principal food [4, 23, 29].

3.2. Mineral Profile of SGF, Raw and Processed Potato Powder, and Supplemented Chapatis. Potato powder embodies greater magnitudes of calcium (Ca), potassium (K), sodium (Na), magnesium (Mg), phosphorus (P), iron (Fe), and zinc (Zn), which might help in preventing various nutritional and health complications [11]. Our results present significantly higher amounts of Ca, Na, and K in raw and processed potato powder when compared with the SGF (Table 2). Ca concentration recorded in raw and processed potato powder insignificantly differed from each other, i.e., 61.5 mg/100 g, and 59 mg/100 g, respectively, while the significantly lower concentration of Ca was observed in SGF, i.e., 42.5 mg/100 g. Likewise, the amount of Na and K was also lower in SGF, i.e., 5.8 mg/100 g and 445 mg/100 g, respectively, than its counterpart raw and processed potato powder carrying significantly ($p < 0.05$) higher amounts of Na (47.3–50 mg/100 g) and K (973–987 mg/100 g). Raw and processed potato

powder was observed relatively low in essential micro-minerals including Fe (1.51–1.55 mg/100 g) and Zn (0.76–0.87 mg/100 g) (Table 2). Substituting SGF with processed potato powder significantly improved Ca contents of 100% SGF-based flatbread from 29.7 mg/100 g to 33.5 mg/100 g anticipating a 13% increment at 10% supplementation (Table 2). Mean values for Na contents of raw and processed potato powder varied between 47 and 50 mg/100 g, which were markedly higher than observed in SGF, i.e., 5.7 mg/100 g. Na contents of the flatbread were also progressively increased from 2.8 mg/100 g to 6.3 mg/100 g at 10% potato powder supplementation, while the rate of increment in K levels of flatbread at the same supplementation level was ~24%. The amount of Fe and Zn in potato powder-supplemented flatbreads were insignificantly different ($p \geq 0.05$) from SGF and SGF-based flatbreads that may be associated with lower contents of referred minerals in potato powder (Table 2).

Results suggest potato powder supplementation anticipates significant improvement in electrolyte contents of the supplemented flatbreads. Earlier, potato powder and the peel fraction of the tuber crop have been suggested as promising sources of Ca and K and trace minerals including Fe and Zn, and their dietary intake to support the prevention of micronutrient inadequacies [5, 30]. Supplementation of wheat flour with noncereal flour-like amaranth aimed at improving nutritional attributes of the baked chapatis was reported by Banerji et al. [31]. The study referred to significant ($p < 0.05$) increment in Ca, Na, K, Fe, and Zn in wheat–amaranth composite flatbreads from 68 to 139 (104% ↑), 493 to 503(2% ↑), 383 to 497(30% ↑), 4.3 to 7.5 (74% ↑), and 2.6 to 3.1 (19% ↑) mg/100 g, respectively, at 40% substitution level.

3.3. Reduction in Antinutrients in Processed Potato Powder and Supplemented Chapatis.

Dehydrated tubers like potatoes may be ranked among vegetables bearing a high load of intrinsic toxicants including oxalates, alkaloids, tannins, cyanogenic glycosides, and phytates, which might pose the risks of adverse health effects such as dizziness, depression, gastrointestinal ailments, kidney stones, vomiting, anemia, rickets, osteoporosis, osteomalacia, and intestinal inflammation [32–34]. Our work identified raw potato powder to hold higher amounts of intrinsic toxicants like alkaloids, oxalates, tannins, and phytates, while the microwave heat treatment of the powder was found to significantly reduce the load (Table 3). The rate of reduction in toxicants was in a range between 76 and 84%, while an individual decline in a load of alkaloids was 76% (60 mg/100 g to 14.5 mg/100 g), oxalates was 80% (31.2 mg/100 g to 6.2 mg/100 g), tannins was 84% (91.4 mg/100 g to 14.6 mg/100 g), and phytates was 82% (44.9 mg/100 g to 7.9 mg/100 g) (Table 3). A threshold level of phytic acid in food is suggested as lesser than 25 mg per 100 g of phytate-containing food [35]. Likewise, a reasonable goal to limit the dietary intake of oxalates by the patients with enteric hyperoxaluria is less than 100 mg daily [36]. Microwave treatment of the raw potato powder brought a significant decline in phytate and oxalate contents

of the processed potato powder making it safer for the consumers with suspected health complications like iron deficiency, anemia, and hyperoxaluria. Unlike potato powder, SGF in this study was not detected for the listed toxicants, and hence, there was a meager transfer of phytates, oxalates, tannins, and alkaloids from the processed potato powder to the baked flatbread. The results suggested a consistent increment in intrinsic toxicant load in composite flour-baked flatbread with an increasing level of potato powder supplementation (Table 3). Composite flour flatbreads were observed to hold alkaloids, oxalates, tannins, and phytates up to 3.1 mg/100 g, 0.7 mg/100 g, 1.6 mg/100 g, and 0.8 mg/100 g, respectively, at 10% supplementation of the microwave-treated potato powder. The lowest concentrations of the listed nutrient inhibitors were recorded in flatbreads developed with 2.5% potato powder supplementation. Earlier studies validate alkali treatment, soaking, boiling, fermentation, microwaving, and blanching to significantly alter antinutrient load in foods [21, 33]. A study by Rytel et al. [37] elucidated thermally processed potato chips, potato purees, and French fries to reduce total alkaloid load by 84, 83, and 97%, respectively, while Omayio et al. [38] and Donald [39] reported a significant ($p < 0.05$) decline in alkaloids of blanched, boiled, and microwaved potatoes from 39 to 94%. Likewise, shorter cooking duration as has been practiced for microwave heating and cooking under vacuum has also been reported to reduce the production of undesirable reaction products during potato cooking [40]. A majority of the antinutrients are reported to make complexes with food components including proteins and microelements. At an instant, relatively large proteins with hydrophobic properties form complexes with tannins [41, 42]. Alike, the phytic acid being a negatively charged structure generally binds with the charged food components, e.g., metal ions including Fe, Zn, Mn, Mg, and Ca [43]. Microwave heating instantaneously generates heat within the product by molecular motion and disrupts hydrogen bonding. Such treatment does not merely promote the migration of dissolved ions but also affects protein structures that may lead to the dissolution of antinutrient–nutrient bonds and improved bioavailability of the nutrients.

3.4. Hunter Color Lab, Instrumental Texture, and Puffing.

Color is a pivotal physical parameter that unswervingly impacts nutritional quality, edibility, and consumer preference. Potato powder embodies starch alongside natural pigments like carotenoids, beta-carotene, and anthocyanin, which enhances the attractive appeal of foods and explicates antioxidant properties [44]. The data presented in Table 4 suggest raw potato powder to exhibit significantly ($p < 0.05$) higher L^* and b^* values, i.e., 88.3 and 14.5 than recorded for processed potato powder and SGF. The study exhibited a significant ($p < 0.05$) increase in a^* values from 1.9 to 2.3 (21% ↑) and b^* values from 10.9 to 13.2 (21% ↑), while a gradual decline in L^* values from 83 to 72 (13% ↓) was noticed on maximum replacement of SGF with processed potato powder (Table 4). An increase in a^* and b^* values in processed potato powder-supplemented chapatis could be

TABLE 2: Mineral composition of straight-grade flour, raw and processed potato powder, and supplemented chapatis (mg/100 g).

Treatments	Ca	Na	K	Fe	Zn
SGF	42.50 ± 0.50^b	5.75 ± 0.25^c	445.00 ± 2.00^c	3.77 ± 0.04^a	3.94 ± 0.02^a
Raw PP	61.50 ± 0.71^a	49.59 ± 0.39^a	986.50 ± 0.71^a	1.55 ± 0.02^b	0.87 ± 0.01^b
Processed PP	59.00 ± 0.71^a	47.34 ± 1.27^b	973.30 ± 1.41^b	1.51 ± 0.14^b	0.76 ± 0.04^c
T_0	29.71 ± 0.22^{cd}	2.78 ± 0.01^d	375.80 ± 0.28^e	3.08 ± 0.01^a	3.17 ± 0.07^a
T_1	29.24 ± 0.34^d	3.11 ± 0.02^d	392.59 ± 2.25^d	3.10 ± 0.14^a	3.07 ± 0.03^a
T_2	30.47 ± 0.67^c	4.13 ± 0.19^c	417.18 ± 1.66^c	3.16 ± 0.26^a	3.08 ± 0.02^a
T_3	32.21 ± 0.30^b	5.20 ± 0.28^b	439.76 ± 3.91^b	3.30 ± 0.38^a	3.14 ± 0.08^a
T_4	33.45 ± 0.64^a	6.26 ± 0.38^a	465.85 ± 1.20^a	3.41 ± 0.49^a	3.25 ± 0.21^a

Values are means ± S.D. ($n = 2$). Values having identical lettering in each column are nonsignificant at $p > 0.05$. $T_0 = 100\%$ straight-grade wheat flour chapatis (control), $T_1 = 2.5\%$ processed potato powder (PP), $T_2 = 5\%$ processed PP, $T_3 = 7.5\%$ processed PP, and $T_4 = 10\%$ processed PP.

TABLE 3: Antinutrient contents of straight-grade flour, raw and processed potato powder, and supplemented chapatis (mg/100 g).

Treatments	Alkaloids	Oxalates	Tannins	Phytates
SGF	ND**	ND**	ND**	ND**
Raw PP	59.98 ± 0.03^a	31.22 ± 0.40^a	91.39 ± 1.75^a	44.92 ± 0.80^a
Processed PP	14.49 ± 0.01^b	6.19 ± 0.80^b	14.59 ± 1.41^b	7.89 ± 0.54^b
Reduction)	(76)	(80)	(84)	(82)
T_0	ND**	ND**	ND**	ND**
T_1	0.77 ± 0.04^d	0.18 ± 0.02^d	0.38 ± 0.03^d	0.22 ± 0.04^d
T_2	1.55 ± 0.07^c	0.34 ± 0.01^c	0.76 ± 0.05^c	0.42 ± 0.05^c
T_3	2.37 ± 0.18^b	0.45 ± 0.08^b	1.19 ± 0.15^b	0.64 ± 0.08^b
T_4	3.11 ± 0.16^a	0.66 ± 0.02^a	1.55 ± 0.14^a	0.81 ± 0.03^a

Values are means ± S.D. ($n = 2$). Values having identical lettering in each column are nonsignificant at $p > 0.05$. $T_0 = 100\%$ straight-grade wheat flour chapatis (control), $T_1 = 2.5\%$ processed potato powder (PP), $T_2 = 5\%$ processed PP, $T_3 = 7.5\%$ processed PP, and $T_4 = 10\%$ processed PP. **Not detected.

TABLE 4: Instrumental texture, Hunter Color Lab and puffing of straight grade flour, raw and processed potato powder, and supplemented chapatis.

Treatments	Hunter Color Lab					Instrumental texture			Puffing height (cm)
	L^*	a^*	b^*	Hue	Chroma	Hardness (N)	Springiness (mm)	Gumminess (N, mm)	
SGF	80.93 ± 0.28^c	2.18 ± 0.05^a	11.85 ± 0.07^b	79.56 ± 0.42^b	12.05 ± 0.08^b	—	—	—	—
Raw PP	88.33 ± 0.47^a	0.44 ± 0.02^b	14.45 ± 0.64^a	88.22 ± 0.16^a	14.46 ± 0.64^a	—	—	—	—
Processed PP	87.10 ± 0.14^b	0.31 ± 0.01^b	10.61 ± 0.54^b	88.32 ± 0.01^a	10.61 ± 0.54^b	—	—	—	—
T_0	82.82 ± 0.83^a	1.89 ± 0.01^c	10.95 ± 0.07^e	80.18 ± 0.03^e	11.11 ± 0.07^e	3.17 ± 0.25^e	1.27 ± 0.04^a	3.10 ± 0.14^a	6.35 ± 0.07^a
T_1	80.10 ± 0.14^b	1.73 ± 0.04^d	11.56 ± 0.02^d	80.66 ± 0.01^d	11.69 ± 0.01^d	4.85 ± 0.07^d	1.11 ± 0.01^b	2.32 ± 0.03^b	5.83 ± 0.10^b
T_2	77.15 ± 0.21^c	1.84 ± 0.03^c	12.11 ± 0.02^c	80.92 ± 0.04^c	12.25 ± 0.03^c	5.94 ± 0.06^c	1.00 ± 0.02^c	1.95 ± 0.05^c	4.60 ± 0.14^c
T_3	75.52 ± 0.03^d	2.05 ± 0.07^b	12.67 ± 0.04^b	81.27 ± 0.05^b	12.84 ± 0.05^b	6.95 ± 0.08^b	0.78 ± 0.03^d	1.70 ± 0.03^d	3.87 ± 0.13^d
T_4	72.06 ± 0.08^e	2.32 ± 0.06^a	13.22 ± 0.04^a	81.51 ± 0.05^a	13.43 ± 0.04^a	7.89 ± 0.13^a	0.53 ± 0.03^e	1.47 ± 0.07^e	2.68 ± 0.26^e

Values are means ± S.D. ($n = 2$). Values having identical lettering in each column are nonsignificant at $p > 0.05$. $T_0 = 100\%$ straight-grade wheat flour chapatis (control), $T_1 = 2.5\%$ processed potato powder (PP), $T_2 = 5\%$ processed PP, $T_3 = 7.5\%$ processed PP, and $T_4 = 10\%$ processed P.

linked with higher magnitudes of phenolics, anthocyanins, beta-carotene, reducing sugars, and to some extent from the products of Maillard reaction [6, 44]. A study by Banerji et al. [31] on flatbread prepared from wheat-amaranth composite flour (60 : 40) anticipates a significant increase in a^* values from 2.5 to 3.5 (40% ↑) and b^* values from 16.4 to 17.4 (6% ↑) while a decrease in L^* values from 64 to 62 (3% ↓).

Textural features of processed potato powder-substituted chapatis delineated a significant ($p < 0.05$) increase in hardness (3.2–7.9 N, 147% ↑) at 10% SGF substitution. Hardness is measured as an index of all-inclusive textural attributes. Springiness and gumminess of processed potato powder-supplemented chapatis were also significantly ($p < 0.05$) declined from 1.3 to 0.5 mm (58% ↓) and 3.1 to 1.5 mm (53% ↓), respectively, at 10% SGF substitution levels (Table 4). Earlier, studies by Liu et al. [23] and Ben Jeddou et al. [27] reported a linear increase in hardness of potato peel powder-based cakes from 0.37 to 0.74 mm (100% ↑) and a significant reduction in springiness from 0.4 to 0.2 mm (50% ↓) at ~10% supplementation.

Puffing is an important quality parameter indicating the physical quality of the baked flatbread [45]. The results from
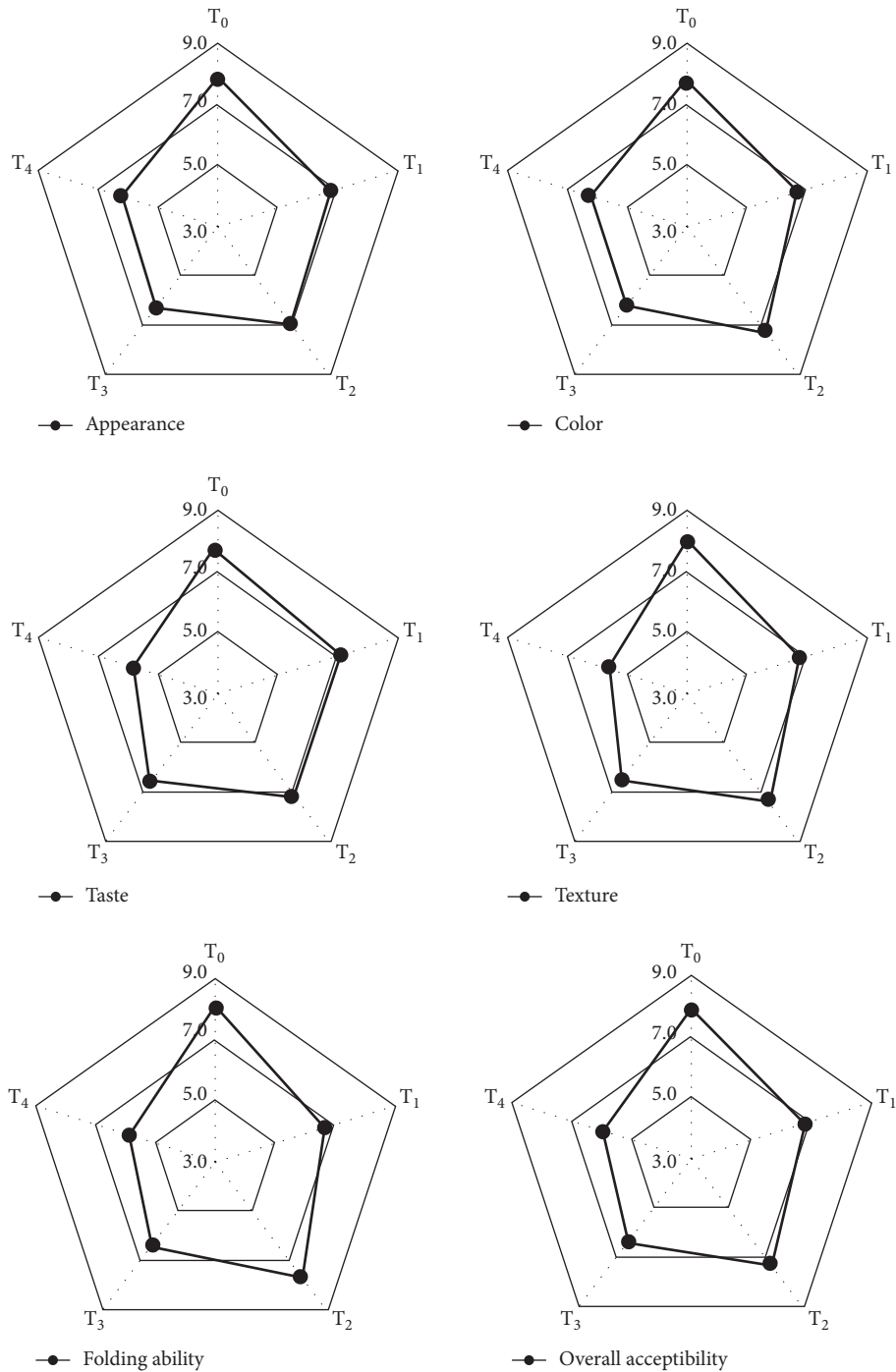
FIGURE 1: Sensory evaluation of straight-grade flour, raw and processed potato powder, and supplemented chapatis.

this study elaborated a significant ($p < 0.05$) decrease in puffed height of the processed potato powder-supplemented flatbread from 6.4 mm (100% SGF) to 2.7 cm at 10% potato powder supplementation (Table 4). Comparable findings for puffing were reported by Cheng and Bhat, [45] wherein supplementation of jering seed flour at substantially higher amounts in wheat flour resulted in a significant decline of the puffed height of flatbreads. Reduction in puffing traits of composite flours may be linked with the presence of higher magnitudes of fibers, nongluten proteins, stronger

intermolecular bonds, and low water-holding ability of nonwheat flours, which results in low steam formation and consequently reduced puffed height [45, 46].

3.5. Organoleptic Attribute Assessment of Processed Potato Powder-Supplemented Chapatis. Sensory attributes are incumbent parameters for evaluating the edibility of value-added foods. Data on the appearance of processed potato powder-supplemented flatbreads revealed a maximum

sensory score for control ~7.8 followed by the product prepared at 5% processed potato powder supplementation bearing an overall acceptability score of 6.9. Color being an imperative quality attribute that enhances the eye appeal and acceptability of finished goods was assigned the highest score of 7.7 and for the control followed by 5% potato powder-supplemented flatbreads that were assigned a 7.2 color score (Figure 1). Substituting wheat flour with potato powder ~10% was observed to drastically affect all sensory attributes of the baked flatbread potato powder supplementation. Contrarily, potato powder supplementation ~5% was found to anticipate better acceptability of the baked product for various sensory attributes. The color of the potato powder-supplemented product was ranked lower at a high degree when compared with the normal control that may be linked with color pigments of the potato powder and products of Maillard reaction generated during baking and microwave heating. Varying degrees of sensory acceptability of composite flour-based flatbreads have been reported earlier emphasizing sensory properties and the physical and biochemical composition of the supplementing ingredients to yield either acceptable or nonacceptable sensory scores. At an instant, a significant decline in the taste of processed potato powder-supplemented flatbread at ≥a 7.5% level of supplementation may be ascribed to the tannins that contribute astringency to the product with increasing concentration. A similar response was documented by Menon et al. [47] linking the hydrolyzable and nonhydrolyzable tannins to significantly alter the taste and color of the bread. Albeit the sensory score of SGF-processed potato powder-supplemented flatbreads was notably decreased with increasing potato powder supplementation levels, the edibility of the product remained acceptable at a 9-point hedonic scale. A higher texture acceptability score may be yielded at processed powder supplementation below 7.5%, and a similar proposal was made by Joshi et al. [6] suggesting better texture acceptability of the muffins carrying grilled potato powder at a level below 10%. Significant decline in texture score of the processed powder-supplemented flatbread may be ascribed to higher fiber contents of the product and reduced water-holding capacity of the potato powder. In line with the findings of Ben Jeddou et al. [27] on sensory acceptability of potato peel powder-supplemented cakes, a higher consumer acceptability score for SGF-processed potato powder composite flatbread may be achieved at 5% potato powder supplementation.

4. Conclusions

Microwave-treated potato powder supplementation in flatbread demarcated increased nutritional value of the baked good suggesting commercial applicability of potato powder as a natural ingredient for value-added product development. With a least to nonsignificant effect on the nutritional composition of potato powder, microwave heat treatment significantly reduced antinutrients in potato powder and the flatbreads. Furthermore, the processed potato powder addition in supplemented flatbreads below 7.5% was found to enhance its nutritional traits mildly to

moderately affecting sensory traits of the finished goods. It may be suggested that microwave heating at 1.1 kW for 2 minutes mitigates antinutrient load in potato powder and helps in improving dietary fiber and microelement concentrations in wheat-potato powder composite conventional baked goods of South Asia. Partial substitution of wheat flour with processed potato powder in developing traditional foods may further reduce the dietary burden on conventional cereals and promote food diversification.

Data Availability

The dataset supporting the conclusions of this article is included within the article.

Disclosure

Conflicts of Interest

The authors declare no conflicts of interest.

Acknowledgments

References

[1] M. Shahbandeh, *Potato Industry–Statistics and Facts*, Statista, Hamburg, Germany, 2021, https://www.statista.com/topics/2379/potato-industry/.

[2] L. Kaur and J. Singh, "Novel applications and non-food uses of potato: future perspectives in nanotechnology," in *Advances in Potato Chemistry and Technology*, pp. 425–445, Academic Press, Cambridge, MA, USA, 2009.

[3] K. Whitney and S. Simsek, "Potato flour as a functional ingredient in bread: evaluation of bread quality and starch characteristics," *International Journal of Food Science and Technology*, vol. 55, no. 12, pp. 3639–3649, 2020.

[4] M. Khaliduzzaman, M. Shams-Ud-Din, and M. N. Islam, "Studies on the preparation of chapatti and biscuit supplemented with potato flour," *Journal of the Bangladesh Agricultural University*, vol. 8, no. 1, pp. 153–160, 2010.

[5] H. Zhang, F. Xu, Y. Wu, H.-h. Hu, and X.-f. Dai, "Progress of potato staple food research and industry development in China," *Journal of Integrative Agriculture*, vol. 16, no. 12, pp. 2924–2932, 2017.

[6] A. Joshi, V. R. Sagar, S. Sharma, and B. Singh, "Potentiality of potato flour as humectants (anti-staling agent) in bakery product: muffin," *Potato Research*, vol. 61, no. 2, pp. 115–131, 2018.

[7] M. S. Hossain, F. Ahmed, A. T. M. Abdullah, M. A. Akbor, and M. A. Ahsan, "Public health risk assessment of heavy metal uptake by vegetables grown at a waste-water-irrigated

site in Dhaka, Bangladesh," *Journal of Health and Pollution*, vol. 5, no. 9, pp. 78–85, 2015.

[8] N. P. Silva-Beltrán, C. Chaidez-Quiroz, O. López-Cuevas et al., "Phenolic compounds of potato peel extracts: their antioxidant activity and protection against human enteric viruses," *Journal of Microbiology and Biotechnology*, vol. 27, no. 2, pp. 234–241, 2017.

[9] R. Ezekiel, N. Singh, S. Sharma, and A. Kaur, "Beneficial phytochemicals in potato–a review," *Food Research International*, vol. 50, no. 2, pp. 487–496, 2013.

[10] A. Popova and D. Mihaylova, "Antinutrients in plant-based foods: a review," *The Open Biotechnologuy Journal*, vol. 13, no. 1, pp. 68–76, 2019.

[11] O. A. Okhonlaye, K. A, and A. O. Helen, "Changes in proximate and antinutrient contents of Irish potato peels fermented with *penicillium chrysogenum* and *bacillus subtilis*," *South Asian Journal of Research in Microbiology*, vol. 6, no. 1, pp. 25–32, 2020.

[12] M. Hendek Ertop and M. Bektaş, "Enhancement of bio-available micronutrients and reduction of antinutrients in foods with some processes," *Food and Health*, vol. 4, no. 3, pp. 159–165, 2018.

[13] O. T. Adepoju, O. Boyejo, and P. O. Adeniji, "Effects of processing methods on nutrient and antinutrient composition of yellow yam (*Dioscorea cayenensis*) products," *Food Chemistry*, vol. 238, pp. 160–165, 2018.

[14] M. A. Khan, C. Mahesh, A. D. Semwal, and G. K. Sharma, "Effect of spinach powder on physico-chemical, rheological, nutritional and sensory characteristics of chapati premixes," *Journal of Food Science & Technology*, vol. 52, no. 4, pp. 2359–2365, 2015.

[15] B. Liu, W. Gu, A. Y. Yang et al., "Promoting potato as staple food can reduce the carbon–land–water impacts of crops in China," *Nature Food*, vol. 2, no. 1, pp. 570–577, 2021.

[16] S. Akhtar, M. Waseem, N. Ahmad et al., "Polyphenol-rich extracts of traditional culinary spices and herbs and their antibacterial activity in minced beef," *Journal of Food Quality*, vol. 2019, Article ID 1702086, 9 pages, 2019.

[17] T. V. Klug, E. Collado, A. Martínez-Sánchez et al., "Innovative quality improvement by continuous microwave processing of a Faba beans pesto sauce," *Food and Bioprocess Technology*, vol. 11, no. 1, pp. 561–571, 2018.

[18] LatimerJr., *Official Methods of Analysis (Moisture–Protocol No. 925.10, Crude Ash–Protocol No. 923.03, Fat–Protocol No. 920.85, Fiber - Protocol No. 32-10, and Protein–Protocol No. 920.87)*, Association of Official Analytical Chemists (AOAC), Gaithersburg, MD, USA, 19th edition, 2019.

[19] M. Waseem, S. Akhtar, M. F. Manzoor et al., "Nutritional characterization and food value addition properties of dehydrated spinach powder," *Food Sciences and Nutrition*, vol. 9, no. 2, pp. 1213–1221, 2021.

[20] G. I. Onwuka, "Soaking, boiling and antinutritional factors in pigeon peas (*Cajanus cajan*) and cowpeas (*Vigna unguiculata*)," *Journal of Food Processing and Preservation*, vol. 30, no. 1, pp. 616–630, 2006.

[21] K. Amin, S. Akhtar, and T. Ismail, "Nutritional and organoleptic evaluation of functional bread prepared from raw and processed defatted mango kernel flour," *Journal of Food Processing and Preservation*, vol. 42, no. 4, Article ID 13570, 2018.

[22] W. Haug and H.-J. Lantzsch, "Sensitive method for the rapid determination of phytate in cereals and cereal products," *Journal of the Science of Food and Agriculture*, vol. 34, no. 12, pp. 1423–1426, 1983.

[23] X. L. Liu, M. U. Tai-hu, S. Hong-nan, Z. Miao, and C. Jing-wang, "Influence of potato flour on dough rheological properties and quality of steamed bread," *Journal of Integrative Agriculture*, vol. 15, no. 1, pp. 2666–2676, 2016.

[24] M. Kiumarsi, M. Shahbazi, S. Yeganehzad, D. Majchrzak, O. Lieleg, and B. Winkeljann, "Relation between structural, mechanical and sensory properties of gluten-free bread as affected by modified dietary fibers," *Food Chemistry*, vol. 277, no. 1, pp. 664–673, 2019.

[25] R. P. Rao, K. Leelavathi, and R. Shurpalekar, "Test baking of chapati- development of a method," *Cereal Chemistry*, vol. 63, no. 4, pp. 297–303, 1986.

[26] V. Bártová, J. Bárta, A. Brabcová, Z. Zdráhal, and V. Horáčková, "Amino acid composition and nutritional value of four cultivated South American potato species," *Journal of Food Composition and Analysis*, vol. 40, no. 1, pp. 78–85, 2015.

[27] K. Ben Jeddou, F. Bouaziz, S. Zouari-Ellouzi et al., "Improvement of texture and sensory properties of cakes by addition of potato peel powder with high level of dietary fiber and protein," *Food Chemistry*, vol. 217, no. 1, pp. 668–677, 2017.

[28] A. C. Kapoor, S. L. Desborough, and P. H. Li, "Potato tuber proteins and their nutritional quality," *Potato Research*, vol. 18, no. 3, pp. 469–478, 1975.

[29] F. Yuksel and O. H. Campanella, "Textural, rheological and pasting properties of dough enriched with einkorn, cranberry bean and potato flours, using simplex lattice mixture design," *Quality Assurance and Safety of Crops & Foods*, vol. 10, no. 4, pp. 389–398, 2018.

[30] F. Zhu and J. He, "Physicochemical and functional properties of Maori potato flour," *Food Bioscience*, vol. 33, no. 1, Article ID 100488, 2020.

[31] A. Banerji, L. Ananthanarayan, and S. Lele, "Rheological and nutritional studies of amaranth enriched wheat chapatti (Indian flat bread)," *Journal of Food Processing and Preservation*, vol. 42, no. 1, Article ID 13361, 2018.

[32] G. A. Otunola and A. J. Afolayan, "Nutritional evaluation of *Kedrostis Africana* (L.) Cogn.: an edible wild plant of South Africa," *Asian Pacific Journal of Tropical Biomedicine*, vol. 7, no. 5, pp. 443–449, 2017.

[33] D. Lo, H. Wang, W. Wu, and R. Yang, "Anti-nutrient components and their concentrations in edible parts in vegetable families," *CAB Reviews*, vol. 13, no. 15, pp. 1–30, 2018.

[34] B. T. Olawoye and S. O. Gbadamosi, "Effects of different treatments on in vitro protein digestibility, anti-nutrients, antioxidant properties, and mineral composition of *Amaranth viridis* seed," *Cogent Food and Agriculture*, vol. 94, no. 1, pp. 1–14, 2017.

[35] S. Onomi, Y. Okazaki, and T. Katayama, "Effect of dietary level of phytic acid on hepatic and serum lipid status in rats fed a high-sucrose diet," *Bioscience, Biotechnology, and Biochemistry*, vol. 68, no. 6, pp. 1379–1381, 2004.

[36] A. Hesse, H. G. Tiselius, R. Siener, and B. Hoppe, *Urinary Stones: Diagnosis, Treatment, and Prevention of Recurrence*, Karger, Basel, Switzerland, 3rd edition, 2009.

[37] E. Rytel, A. Tajner-Czopek, A. Kita, A. Z. Kucharska, A. S. Ol-Łeztowska, and K. Hamouz, "Content of anthocyanins and glycoalkaloids in blue-fleshed potatoes and changes in the content of a-solanine and a-chaconine during manufacture of fried and dried products," *International Journal of Food Science and Technology*, vol. 53, no. 1, pp. 719–727, 2018.

[38] D. Omayio, G. Abong, and M. Okoth, "A review of occurrence of glycoalkaloids in potato and potato products," *Current Research in Nutrition and Food Science Journal*, vol. 4, no. 3, pp. 195–202, 2016.

[39] G. Donald, "Potatoes, tomatoes, and solanine toxicity (*Solanum tuberosum* L., and *Solanum lycopersicum* L.)," *Medical Toxicology of Natural Substances: Foods, Fungi, Medicinal Herbs, Toxic Plants, and Venomous Animal*, pp. 77–83, John Wiley & Sons, Inc., Hoboken, NJ, USA, 2008.

[40] S. S. Jayanty, K. Diganta, and B. Raven, "Effects of cooking methods on nutritional content in potato tubers," *American Journal of Potato Research*, vol. 96, no. 2, pp. 183–194, 2019.

[41] K. Raes, D. Knockaert, K. Struijs, and J. Van Camp, "Role of processing on bioaccessibility of minerals: influence of localization of minerals and anti-nutritional factors in the plant," *Trends in Food Science & Technology*, vol. 37, no. 1, pp. 32–41, 2014.

[42] M. Samtiya, R. E. Aluko, and T. Dhewa, "Plant food anti-nutritional factors and their reduction strategies: an overview," *Food Production, Processing and Nutrition*, vol. 2, no. 1, pp. 1–14, 2020.

[43] F. Grases, R. M. Prieto, and A. Costa-Bauza, "Dietary phytate and interactions with mineral nutrients," in *Clinical aspects of Natural and Added Phosphorus in Foods*, pp. 175–183, Springer, New York, NY, USA, 2017.

[44] J. Lachman, K. Hamouz, and M. Orsak, "Colored potatoes," in *Advances in Potato Chemistry and Technology*, J. Singh and L. Kaur, Eds., pp. 249–281, Academic Press, London, UK, 2nd edition, 2016.

[45] Y. F. Cheng and R. Bhat, "Physicochemical and sensory quality evaluation of chapati (Indian flat bread) produced by utilizing underutilized Jering (*Pithecellobium jiringa* Jack.) legume and wheat composite flour," *International Food Research Journal*, vol. 22, no. 6, pp. 2244–2252, 2015.

[46] K. R. Parimala and M. L. Sudha, "Wheat-based traditional flat breads of India," *Critical Reviews in Food Science and Nutrition*, vol. 55, no. 1, pp. 67–81, 2015.

[47] L. Menon, S. D. Majumdar, and U. Ravi, "Mango (*Mangifera indica* L.) kernel flour as a potential ingredient in the development of composite flour bread," *Indian Journal of Natural Products and Resources*, vol. 5, no. 1, pp. 75–82, 2014.

WILEY | Hindawi

Research Article

Intrusion Detection Using Machine Learning for Risk Mitigation in IoT-Enabled Smart Irrigation in Smart Farming

Abhishek Raghuvanshi ![ORCID],[1] **Umesh Kumar Singh** ![ORCID],[2] **Guna Sekhar Sajja** ![ORCID],[3] **Harikumar Pallathadka** ![ORCID],[4] **Evans Asenso** ![ORCID],[5] **Mustafa Kamal** ![ORCID],[6] **Abha Singh** ![ORCID],[6] **and Khongdet Phasinam** ![ORCID][7]

[1]*Mahakal Institute of Technology, Ujjain, India*
[2]*Institute of Computer Sciences, Vikram University, Ujjain, India*
[3]*University of the Cumberlands, Williamsburg, KY, USA*
[4]*Manipur International University, Imphal, Manipur, India*
[5]*Department of Agricultural Engineering, University of Ghana, Accra, Ghana*
[6]*Department of Basic Sciences, College of Science and Theoretical Studies, Saudi Electronic University, Dammam 32256, Saudi Arabia*
[7]*Pibulsongkram Rajabhat University, Phitsanulok, Thailand*

Correspondence should be addressed to Evans Asenso; easenso@ug.edu.gh

The majority of countries rely largely on agriculture for employment. Irrigation accounts for a sizable amount of water use. Crop irrigation is an important step in crop yield prediction. Field harvesting is very reliant on human supervision and experience. It is critical to safeguard the field's water supply. The shortage of fresh water is a major challenge for the world, and the situation will deteriorate further in the next years. As a result of the aforementioned challenges, smart irrigation and precision farming are the only viable solutions. Only with the emergence of the Internet of Things and machine learning have smart irrigation and precision agriculture become economically viable. Increased efficiency, expense optimization, energy maximization, forecasting, and general public convenience are all benefits of the Internet of Things (IoT). As systems and data processing become more diversified, security issues arise. Security and privacy concerns are impeding the growth of the Internet of Things. This article establishes a framework for detecting and classifying intrusions into IoT networks used in agriculture. Security and privacy are major concerns not only in agriculture-related IoT networks but in all applications of the Internet of Things as well. In this framework, the NSL KDD data set is used as an input data set. In the preprocessing of the NSL-KDD data set, first all symbolic features are converted to numeric features. Feature extraction is performed using principal component analysis. Then, machine learning algorithms such as support vector machine, linear regression, and random forest are used to classify preprocessed data set. Performance comparisons of machine learning algorithms are evaluated on the basis of accuracy, precision, and recall parameters.

1. Introduction

Agriculture is very important to the country's economic well-being because it provides food for everyone. One of the most important things that happened in the country is linked to it. If a country has a lot of farmers, it is thought to be both economically and socially wealthy. Agriculture is the main source of jobs in most countries. When there are a lot of people on a big farm, they often need help with planting and caring for the animals. These large farms can use nearby processing facilities to finish and improve their agricultural goods [1]. As human civilization has progressed, there have been big changes in agricultural output. These changes have made it possible to use less resources and carry out less work.

Despite this, demand and supply have never been able to meet due to the high population density. In 2050, the world's population is expected to grow to 9.8 billion people, a 25 percent increase over the current amount [1]. There is a strong likelihood that the majority of population growth will occur in developing countries [2].

Despite this, 70 percent of the world's population is anticipated to live in cities by 2050, up from 49 percent now [3]. In addition, as incomes rise, so will the need for food, particularly in developing countries. As a result, these countries will become more aware of the quality of their food and diet. As a result, consumers' tastes may move away from grains and cereals toward legumes and, eventually, meat.

In agriculture, water is a valuable yet finite natural resource [4–6]. In a country like India, a considerable amount of water is used for irrigation [7]. Many environmental conditions influence crop productivity, including air temperature, soil temperature, and humidity [8]. Crop irrigation is an important component in affecting crop output [8]. Farmers rely substantially on human supervision and experience for harvesting fields [9]. The water supply for the field must be preserved [10]. In today's globe, water scarcity is a big issue. It is already a problem for people all across the world [11, 12]. The scenario could get even worse in the coming years.

Smart farming is a term that refers to a well-known and better way to run a farm that has become more common in modern farming. Agricultural and information technologies are used to keep an eye on the health and production of crops. This includes keeping an eye on field crop conditions and other indicators [13, 14]. Finally, the goal of smart farming is to cut the cost of agricultural inputs while still keeping the quality of the end product the same. If you use a lot of pesticide or fertilizer at the same time, the whole field is treated as a single unit.

The principal sources of natural water resources are rainwater, subterranean water, and surface water. 96.5 percent of the world's water is found in the oceans. Only 0.001 percent of the remaining water on the globe can be found in clouds, mist, and precipitation, which is 1.7 percent of the world's total water supply. The majority of the world's surface water is found in the ocean, which is made up of salt water. Therefore, there is a shortage of fresh water in most of the countries around the world. The survival of all ecosystems depends on the availability of fresh water. According to the World Resources Institute (WRI), most of the countries are expected to face water scarcity in upcoming years [15]. There is a considerable impact on downstream ecosystems due to the vast majority of freshwater being used for agricultural and industrial uses. There is a need to utilize fresh water in such a way that the upcoming generations do not get affected by the scarcity of fresh water.

The soil contains a variety of soil types, including sandy, salty, and clayey soils. Each type of soil has its own advantages and disadvantages. A good example of this is sandy soil, which has a high capacity for drainage. Drainage, on the other hand, swiftly removes nutrients from the soil. The soil's properties are crucial to determining how much water a plant needs [16].

Agricultural jobs, in particular, can benefit greatly from data mining approaches. One of these operations is the use of association rule restrictions to regulate water use in agricultural areas. In addition, the Internet of Things has made smart farming possible by various data acquisition and storage techniques. Field values for optimal plant irrigation are collected by smart sensor networks in modern irrigation systems. Machine learning is used in a wide range of real-world applications such as smart farming, smart healthcare, smart logistics, and smart production. In the framework [17], data are acquired using soil and moisture sensors, and then they are stored on a centralized cloud server. On a cloud server, various analytics are performed using machine learning algorithms. This framework provides the exact water quantity required for a particular crop. This framework is shown in Figure 1.

An IoT-enabled global smart city concept is possible. There are many different types of intelligent communities, such as smart homes, smart farms, smart environments, smart fitness, and smart governance, for example. Additionally, the Internet of Things is employed in the oil and gas extraction, manufacturing, and refining industries. The Internet of Things (IoT) improves efficiency, optimizes costs, maximizes energy utilization, maintains forecasts, and provides a great deal of convenience for the general public. Security concerns are increasing as more and more systems and data processing become more diversified. Security and privacy concerns are the primary impediments to the growth of the Internet of Things.

Computer security is the act of securing computer systems from external threats in order to ensure the confidentiality, integrity, and availability of computing resources. When an intrusion occurs, the network resources and the victim server are put in danger [18]. System administrators can take action if intrusions are detected by the intrusion detection system (IDS) because it monitors and reports on intrusions. As the number of cyberattacks has risen, so has people's mistrust of the Internet. A denial of service (DoS) is a well-executed security attack (DoS).

It is possible to use IDS to detect attacks from the outside as well as from within a company's computer network. It looks like a burglar alarm, but an intrusion detection system is different. It is proposed in this article a framework for detecting and categorizing intrusions into Internet of Things networks that are utilized in agriculture. Security and privacy are important considerations not only in IoT networks linked to agriculture but also in all Internet of Things applications in general. As an input data set, the NSL KDD data set is used in this technique and is available online [19]. The NSL-KDD data collection is preprocessed by first translating all symbolic features to numeric features and then transforming all numeric features to symbolic features. In order to extract features, principal component analysis is utilized. After that, the preprocessed data set is categorized using machine learning methods such as support vector machine, linear regression, and random forest to determine its classification. When comparing the performance of machine learning algorithms, the accuracy, precision, and recall measurements are taken into consideration.
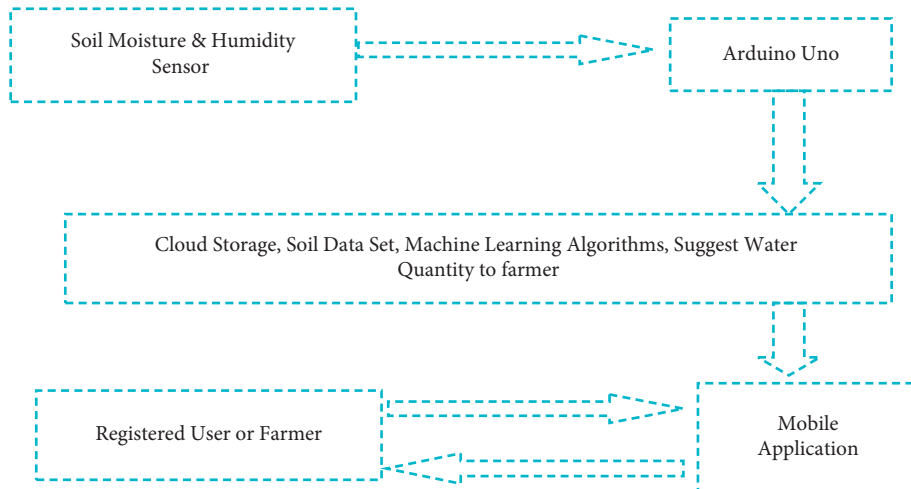
FIGURE 1: A framework for smart irrigation.

2. Literature Survey

2.1. Review of Existing Irrigation Systems. A wide range of industries, including the military and agriculture, rely on wireless sensor networks (WSNs). A lot of research is going on the power consumption of wireless sensor network. Metaheuristics and WSN life spans were also examined in their research. Using metaheuristic algorithms, they propose a transition, evaluation, and determination procedure that helps to find the optimal solution to the problem.

It is clear from their explanation that the metaheuristic method requires a thorough comprehension of the many field characteristics and domain expertise associated with the longevity problem. Metaheuristic algorithms have already been studied by a large number of academics. Even though these strategies increase the WSN's effectiveness, there are still a number of issues that need to be addressed. Contingency planning may lead to a reduction of sensors or cluster heads. Furthermore, metaheuristic approaches are meant for optimization and are not suitable to solve scalable problems.

According to Li et al. [20], the nodes should be as small as possible to enhance connection and coverage. The proposed method is compared to other existing methods to perform the similar task. The efficacy of the suggested strategy was proven in four unique instances using two well-known ways.

WSN nodes are used in mobile network topologies when a significant level of communication frequency is required. Hassan and colleagues explored the use of frequencies for industrial, scientific, and medical (ISM) objectives [21]. The premise of their reasoning is frequency reuse at sensor nodes along busy pathways. In order to spread the load across the macro cells, we employed the CR approach. In turn, this results in a reduced crash area and greater space for passengers in their suggested design. Using an underground sensor network, soil humidity and temperature may be monitored in real time. Thus, sensors and power adjustments for input setup and regular energy maintenance are appropriately installed and maintained [22].

Verma et al. [23] investigated the use of wireless sensors for irrigation scheduling. Using a sensor array and sensor network-based accuracy technologies, they are able to predict real-time watering demands in the soil and so save unnecessary watering. For irrigation systems to function more efficiently, data transmission demands improved energy savings. Multiple access time division (MATD) is claimed by Ushakov et al. [24] to be more efficient for data transfer in WSN irrigation systems (TDMA). Energy is saved by immediate transmission and the addition of data. TDMA also enhances the performance of the network.

Goumopoulos et al. [25] developed an ontological technique for a wireless sensor or actuator-based autonomous zone irrigation system. In precision agriculture, plants communicate with one other in order to preserve water. Detecting node problems in the network is the primary goal of this system, which employs many machine learning approaches. In the past, irrigation activities were made more automated and user-friendly by creating end-user apps.

Cotton crops can be irrigated more efficiently according to a system devised by Rakhra et al. [26]. Researchers have used a wide range of data sets to predict the exact amount of water decided for a particular combination of soil. The output of the analytical study is made available to the farmers or other users by a mobile application.

Lopez et al. [27] investigated the agricultural uses of wireless sensor networks. Time-dependent agriculture industry characteristics were discussed extensively in their debate. As a consequence, they compiled a list of sensors that may be used to monitor agricultural factors. In the end, they looked at a variety of communication networks and made comparisons.

According to [28, 29], field productivity can be improved by sending out notifications in the form of text messages or emails when certain variables have been measured over a threshold. Some sensors, such as those used to assess agricultural fields' statistical features, were thoroughly examined, as were the products they are linked to and the specifications attached to them. The model had sensors for

soil water content, soil moisture content, soil electrical conductivity, pH, temperature, and wind speed.

Dou et al. [30] designed an ecofriendly framework to implement the basic functions of smart agriculture including the optimization of farming resources, decision support, and land surveillance. Water and fertilizer consumption may be maximized while crop yields can be improved at the same time thanks to a new technique they have devised.

Deepika and Rajapirian [31] have created a wireless sensor network prototype for precision agriculture that makes use of a constrained power source. For their model, they employed sand soil with varying amounts of water in order to demonstrate the impacts of off-the-shelf technology.

According to Deepika and Rajapirian [32], a research study on the current status of precision agriculture's wireless sensor networks assessed some of the more cutting-edge possibilities. In order to monitor a plant, an FPGA-based control system is employed. Imam et al. [33] examined various issues and challenges related to wireless sensor networks and sensors for IoT-based agriculture in order to optimize farmer advantages. In precision agriculture, microcontroller families and sensor nodes were compared. Researchers also detailed the demands of relative humidity sensors and their interfaces.

2.2. Review of Existing Intrusion Detection Methods.
Computational intelligence is a new generation of information systems that are being built with the help of soft computing [34]. With a soft computing system, you can build intelligent machines that can solve complicated real-world issues that cannot be mathematically modeled because they are too hard to model. In order to attain a likeness to human decision-making, it uses tolerance for approximation, ambiguity, imprecision, and partial reality [35]. Soft computing methods for intrusion detection are summarized in this section. The research is broken into four sections: fuzzy logic, neural networks, evolutionary algorithms, and artificial immune systems. Intrusion detection has yet to benefit from the use of coupled map lattices.

Since its inception in Holland, the genetic algorithm (GA) has been shown to be a flexible and effective search engine. Evolution in the wild is simulated using computer technology. As a stochastic global search process, the GA is based on the survival of the fittest principle and creates ever-closer approximations to a solution.

New solutions are generated every generation by selecting people based on their performance in the issue area and spawning children. Individuals that are better suited to the problem area than their predecessors can be formed by using this method of recruiting new employees [36]. The fitness function provides an indication of how people did in the issue area.

As a result of the flocking and schooling behavior of birds and fish [37], they created PSO in 1995 [38]. Artificial life, psychology, physics, and computer science all played a role in the development of PSO in some capacity. A "population" of particles moves around the problem region

at specific rates in order to solve it. Particle velocities are adjusted via stochastic calibration based on their prior best position and their best nearby position.

Both the particle best and the neighborhood best are calculated using a user-defined fitness function. As each particle moves, it naturally results in a near-ideal solution or a near-optimum solution. "Swarm" is used to describe the movement of particles in the issue room, rather than a flock of birds or school of fish.

As an approximation logic known as fuzzy logic (FL), two-valued logic is expanded to include operations on fuzzy sets, such as equalization, enclosure, complementation, intersection, and union, in the context of fuzzy logic. Machine learning optimization and classification paradigms based on evolutionary processes like genetics and natural selection are used in evolutionary computing. In the field of evolutionary computing, concepts such as genetic algorithms, evolutionary programming, genetic programming, and evolution techniques are all included. Genetic algorithms are the most frequently used in applications [39].

The hidden naive Bayes classifier (HNB) is more adaptable than the classic naive Bayesian classifier. In the HNB model, the hidden parent of each attribute is specified by adding a new layer. The structural properties of HNB can be inferred using naive Bayes. Hidden parents are created for each trait so that the forces of its other characteristics can be brought together. The average of weighted one-dependence estimators [40] is used to describe hidden parents.

The support vector machine (SVM) is a classification method based on statistical learning theory (SLT). Hyperplane classifiers are another example of this. Using SVM, an ideal hyperplane maximizes the difference between two groups while minimizing any overlap.

There are several layers of latent variables (hidden units) in DBNs in machine learning, and the relations between the levels but not the units inside each layer are generative graph models or deep neural networks.

A model created by researchers in [42] can be used to select the features of an intrusion detection system. Using genetic algorithms and PSO, the data set has an accuracy percentage of 91.75%.

3. Methodology

Figure 2 presents a framework for intrusion detection and classification system for IoT network for agriculture fields. The main components of this framework are IDS data set, data preprocessing algorithm, machine learning algorithms, and prediction module.

In preprocessing of the NSL-KDD data set, firstly all symbolic features are converted to numeric features. The target class is also allocated unique numbers. Continuous numeric features such as duration (duration of connection) and SRC bytes (data bytes) present in the dataset are normalized using z-score normalization. Feature extraction is carried out using the principle component analysis (PCA) approach in this article. Data analysis and compression may benefit from PCA's linear approach to dimensionality reduction [30]. It is based on finding orthogonal linear
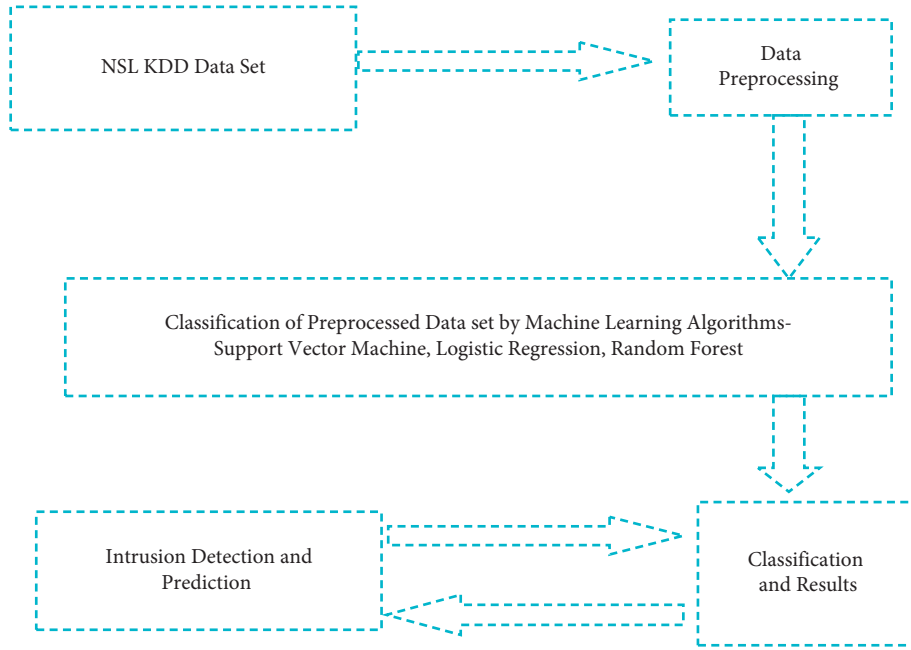
Figure 2: A framework for IDS for IoT networks for agriculture fields.

combinations of the original characteristics with the greatest variance in order to convert a large number of uncorrelated features.

3.1. Support Vector Machine Approach. When it comes to handling two-class categorization problems, a support vector machine (SVM) is the most common method. It is possible to perform classification and regression with SVM in addition to other uses. In addition, SVM uses the kernel phenomenon to alter the data before determining an appropriate boundary between the most likely outcomes. In addition, the decision line between the two classes on a graph must be wide enough to be discernible. SVM creates an ideal boundary that divides the new data point into the correct categories. For that reason, the hyperplane is often referred to as the ideal boundary.

3.2. Logistic Regression. Logistic regression is the technique used to link a dependent variable to one or more independent variables. In some contexts, the dependent variable and the independent variable are referred to as predictors and predictors, respectively. Temperature and humidity differential, soil moisture, and pH rate are variables independent of plant type prediction (c). The following formula has been established:

$$Y = B_0 + B_1X_1 + B_2X_2 + B_3X_3. \tag{1}$$

3.3. Random Forest. All of the predictors in a random forest are built from random variables with the same distribution across all the trees in the forest. The forest's generalization error decreases as time passes. In the woods, there is a record number of trees.

The generalization error of a tree classifier forest depends on the relative strength of the individual forest trees and their comparison. As compared to AdaBoost, using a random selection of features to split each node results in error rates that are more stable. Variance, frequency, and consistency of internal measurements are used to indicate the reaction to an increase in the number of attributes that are split. The parameter importance estimate is also based on external measurements. Regression is based on the same principles.

4. Results and Analysis

In fact, the NSLKDD dataset is used for anomaly detection. This enhanced version of the KDDCUP99 dataset has no redundancy, no duplication of records, and a lower complexity level than NSLKDD [43]. Twenty percent of the NSLKDD dataset is training data (25192 records), and the remaining eighty percent is testing data (100781 records). In this paper, we use only 20% of the training data to generate decision rules. In the experimental analysis, three classification algorithms, namely, SVM-support vector machine, logistic regression, and random forest classifiers, are used. To calculate accuracy the following formulae were used:

$$\text{accuracy} = \frac{(TP + TN)}{(TP + TN + FP + FN)},$$

$$\text{precision} = \frac{TP}{(TP + FP)}, \tag{2}$$

$$\text{recall} = \frac{TP}{(TP + FN)},$$

where TP represents true positive, TN represents true negative, FP represents false positive, and FN represents false negative.

TABLE 1: Accuracy of machine learning algorithms.

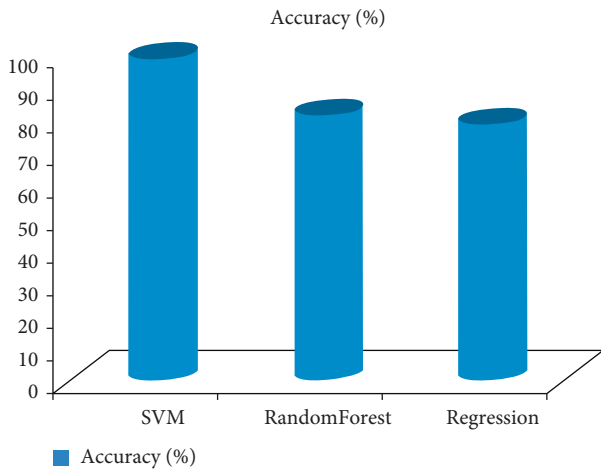| Accuracy results of machine learning algorithms	
Machine learning algorithms	Accuracy (%)
SVM	98
RF	85
Logistic regression	78

FIGURE 3: Accuracy of classifiers.
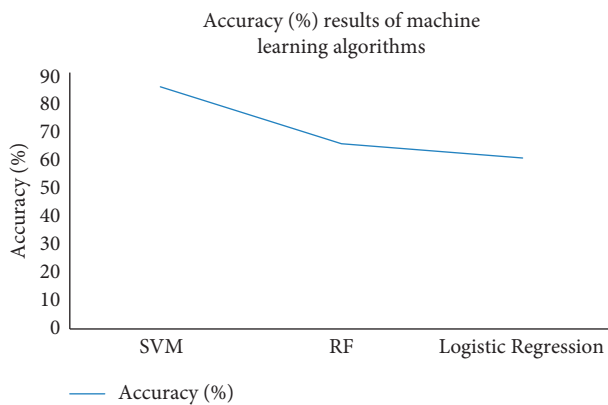
FIGURE 4: Graphical representation of the accuracy results of machine learning algorithms.

FIGURE 5: Precision of classifiers for intrusion classification for agriculture fields.
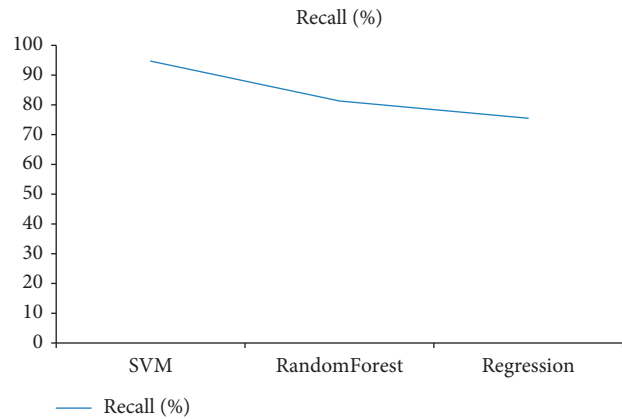
FIGURE 6: Recall of classifiers for intrusion classification for agriculture fields.

The results proved that the accuracy of the SVM classifier is better than that of the random forest and logic regression algorithms. It is shown in Table 1 and Figure 3. Also, Figure 4 shows a graphical representation of the accuracy results of machine learning algorithms.

Precision and recall parameters are also used to measure the performance of machine learning algorithms. Precision and recall of SVM, random forest, and logistic regression for intrusion detection of agriculture fields are shown below in Figures 5 and 6.

In this graph, SVM exceeds random forest and logistic regression in terms of machine learning algorithm accuracy. The accuracy of SVM is higher than 98%, but random forest and logistic regression accuracy is less than 78%.

5. Conclusion

Agriculture is crucial to the country's economic well-being since farmers produce food for everyone. It connects a varied spectrum of enterprises around the country. A country with a sizable agricultural sector is considered wealthy economically and socially. Agriculture is critical in the majority of countries as a source of employment. Irrigation accounts for a sizable portion of overall water use in a country like India. Among the several elements affecting crop productivity are the surrounding environment's temperature, soil temperature, and relative humidity. Agricultural irrigation is crucial in crop production since it has a direct effect on crop yield. Harvesting fields successfully is highly dependent on human supervision and experience. It is vital to safeguard the field's water supply at all costs. Water scarcity is a significant issue in contemporary civilization. The issue is global in scope, affecting individuals on a daily basis. As a result, we are concerned about the possibility of the situation deteriorating worse in the next few years. To address the issues highlighted above, smart irrigation and precision

farming are the answer. Smart irrigation and precision agriculture are only possible with the development of the Internet of things and machine learning. Numerous benefits accrue from the Internet of Things, including enhanced efficiency, cost optimization, optimal energy consumption, forecasting, and convenience for the general public (IoT). The diversity of data processing technologies and methodologies raises issues regarding their dependability and security. Concerns about security and privacy are impeding mainstream adoption of the Internet of Things. This article proposes a system for detecting and categorizing intrusions into IoT networks in agricultural regions. SVM has a precision of greater than 98 per cent; however, random forest and logistic regression have a precision of less than 78 percent.

Data Availability

The data supporting this research article are available from the corresponding author on reasonable request.

Conflicts of Interest

The authors declare that they have no conflicts of interest.

References

[1] M. Schnfeld, R. Heil, and L. Bittner, *Big Data on a FarmSmart Farming, Big Data in Context*, T. Hoeren and B. Kolany-Raiser, Eds., Springer, Berlin, Germany, 2018.

[2] R. Varghese and S. Sharma, "Affordable smart farming using IoT and machine learning," in *Proceedings of the IEEE Second International Conference on Intelligent Computing and Control Systems (ICICCS)*, pp. 645–650, Madurai, India, June 2018.

[3] R. Manne and S. C. Kantheti, "Application of artificial intelligence in healthcare: chances and challenges," *Current Journal of Applied Science and Technology*, vol. 40, no. 6, pp. 78–89, 2021.

[4] C. Kamienski, J.-P. Soininen, M. Taumberger et al., A. Torre Neto, "Smart water management platform: IoT-based precision irrigation for agriculture," *Sensors*, vol. 19, no. 2, Article ID 276, 2019.

[5] L. Wang, W. Wu, J. Xiao, Q. Huang, and Y. Hu, "Effects of different drip irrigation modes on water use efficiency of pear trees in northern China," *Agricultural Water Management*, vol. 245, Article ID 106660, 2020.

[6] K. S. Sahoo, D. Puthal, M. Tiwary et al., "Efficient switch migration-based load balancing for multi-controller SDN in IoT," *IEEE Internet of Things Journal*, vol. 7, no. 7, pp. 5852–5860, 2019.

[7] N. K. Nawandar and V. R. Satpute, "IoT based low cost and intelligent module for smart irrigation system," *Computers and Electronics in Agriculture*, vol. 162, no. 4, pp. 979–990, 2019.

[8] C. M. Bavougian and P. E. Read, "Mulch and groundcover effects on soil temperature and moisture, surface reflectance, grapevine water potential, and vineyard weed management," *PeerJ*, vol. 6, no. 1, Article ID e5082, 2018.

[9] D. Glaroudis and P. Chatzimisios, "Survey, comparison and research challenges of IoT application protocols for smart farming," *Computer Networks*, vol. 168, no. 4, Article ID 107037, 2020.

[10] D. Liu, Q. Jia, J. Li, P. Zhang, X. Ren, and Z. Jia, "Increased photosynthesis and grain yields in maize grown with less irrigation water combined with density adjustment in semi-arid regions," *PeerJ*, vol. 8, no. 1, Article ID e9959, 2020.

[11] P. Fremantle and P. Scott, "A survey of secure middleware for the Internet of Things," *PeerJ Computer Science*, vol. 3, no. 15, Article ID e114, 2017.

[12] J. M. Schleicher, M. Vögler, C. Inzinger, and S. Dustdar, "Modeling and management of usage-aware distributed datasets for global smart city application ecosystems," *PeerJ Computer Science*, vol. 3, no. 11, Article ID e115, 2017.

[13] W. Tao, L. Zhao, G. Wang, and R. Liang, "Review of the internet of things communication technologies in smart agriculture and challenges," *Computers and Electronics in Agriculture*, vol. 189, Article ID 106352, 2021.

[14] A. Rehman, T. Saba, M. Kashif, S. M. Fati, S. A. Bahaj, and H. Chaudhry, "A revisit of internet of things technologies for monitoring and control strategies in smart agriculture," *Agronomy*, vol. 12, Article ID 127, 2022.

[15] M. C. Dash and S. P. Dash, *Fundamental of Ecology*pp. 281–284, McGraw-Hill Publication, New York, NY, USA, 3rd edition, 2009.

[16] S. F. da Costa Bezerra, A. S. M. Filho, F. C. Delicato, and A. R. da Rocha, "Processing complex events in fog-based internet of things systems for smart agriculture," *Sensors*, vol. 21, no. 21, Article ID 7226, 2021.

[17] K. Phasinam, T. Kassanuk, P. P. Shinde et al., "Application of IoT and cloud computing in automation of agriculture irrigation," *Journal of Food Quality*, vol. 2022, Article ID 8285969, 8 pages, 2022.

[18] B. B. Zarpelão, R. S. Miani, C. T. Kawakani, and S. C. de Alvarenga, "A survey of intrusion detection in Internet of Things," *Journal of Network and Computer Applications*, vol. 84, pp. 25–37, 2017.

[19] C.-W. Tsai, T.-P. Hong, and G.-N. Shiu, "Metaheuristics for the lifetime of WSN: a review," *IEEE Sensors Journal*, vol. 16, no. 9, pp. 2812–2831, 2016.

[20] S. Li, J. Gao, Q. Zhu, L. Zeng, and J. Liu, "A dynamic root simulation model in response to soil moisture heterogeneity," *Mathematics and Computers in Simulation*, vol. 113, pp. 40–50, 2015.

[21] F. Hassan, A. Roy, and N. Saxena, "Convergence of WSN and cognitive cellular network using maximum frequency reuse," *IET Communications*, vol. 11, pp. 664–672, 2016.

[22] X. Dong, M. C. Vuran, and S. Irmak, "Autonomous precision agriculture through integration of wireless underground sensor networks with center pivot irrigation systems," *Ad Hoc Networks*, vol. 11, no. 7, pp. 1975–1987, 2013.

[23] N. Verma, M. Rakhra, M. W. Bhatt, and U. Garg, "Engineering technology characterization of source solution for ZnO and their data analytics effect with aloe vera extract," *Neuroscience Informatics*, vol. 2, no. 3, Article ID 100015, 2022.

[24] D. Ushakov, V. Fedorchenko, V. Fedorchenko, N. Fedorchenko, V. Rybachok, and M. Bazhenov, "Brief geographical and historic overview of tourism transnationalization," *Geojournal of Tourism and Geosites*, vol. 31, no. 3, pp. 1180–1185, 2020.

[25] C. Goumopoulos, B. O'Flynn, and A. Kameas, "Automated zone-specific irrigation with wireless sensor/actuator network and adaptable decision support," *Computers and Electronics in Agriculture*, vol. 105, pp. 20–33, 2014.

[26] M. Rakhra, R. Singh, T. K. Lohani, and M. Shabaz, "Meta-heuristic and machine learning-based smart engine for renting and sharing of agriculture equipment," in *Mathematical Problems in Engineering*, D. Singh, Ed., vol. 2021, Article ID 5561065, 13 pages, 2021.

[27] J. A. López, A. J. Garcia-Sanchez, F. Soto, A. Iborra, F. Garcia-Sanchez, and J. Garcia-Haro, "Design and validation of a wireless sensor network architecture for precision horticulture applications," *Precision Agriculture*, vol. 12, no. 2, pp. 280–295, 2011.

[28] R. K. Kodali, N. Rawat, and L. Boppana, "WSN sensors for precision agriculture," in *Proceedings of the Region 10 Symposium*, pp. 651–656, Kuala Lumpur, Malaysia, April 2014.

[29] D. Ushakov, M. Vinichenko, and E. Frolova, "Environmental capital: a reason for interregional differentiation or a factor of economy stimulation (the case of Russia)," *IOP Conference Series: Earth and Environmental Science*, vol. 272, no. 3, Article ID 32111, 2019.

[30] C. Dou, L. Zheng, W. Wang, and M. Shabaz, "Evaluation of urban environmental and economic coordination based on discrete mathematical model," in *Mathematical Problems in Engineering*, D. Singh, Ed., vol. 2021, Article ID 1566538, 11 pages, 2021.

[31] G. Deepika and Rajapirian, "Wireless sensor network in precision agriculture: a survey, emerging trends in engineering, technology and science (ICETETS)," in *Proceedings of the International Conference on IEEE*, pp. 1–4, Pudukkottai, India, February 2016.

[32] S. A. Imam, A. Choudhary, and S. Achan, "Design issues for wireless sensor networks and smart humidity sensors for precision agriculture: a review," in *Proceedings of the 2015 International Conference on Soft Computing Techniques and Implementations-(ICSCTI)*, pp. 181–187, Faridabad, India, October 2015.

[33] O. Sivash, D. Ushakov, and M. Ermilova, "Investment process resource provision in the agricultural sector," *IOP Conference Series: Earth and Environmental Science*, vol. 272, no. 3, Article ID 32118, 2019.

[34] A. Patel and A. Jain, "A study of various Black Hole Attack techniques and IDS in MANET," *International Journal of Advanced Computer Technology*, vol. 4, no. 3, pp. 58–62, 2015.

[35] J. Visumathi and K. L. Shunmuganathan, "A computational intelligence for evaluation of intrusion detection system," *Indian Journal of Science and Technology*, vol. 4, no. 1, 2011.

[36] B. Wang, X. Yao, Y. Jiang, C. Sun, and M. Shabaz, "Design of a real-time monitoring system for smoke and dust in thermal power plants based on improved genetic algorithm," in *Journal of Healthcare Engineering*, Dr. D. Singh, Ed., vol. 2021, Article ID 7212567, 10 pages, 2021.

[37] S. Mohanasundaram, E. Ramirez-Asis, A. Quispe-Talla, M. W. Bhatt, and M. Shabaz, "Experimental replacement of hops by mango in beer: production and comparison of total phenolics, flavonoids, minerals, carbohydrates, proteins and toxic substances," *International Journal of System Assurance Engineering and Management*, 2021.

[38] M. S. Almahirah, M. Jahan, S. Sharma, and S. Kumar, "Role of market microstructure in maintaining economic development," *Empirical Economics Letters*, vol. 20, no. 2, pp. 01–14, 2021.

[39] A. Chaudhary, V. N. Tiwari, and A. Kumar, "Analysis of fuzzy logic based intrusion detection systems in mobile ad hoc networks," *International Journal of Information Technology*, vol. 6, no. 1, 2014.

[40] P. Nagar, H. K. Menaria, and M. Tiwari, "Novel approach of intrusion detection classification deeplearning using SVM. In first international conference on sustainable technologies for computational intelligence," *Advances in Intelligent Systems and Computing*, Springer, Singapore, 2020.

[41] M. A. Salama, H. F. Eid, R. A. Ramadan, A. Darwish, and A. E. Hassanien, "Hybrid intelligent intrusion detection scheme," *Advances in Intelligent and Soft Computing*, vol. 96, pp. 293–303, 2011.

[42] M. W. Sherwood and J. L. Pollard, "The risk-adjusted return potential of integrating ESG strategies into emerging market equities," *Journal of Sustainable Finance & Investment*, vol. 8, no. 1, pp. 26–44, 2018.

[43] S. Revathi and D. A. Malathi, "A detailed analysis on NSL-KDD dataset using various machine learning techniques for intrusion detection," *International Journal of Engineering Research and Technology*, vol. 2, no. 12, pp. 1848–1853, 2013.

WILEY | Hindawi

Research Article

Application of IoT and Cloud Computing in Automation of Agriculture Irrigation

Khongdet Phasinam [ID],[1] Thanwamas Kassanuk [ID],[2] Priyanka P. Shinde [ID],[3] Chetan M. Thakar [ID],[4] Dilip Kumar Sharma [ID],[5] Md. Khaja Mohiddin [ID],[6] and Abdul Wahab Rahmani [ID][7]

[1]*Faculty of Food and Agricultural Technology, Pibulsongkram Rajabhat University, Phitsanulok, Thailand*
[2]*School of Agriculture & Food Engineering, Faculty of Food and Agricultural Technology, Pibulsongkram Rajabhat University, Phitsanulok, Thailand*
[3]*Department of MCA, Government College of Engineering, Karad, India*
[4]*Department of Mechanical Engineering, Government College of Engineering, Karad, Maharashtra, India*
[5]*Department of Mathematics, Jaypee University of Engineering and Technology, Guna, MP, India*
[6]*Bhilai Institute of Technology, Raipur, Chhattisgarh, India*
[7]*Isteqlal Institute of Higher Education, Kabul, Afghanistan*

Correspondence should be addressed to Abdul Wahab Rahmani; ab.wahab.professor@isteqlal.edu.af

All living things, including plants, animals, and humans, need water in order to live. Even though the world has a lot of water, only about 1% of it is fresh and usable. As the population has grown and water has been used more, fresh water has become a more valuable and important resource. Agriculture uses more than 70% of the world's fresh water. People who work in agriculture are not only the world's biggest water users by volume, but also the least valuable, least efficient, and most subsidized water users. Technology like smart irrigation systems must be used to make agricultural irrigation more efficient so that more water is used. A system like this can be very precise, but it needs information about the soil and the weather in the area where it is going to be used. This paper analyzes a smart irrigation system that is based on the Internet of Things and a cloud-based architecture. This system is designed to measure soil moisture and humidity and then process this data in the cloud using a variety of machine learning techniques. Farmers are given the correct information about water content rules. Farming can use less water if they use smart irrigation.

1. Introduction

Water is an important natural resource for agriculture, but it is limited [1–3]. A large portion of water in a country like India is needed for irrigation [4]. Crop irrigation is a significant component in influencing crop productivity, as it is affected by a variety of environmental factors such as air temperature, soil temperature, humidity, and soil moisture [5]. For harvesting fields, farmers rely heavily on human supervision and experience [6]. The field's water supply must be maintained [7]. Water scarcity is a major concern in today's world. People all throughout the world are already suffering from such scarcity [8, 9]. In the future years, the situation may worsen.

Rainwater, subsurface water, and surface water are the primary sources of natural water resources. The oceans contain 96.5 percent of the planet's water. The remaining water in the world is available as 1.7 percent in groundwater, 1.7 percent in glaciers and ice caps, a minor fraction in other bodies of water, and 0.001 percent in the air as mist, clouds, and precipitation [10]. In summary, the ocean, which is salt water, contains the majority of the world's surface water. As a result, overall fresh water availability is a rare resource.

Furthermore, fresh water is a critical natural resource that is required for the survival of all ecosystems. However, from a global viewpoint, just 2.53 percent of the entire water body is now available as fresh water [11]. According to a new

analysis by ecologist Dash and Dash [12], the majority of the world's population may suffer a water crisis by 2025. On the other hand, the bulk of fresh water is used for irrigation and industrial purposes, which has a significant influence on downstream ecosystems. As a result, the use of finite fresh water resources must be carefully regulated in order to prevent having a negative influence on water availability for future generations.

According to Hegde [13], Figure 1 shows that 81 percent of India's fresh water is used for irrigation, 13 percent for industry, and 6 percent for domestic use. Human water consumption is expected to increase by up to 26% by 2025 [14].

This data demonstrates the poor use of water resources, particularly in agriculture [15]. As a result, there is a critical need to develop strategies to increase the efficiency of fresh water utilization in agriculture. Agriculture is the backbone and most significant gift to human life not only in India, but also across the world. However, the bulk of the world's cropland suffers from a severe lack of irrigation water. Drip irrigation systems have been created by researchers in such a scenario to minimize water use in arid locations. This is due to the lack of standards and systematic approaches for utilizing water and power in a positive manner. As a result, farmers' overheads for conventional drip irrigation have increased, and they must personally visit and monitor the farms on a regular basis.

The same technologies are now being used in Pennsylvania to figure out how much work will be done. A lot of research has been done in the past to make the process of figuring out how many grapes, wheat, or fruit to make easier. Most of these studies use computer vision and other technologies that work with them. The most important thing about PA is that real-time information can be found. Before harvesting crops, a production estimate creates a very important production database.

Such a database allows PA to be used for more than its original goals. It can be used for resource management, harvesting workforce estimation, harvesting time, postharvest problems, storage, and transportation. In addition, production counts have been found to help with financial decisions like figuring out how much to charge for a product, when to sell it, and how much profit or loss it will make.

A crop requires a set amount of water at defined times during its growing period. Irrigation aids crop growth in agriculture. Irrigation is the technique of artificially watering crops. This approach is especially useful in locations with little or inconsistent rainfall. Water is essential to the survival of plants in a variety of ways. Understanding the soil-water-plant link is required to comprehend the various water management strategies under different climatic situations.

There are several types of soil, such as sandy, silty, and clay. Each soil type has its own set of pros and downsides. The sandy soil, for example, has a high drainage capacity. The nutrients, on the other hand, are quickly taken away by the drain. However, because the particles in silty soil are tiny, they may store water for a considerably longer amount of time. However, this soil has a limited capacity to drain water. As a result, for effective agricultural techniques, the soil must
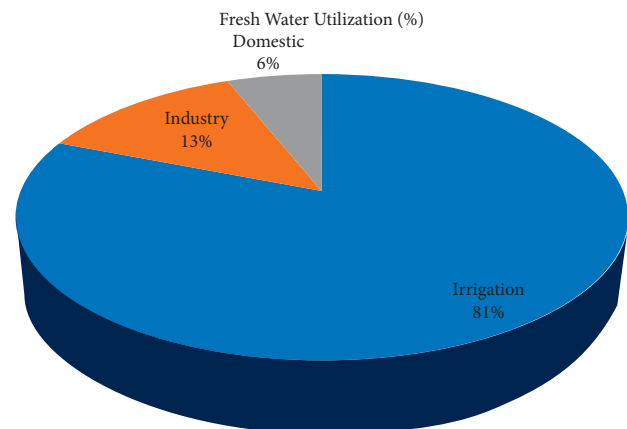

FIGURE 1: Fresh water utilization [13].

be good in all aspects, such as drainage, nutrient retention, and water retention. As a result, it is critical to understand the soil qualities in order to regulate the water requirements.

Furthermore, data mining techniques can substantially benefit the decision-making process for many agricultural tasks. The application of association rule regulations to manage the amount of water in agricultural areas is one of these operations. In addition, wireless sensor networks have evolved as a new precision agriculture approach. In current irrigation systems, smart sensor networks are used to collect field values for optimal plant irrigation. In many industries, including agriculture, healthcare, and logistics, machine learning [14] is an important method. This article also uses a machine learning-based system to reduce fresh water waste.

2. Literature Survey

2.1. Review of WSN in Agriculture. Wireless sensor networks (WSNs) play an important role in a variety of industries, including military and agricultural uses in everyday life. Tsai et al. [15] investigated the lifetime property of WSN, which is the time it takes for the sensor to run out of energy. They also explored a metaheuristic approach and how it deals with the WSN lifetime problem. They suggest a metaheuristic algorithm that operates in three phases: transition, evaluation, and determination, which aid in the selection of the best solution to the issue.

It is obvious from their explanation that understanding the different field parameters and domain expertise linked to the longevity problem are required for executing the metaheuristic method. Many scholars have already researched numerous metaheuristic algorithms. Even if the adoption of these techniques improves the performance of the WSN, there are still some outstanding concerns that require additional investigation. When contingency is considered, for example, the number of sensors or cluster heads might be minimized. Furthermore, while most metaheuristic methods are designed with optimization in mind, they may not perform well when used to solve lifespan problems.

WSN node deployment must be both efficient and significant. Li et al. [16] introduced a novel approach for effective sensor node deployment in wireless networks,

dubbed the Efficient Dynamic Deployment Approach of Sensor Nodes (EDSNDA), in which the needs of sensor node connection and coverage are considered by reducing node size as much as possible. The algorithm is compared to two other methods: Max-Cov and Min-Cov. Both of these methods are well known, and they employed four dynamic programming models for four distinct circumstances to demonstrate that their suggested technique outperforms the other existing models.

WSN nodes in mobile network architecture are utilized for communication when a large quantity of frequency is required. Hassan et al. [17] explored frequency reuse, which involves reusing a frequency for industrial, scientific, and medical (ISM) applications. Their debate is based on frequency reuse, which is done at sensor nodes located along busy pathways. The CR algorithm was utilized to disperse the load to the macrocells. Their suggested model has a reduced collision domain and can accommodate a larger number of users.

For farmers to enhance their yield, precision farming is vital. In such situations, the use of WSN may be very helpful in determining suitable decisions that support the irrigation requirements and crop output projections by farmers and other agricultural players, such as government irrigation agencies. A self-contained agricultural precision system based on central pivot irrigation systems was established by Dong et al. [18]. The technology uses an underground sensor network to monitor field characteristics such as soil humidity and temperature. This ensures that the sensors are installed and power adjustments are made for the input configuration and regular energy maintenance.

The use of wireless sensors for efficient irrigation planning was addressed by Vellidis et al. [19]. A sensor array system is used in their design to measure soil temperature and moisture so that watering requirements may be predicted in real time, merging the sensor array with sensor network-based accuracy technology.

In irrigation systems, data transmission requires more energy and hence energy conservation in order to enhance irrigation efficiency. According to Nesa Sudha et al. [20], the use of the Multiple Access Time Division allows more efficient transmission of data into WSN irrigation systems (TDMA). Energy is conserved in two ways: from the node to the sink node direct transfer and the addition of data. The network's performance is also improved via TDMA.

Goumopoulos et al. [21] suggested a novel automated zone irrigation system based on wireless sensors or actuators coordinated through an ontological approach. Precision agriculture, which is employed in this approach, is based on speaking plants in order to save more water. This system detects node failures in the network and uses various machine learning methods to improve system performance. Many end-user apps have been created in the past to improve the automation and user friendliness of irrigation tasks.

Vellidis et al. [19] created a technique for optimum cotton crop irrigation. The soil-water balance was computed in their method using data sets from a variety of cotton producing sites. Using the data sets, the authors created an Android mobile application. Furthermore, their application was designed to collect weather data from weather stations in and around the places where it was utilized. The program estimated the irrigation requirements and automatically planned the irrigation systems using the in-built data and the downloaded meteorological data in order to enhance cotton production.

Abbasi et al. [22] examined wireless sensor network applications and their need in the agricultural arena. They spoke about numerous criteria for the agriculture industry that is dependent on time variation features. Furthermore, they offered a quick study in the form of a table containing several types of sensors utilized for agriculture-related variables. Finally, they compared communication systems with varying capacities and features.

López et al. [23] suggested globally developed wireless sensor network architecture to monitor horticulture crops and ensure a high degree of sensor node power. This architecture is heavily reliant on the Berkeley Medium Access Control (B-MAC) protocol, and it takes into account various components such as base station, gateway, soil mote, water mote, and environmental conditions, and it interconnects the properties in order to achieve better throughput and reduce delays.

According to Kodali et al. [24], data accumulation in the gateway and processing will result in some warnings in the form of messages or emails indicating that the measured variables have passed the threshold, which boosts field productivity by lowering agricultural input. They focused on a number of sensor types that were used to determine statistical characteristics of agricultural fields, and they offered an elaborative description of the sensors and their specifications connected to commercial goods while keeping precision agriculture in mind. In addition, the model took into account soil water content sensors, soil moisture content sensors, soil electrical conductivity sensors, PH sensors, weedseeker sensors, temperature sensors, and wind speed sensors.

Because of a lack of decision support systems in the precision agriculture industry, Kassim et al. [25] created an eco-friendly WSN solution called the intelligent greenhouse monitoring system to address difficulties such as farming resource optimization, decision support, and land monitoring. Their approach optimizes the use of water and fertilizer while also increasing the output of the system's crops. They discussed the environmental elements that influence plant development.

Jao et al. [26] created a prototype model of wireless sensor networks for precision agriculture to gather soil moisture content while using a restricted battery supply. Sand soil with varying water amounts was utilized in their model to demonstrate outcomes using off-the-shelf hardware components.

Deepika and Rajapirian [27] conducted a survey of wireless sensor networks in precision agriculture, explaining both current and innovative technologies. For plant monitoring, this model is considered field programmable gate array-based control.

Imam et al. [28] offered an assessment of design difficulties for wireless sensor networks and smart humidity sensors for precision agriculture, with the goal of

maximizing farmer advantages. They conducted a comparison study on the utilization of microcontroller families and sensor node units in precision agriculture. Furthermore, they defined and tabulated the needs of the relative humidity sensor, as well as modeling and interface methodologies.

2.2. Reviews on Water Conservation. Water conservation is critical in agriculture. As a result, several scholars conducted studies in order to discover novel strategies for water conservation. Abubaker et al. [29] conducted trials in several seasons for sessional analysis based on dry and wet seasons, as well as studying the impact of five water collecting systems. Their model took into account the moisture content of the soil in three seasons, namely, sowing, midseason, and after harvest, at four different depths, and they demonstrated that their technique is effective for reducing water usage and improving productivity.

Gutierrez et al. [30] created an algorithm for successful plant soil temperature management, which was written on a microcontroller. It makes use of a solar cell and a communication link based on a cellular Internet interface. The authors conducted the studies for 136 days, and the results showed that their proposed irrigation approach reduced water use by up to 90% when compared to typical agricultural methods.

Gajendran et al. [31] used distributed clustering to explain the efficiency and latency of information collecting mechanisms. The algorithm generates the threshold value depending on the transmission distance, and this overall mechanism aids in the development of a robust information delivery mechanism to the base station, reducing packet loss. When compared to traditional agricultural techniques, drip irrigation technology helps to reduce crop water demand.

Grace et al. [32] offered a work based on a wireless control system that was utilized to operate drip irrigation without the assistance of a human. The primary benefit of their model was the ability to acquire rain information.

Gaddam et al. [33] presented a drought monitoring system for wireless networks that would assess meteorological and soil parameters to anticipate and diagnose drought situations. Their model was capable of collecting and analyzing data for optimal water conservation.

Figueroa and Pope [34] introduced three unique methods for determining root system water consumption from soil moisture sensor time series data: Top Rule Pattern, Prevalidated Top Rule Pattern, and Series String Comparison. The authors compared the algorithms to an actual deployed method, Density Histogram.

Li et al. [35] developed a dynamic root design to mimic the interplay of root development and soil water flow. Their suggested model's goal was to realistically describe a three-dimensional root system that could then be connected with a soil model. This model was used to characterize the dynamic interactions of the root system with soil processes such as water transport and local soil characteristics with rooting patterns and tropisms.

Mert and Adnan [36] investigated the effect of thermal behavior on green roofs, popularly known as roof gardening.

To assess both the external and internal conditions, data is collected utilizing soil moisture sensors and temperature sensors. Following an analysis of the data produced by the sensors, their green roof system reduced both the summer and winter extreme temperature effects to a certain extent, and the study revealed that extreme temperature fluctuations on the surface of the green roof and the building envelope are reduced by 79 percent by the green roof system.

Vazhachirackal [37] examined many conceptions of city farming as well as technical and nontechnical elements. The author's study on roof gardening in the metropolitan zone gave valuable assistance for urban food production. This approach also has significant social and economic benefits, since it adds to money generation, as well as environmental advantages.

Rao [38] did terrace garden research, which included the ecological value of terrace gardening by balancing out the ecology, exploitation of open space, trash recycling, energy conservation, and several other terrace gardening applications. They demonstrated that green roof or terrace gardening is a necessity in today's environment.

Besbes et al. [39] provided a model of the heat and mass transfer processes that occur on roofs, and the study was carried out using four different types of roofs, each with a different soil type employed for vegetation and thermal movement of the roof. The experiment resulted in diverse behavioral changes on different roofs, and the results revealed that a light roof with no vegetation exhibits high thermal discomfort, whereas growing plants on the roofs exhibits lower thermal discomfort. Similar work is done by researchers in [40, 41]. These all are proving the importance of Internet of Things in making precision agriculture efficient.

3. Methodology

This section presents a framework for smart irrigation. This framework is shown in Figure 2. The main components of this framework are soil moisture and humidity sensor, Raspberry Pi, central cloud storage, soil data set, machine learning techniques, and mobile applications.

3.1. The Major Components of the Proposed Framework

3.1.1. Raspberry Pi. The core is an ARM11 CPU. A single core 32-bit ARM11 CPU is employed in this system. It has 512 MB of RAM. This board has USB connections, an Ethernet port, an HDMI port, and an SD card slot. It is simple to connect this board to the Internet by utilizing the Ethernet or USB ports. For environmental parameter monitoring, various sensing devices are interfaced with common purpose input output (GPIO). We offer 5 V, 1 A power to the "Raspberry Pi" via the micro-USB port. Essentially, an SD Card with a memory capacity of 8 GB is used to save files such as applications required for the project with the assistance of the operating system [30].

A "Raspberry Pi" board is utilized as a keyboard and mouse through USB ports. For a display, we utilize the "Raspberry Pi" board as the HDMI port, which primarily
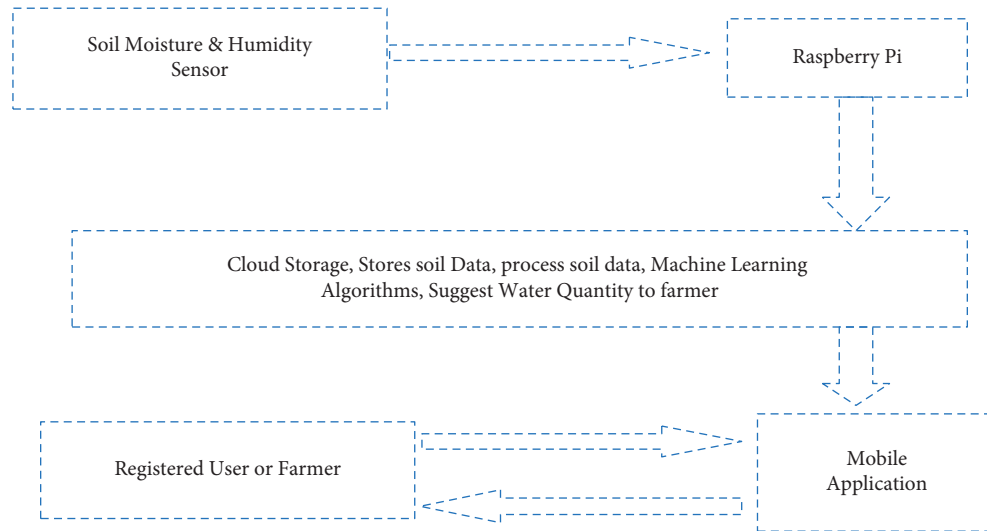
FIGURE 2: A framework for smart irrigation.

converts HDMI ports to VGA cables. The Ethernet port is used to connect the machine to the Internet through LAN. There is also a normal 3.5 mm small analog audio connector and a regular RCA-type connection on this board. This board also has a 15-pin CSI (Camera Serial Interface) connection for camera module interface and a 15-pin DSI (Display Serial Interface) connection for LED or LCD display interface.

3.1.2. DHT11/DHT22 Humidity Sensor. This is a moisture and humidity sensor. It is used to continually check the amount of humidity and moisture in the soil. This detected data is saved in the cloud via the Raspberry Pi [32].

3.1.3. YL-69 Soil Moisture Sensor. This sensor is used to determine the soil's water content. It is commonly utilized in agriculture, water systems, greenhouses, and other research center activities that need exact estimations of soil water levels. It is separated into two sections: an electrical board that houses the hardware and a dirt mugginess test. The sensor works by producing a potential distinction that is exactly proportional to the dielectric permittivity of water. Variations in voltage can be interpreted as changes in dielectric permittivity and hence as changes in water levels [31].

3.1.4. Cloud Storage. All soil related data is stored in centralized cloud storage. Climate data of that region is also stored in cloud. This cloud has machine learning algorithms like SVM, random forest, and Naïve Bayes. Machine learning algorithms are applied on soil data and climate data to obtain the correct quantity of data required by a particular crop and then this information is made available to registered user by mobile applications. Registered user can view predictions of machine learning. Registered user can set humidity and moisture level for his crop.

3.2. Machine Learning Algorithms

3.2.1. Support Vector Machine Classifier. Support vector machines are associated with learning algorithms which learn from data to decipher patterns in classification and regression analysis. SVM models aim to find fresh water saved in smart irrigation in the different classes as wide as possible so that when a new sample comes in, it is classified based on which side of the gap they fall in.

3.2.2. Random Forests. Random forest is a powerful ensemble learning algorithm often used in classification tasks. It classifies based on the results obtained from the myriad of decision trees it generates while training, where the mode of the targeted outputs from each decision tree is the output of the forest. Random forest generates decision trees on random samples of the training data, thereby reducing the variance in the overall model improving its performance and controlling overfitting.

3.2.3. Naïve Bayes. Naïve Bayes is a probabilistic classifier based on Bayes theorem, with the features being independent of each other. Each feature is considered to contribute to the probability of any given test instance to belong to a particular class.

4. Results

A data set of 330 soil records was created for experimental analysis. This includes soil moisture and humidity details for specific crops in specific regions. Climate data for regions was also part of the data set. In an experimental study, three machine learning algorithms were used: SVM, random forest, and Naïve Bayes.

The accuracy results of machine learning algorithms are shown below in Figure 3: other results are presented in Figures 4 and 5, and Tables 1 and 2.
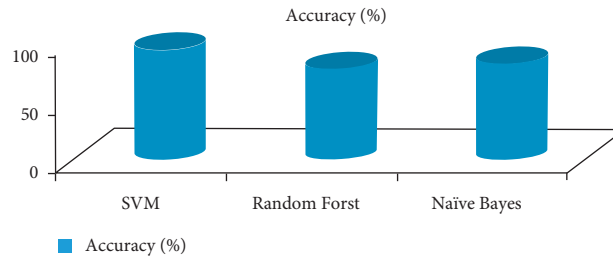
Figure 3: Accuracy of machine learning algorithms.
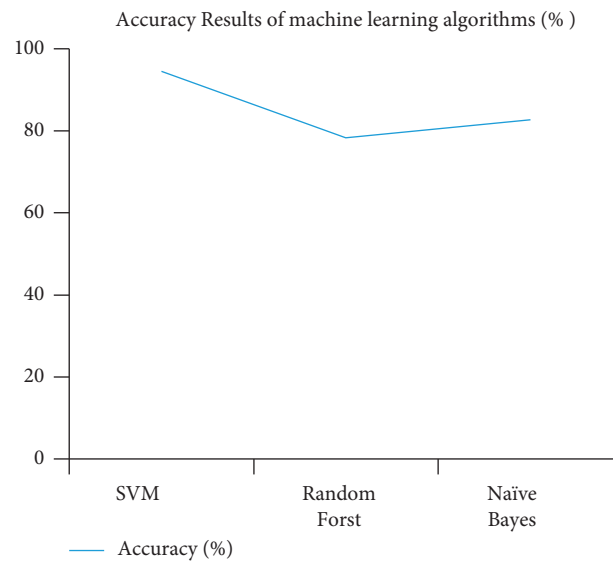
Figure 4: Graphical representation of accuracy results of machine learning algorithms.
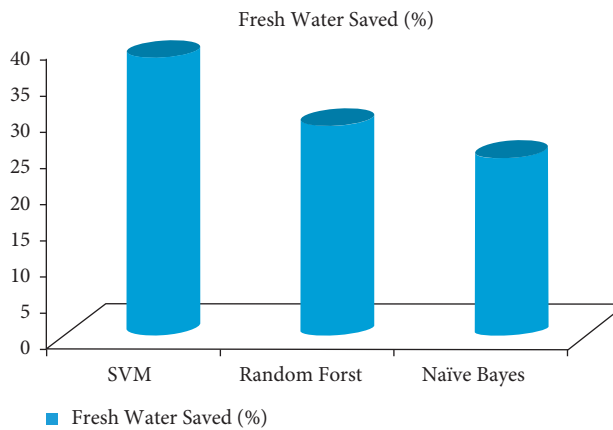
Figure 5: Fresh water saved in smart irrigation.

In this graph, SVM's accuracy result of machine learning algorithms is better than random forest and Naïve Bayes. The result of SVM is more than 80%, but on the other hand, random forest and Naïve Bayes accuracy results are less than 77.5%.

Due to proper water content suggestion for a particular crop, the fresh water saved by algorithms is as follows.

In this graph shown in Figure 6, SVM machine learning algorithms show that fresh water saved in smart irrigation is better than random forest and Naïve Bayes. The result of SVM is more than 35%, but on the other hand, random forest and Naïve Bayes accuracy results are less than 30%.

Table 1: Accuracy of machine learning algorithms.

Accuracy results of machine learning algorithms	
Machine learning algorithms	Accuracy (%)
SVM	88
Random forest	70
Naïve Bayes	76

Table 2: Fresh water saved in smart irrigation.

Fresh water saved in smart irrigation	
Machine learning algorithms	Fresh water saved (%)
SVM	37
RF	26
Naïve Bayes	22
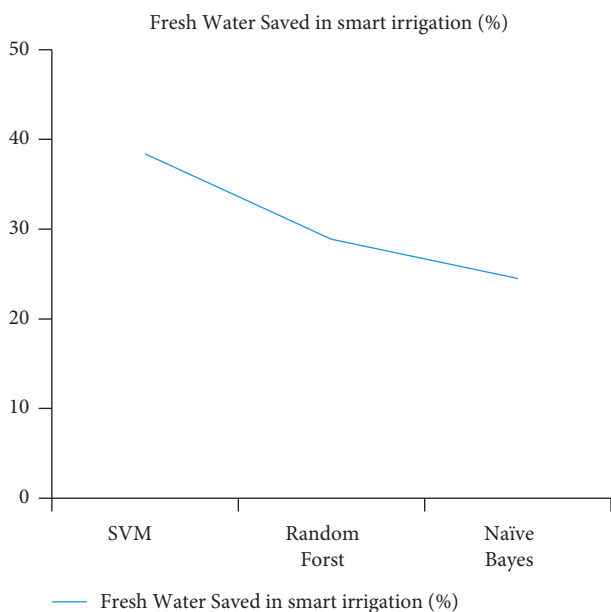
Figure 6: Graphical representation of fresh water saved in smart irrigation.

5. Conclusion

Agriculture, according to the Food and Agriculture Organization of the United Nations (FAO), is not only the world's largest water consumer in terms of volume, but also a low-value, low-efficiency, and extensively subsidized user of water. Because of this, there is an urgent need to increase the efficiency of agricultural irrigation by utilizing technology such as smart irrigation systems. The precision of such a system, on the other hand, is dependent on soil data from that region, as well as climatic data from that region, to be effective. This article describes a smart irrigation system that is based on the Internet of Things and cloud computing architecture. In this framework, machine learning algorithms were utilized to anticipate the proper amount of fresh water required for a crop to be cultivated. As a result, a significant amount of fresh water is saved. The agricultural sector will be transformed as a result of smart irrigation.

5.1. Future Work. Although the systems described in the previous part make the IoT and cloud computing concept practicable, a significant amount of research is still necessary. This section examines the technical issues that now plague IoT systems. Later on, a novel concept of IoT and cloud architecture was developed to meet all necessary parts that are missing in existing architecture. Before the Internet of Things can be extensively adopted and deployed across all sectors, a thorough understanding of industrial characteristics and needs on cost, security, privacy, and risk is required.

Data Availability

The data shall be made available on request.

Conflicts of Interest

The authors declare that they have no conflicts of interest.

References

[1] C. Kamienski, J.-P. Soininen, M. Taumberger et al., "Smart water management platform: Iot-based precision irrigation for agriculture," *Sensors*, vol. 19, no. 2, p. 276, 2019.

[2] L. Wang, W. Wu, J. Xiao, Q. Huang, and Y. Hu, "Effects of different drip irrigation modes on water use efficiency of pear trees in northern China," *Agricultural Water Management*, vol. 245, Article ID 106660, 2020.

[3] K. S. Sahoo, D. Puthal, M. Tiwary et al., "Esmlb: efficient switch migration-based load balancing for multi-controller SDN in IoT," *IEEE Internet of Things Journal*, vol. 7, no. 7, pp. 5852–5860, 2019.

[4] N. K. Nawandar and V. R. Satpute, "IoT based low cost and intelligent module for smart irrigation system," *Computers and Electronics in Agriculture*, vol. 162, no. 4, pp. 979–990, 2019.

[5] C. M. Bavougian and P. E. Read, "Mulch and groundcover effects on soil temperature and moisture, surface reflectance, grapevine water potential, and vineyard weed management," *PeerJ*, vol. 6, no. 1, Article ID e5082, 2018.

[6] D. Glaroudis, A. Iossifides, and P. Chatzimisios, "Survey, comparison and research challenges of IoT application protocols for smart farming," *Computer Networks*, vol. 168, no. 4, Article ID 107037, 2020.

[7] D. Liu, Q. Jia, J. Li, P. Zhang, X. Ren, and Z. Jia, "Increased photosynthesis and grain yields in maize grown with less irrigation water combined with density adjustment in semi-arid regions," *PeerJ*, vol. 8, no. 1, Article ID e9959, 2020.

[8] P. Fremantle and P. Scott, "A survey of secure middleware for the internet of things," *PeerJ Computer Science*, vol. 3, no. 15, p. e114, 2017.

[9] J. M. Schleicher, M. Vögler, C. Inzinger, and S. Dustdar, "Modeling and management of usage-aware distributed datasets for global smart city application ecosystems," *PeerJ Computer Science*, vol. 3, no. 11, p. e115, 2017.

[10] C. E. LaCanne and J. G. Lundgren, "Regenerative agriculture: merging farming and natural resource conservation profitably," *PeerJ*, vol. 6, Article ID e4428, 2018.

[11] I. A. Shiklomanov and J. C. Rodda, *World Water Resources at the Beginning of the Twenty-First Century*, Cambridge University Press, Cambridge, UK, 2004.

[12] M. C. Dash and S. P. Dash, *Fundamental of Ecology*, McGraw-Hill Publication, Chennai, India, 3rd edition, 2009.

[13] N. G. Hegde, "Water scarcity and security in India," in *Proceedings of the 2012 BAIF-Indian Science Congress*, pp. 1–19, Kolkata, India, 2012.

[14] R. Manne and S. C. Kantheti, "Application of artificial intelligence in healthcare: chances and challenges," *Current Journal of Applied Science and Technology*, vol. 40, no. 6, pp. 78–89, 2021.

[15] C.-W. Tsai, T.-P. Hong, and G.-N. Shiu, "Metaheuristics for the lifetime of WSN: a review," *IEEE Sensors Journal*, vol. 16, no. 9, pp. 2812–2831, 2016.

[16] S. Li, J. Gao, Q. Zhu, L. Zeng, and J. Liu, "A dynamic root simulation model in response to soil moisture heterogeneity," *Mathematics and Computers in Simulation*, vol. 113, pp. 40–50, 2015.

[17] F. Hassan, A. Roy, and N. Saxena, "Convergence of WSN and cognitive cellular network using maximum frequency reuse," *IET Communications*, vol. 11, pp. 664–672, 2016.

[18] X. Dong, M. C. Vuran, and S. Irmak, "Autonomous precision agriculture through integration of wireless underground sensor networks with center pivot irrigation systems," *Ad Hoc Networks*, vol. 11, no. 7, pp. 1975–1987, 2013.

[19] G. Vellidis, V. Liakos, J. H. Andreis et al., "Development and assessment of a smartphone application for irrigation scheduling in cotton," *Computers and Electronics in Agriculture*, vol. 127, pp. 249–259, 2016.

[20] M. Nesa Sudha, M. L. Valarmathi, and A. S. Babu, "Energy efficient data transmission in automatic irrigation system using wireless sensor networks," *Computers and Electronics in Agriculture*, vol. 78, no. 2, pp. 215–221, 2011.

[21] C. Goumopoulos, B. O'Flynn, and A. Kameas, "Automated zone-specific irrigation with wireless sensor/actuator network and adaptable decision support," *Computers and Electronics in Agriculture*, vol. 105, pp. 20–33, 2014.

[22] A. Z. Abbasi, N. Islam, and Z. A. Shaikh, "A review of wireless sensors and network applications in agriculture," *Computer Standards & Interfaces*, vol. 36, no. 2, pp. 263–270, 2014.

[23] J. A. López, A. J. Garcia-Sanchez, F. Soto, A. Iborra, F. Garcia-Sanchez, and J. Garcia-Haro, "Design and validation of a wireless sensor network architecture for precision horticulture applications," *Precision Agriculture*, vol. 12, no. 2, pp. 280–295, 2011.

[24] R. K. Kodali, N. Rawat, and L. Boppana, "WSN sensors for precision agriculture," in *Proceedings of the 2014 Region 10 Symposium*, Kuala Lumpur, Malaysia, 2014.

[25] M. R. M. Kassim, I. Mat, and A. N. Harun, "Wireless sensor network in precision agriculture application," in *Proceedings of the 2014 International Conference on Computer, Information and Telecommunication Systems (CITS)*, Jeju, Republic of Korea, 2014.

[26] J. Jao, B. Sun, and K. Wu, "A prototype wireless sensor network for precision agriculture," in *Proceedings of the IEEE 33rd International Conference on Distributed Computing Systems Workshops*, Philadelphia, PA, USA, 2013.

[27] G. Deepika and P. Rajapirian, "Wireless sensor network in precision agriculture: a survey," in *Proceedings of the 2016 International Conference on IEEE Emerging Trends in Engineering, Technology and Science (ICETETS)*, Pudukkottai, India, 2016.

[28] S. A. Imam, A. Choudhary, and V. K. Sachan, "Design issues for wireless sensor networks and smart humidity sensors for precision agriculture: a review," in *Proceedings of the 2015 International Conference on Soft Computing Techniques and Implementations-(ICSCTI)*, Faridabad, India, 2015.

[29] B. M. A. Abubaker, Y. Shuang-En, S. Guang-Cheng, and M. Alhadi, "Impact of different water harvesting techniques on soil moisture content and yield components of sorghum," *Pakistan Journal of Agricultural Sciences*, vol. 51, 2014.

[30] J. Gutierrez, J. F. Villa-Medina, A. Nieto-Garibay, and M. A. Porta-Gandara, "Automated irrigation system using a wireless sensor network and GPRS module," *IEEE Transactions on Instrumentation and Measurement*, vol. 63, no. 1, pp. 166–176, 2014.

[31] E. Gajendran, S. B. Prabhu, and M. Pradeep, "An analysis of smart irrigation system using wireless sensor," *Multidisciplinary Journal of Scientific Research &Education*, vol. 3, no. 3, pp. 230–234, 2017.

[32] K. V. Grace, S. Kharim, and P. Sivasakthi, "Wireless sensor-based control system in agriculture field," in *Proceedings of the 2015 Global Conference on Communication Technologies (GCCT)*, Thuckalay, India, 2015.

[33] A. Gaddam, M. Al-Hrooby, and W. F. Esmael, "Designing a wireless sensors network for monitoring and predicting droughts," in *Proceedings of the 8th International Conference on Sensing Technology*, Liverpool, UK, 2014.

[34] M. Figueroa and C. Pope, "Root system water consumption pattern identification on time series data," *Sensors (Basel, Switzerland)*, vol. 17, pp. 1–21, 2017.

[35] Y. Li, W. Gao, C. Wu, and Y. Wang, "Deployment of sensors in WSN: an efficient approach based on dynamic programming," *Chinese Journal of Electronics*, vol. 24, no. 1, pp. 33–36, 2015.

[36] E. K. S. I. Mert and U. Z. U. N. Adnan, "Investigation of thermal benefits of an extensive green roof in Istanbul climate," *Scientific Research and Essays*, vol. 8, pp. 623–632, 2013.

[37] P. J. Vazhachirackal, "Balcony and terrace gardens in urban greening and local food production, scenarios from Mumbai metropolitan region (MMR), India," *International Journal of Food, Agriculture and Veterinary Sciences*, vol. 4, 2014.

[38] P. Rao, "Role of terrace garden in sustainability and environment," *International Journal of Management*, vol. 4, pp. 19–22, 2016.

[39] K. Besbes, A. Zoughaib, R. Bouchie, and S. Farkh, "Green roofs impact on buildings cooling load," in *Proceedings of the 2012 International High Performance Buildings Conference*, West Lafayette, IN, USA, 2012.

[40] L. M. Fernández-Ahumada, J. Ramírez-Faz, M. Torres-Romero, and R. López-Luque, "Proposal for the design of monitoring and operating irrigation networks based on IoT, cloud computing and free hardware technologies," *Sensors*, vol. 19, no. 10, p. 2318, 2019.

[41] L. García, L. Parra, J. M. Jimenez, J. Lloret, and P. Lorenz, "IoT-based smart irrigation systems: an overview on the recent trends on sensors and IoT systems for irrigation in precision agriculture," *Sensors*, vol. 20, no. 4, p. 1042, 2020.

WILEY | Hindawi

Research Article

Protective Effects of Honey-Processed *Astragalus* on Liver Injury and Gut Microbiota in Mice Induced by Chronic Alcohol Intake

Jingxuan Zhou [iD],[1] **Nanhai Zhang** [iD],[1] **Liang Zhao** [iD],[2] **Mohamed Mohamed Soliman** [iD],[3] **Wei Wu,**[4] **Jingming Li,**[5] **Feng Zhou** [iD],[1] and **Liebing Zhang** [iD][1]

[1]*Beijing Key Laboratory of Functional Food from Plant Resources, College of Food Science and Nutritional Engineering, China Agricultural University, 17 Tsinghua East Road, Beijing 10083, China*
[2]*Beijing Engineering and Technology Research Center of Food Additives, Beijing Technology and Business University (BTBU), 11 Fucheng Road, Beijing 100048, China*
[3]*Clinical Laboratory Sciences Department, Turabah University College, Taif University, Taif, Saudi Arabia*
[4]*College of Engineering, China Agricultural University, 17 Tsinghua East Road, Beijing 10083, China*
[5]*Center for Viticulture and Enology, College of Food Science and Nutritional Engineering, China Agricultural University, 17 Tsinghua East Road, Beijing 10083, China*

Correspondence should be addressed to Feng Zhou; zf@cau.edu.cn and Liebing Zhang; lbzhang@cau.edu.cn

Honey-processed *Astragalus* (HPA) is a mixture of *Astragalus* and honey, which is a processed product of Chinese medicine. It has the active ingredients of *Astragalus* and the unique effects of honey. However, the mechanism of HPA for improving alcoholic liver disease (ALD) is not clear. The purpose of this study is to explore the ameliorating effect and mechanism of HPA (4 and 8 g/kg bw) on alcoholic liver injury. Two doses of HPA were orally administered to alcohol-treated mice for four weeks. The results showed that HPA could effectively reduce triglycerides (TG) by 59% and free fat acid (FFA) and total cholesterol (TC) in serum and hepatic were reduced by least 25.9%. HPA could cause a decrease in serum low-density lipoprotein cholesterol (LDL-C) from 0.145 mM to 0.117 mM, and the serum high-density lipoprotein cholesterol (HDL-C) was increased. After alcohol-treated mice were supplemented with HPA, antioxidant markers (superoxide dismutase (SOD), catalase (CAT), glutathione (GSH), and Glutathione peroxidase (GSH-Px)), liver function index (alanine aminotransferase (ALT), aspartate aminotransferase (AST), and alkaline phosphatase (ALP)), proinflammatory cytokines (tumor necrosis factor-α (TNF-α), interleukin-6 (IL-6), and interleukin-1β (IL-1β)), and liver tissue were all significantly improved. This is related to the fact that HPA can promote the expression of oxidative stress-related genes and inhibit the expression of inflammation-related genes. In addition, HPA could also regulate the disturbance of the intestinal microflora. In general, HPA could significantly improve the accumulation of serum and liver lipids caused by alcohol and the imbalance of intestinal flora in mice. It could also improve liver function, oxidative stress, and inflammation.

1. Introduction

Alcohol-related diseases are one of the most common preventable diseases in the world [1]. More than 3 million people around the world die from alcoholism every year [2]. Alcohol injury can cause damage to many end-organs and systems in the body, and alcoholic liver disease (ALD) is an important manifestation of liver injury [3]. ALD can develop from asymptomatic to alcoholic fatty liver, liver cirrhosis, and even alcoholic hepatitis and hepatocellular carcinoma [2, 4]. There is evidence that the development mechanism of ALD is closely related to oxidative stress, inflammatory development, and intestinal microflora disorders [5]. Although drugs such as disulfiram, naltrexone, and corticosteroids are used in abstinence treatment, some drugs are not approved for ALD treatment. Corticosteroids are effective only in the short term in 50% patients with ALD [6, 7]. Due to the personal differences of patients and adverse reactions

caused by drugs still exist, so it is common to choose natural products with low side effects and good tolerance to achieve the improvement of ALD.

Astragalus (Huangqi, Astragalus membranaceus Beg. var. mongholicus (Beg.)) appears in people's field of vision as a common healthcare traditional Chinese medicine because of its antioxidant, anti-inflammatory, and other biological activities [8–10]. Astragalus extracts can improve lipo-polysaccharide-induced liver injury by inhibiting the formation of lipid peroxides and proinflammatory factors [11]. Our previous studies showed that Astragalus polysaccharides and Astragalus saponins could improve liver injury in ALD mice [12]. As a safe alternative sweetener, honey could reduce triglycerides (TG), total cholesterol (TC), and low-density lipoprotein cholesterol (LDL-C) [13]. Data showed that honey could improve liver injury by regulating oxidative stress markers: catalase (CAT), glutathione (GSH), malondialdehyde (MDA), superoxide dismutase (SOD), and liver function [14, 15]. Honey-processed Astragalus (HPA) is a mixture of astragalus and honey [16]. Some studies have shown that after the combination of honey and Astragalus, the structure of the active components of Astragalus has changed, and the efficacy of HPA was stronger than that of Astragalus [16, 17]. In addition, HPA had a certain anti-inflammatory effect [16, 17]. HPA could not only improve the inflammatory response but also regulate the gut microbial flora diversity of colitis mice [18].

However, the mechanism and research of HPA alleviating ALD are still poorly understood. In view of the above biological activities of HPA, we speculate that HPA may have a beneficial effect on improving ALD. Therefore, this study aims to evaluate the improvement effect of HPA (Hunyuan, Shanxi Province) on alcohol-induced liver injury in mice and the effect of reducing serum and hepatic lipids. In addition, explore the mechanism of inhibiting oxidative stress, inflammation, and the influence of intestinal flora in alcohol-treated mice.

2. Materials and Methods

2.1. Materials and Chemicals.
Honey-processed Astragalus was provided by Ze Qingqi Industry Development Co., Ltd. (Shanxi, China). Edible alcohol was purchased from Henan Xinheyang Alcohol Co., Ltd. (Henan, China). The assay kits of CAT, SOD, GSH, MDA, γ-glutamyl transpeptidase (γ-GT), glutathione peroxidase (GSH-Px), and free fat acid (FFA) and the commercial enzyme-linked immunosorbent assay (ELISA) kits of tumor necrosis factor-α (TNF-α), interleukin-6 (IL-6), and interleukin-1β (IL-1β) were bought from Beijing Sinouk Institute of Biological Technology (Beijing, China). The commercial assay kits of TG, TC, high-density lipoprotein cholesterol (HDL-C), LDL-C, alanine aminotransferase (ALT), aspartate aminotransferase (AST), and alkaline phosphatase (ALP) were purchased from Biosino Bio-Technology and Science Inc. (Beijing, China). FastQuant RT Kit and SuperReal PreMix Plus with SYBR Green were purchased from Tiangen Biotech Co. Ltd. (Beijing, China). E.Z.N.A.® soil DNA Kit was bought from Omega Bio-tek (Norcross, GA, USA). AxyPrep DNA Gel

Extraction Kit was provided by Axygen Biosciences (Union City, CA, USA). Other reagents, such as ethanol, hydrochloric acid, chloroform, acetone, and NaOH, were all of analytical grade.

2.2. Animals and Experimental Design.
Forty-eight 5-week-old male ICR mice (20 ± 1 g of weight) were all bought from Beijing Vital River Laboratory Animal Technology Co., Ltd. (Beijing, China; Certificate no. SCXK (Beijing) 2016-0006). The mice were kept in separate cages with fed food and water ad libitum. The mice were housed in a controlled environment with 40–55% humidity and a 12 h light/dark cycle at 22–24°C. All animal procedures act up to the Animal Ethics Committee of the Beijing Key Laboratory of Functional Food from Plant Resources and the guidelines for the care and use of laboratory animals of the National Institutes of Health.

All mice were randomly divided into normal group (NG), model group (MG), HPA low-dose group (HPAL), and HPA high-dose group (HPAH) after adaption for 1 week ($n = 12$ each group). The mice in the NG and MG were orally distilled water for the following 4 weeks. After 1 hour of treatment with distilled water, the MG were given orally 10 mL/kg body weight (bw) of 50% alcohol. In the HPAL and HPAH, HPA was formulated into a solution with a mass fraction of 40% and 80% (HPA was dissolved in distilled water). First, all mice were given orally the same dose alcohol as MG. Then, the HPAL and HPAH were administrated with 40% and 80% of HPA solution by oral route respectively (10 mL/kg bw) after treatment with 50% alcohol 1 hour later. The mice were weighted every three days, and the perfusion volume was adjusted based on the body weight. After the fourth week of feeding, the mice were weighed and recorded for the last time. The mice were fasted for 12 hours with water freely before the blood samples were taken. The blood samples were taken from the orbital venous plexus of the mice and stored at 4°C for 12 hours. The liver tissue was weighed immediately after the mice were killed and the liver index was calculated [liver index (%) = liver weight (g)/final body weight (g) × 100%]. The liver sample was divided into two parts: one part was immersed in 10% formalin solution for histopathology; the other part was used for biochemical determination and stored at −80°C. Colon contents were collected and stored at −80°C for intestinal microbiota analysis.

2.3. Analysis of Biochemical Indicators in Serum and Hepatic.
The serum was obtained after the blood samples centrifuged at 4°C with 4000 g for 15 minutes. According to the test kits, the levels of serum TC, TG, FFA, HDL-C, LDL-C, AST, ALT, APL, and γ-GT were tested by the Mindray BS-420 automatic biochemical analyzer (Shenzhen Mindray Biomedical Electronics Co., Ltd.). According to the method of Zhao et al. [19], the liver sample was homogenized, and then liver lipids were extracted from liver homogenate. The hepatic TC, TG, and FFA were determined by the same corresponding detection kits for detection with serum TC, TG, and FFA. The activities of SOD, CAT, GSH, GSH-Px, and the level of MDA

in liver were detected using the corresponding assay kits. The contents of TNF-α, IL-6, and IL-1β were measured following the instructions of the corresponding ELISA kits. The BCA kit was used to measure the concentration of total protein in liver homogenate.

2.4. Analysis of Real-Time PCR.
The total liver RNA was extracted by using TRIpure reagent according to the instruction and reverse-transcribed into cDNA by using FastQuant RT Kit. The levels of mRNA expression were measured according to the kit manufacturer's instruction by SuperReal PreMix Plus with SYBR Green [20]. Glyceraldehyde-3-phosphate dehydrogenase (GAPDH) as the internal reference was measured to normalize mRNA expression. The appropriate primers are shown in Table 1. The relative mRNA expression was calculated by the $2^{-\Delta\Delta Ct}$ method (relative expression = $2^{-\Delta\Delta Ct}$ (ΔCt (test) = Ct (target, test) – Ct (ref, test), ΔCt (calibrator) = Ct (target, calibrator) – Ct (ref, calibrator), $\Delta\Delta Ct = \Delta Ct$ (test) – ΔCt (calibrator))) [21].

2.5. Histological Analysis.
The extracted livers were fixed in 10% (v/v) formalin solution for 24 h, before the samples were cut into slices. Then, the slices were embedded in paraffin. The slices were stained with hematoxylin and eosin (H&E) and Masson. Finally, the sections were placed under a light microscope (BA-9000, Osaka, Japan) for observation.

2.6. Analysis of Gut Microbiota.
The genome of fecal flora was extracted by using the DNA extraction kit, and the DNA samples were determined by NanoDrop2000 spectrophotometer (Thermo Fisher Scientific, Waltham, MA, USA). The V3-V4 region of the bacterial 16S rDNA genes was amplified using the barcoded universal primers (338F: 5′-ACTCCTACGGGAGGCAGCAG-3′; 806R: 5′-GGAC-TACHVGGGTWTCTAAT-3′). The amplified products were confirmed by agarose gel electrophoresis for completeness and purified by AxyPrep DNA Gel Extraction Kit. The amplified products library was paired-end-sequenced on Illumina Miseq platform (Illumina, San Diego, CA, USA). Gut microbiota analysis was completed by Majorbio Bio-Pharm Technology Co., Ltd. (Shanghai, China).

2.7. Statistical Analysis.
The results of the animal experiment were presented as mean ± standard deviation (SD). SPSS 25.0 was used to evaluate the statistical analysis between model and other groups by independent-samples T test using SPSS 25.0 (SPSS Inc., Chicago, USA). The figures were drawn by GraphPad Prism version 8.0 (La Jolla, CA, USA). $p < 0.05$ was recognized as statistically significant and $p < 0.01$ were regarded as highly statistically significant.

3. Result

3.1. Effect of HPA on Food Intake, Body Weight, and Hepatic Index in ALD Mice.
As shown in Table 2, the final body weight and food intake of alcohol-treated mice were significantly lower than the NG ($p < 0.01$). The hepatic index in the MG was lower than that in the NG ($p < 0.05$). Only the high-dose HPA could clearly decrease the hepatic index compared to the MG ($p < 0.05$).

3.2. Effect of HPA on Lipids of Serum and Hepatic in ALD Mice.
Figures 1(a)–1(e) present the influence of HPA on the serum lipids (TC, TG, FFA, HDL-C, and LDL-C). Compared with the NG, the levels of serum of TC, TG, FFA, and LDL-C in alcohol-treated mice were apparently increased ($p < 0.01$). Serum HDL-C in the MG was significantly reduced by 25.3% (versus NG, $p < 0.01$). As displayed in Figures 1(f)–1(h), the contents of hepatic lipids (TC, TG, and FFA) in the MG were obviously higher than that in the NG ($p < 0.01$). The levels of serum and hepatic lipids in all treatment groups were improvement apparently (versus MG, $p < 0.01$). The contents of serum TG and hepatic TG in the HPAH could reduce by more than 59% (versus MG, $p < 0.01$). As Figures 1(a)–1(h), the high-dose HPA had the best improvement effect on the lipids of serum and hepatic in ALD mice.

3.3. Effect of HPA on Hepatic Function in ALD Mice.
Figure 2 shows that the activities of ALT, AST, ALP, and γ-GT in the MG were apparently higher than that in the NG ($p < 0.01$). The HPA could reduce the levels of these indexes (versus MG, $p < 0.01$). In particular, the improvement effect of high dose HPA was the best, reducing AST (18.82%), ALT (23.67%), ALP (31.76%), and γ-GT (26.66%), respectively.

3.4. Effect of HPA on the Hepatic Oxidative Stress in ALD Mice.
As shown in Figures 3(a)–3(e), there was a significant plummet in the CAT, SOD, GSH, and GSH-Px contents that occurred in alcohol-treated mice, and the MDA level had an apparently elevation (versus NG, $p < 0.01$). After treatment with HPA, the content of oxidation markers in the liver of ALD mice was significantly improved (versus MG, $p < 0.01$). In terms of SOD, GSH-Px, and MDA, the improvement effect of the HPAH was better than that of the HPAL. Especially, high dose of HPA could reduce the MDA level in ALD mice to 60% of the original (Figure 3(e), $p < 0.01$). In addition, HPAL had the best improvement effect on CAT and GSH, and low dose of HPA could increase the level of CAT in ALD mice by 0.27 times (versus MG, $p < 0.01$).

3.5. Effect of HPA on Inflammation Response in ALD Mice.
As shown in Figures 4(a)–4(c), the effect of HPA on the level of inflammatory factors in ALD mice was evaluated. The level of inflammatory factors (IL-1β, IL-6, and TNF-α) increased significantly in alcohol-treated mice (versus NG, $p < 0.01$). The three indexes in the treatment groups were obviously decreased (versus MG, $p < 0.01$). In the levels of IL-1β and TNF-α, the HPAH had the best improvement effect. The HPAH not only reduced the values of IL-1β from 7.77 to 3.86 pg/mg pro but also reduced the TNF-α index by 4.12 pg/mg pro (versus MG, $p < 0.01$). Compared with the MG, the content of IL-6 in the HPAL was only 0.67 times that in the MG (Figure 4(b)).

TABLE 1: Primer sequences of genes used for qRT-PCR.

Gene	Forward primer (5′-3′)	Reverse primer (5′-3′)
Gapdh	TCTCCTGCGACTTCAACA	TGTAGCCGTATTCATTGTCA
Keap1	CAGATTGACAGCGTGGTT	GCAGTGTGACAGGTTGAA
Nfe2l2	GTGCTCCTATGCGTGAAT	TCTTACCTCTCCTGCGTATA
Hmox1	AGGTCCTGAAGAAGATTGC	TCTCCAGAGTGTTCATTCG
Nqo1	ATGAAGGAGGCTGCTGTA	AGATGACTCGGAAGGATACT
Tlr4	TGACATTCCTTCTTCAACCA	CACAGCCACCAGATTCTC
Myd88	CCGTGAGGATATACTGAAGG	TTAAGCCGATAGTCTGTCTG
Nfkb1	AGACAAGCAGCAGGACAT	CCAGCAACATCTTCACATC

TABLE 2: Effects of AP and AS on body weight, food intake, and liver index of mice.

Groups	Initial weight (g)	Final weight (g)	Food intake (g/d)	Hepatic index (%)
NG	28.38 ± 1.17	34.09 ± 2.97	4.92 ± 0.46	3.63 ± 0.22
MG	28.55 ± 1.49	$28.98 \pm 2.00^{**}$	$3.63 \pm 0.66^{**}$	$3.99 \pm 0.11^{*}$
HPAL	28.90 ± 1.69	28.98 ± 1.17	3.28 ± 0.73	3.82 ± 0.16
HPAH	28.74 ± 1.32	28.63 ± 1.98	3.20 ± 0.68	$3.73 \pm 0.22^{\#}$

Data were expressed as mean $\pm$ SD ($n = 12$). $^{**} p < 0.01$ and $^{*} p < 0.05$, versus NG; $^{\#} p < 0.05$, versus MG.
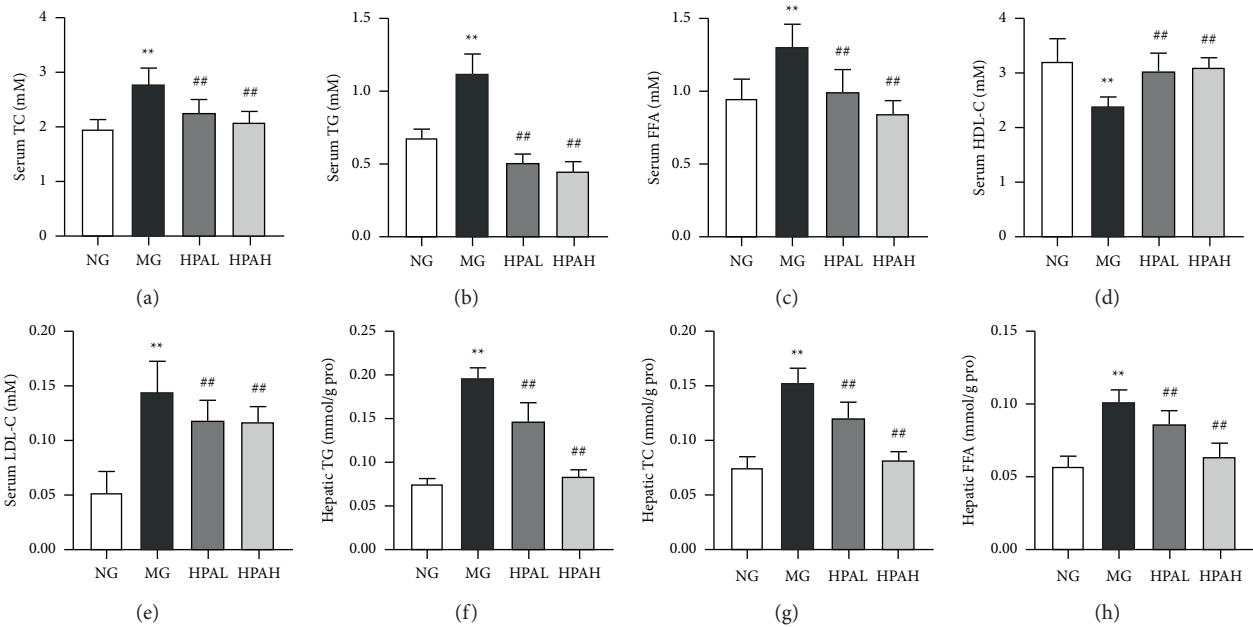

FIGURE 1: Effect of HPA on the serum and liver lipids in ALD mice. (a) Serum TG; (b) serum TC; (c) serum HDL-C; (d) serum LDL-C; (e) serum FFA; (f) hepatic TG; (g) hepatic TC; (h) hepatic FFA. Data were expressed as mean $\pm$ SD ($n = 12$). $^{**} p < 0.01$, versus NG; $^{\#} p < 0.05$ and $^{\#\#} p < 0.01$, versus MG.

3.6. Effect of HPA on Oxidative Stress and Inflammation-Related Gene Expression in ALD Mice. Figure 5 shows the effect of HPA on gene expression in inflammatory signal pathway (TLR4 (Tlr4), Myd88 (Myd88), and NF-κB (Nfkb1)) and oxidative stress signal pathway (Kelch-like ECH-associated protein 1 (Keap1 (Keap1)), NF-E2-related factor 2 (NRF2 (Nfe2l2)), heme oxygenase 1 (HO-1 (Hmox1)), and NADPH quinone dehydrogenase 1 (NQO1 (Nqo1)) in alcohol-treated mice. After the mice were treated by alcohol, the mRNA expression of Keap1, Nfe2l2, Hmox1, and Nqo1 was significantly downregulated, while the mRNA expression of Tlr4, Myd88, and Nfkb1 was significantly upregulated (versus NG, $p < 0.01$). It has been observed that the HPA could obviously reduce the

expression of Keap1, Nfe2l2, Hmox1, and Nqo1 and clearly increased the expression of Tlr4, Myd88, and Nfkb1 (vs. MG, $p < 0.01$). Compared with the MG, the genes related to oxidative stress in the HPAH increased more than 2 times, and the genes related to inflammation in the HPAH decreased by more than 36.6%. Therefore, it can be seen that HPAH reduced the expression of inflammation-related genes and at the same time promotes the expression of antioxidant-related genes.

3.7. Effect of AP and AS on Histopathological Variations of Livers in ALD Mice. In order to confirm that the HPA has improvement effect on ALD, hepatic sections were stained
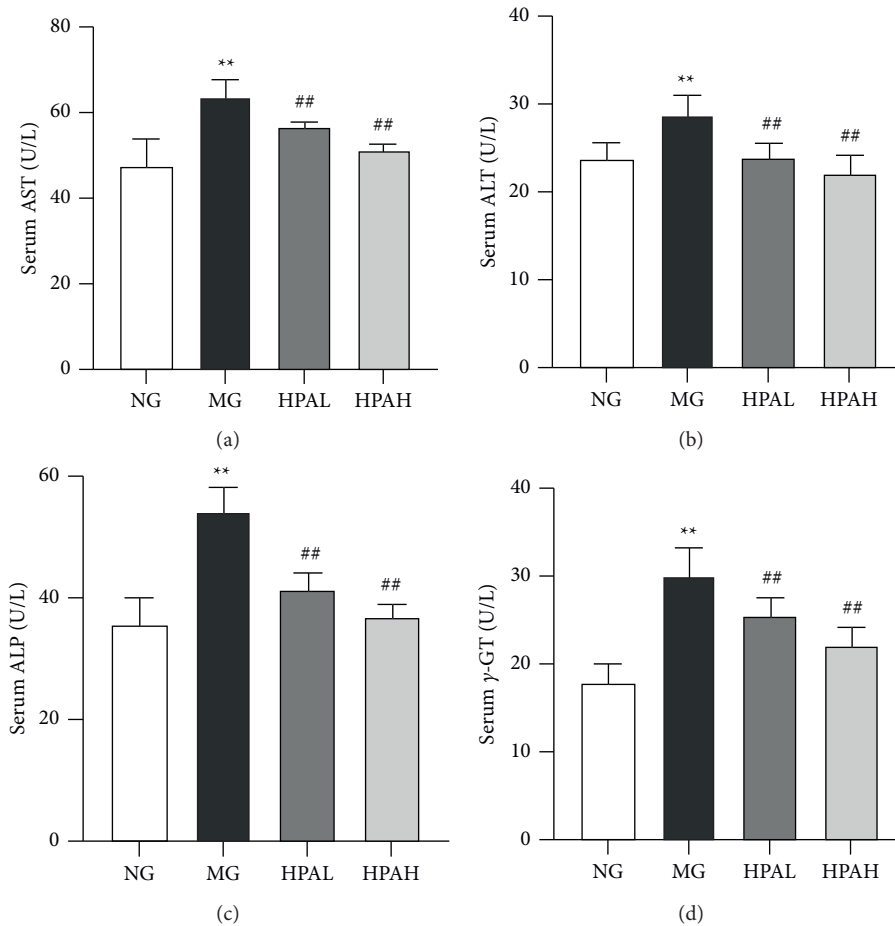
FIGURE 2: Effect of HPA on the hepatic function in ALD mice. (a) Serum AST; (b) serum ALT; (c) serum ALP; (d) serum γ-GT. Data were expressed as mean $\pm$ SD ($n = 12$). $^{**}p < 0.01$, versus NG; $^{\#}p < 0.05$ and $^{\#\#}p < 0.01$, versus MG.

by H&E and Masson and pathological observations were performed. As presented in Figure 6, the structure of hepatocytes and the arrangement of hepatic cords in the NG were normal, and there was no edema and inflammatory infiltration. At the same time, there was no accumulation of collagen fibers in liver tissue. However, the structure of hepatocytes and hepatic cords of alcohol-fed mice were disordered, and there was obvious inflammatory cell infiltration. At the same time, hepatocytes were accompanied by severe accumulation of collagen fibers. After the intervention of HPA, the structure of hepatocytes and hepatic cords was not arranged neatly; there were a small amount of inflammatory cell infiltration and collagen fibers accumulated. But compared with the MG, it had obvious improvement effect.

3.8. Effects of HPA on the Changes of the Gut Microbiota Composition in ALD Mice. In Figure 7(a), the Venn chart shows that the NG, MG, HPAL, and HPAH had a total of 104 OTUs at the genus level. Figures 7(b) and 7(c) show the composition of intestinal flora in each group of mice at the genus and phylum levels. At the genus level (Figure 7(c)), the dominant bacteria in the NG mice were

norank_f_Muribaculaceae and *Lactobacillus*, accounting for 29.36% and 21.25% respectively. While, in the MG, the dominant bacteria were *Lactobacillus* (35.24%), *norank_f_Muribaculaceae* (25.77%), and *Faecalibaculum* (5.80%). After being treated with HPA, the abundance of *Feacalibaculum* and *norank_f_Muribaculaceae* were decreased to some extent, and the abundance of *Prevotellaceae* was increased (versus MG). At the phylum level (Figure 7(b)), the abundance of Firmicutes in MG was significantly increased, and the content of *Bacteroidota* was decreased (versus NG). Compared with the MG, the abundance of Firmicutes was decreased, and the *Verrucomicrobiota* was increased.

The correlation between gut microbial flora and biochemical indicators is shown in Figure 7(d). There were both positive and negative correlations between serum lipids indexes and each colony. The *Romboutsia* was positively correlated with AST and hepatic TC ($p \leq 0.001$). The relative abundance of *Turicibacter* was significantly positively correlated with IL-6, and it was negatively correlated with SOD ($p \leq 0.001$). Both *unclassified_k__norank_d__Bacteria* and *Bifidobacterium* showed positive correlation with serum LDL-C, while *norank_f__Erysipelotrichpaceae, norank_-f__Lachnospiraceae,* and *Colidextribacter* were negatively
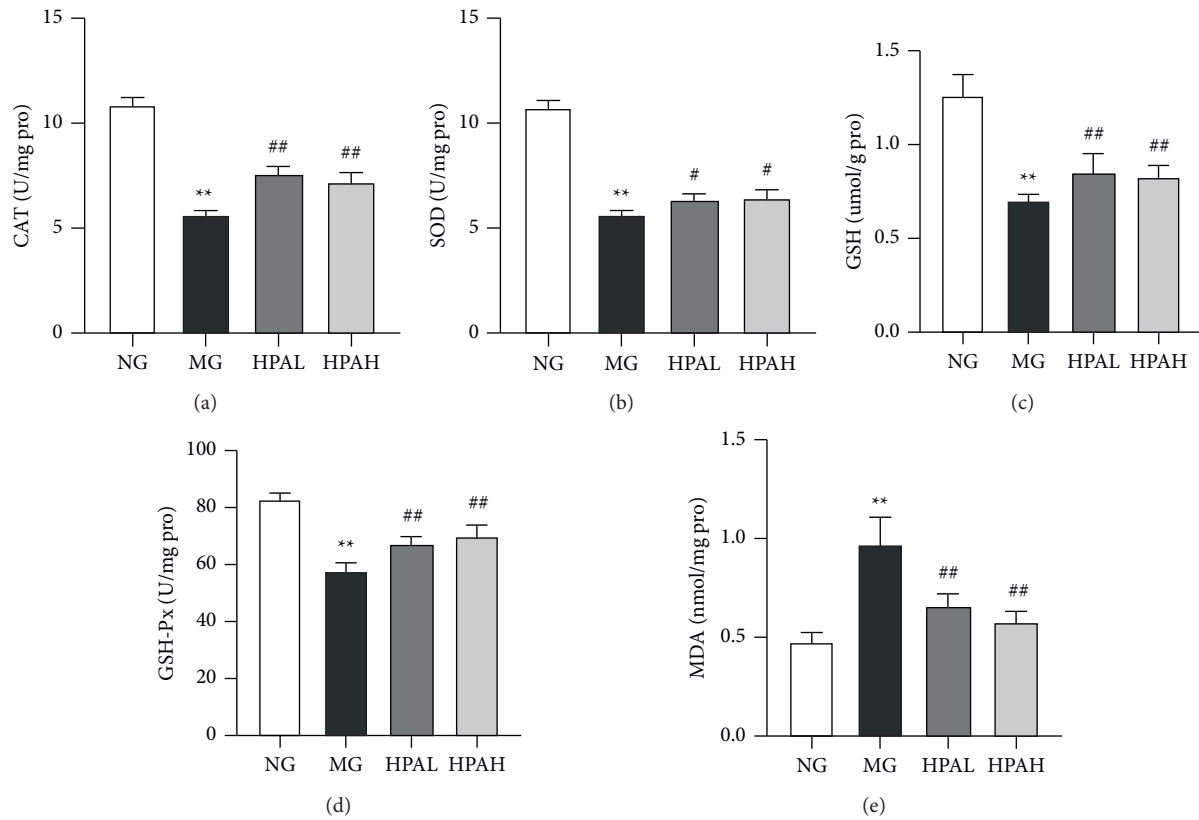
FIGURE 3: Effect of HPA on the antioxidant capacities in ALD mice. (a) CAT activity; (b) SOD activity; (c) GSH activity; (d) GSH-Px activity; (e) MDA level. Data were expressed as mean ± SD ($n = 12$). **$p < 0.01$, versus NG; #$p < 0.05$ and ##$p < 0.01$, versus MG.
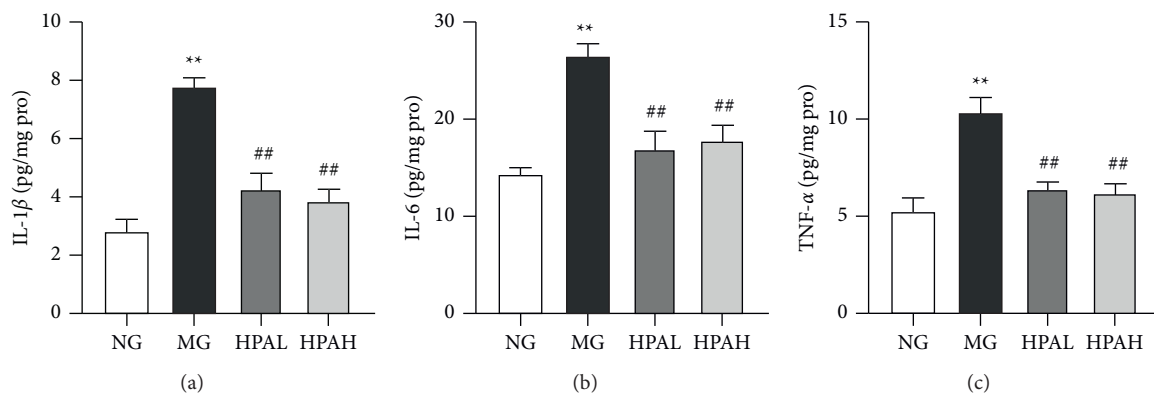
FIGURE 4: Effect of HPA on inflammation response in ALD mice. (a) Hepatic IL-1β; (b) hepatic IL-6; (c) hepatic TNG-α. Data were expressed as mean ± SD ($n = 12$). **$p < 0.01$, versus NG; #$p < 0.05$ and ##$p < 0.01$, versus MG.

correlated with serum LDL-C ($p \leq 0.001$). *Colidextribacter* was negatively correlated with TNF-α and hepatic FFA ($p \leq 0.001$). The relative abundance of *Roseburia* was obviously negatively correlated with ALP ($p \leq 0.001$).

4. Discussion

ALD is the leading cause of global liver disease, and its risk increases with increased dose and duration of alcohol consumption [22, 23]. Some scholars have pointed out that oxidative stress and inflammatory cytokines could directly

or indirectly make the development of ALD more serious [24, 25]. In this study, the alcohol-induced ALD mice model was established. The purpose of experiment was to explain the mechanism of HPA to improve ALD in mice by studying detected liver index, blood lipids, oxidation markers, and inflammatory factors. In addition, the regulatory effect of HPA on intestinal microflora in ALD mice was also investigated.

The final weight, food intake, and hepatic index in the MG were significantly different from those in the NG (Table 1). After treatment with high-dose HPA, the liver

Figure 5: Effect of HPA on oxidative stress and inflammation-related gene expression in ALD mice. (a) *Keap*1; (b) *Nfe*2l2; (c) *Nqo*1; (d) *Homx*1; (e) *Tlr*4; (f) *Myd*88; (g) *Nfkb*1. Data were expressed as mean ± SD ($n = 12$). $^{**}p < 0.01$, versus NG; $^{##}p < 0.01$, versus MG.
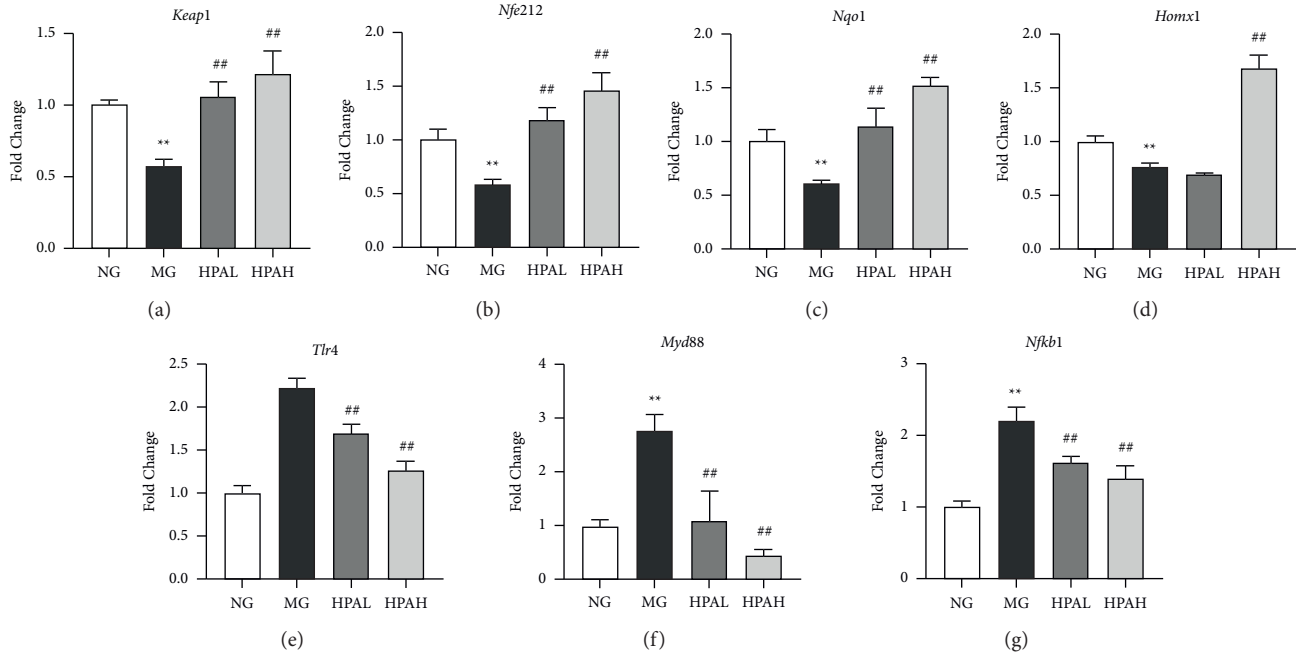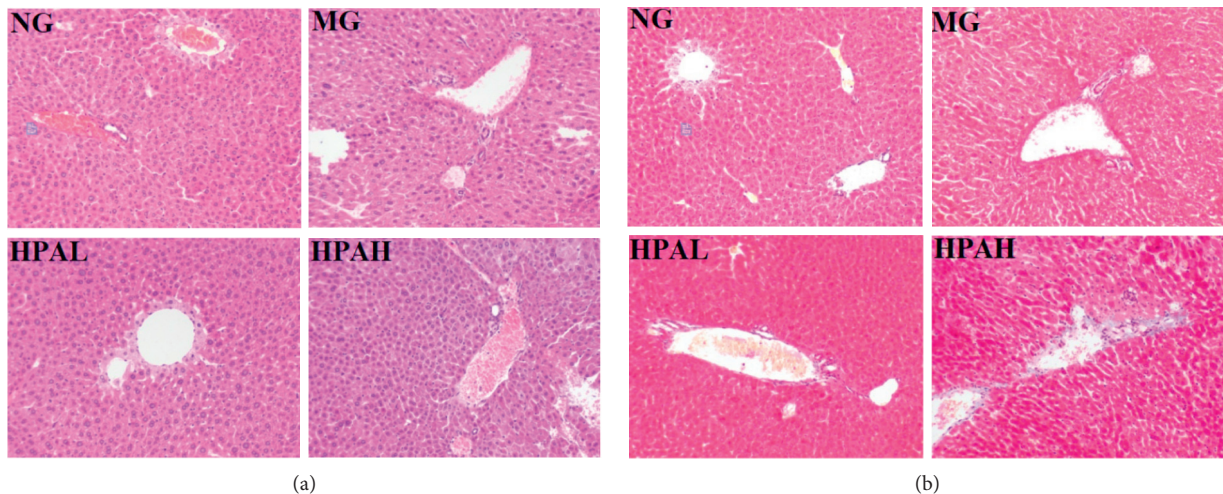

Figure 6: Histopathological detection of livers in ALD mice. (a) H&E staining in liver (×200 magnification); (b) Masson staining in liver (×200 magnification).

index was obviously reduced (versus MG). However, there was no significant change in these indexes between the HPAL and the MG. This shows that the liver index decreases with the increase of the HPA.

Some studies have shown that alcoholic liver injury could cause excessive accumulation of lipids in serum and liver, resulting in dyslipidemia in the body and the formation of alcoholic fatty liver [26, 27]. The current results showed that both high-dose and low-dose HPA could significantly improve the abnormalities of serum lipids and liver lipids (TC, TG, and FFA) caused by alcohol (versus MG, Figures 1(a)–1(h)). HPA could obviously reduce the content of LDL-C and increased the content of HDL-C; this result

was consistent with the study of Sadeghi et al. [28]. High-dose HPA had the best effect in improving blood lipids.

The activities of AST, ALT, ALP, and γ-GT will increase with alcohol intake, thus aggravating the degree of liver injury, so they are important indicators for evaluating liver function [29, 30]. The results showed that all treatment groups could clearly reduce the levels of the above four indexes (Figure 2). Therefore, HPA could improve liver dysfunction cause by alcohol, and the improvement effect of high-dose HPA was the best.

Oxidative stress refers to the imbalance between reactive oxygen species and antioxidants, which can be exacerbated by excessive alcohol intake [25, 31]. In a normal
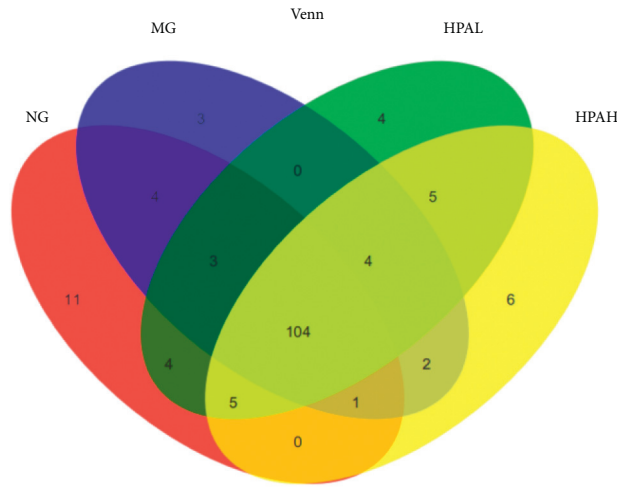
(a)
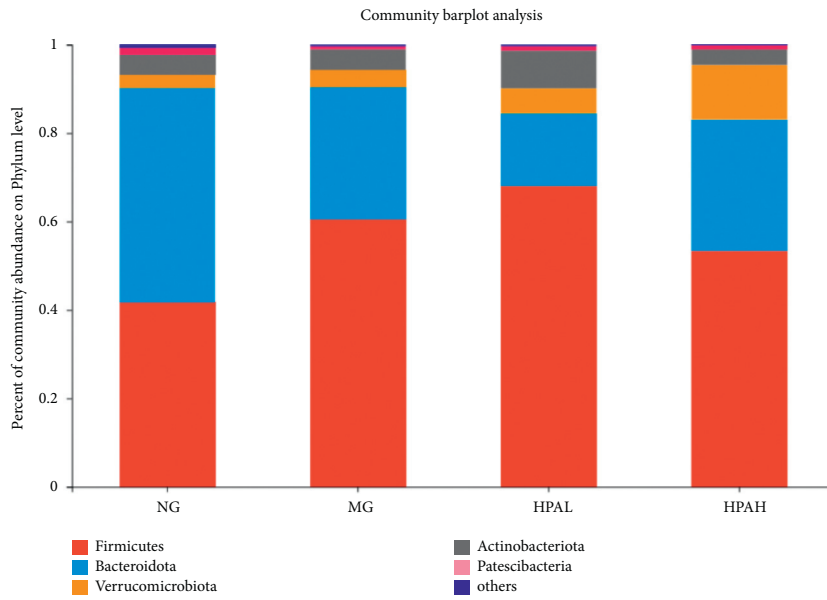
(b)

Figure 7: Continued.

(c)

FIGURE 7: Continued.

Spearman Correlation Heatmap
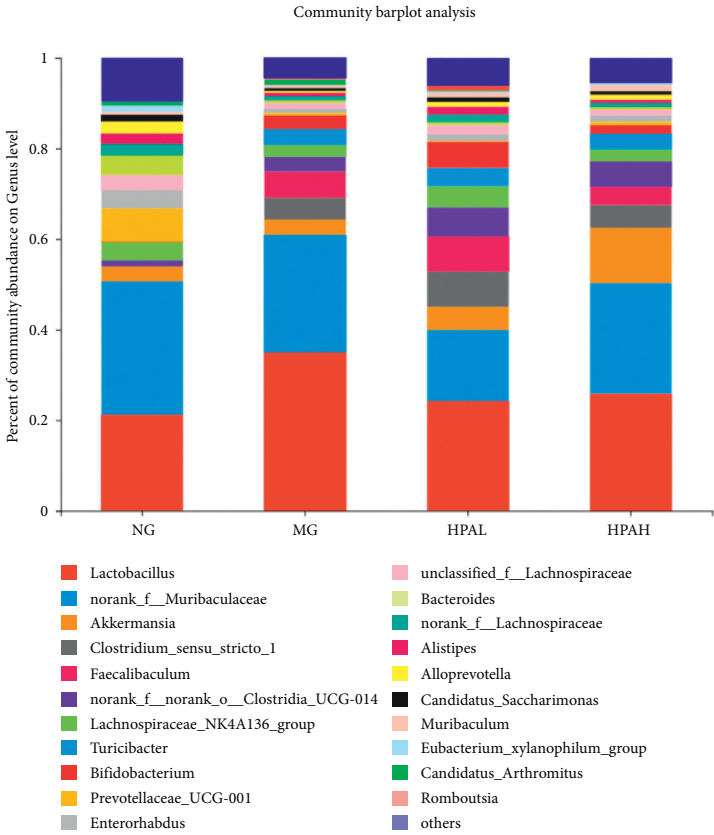
(d)
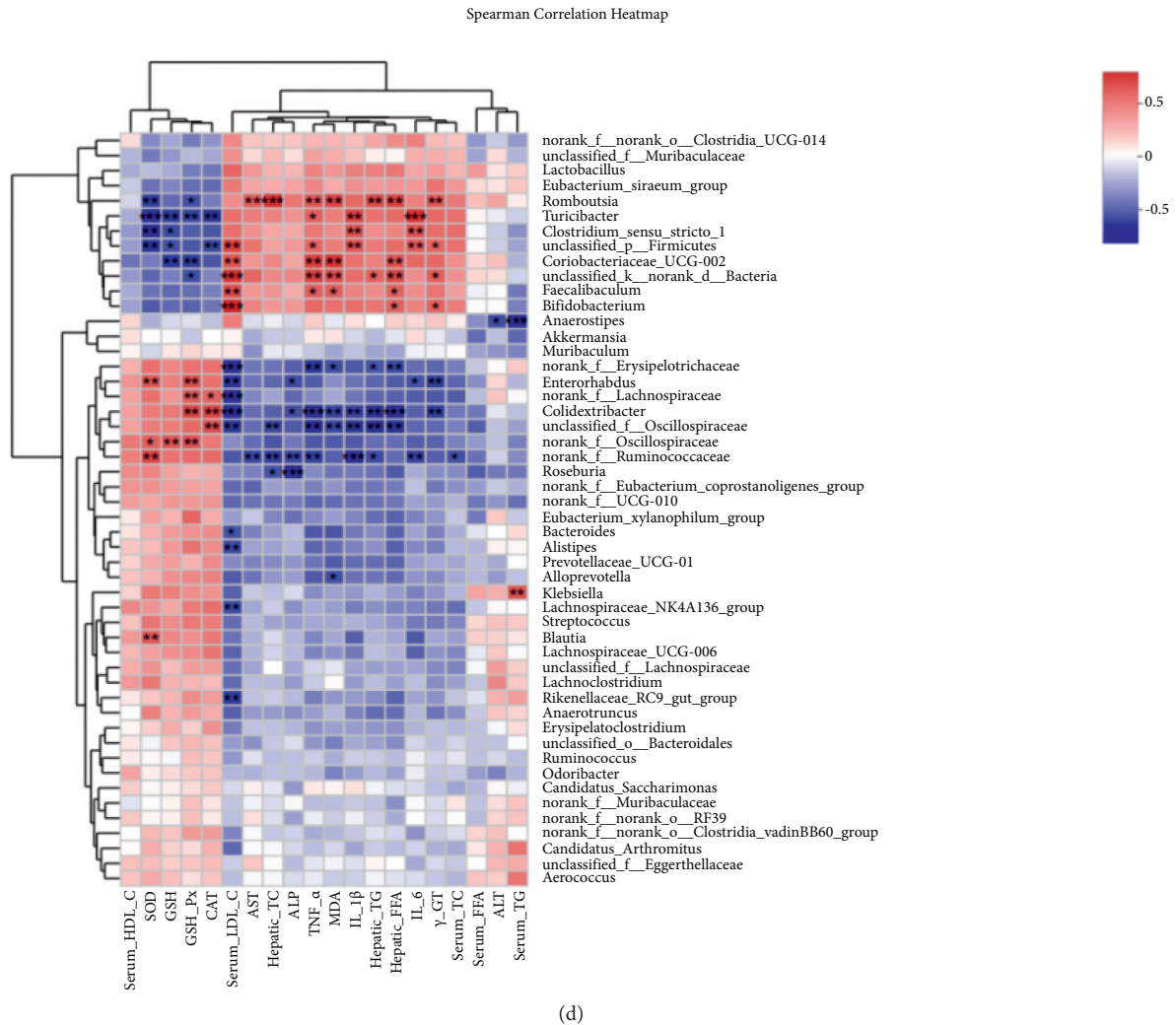
Figure 7: Effects of HPA on the changes of the colonic microbiota composition in ALD mice. (a) Venn diagrams of HPA; (b) percent of community abundance at phylum level; (c) percent of community abundance at genus level; (d) heatmap of spearman's correlation analysis of the biological parameters and relative abundance of colonic microbiota at species level. $^{***}p \leq 0.001$ and $^{**}p \leq 0.01$.

physiological environment, antioxidants are present in human cells to eliminate harmful free radicals, such as CAT, SOD, and GSH [32]. KEAP1/NRF2 is a classical oxidative stress pathway, in which NRF2 is a key transcription factor in the process of oxidative stress [33, 34]. After NFR2 is isolated into the nucleus, it binds to the ARE site to activate the expression of downstream *Hmox*-1 and *Nqo*1 gene, thus increasing the production of antioxidant enzymes and regulating the level of oxidative stress [35]. Figure 3 shows that the levels of oxidative stress markers were significantly increased in all treatment groups (versus MG). Interestingly, the low-dose HPA had a good effect on CAT and GSH levels; the high-dose HPA had the good effect on SOD and GSH-Px. In addition, HPA could obviously reduce the level of MDA in alcohol-treated mice (versus MG). At the genetic level, HPA could apparently enhance the expression of antioxidant genes (Figures 5(a)– 5(d)), so as to improve the effects on oxidative stress caused by ALD.

Continuous intake of alcohol activates proinflammatory cytokines, leading to liver inflammation [36]. When NF-κB is transferred from the cytoplasm to the nucleus, it releases inflammatory mediators, including IL-1β, IL-6, and TNF-α [37]. These inflammatory mediators disrupt the balance between proinflammatory and anti-inflammatory factors, so they play an important role in the pathogenesis of ALD [38]. Excessive ethanol intake will increase the level of toxin in the body; the TLR4 was activated and then the expression level of *Myd*88 gene signal pathway was increased, leading to liver inflammation [39]. In particular, the levels of IL-1β, IL-6, and TNF-α in alcohol-treated mice decreased significantly after HPA treatment (Figures 4(a)–4(c)). In the report of Liao et al. [17], HPA also reduced the inflammatory cytokines in alcohol-induced ALD mice, which is consistent with our results. In Figures 6(a) and 6(b), the expression of genes related to inflammation was decreased in all treatment groups, and the improvement effect of high-dose HPA was the best.

It has been reported that long-term alcohol intake can lead to a disorder in the abundance of intestinal microflora [30]. In the intestinal microflora, there have been beneficial and harmful bacteria. Among them, *Faecalibaculum* is a representative genus of intestinal bacteria in alcoholic liver injury, which has the effect of promoting inflammation [40]. *norank_f_Muribaculaceae* has a great relationship with human obesity; the higher its abundance is, the thinner the person is [41]. *Akkermansia* can reduce intestinal permeability, and as its abundance increases, so does the content of lipopolysaccharide [42]. In this experiment, the results showed that the abundance of harmful bacteria (*norank_f_Muribaculaceae*, *Faecalibaculum*, and *unclassified_p_Firmicutes*) in alcohol-treated mice was increased. After treatment with HPA, the harmful bacteria abundance was decreased, and the beneficial bacteria (*Akkermansia*) was increased. The results showed that HPA could improve the intestinal microbial disorder caused by alcohol by changing the abundance of intestinal flora.

In this study, we found that HPA could reduce the indexes of serum and liver lipid in alcohol-treated mice. HPA could improve liver inflammation and oxidative stress in ALD mice by promoting or inhibiting the expression of inflammatory factors and antioxidative stress genes. After the ALD mice were treatment by HPA, the beneficial bacteria were increased and harmful bacteria were reduced.

5. Conclusion

In general, HPA could improve the lipid accumulation in serum and liver caused by alcohol and also inhibit the development of inflammatory factors and liver fibrosis. On the contrary, HPA could improve the activities of liver function and oxidation markers and regulate the imbalance of intestinal microflora. Quantitative RT-PCR results showed that HPA could alleviate oxidative stress and inflammation of ALD through two signal pathways: KEAP1/NRF2 and TLR4/MyD88/NF-κB. In addition, high-dose HPA showed a more prominent effect. This project provided a theoretical basis for HPA in the treatment of alcoholic liver disease. At the same time, it provides a certain theoretical basis for the subsequent exploration of the functions of the monomer components in HPA. It also provides new ideas for the treatment or prevention of ALD. In the future, we will study the effective monomer components in HPA.

Data Availability

The data used to support the findings of this study are available from the corresponding author upon request.

Disclosure

Jingxuan Zhou and Nanhai Zhang share first authorship.

Conflicts of Interest

The authors declare that the research was conducted in the absence of any commercial or financial relationships that could be construed as potential conflicts of interest.

Authors' Contributions

JZ and NZ performed the experiments and wrote the manuscript. LZhao revised the manuscript. WW and JL supervised the project. FZ and LZhan contributed to conception and design the project. FZ, JL, LZhan, and M.M. Soliman contributed to acquisition of the financial support for the project. All authors have read and agreed to the published version of the manuscript. Jingxuan Zhou and Nanhai Zhang have contributed equally to this work.

Acknowledgments

References

[1] J. Rehm, A. V. Samokhvalov, and K. D. Shield, "Global burden of alcoholic liver diseases," *Journal of Hepatology*, vol. 59, no. 1, pp. 160–168, 2013.

[2] J. S. Bajaj, "Alcohol, liver disease and the gut microbiota," *Nature Reviews Gastroenterology & Hepatology*, vol. 16, no. 4, pp. 235–246, 2019.

[3] P. Mathurin and R. Bataller, "Trends in the management and burden of alcoholic liver disease," *Journal of Hepatology*, vol. 62, no. 1, pp. S38–S46, 2015.

[4] Y. Lv, K. F. So, and J. Xiao, "Liver regeneration and alcoholic liver disease," *Annals of Translational Medicine*, vol. 8, no. 8, Article ID 567, 2020.

[5] L. Zhao, A. Mehmood, D. Yuan et al., "Protective mechanism of edible food plants against alcoholic liver disease with special mention to polyphenolic compounds," *Nutrients*, vol. 13, no. 5, Article ID 1612, 2021.

[6] V. Rosato, L. Abenavoli, A. Federico, M. Masarone, and M. Persico, "Pharmacotherapy of alcoholic liver disease in clinical practice," *International Journal of Clinical Practice*, vol. 70, no. 2, pp. 119–131, 2016.

[7] A. K. Singal, R. Bataller, J. Ahn, P. S. Kamath, and V. H. Shah, "ACG clinical guideline: alcoholic liver disease," *American Journal of Gastroenterology*, vol. 113, no. 2, pp. 175–194, 2018.

[8] K. K. Auyeung, Q.-B. Han, and J. K. Ko, "Astragalus membranaceus: a Review of its protection against inflammation and gastrointestinal cancers," *The American Journal of Chinese Medicine*, vol. 44, no. 1, pp. 1–22, 2016.

[9] T. Nozaki, J. Minaguchi, K. Takehana, and H. Ueda, "Anti-diabetic activities of traditional Chinese herbal medicine in streptozotocin-induced diabetic rats," *Okajimas Folia Anatomica Japonica*, vol. 93, no. 4, pp. 111–118, 2017.

[10] L. Yang, X. Han, F. Xing et al., "Total flavonoids of astragalus attenuates experimental autoimmune encephalomyelitis by suppressing the activation and inflammatory responses of microglia via JNK/AKT/NFκB signaling pathway," *Phytomedicine*, vol. 80, Article ID 153385, 2021.

[11] W.-Y. Sun, W. Wei, S.-Y. Gui, L. Wu, and H. Wang, "Protective effect of extract fromPaeonia lactifloraandAstragalus membranaceusagainst liver injury induced by Bacillus calmette-guérin and lipopolysaccharide in mice," *Basic and*

Clinical Pharmacology and Toxicology, vol. 103, no. 2, pp. 143–149, 2008.

[12] J. Zhou, N. Zhang, L. Zhao et al., "Astragalus polysaccharides and saponins alleviate liver injury and regulate gut microbiota in alcohol liver disease mice," *Foods*, vol. 10, no. 11, Article ID 2688, 2021.

[13] N. Ramli, K.-Y. Chin, K. Zarkasi, and F. Ahmad, "A review on the protective effects of honey against metabolic syndrome," *Nutrients*, vol. 10, no. 8, Article ID 1009, 2018.

[14] H. Laaroussi, M. Bakour, D. Ousaaid et al., "Protective effect of honey and propolis against gentamicin-induced oxidative stress and hepatorenal damages," *Oxidative Medicine and Cellular Longevity*, vol. 2021, Article ID 9719906, 19 pages, 2021.

[15] N. S. Nayan, M. A. M. Yazid, K. Nallappan et al., "In vitro modulation of endogenous antioxidant enzyme activities and oxidative stress in autism lymphoblastoid cell line (ALCL) by stingless bee honey treatment," *Oxidative Medicine and Cellular Longevity*, vol. 2020, Article ID 4539891, 7 pages, 2020.

[16] M. Xiao, H. Chen, Z. Shi, Y. Feng, and W. Rui, "Rapid and reliable method for analysis of raw and honey-processed astragalus by UPLC/ESI-Q-TOF-MS using HSS T3 columns," *Analytical Methods*, vol. 6, no. 19, pp. 8045–8054, 2014.

[17] J. Liao, C. Li, J. Huang et al., "Structure characterization of honey-processed astragalus polysaccharides and its anti-inflammatory activity in vitro," *Molecules*, vol. 23, no. 1, Article ID 168, 2018.

[18] J. Wu, C. Li, L. Bai et al., "Structural differences of polysaccharides from Astragalus before and after honey processing and their effects on colitis mice," *International Journal of Biological Macromolecules*, vol. 182, pp. 815–824, 2021.

[19] L. Zhao, N. Zhang, D. Yang et al., "Protective effects of five structurally diverse flavonoid subgroups against chronic alcohol-induced hepatic damage in a mouse model," *Nutrients*, vol. 10, no. 11, Article ID 1754, 2018.

[20] H.-Y. Koo, M. A. Wallig, B. H. Chung, T. Y. Nara, B. H. S. Cho, and M. T. Nakamura, "Dietary fructose induces a wide range of genes with distinct shift in carbohydrate and lipid metabolism in fed and fasted rat liver," *Biochimica et Biophysica Acta-Molecular Basis of Disease*, vol. 1782, no. 5, pp. 341–348, 2008.

[21] S. C. Taylor, K. Nadeau, M. Abbasi, C. lachance, M. Nguyen, and J. Fenrich, "The ultimate qPCR experiment: producing publication quality, reproducible data the first time," *Trends in Biotechnology*, vol. 37, no. 7, pp. 761–774, 2019.

[22] G. E. Arteel, "Liver-lung axes in alcohol-related liver disease," *Clinical and Molecular Hepatology*, vol. 26, no. 4, pp. 670–676, 2020.

[23] X. Chi, C. Q. Pan, S. Liu, D. Cheng, Z. Cao, and H. Xing, "Regulating intestinal microbiota in the prevention and treatment of alcohol-related liver disease," *Canadian Journal of Gastroenterology and Hepatology*, vol. 2020, Article ID 6629196, 10 pages, 2020.

[24] H. Kawaratani, T. Tsujimoto, A. Douhara et al., "The effect of inflammatory cytokines in alcoholic liver disease," *Mediators of Inflammation*, vol. 2013, Article ID 495156, 10 pages, 2013.

[25] H. K. Tan, E. Yates, K. Lilly, and A. D. Dhanda, "Oxidative stress in alcohol-related liver disease," *World Journal of Hepatology*, vol. 12, no. 7, pp. 332–349, 2020.

[26] H. Chen, F. Shen, A. Sherban et al., "DEP domain-containing mTOR-interacting protein suppresses lipogenesis and ameliorates hepatic steatosis and acute-on-chronic liver injury in alcoholic liver disease," *Hepatology*, vol. 68, no. 2, pp. 496–514, 2018.

[27] Y. Song, X. Wu, D. Yang et al., "Protective effect of andrographolide on alleviating chronic alcoholic liver disease

in mice by inhibiting nuclear factor kappa B and tumor necrosis factor Alpha activation," *Journal of Medicinal Food*, vol. 23, no. 4, pp. 409–415, 2020.

[28] F. Sadeghi, M. Akhlaghi, and S. Salehi, "Adverse effects of honey on low-density lipoprotein cholesterol and adiponectin concentrations in patients with type 2 diabetes: a randomized controlled cross-over trial," *Journal of Diabetes and Metabolic Disorders*, vol. 19, no. 1, pp. 373–380, 2020.

[29] Y. Sutoh, T. Hachiya, Y. Suzuki et al., "ALDH2 genotype modulates the association between alcohol consumption and AST/ALT ratio among middle-aged Japanese men: a genome-wide G×E interaction analysis," *Scientific Reports*, vol. 10, no. 1, Article ID 16227, 2020.

[30] M. Zahid, M. Arif, M. A. Rahman, and M. Mujahid, "Hepatoprotective and antioxidant activities of Annona squamosa seed extract against alcohol-induced liver injury in Sprague Dawley rats," *Drug and Chemical Toxicology*, vol. 43, no. 6, pp. 588–594, 2020.

[31] A. Michalak, T. Lach, and H. Cichoż-Lach, "Oxidative stress-a key player in the course of alcohol-related liver disease," *Journal of Clinical Medicine*, vol. 10, no. 14, Article ID 3011, 2021.

[32] L. Zhao, A. Mehmood, M. M. Soliman et al., "Protective effects of ellagic acid against alcoholic liver disease in mice," *Frontiers in nutrition*, vol. 8, Article ID 744520, 2021.

[33] J. Sun, Z. Hong, S. Shao et al., "Liver-specific Nrf2 deficiency accelerates ethanol-induced lethality and hepatic injury in vivo," *Toxicology and Applied Pharmacology*, vol. 426, Article ID 115617, 2021.

[34] M. Yamamoto, T. W. Kensler, and H. Motohashi, "The KEAP1-NRF2 System: a thiol-based sensor-effector apparatus for maintaining redox homeostasis," *Physiological Reviews*, vol. 98, no. 3, pp. 1169–1203, 2018.

[35] A. Loboda, M. Damulewicz, E. Pyza, A. Jozkowicz, and J. Dulak, "Role of Nrf2/HO-1 system in development, oxidative stress response and diseases: an evolutionarily conserved mechanism," *Cellular and Molecular Life Sciences*, vol. 73, no. 17, pp. 3221–3247, 2016.

[36] N. Hosseini, J. Shor, and G. Szabo, "Alcoholic hepatitis: a review," *Alcohol and Alcoholism*, vol. 54, no. 4, pp. 408–416, 2019.

[37] Q.-H. Huang, L.-Q. Xu, Y.-H. Liu et al., "Polydatin protects rat liver against ethanol-induced injury: involvement of CYP2E1/ROS/Nrf2 and TLR4/NF-κB p65 pathway," *Evidence-based Complementary and Alternative Medicine*, vol. 2017, Article ID 7953850, 14 pages, 2017.

[38] B. Gao, "Hepatoprotective and anti-inflammatory cytokines in alcoholic liver disease," *Journal of Gastroenterology and Hepatology*, vol. 27, pp. 89–93, 2012.

[39] S. Patel, R. Behara, G. Swanson, C. Forsyth, R. Voigt, and A. Keshavarzian, "Alcohol and the intestine," *Biomolecules*, vol. 5, no. 4, pp. 2573–2588, 2015.

[40] V. B. Dubinkina, A. V. Tyakht, V. Y. Odintsova et al., "Links of gut microbiota composition with alcohol dependence syndrome and alcoholic liver disease," *Microbiome*, vol. 5, no. 1, Article ID 141, 2017.

[41] D. Hou, Q. Zhao, L. Yousaf, J. Khan, Y. Xue, and Q. Shen, "Consumption of mung bean (Vigna radiata L.) attenuates obesity, ameliorates lipid metabolic disorders and modifies the gut microbiota composition in mice fed a high-fat diet," *Journal of Functional Foods*, vol. 64, Article ID 103687, 2020.

[42] J. Fan, Y. Wang, Y. You et al., "Fermented ginseng improved alcohol liver injury in association with changes in the gut microbiota of mice," *Food & Function*, vol. 10, no. 9, pp. 5566–5573, 2019.

WILEY | Hindawi

Research Article

Extraction, Purification, Optimization, and Application of Galactomannan-Based Edible Coating Formulations for Guava Using Response Surface Methodology

Ammara Ainee [ID],[1] **Sarfraz Hussain,**[1] **Muhammad Nadeem,**[1] **Asaad R. Al-Hilphy,**[2] **and Azhari Siddeeg** [ID][3]

[1]*Institute of Food Science and Nutrition (IFSN), University of Sargodha, Sargodha, Pakistan*
[2]*Department of Food Science, College of Agriculture, University of Basrah, Basrah, Iraq*
[3]*Department of Food Engineering and Technology, Faculty of Engineering and Technology, University of Gezira,*
 Wad Medani, Sudan

Correspondence should be addressed to Ammara Ainee; ammara.ainee@uos.edu.pk and Azhari Siddeeg;
azhari_siddeeg@uofg.edu.sd

Galactomannan from fenugreek and guar seeds were extracted, purified, and used in edible coatings, optimized via response surface methodology. The results showed that the emulsifying capacity and stability of fenugreek galactomannan (FG) and guar galactomannan (GG) increased with increase in the concentration of galactomannan up to 0.5–1%. The average optimized values of FG and GG in edible coatings were predicted to be 1.71% and 2.11% for weight loss, 0.72% and 2.14% for firmness, 1.02% and 1.44% for TSS, 0.83% and 1.36% for pH, 1.03% and 1.44% for acidity, respectively. Significant decrease in weight loss and maximum retention of firmness was observed in coated guava. The TSS increased up to a certain storage period in all treatments and decreased as the storage period progressed, whereas pH exhibited an increasing trend while a significant decrease in acidity was observed. The findings revealed that the shelf life of guava could considerably be improved by incorporating 1.24% galactomannan from GG and 1.01% from FG in the edible coating.

1. Introduction

Guava (*Psidium guajava* L.) is a well-renowned fruit in Pakistan [1]. Guava quickly softens and thus has poor shelf stability that is susceptible to shipping and storage damage [2–4]. The guava's shelf life varies with the ambient temperature from three to five days [5]. Between harvest and consumption, significant losses are rendered in the quality and quantity of fruits and vegetables [6]. Food packaging innovations can help alleviate changing market demands such as consumer choice for safe and high-quality food items, and the decrease in environmental adverse effects of food packaging [7]. The need for a replacement for synthetic packaging with bio-based polymers is important.

Edible coatings can significantly increase shelf life and enhance food quality by the reduction in weight and moisture loss, creating barrier properties against oil, gas, aroma, and flavor. The preservation of mechanical, rheological attributes, food color, and appearance of food are also improved. It is an environmentally friendly invention [6, 8]. Edible coatings generate a protective environment around the fruits and vegetables [9].

Galactomannans, water-soluble heterogeneous polysaccharides found in many leguminous seeds and mainly consists of mannose and galactose. They differ from each other by the mannose/galactose ratio. Fenugreek, guar gum, locust bean gum, and alfalfa are the most common sources of galactomannans [10]. It finds applications in different sectors (pharmaceutical, textile, cosmetics, biomedical, and food) due to its versatile characteristics and nontoxic effect. In the food industry, galactomannans are extensively used in film/coating formulation, dietary,

powdered and baby foods, soups, seasoning, sauces, meat, bakery, and dairy products [11].

Extraction and utilization of polysaccharides from plant and animal sources have gained significant attention in recent times because of their stability, biodegradability, and ecologically friendly. Guar gum is a natural polysaccharide [12]. Guar gum is extracted from the endosperm of guar seeds belongs to the family Leguminosae and is commonly known as guar, guaran, or cluster bean [13]. The chief suppliers of guar throughout the world are Pakistan and India, where 80% of the total guar is produced [14]. Guar gum is expensive and forms a viscous gel in cold water, so it is extensively used in different food products and industries as a stabilizer as well as an emulsifying and thickening agent [15].

Fenugreek (*Trigonella foenum-graecum*) is a popular spice consumed globally and commonly known as "Methi" [16]. It is widely grown in Pakistan, Turkey, China, Egypt, India, and the Mediterranean [17]. The seeds of fenugreek are rich in gum, fiber, alkaloids, flavonoids, saponins, and volatile compounds [18]. The plant seeds are a good source of polysaccharides [19]. In the past, fenugreek use in the manufacture of food has been increased by its emulsifying, thickening, and stabilizing properties in many food products [20].

The ripening process continues in guava even after detaching from trees and respire at a higher rate due to climacteric in nature. Due to short shelf life, marketing and subsequent storage of guava are difficult. Therefore, some treatments that can extend shelf life and conserve the quality of guava fruits are required (Anjum et al.) [21]. The study of postharvest physiology is of immense importance. The shelf life of fresh fruit is short at room temperature without any pre or posttreatment during storage. Reduction in losses and waste of fresh guava is essential for the fact that this fruit provides vital nutrients. Keeping in view the above-mentioned facts, current research work was carried out to improve the quality characteristics and extend the shelf life of local variety (Gola) of guava during the storage period by optimization of polysaccharides levels in edible coatings through the response surface methodology (RSM). Thus optimum galactomannan-based coating formulation was the main objective of the study and to study the effect of coating on quality attributes as well as shelf stability of guava.

2. Materials and Methods

2.1. Raw Materials. Fenugreek and guar seeds were purchased from the local market of Sargodha, Punjab, Pakistan. Freshly picked guava cv gola, for coating purposes, was purchased from guava orchard at Sargodha district, Punjab province (Figure 1). The ripe fruits were selected along with the stem, uniform size, color, free of any physical damage and fungal infestation, further followed by manual sorting and grading in the laboratory. Olive oil (extra light) and glycerin were purchased from the market at Sargodha. Chemicals including ethanol, isopropanol, and NaCl were purchased from Sigma-Aldrich, Germany available in the local market.

2.2. Extraction and Purification of Polysaccharide from Guar and Fenugreek Seeds. The seeds of guar and fenugreek were soaked separately in water overnight at room temperature. The polysaccharide extraction and purification were carried out according to the method described by [19]. Cleaned whole seeds were crushed and immersed for 24 hrs at 50°C in a 5% salt solution having 3 pH adjusted by acetic acid. The polysaccharides were extracted separately by muslin cloth. Crude gums were purified by the addition of IPA spirit (a blend of 10% isopropanol and 90% ethanol) in a ratio of 3 : 1 by volume with continuous stirring followed by centrifugation at 6000 rpm for 7 min. The white precipitate obtained from both gums was filtered by muslin cloth. The pomace of seeds was again immersed in a 5% salt solution of 3 pH until the maximum gum was extracted following the purification procedure. The purified polysaccharides were dried in an oven at 50°C for 24 hrs. The purified dried polysaccharide was weighed and stored in airtight jars at a cool dry place for further utilization and analysis (supplementary Figures 1–6).

2.2.1. Emulsifying Properties. The emulsifying capacity (EC) and stability of the polysaccharides were determined according to [19] with some minor modifications. Suspension (60 ml) of each gum was prepared with an increase in the galactomannan concentration (0.5, 0.75, 1.0% w/v), at the same commercial olive oil level (6 ml) homogenized at 10,000 rpm for 1 min. The suspensions were then centrifuged at 1300 rpm for 5 min. EC was calculated as

$$\text{emulsion capacity (\%)} = \frac{\text{emulsion volume}}{\text{total volume}} \times 100. \quad (1)$$

Emulsion stability (ES) against high temperatures were determined in the emulsions that were heated in a water bath at 80°C for 30 min and centrifuged at 1300 rpm for 5 min. The ES was calculated as

$$\text{emulsion stability (\%)} = \frac{\text{final emulsion volume}}{\text{initial volume}} \times 100. \quad (2)$$

2.3. Edible Coating Formulation. The coatings were prepared following the protocol of Vishwasrao and Ananthanarayan [2] with minor modifications. Purified polysaccharides extracted from fenugreek and guar seeds were used in the formulations of coating as a source of thickening, gelling, and stabilizing agent, glycerol as a plasticizer, olive oil as hydrophobic phase, and distilled water to make the edible coating. Measured amounts of guar galactomannan (GG) and fenugreek galactomannan (FG) powder were dissolved in 100 ml distilled water according to the treatment plan created by the central composite design and stirred by hot plate magnetic stirrers to form a gel, and then emulsifying agent (glycerol) was added. After the addition of oil, the mixture was homogenized for 5 min to get physically and chemically stable, inert, and nongreasy emulsion (Table 1). Emulsions prepared were cooled at room temperature and were kept in clean, dried, and airtight glass bottles for further application for one week.

FIGURE 1: The geographic location of procurement of guava fruits.

TABLE 1: Edible coating formulations from fenugreek galactomannan and guar galactomannan through central composite design.

Treatments	Fenugreek galactomannan (g/100 ml)	Guar galactomannan (g/100 ml)	Olive oil (ml/100 ml)	Glycerin (ml/100 ml)	Distilled water (ml/100 ml)
EC_0			Control		
EC_1	1.00	1.5	5	0.3	92.2
EC_2	1.00	0.80	5	0.3	92.9
EC_3	0.30	1.50	5	0.3	92.9
EC_4	1.00	1.50	5	0.3	92.2
EC_5	1.00	2.20	5	0.3	91.5
EC_6	1.71	1.50	5	0.3	91.49
EC_7	1.00	1.50	5	0.3	92.2
EC_8	0.50	1.00	5	0.3	91.2
EC_9	1.00	1.50	5	0.3	92.2
EC_{10}	1.00	1.50	5	0.3	92.2
EC_{11}	1.50	1.00	5	0.3	92.2
EC_{12}	0.50	2.00	5	0.3	92.5
EC_{13}	1.00	1.50	5	0.3	92.5
EC_{14}	1.5	2.00	5	0.3	91.2

2.4. Preparation of Fruit Samples. Selected guavas were washed, rinsed, dried, and dipped in chlorinated water (chlorine level up to 150 ppm). After that guavas were divided into ten lots, each carrying an equal number (15 No) of fruits, and were coated by emulsion, prepared according to the treatment formulation except EC_0 (control), via the dipping method. Each fruit was dipped for one minute, twisted, and placed in baskets, then allowed to dry for 20 minutes at room temperature. Before dipping guava in the solution, the mixture was homogenized to get a uniformly dispersed emulsion. The coated guavas were placed in baskets at the storage temperature of $24 \pm 5°C$ and stored for about 20 days.

2.5. Physico-Chemical Analysis. The weight of each coated and uncoated fruit was recorded by the electronic weighing balance, on 1st day of the experiment and after every 5 days interval for 20 days and the weight loss percentage were calculated. The fruit firmness was measured by using a penetrometer (model GY-2, Walfront, USA) and expressed as kg/cm^2. A refractometer (RHB-32 ATC model, China)

was used for the determination of total soluble solids (TSS) of the guava fruit juice and expressed as Brix. acidity (acetic acid) was determined by titrating the juice against 0.1 M sodium hydroxide solution and six drops of phenolphthalein until the color changed to faint pink color. The volume of NaOH used was noted to get the value of acid (in grams per 100 mL). A digital calibrated pH meter (PH-8414 model) was used to measure the pH of juice according to the standard method [22]. The experiment was performed in triplicate; three fruits were taken each time after every five days.

2.6. Statistical Analysis. Multiple regressions to fit second-order polynomial equation through response surface methodology was applied to estimate the responses of fenugreek and guar gum used as independent variables during storage. Central composite design was used to optimize the levels of independent variables using Minitab 16 statistical software. Response surface graphs were generated to see the effects of independent variables on dependent variables. The data were analyzed by Nadeem et al. [23].

3. Results and Discussion

3.1. Emulsifying Properties.

Due to high surface energy on the contact surface of oil and water molecules, thermodynamic emulsions are unstable and can result in the complete separation of two immiscible layers by coalescence; therefore, the stability of emulsions was examined. Emulsions prepared with high concentrations of galactomannan have been found to be more stable and have higher emulsion capacity [19].

Emulsions containing various concentrations of galactomannan (0.5, 0.75, 1.0% w/v) showed pronounced emulsifying property which increased with increasing galactomannan concentration up to 1.0% but the FG showed slightly lower than GG. The emulsion stability (ES) and emulsion capacity (EC) of guar galactomannan and fenugreek galactomannan are shown in Table 2. GG provided an excellent emulsion stabilization effect during two weeks of storage period at $25°C$ as compared to FG. Moreover, emulsions with 0.5% of GG and FG could even maintain the emulsification stability up to 94% and up to 97% over two weeks, respectively.

As the concentration of polysaccharides increases, the globules become more strongly enclosed in polymeric conformation. Higher polymer concentrations provide good viscosity to the aqueous phase, which further prevents the mobility of the globules and slows their amalgamation. The emulsifying properties of the hydrocolloids are either due to their interface behavior or their viscosity modifying properties that further inhibit the contact of the globules which also allows more time for the polymer to be absorbed in the interface [24].

3.2. Physico-Chemical Properties.

Polysaccharides from guar galactomannan and fenugreek galactomannan were used in different levels to increase the shelf-life of guava. The effect of fenugreek and guar galactomannan on the physicochemical properties of guava fruit during storage (at 0, 5, 10, 15, and 20 days) was assessed. The RSM was applied to estimate the responses of fenugreek and guar galactomannans used as independent variables during storage.

3.3. Weight Loss.

Weight loss in guava during ripening is due to both transpiration and respiration. Weight loss results in textural changes and surface shrinkage that adversely affects the shelf life of climacteric fruits and vegetables. The models were developed for weight loss of guava fruit as affected by independent variables during 20 days storage. The results depicted in Table 3 and Figure 2 revealed the significant effect of fenugreek galactomannan and guar galactomannan on weight loss in guava fruits during 20 days. The linear terms of FG and GG have a statistically significant ($p < 0.05$) effect for weight loss during the storage period. The FG^2 and GG^2 quadratic terms are found significant at 5, 10, 15, and 20 days storage intervals. The coefficients of determination (R^2) were studied as above 90% at most of the storage intervals, therefore it could be assured that models are well fitted and the coefficients of polynomial equations were calculated by

the equations given at the top of each graph (Figure 1). Optimized average values of fenugreek and guar galactomannan in the edible coating were found to be 1.70% and 2.10%, respectively. A decrease in weight loss was observed in edible-coated guava fruits during storage intervals. These results were found parallel to the findings of previously reported studies [25, 26]. Edible coatings reduced the respiration rates, water loss, and oxidation reaction rates by making a semipermeable barrier against oxygen (O_2), carbon dioxide (CO_2), moisture, and solute movement. The cumulative loss in weight increased gradually in all the treatments by advancement in storage duration. Coatings act as a barrier to desiccation and lead to maintained fresh weight of fruits (Khaliq et al.) [27]. Increased concentrations of polysaccharides allowed the formation of a thick layer around the fruit surface which retains firmness by reducing the loss of moisture and gas permeability. In this work, physiological weight loss was probably lower in coated fruits due to inhibited desiccation.

3.4. Firmness.

Firmness is associated with water content and metabolic changes that occur in fruits and it is an important parameter that affects consumer acceptability [28]. The models were developed for the firmness of guava fruit as affected by fenugreek galactomannan and guar galactomannan during 20 days storage (Figure 3). The statistical analysis by applying the analysis of variance technique to the full regression of model (Table 4) shows a significant effect of FG and guar galactomannan. However, linear and quadratic terms of FG and GG are observed to positively change the firmness of fruits at 5, 10, 15, and 20th day of storage intervals, whereas at 1st day of storage have no effect. When the interaction of these two terms (FG $*$ GG) was studied, it was found negative for all storage intervals. The coefficients of determination (R^2) were more than 85%, indicating well-fitted response models. The data showed that FG and guar galactomannan contributed toward firmness in guava fruit at 5 to 20 days storage intervals (Figure 2). For good firmness, optimized average values of fenugreek galactomannan and guar galactomannan in the edible coating were predicted to be 0.72% and 2.14%, respectively. The results showed that the optimized formulation was effective in maintaining the firmness of the guava fruit. The above-given results of firmness were similar to previous study results [29]. Another research reported a few variations in texture changes during the storage period [30]. Moreover, the edible coating is helpful in maintaining firmness [31].

3.5. TSS.

The regression coefficients of variables in models showed that fenugreek galactomannan and guar galactomannan did not contribute toward change in TSS in guava fruits at the start of storage, but after that contributed significantly from 5th to 20 days storage intervals. The effect of linear terms of FG and GG are statistically significant ($p < 0.05$) for TSS at all days of storage intervals except the start of the study (Figure 4 and supplementary Table 1). The X^2 quadratic terms are found significant at 5, 10, 15, and 20 days storage intervals, whereas, the quadratic terms for FG^2

TABLE 2: Emulsion capacity and stability of fenugreek galactomannan and guar galactomannan.

Galactomannan	Concentration (g) (% w/v)	Emulsion capacity (%)	Emulsion stability (%)
Fenugreek	1.0	98.23 ± 0.15	97.17 ± 0.11
	0.75	96.73 ± 0.15	95.87 ± 0.15
	0.5	94.8 ± 0.1	94.57 ± 0.35
Guar	1.0	98.83 ± 0.15	99.06 ± 0.06
	0.75	97.13 ± 0.06	98.83 ± 0.15
	0.5	95.95 ± 0.02	97.5 ± 0.1

TABLE 3: Analysis of variance (sum of the square) for response surface model of weight loss of guava fruits during storage.

SOV	Df	Days			
		5	10	15	20
Model	5	22.8021^*	8.4648^*	22.5618^*	13.5515^*
Linear	2	1.6024^*	0.1901^*	0.0951^*	1.1588^*
FG	1	1.1915^*	0.1321^*	0.0882^*	1.1581^*
GG	1	0.4109^*	0.0580^*	0.0069^*	0.0006^*
Square	2	21.1907^*	8.2195^*	19.5255^*	8.5903^*
FG * FG	1	20.5353^*	0.3314^*	10.9630^*	1.1501^*
GG * GG	1	12.3077^*	6.4152^*	19.0467^*	7.7648^*
2-way interaction	1	0.0090^{ns}	0.0552^{ns}	2.9412^{ns}	3.8025^{ns}
FG * GG	1	0.0090^{ns}	0.0552^{ns}	2.9412^{ns}	3.8025^{ns}
Error	3	0.6967	3.8930	11.6652	6.3300
Total	8	23.4988	12.3578	34.2270	19.8815
R-square (%)		94.04	88.50	95.92	88.16

If $p > 0.05$, ^{NS}non-significant ($p > 0.05$); $p > 0.05$, *significant; and $p > 0.01$, **highly significant fenugreek galactomannan (FG), guar galactomannan (GG).
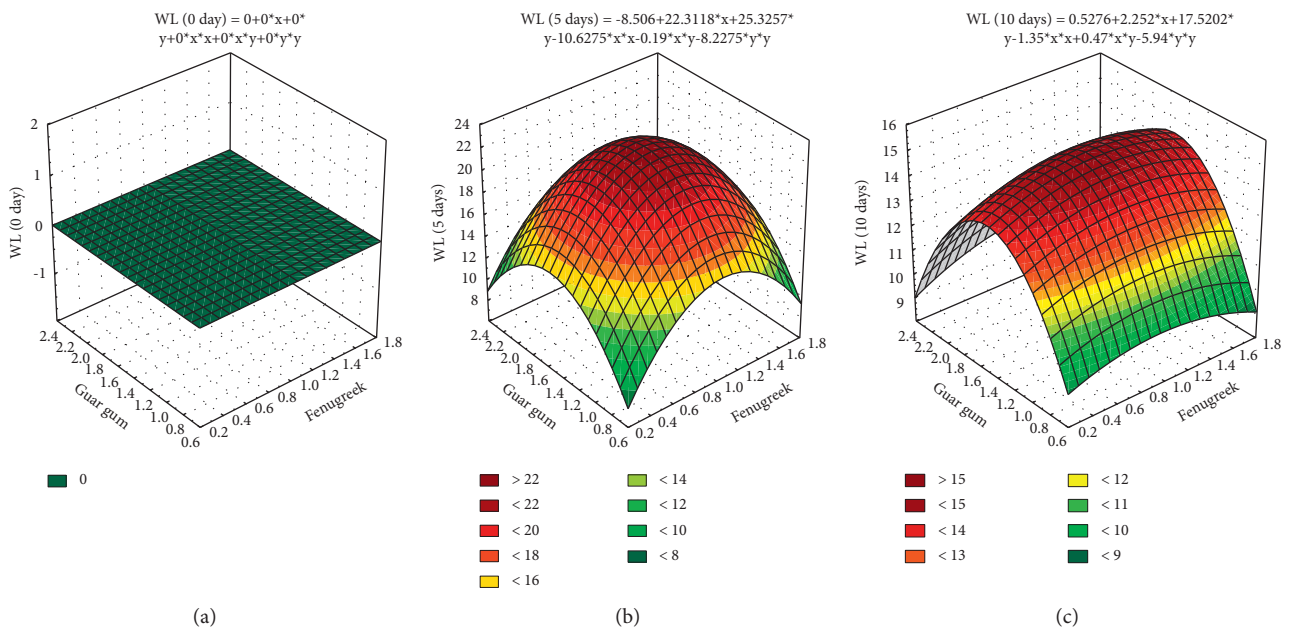

(a)

(b)

(c)

FIGURE 2: Continued.

WL (15 days) = -15.1509+20.465*x+34.0764* y-7.765*x*x-3.43*x*y-10.235*y*y

WL (20 days) = 5.8036-0.059*x+15.7227* y-2.515*x*x+3.9*x*y-6.535*y*y
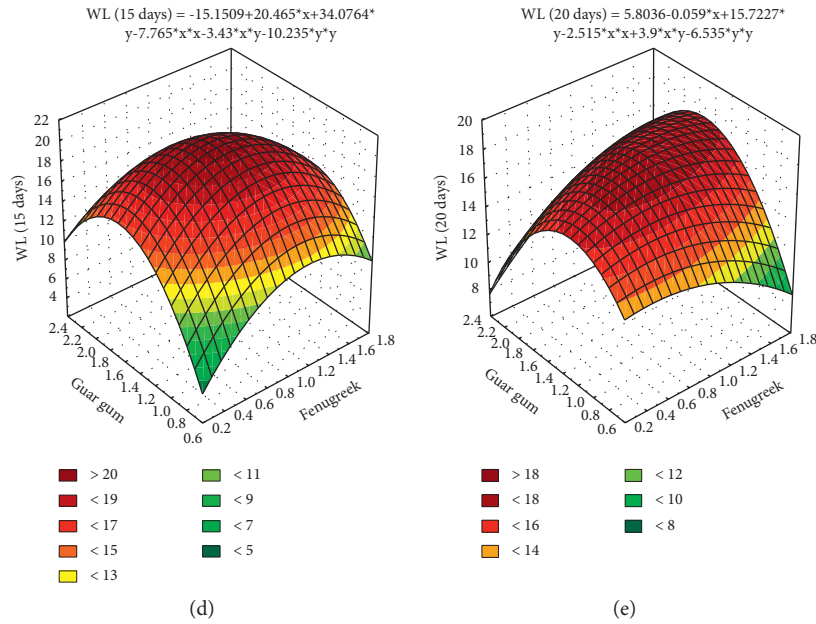
(d)	(e)

FIGURE 2: Response surface plot showing the impact of guar galactomannan and fenugreek galactomannan on weight loss of guava fruit during storage. (a) WL (0 days) = $0 + 0 * x + 0 * y + 0 * x * x + 0 * x * y + 0 * y * y$. (b) WL (5 days) = $-8.506 + 22.3118 * x + 25.3257 * y - 10.6275 * x * x ^- 0.19 * x * y - 8.2275 * y * y$. (c) WL (10 days) = $0.5276 + 2.252 * x + 17.5202 * y ^- 1.35 * x * x + 0.47 * x * y ^- 5.94 * y * y$. (d) WL (15 days) = $-15.1509 + 20.465 * x + 34.0764 * y - 7.765 * x * x - 3.43 * x * y ^- 10.235 * y * y$. (e) WL (20 days) = $5.8036 - 0.059 * x + 15.7227 * y ^- 2.515 * x * x + 3.9 * x * y ^- 6.535 * y * y$.

Firmness (0 day) = 1.2139+0.0894*x+0.1001*y -0.021*x*x-0.025*x*y-0.02*y*y

Firmness (5 days) = 1.6352-0.1771*x- 0.2629*y+0.0912*x*x-0.004*x*y+0.0902*y*y

Firmness (10 days) = 1.9224-0.3913*x-0.536*y +0.201*x*x+0.001*x*y+0.182*y*y
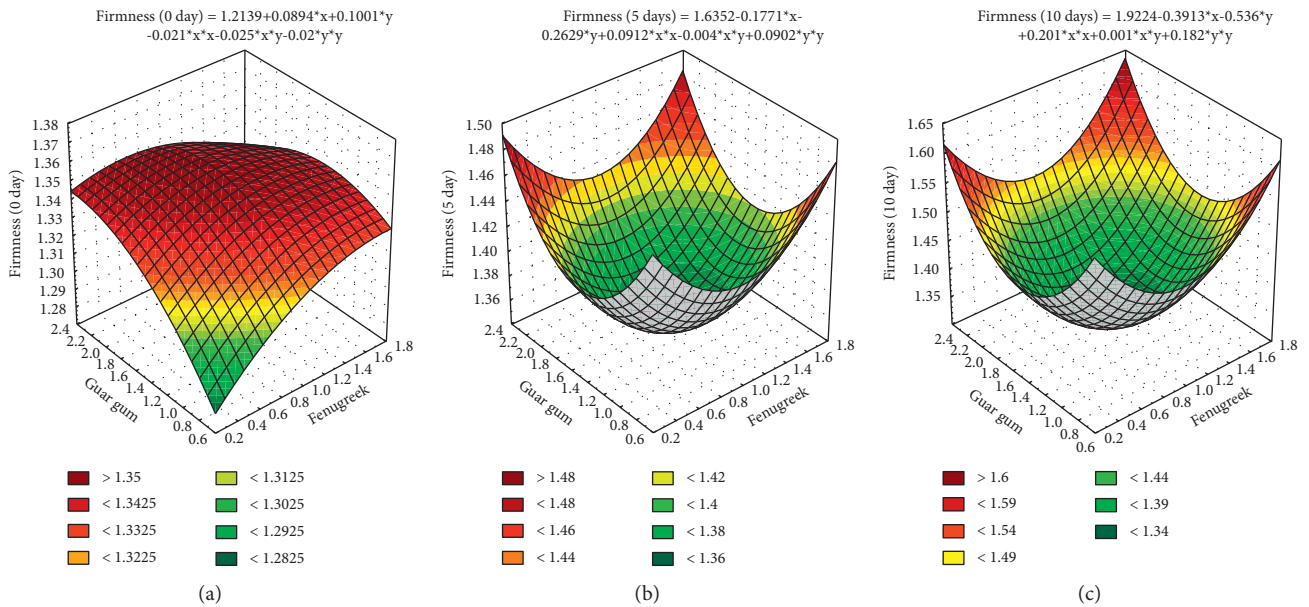
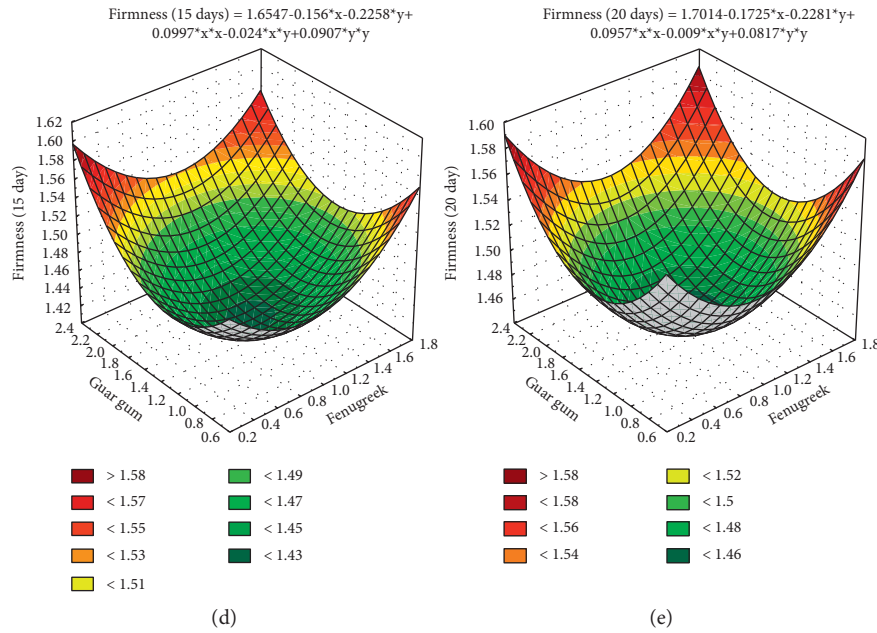|		
(a)	(b)	(c)

FIGURE 3: Continued.

FIGURE 3: Response surface plot showing the impact of guar galactomannan and fenugreek galactomannan on the firmness of guava fruit during storage. (a) Firmness (0 days) $= 1.2139 + 0.0894 * x + 0.1001 * y - 0.021 * x * x - 0.025 * x * y - 0.02 \times y * y$. (b) Firmness (5 days) $= 1.6352 - 0.1771 * x - 0.2629 * y + 0.0912 * x * x - 0.004 * x * y + 0.0902 * y * y$. (c) Firmness (10 days) $= 1.9224 - 0.3913 * x - 0.536 * y + 0.201 * x * x + 0.001 * x * y + 0.182 * y * y$. (d) Firmness (15 days) $= 1.6547 - 0.156 * x - 0.2258 * y + 0.0997 * x * x - 0.024 * x * y + 0.0907 * y * y$. (e) Firmness (20 days) $= 1.7014 - 0.1725 * x - 0.2281 * y + 0.0957 * x * x - 0.009 * x * y + 0.0817 * y * y$.

TABLE 4: Analysis of variance (sum of the square) for response surface model of fruit firmness during storage.

SOV	Df	Days				
		0	5	10	15	20
Model	5	0.000902^{ns}	0.001865^{*}	0.008777^{*}	0.003303^{*}	0.002014^{*}
Linear	2	0.000652^{ns}	0.000031^{*}	0.000537^{ns}	0.001122^{*}	0.000194^{ns}
Fenugreek (FG)	1	0.000197^{ns}	0.000001^{*}	0.000297^{ns}	0.000114^{*}	0.000060^{ns}
Guar gum (GG)	1	0.000455^{ns}	0.000030^{ns}	0.000240^{ns}	0.001009^{*}	0.000134^{ns}
Square	2	0.000094^{ns}	0.001830^{*}	0.008240^{ns}	0.002036^{ns}	0.001799^{*}
FG * FG	1	0.000080^{ns}	0.001514^{*}	0.007346^{*}	0.001809^{*}	0.001667^{*}
GG * GG	1	0.000073^{ns}	0.001481^{*}	0.006023^{ns}	0.001497^{ns}	0.001215^{*}
2-way interaction	1	0.000156^{ns}	0.000004^{ns}	0.000000^{ns}	0.000144^{*}	0.000020^{ns}
FG * GG	1	0.000156^{ns}	0.000004^{ns}	0.000000^{ns}	0.000144^{*}	0.000020^{ns}
Error	3	0.002181	0.000239	0.002070	0.000497	0.001094
Total	8	0.003083	0.002104	0.010847	0.003800	0.003108
R-square (%)		29.26	88.64	90.91	96.92	94.79

If $p > 0.05$, ^{NS}non-significant ($p > 0.05$); $p < 0.05$, *significant; and $p < 0.01$, ** highly significant fenugreek galactomannan (FG), guar galactomannan (GG).

and GG^2 are found significant at the 5th and 10th days. The interaction of two variables (XY) was nonsignificant at the start of the study and then significant effect on the TSS of guava fruits at various storage intervals. The coefficient of determination (R^2) was low on the 1st day and then was above 80% after the 5th day, indicating that models are well fitted (Figure 3). The average optimized levels of fenugreek and guar galactomannan in the edible coating were found to be 1.02 and 1.44%, respectively. The effect of edible coating on Brix of guava described that the total soluble solid increased up to a certain storage period in all the treatments and thereafter reduced as the storage period progressed. These results are consistent with previous findings [26]. The initial increase in TSS during storage was mainly due to the conversion of starch into soluble forms of sugars and the subsequent decrease in TSS was due to rapid utilization of reducing sugar and other organic metabolites [5].

3.6. pH. The regression coefficients of variables showed that FG and GG significantly affected the change in pH of guava fruits during storage. The effect of linear terms of fenugreek galactomannan and guar galactomannan are statistically significant ($p < 0.05$) for pH at all days of storage intervals (supplementary Figure 7 and supplementary Table 2). The X^2 quadratic terms (FG^2 and GG^2) are found significant at 5, 10, 15, and 20 days' storage intervals. The interaction of two variables (FG * GG) shows a significant effect on the pH of

TSS (0 day) = 7.9302+3.3043*x+5.9604*y-1.2*x*x-0.9*x*y-1.7*y*y

(a)

TSS (5 days) = 6.3321+4.8086*x+6.5104*y-1.625*x*x-1.4*x*y-1.725*y*yt

(b)

TSS (10 days) = 1.2367+14.3253*x+9.4129*y-7.125*x*x+0.4*x*y-3.625*y*y

(c)

TSS (15 days) = 10.479-0.0644*x+11.2362*y-4.675*x*x+7.2*x*y-6.575*y*y

(d)

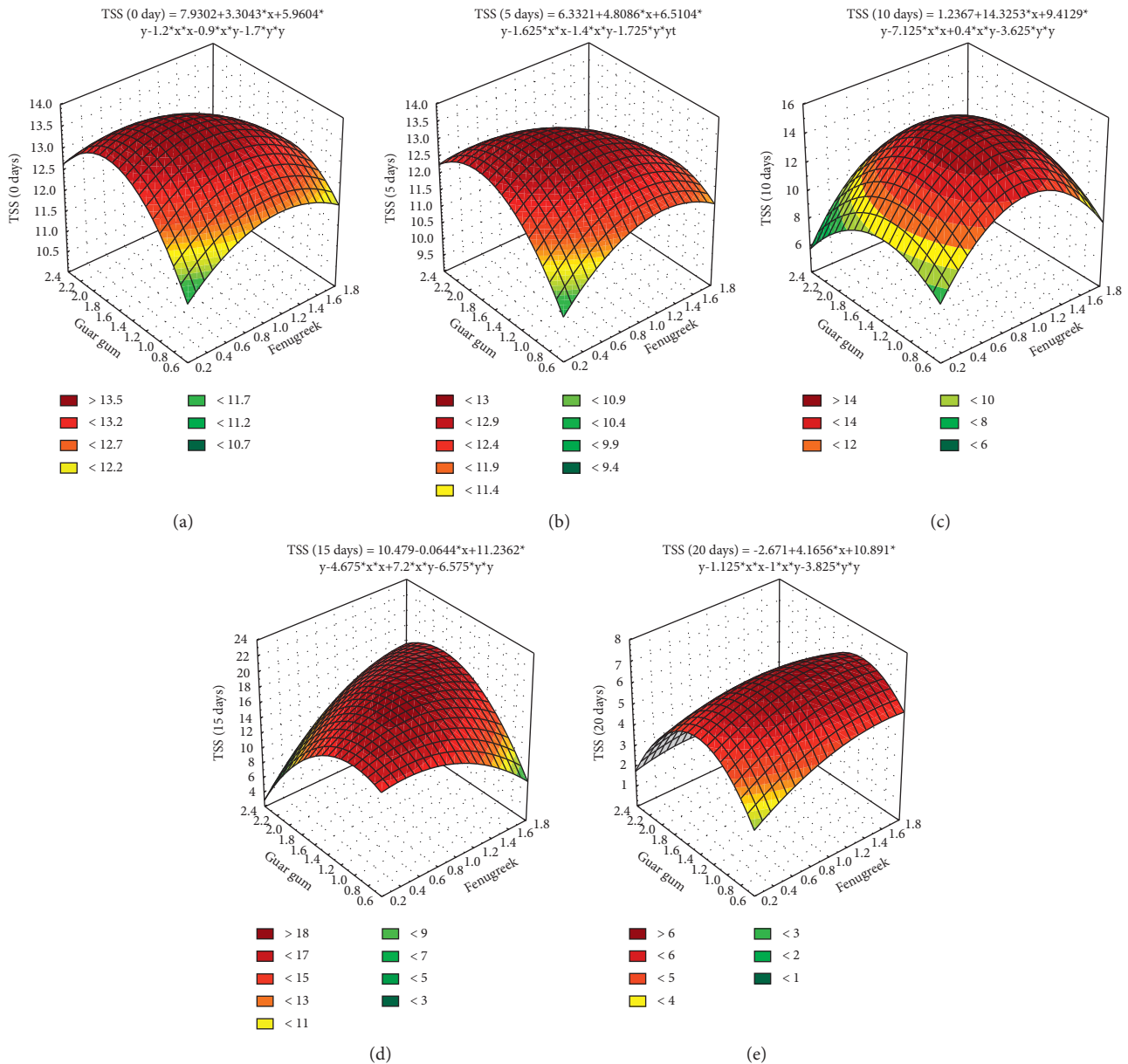TSS (20 days) = -2.671+4.1656*x+10.891*y-1.125*x*x-1*x*y-3.825*y*y

(e)

FIGURE 4: Response surface plot showing the impact of guar galactomannan and fenugreek galactomannan on TSS of guava fruit during storage. (a) TSS (0 days) = $7.9302 + 3.3043 * x + 5.9604 * y - 1.2 * x * x - 0.9 * x * y - 1.7 * y * y$. (b) TSS (5 days) = $6.3321 + 4.8086 * x + 6.5104 * y - 1.625 * x * x - 1.4 * x * y - 1.725 * y * y$. (c) TSS (10 days) = $1.2367 + 14.3253 * x + 9.4129 * y - 7.125 * x * x + 0.4 * x * y - 3.625 * y * y$. (d) TSS (15 days) = $10.479 - 0.0644 * x + 11.2362 * y - 4.675 * x * x + 7.2 * x * y - 6.575 * y * y$. (e) TSS (20 days) = $-2.671 + 4.1656 * x + 10.891 * y - 1.125 * x * x - 1 * x * y - 3.825 * y * y$.

guava fruits at all storage intervals. The coefficient of determination (R^2) was 99.10% on the 1st day, 96.78% on the 5th day, 75.58% on the 10th day, 88.48% on the 15th day, and 82.13% on the 20th day, indicating that models are well fitted (supplementary Figure 7).

A similar increasing trend in pH values of the galactomannan coated guavas throughout the storage period has been observed in the previously reported study [32]. Moreover, another study reported a minor raise in pH values after eight days of storage time [30]. That variation was occurred owing to the decrease in the amount of malic acid, because of the rise in respiration rate during cutting and

peeling. The average optimized levels of fenugreek galactomannan and guar galactomannan in the edible coating were 0.83% and 1.36%, respectively. The increased pH value was due to the development of organic acids through maturity or storage period [27].

3.7. Acidity. The regression coefficients of variables in models showed that the FG and GG did not contribute toward change in acidity in guava fruits at the start of storage but after that contributed significantly from 5th to 20 days storage intervals. The effect of linear terms of fenugreek galactomannan and

guar galactomannan are statistically significant ($p < 0.05$) for acidity at all days of storage intervals except the start of the study (supplementary Figure 8 and supplementary Table 3). The X^2 quadratic terms are found significant at 5, 10, 15, and 20 days storage intervals, whereas the quadratic terms for FG^2 and GG^2 are found significant at 5th and 10th days. The interaction of two variables (XY) shows a nonsignificant effect at the start and a significant effect on the acidity of guava fruits after 5 days storage intervals. The coefficients of determination (R^2) were well enough for well-fitted models (supplementary Figure 8). A significant decrease in acidity was observed at 5, 10, and 20 days of storage. The increase in pH and decrease in acidity in coated fruits was due to the reduction in respiration rate of fruits and consequently limit the over consumption of organic acids in respiration reactions [33]. The average optimized levels of fenugreek galactomannan and guar galactomannan in edible coating were 1.03% and 1.44%, respectively. The reduction of organic acids leads to decline of TA that subsequently results in increased juice pH of guava fruits [34]. The influence of treatments and storage times was significant on titratable acidity (TA) of guava fruits. Overall, the TA was progressively decreased but the reduction was significantly higher in control than the treated guava fruits.

4. Conclusion

According to the present study, 1.24 g guar galactomannan and 1.01 g fenugreek galactomannan in edible coating appeared to be the optimum coating formulation for improving the postharvest quality of guava fruit. The response surface methodology was observed as an effective statistical tool to discriminate the interactive effects of independent variables. The FG and GG-based edible coating significantly reduced the weight loss and TSS. Moreover, the coated fruit was fresh, firmer, and low in TA during storage. Thus, the RSM could be effectively used to optimize edible coating formulations leading to the overall enhancement of the quality and shelf-life of guava fruit.

Abbreviations

CO_2: Carbon dioxide
CCD: Central composite design
EC: Emulsifying capacity
ES: Emulsion stability
FG: Fenugreek galactomannan
GG: Guar galactomannan
RSM: Response surface methodology
TSS: Total soluble solids
O_2: Oxygen.

Data Availability

The dataset supporting the conclusions of this article is included in the manuscript.

Additional Points

Practical Application. Galactomannan-based edible coating can be served as environmentally friendly packaging by replacing the use of chemicals and reducing packaging waste in the food industry.

Conflicts of Interest

The authors declare that they have no conflicts of interest.

Acknowledgments

Supplementary Materials

Supplementary Figure 1: extraction and purification of guar galactomannan. Supplementary Figure 2: extraction and purification of fenugreek galactomannan. Supplementary Figure 3: XRD pattern of guar galactomannan. Supplementary Figure 4: XRD pattern of fenugreek galactomannan. Supplementary Figure 5: FTIR spectra of guar galactomannan. Supplementary Figure 6: FTIR spectra of fenugreek galactomannan. Supplementary Figure 7: response surface plot showing the impact of guar galactomannan and fenugreek galactomannan on pH of guava fruit during storage. Supplementary Figure 8: response surface plot showing the impact of guar galactomannan and fenugreek galactomannan on the acidity of guava fruit during storage. Supplementary Table 1: analysis of variance (sum of the square) for response surface model of fruit firmness during storage. Supplementary Table 2: analysis of variance (sum of the square) for response surface model of fruit TSS during storage. Supplementary Table 3: analysis of variance (sum of the square) for response surface model of fruit pH during storage. Supplementary Table 4: analysis of variance (sum of the square) for response surface model of fruit acidity during storage. (*Supplementary Materials*)

References

[1] S. Noonari, I. N. Memon, H. Wagan, I. Mushtaque, and M. Ismail, "Performance of guava orchards production and marketing in Sindh Pakistan," *Academy of Agriculture Journal*, vol. 1, no. 1, 2016.

[2] C. Vishwasrao and L. Ananthanarayan, "Postharvest shelf-life extension of pink guavas (*Psidium guajava* L.) using HPMC-based edible surface coatings," *Journal of Food Science and Technology*, vol. 53, no. 4, pp. 1966–1974, 2016.

[3] L. J. Babatola and G. Oboh, "Extract of varieties of guava (Psidium guajava L.) leaf modulate angiotensin-1-converting enzyme gene expression in cyclosporine-induced hypertensive rats," *Phytomedicine*, vol. 1, no. 4, Article ID 100045, 2021.

[4] Y. Suwanwong and S. Boonpangrak, "Phytochemical contents, antioxidant activity, and anticancer activity of three common guava cultivars in Thailand," *European Journal of Integrative Medicine*, vol. 42, Article ID 101290, 2021.

[5] A. Singh, D. S. Kachway, V. S. Kuschi, G. Vikas, N. Kaushal, and A. Sigh, "Edible oil coatings prolong shelf life and improve quality of guava (*Psidium guajava* L.)," *International Journal of Pure & Applied Bioscience*, vol. 5, no. 3, pp. 837–843, 2017.

[6] R. K. Dhall, "Advances in edible coatings for fresh fruits and vegetables: a review," *Critical Reviews in Food Science and Nutrition*, vol. 53, no. 5, pp. 435–450, 2013.

[7] J.-W. Han, L. Ruiz-Garcia, J.-P. Qian, and X.-T. Yang, "Food packaging: a comprehensive review and future trends," *Comprehensive Reviews in Food Science and Food Safety*, vol. 17, no. 4, pp. 860–877, 2018.

[8] M. Lacroix and K. D. Vu, "Edible coating and film materials," in *Innovations in Food Packaging*, pp. 277–304, Academic Press, Cambridge, MA, USA, 2014.

[9] G. I. Olivas, J. E. Dávila-Aviña, N. A. Salas-Salazar, and F. J. Molina, "Use of edible coatings to preserve the quality of fruits and vegetables during storage," *Stewart Postharvest Review*, vol. 3, no. 6, pp. 1–10, 2008.

[10] D. Mudgil, "The interaction between insoluble and soluble fiber," in *Dietary Fiber for the Prevention of Cardiovascular Disease*, pp. 35–59, Academic Press, Cambridge, MA, USA, 2017.

[11] M. A. Cerqueira, A. I. Bourbon, A. C. Pinheiro et al., "Galactomannans use in the development of edible films/coatings for food applications," *Trends in Food Science & Technology*, vol. 22, no. 12, pp. 662–671, 2011.

[12] G. Dodi, D. Hritcu, and M. I. Popa, "Carboxymethylation of guar gum: synthesis and characterization," *Cellulose Chemistry and Technology*, vol. 45, no. 3, p. 171, 2011.

[13] D. Mudgil, S. Barak, and B. S. Khatkar, "Guar gum: processing, properties and food applications-a review," *Journal of Food Science and Technology*, vol. 51, no. 3, pp. 409–418, 2014.

[14] A. H. Bahar, M. A. Ismail, A. H. Sulaiman, and S. Ali, "Characteristic evaluation of some guar (*Cyamopsis tetragonoloba* [L] taub) genotypes grown under rain-fed conditions at zalingei area," *ARPN Journal of Science and Technology*, vol. 5, no. 5, pp. 215–218, 2015.

[15] N. T. Farah, K. Ariba, Sirajuddin, and I. A. Hassan, "Analytical characterization of guar and guar gum produced in sindh, Pakistan," *Food Science and Nutrition Technology*, vol. 1, no. 2, pp. 2574–2701, 2016.

[16] K. Srinivasan, "Fenugreek (*Trigonella foenum-graecum*): a review of health beneficial physiological effects," *Food Reviews International*, vol. 22, no. 2, pp. 203–224, 2006.

[17] J. X. Jiang, L. W. Zhu, W. M. Zhang, and R. C. Sun, "Characterization of galactomannan gum from fenugreek (*Trigonella foenum-graecum*) seeds and its rheological properties," *International Journal of Polymeric Materials*, vol. 56, no. 12, pp. 1145–1154, 2007.

[18] N. Khorshidian, M. Yousefi Asli, M. Arab, A. Adeli Mirzaie, and A. M. Mortazavian, "Fenugreek: potential applications as a functional food and nutraceutical," *Nutrition and Food Sciences Research*, vol. 3, no. 1, pp. 5–16, 2016.

[19] F. Rashid, S. Hussain, and Z. Ahmed, "Extraction purification and characterization of galactomannan from fenugreek for industrial utilization," *Carbohydrate Polymers*, vol. 180, pp. 88–95, 2018.

[20] N. D. Işıklı and E. Karababa, "Rheological characterization of fenugreek paste (çemen)," *Journal of Food Engineering*, vol. 69, no. 2, pp. 185–190, 2005.

[21] M. A. Anjum, H. Akram, M. Zaidi, and S. Ali, "Effect of gum Arabic and aloe vera gel based edible coatings in combination with plant extracts on postharvest quality and storability of "Gola" guava fruits," *Scientia Horticulturae*, vol. 271, Article ID 109506, 2020.

[22] AACC, *Approved Methods of Analysis*, The American Association of Cereal Chemist, Saint Paul, MN, USA, 2000.

[23] M. Nadeem, F. Muhammad Anjum, M. A. Murtaza, and G. Mueen-ud-Din, "Development, characterization, and optimization of protein level in date bars using response surface methodology," *The Scientific World Journal*, vol. 2012, Article ID 518702, 10 pages, 2012.

[24] R. Malviya, P. K. Sharma, and S. K. Dubey, "Antioxidant potential and emulsifying properties of Kheri (Acacia chundra, Mimosaceae) gum polysaccharide," *Marmara Pharmaceutical Journal*, vol. 21, no. 3, p. 701, 2017.

[25] N. Azarakhsh, A. Osman, H. M. Ghazali, C. P. Tan, and N. Mohd Adzahan, "Optimization of alginate and gellan-based edible coating formulations for fresh-cut pineapples," *International Food Research Journal*, vol. 19, no. 1, 2012.

[26] P. Dutta, N. Bhowmick, S. Khalko, A. Ghosh, and S. K. Ghosh, "Postharvest treatments on storage life of guava (*Psidium guajava* L.) in himalayan terai region of West Bengal, India," *International Journal of Current Microbiology and Applied Science*, vol. 6, no. 3, pp. 1831–1842, 2017.

[27] G. Khaliq, H. T. Abbas, I. Ali, and M. Waseem, "Aloe vera gel enriched with garlic essential oil effectively controls anthracnose disease and maintains postharvest quality of banana fruit during storage," *Horticulture Environment and Biotechnology*, vol. 60, no. 5, 2019.

[28] M. A. Rojas-Graü, M. S. Tapia, and O. Martín-Belloso, "Using polysaccharide-based edible coatings to maintain quality of fresh-cut Fuji apples," *LWT-Food Science and Technology*, vol. 41, no. 1, pp. 139–147, 2008.

[29] J. Y. Lee, H. J. Park, C. Y. Lee, and W. Y. Choi, "Extending shelf-life of minimally processed apples with edible coatings and antibrowning agents," *Lebensmittel-Wissenschaft und-Technologie-Food Science and Technology*, vol. 36, no. 3, pp. 323–329, 2003.

[30] D. Albanese, L. Cinquanta, and M. Dimatteo, "Effects of an innovative dipping treatment on the cold storage of minimally processed Annurca apples," *Food Chemistry*, vol. 105, no. 3, pp. 1054–1060, 2007.

[31] G. Oms-Oliu, R. Soliva-Fortuny, and O. Martín-Belloso, "Edible coatings with antibrowning agents to maintain sensory quality and antioxidant properties of fresh-cut pears," *Postharvest Biology and Technology*, vol. 50, no. 1, pp. 87–94, 2008.

[32] R. Sothornvit, "Effect of edible coating on the qualities of fresh guava," *Acta Horticulturae*, vol. 1012, pp. 453–459, 2012.

[33] F. D. Soares, T. Pereira, M. O. Maio Marques, and A. R. Monteiro, "Volatile and non-volatile chemical composition of the white guava fruit (Psidium guajava) at different stages of maturity," *Food Chemistry*, vol. 100, no. 1, pp. 15–21, 2007.

[34] R. Etemadipoor, A. Ramezanian, A. Mirzaalian Dastjerdi, and M. Shamili, "The potential of gum Arabic enriched with cinnamon essential oil for improving the qualitative characteristics and storability of guava (Psidium guajava L.) fruit," *Scientia Horticulturae*, vol. 251, pp. 101–107, 2019.